New chiral, tridentate, phosphine group containing ferrocenyl ligands for asymmetric catalysis with non-noble metals

Uchchhal Bandyopadhyay

THÈSE

En vue de l'obtention du

DOCTORAT DE L'UNIVERSITÉ DE TOULOUSE

Délivré par l'Université Toulouse 3 - Paul Sabatier

Présentée et soutenue par

Uchchhal BANDYOPADHYAY

Le 22 Juillet 2021

Nouveaux ligands ferrocéniques chiraux tridentes contenant des groupements phosphine pour la catalyse asymétrique avec des métaux non-nobles

[New chiral, tridentate, phosphine group containing ferrocenyl ligands for asymmetric catalysis with non-noble metals]

Ecole doctorale : **SDM - SCIENCES DE LA MATIERE - Toulouse**

Spécialité : **Chimie Organométallique et de Coordination**

Unité de recherche :
LCC - Laboratoire de Chimie de Coordination

Thèse dirigée par
Rinaldo POLI et Eric MANOURY

Jury
M. Mathieu Sauthier, Rapporteur
Mme Emmanuelle Schulz, Rapporteure
M. Petr Štěpnička, Examinateur
Mme Montserrat Gomez, Examinatrice
M. Rinaldo Poli, Directeur de thèse
M. Eric Manoury, Co-directeur de thèse

Année: 2021

THESE

Présentée

DEVANT L'UNIVERSITE PAUL SABATIER DE TOULOUSE III (Sciences)

En vue de l'obtenion

DU DOCTORAT DE L'UNIVERSITE PAUL SABATIER

(Spécialité: Chimie Organométallique)

par

UCHCHHAL BANDYOPADHYAY

'New chiral, tridentate, phosphine group containing ferrocenyl ligands for asymmetric catalysis with non-noble metals'

Composition du Jury:

M. Mathieu Sauthier, Université Lille I	Rapporteur
Mme. Emmanuelle Schulz, ICMMO-CNRS, Orsay	Rapporteure
M. Petr Štěpnička, Charles University in Prague	Examinateur
Mme. Montserrat Gomez, Université Toulouse III	Examinatrice
M. Rinaldo Poli, INP- Toulouse	Directeur de thèse
M. Eric Manoury, LCC- CNRS	Co-directeur de thèse

Recherches effectuees au Laboratoire de Chimie de Coordination du CNRS
205, Route de Narbonne- 31077, TOULOUSE Cedex 4.

Acknowledgements

I acknowledge Dr. Azzedine Bousseksou, first of all, for hosting me for a 3.5-year thesis at the Laboratoire de Chimie de Coordination (LCC)-CNRS at Universite Paul Sabitier in Toulouse.
I would also like to thank the members of the jury, Prof. Mathieu Sauthier, Dr.Emmanuelle Schulz, Prof. Montserrat Gomez, Prof. Petr Štěpnička for doing me the honor of judging my work. I would like to thank my thesis supervisors, Prof. Rinaldo Poli and Dr. Eric Manoury, for their daily support, regular scientific input and for the confidence they have placed in me, which has enabled me to make good progress on a scientific level. I sincerely thank Prof. Basker Sundararaju, IIT Kanpur for recommending me to join LCC and work on this colaborative project. I also acknowledge 'Centre Franco-Indien pour la Promotion de la Recherche Avancée' (CEFIPRA) for providing the financial support.

I would like to thank the members of the different NMR departments: Antoine Bonnet, David Paryl, Christian Bijani and Francis Lacassin; Laure Vendier, Carine Duhayon, and Sonia Melet for the XRD- service. I heartily express my gratitude to Dr. Jean Claude Daran for the crystal data analysis and structure determination. My thanks also go to the members of the joint mass spectroscopy service at Paul Sabatier University. I would like to thank Nataly Aulier**,** Stéphanie Seyrac from Personnel Management Department and general secretary Patricia Fouquereau; for taking care of the relevant administrative procedures, when needed.
A big thank you to all the members of my beloved G team for persisting a healthy and vibrant atmosphere that helped me a lot to grow both, professionally and mentally. I shared good times and had very enriching scientific discussions. My sincere thank goes to Sandrine Vincendeau (for your very kind co-operation in any lab related doubts or situations), Agnès Labande (especially, for helping me out with the doctoral school procedures), Eric Deydier, Pascal Guillo, Dominique Agustin, Catherine Audin, Florence Gayet, Yun Wang, Hui Wang, Jirong Wang, Lucas Thevenin, Ramakrishna Gandikota (for teaching me a lot of research oriented techniques), Abdelhak Lachguar (for a lot of work sharing and finally for the combined paper), Maxime Michelas, Chantal Abou Fayssal, Meenu Murali, Lionel Crane, Julian Sobieski, Mehdi Ech-Chariy.
My father has been the unsung hero behind my entire academic journey. His sacrifices, love, struggle, support and faith have brought me the place where I am. I express my sincere gratitude, love and respect to him. I want to say if you were not there this might not be happened. Thank you

also to my family and relatives for being there and supporting me through good times and bad. My sincere gratitude to all my teachers from school and college. There is little everything in my thesis from what I learnt from all my teachers.

I like to thank all the people whom I met in Toulouse. The presence of all of you around me and kind co-operations in different situations, time to time, helped me to fix several things and made me feel comfortable. Above all, I enjoyed all of your company, a lot. In this regard I especially mention Dr. Ramakrishna Gandikota, once again, and his wife Renuka Gandikota, for their constant support and helping hands which drove me through difficult circumstances. I express sincere gratitude to both of you and love for your son, little Ruthwik. A special thanks to Dr. Rudraditya Sarkar, for all the Friday night dinners. My sincere thank goes to my other seniors- Dr. Subhadip Chakrabory, Dr. Ramaraj Ayyappan, Dr. Sravani Teja Bulusu, Dr. Pritam Das, Dr. Kuntal Bhandari and my beloved friends and juniors- Priyanka, Sayantan, Ashraful, Radhika, Prathwi, Mohor, Meenu, Dipti and Ashwin. I would like to mention 'Toulouse Cricket Club' which has been indivisible part of my life in Toulouse. Practicing cricket as a physical exercise and mental relaxation during the Sundays has been very effective for me, throughout. I thank my fellow club members, Philippe (the President), Christophe, Darshan, Tanjil, Rayhan, Tanveer, Sam, Saqline, Tithir, Ruaridh and everyone I forgot. I spent some quality time in our playground with all of you guys.

I also thank my friends back in India. A big thanks to the people of Serampore, Hooghly (Sukanto, Rajesh, Chintu…….) for always being there as true friends and for the all the good memories we shared together. I thank all of friends and classmates from school and college for their warm company.

A sincere thank you to everyone!!

Contents

Abbreviations and Symbols

1) Symbols

δ= Chemical Shift
s= Singlet
d= Doublet
t= Triplet
q= Quartet
dd= Doublet of doublet
dt= Doublet of triplet
br= Broad
hept= Heptet
J= Coupling Constant
J_{CP}= Coupling Constant for coupling between proton and phosphorous
(M)= Molar
g= Gram
mmol= Milimol
h= Hour
(R_P/ S_P) = Planar chirality with absolute configuration- *R/ S*
(S_P)= chiral phosphine
ppm= Parts per Million
MHz= Mega Hertz
Hz= Hertz

2) Abbreviations

NMR= Nuclear Magnetic Resonance
TLC= Thin Layer Chromatography
DCI-CH_4= Desorption Chemical Ionization (by CH_4)
DH= Direct Hydrogenation
TH= Transfer Hydrogenation
ATH= Asymmetric Transfer Hydrogenation
BH= Borrowing Hydrogen
CBS= Corey-Baksi-Shibata
quat.= Quarternary
Subst.= Substituted
equiv.= Equivalent
rac= Racemic
S/C= Substrate-catalyst molar ratio
TON= Turn Over Number
TOF= Turn Over Frequency
Ee= Enatiomeric excess
er= Enatiomeric ratio
dr= diastereomeric ratio

3) Chemical Compound Abbreviations

Cp= Cyclopentadienyl

Fc= Ferrocenyl
Ar= Aromatic
^{i}pr= Isopropyl
^{t}Bu= Tertiary butyl
Bn= Benzyl
Py= Pyridyl
Ts= Tosyl
DABCO= 1,4-Diazabicyclo(2,2,2)octane
DCM= Dichloromethane
DEAD= Diethyl Aza Dicarboxylate
TMSCl= Trimethyl Silyl Chloride
TBAF= Tetrabutyammonium fluoride
PTSA= *p*-toluenesulphonic acid
THP= Tetrahyropyran
DHP= Dihyropyran
THF= Tetrahydrofuran
BOC= tert-butyloxycarbonyl
CBz= benzyl chloroformate
SAMP= *(S)*-1-amino-2-methoxymethylpyrrolidine
BAr_F= tetrakis(3,5-bis(trifluoromethyl)phenyl)borate

Résumé des travaux de recherche

Introduction

La catalyse suscite de l'intérêt depuis plusieurs décennies car elle permet de réaliser de nombreuses réactions dans de meilleures conditions, c'est-à-dire avec moins d'énergie, une meilleure économie d'atomes et avec des réactifs moins dangereux. En outre, certaines réactions catalytiques peuvent être des réactions énantiosélectives, ce qui présente un intérêt considérable en raison de l'importance des composés énantiomériquement enrichis dans de nombreux domaines tels que l'agrochimie, la pharmacie et l'industrie des matériaux. Il est évidemment très important de développer des catalyseurs chiraux offrant une énantiosélectivité et une productivité élevée. Les catalyseurs à base de métaux de transition se sont avérés être les systèmes les plus polyvalents et les plus compétents pour fournir une excellente productivité et une énantiosélectivité dans différents types de réactions organiques asymétriques au cours des dernières décennies. Ces catalyseurs consistent en général en un centre métallique coordonné à un ligand organique chiral monodenté ou polydenté. Dans la recherche actuelle, les métaux de transition non nobles ou de première rangée sont de plus en plus souvent introduits dans la recherche de solutions plausibles à de nombreux problèmes, comme l'épuisement rapide des métaux de transition nobles ou plus lourds (2e/3e période), la crise environnementale, *etc.* Les réactions catalytiques pilotées par des métaux non nobles avec des ligands chiraux existants, ainsi que de nouveaux ligands spécialement développés, sont étudiées à un rythme croissant afin de trouver un ajustement approprié. À cet égard, les ligands tridentés chiraux attirent de plus en plus l'attention à la suite de leur succès rapide au cours des dernières années.

Nous avons été très intéressés par les réalisations importantes obtenues avec des ligands chiraux possédant un squelette ferrocénique et une chiralité planaire associée et, en particulier, ceux contenant une phosphine (par exemple, JOSIPHOS et FOXAP) dans le domaine de la catalyse asymétrique homogène à base de métaux de transition au cours des dernières décennies. En outre,

les ligands ferrocéniques tridentes chiraux contenant des phosphines et les catalyseurs à base de métaux non nobles ont conduit à quelques réalisations récentes intéressantes dans les réactions asymétriques d'hydrogénation-déshydrogénation, d'alkylation, de cycloaddition, *etc.* Cependant, le nombre de ces ligands tridentes est encore assez limité, ce qui nous a motivés à développer quelques nouveaux composés supplémentaires. Cependant, le nombre de ces ligands tridentes est encore assez limité, ce qui nous a incités à développer quelques nouveaux composés supplémentaires. Ainsi, dans cette thèse, nous avons conçu un certain nombre de familles de ligands phosphine tridentes ferrocéniques à chiralité planaire.

Objectifs de la thèse et état de l'art

Les progrès très récents de la méthodologie de l'"emprunt d'hydrogène" décrivent l'activation temporaire d'alcools primaires et secondaires en son analogue carbonyle. L'intermédiaire subit une réaction de condensation avec un autre substrat suivie d'une hydrogénation, conduisant à un produit plus complexe, difficile à obtenir en une seule étape. La version asymétrique de cette méthodologie n'est pas explorée autant que ses versions non asymétriques. Par conséquent, l'objectif global de notre projet est de développer des versions asymétriques des réactions catalytiques par "'emprunt d'hydrogène" en utilisant les ligands ferrocéniques à chiralité planaire tridentes à base de phosphine et leurs complexes métalliques comme catalyseurs. La stratégie consiste à réunir l'expertise des groupes français et indien (Prof. Basker Sundararaju, IITK ,Inde) pour atteindre des objectifs réalistes mais stimulants. Le choix des objectifs est motivé par le problème de l'épuisement rapide des combustibles fossiles et des métaux nobles, ces derniers étant la source des catalyseurs les plus courants, bien qu'ils soient de moins en moins disponibles. Par conséquent, le développement de procédés faisant appel à des métaux abondants dans la terre et utilisant des ressources renouvelables pour l'énergie et la durabilité est d'un grand intérêt actuel. À

cet égard, les métaux de transition ou les métaux non nobles (Cobalt, manganèse, fer principalement) sont choisis pour la conception de catalyseurs.

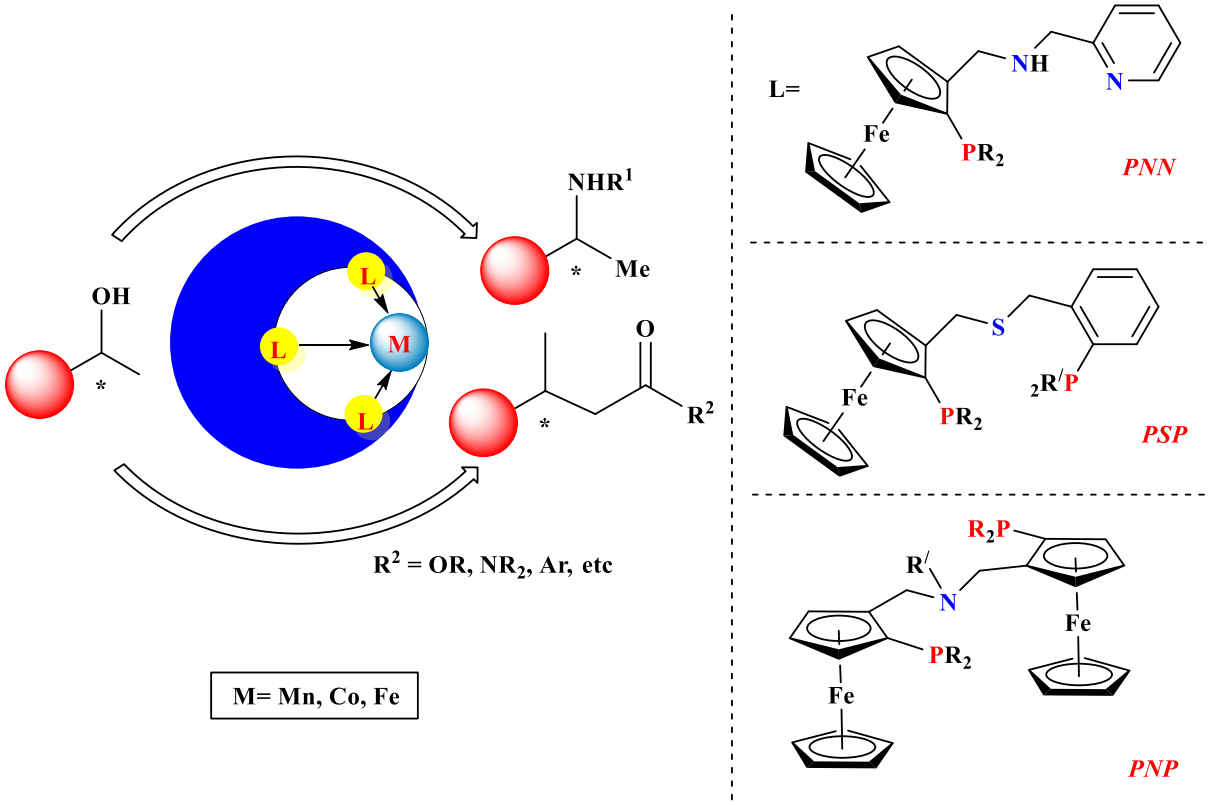

Schème 1 : Aperçu général de notre réaction cible et du développement de catalyseurs

Cette thèse décrit la synthèse de quelques familles de ligands ferrocéniques planaires tridentés et chiraux contenant des phosphines (par exemple, PNN, PNP, PSP, *etc.*), ce qui constitue l'objectif principal du projet. Plusieurs autres composés organiques ou organométalliques, formés soit comme intermédiaires de synthèse, soit comme sous-produits au cours de synthèses de ligands multi-étapes, sont également mentionnés en détail dans cette thèse.

Résumé du chapitre 1

Un aperçu bibliographique est présenté dans ce chapitre. Cette vue d'ensemble comprend une brève description de la justification de la catalyse à base de métaux non nobles dans les domaines récents de la catalyse et une brève idée de l'hydrogénation et de l'hydrogénation de transfert, dans les sections précédentes (sections 1.1 et 1.2). Dans les sections suivantes, un bon nombre de ligands

bidentes non-ferrocéniques et ferrocéniques contenant une fonction phosphine ont été présentés ainsi que leur application dans l'hydrogénation asymétrique ou l'hydrogénation de transfert avec les métaux de transition (section 1.2.1 et 1.2.2). La section comprend également les avancées récentes concernant les ligands ferrocéniques tridentes contenant une fonction phosphine et leurs applications dans le même domaine catalytique. Les sections suivantes (sections 1.3 et 1.4) décrivent brièvement la méthodologie "Borrowing Hydrogen". La description comprend l'idée générale et le mécanisme de ce processus catalytique, les avancées récentes des systèmes de catalyseurs métalliques à base de ligands pour les substrats typiques (par exemple, les alcools primaires et secondaires). Quelques exemples de la méthodologie asymétrique "Borrowing Hydrogen" catalysée par des catalyseurs métalliques à base de ligands chiraux, qui présente un intérêt majeur, ont été présentés dans les sections 1.4.

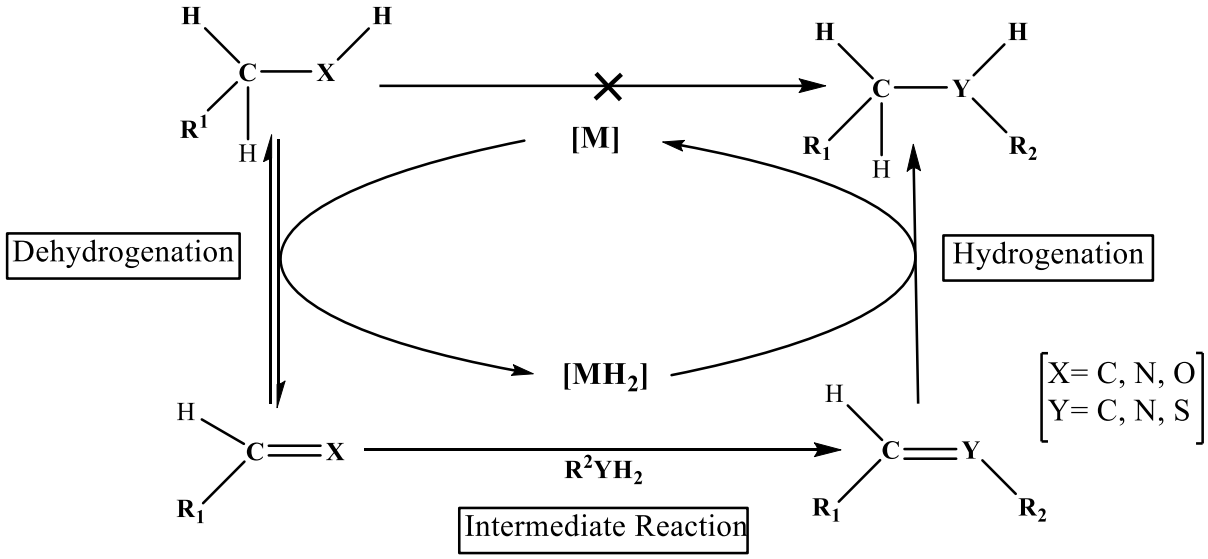

Schème 2: Mécanisme général de la méthodologie d'emprunt d'hydrogène

Résumé du chapitre 2

Le chapitre commence par la description des protocoles de synthèse précédemment rapportés et conçus pour les ligands ferrocéniques bidentes contenant un groupe phosphine. Il est ensuite directement orienté vers la discussion des résultats obtenus.

Les recherches synthétiques primaires ont commencé par la synthèse du (2-diphénylthiophosphinoferrocényl)méthanol **2-29**. Il s'agit de l'intermédiaire de synthèse le plus important pour tous les ligands que nous avons conçus. Il a été synthétisé à la fois dans ses versions racémiques et énantiomériquement pures en utilisant un protocole bien établi comprenant trois-quatre étapes. La synthèse détaillée a été décrite dans le chapitre 2.

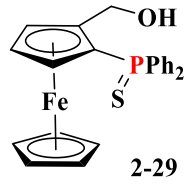

2-29

(rac and R/S_p)

Schème 3 : Structure chimique du (2-diphénylthiophosphinoferrocényl)methanol

Les proligands ferrocéniques de type PNP **2-51**, ont été synthétisés par le Dr. Lucie Routaboul, précédemment. Ces composés contiennent deux unités identiques ortho-(thiodiphénylphosphino)-ferrocénylméthyle reliées par une unité amine tertiaire. La synthèse a été réalisée par substitution nucléophile du sel de pyridinium de l'alcool **2-29** à reflux soit par une amine simple (benzylamine) soit par les amines **2-42**. La synthèse a été reproduite dans cette thèse car elle n'a pas été explorée dans aucun type de catalyse jusqu'à présent.

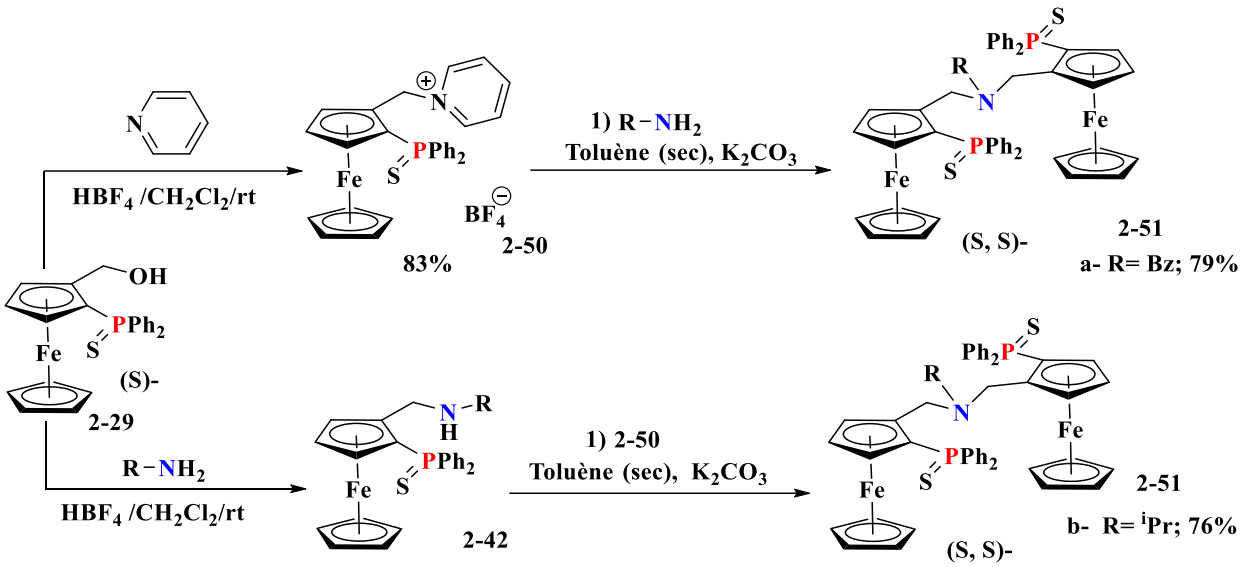

Schème 4 : Synthèse des proligands PNP **2-51**

La famille suivante de ligands est constituée d'amines tertiaires ferrocéniques contenant une fonvtion phosphine avec le modèle de coordination P,N,N-. Nous avons conçu deux types de ligands : le ligand **2-1** qui est un simple type PNN, tandis que le ligand **2-39** contient un bras latéral pyridyle modifié avec un groupe 2-hydroxyle. Le modèle du ligand **2-39** a été inspiré par la propriété tautomérique des 2-hydroxypyridones et, par conséquent, la capacité de fournir une bi-fonctionnalité métal-ligand dans certaines conditions catalytiques.

Schème 5 : Formule chimique de deux ligands de type PNN

Les formes de proligands protégés par une phosphine **2-28**, du ligand 2-1 ont été préparées par couplage de l'alcool **2-29** et de certains dérivés de la 2-picolylamine, dans les conditions bien connues de la réaction de Mitsunobu. Les trois proligands synthétisés sont caractérisés de manière approfondie par RMN multinucléaire, HRMS et cristallographie par diffraction des rayons X sur

monocristaux. Les dérivés de 2-picolylamine (**2-30**) utilisés comme partenaires de couplage sont soit utilisés à partir de sources disponibles dans le commerce, soit synthétisés au préalable à partir de 2-picolylamine simple.

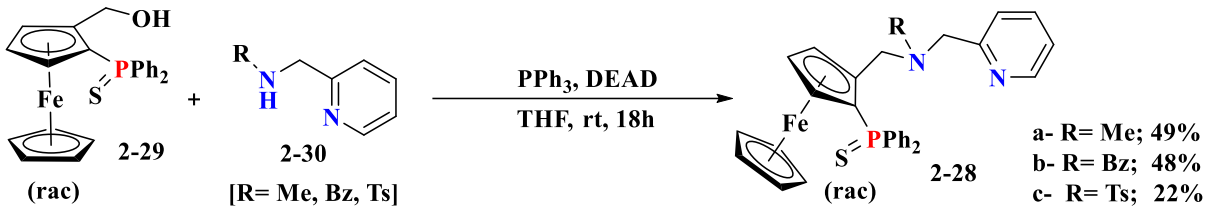

Schème 6 : Synthèse de différents proligands PNN **2-28** dans les conditions de ma réaction de Mitsunobu

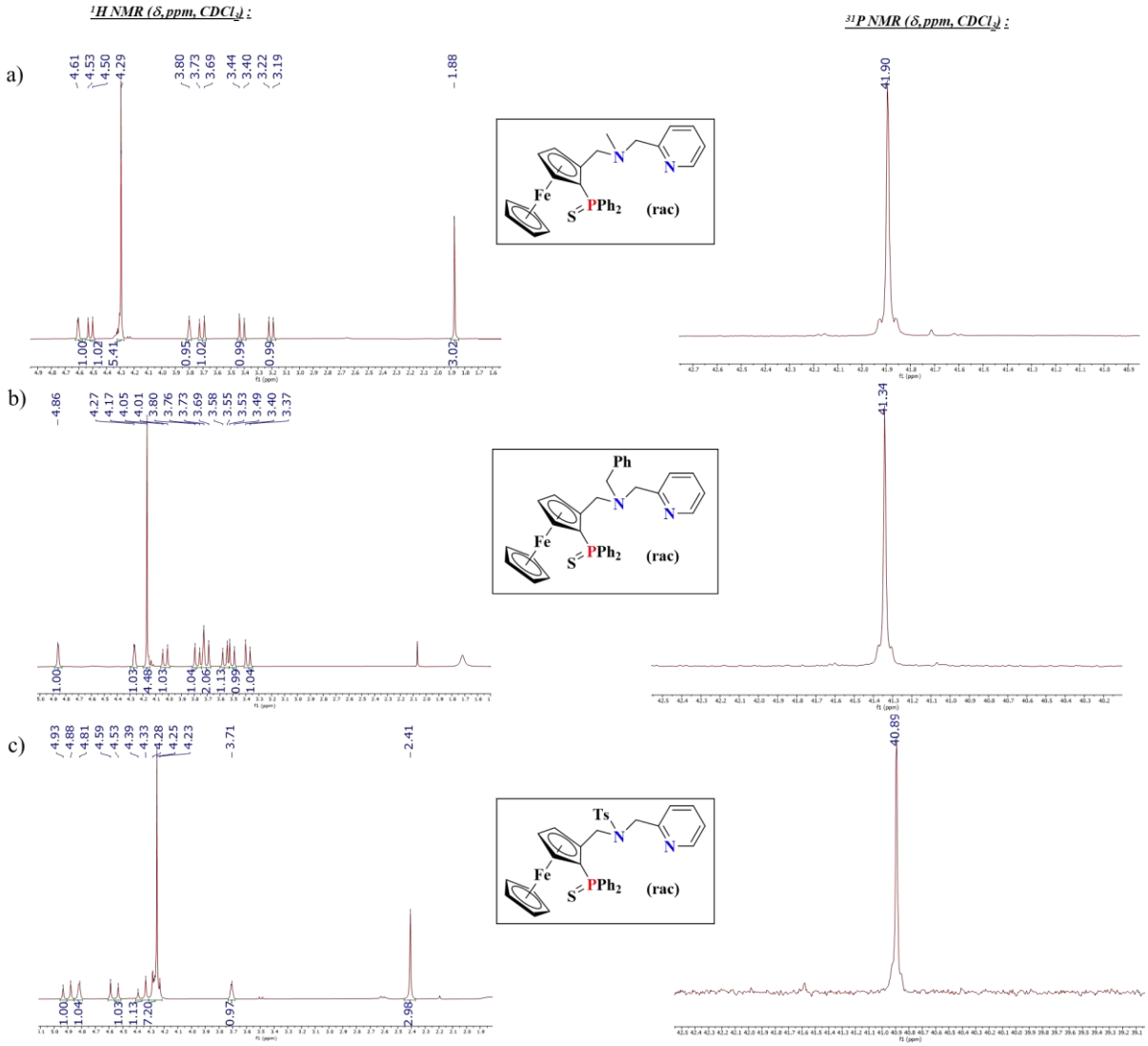

Figure 1 : Spectres RMN ^{1}H (Cp et région aliphatique) et ^{31}P de **2-28a**, **2-28b** et **2-28c**

La protection par le soufre de la fonction phosphine dans **2-28a** (R=Me) a été supprimée par une réaction d'échange avec $P(NMe_2)_3$ à des températures élevées pour obtenir le ligand **2-1** contenant une phosphine libre activée (R=Me). Le ligand activé a été caractérisé par RMN multinucléaire. Pour les deux autres proligands, le processus est en cours d'investigation pour le moment.

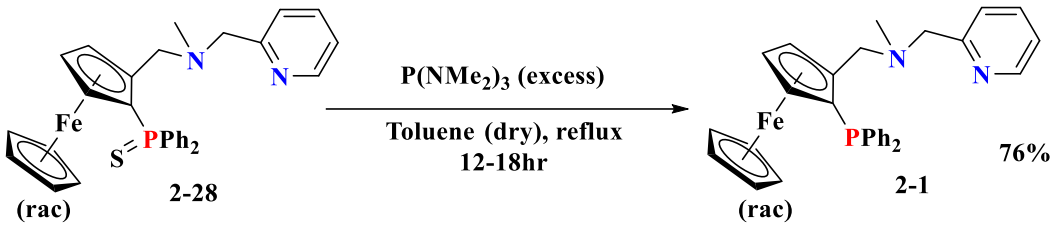

Schème 7 : Déprotection de la fonction phosphine du ligand **2-28a** (R= Me)

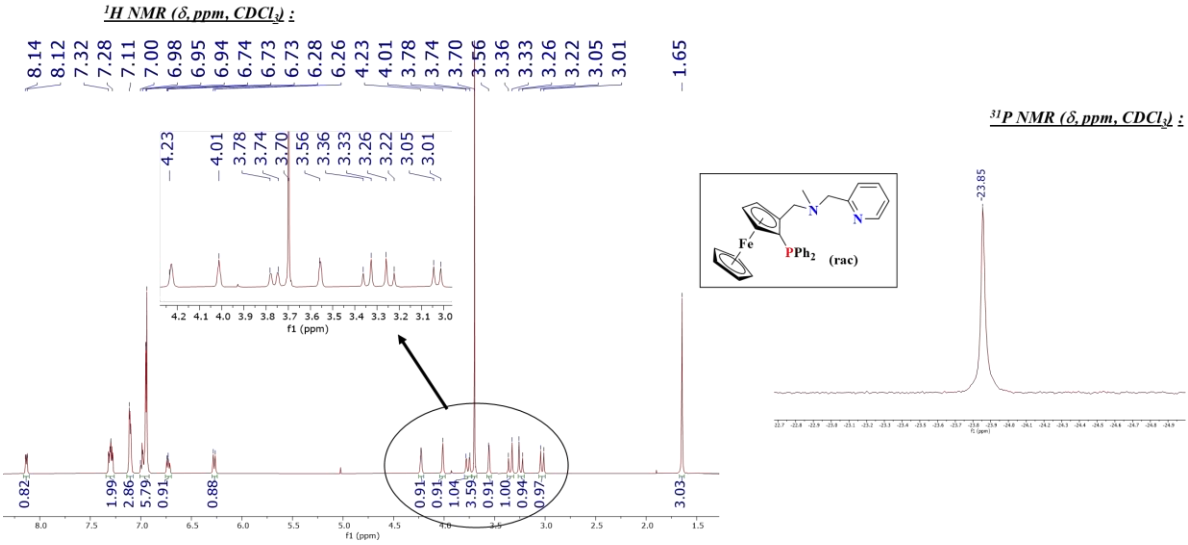

Figure 2: Spectres de RMN ^{1}H et ^{31}P de **2-1** (R= Me)

Dans la section suivante de ce chapitre, une 6-méthoxy pyridine fonctionnalisée avec un bras CH_2Br et CH_2OTs approprié en position 2 comme intermédiaires de synthèse pour le ligand **2-39** ont été préparés en suivant 2-3 étapes avec les optimisations nécessaires. Le groupe 6-méthoxy représente la forme protégée du groupe hydroxyle. Cette protection a été faite intentionnellement au début du processus de synthèse et est destinée à être retirer à un stade ultérieur si nécessaire.

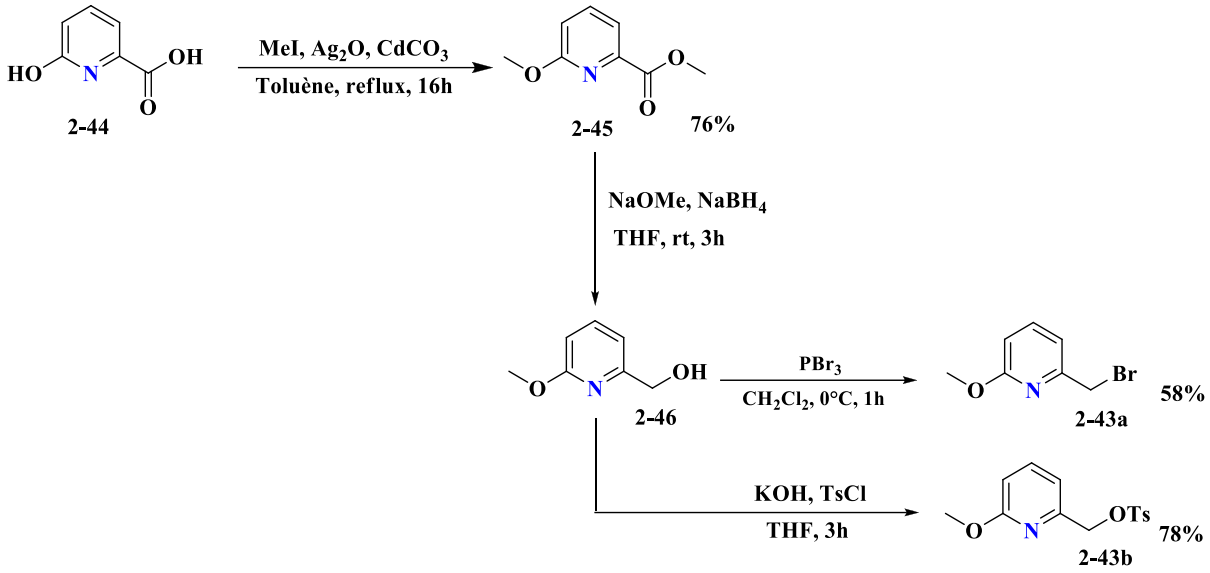

Schème 8 : Preparation of Bromo and Tosyl intermediates **2-43**

L'intermédiaire tosyle **2-43b** a été mis à réagir avec les amines **2-42** pour obtenir les proligands hydroxyles protégés **2-40** en présence d'une base. Deux proligands ont été synthétisés et caractérisés par RMN multinucléaire, HRMS et DRX (pour l'un d'entre eux). La synthèse est optimisée jusqu'à ce stade pour le moment. Une déprotection par un groupement hydroxyle suivie d'une déprotection de la phosphine sont actuellement étudiées.

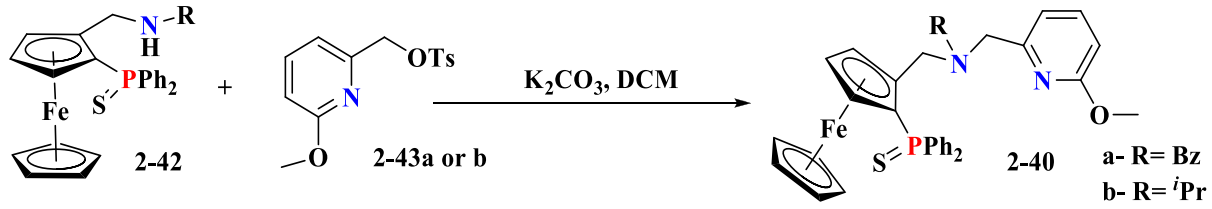

Schème 9 : Synthèse des proligands PNN modifiés **2-40** sous forme hydroxyles protégés

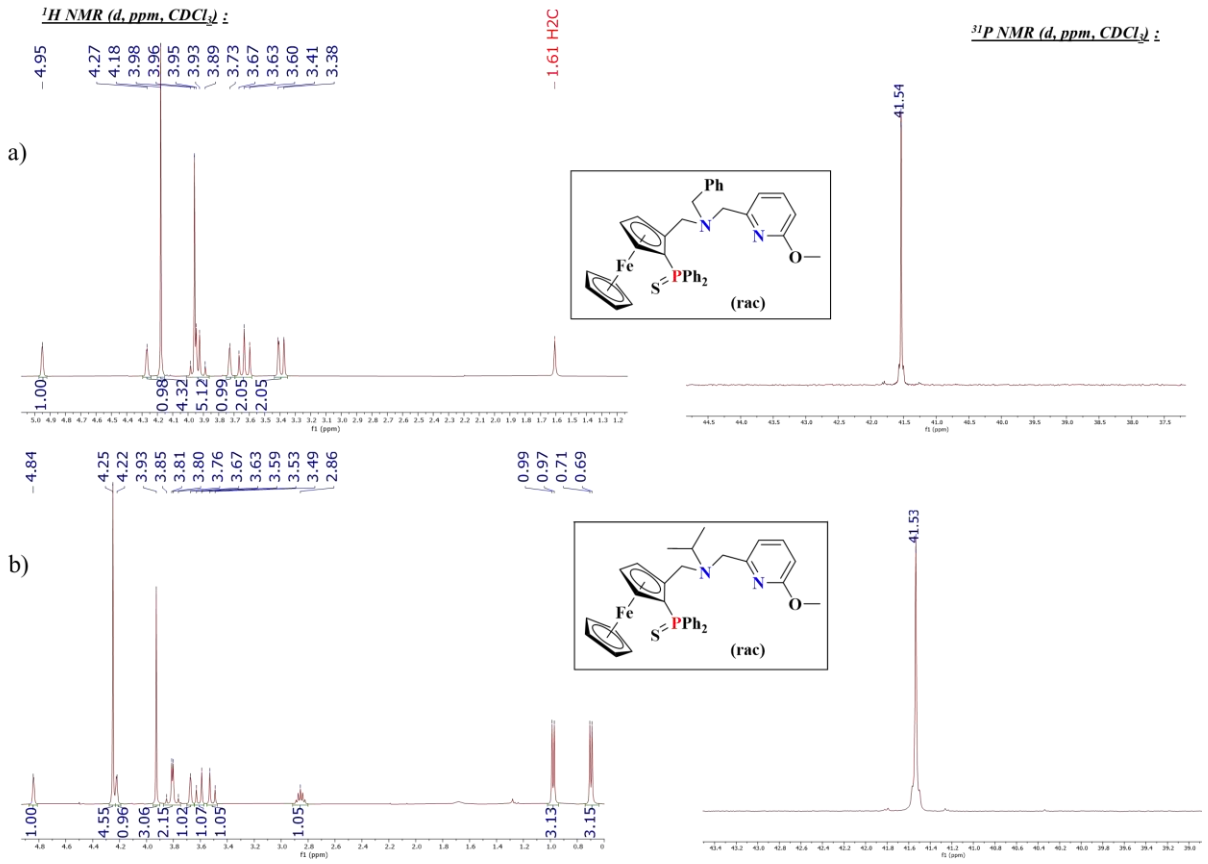

Figure 3 : Spectres RMN ^{1}H (Cp et région aliphatique) et ^{31}P de **2-40a** et **2-40b**

Résumé du chapitre-3

Le terme 'bi-fonctionnalité métal-ligand' qui a été introduit auparavant dans cette thèse, a été brièvement décrit au début de ce chapitre. La synthèse de quelques ligands ferrocéniques tridentés contenant des phosphines a été présentée dans la section suivante. Ensuite, les travaux qui ont été réalisés ont été décrits.

Deux ligands tridentes contenant de la phosphine (**3-9** et **3-10**) avec des amines secondaires attachées ont été conçus avec la capacité potentielle de bi-fonctionnalité métal-ligand par le centre 'N-H'.

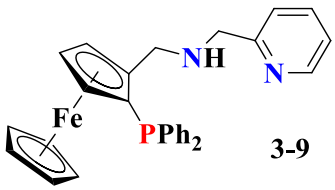

3-9

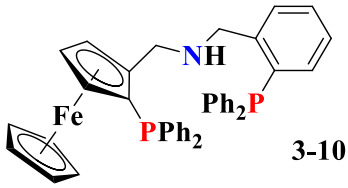

3-10

Schème 10: Formule moléculaire des deux ligands conçus

L'amine **3-35**, l'intermédiaire de synthèse du ligand **3-10**, a été préparée au préalable en suivant quelques étapes à partir du 2-bromobenzonitrile.

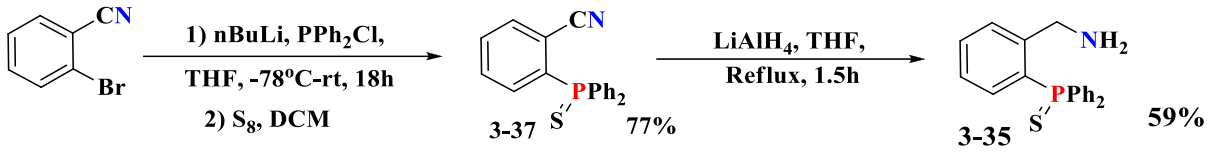

Schème 11 : Synthèse de l'ortho-(thiodiphénylphosphino)-benzylamine **3-35**

Deux proligands **3-32** et **3-34** ont été préparés par couplage de **2-29** avec la 2-picolylamine et l'amine **3-35**, respectivement ; en condition acide fort (HBF_4).

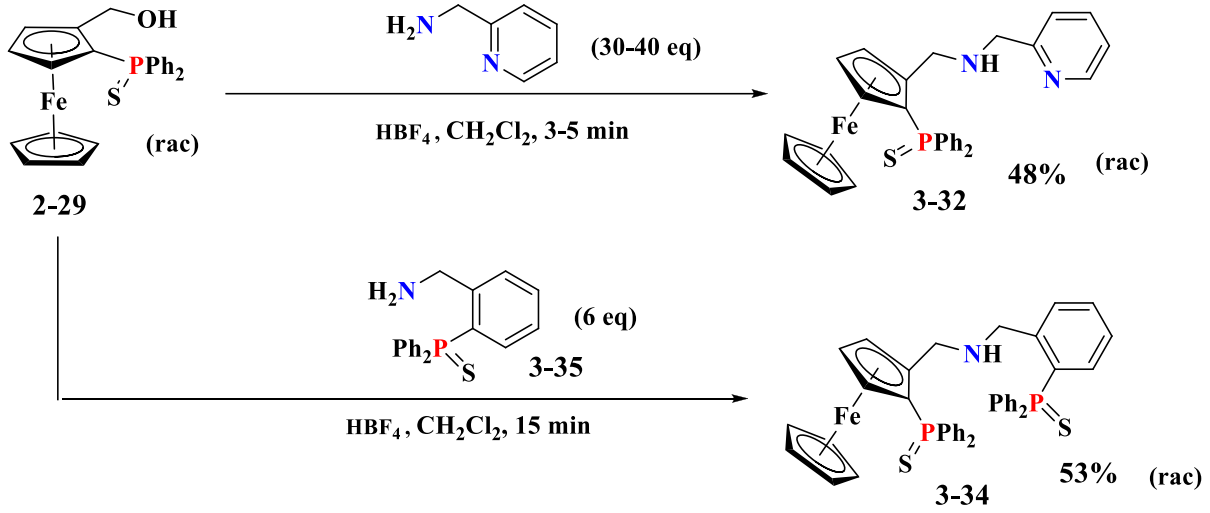

Schème 12 : Synthèse des proligands **3-32** et **3-34**

Ces deux proligands ont été caractérisés par RMN multinucléaire, HRMS et DRX. La déprotection par la phosphine est actuellement à l'étude.

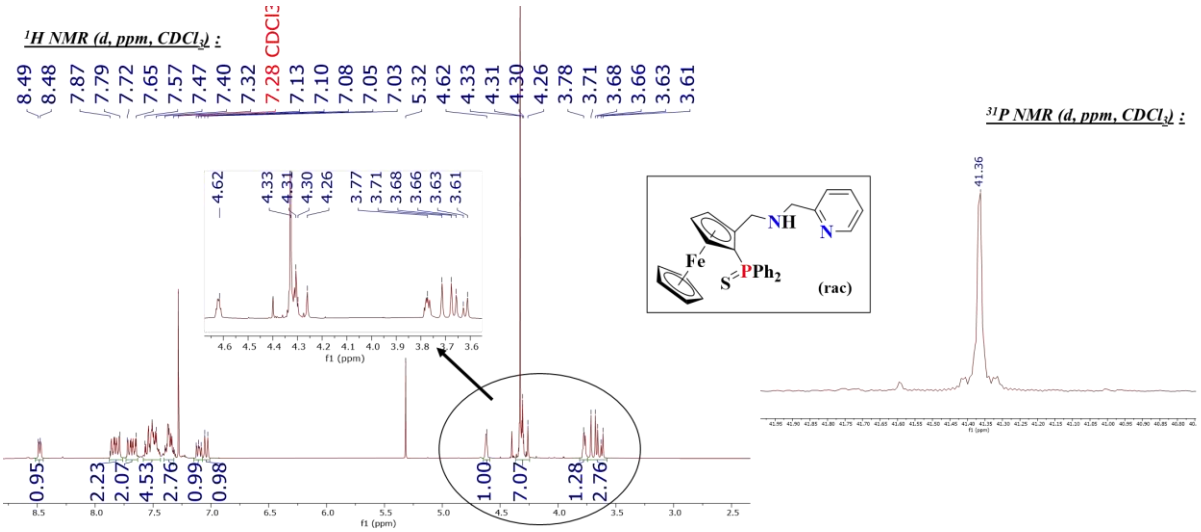

Figure 4 : Spectres de RMN de ^{1}H et ^{31}P de **3-32**

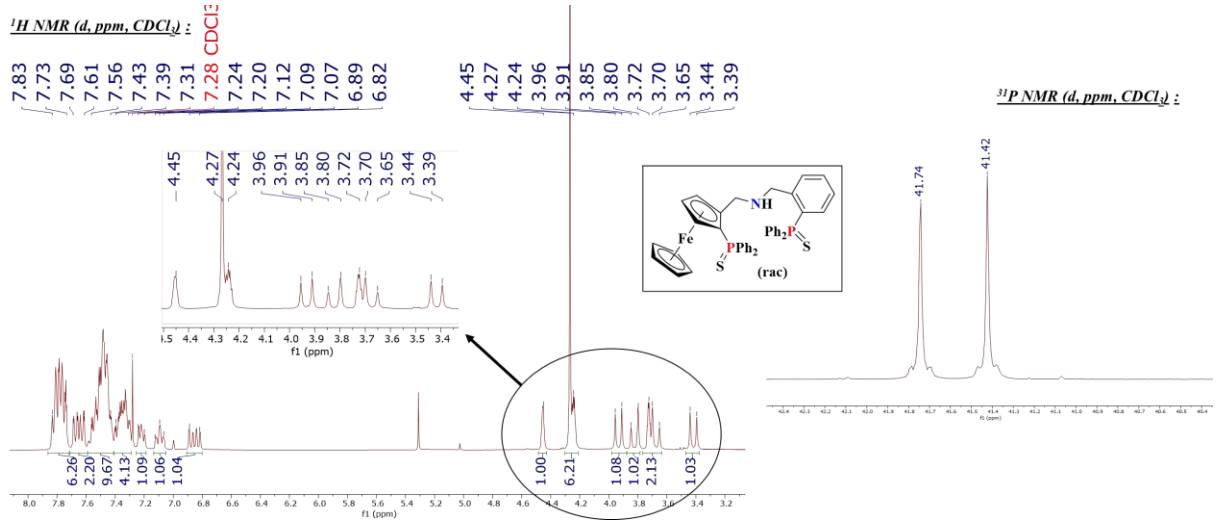

Figure 5 : Spectres de RMN de ^{1}H et ^{31}P de **3-34**

Tous les autres intermédiaires de synthèse qui interviennent dans la synthèse de **3-32** et **3-34** ont été caractérisés par RMN multinucléaire, HRMS et cristallographie par diffraction des rayons X (dans quelques cas), également. Quelques sous-produits, formés dans des conditions de synthèse autres que celles qui ont été optimisées, ont également été caractérisés. Ils ont été décrits dans les chapitres principaux.

Résumé du chapitre-4

Dans ce chapitre, deux ligands ferrocéniques thioéther légèrement différents contenant de la phosphine ont été conçus. Le changement de l'atome de coordination du donneur dur - azote - au donneur mou - soufre - a servi de motivation principale pour examiner les changements dans le comportement catalytique des ligands. Au début du chapitre, certains ligands ferrocéniques thioéther contenant de la phosphine, rapportés précédemment, ont été mis en évidence en termes de protocoles de synthèse.

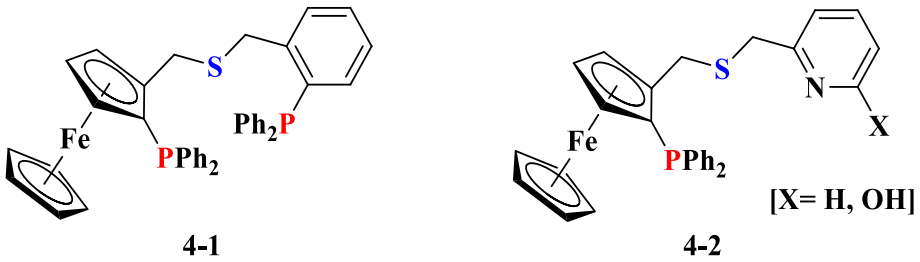

Schème 13 : Formule moléculaire des deux ligands phosphine thioéther

Du point de vue de la rétrosynthèse du ligand **4-1**, il était prévu de préparer l'ortho-(thiodiphénylphosphino)-benzylmercaptan **4-39** comme intermédiaire de synthèse. Ainsi, le thioacétate **4-46** a été synthétisé comme précurseur de son analogue thiol **4-39** en suivant quelques étapes de synthèse, en partant du méthyl -2- bromobenzoate.

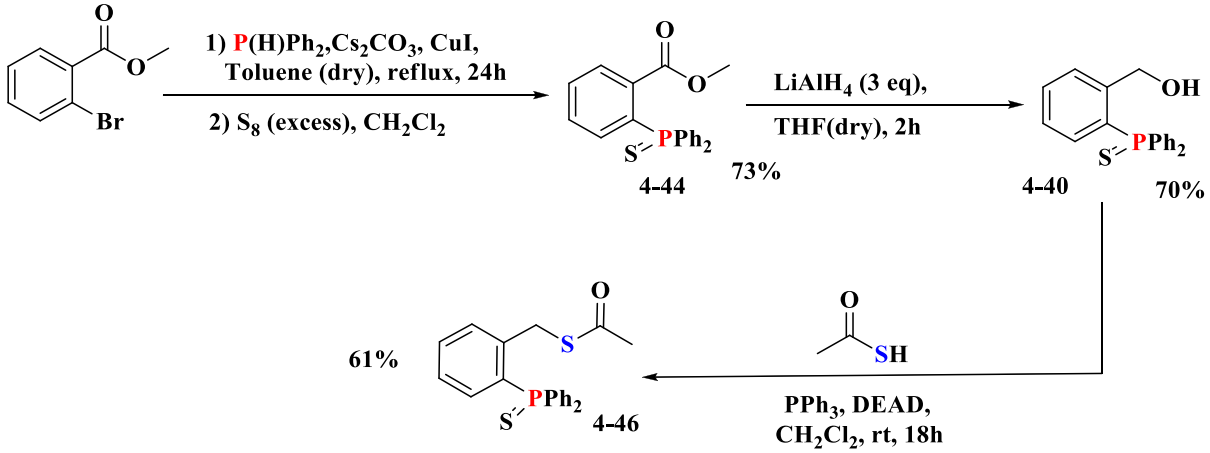

Schème 14 : Synthèse du thioacétate **4-46**

Après une brève étude de la littérature, on a compris que la synthèse des thiols a toujours été difficile car les thiols peuvent facilement former le disulfure correspondant en s'oxydant à l'air. En fait, la formation du disulfure **4-48** et du thiol monomère **4-39** a été observée dans notre cas, en fonction des conditions de réaction. Le thiol monomère **4-39** s'est avéré prédominant dans des conditions réductrices ($LiAlH_4$) de l'analogue thioacétate **4-46**, alors que le disulfure **4-48** s'est formé dans la plupart des conditions basiques douces (NaOH aqueux, NaOMe, *etc.*). Les deux espèces ont été caractérisées par RMN, HRMS et cristallographie par diffraction des rayons X.

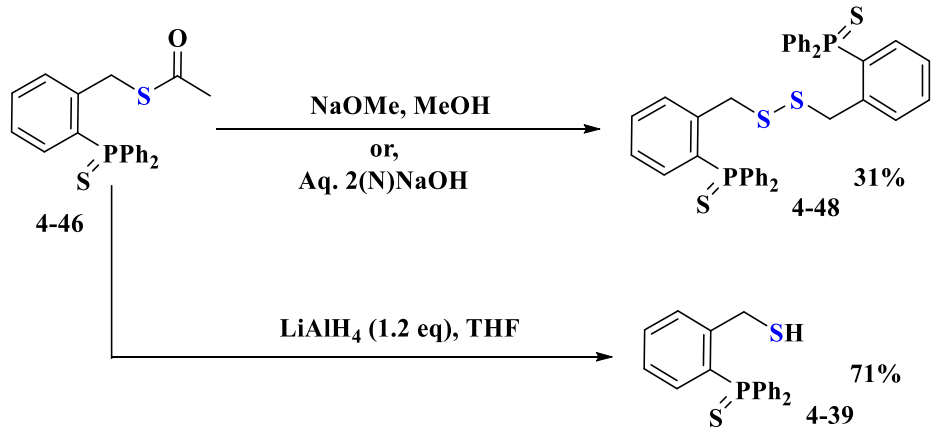

Schème 15 : Formation de **4-48** ou **4-39** selon les conditions de réaction

Le ligand PSP souhaité a été facilement synthétisé sous forme racémique et énantiomériquement pure en utilisant le thiol **4-39** dans des conditions HBF_4. Le ligand a également été caractérisé par RMN, HRMS et cristallographie par diffraction des rayons-X.

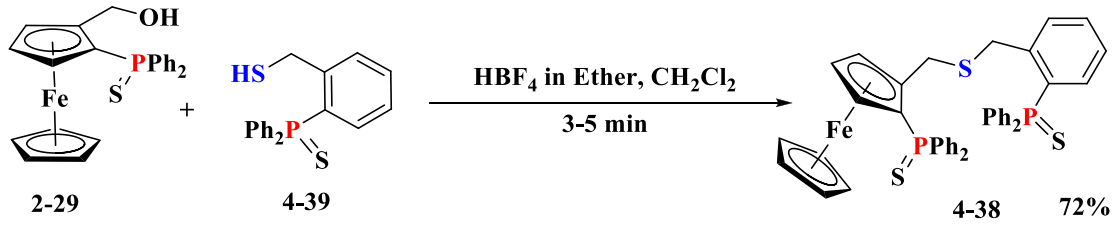

Schème 16 : Synthèse du proligand P,S,P **4-38**

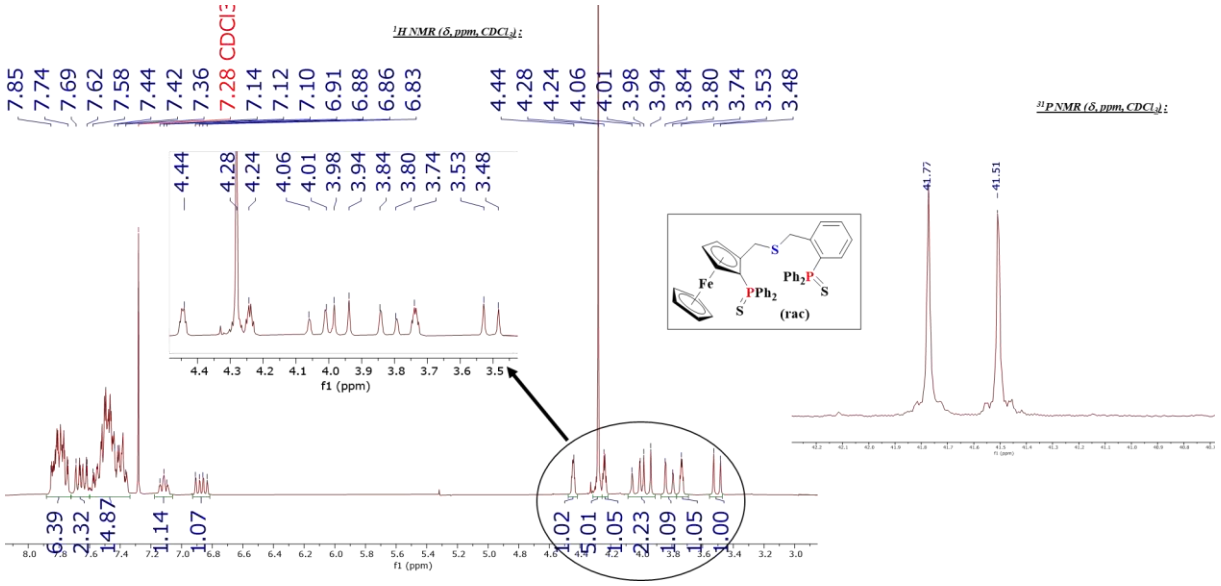

Figure 6 :Spectres de RMN 1H et 31P de **4-38**

La déprotection de la phosphine a été faite pour le proligand **4-38** pour obtenir la forme **4-1** du ligand activé. Le ligand activé a également été caractérisé par RMN multinucléaire.

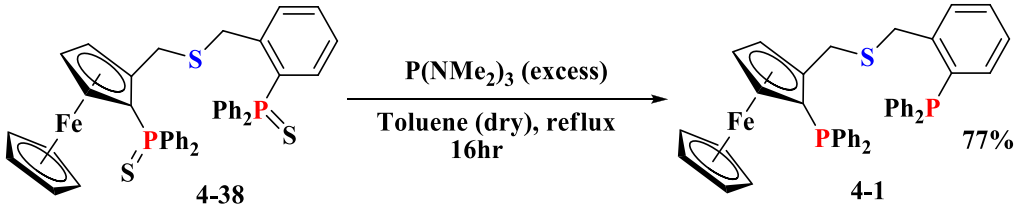

Schème 17 : Désulfuration du ligand P,S,P protégé **4-38**

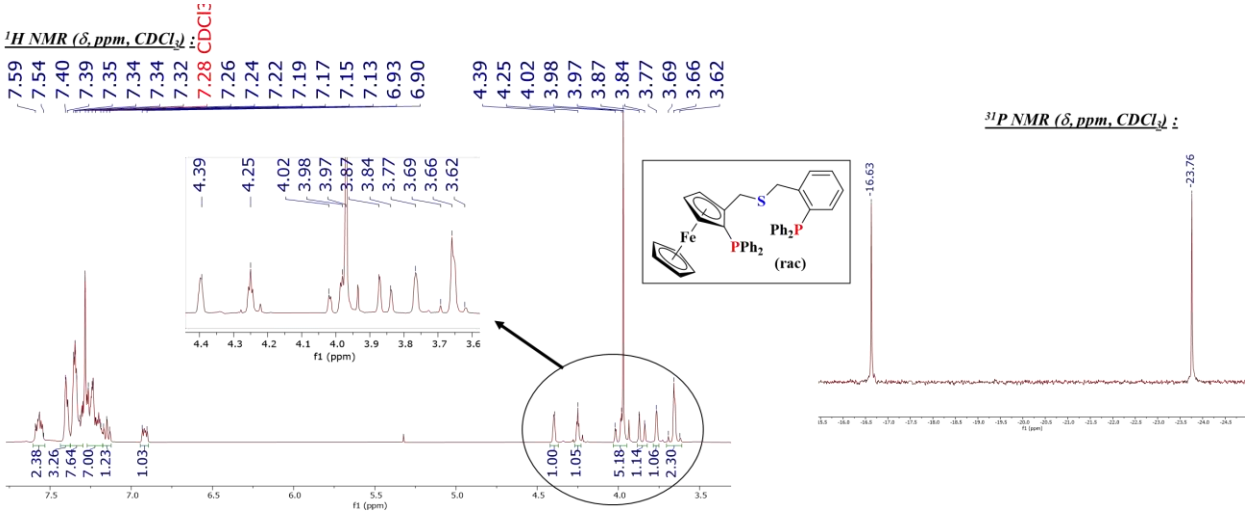

Figure 7 : Spectres de RMN ^{1}H et ^{31}P de **4-1**

Les expériences sur la synthèse des thiols nous ont permis d'aborder différemment la synthèse du second ligand **4-2**. Nous avons décidé de préparer le thiol ferrocénique et de réaliser l'alkylation du thiolate en fonction des besoins. De cette manière, cela permettra d'apporter plus de diversité en termes de développement de ligands du même type.

Lors de la tentative de synthèse du thiol **4-51** à partir de son analogue thioacétate **4-54**, il a été observé que la stabilité aérienne du thiol monomère est transitoire. Bien que l'espèce primaire formée après l'achèvement de la réaction soit le thiol monomère, une dimérisation importante a été détectée lors du stockage dans des conditions ambiantes.

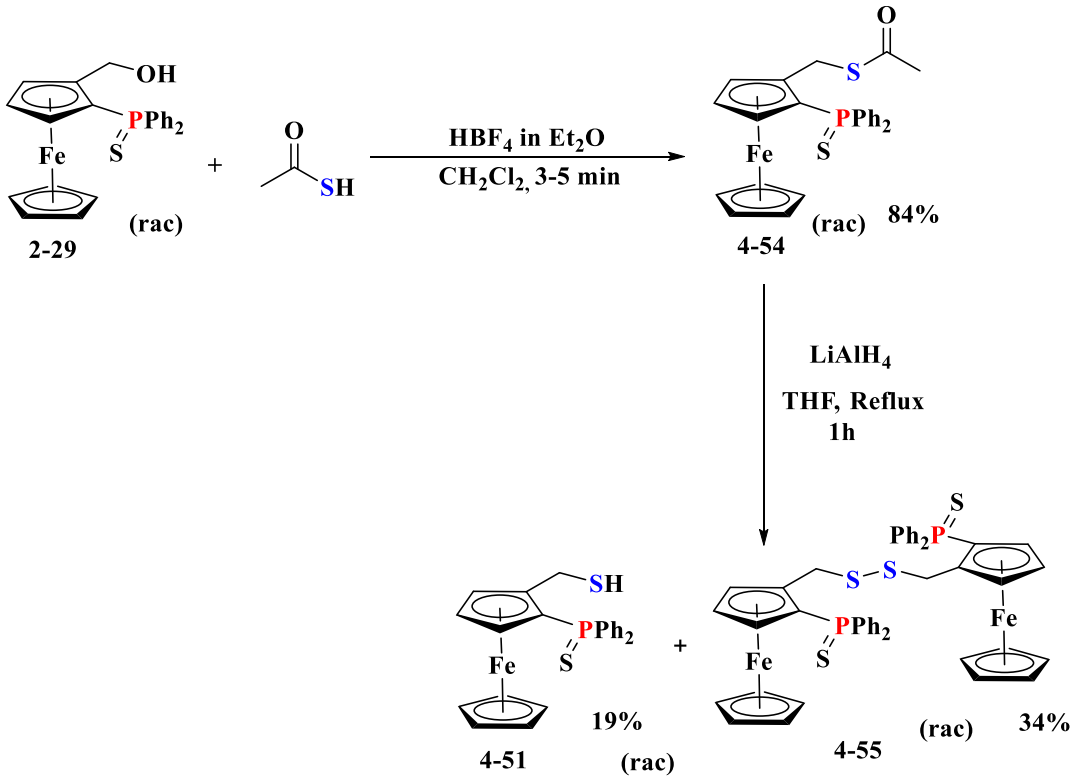

Schème 18 : Formation de thiol **4-51** et disulfure **4-55**

Tant le thiol **4-51** que l'espèce disulfure **4-55** ont pu être caractérisés. De plus, le disulfure a été caractérisé par RMN multinucléaire à la fois dans le mélange de diastéréoisomères et dans la forme pure énantiomère. Le thiol monomère **4-51** a également été caractérisé par cristallographie aux rayons X.

La synthèse du ligand a été planifiée avec une approche " one pot " concernant la stabilité aérienne des espèces thiol monomères. En conséquence, après la réduction du thioacétate **4-54** suivie de l'élaboration, l'espèce thiol **4-51** nouvellement formée a été alkylée *in situ* avec des tosylates de pyridyle **2-43** en présence de NaH. Deux proligands **4-49** ont été synthétisés par cette approche d'alkylation réductrice «one pot».

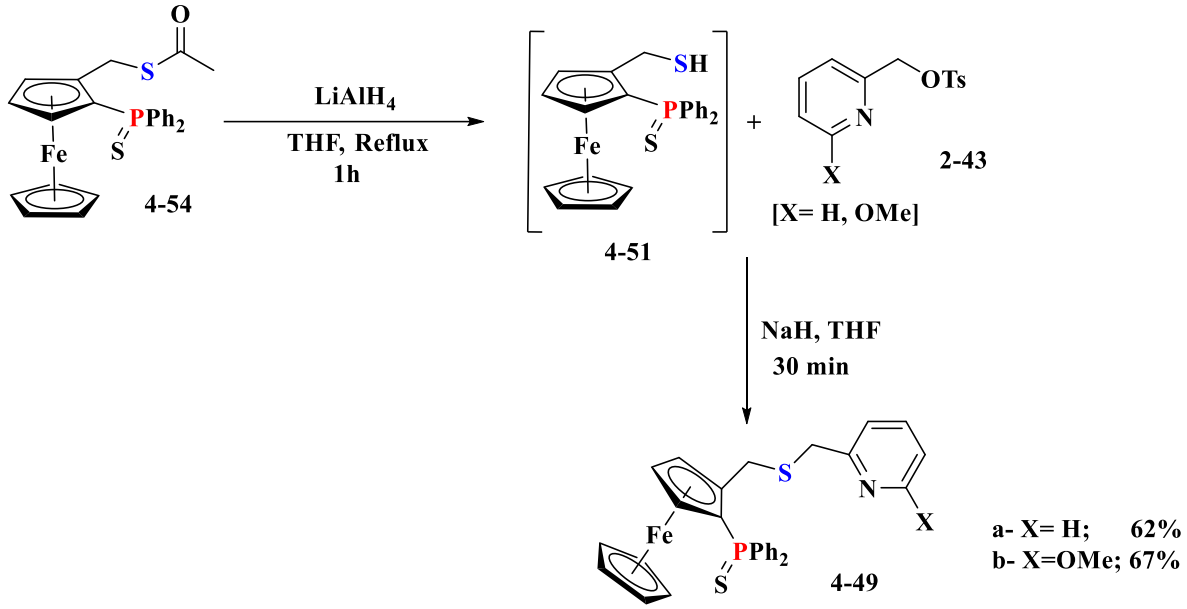

Schème 19 : Synthèse des ligands PSN protégés **4-49** (les rendements sont calculés par rapport à **4-54**)

Ces deux proligands ont été caractérisés par RMN multinucléaire et HRMS. L'optimisation des conditions de réaction est en cours.

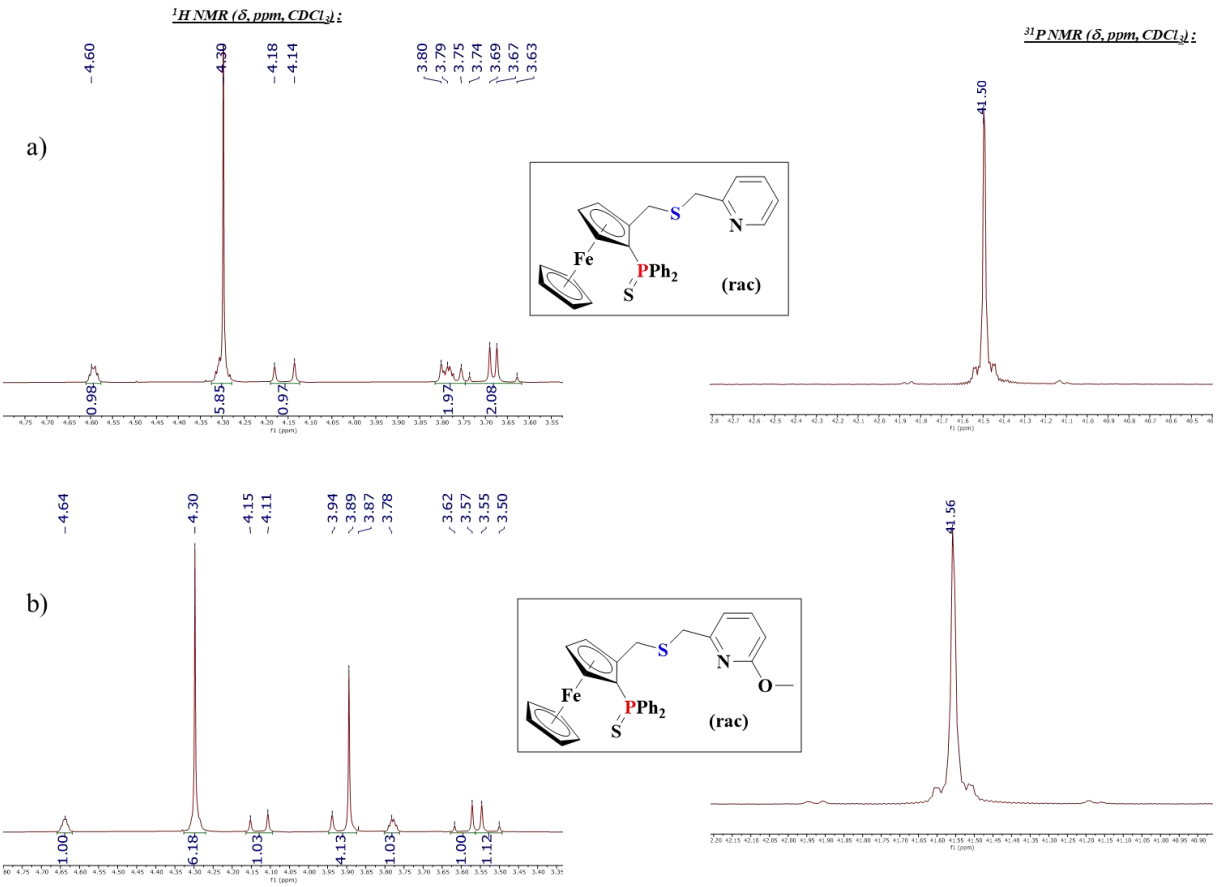

Figure 8 : Spectres RMN ^{1}H (Cp et région aliphatique) et ^{31}P de **4-49a** et **4-49b**

Cette approche d'alkylation réductrice « one pot » a été étendue à la synthèse de quelques autres espèces de phosphine-thioéther. Deux autres composés **4-56** et **4-57** ont été préparés, qui sont jusqu'à présent non décrits.

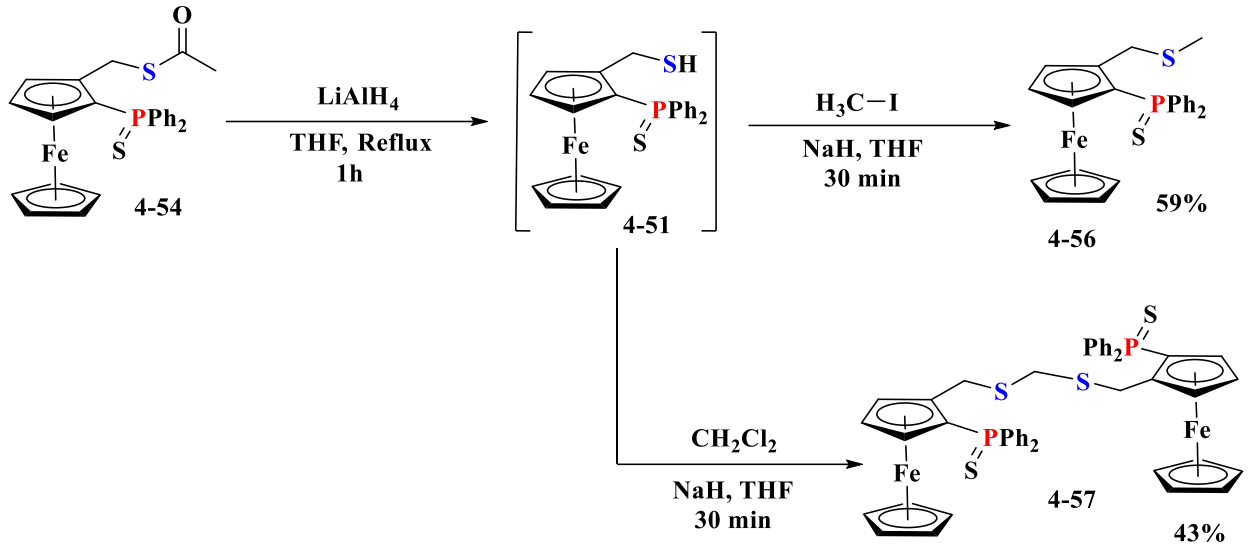

Schème 20 : Synthèse de deux thioéthers différents

Conclusion et perspectives

De nouvelles familles de ligands tridentés chiraux planaires contenant une phosphine sous leur forme protégée par un PS ont été synthétisées et sont décrites dans cette thèse.

Les proligands de la famille PNP **2-51**, inexplorés à ce jour pour des applications catalytiques, ont été produits selon la méthode développée par le Dr. Lucie Routaboul. En dehors de cela, tous les proligands n'ont pas été décrits précédemment. Ils ont été caractérisés par RMN multinucléaire et HRMS. En outre, au moins un membre de chaque famille a été caractérisé structurellement par diffraction des rayons X, à l'exception de la famille PSN, pour laquelle des monocristaux n'ont pas encore été obtenus. Une perspective à court terme de ce travail est l'optimisation et la mise à l'échelle des diverses synthèses de ligands, pour l'exploration ultérieure de leur potentiel catalytique.

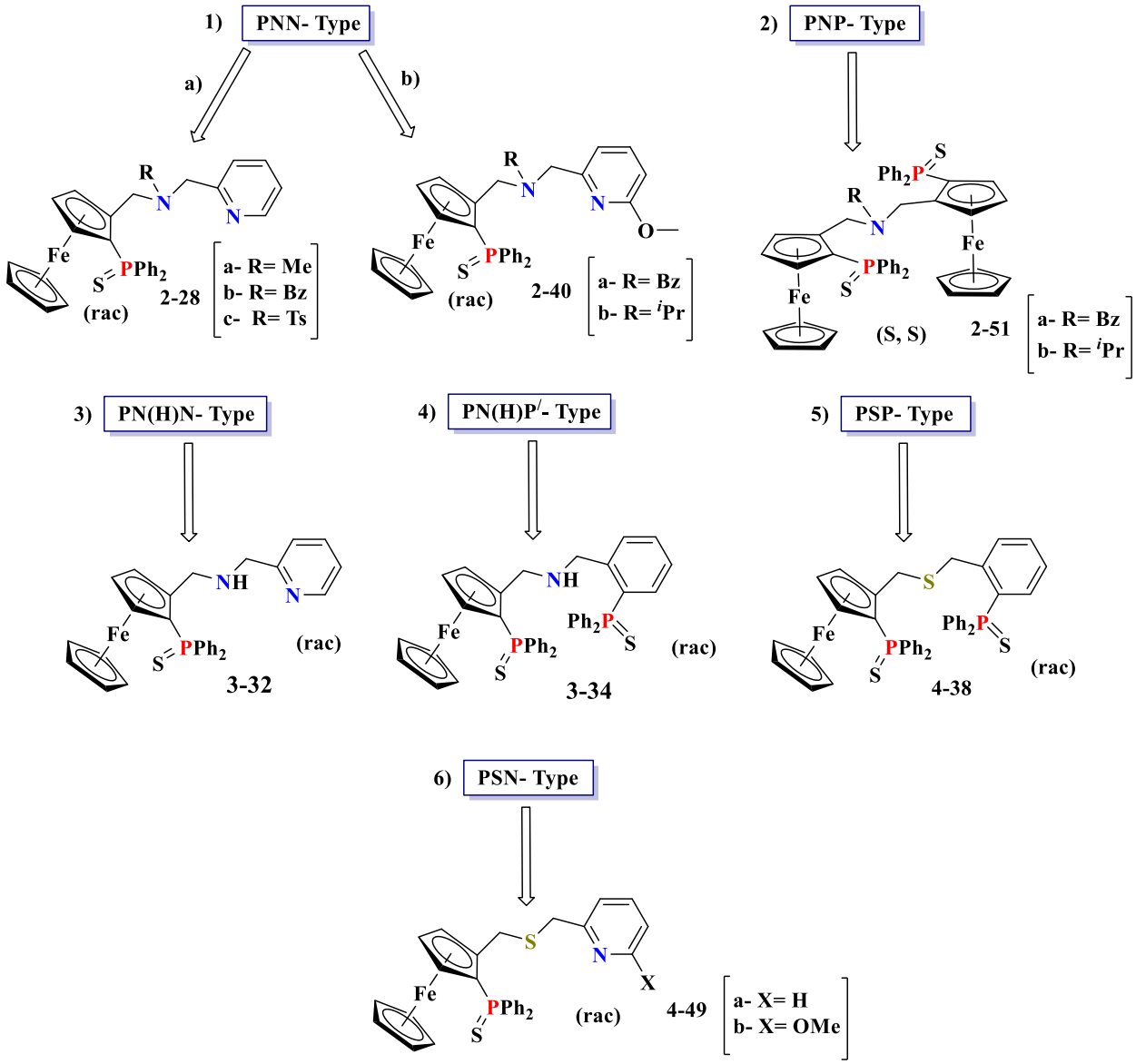

Schème 21 : Familles de ligands tridentés contenant des phosphines

La synthèse de ces ligands contenant des phosphines nécessite un certain nombre d'intermédiaires organiques et ferrocéniques de synthèse. Plusieurs de ces intermédiaires ont été préparés selon des procédures standards, ne nécessitant pas d'optimisations importantes. Les intermédiaires précédemment non rapportés (tant organiques que ferrocéniques) ont été soigneusement caractérisés par RMN, spectrométrie de masse et, dans la plupart des cas, également par DRX. Diverses réactions organiques (réaction de Mitsunobu, réduction, tosylation, méthode HBF_4, *etc*.)

ont été examinées à des fins d'optimisation. Quelques-unes d'entre elles n'ont pas fonctionné tandis que d'autres ont conduit à la formation de sous-produits inattendus. Quelques-uns d'entre eux ont pu être isolés et entièrement caractérisés.

Cependant, des solutions appropriées pour quelques problèmes de synthèse associés aux proligands ciblés n'ont pas encore été trouvées. La déprotection de la fonction ortho-méthoxy dans le cycle pyridine des proligands PNN **2-40** n'a pas encore réussi. En raison du temps limité, la déprotection P=S de quelques ligands (par exemple **2-28b**, **c**, **3-32**, **3-34**, **4-49**) doit encore être réalisée. Les efforts dans ces directions sont en cours et nous sommes confiants dans le succès final.

Le nouveau protocole de préparation du thioéther ferrocénique (voir chapitre 4, section 4-10), c'est-à-dire l'alkylation du thiolate ferrocénique généré *in situ* (à partir du thioacétate ferrocénique) par NaH, élimine l'utilisation des espèces thiols correspondantes comme nucléophiles pour la substitution, puisque le thiolate ferrocénique agit comme nucléophile et substitue une autre espèce électrophile présente dans le milieu (par exemple, CH_3I, CH_2Cl_2, *etc.*). Cette nouvelle procédure présente des avantages par rapport à la méthode compétitive et bien établie du HBF_4 (qui nécessite inévitablement une espèce thiol comme nucléophile), conduisant potentiellement à la génération d'une grande famille de thioéthers ferrocéniques structurellement diversifiés, mais elle est également associée à quelques limitations telles que des rendements plus faibles. L'optimisation et l'étude de l'influence de la nature du substrat sur les performances de la réaction font partie des perspectives à court terme.

Des tentatives préliminaires de complexation pour quelques-uns de ces ligands ont donné des résultats prometteurs. Par exemple, on a constaté que le ligand PSP **4-1** déplaçait le CO dans $MnBr(CO)_5$ et donnait un produit tricarbonyle, selon le spectre infrarouge. Cependant, une

caractérisation plus poussée (RMN, masse, DRX) de l'une des espèces proposées est nécessaire. Par conséquent, en raison du manque de preuves concluantes, ces complexes n'ont pas été décrits dans les chapitres principaux. L'optimisation des réactions de complexation et la caractérisation des produits sont en cours.

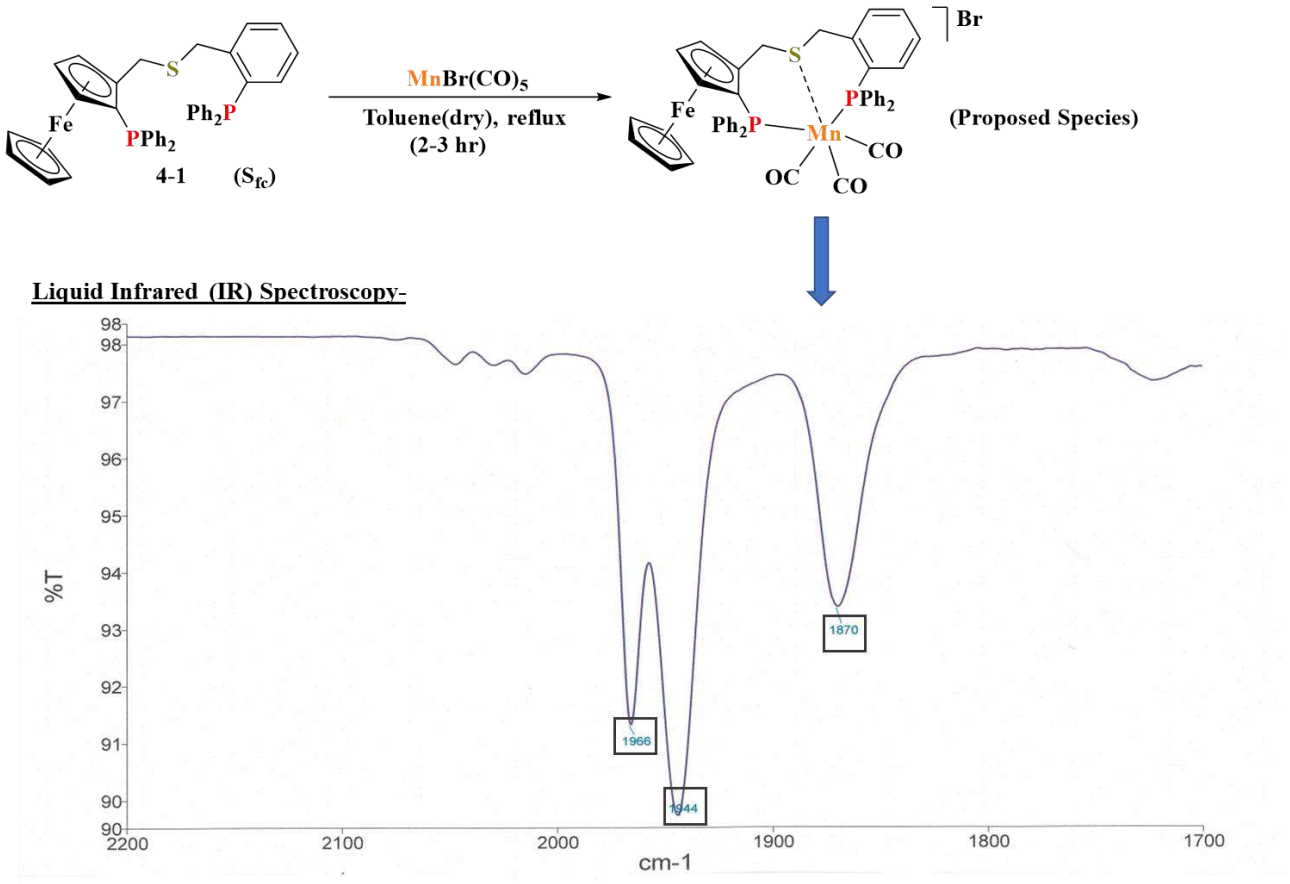

Schème 22 : Détection d'une espèce métal-tricarbonyle par spectroscopie IR

Quelques ligands protégés dans leurs formes racémiques et énantiomériquement pures ont été envoyés au laboratoire de notre collaborateur indien (Prof. Basker Sundararaju, IIT Kanpur, Inde) pour tester les activités catalytiques en présence de précurseurs de métaux non nobles. Les premières études catalytiques seront réalisées avec la génération *in situ* des espèces actives à partir des ligands et des précurseurs métalliques appropriés, en commençant par la version racémique

pour l'optimisation des conditions de réaction. Les investigations seront ensuite étendues aux versions asymétriques pour les meilleurs systèmes catalytiques.

General Introduction

Catalysis gained attention for several decades because it allows to carry out many reactions in better conditions, meaning- with less energy, better atom economy and sustainability. In addition, some catalytic reactions can be enantioselective reactions which is of tremendous interest because of the importance of enantiomerically enriched compounds in many fields like agrochemical, pharmaceutical, materials industry. To develop chiral catalysts that provide high enantioselectivity and productivity is obviously very relevant. Transition metal-based catalysts are proven to be the most versatile and competent systems to provide excellent productivity and enantioselectivity in different kind of asymmetric organic reactions throughout the past few decades. These catalysts consist in general of a metal center coordinated to a monodentate or polydentate chiral organic ligand. In modern day research, non-noble or first row transition metals are introduced more often for the pursuit of plausible solutions for many problems, like the fast depletion of noble or heavier ($2^{nd}/3^{rd}$ row) transition metals, the environmental crisis, *etc*. Catalytic reactions driven by non-noble metals with existing chiral ligands, as well as specially developed new ligands, are being investigated at a growing pace in order to find a proper fit. In this regard, chiral tridentate ligands are gaining more and more attention following their rapid success in the past decade.

We have been highly intrigued by the profound accomplishments of chiral ligands with a phosphine-containing planar chiral ferrocene backbone (for example, JOSIPHOS and FOXAP) in the field of homogeneous transition metal-based asymmetric catalysis throughout the past few decades. In addition, chiral tridentate phosphine-containing ferrocenyl ligands and non-noble metal-based catalysts have led to a few interesting recent achievements in asymmetric hydrogenation-dehydrogenation, alkylation, cycloaddition reactions, *etc.* However, the number of these tridentate ligands is still rather limited, motivating us to develop a few additional new members. Hence, a number of planar chiral tridentate phosphine-containing ferrocenyl ligand families such as PNP, PNN, PSP, PSN, *etc*., were designed and synthesized during this thesis. The potential catalytic applications in asymmetric C-C and C-N bond formation reactions starting from alcohols, using the recently developed 'Borrowing Hydrogen' strategy, is proposed as a perspective.

Chapter-1: Bibliographic Overview

1. 1) Introduction

'Sustainability' is the central theme of modern-day research as it corresponds to the balanced utilization of the limited resources stored in our planet. This ensures our existence and transfers a healthy environment to the future generation for a high life standard. In the chemical research field, catalysis is one of the means of sustainability. In a more specific way, traditional organic reactions, despite their efficiency, often requires long reaction times and precise separation techniques. These produce significant amount of chemical wastes at the end, which is a real threat to the environment. Catalysis circumvents a few of these issues by providing atom-economical synthetic methods (reusable metal catalyst, easy separation techniques *etc.*). Transition metal-based homogenous catalysis has been fascinating over the past decades and keeps on attracting interest because it increases the productivity and selectivity of a wide range of processes in the industrial, pharmaceutical, agrochemical fields.

Noble and Non-noble metals in catalysis. Noble metals are those metals that- resist corrosion and oxidation in moist air. Most of these metals belong to the 2nd or, 3rd row transition metal series (4d or 5d) of the periodic table (*e.g.* Ru, Rh, Ir, Os, Re *etc.*). The resources of these metals are limited. A few of these metals of low occurrence on earth are considered as precious metals (*e.g.* Ag, Au, Hg *etc*.) and possess high economic value. Noble metals have been highly successful in different homogenous transition metal-based catalyses for last few decades. However, the resources of noble metals are depleting abruptly following their rapid consumption. In addition to that, these metals are toxic to the environment.[1a]

Transition metals that belong to the 3d transition series of the periodic table are known as base metals (*e.g.* Fe, Mn, Co, Ni *etc*.). They are not resistant to corrosion, are sensitive towards air oxidation and are considered as non-noble metals. There are certain justifications behind the emerging interest of involvement of these metals into homogeneous catalysis. These metals are earth-abundant and, therefore, inexpensive. They are biocompatible, particularly valuable for pharmaceutical industry and environmentally benign in most cases.[1a]

The current focuses of research highly incline towards green chemistry to cope with few environmental issues like- rapid depletion of fossil fuel which is the main source of energy, abrupt change in global climate as an inevitable consequence of pollution *etc.* Non-noble metal-based

homogenous catalysis is becoming the cornerstone in green chemistry. Seminal developments in different sectors of homogenous catalysis (*e.g.* hydrogenation-dehydrogenation, hydrosilylation, C-H bond activation *etc*.) with Fe,[1] Mn,[2] Co,[3] Ni[4] are further accelerating the upbringings.

Alcohols as the feedstock of Sustainable chemistry. Alcohols constitute a major family of products derived from biomass and are considered as a potential alternative for fuel production.[5] Apart from that, being abundant and a potential source of carbon atoms, they can be transformed into diverse range organic compounds that are essential in many areas such as industrial commodities (*e.g.* fragrances, sweeteners, surfactants, inks, paints *etc*.), valuable synthetic intermediates for other compounds, fine chemicals *etc.*[6] Nevertheless, alcohols typically have a rather low reactivity as alkylating agents because the hydroxyl group (-OH) is sluggish to be replaced by nucleophilic reagents. Thus, it is necessary to transform alcohols into derivatives bearing good leaving groups (*e.g.* halides, tosylates, triflates, sulfonates *etc.*), in order to carry out very efficient alkylation reactions.[6b, 7] There are examples of transition metal catalyzed oxidation of alcohols to produce corresponding carbonyl compounds, which are more reactive than alcohol precursors, for further use.[8] Besides, simple alcohols (*e.g.* isopropyl alcohol, methanol) are one of the main sources of hydrogen in metal-catalyzed transfer hydrogenation reactions (see section 1.2).[9] However, the modern-day approach of sustainable and green chemistry has helped to discover methods that can temporarily activate the alcohols and ultimately produce β- alkylated products that are otherwise difficult to obtain via single step transformations.[10] This approach, known as 'Borrowing Hydrogen' methodology, anchors the way towards transition metal catalyzed new C-C and C-N bond formation leading to new products starting from an alcohol (See section 1.3 and 1.4). Hence, alcohols can be considered as the feedstock of modern-day sustainable chemistry.

Importance of chiral amines. Amines are another extremely important class of organic compounds as they are used as intermediates to prepare several drugs, polymers, food additives *etc*. They also represent one of the most abundant families of organic compounds including a huge number of natural products, biologically and pharmacologically active compounds (*e.g.* amino acids, alkaloids, nucleotides *etc.*). Amines are associated with the inherent property of hydrogen bonding and thus chiral amines are powerful pharmacophores.[11] The construction of C-N bond which give rise to amines can be carried out by several N-alkylation methods at hand.[12] However,

few disadvantages like- the use of hazardous chemicals, over alkylation, chemical waste generation *etc*. are inevitably associated with the traditional methods. Therefore, various transition metal-catalyzed methods (such as-Pd and Cu catalyzed amination of aryl halides, hydroamination, reductive amination *etc*.) to eliminate those disadvantages have emerged rapidly during the past decade[13] and a few of these methods are applied in large scale syntheses of pharmaceuticals.[14] The synthesis of chiral amines, apart from the traditional ways,[15] is less explored due to hitherto unavailability of competent procedures. Very recent advances with Borrowing Hydrogen Alkylation methods were proven to be successful in that respect, which inspires further investigations (see Section-1.3 and 1.4). With the help of this method simple alcohols can be converted to an amine in one pot. Various research groups are now interested in further exploring this particular area of research.

1. 2) Hydrogenation and Transfer hydrogenation- A Brief Overview

Among all the catalytic reactions driven by transition metals, hydrogenation is one of the significant and practical tools because of its wide applicability to a number of organic substrates (olefins, ketones, imines *etc*.).

A catalyst selectivity (regio and stereoselectivity) is mostly governed by the nature of ligand coordinated to the metal. Hence, the design of an efficient coordinating ligand is a factor of major importance. The structural nature of the ligand highly influences the steric and electronic environment around the metal center, which therefore, reflects onto the productivity and selectivity. In this regard, phosphorus-based homo- and hetero- functional multidentate ligands are one of the most successful ligand families for hydrogenation, allylic substitution and hydrosilylation *etc*.[16] However, in view of the objectives of this thesis, the subsequent discussion will be mostly focused on hydrogenation and on the efficient phosphorus-based ligands for that process.

1.2. 1) Definitions and Mechanisms

The addition of hydrogen atoms across multiple bonds through dihydrogen gas as donor is known as hydrogenation or direct hydrogenation (DH). The earliest major breakthrough in this field was contributed by Paul Sabatier towards the end of the 19th century, when he discovered that hydrogen addition could be possible across organic unsaturated bonds with trace amounts of Nickel, present

as catalyst.[17] This revolutionary work, back in that time, brought a number of prospects among the hydrogenation-based industrial processes including his own method to hydrogenate CO_2 to form CH_4 and O_2-the Sabatier process. The Nobel Prize in Chemistry in 1912 was awarded to him "for his method of hydrogenating organic compounds in the presence of finely disintegrated metals".[18] However, homogeneous metal-catalyzed hydrogenation was started to grow since 1960's and slowly, turned out as one of the most developed and important method to incorporate hydrogen atoms in multiple bonds (discussed later).

The mechanism of hydrogenation follows the sequence of initial activation of dihydrogen on the metal catalyst generating metal hydride and subsequent transfer of hydrogen to the unsaturated substrates. The metal hydride species formation takes place after an initial intermediate dihydrogen complex following three possible pathways:[19]

1) Heterolytic splitting generating a metallic monohydride and a pronated base (Scheme 1. 1, Path 1)

2) Oxidative addition to metal center providing a dihydride complex (Scheme 1. 1, Path 2)

3) Heterolytic splitting generating a metallic monohydride and a pronated ligand (Scheme 1. 1, Path 3)

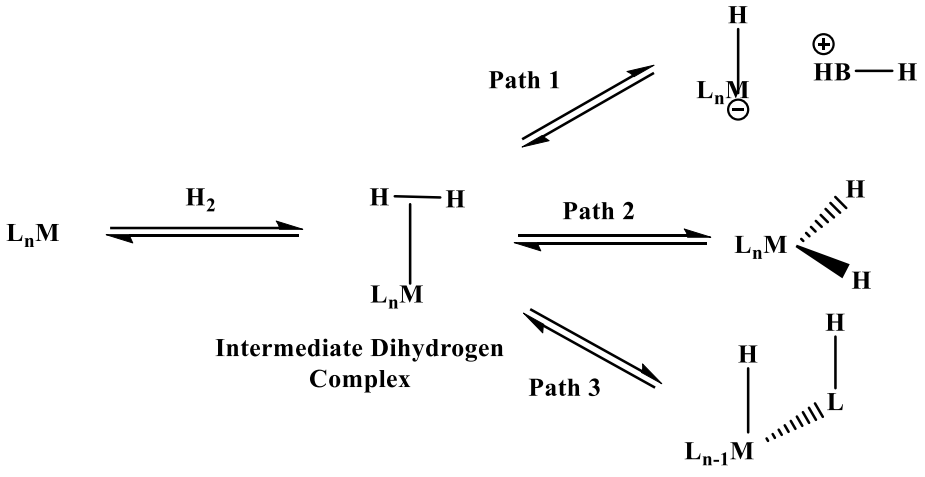

Scheme 1. 1: Metal Hydride Species Formation

There are two possible mechanistic pathways by which hydrogen transfer might take place to hydrogenate a polar unsaturated bond (*e.g.* ketone, imine *etc.*). These two pathways are:

1) Inner-sphere pathway where the substrate coordinates to the metal and subsequent hydride transfer takes place [Scheme 1. 2, a)].

2) Outer-sphere pathway where a concerted hydrogen transfer to substrate occurs without metal coordination. In this pathway, the ancillary ligand, co-ordinated to metal, most likely facilitates the hydrogenation step by transferring hydrogen [Scheme 1.2, b)].

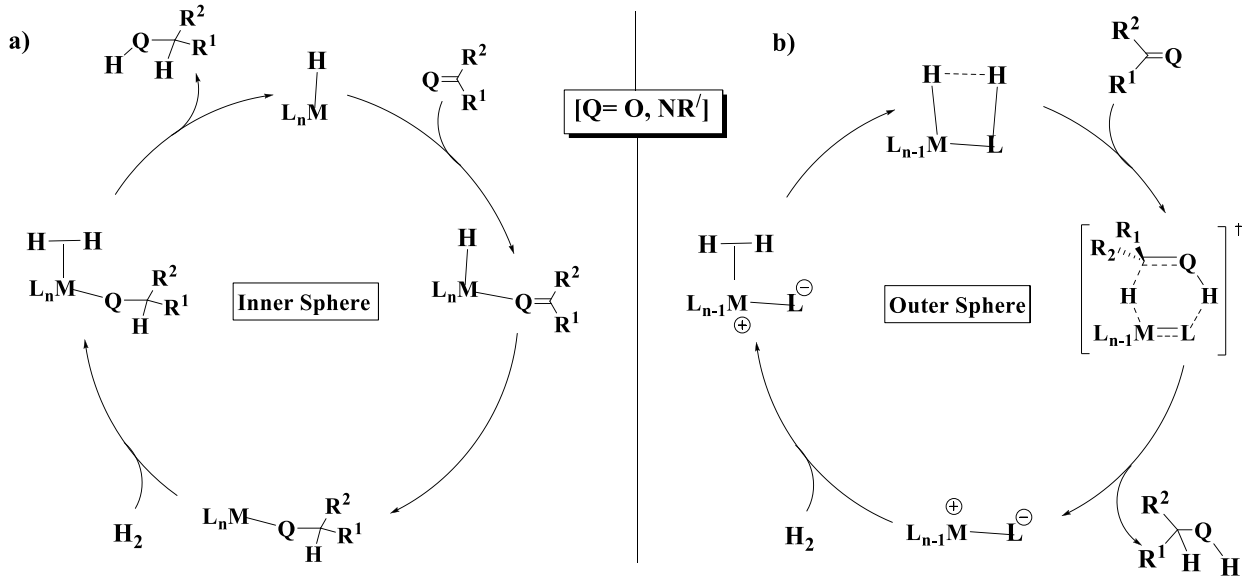

Scheme 1. 2: Mechanisms of hydrogenation for polar C=Q (ketones, imines) bonds

Transfer hydrogenation (TH) uses hydrogen donors other than gaseous hydrogen. Since, hydrogen gas is flammable and explosive, strict safety measures have to be followed while handling it. TH circumvents this issue by employing organic compounds as hydrogen donors. Common hydrogen donors for TH are primary or secondary alcohols like methanol, benzyl alcohol or propan-2-ol and formic acid and its salts. Isopropanol/ base and Formic acid / NEt_3 (Triethylammonium formate or, TEAF) are the most used, so far.[20]

The mechanism of TH can be classified into two major categories, as follows:[21]

1) Direct Hydrogen Transfer- This mechanism was proposed for the Meerwein- Ponndorf-Verley (MPV) reduction where aluminium isopropoxide was used to directly transfer hydrogen from isopropanol to a ketone.[22] In this pathway, alkoxide transfers its β-H atom to the electrophilic carbonyl group through a 6-membered cyclic transition state where the metal acts as

scaffold and thereby avoiding metal-hydride intermediate (Scheme 1. 3). The reduction can be reversed by using acetone as a hydrogen acceptor, which was proposed by Oppenauer.[23] Combination of the two processes, known as MPVO systems, are mostly restricted to Al-, and Sn-catalyzed process and rarely followed by late transition-metal systems.[24]

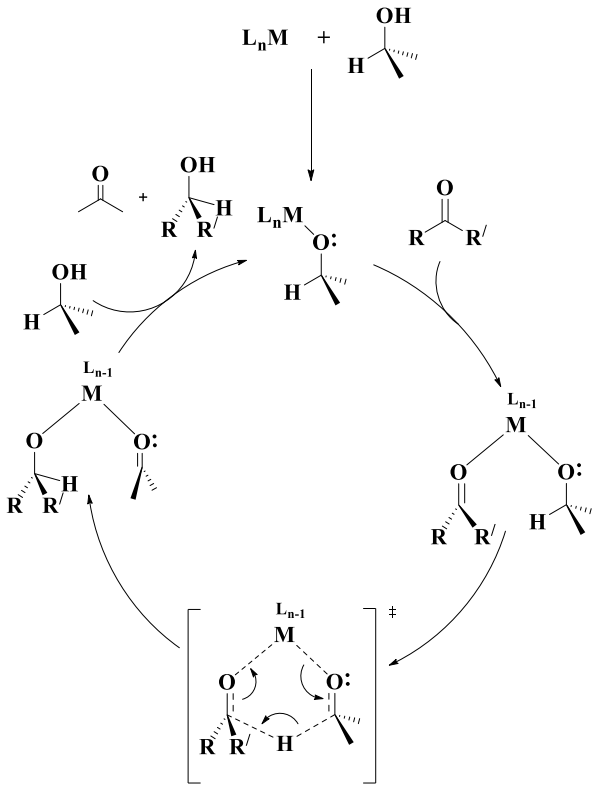

Scheme 1. 3: MPVO System

2) Hydridic Route– This route can be considered as more generalized route to hydrogenate carbonyls and other unsaturated polar bonds like imines, using various other transition metal complexes (*e.g.* Ru, Rh, Ir *etc.*) as catalysts. The hydrogen donor species (*e.g.* isopropanol) is oxidized at first giving rise to the metal hydride species. The overall mechanism, again, can be classified into two categories. The first one is the inner sphere hydrogen transfer where the substrate coordinates to the metal [Scheme 1. 4, a)]. The second one is the outer sphere hydrogen transfer which follows a direct concerted transfer hydrogenation from the complex to the substrate [Scheme 1. 4, b)]. Both steps and the subsequent hydride insertion are common with hydrogenation mechanism as shown in Scheme 1.2. However, the mechanistic feature of both routes involves the necessity of a metal hydride intermediate. Several hydrido complexes were isolated from transition metal catalyzed transfer hydrogenation reaction mixtures.[21, 25]

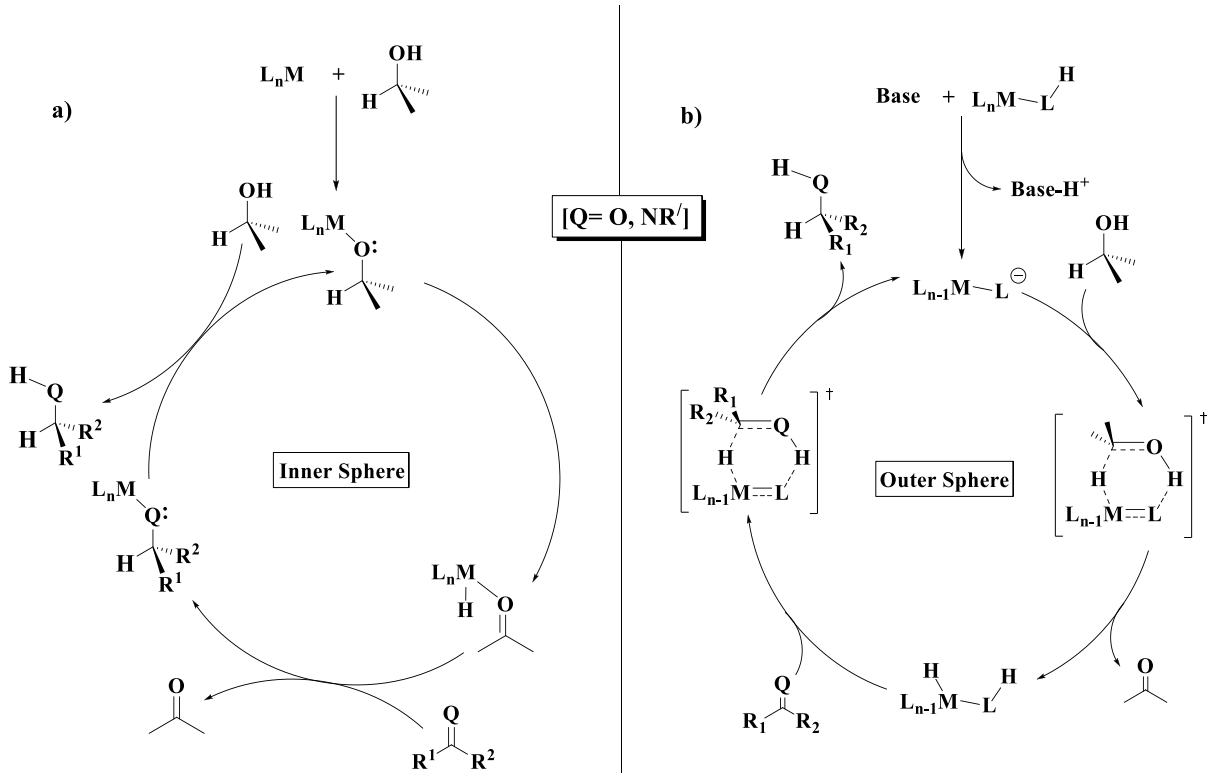

Scheme 1. 4: Two hydridic mechanisms of transfer hydrogenation for polar C=Q (ketones, imines) bonds

C=C double bond reductions are favorable reactions as they give rise to alkanes, which are thermodynamically more stable. However, TH of simple alkenes is found to be sluggish in the presence of alcohols as hydrogen donors, whereas, conjugated double bonds (*e.g.* conjugated acid derivatives, α,β-unsaturated carbonyls *etc.*) were effectively reduced in such cases. For α,β-unsaturated carbonyls the initial chemoselectivity is directed towards the C=O reduction. The chemoselectivity can be reversed towards the C=C reduction with the increase of bond polarity by attaching additional electron withdrawing substituent in the side chain of the unsaturated compounds.[26] In the coming sections various related examples will be presented. Nevertheless, transfer hydrogenation of alkynes is found to be resistant in similar conditions.[26]

Transfer of hydrogen in a stereoselective manner, induced by chiral ligands or additives, makes the process asymmetric and is termed "Asymmetric Hydrogenation" or "Asymmetric Transfer Hydrogenation (ATH)" (Scheme 1. 5). The effective way to produce enantiomerically pure organic compounds that are useful for biological applications, for drug synthesis *etc*.; starting from prochiral and easily available unsaturated counterparts, is the key point for rapid enrichment in this research area. Along with this, the implementation of green synthetic procedure (biphasic,

heterogeneous catalysis) and the design of environmentally friendly catalysts (non-toxic, recyclable) attract growing attention in both academic and industrial research.

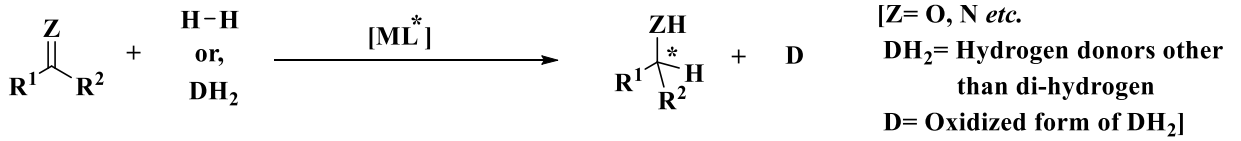

Scheme 1. 5: Asymmetric (Transfer) Hydrogenation

Catalyst design for hydrogenation and transfer hydrogenation started to evolve from the pioneering work of Wilkinson (1966), who discovered the first ever efficient homogenous catalyst for hydrogenation, $[RhCl(PPh_3)_3]$.[27] Later on, valuable contributions for ligand and catalyst design and for substrate scope were provided by a number of research groups across the globe. A huge library of efficient ligands proven to be excellent is available now. The catalyst design was extended to other noble metals (Ru, Ir, Pt, Pd) and more recently to non-noble metals (Mn, Co, Fe, Ni *etc*.). Substrates ranging from α-dehydroamino acids, functional olefins, ketones, imines to non-functionalized olefins have progressively attracted attention. A brief review pointing out a selection of the most successful chiral ligands are discussed below.

1.2. 2) High Performance Phosphorous containing Chiral Non-ferrocenyl bidentate and tridentate ligands for Hydrogenation: Brief Review

The earliest report of asymmetric hydrogenation corresponds to the work of Knowles, where the PPh_3 moiety of Wilkinson's catalyst was replaced by the chiral monophosphine *(-)*-PPhMe(^{n}Pr) and $PhP(CH_2CHMeEt)_2$.[28] Then, the first biphosphine ligands, *(S,S)*-DIOP (**1-1**) and *(S,S)*-DIPAMP (**1-2**), were reported for Rh- catalyzed asymmetric hydrogenation and transfer hydrogenation reported by Kagan (1971)[29] and Knowles (1977),[30] respectively. The DIPAMP-based Rh-catalyst was later utilized for the industrial synthesis of L-DOPA, developed by Monsanto[30c] (Scheme 1. 6). Other C_2-symmetric bisphospholane ligands, *(R,R)*-DuPhos (**1-3**) and *(R,R)*-BPE (**1-4**), developed by Burk *et al.* (1991) were successful for the Rh-catalyzed hydrogenation of (*R)*-(acylamino)acrylic acids, enamides, enol acetates, α-keto esters, unsaturated carboxylic acids, and itaconic acid.[31]

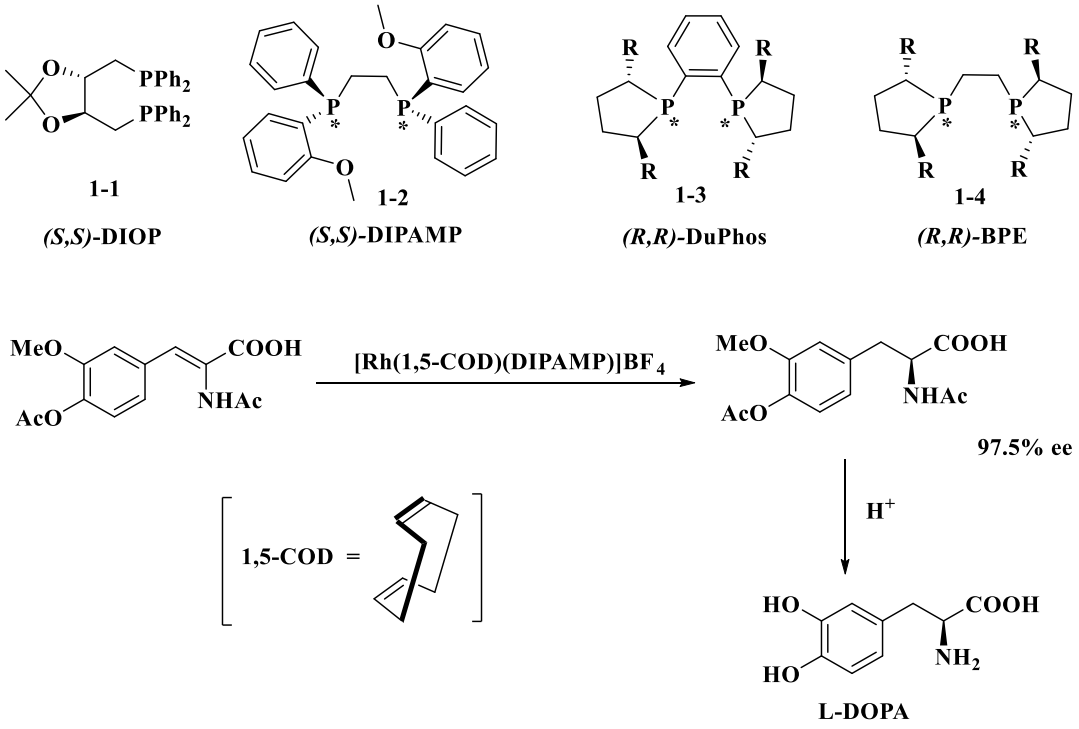

Scheme 1. 6: Earlier Phosphine-based Ligands and synthesis of L-DOPA

BINAP and Related Ligands

The discovery of C_2-symmetric BINAP ligand (**1-5**) developed by Noyori *et al.* (1989), is considered as one of the landmarks of hydrogenation because of the very first extended utilization of metals (Rh, Ru) and wide substrate scope ranging from substituted olefins, β-keto esters, aromatic and aliphatic ketones *etc*.[32] Atropisomerism associated to the C_2-symmetry is the origin of axial chirality in this diphosphine ligand. The Ru-BINAP system was proven more competent than the Rh-BINAP catalyst as, in case of the Ru-BINAP system, the catalytic pathway follows the inner sphere or monohydride mechanism, whereas the Rh-BINAP catalyst follows the inner-sphere dihydride pathway.[33] This key difference allowed the Ru-BINAP system to hydrogenate efficiently with high enantioselectivies covering a large substrate scope including substituted olefins (α-arylacrylic acids, α, β- and α, β, γ-unsaturated acids *etc*.), allylic and homo allylic alcohols, β-keto esters, aromatic and aliphatic ketones *etc*. Inspired by the work of Noyori with the seminal BINAP chemistry, a number of research groups developed many modified ligands with atropisomeric aryl biphosphines.[16d] A few selected examples are described below and shown in Scheme 1.7.

Miyashima *et al.* reported BICHEP ligand (**1-6a**), which was successfully applied to Ru- and Rh-catalyzed asymmetric hydrogenation.[34] BIPHEMP (**1-6b**)[35] and MeO-BIPHEP (**1-6c**)[36] developed by Schmidt and coworkers have also shown good catalytic activity for asymmetric hydrogenation. A modified BINAP ligand, H8-BINAP (**1-7**), developed by Takaya provided enantioselectivity even better than BINAP for Ru-catalyzed hydrogenation of unsaturated carboxylic esters.[37]

Dibenzofuran based bisphosphine BIFAP ligand (**1-8**), were developed by Hiemstra *et al.* This ligand showed excellent enantioselectivity for Ru-catalyzed hydrogenation of methyl acetoacetate (ee >99%; depending on the analytical technique). They proposed that the enantioselectivity is most likely governed by the dihedral angle of the biaryl backbone.[38] Later on, SEGPHOS **(1-10)** with a narrower dihedral angle than BINAP lead to better enantioselectivity for the Ru-catalyzed hydrogenation of carbonyl compounds (ee >99%).[39] Zhang *et al*. developed Cn-TunaPhos ligands (**1-12**) with tunable bite angles in order to test the impact of this angle on enantioselectivity. C_4-TunaPhos exhibited comparable or better enantioselectivity (depending upon the substrate) than BINAP for the Ru-catalyzed hydrogenation of β-keto esters,[40] whereas, C_2-TunaPhos was the best ligand for Ru-catalyzed hydrogenation of enol acetates (ee up to 99.2%).[41]

Benincori *et al.* prepared BITINAP (**1-11a**) and TetraMe-BITINAP (**1-11b**) ligands by changing the aromatic rings (relative to BINAP or BIPHEMP) to heterocyclic benzothiophene ring. These ligands were successfully used for the Ru-catalyzed asymmetric hydrogenation of β-keto esters (ee up to 99%).[42] P-PHOS (**1-9**) ligands with heteroaromatic pyridyl ring, developed by Chan and co-workers, have shown good enantioselectivity for the Ru-catalyzed asymmetric hydrogenation of β-keto esters (ee up to 98.5%), α-arylacrylic acids (ee up to 96.2%) and substituted β-(acylamino)acrylates (ee up to 99.7%).[43]

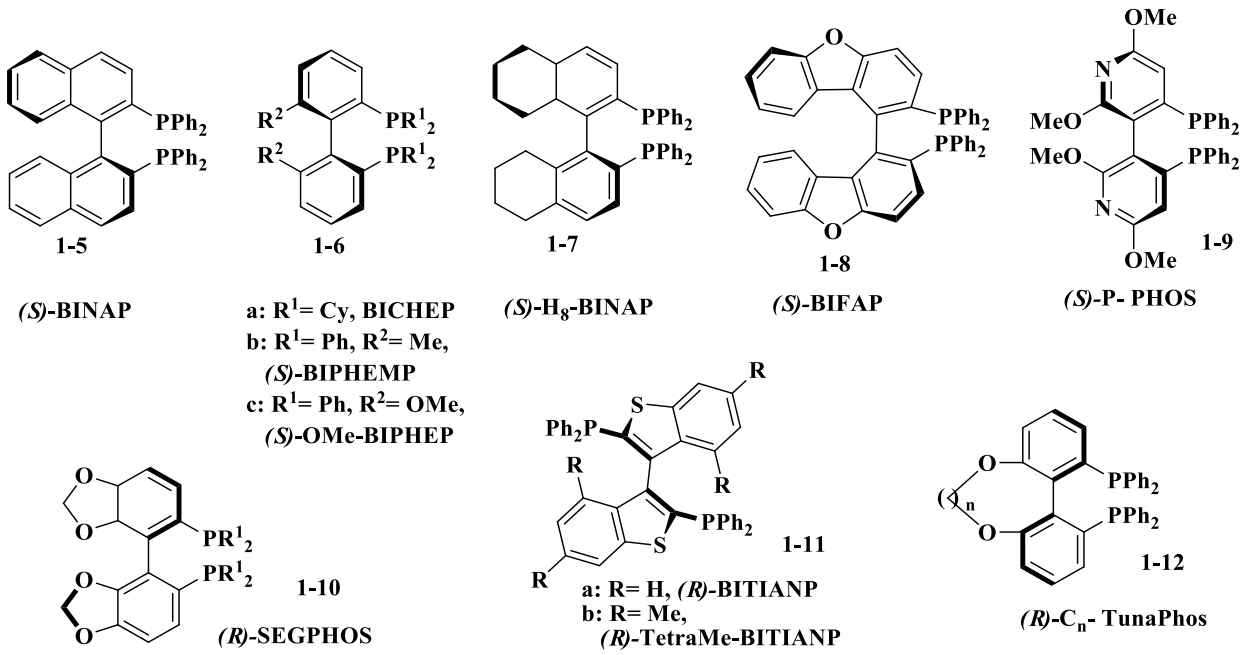

Scheme 1. 7: BINAP and related ligands

PHOX and related Ligands

Chiral enantiopure **Ph**osphanodihydro**ox**azolines (PHOX) ligands (Scheme 1. 8) were developed by Pfaltz and co-workers (1997).[44] These ligands are simple phosphines with an attached chiral oxazoline ring. The ligand designing was highly motivated by Crabtree's catalyst- $[Ir(COD)(Py)PCy_3]PF_6$, which is a cationic Ir-complex with monophosphane and pyridine as ligand and efficiently hydrogenated tri- and tetra-substituted olefins.[45] PHOX ligands were introduced in order to design an electronically similar chiral catalyst to examine the asymmetric hydrogenation of prochiral substrates of the same kind (unfunctionalized olefins).

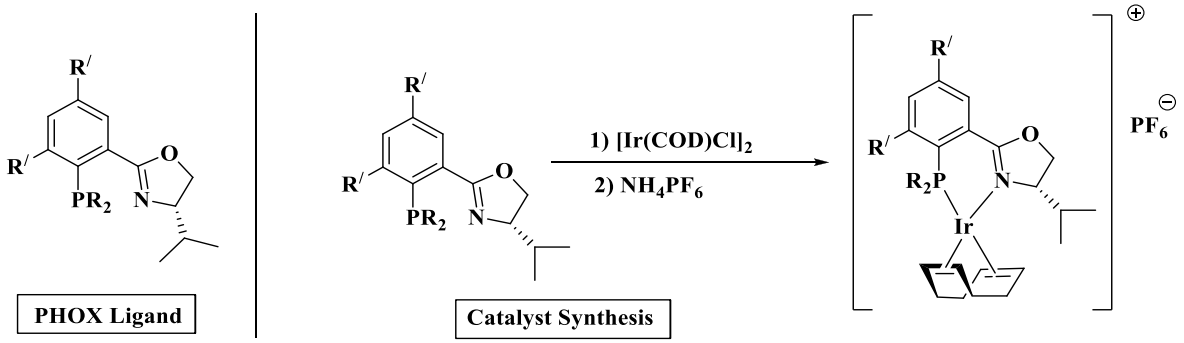

Scheme 1. 8: General structure of PHOX ligands and its Ir-catalyst synthesis

PHOX ligand-based chiral Ir-catalysts- **1-13** have ultimately been successful in the asymmetric hydrogenation of several unfunctionalized tri-substituted olefins with variable catalyst loading (0.1-4 mol%). Excellent yields and enantioselectivities (> 99%) were achieved. The asymmetric hydrogenation of imines has been moderately effective with these catalysts (yield up to 89%) under a relatively high dihydrogen pressure (100 bar) (Scheme 1. 9).[44, 46]

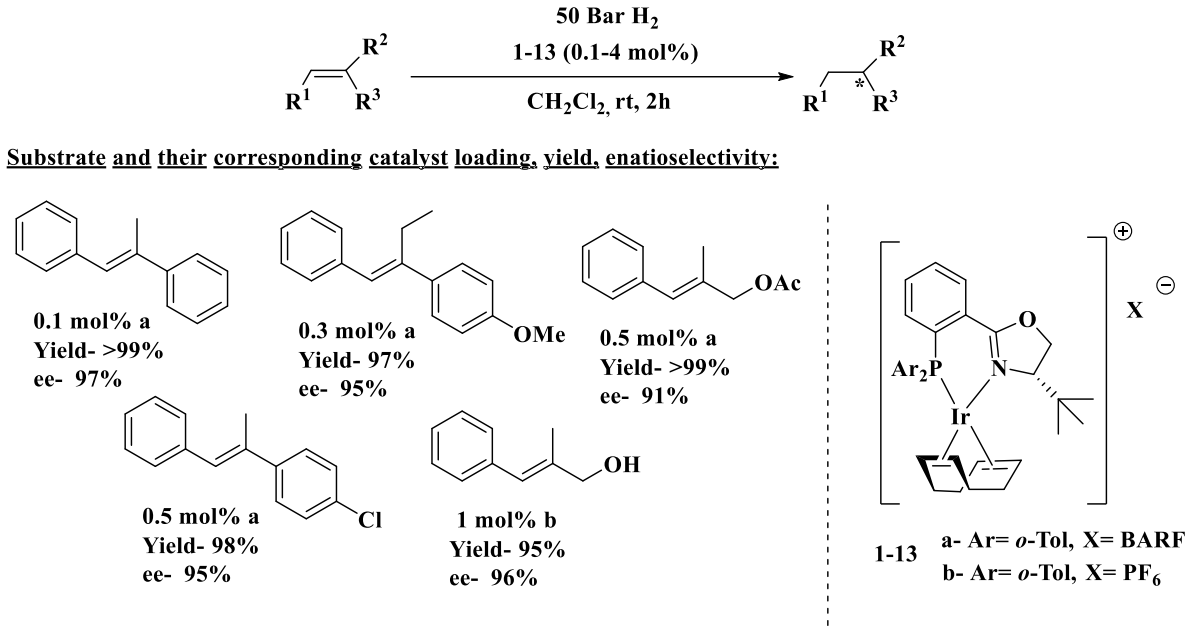

Scheme 1. 9: Asymmetric hydrogenation of substituted olefins by PHOX-based Ir-catalyst

The success of PHOX-Ir complex prompted successive developments of various similar kind of P,N ligands. Among them PyrPHOX (**1-14**),[47] phosphinite-oxazolines (**1-15**),[48] phosphine-imidazolines (PHIM) (**1-16**),[49] threonine derived phosphinite-oxazolines (**1-17**),[50] and JM-phos (**1-18**)[51] are the most significant ones (Scheme 1. 10). The catalytic systems obtained with these ligands after coordination with $[Ir(COD)Cl]_2$ were very efficient giving excellent yields (>99%) and enantioselectivities (94-99%) for the asymmetric hydrogenation of unfuntionalized tri-substituted olefins for different substrate to catalyst ratios (up to 1000:1).

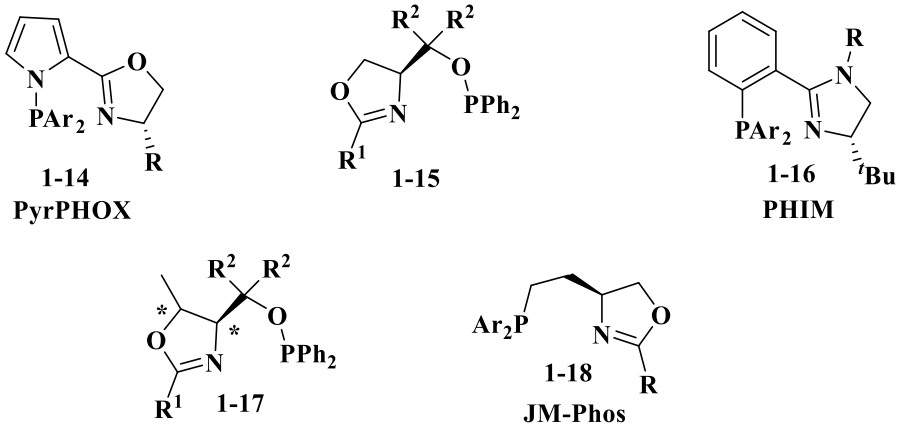

Scheme 1. 10: Other ligands inspired by PHOX

Dieguez *et al*. developed a series of chiral pyranoside phosphite-oxazolines (LP-Ox) ligands (Scheme 1. 11).[52] The motivation for this design came from the need of a catalyst that can attain high asymmetric induction in the hydrogenation of a broader substrate scope of unfunctionalised olefins, especially olefins without any neighboring polar group. Ir -complexes of these ligands brought excellent enantioselectivities and yields for the asymmetric hydrogenation of tri-substituted unfunctionalized olefins. They also proved successful for highly challenging disubstituted olefins with or without polar groups attached to side chain. Excellent catalytic activities (up to 100% conversion) and enantioselectivities were attained under relatively milder condition (1 bar H_2).[53] The reactivity is mostly dependent on the steric properties of the oxazoline substituent and of the substituents at the *ortho*-positions of the biaryl phosphite moiety.

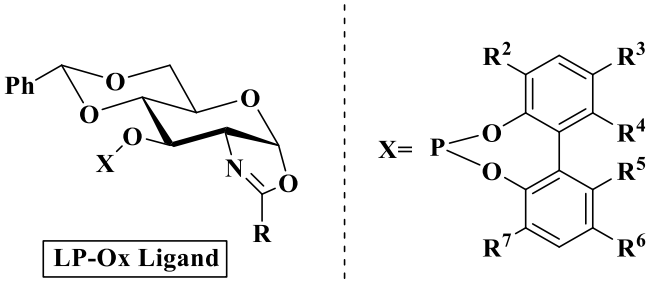

Scheme 1. 11: Structure of LP-OX Ligand

A new efficient family of ligands-**1-19**, where the oxazoline group of LP-ox was replace by a thiazoline moiety was also developed by the same research group.[54] The variation of steric property and basicity of the N-donor group as a result of the O/S replacement reflected to improved

enantioselectivities for Z-tri-substituted olefins with or without a neighboring polar group and 1,1-disubstituted terminal olefins (Scheme 1. 12).

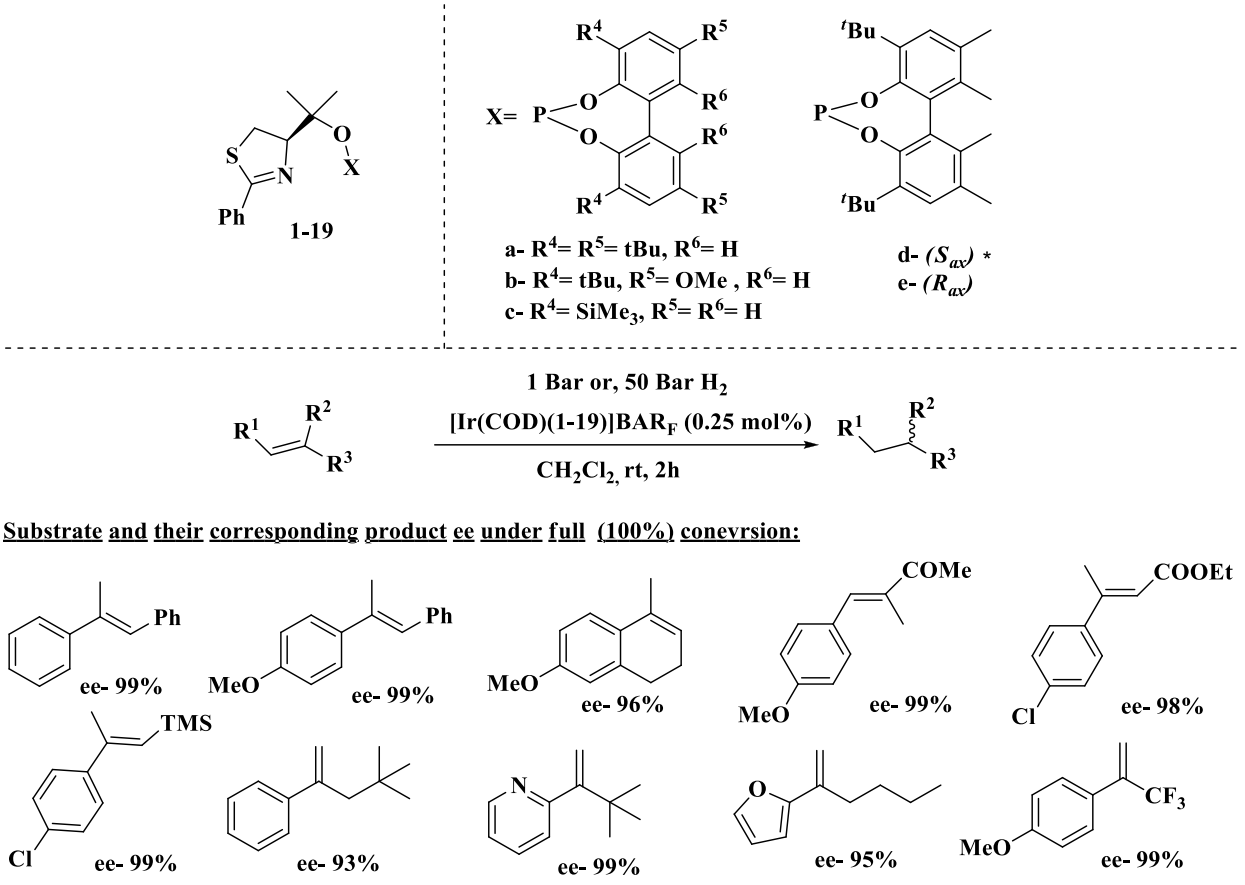

Scheme 1. 12: Asymmetric Hydrogenation with Thiazoline-phosphinite Ligands

PNN and PNP Ligands

Clarke and co-workers developed P,N,N ligands based on a 1,2-cyclohexane diamine scaffold, **1-20** and **1-21** (Scheme 1. 13).[55] Ru-complexes of these ligands were tested in the hydrogenation of a few phenyl alkyl ketones. A decent level of enantioselectivity was observed with phenyl *tert*-butyl ketone (ee of the product up to 67% for **1-21** and up to 85 for **1-20** with X= 3,5-di-t-butyl). An analogous ligand **1-22** was developed by the same group based on the *t*-stilbenediamine scaffold. It was also proved to be efficient in the enantioselective Ru-catalyzed hydrogenation of ketones (ee up to 80% in the hydrogenation of phenyl *tert*-butyl ketone).[56] More recently, ligand

* *(S_{ax}/ R_{ax})*= Abosolute configuration of the axial chirality of the biphenyl ring

1-20 was used in the Ir-catalyzed hydrogenation and transfer hydrogenation of alkyl aryl ketones. Good enantioselectivities were, in particular, obtained with the alkyl group of the ketone substrate being 4-piperidyl (ee in the 75-96% range) or cyclohexyl (ee up to 98%). [57]

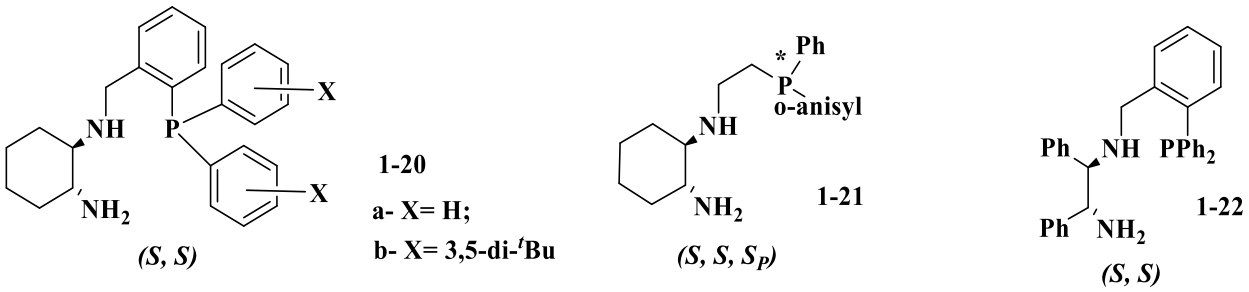

Scheme 1. 13: PNN ligands developed by Clarke

Morris and coworkers synthesized the chiral PNP ligands **1-23**.[58] Fe-complexes of the ligand after treatment with $LiAlH_4$ followed by *t*-amylOH yield monohydride complexes- **1-25** as the precatalyst for the asymmetric hydrogenation of ketones. They proposed that the dihyride complexes-**1-26**, formed after activation of **1-25** with a base (KO^tBu) under dihydrogen pressure, acts as real hydrogenation catalyst.[59] The same catalytic systems could also be obtained directly from ligands **1-23** (Scheme 1. 14).[60]

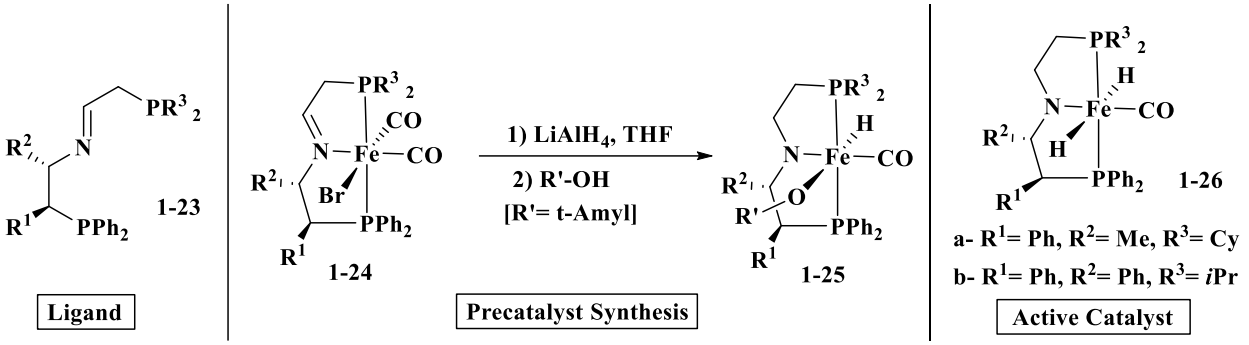

Scheme 1. 14: Ligand and Active catalyst of PNP Ligands developed by Morris

These catalytic systems proved to be very efficient in the asymmetric hydrogenation of aryl alkyl ketones with low amounts of catalysts (typically 0.1mol%) and high enantioselectivities (ee=86-96%)[58b] and for the asymmetric hydrogenation of activated imines (N-phosphinoyl and N-tosylimines) to yield the corresponding amines with high enantiomeric excesses (in the 90-98% range for most substrates, see Table 1. 1).[61]

Table 1. 1: Short summery of Catalytic activity of Catalyst designed by Morris

Substrate	Catalyst and loading of catalyst	H_2 Pressure	Yield (%)	ee (%)
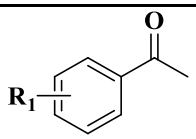	**1-26a** (0.1 mol%)	5 atm	95-99	76-82 *(S)*
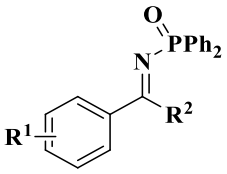	**1-26b** (3 mol%)	30 bar	59-85	92-98 *(S)*
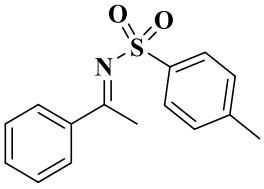	**1-26b** (3 mol%)	30 bar	82	97 *(S)*

Chiral polydentate phospholanes have been efficient for the Rh-catalyzed asymmetric hydrogenation of substituted olefins (ee up to 90%) but poor results were obtained for the asymmetric hydrogenation of ketones.[62]. Beller *et al*. revised the synthesis of a chiral tridentate PNP ligand **1-27** bearing two stereogenic phospholane rings (Scheme 1. 15) and tested them in the asymmetric hydrogenation of ketones with various metals (Mn, Re, Ru, Fe).[63] The Mn and Fe-based catalytic systems (**1-28** and **1-29**) were proven rather efficient, for the asymmetric hydrogenation of cyclic aliphatic ketones (average ee 30-70% and conversion up to 99% in both cases).

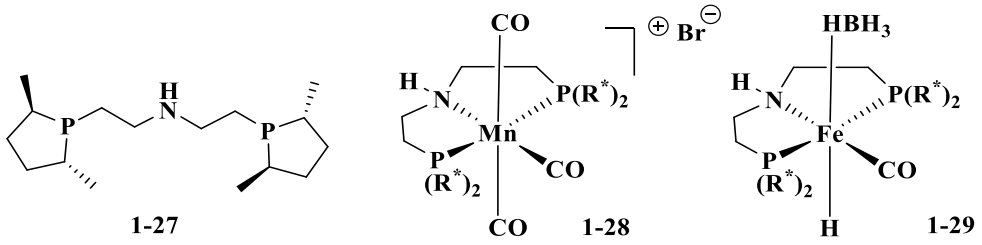

Scheme 1. 15: PNP ligand and complex developed by Beller and co-workers.

Phosphorous-Sulphur Ligands

Phosphorus containing thioether ligands have been relatively less studied with respect to P,N; P,P; or P,N,N analogues. Most ligands developed so far mostly are phosphite or phosphinite- based, rather than phosphine-based. The major catalytic tests of these ligands were restricted to allylic substitution reactions until the last decade. However, more recently phosphite/ phosphinite-thioether ligands have shown excellent performance in the asymmetric hydrogenation of different types of olefins with different non-noble metals.

Gladiali *et al.* (1994), reported phosphine-thioether ligands **1-30** (Scheme 1. 16), having the BINAP scaffold with one phosphine group replaced by a thioether group and their Pd and Rh complexes.[64] The Rh-catalyzed hydrogenation of functionalized olefins was carried out with moderate yield and enantioselectivity (ee up to 60%).[65]

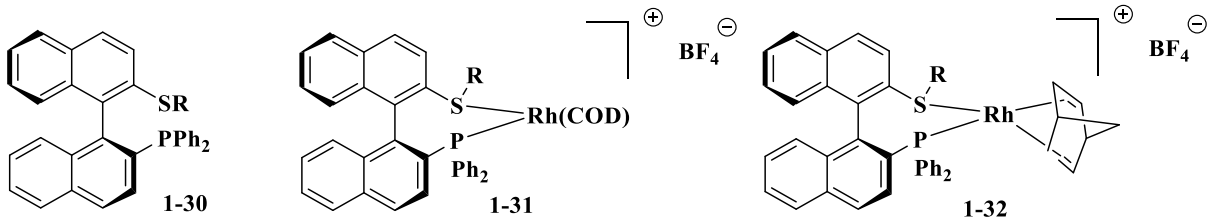

Scheme 1. 16: Phosphine- thioether ligands based on BINAP Scaffold and corresponding metal complexes

Evans *et al*. have developed efficient Phosphinite-thioether ligands **1-33** and **1-34.** Rh-complexes of these ligands successfully hydrogenated functionalized olefins such as tetra substituted enamides with very high enantioselectivities (ee up to 98%) (Scheme 1. 17).[66]

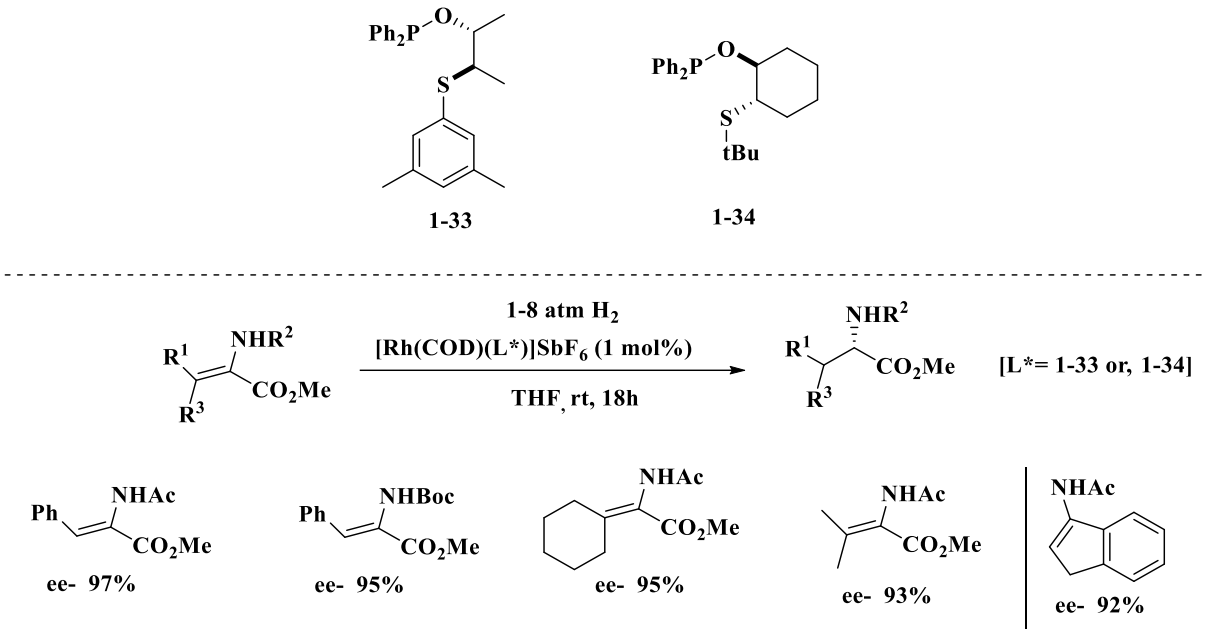

Scheme 1. 17: Ligands developed by Evans and catalytic applications

Dieguez *et al*. recently replaced the phosphinite moiety in Evans ligand with biaryl phosphite moieties and developed a number of phosphite-thioether ligands, **1-35** (Scheme 1. 18).[67] A lower air sensitivity and a greater flexibility of the biaryl phosphite group in **1-35**, which can easily accommodate a wide range of substrates with diverse steric demand in the chiral pocket of the catalyst, was the major motivation for designing this kind of ligands.[68]

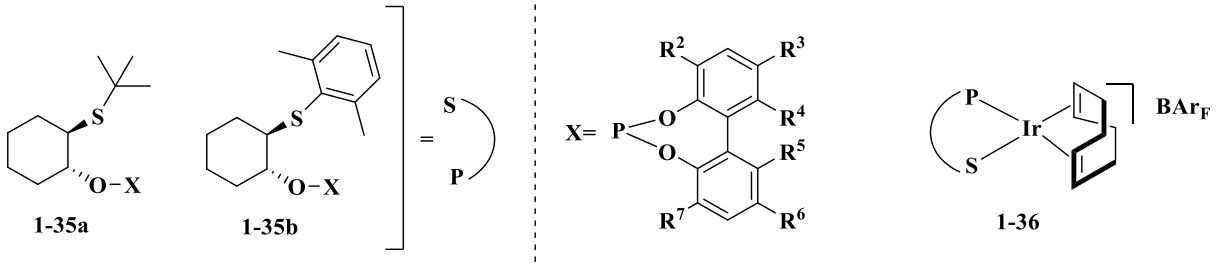

Scheme 1. 18: Phosphite-thioether ligands developed by Dieguez *et al.*

These ligands were successfully utilized in Ir-catalyzed hydrogenation of several *(E)*-unfunctionalized alkenes and 1,1-disubstituted alkenes (Scheme 1. 19). Notably, they allowed extension to the hydrogenation of terminal aryl substituted boronic esters with excellent enantioselectivity (ee up to 98%).

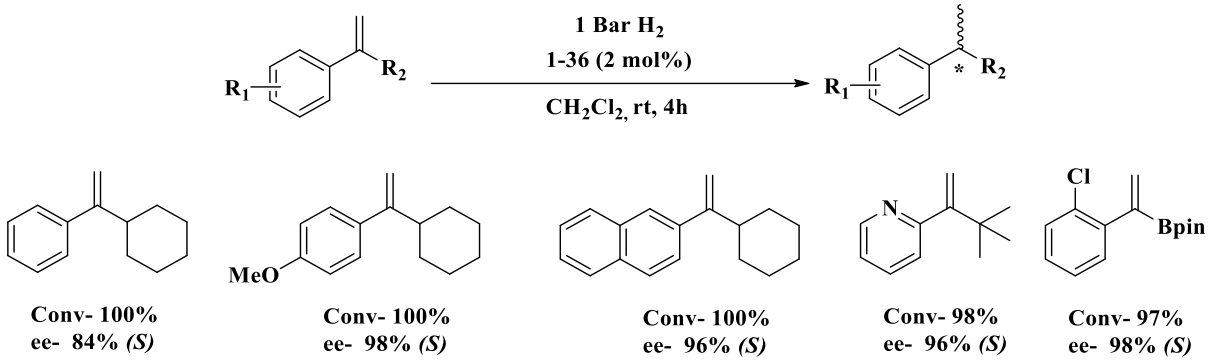

Scheme 1. 19: Asymmetric hydrogenation with Ir-complex of phosphite-thioether ligands

They also reported phosphinite/ phosphite-thioether ligands (**1-37** and **1-38**, see Scheme 1. 20) derived from aryl glycidol and their application with excellent catalytic activities in the Pd-catalyzed hydrogenation of functionalized (ee up to 97%) and unfunctionalized olefins (ee up to 99%).[69]

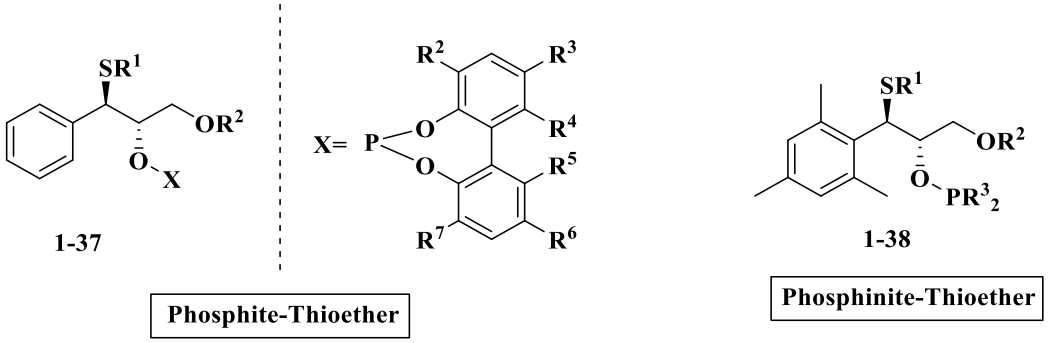

Scheme 1. 20: Ligands derived from aryl glycidol

A large library of furanoside phosphite/ phosphinite/ phosphine-thioether ligands has been developed by Dieguez *et al*. (Scheme 1. 21). These were the first non-N-donor heterodentate ligands applied to the Ir-catalyzed hydrogenation of unfunctionalized olefins. The phosphite variants, **1-39**, were proven to afford excellent enantioselectivities (ee up to 99%) for Ir-catalyzed asymmetric hydrogenation of *(E)*- and *(Z)*-unfunctionalized olefins even with poorly co-coordinative groups (*e.g.* α,β- unsaturated esters and vinyl boronates).[70]

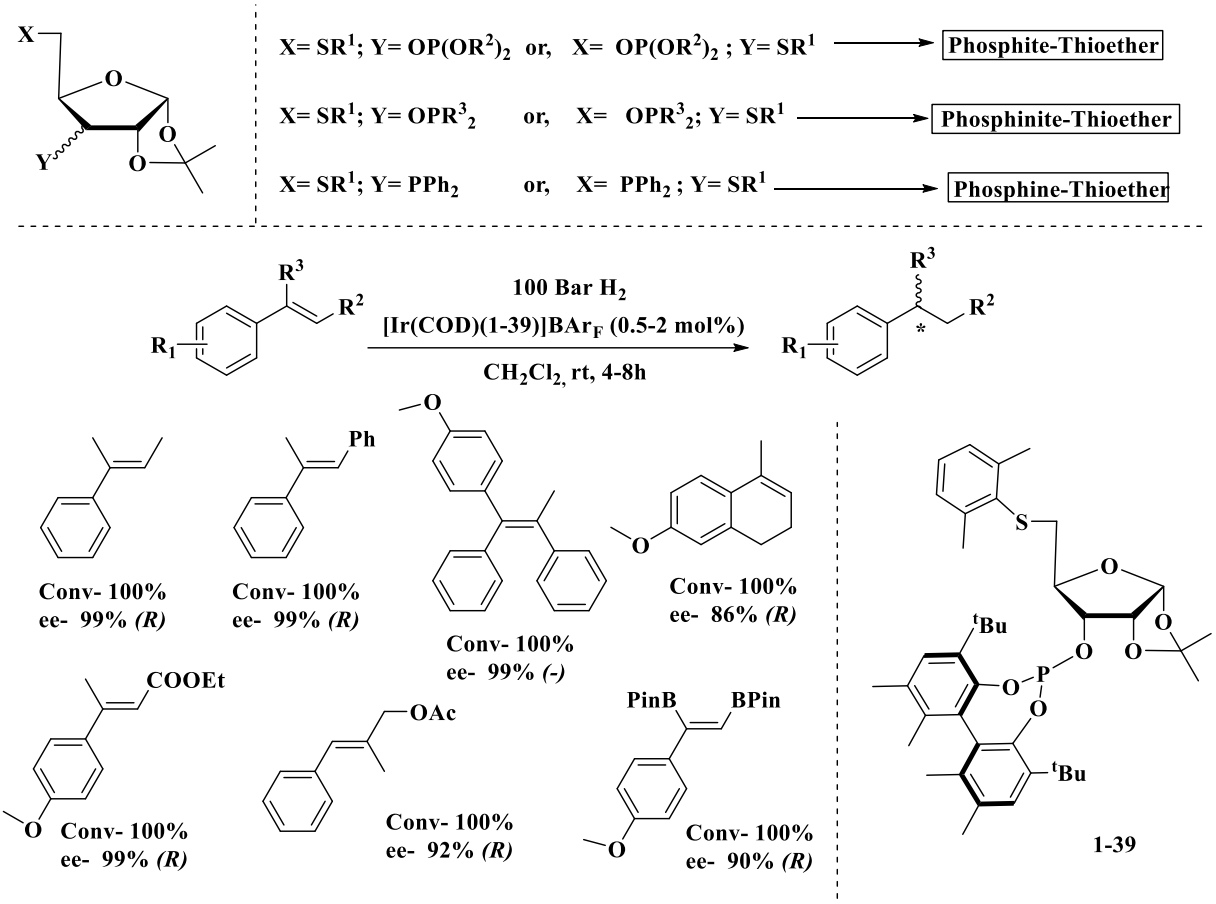

Scheme 1. 21: General ligand formula of furanoside based P,S- ligands and catalytic results with the best one

Phosphite-thioether ligands- **1-40** and **1-41 (**Scheme 1. 22**)**, prepared from available L-*(+)*-Tartaric acid and D-*(-)*-Mannitol developed by same group. These ligands also gave excellent enantioselectivity for Ir-catalyzed asymmetric hydrogenation of unfunctionalized tri-substituted olefins and asymmetric hydrogenation of cyclic β-enamides (ee up to 99% in both cases).[71]

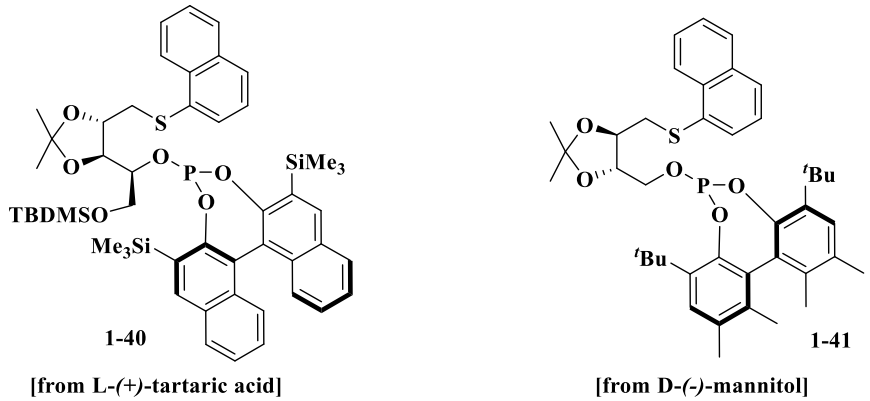

Scheme 1. 22: Phosphite-thioether ligands based on L-*(+)*-Tartaric acid and D-*(-)*-Mannitol

SpiroAP, SpiroPAP and SpiroSAP

Xie, Zhou *et al.* (2010) reported chiral spiro aminophosphine ligands known as SpiroAP (**1-42**).[72] Later on, a family of spiro tridentate ligands, called SpiroPAP (**1-43**), Oxa-SpiroPAP (**1-44**), and SpiroSAP (**1-45** and **1-46**) were prepared by sidearm modification (Scheme 1. 23).[73]

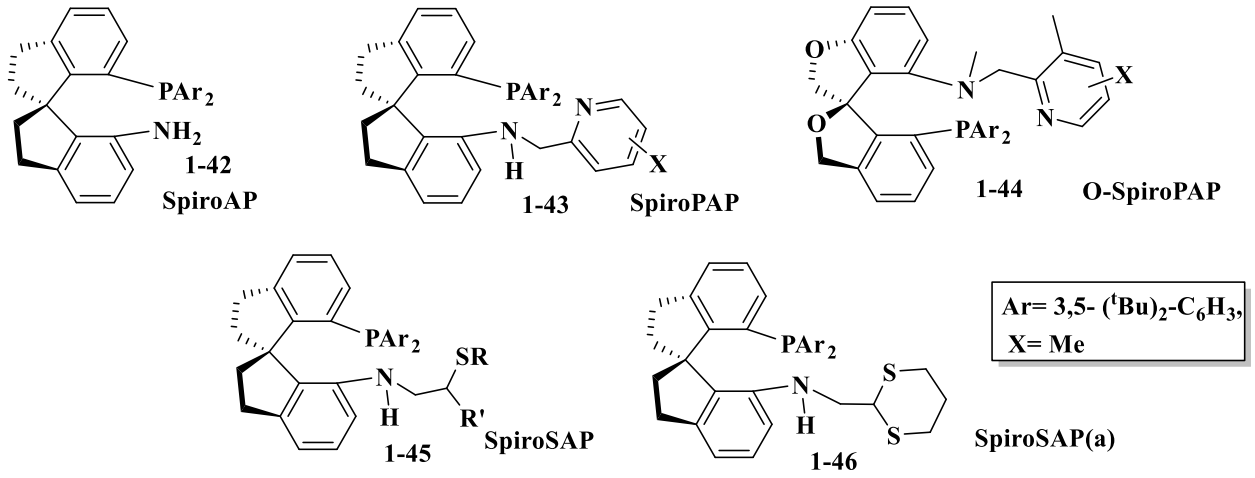

Scheme 1. 23: Spiro ligand family and the most effective Variant

SpiroAP Ligand- **1-42** was used for Ir-catalysed asymmetric hydrogenation of α-arylmethylene Cycloalkanone with high yield and enantioselectivity (yield-99% ; ee up to 97%) [Scheme 1. 24, a)].

Iridium complexes of SpiroPAP- **1-47** were used in the asymmetric hydrogenation of various aryl alkyl and cycloalkyl alkyl ketones with very low loadings (typically S/C= 5000 and TON up to 4.55×10^6) and very high enantioselectivities (ee = 88-99.9%).[73c] This efficient catalytic system

was scaled up for the industrial asymmetric synthesis of Rivastigmine, a drug for the treatment of Alzeimer's disease [Scheme 1. 24, b)].[74] These complexes were also used in the asymmetric hydrogenation of β-ketoesters with once again very high catalytic activities (typically S/C= 1000 and TON up to $1.23x10^6$) and high enantioselectivities (ee in the 88-95.8% range),[75] of heteroaryl δ-ketoesters (for S/C= 1000, yield in the 92-97% range and ee in 96.7-99.9% range),[76] of alkyl and aryl α-ketoacids (for S/C= 1000, yield in the 92-98% range and ee in the 56-98% range),[77] in the hydrogenation of racemic α-substituted lactones to yield chiral diols by Dynamic Kinetic Resolution (yields = 82-95%, ee = 69-95%)[78] and in the asymmetric transfer hydrogenation of ketones (for S/C= 1000, yields=90-99% range and ee=80-98% range).[79]

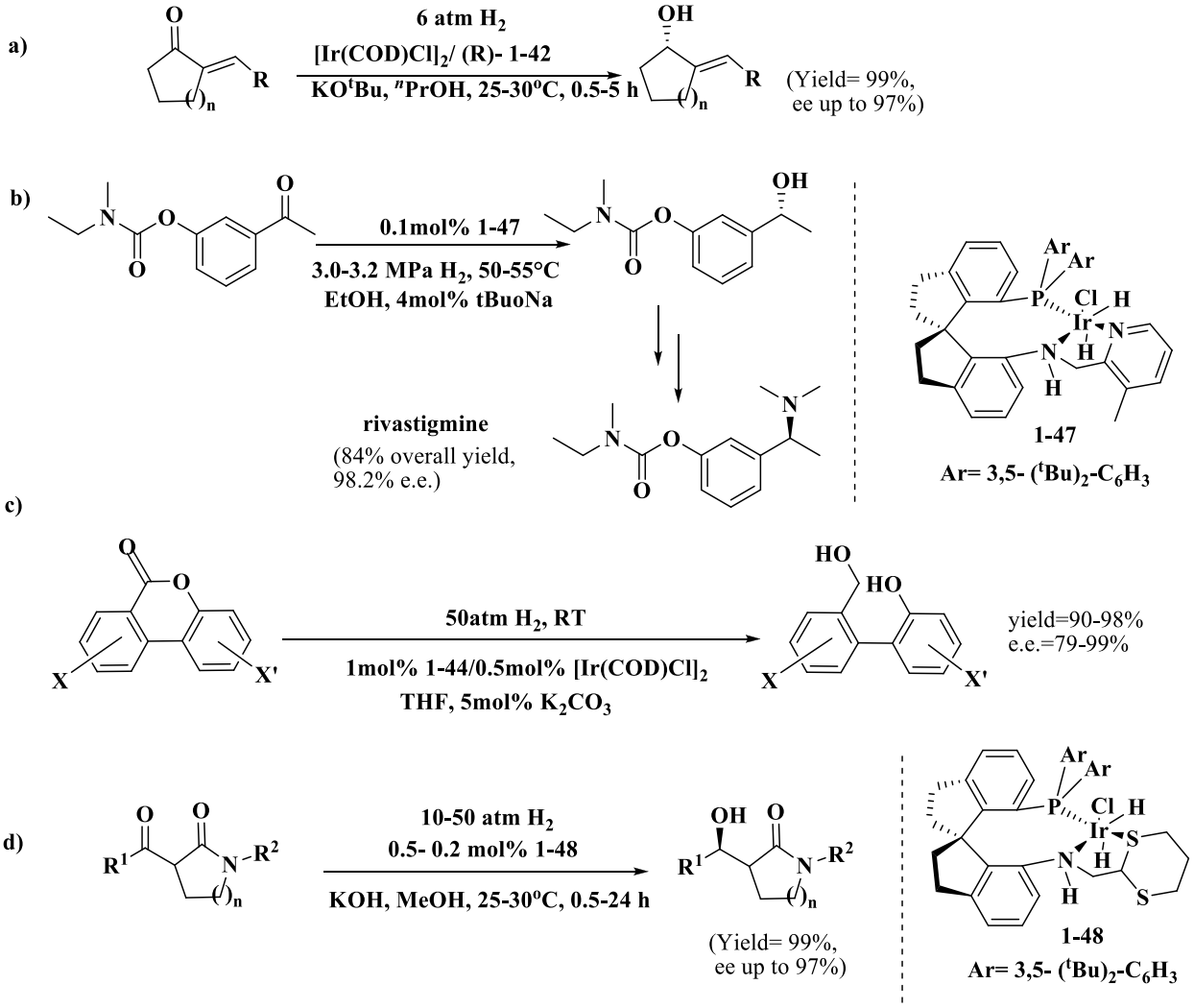

Scheme 1. 24: Few applications of Spiro ligands in Ir catalyzed Asymmetric Hydrogenation

O-SpiroPAP ligands- **1-44** were used in the iridium-catalyzed hydrogenation of bridged biaryl lactones to axially chiral compounds with high yields (up to 99%) and enantioselectivities (ee > 99%) [Scheme 1. 24, c)].[73a]

PNS analogue of the SpiroPAP ligand family, SpiroSAP (**1-45, 1-46**) were used in the asymmetric Ir-catalyzed hydrogenation of β-alkyl-β-ketoesters (yield = 91-98%, ee = 95-99.9% with **1-46**) [73b] and in the hydrogenation of racemic β-ketolactams and of ketoesters (yield=87-99%, TON up to 5000, syn/anti from 97/3 to 99/1, ee = 83-99.9% with **1-46**) by Dynamic Kinetic Resolution[Scheme 1. 24, d)].[80]

1.2. 3) High Performance Phosphine containing Ferrocenyl bidentate and tridentate ligands for Hydrogenation: Brief Review

Chiral ferrocene derivatives have a prolonged history of over four decades as ligands for asymmetric catalysis, especially because of their easily accessible planar chirality and of the ferrocene scaffold specific stereo-electronic properties. Because of these advantages, the quest for ligands is still on. The starting point was undoubtedly the pioneering discovery of Ugi's amine back in 1970, which allowed the synthesis of a number of substituted phosphine-containing planar chiral ferrocenyl ligands (see Chapter-2). PPFA (**1-49**), BPPFA (**1-50**), Bophoz (**1-51**) (Scheme 1. 25), Josiphos *etc.* appeared in the initial stages of this ligand family development. BPPFA, developed by Hayashi (1980) was effective for hydrogenation of functionalized olefin with $[RhCl(NBD)]_2$ with ee up to 98%, although requiring but long reaction time (30 h) and a high H_2 pressure (100 atm).[81] Bophoz developed by Boaz (2002), in combination with $[Rh(COD)_2]OTf$, hydrogenates dehydro-α-amino acid derivatives with ees up to 99%.[82]

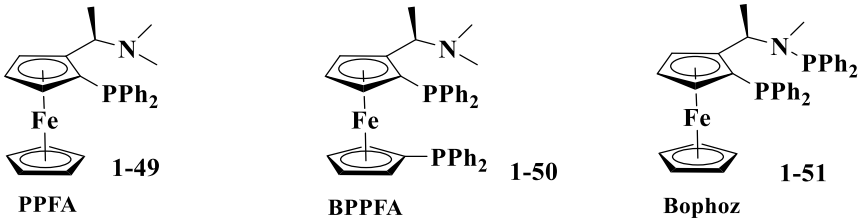

Scheme 1. 25: General structure of PPFA, BPPFA, Bophoz

Among the 1,2- substituted ligands, the Josiphos family has been most successful for catalytic asymmetric hydrogenation. A few ligands in this family have been synthesized by other pathways than the Ugi's amine approach. The FOXAP family has been the most effective among them for

hydrogenation. Ferrocenyl phosphine thioether ligands that combines two soft P- and S- centers were proven effective in certain asymmetric hydrogenations. Ligands of this particular type are derived either from Ugi Amine or other approaches (See Chapter-4). Tridentate ligands of similar types are part of modern-day ferrocenyl ligand development. In the following sections we will briefly discuss the effective 1,2- substituted phosphine-containing ferrocenyl ligands towards metal catalyzed asymmetric hydrogenation or transfer hydrogenation.

Josiphos and related ligands

Josiphos is a type of C_1- symmetric planar chiral ferrocene-based ligands bearing two different phsophine groups. One is directly attached to the ferrocene backbone and the other one on the side chain (Scheme 1. 26).[83]

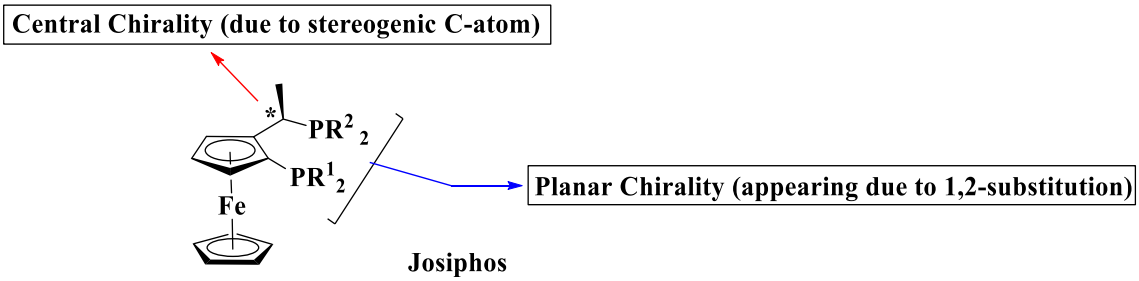

Scheme 1. 26: General structure of Josiphos

Josiphos is the most significant among the ligands derived from further side chain substitution of planar chiral ferrocenyl compounds based on Ugi's amine (See chapter-2). Many variants of Josiphos ligands, differing by the nature of the phosphine groups, have been synthesized. There are three major motivations behind the synthesis of a wide range of josiphos ligands[84]-

1) The scaffold being highly tunable, a variety of substituents with different steric and electronic properties can be incorporated on the Cp ring or on the side chain (both enantiomers) according to the steric and electronic requirement of the catalytic reactions.

2) The Rh-catalyzed hydrogenation of enamide, which was the first catalytic test with a Josiphos ligand was a grand success (ee over 90%, TOF 1000h^{-1})

3) A few of the key intermediates or the synthesis of certain industrially successful organic compounds, like- *(S)*- Metolachlor,[85] *(+)*-Biotin,[86] *(+)-cis*-methyl dihydrojasmonate [87]- were

obtained with high enantioselectivity using catalytic hydrogenation based on Josiphos ligand. This also led to further interest.

Rh and Ir complexes with chiral Josiphos ligands- **1-52** are highly selective for the asymmetric hydrogenation of acetoacetates (yield 100%, ee up to 97%), enamides (yield 100%, ee up to 96%), and itaconic acid derivatives (yield 100%, ee up to 99%).[88] Moderate results were obtained for Ir-catalyzed asymmetric hydrogenation of N-aryl/ alkyl imines and phosphinylimines.[89] Scheme 1. 27 briefly summarizes the most relevant hydrogenation results for the different above-mentioned substrates.

Substrate	Catalyst	Reaction conditions	ee range (%)	Best TON	Best TOF (h^{-1})
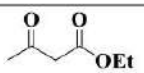	$[Rh(nbd)_2]BF_4$/ **b**	5 bar H_2 r.t.	84-97	100	6
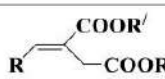	$[Rh(nbd)_2]BF_4$/ **a**	1 bar H_2 25°C	90-99.6	100	200
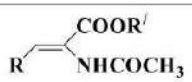	$[Rh(nbd)_2]BF_4$/ **a**	1 bar H_2 25°C	25-97	100	330
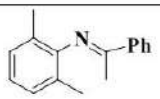	$[Ir(COD)Cl]_2$/ **c**	80 bar H_2 25°C	67-96	200	n.a.
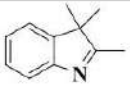	$[Ir(COD)Cl]_2$/ **d**	80 bar H_2 15°C	76-93	250	56
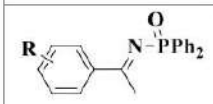	$[Rh(nbd)_2]BF_4$/ **e**	70 bar H_2 60°C	35-99	500	500

* This table is adapted from ref- [84]. TONs and TOFs are calculated by standard experiments; although the values are not optimized.

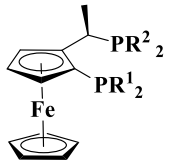

1-52

a- R^1**= Ph,** R^2**= Cy**
b- R^1**= 3,5-**CF_3**Ph,** R^2**= Cy**
c- R^1**= Ph,** R^2**= 4-**CF_3**Ph**
d- R^1**= Xyl,** R^2**= Xyl**
e- R^1**= Cy,** R^2**= Cy**

Scheme 1. 27: Asymmetric Hydrogenation of different substrates with Josiphos ligands

The recent advances with Josiphos include very interesting results. Among the selected ones, Ru or Os based chiral pincer complexes -**1-53**, based on Josiphos ligands, have been proven very effective for the transfer hydrogenation of various alkyl aryl ketones (yield 100%, ee up to 99%) (Scheme 1. 28).[90]

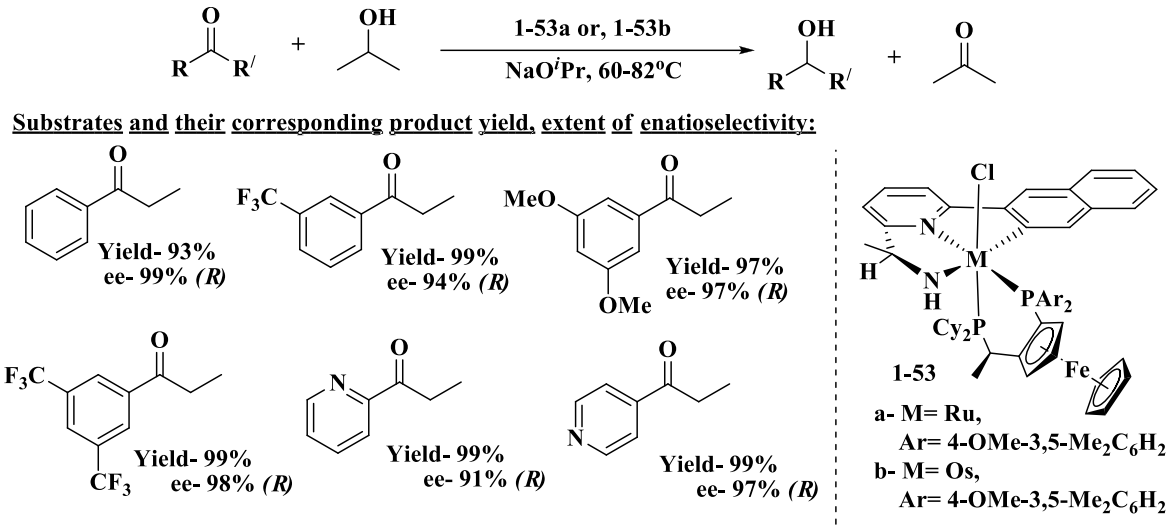

Scheme 1. 28: catalyst **1-53** and its catalytic application towards asymmetric hydrogenation

Tetra-substituted α,β-unsaturated ketones are challenging substrates because of the chemoselectivity issue between C=C and C=O bond hydrogenation. Sheppard *et al.* developed Rh-catalyzed asymmetric hydrogenation systems using Josiphos ligand- **1-54**, which selectively reduces the C=C bond and thus provides optically active ketones with good yield and enantioselectivities (yield 97%, ee up to 96%) (Scheme 1. 29). The presence of a Lewis acid as an additive was very essential to increase the enantioselectivity for the more substituted ketones. Zn $(OTf)_2$ was proven the best so far.[91]

Rh-catalyzed enantioselective hydrogenation of N-alkoxycarbonyl hydrazones in the presence of a Josiphos ligand **1-55** has been reported by scientists from Merck and Co. (Scheme 1. 30). They have tested a number of commercially available chiral ligands (*e.g.* DIOP, Norphos, Duphos, Josiphos *etc.*). Josiphos was proven to be the best one as it afforded good to excellent enantioselectivities for hydrazones attached with different protected groups (BOC, CBz *etc.*).[92]

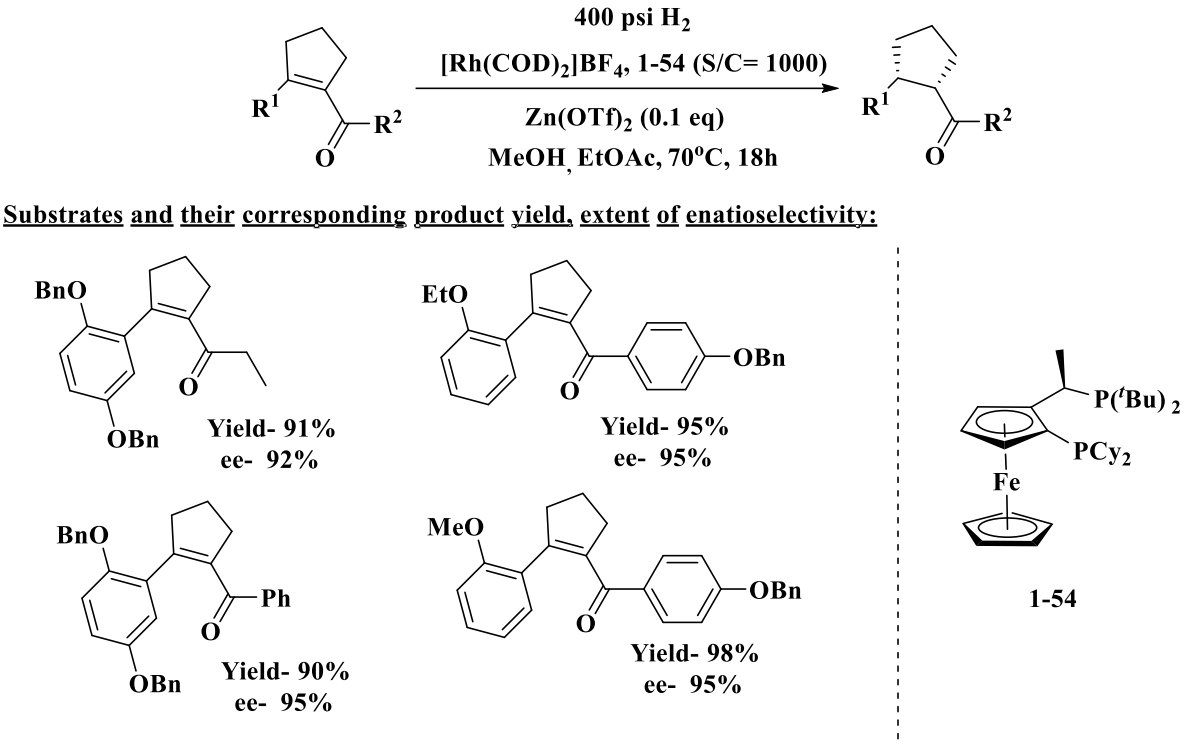

Scheme 1. 29: Asymmetric Hydrogenation of tetra-substituted α, β- unsaturated ketones

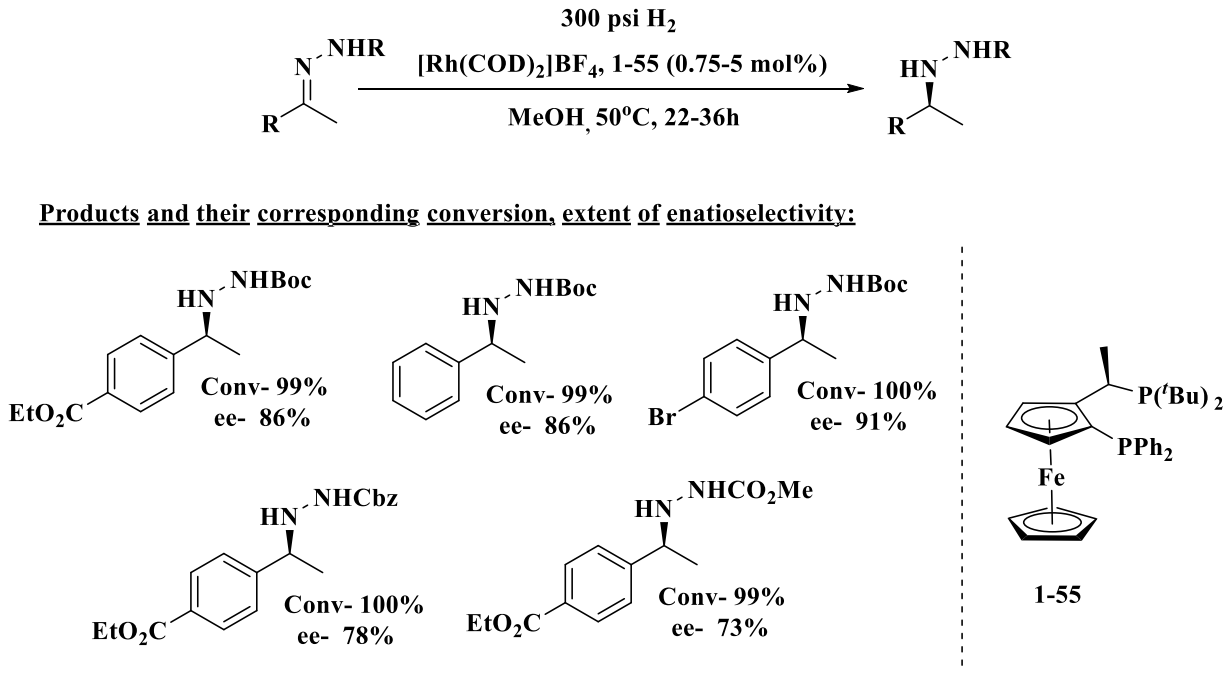

Scheme 1. 30: Asymmetric hydrogenation of protected hydrazones

Zhang and coworkers, very recently developed a very interesting ligand family by attaching a chiral biphenyl phosphine or binaphane moiety into the Josiphos backbone. The ligand is known

as Josiphos-type binaphane (**1-56**). This ligand was successful for the Ir-catalyzed enantioselective hydrogenation of 1-aryl substituted dihydroisoquinolines (ee up to > 99%) (Scheme 1. 31). The resulting products are substituted 1,2,3,4-tetrahydroquinolines, which are very ubiquitous scaffolds in natural products and biologically active compounds.[93]

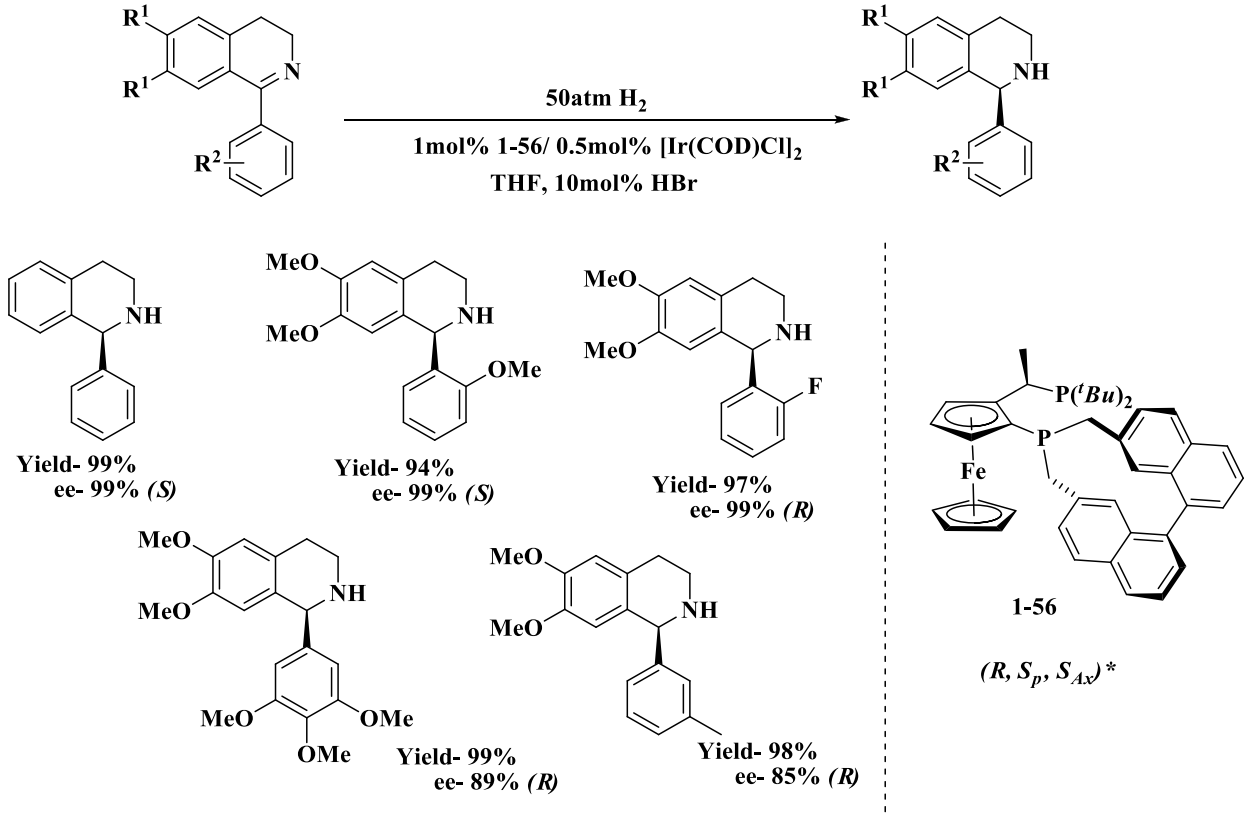

Scheme 1. 31: josiphos-binaphane ligands for asymmetric hydrogenation

Very recently Hu *et al*. developed an analogous ferrocene/indole-based ligand with two different phosphine centers, namely IndoFerroPhos (**1-57**). This ligand was utilized for the [$Rh(COD)_2BF_4$]-catalyzed asymmetric hydrogenation (10 bar H_2) of α-dehydroamino acid esters (yield- > 99%, ee up to 97%)and α-enamides (yield- 85-96%, ee up to 98%) (Scheme 1. 32).[94]

* *(S_{Ax})*= Absolute configuration of axial chirality in binapthyl ring

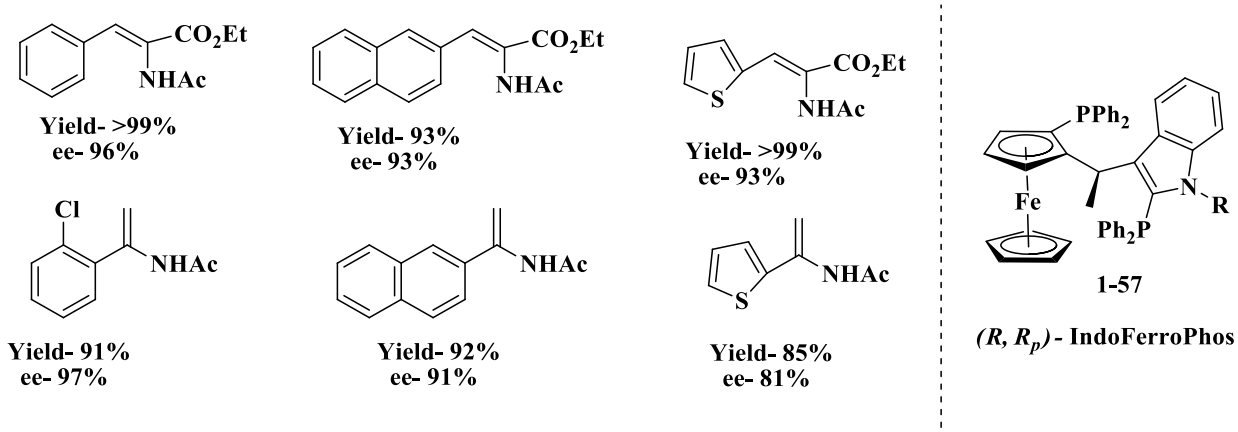

Scheme 1. 32: Catalytic results with IndoFerrophos

FOXAP and related ligands

The ferrocenyl oxazoline-based P,N ferrocenyl or, **F**errocenyl**oxa**zolinyl**p**hosphines (FOXAP) ligands, are widely studied among the other P,N-ferrocenyl ligands (Scheme 1. 33). They were first reported independently by Richards, Sammakia and Umera.[95] The ability to form stable 6-membered chelate rings upon metal co-ordination, association of the oxazoline ring with central chirality and ferrocenyl backbone with planar chirality which provides a better chiral environment during the asymmetric reaction; were the determining factors for the success of this kind of ligand scaffolds. [96]

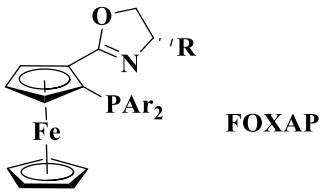

Scheme 1. 33: General structure of FOXAP

Hidai *et al*. after isolating diastereomerically pure FOXAP-based Ru-complexes (**1-58**) utilized them for the hyrosilyltion and transfer hydrogenation of alkyl aryl ketones with excellent yields and enantioselectivities (Scheme 1. 34).[97]

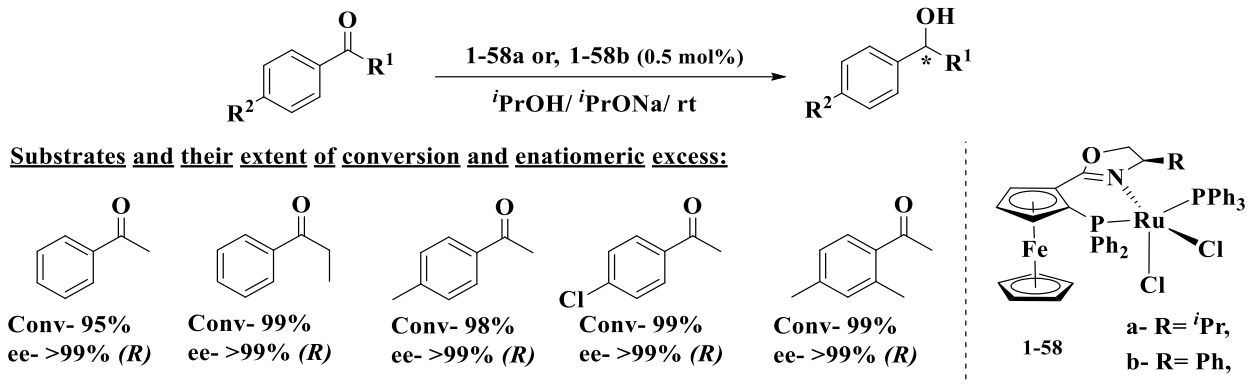

Scheme 1. 34: Transfer hydrogenation with Ru-FOXAP

Naud *et al*. reported the first efficient Ru-catalyzed H_2-hydrogenation of simple aryl alkyl ketones by the FOXAP ligand **1-59** and **1-60 (**Scheme 1. 35**)**. Excellent enatioselectivities and TONs of up to 50,000 were achieved. Similar enantioselectivities (88-99%) were provided by FOXAP ligands with different substituents, proving the main influence of the planar chirality in this case.[98]

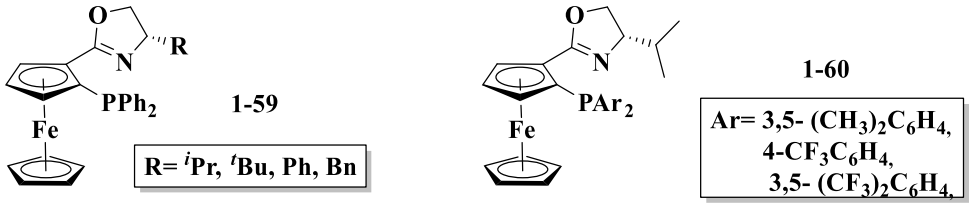

Scheme 1. 35: FOXAP ligands utilized by Naud *et al.* for Ru-catalyzed asymmetric hydrogenation

Chiral amides are useful subunits of various natural products and they are synthetic intermediates for chiral ketones or amines.[99] The FOXAP ligand- **1-61** has been efficient for the Ir-catalyzed asymmetric hydrogenation of α,β-unsaturated amides (ee up to 96%), as shown by Hou *et al*. (Scheme 1. 36).[100]

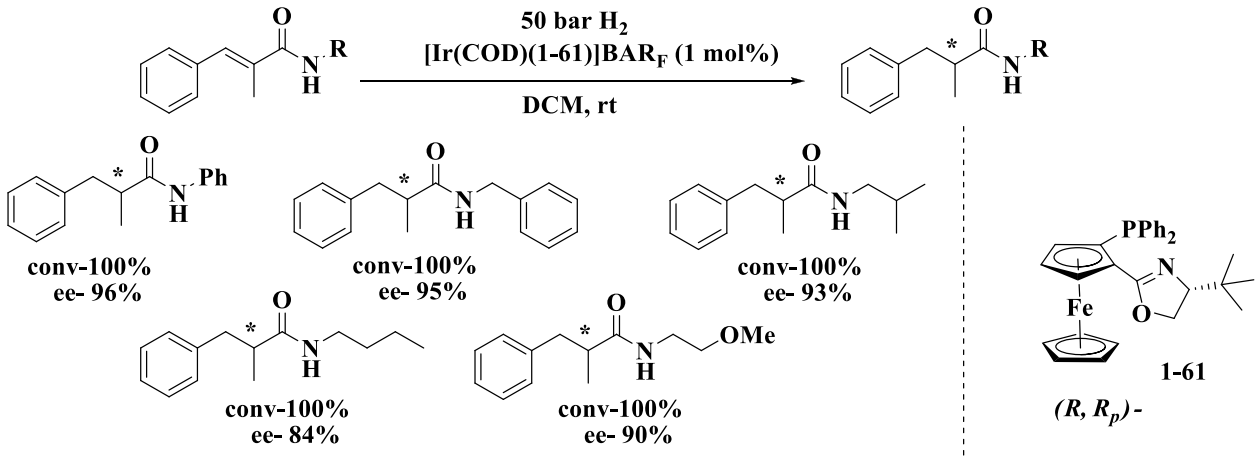

Scheme 1. 36: Hydrogenation of unsaturated amides

Zhou *et al*. have reported an Ir-based catalytic system using the other enantiomer [*(S, S_p)*-**1-62**] of ligand **1-61** for the asymmetric hydrogenation of heteroatomic quinolines to produce chiral tetra-hydroquinolines (Scheme 1. 37) which are structural subunits of alkaloids and other biologically active compounds.[101]

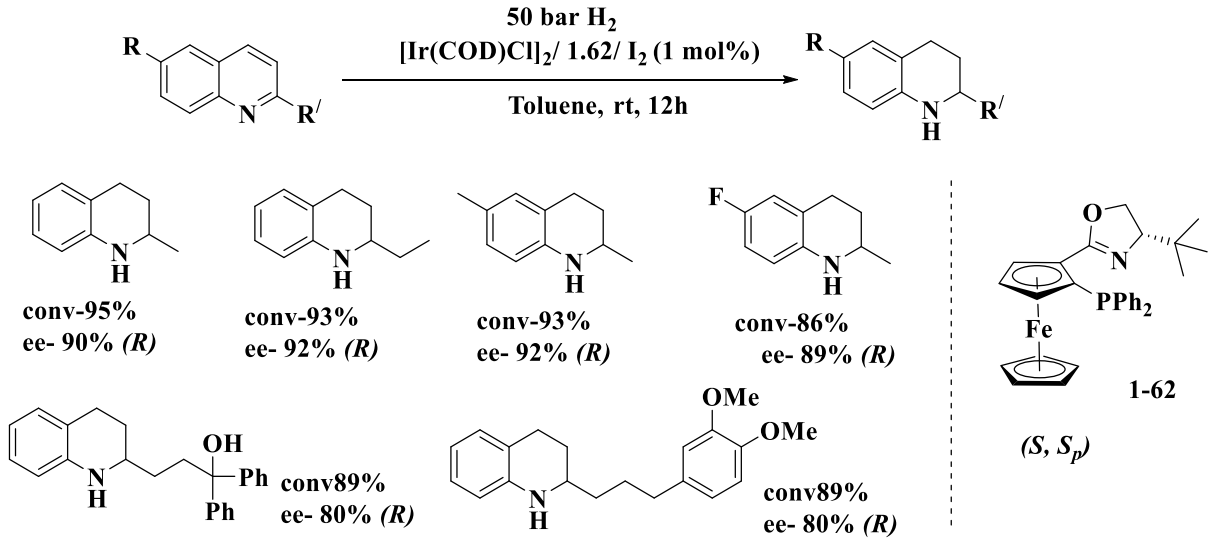

Scheme 1. 37: Hydrogenation of quinolines

Weissensteiener *et al*. synthesized a series of modified FOXAP ligands, namely Raffa-FOX (**1-63- 1-66,** see Scheme 1. 38). These ligands associate the ferrocene planar chirality with the additional central chirality of the side chain (for **1-63, 1-65, 1-66**) and/or of the oxazoline ring (for **1-64, 1-65, 1-66**). For the first two members (**1-63, 1-64**) in Scheme 1. 38, one of this central chirality (either ferrocene side chain or oxazoline ring) has been dropped to bring more structural

variety. However, ligands with three chirality elements have been proven to be most successful. [102]

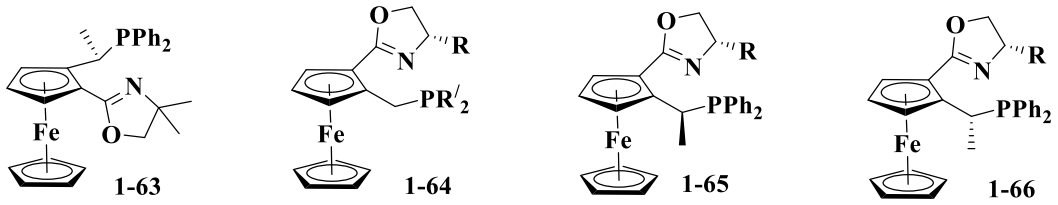

Scheme 1. 38: Raffa-FOX ligands

The Ru-complex of Raffa- FOX ligand- **1-67** was isolated and utilized for asymmetric hydrogenation as well as transfer hydrogenation for several alkyl aryl ketones. The results that were obtained were excellent and mostly comparable for both reactions (Scheme 1. 39).

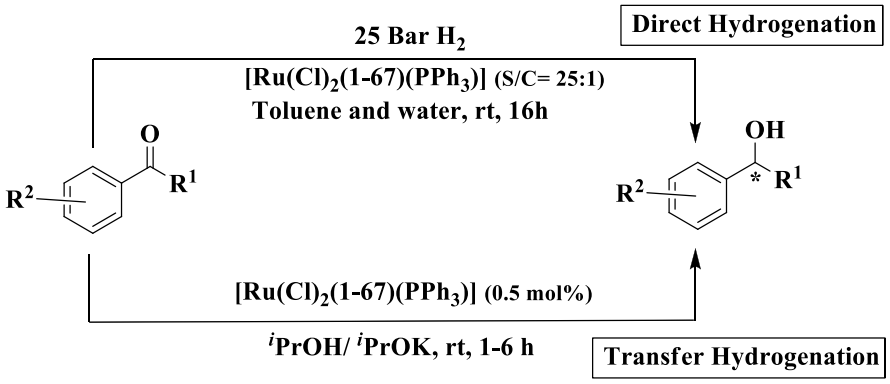

Substrate		Hydrogenation		Transfer Hydrogenation	
		Conversion (%)	ee (%)	Conversion (%)	ee (%)
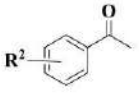	R= H	99	99 (S)	99	98 (S)
	R= 2-F	97	90 (S)	99	50 (S)
	R= 2-Cl	95	91 (S)	>99	75 (S)
	R= 4-CF_3	97	90 (S)	>99	87 (S)
	R= 4-Me	>99	97 (S)	97	98 (S)
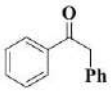		>99	99 (S)	>99	97 (S)

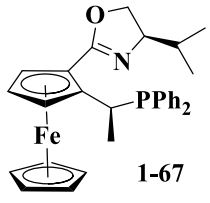

(R, R_{ox}, R_p) *

Scheme 1. 39: Asymmetric hydrogenation with Raffa FOX ligand **1-67**

Taniaphos

Knochel and co-workers developed ferrocenyl ligands **1-68** and **1-69** with heteroatom donors, named Taniaphos (Scheme 1. 40).

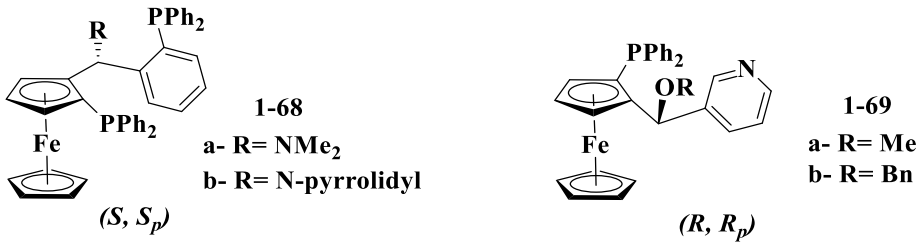

Scheme 1. 40: Taniaphos Ligands developed by Knochel *et al.*

Ligand **1-68** showed good activity in the Ru-catalyzed asymmetric hydrogenation of various aryl and alkyl β-keto esters (ee up to 97%, see Scheme 1. 41) and β-dicarbonyl compounds (ee up to 98%).[103] Rh catalyzed asymmetric hydrogenation of unsymmetrical hydrazones was performed with moderate efficiency (ee up to 65%).[104]

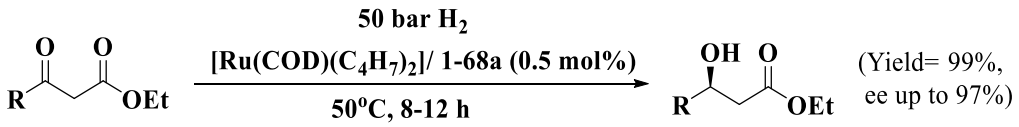

Scheme 1. 41: Asymmetric hydrogenation of β-keto esters using Taniaphos ligands

Ligand **1-69a** has been particularly efficient for the Ir-catalyzed asymmetric hydrogenation of acyclic N-arylamines. A number of substrates with electron withdrawing or electron donating functional group and α-substituted side chains were well-tolerated with very good enantioselectivities (ee up to 99%) (Scheme 1. 42).[105]

* *(R, R_{ox}, R_p)*= Absolute configuration of the central chirality in the side-chain stereogenic carbon *(R)*, in the oxazoline ring stereogenic carbon *(R_{ox})* and planar chirality of ferrocenyl backbone *(R_p)*, respectively

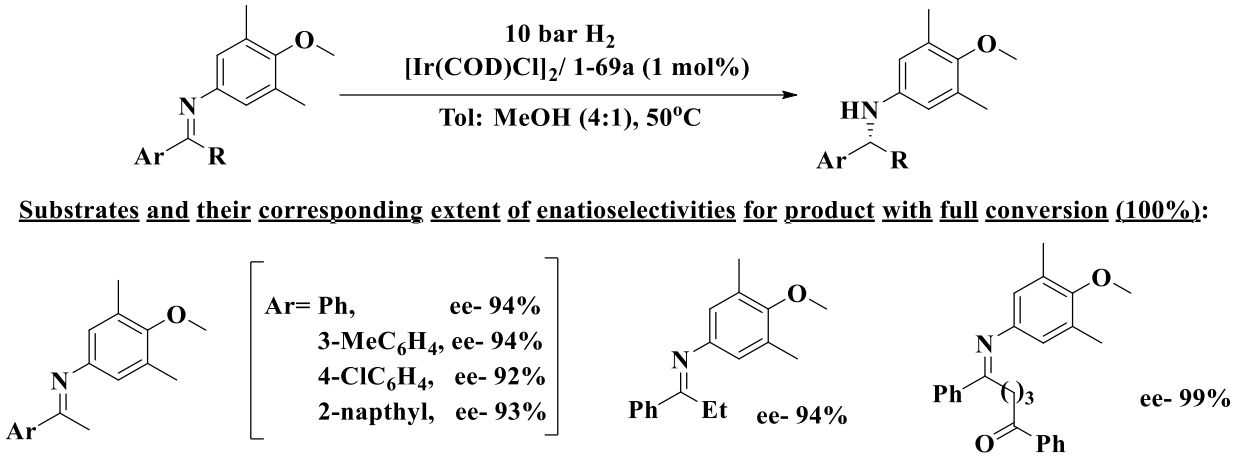

Scheme 1. 42: Asymmetric hydrogenation of acyclic N-arylamines using Taniaphos ligands

Ferrocenyl Phosphine Thioether ligands

There is a handful of examples of ferrocenyl phosphine-thioether ligands for catalytic applications and mostly limited to allylic alkylation (see chapter-4). However, our group has designed a few planar chiral ferrocenyl phosphine thioether ligands- **1-70** (Scheme 1. 43) and studied their co-ordination chemistry with different metals (Pd, Pt, Cu, Ir, Rh).[106]

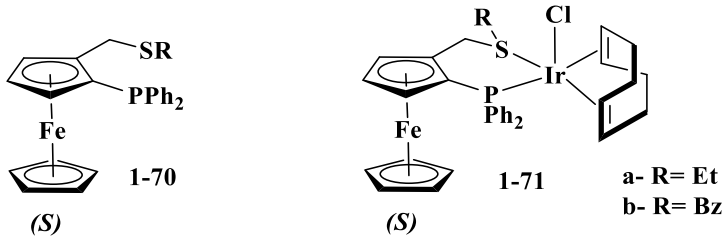

Scheme 1. 43: P,S Ferrocenyl ligands and corresponding Ir- complex developed by our group

Ir-complexes- **1-71** gave excellent enantioselectivities in the asymmetric hydrogenation of several alkyl aryl ketones (yield 99%, ee >99%, see Table 1. 2).[107]

Table 1. 2:Hydrogenation of Alkyl Aryl ketones by **1-71**

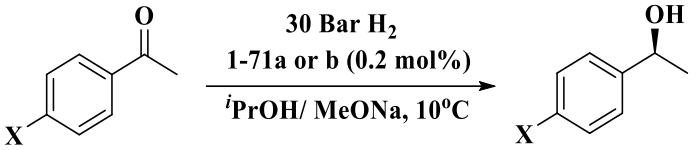

Entry	X	Catalyst	Yield (%)	ee (%)
1	H	**1-71b**	99	87
2	Me	**1-71a**	86	93
3	H	**1-71a**	>99	>99

Dieguez and co-workers very recently compared the activity of three different kinds of ferrocenyl phosphine-thioether ligands towards the Ir-catalyzed asymmetric hydrogenation (100 bar H_2) of minimally functionalized di, tri and tetra-substituted olefins. The ligand selection was based on the variation of the stereoelectronic environment around the thioether group (**1-70**), on the direct attachment of the thioether moiety to the ferrocene backbone (**1-72**) and on the introduction of an additional central chirality at the methylene spacer (**1-73**) (Scheme 1. 44).[108] Moderate and comparable catalytic activities were found for various substrates with 1 mol% catalyst loading (see Table 1. 3).

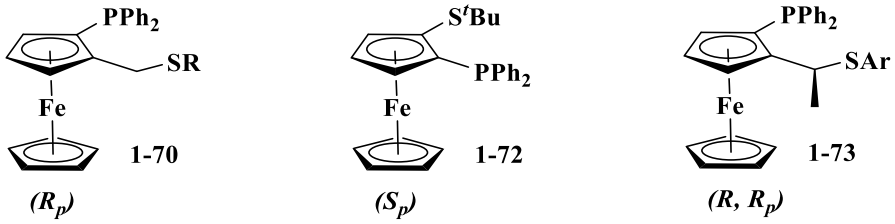

Scheme 1. 44: Ligands selected for asymmetric hydrogenation of olefins

Table 1. 3: Selected catalytic results of the for Ir-catalyzed Asymmetric Hydrogenation at 100 bar H_2 pressure and room temperature with 1 mol% catalyst loading

Substrate	Ligand	Conversion (%)	ee (%)
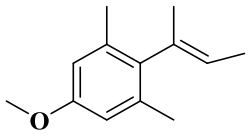	**1-70**	100	11-50
	1-72	100	15
	1-73	100	29-85
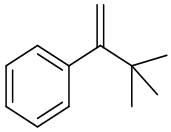	**1-70**	100	16-81
	1-72	100	82
	1-73	100	3-46
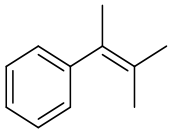	**1-70**	100	6-32
	1-70	100	4
	1-73	100	9-12

Other Ferrocenyl tridentate (PNN, PNP, PNO) ligands: Recent Advances

Phosphine-containing ferrocenyl tridentate ligands received considerable attention along this decade. The success of the analogues bidentate ligands (P,P; P,N; P,S *etc*.) in various catalytic applications has driven the interest to expand the ligating scaffold with an additional donor function to develop a new generation of tridentate ligands (see Scheme 1. 45). Chen, Zhang and co-workers developed new ferrocene-based P,N,N ligands, **1-74**, which are analogues to SpiroPAP and applied them to Ir-catalysed asymmetric hydrogenation of several alkyl aryl ketones.[109] Nearly quantitative yields (96-99%) with good enantioselectivities for the corresponding alcohols

were obtained (for S/C = 2000, ee = 60.8-86.6%). The highest efficient ligand among them, **1-74a**, is mentioned in Scheme 1.45.

Clarke and co-workers prepared a Mn(I)-complex, **1-75,** with **1-74** ligand scaffold.[110] The complex was again utilized for the asymmetric hydrogenation of various aryl alkyl ketones. Similar enantioselectivities (ee up to 91% and over 80% for crowded substrates) for corresponding alcohols were obtained along with quantitative yields.

Zhang *et al.* synthesized **1-76** and an oxidized analogue **1-77**. Ligand **1-76** is analogous to **1-74** where the pyridine moiety is replaced by a benzimidazole group. Manganese complexes of both of these ligands were used in the asymmetric hydrogenation. The system with ligand **1-76** showed good catalytic activity for alkyl aryl ketones (S/C= 1000/1, yield= 95-99%, ee= 49.7-99%).[111] The system with ligand **1-77** executed excellent catalytic activity (TON up to 13000) and high enantioselectivities (ee up to 99%) for unsymmetrical benzophenone derivatives.[112]

Zirakzadeh and co-workers developed $PNP^{/}$- type ferrocenyl ligands **1-78** and their corresponding Fe-complexes- **1-79**, which were used in the Fe-catalyzed hydrogenation of ketones.[113] Good to excellent yields of alcohols were obtained with ee up to 81%. The Mn-complex **1-79c** of the same ligands (**1-78**) were tested in the transfer hydrogenation of ketones and ees in the 20-85% range were obtained.[114]

From the latest work of Zhang *et al.* another new class of ferrocenyl $PNP^{/}$ ligands and their Mn-complexes **1-80** were synthesized.[115] Asymmetric hydrogenation of alkyl aryl ketones was carried out with excellent yield (99%) and enantioselectivity (ee up to 99%) covering a very wide substrate scope (40).

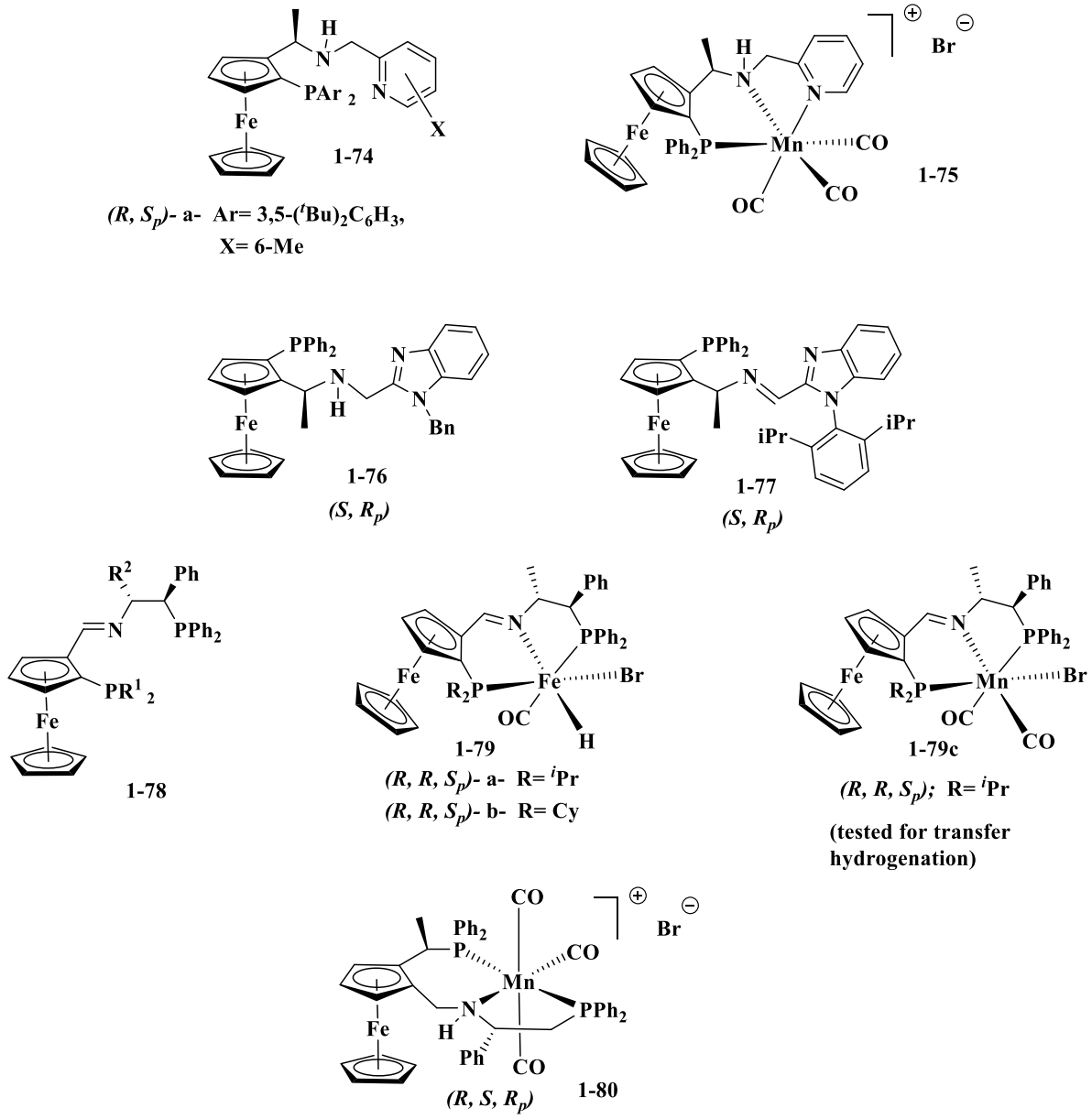

Scheme 1. 45: Ferrocenyl PNP, PNN ligands and their corresponding few metal complexes

Table 1. 4 briefly summarize the extent of asymmetric hydrogenation of simple alkyl aryl ketones and other few parameters (H_2 pressure, metal precursor *etc*.) with the ligands shown in Scheme 1. 45.

Table 1. 4: Summary of results obtained from asymmetric hydrogenation of alkyl aryl ketones using tridentate ferrocenyl ligands and corresponding metal precursors/ complex

Substrate	Pre-catalyst	H_2 Pressure	Catalytic Ratio (mol%)	Yield (%)	ee (%)	No. of Substrates
	1-74 + $[Ir(COD)Cl_2]_2$	20 atm	**1-74=** 0.055 $[Ir(COD)Cl_2]_2$= 0.025	87-91	53.5-86.6 *(R)*	14
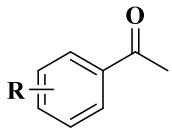	**1-76** + $MnBr(CO)_5$	3 mPa	**1-76=** 0.1 $MnBr(CO)_5$= 0.1	97-99	49-85	~13
	1-79a	20 bar	**1-79a=** 1	61-80	61-81 *(S)*	7
	1-79b	20 bar	**1-79b=** 1	61-96	61-79 *(S)*	7
	1-80	60 bar	**1-80=** 1	40-99	92-99 *(R)*	~20
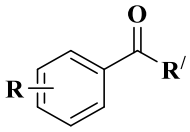	**1-75**	50 bar	**1-75=** 1	85-96	61-91 *(R)*	~12
	1-76 + $MnBr(CO)_5$	3 mPa	**1-76=** 0.1 $MnBr(CO)_5$= 0.1	98-99	67.5-84	4
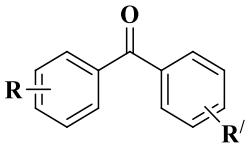	**1-77** + $MnBr(CO)_5$	3 mPa	**1-76=** 0.1 $MnBr(CO)_5$= 0.1	97-99	64-99	~20

A similar class of ferrocenyl aminophosphine ligands, f-Amphox (**1-81**), f-Amphol (**1-82**), f-Ampha (**1-83**) and f-diaphos (**1-84**) were also developed by Zhang and co-workers (Scheme 1. 46).[116]

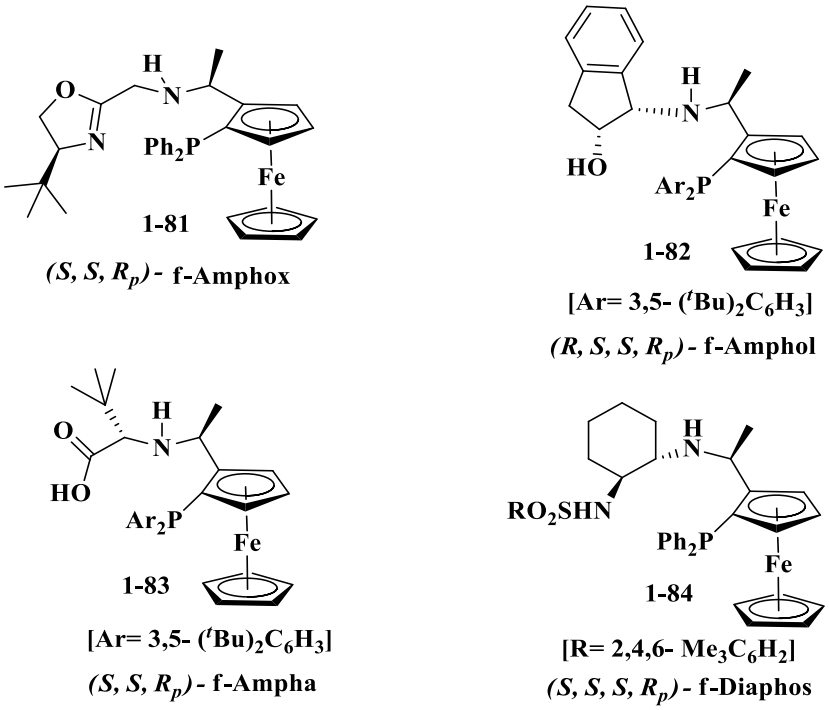

Scheme 1. 46: f-Amphox, f-Amphol, f-Ampha, f-diaphos ligands

These ligands were successfully used in the Ir-catalyzed ($[Ir(COD)Cl_2]_2$) asymmetric hydrogenation of ketones. Quantitative yields of alcohols were obtained for S/C=1000 with ee in the 96-99.9% range. Apart from this, the same catalytic systems were successfully applied with low catalytic loadings (TON up to 10^6) to the asymmetric hydrogenation of relatively less reactive ketones, *i.e.*- α-hydroxy ketones,[117] 2-pyridyl aryl ketones,[118] α-amino ketones,[119] β-ketosulphones,[120] α- ketoesters, [121] simple and α- substituted β-ketoesters[122] *etc* (see Table 1. 5).

Table 1. 5: Summary of results obtained from asymmetric hydrogenation of less reactive ketones using f-amphox, f-Amphol, f-Ampha, f-diaphos ligands and $[Ir(COD)Cl_2]_2$ as metal precursor

Substrate	Ligand	H_2 Pressure	Catalytic Ratio	Conversion or yield (%)	ee (%)
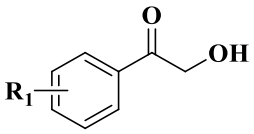	**1-81**	20 atm	**1-81**= 0.1 mol%	Yield= 99	96-99
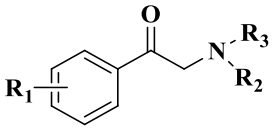	**1-81**	40 atm	S/C= 50,000	Conversion= >99	>99
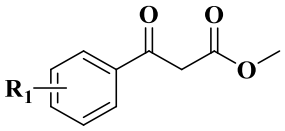	**1-81**	10 bar	**1-81**= 1.1 $[Ir(COD)Cl_2]_2$= 0.5	Yield= 80-96	71-95
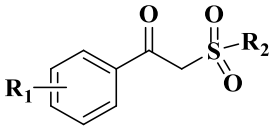	**1-82**	20 atm	S/C= 1000	Conversion= >99 Yield= 98-99	94-99
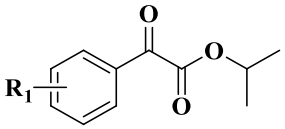	**1-83**	20 atm	S/C= 1000	Yield= 88-99	79-97
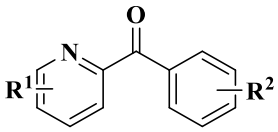	**1-84**	3 mPa	**1=84**= 0.1 mol%	Conversion= 100	97-99

1. 3) Hydrogen Auto-transfer Methodology: New Tool for Alkylations

Early reports by Grigg *et al.*[123] and by Watanbe *et al.*,[124] (1981) on the metal catalyzed (Rh, Ir, Ru) about N-alkylation of amines by alcohol- were the foundations of an ingenious homogeneous catalytic single-step strategy, circumventing the multistep synthesis required for a class of sluggish organic reactions. This strategy, later named 'Borrowing Hydrogen' (BH) or, 'Hydrogen Auto-transfer' methodology, turned out to be interesting due to several factors, including its wide scope in new C-C and C-N bond formation. This methodology combines two transfer hydrogenations (avoiding the direct use of H_2), one in each direction, sandwiching a (generally non-catalyzed)

condensation reaction to produce complex molecules without the isolation of any intermediate. In general, the mechanism of the BH methodology can be divided into three simple steps as follows (Scheme 1. 47).

Dehydrogenation- In the first metal-catalyzed dehydrogenation step, the substrate molecule turns into its corresponding more reactive unsaturated species (*e.g.* alkane to alkene, alcohol to aldehyde or ketone, amine to imine). The hydrogen equivalents are stored in the catalytic system, generally resulting in a hydride species.

Intermediate Reaction- In this step the more activated unsaturated intermediate undergoes a condensation reaction (*e.g.* aldol condensation, imine condensation or Wittig reaction) with a second substrate present in the medium to generate a new unsaturated intermediate with a newly formed C=X bond.

Hydrogenation- The new unsaturated species is reduced by hydrogen stored in the catalytic system generated in the first step, giving rise to the new alkylated final product, which would normally be hard to access from the same starting material by following conventional organic transformations.

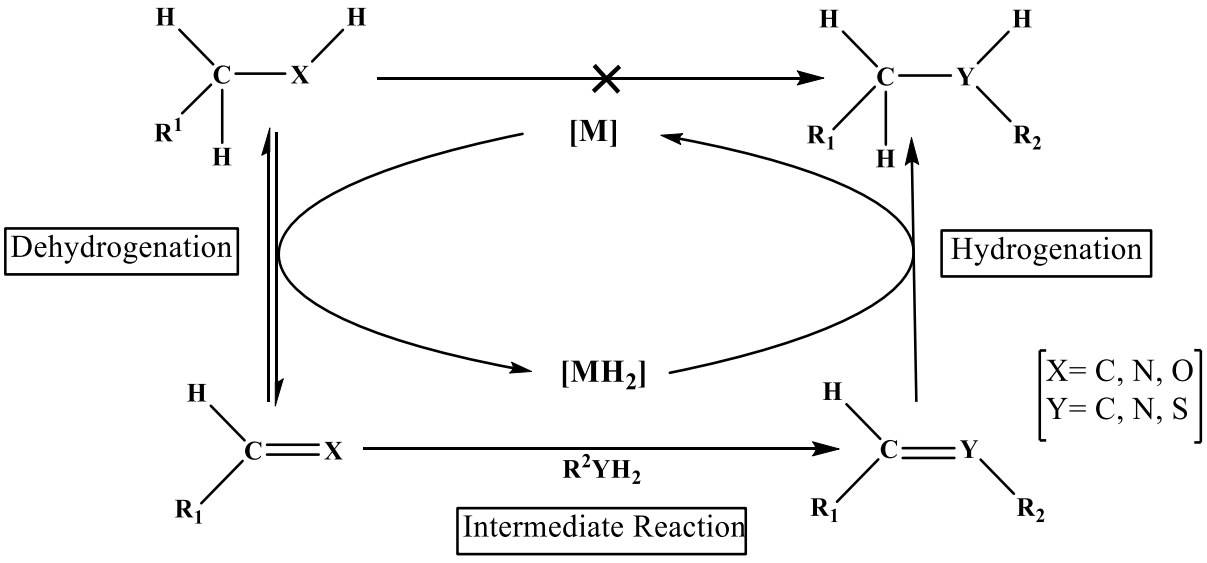

Scheme 1. 47 : General Scheme of Borrowing Hydrogen Methodology

The overall process is classified as one of catalytic dehydrogenation strategies used for chemical synthesis.[125] Since, the hydrogen atoms borrowed from the molecule are further re-incorporated

in the product, the release of deleterious free H_2 gas release (as in the case of acceptor less dehydrogenations) is abolished. Furthermore, the BH methodology also eliminates the use of stoichiometric amounts of a sacrificial hydrogen donor (or, acceptor depending on the reaction), which is necessary for the transfer hydrogenation methods. Another interesting feature is that H_2O is the only byproduct generated during the condensation step. Therefore, because of the simplification of multistep organic syntheses to single-step transformations and the reduced production of chemical waste, the B-H methodology brings a practical, green and atom-economical approach towards the many fundamental reactions (alkylation, amination *etc*.) of organic chemistry. However, a few problems are associated with this method, such as- the necessity of additives (*e.g.* ligands, bases, acids, salts) in the reaction mixture and difficulties in the catalyst/product separation and catalyst recycling.[126]

Homogeneous BH catalysis has since become a wide field of research. It includes the activation of alkanes, alcohols and amines for further C-C or, C-N bond formation through various intermediate organic reactions, such as- metathesis, aldol reaction, Knovenagel condensation, conjugate addition, Wittig reaction *etc*. A number of catalyst systems ranging from traditional Pd, Ru, Ir catalysts ($[Ru(PPh_3)_3(CO)H_2]$, $[Cp^*Ir(Cl)_2]_2$ *etc*.) to bidentate or tridentate ligand- based catalysts have been proven promising. Several review articles have been published highlighting various aspects of this diverse research area.[127] The activation of alcohols as electrophiles for C-X bond forming reactions by means of the BH methodology is the most explored area in this regard.[7b, 127b-d, 127f, 128] Hence, in the context of this thesis objectives, the subsequent discussion will be mostly focused on the selected examples of bidentate or tridentate ligand based metal complexes that have shown good performance for the activation of primary and secondary alcohols for further transformations through the BH process.

Beller *et al*. combining two different Ru-catalysts (Ru-MACHO and the Shvo's Catalyst) reported selective β-Alkylation of 2-arylethanols with methanol. Several functional groups as well as heterocyclic species were well-tolerated under the reaction conditions (Scheme 1. 48).[129]

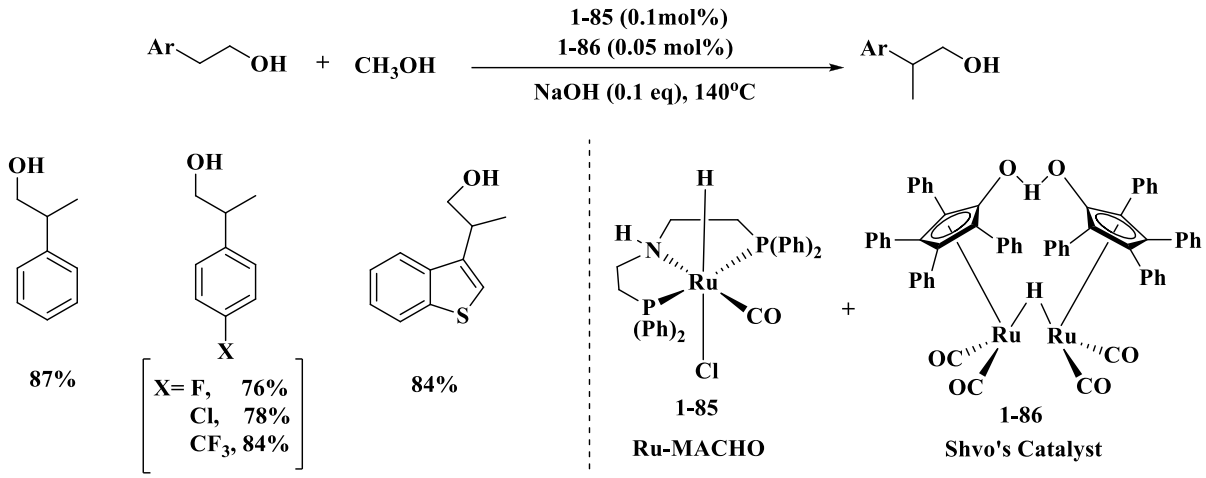

Scheme 1. 48 : BH with Ru-MACHO and Shvo's catalyst

The explicit success of this protocol relies on the cooperative catalysis operated by the combination of the two catalysts (Ru-MACHO and the Shvo's Catalyst). Control experiments with absence of either one resulted drastic decrease in yields. The role of Ru-MACHO was proposed as the main BH- catalyst with the utmost capacity of methanol dehydrogenation, whereas, Shvo's catalyst is mostly responsible for the selective dehydrogenation of 2-pheylethanol. The plausible mechanism thus comprises two different dehydrogenations to aryl ethanol and formaldehyde, a selective aldol condensation and final hydrogenation in a stepwise manner and this is completely directed by the combination of the two Ru-catalyst systems (Scheme 1. 49).[129]

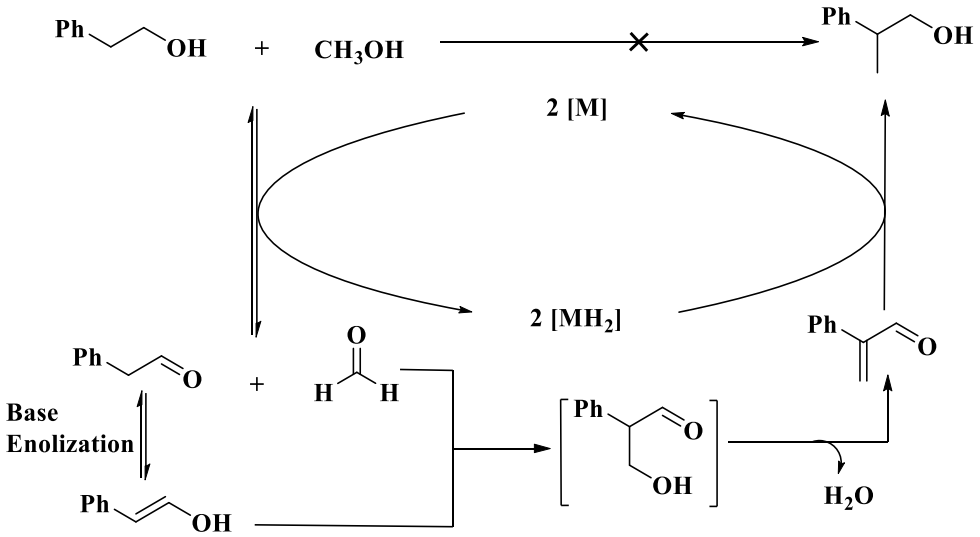

Scheme 1. 49 : Mechanism of the BH catalysis depicted in Scheme 1. 48

The catalytic amination of alcohols with (primary or secondary) amines following the BH-methodology[130] is particularly interesting. This brings the advantage of facile condensation

reaction between amines and aldehydes and eliminates the use of toxic alkyl halides as alkylating agents and the possibility of over alkylation (disadvantage of classical methods). Kempe *et al*. reported iridium complexes- **1-86** and **1-87** of aminopyridine based anionic P,N- ligands (Scheme 1. 50). Quantitative monoalkylation of different types of anilines with benzyl or aliphatic alcohols was observed under mild condition (70 ^{o}C) and low catalyst loading.[131]

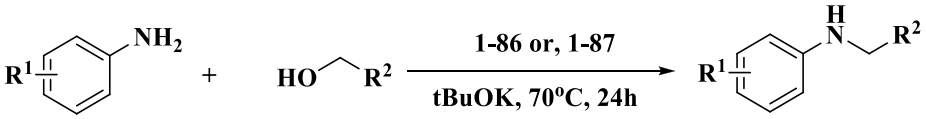

Product	Yield (%)	
	With 1-86	With 1-87
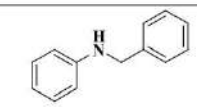	38	92
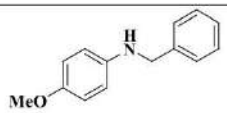	29	92
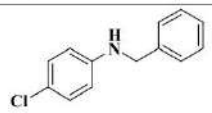	75	98
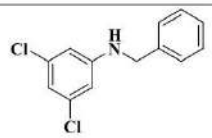	54	98
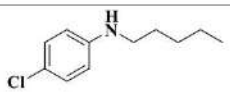	52	98

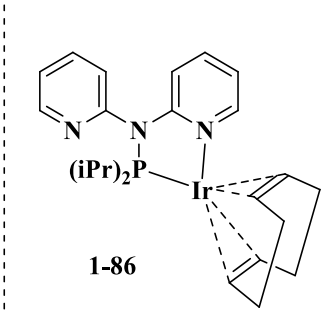

1-86

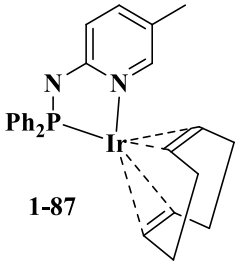

1-87

Scheme 1. 50 : Aminopyridine based Ir Complex for catalytic amination of alcohol

Ammonia (NH_3) has also been employed as aminating agent. Amongst the early contributions, the work from the Milstein group by using based by using the Ru complex **1-88** with a hemi-labile PNP acridine ligand for the amination of simple alcohols (Scheme 1. 51) is a major one. Excellent yields were achieved (up to 96%).[132]

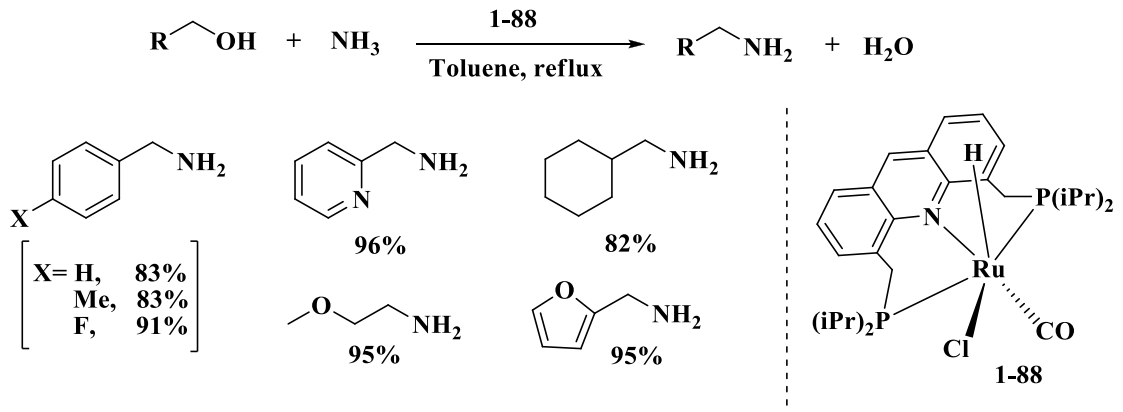

Scheme 1. 51 : Milstein's Catalyst **1-88** for catalytic amination of alcohol with NH_3

Beller and Vogt group independently, used commercially available CataCXium PCy **1-89a** as ligand and $[Ru_3(CO)_{12}]$ to efficiently synthesized different primary amines through catalytic amination of secondary alcohols with ammonia (Scheme 1. 52).[133]

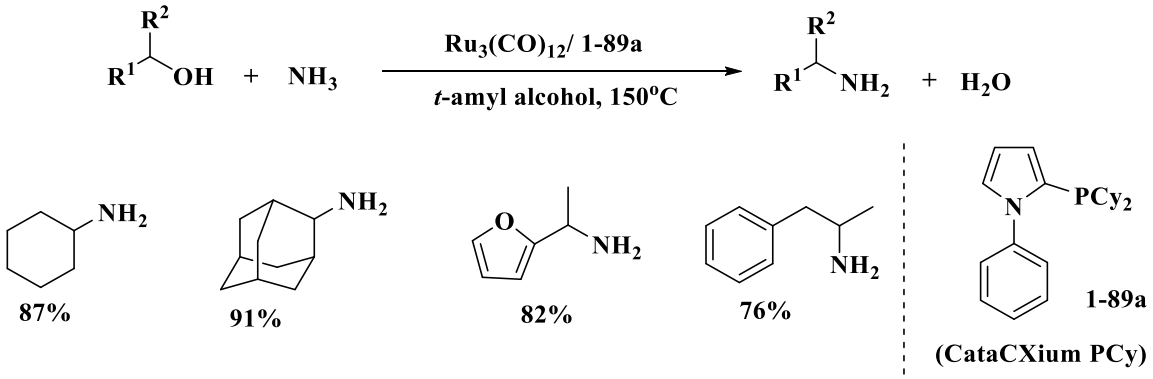

Scheme 1. 52: Catalytic amintation using CataCXium PCy/ $[Ru_3(CO)_{12}]$

Building on these results, the Vogt group carried out a study aimed at selecting a robust catalyst for the amination of bio monoalcohols (*e.g.* menthol, verbenol, borneol *etc.*). A variety of ligands (Scheme 1. 53) were screened. High activity was found for ligand-**1-90** in the presence of $[Ru_3(CO)_{12}]$.[134]

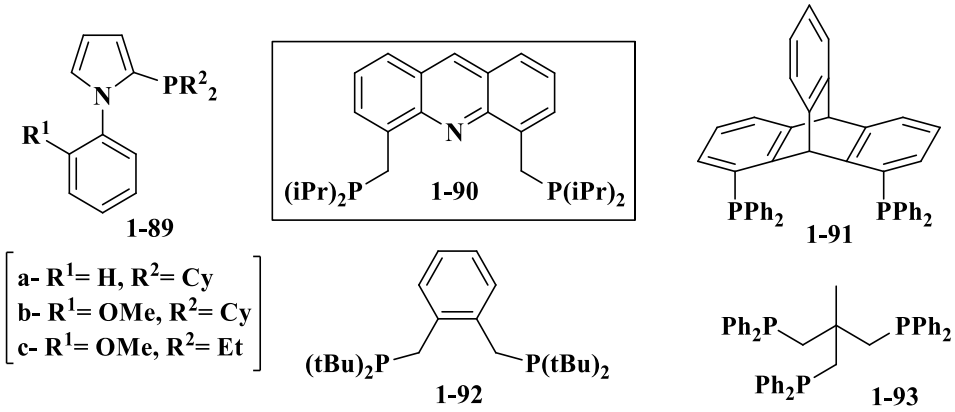

Scheme 1. 53: Ligands that are used for Ru-catalyzed amination of bioalcohols

Generally, the activation of secondary alcohols is relatively difficult than primary alcohols. The reaction in case of primary alcohols becomes easier because of the intermediate step (condensation) is faster for the aldehyde (generated from primary alcohol) than for the ketones (generated from secondary alcohols). Secondary alcohols were found to be activated at very high temperature. Among the few reports, Yu *et al.* synthesized a few pyridyl-supported pyrazolyl-imidazolyl ligands and their corresponding Ru(III)-NNN complexes. The complex **1-94** (Scheme 1. 54) proved efficient for the β-alkylation of a wide variety of secondary alcohols with primary alcohols under solvent-free conditions.[6b]

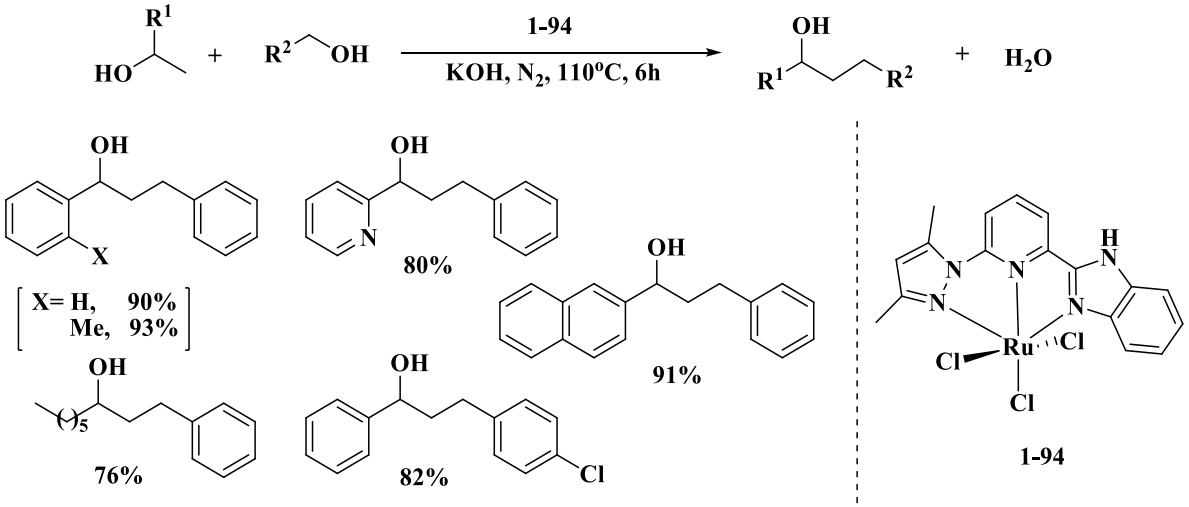

Scheme 1. 54: Yu catalyst for β-alkylation of secondary alcohols

Triphenylphosphino oxazoline-based Ru complex- **1-95,** described by Marichev *et al*. activated primary and secondary alcohols as well as diols (Scheme 1. 55). Correspondingly, secondary, tertiary and N-heterocyclic amines were formed under refluxing conditions. Intramolecular

cyclizations between diamines and diols in the presence of the same complex worked with moderate efficiency to give rise to piperazines, diazocines *etc*.[135]

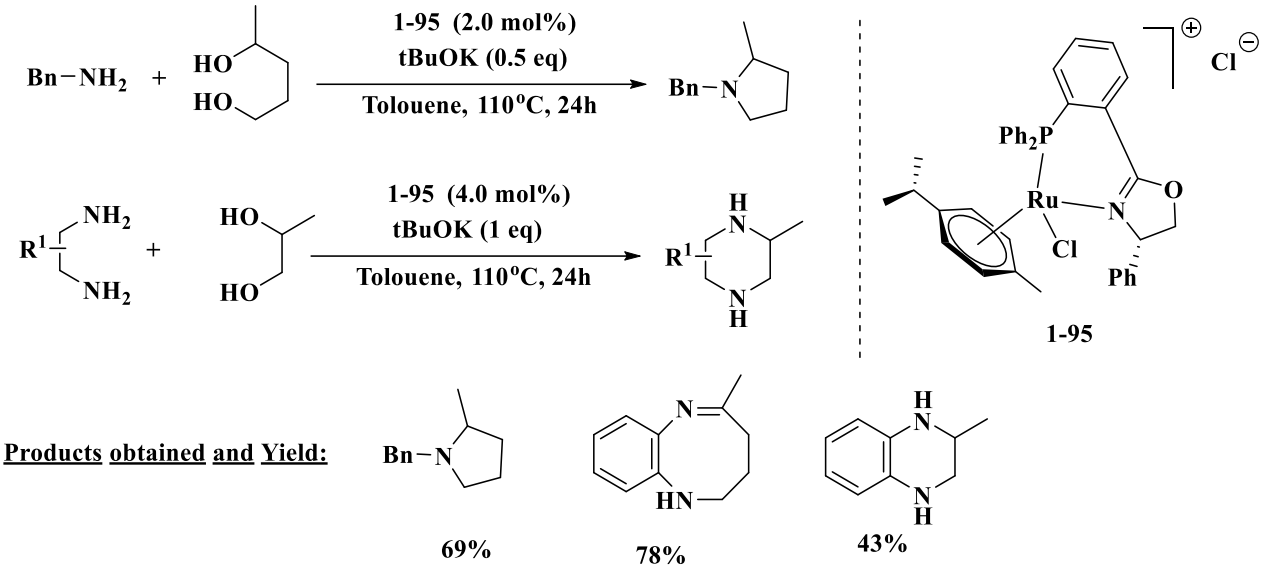

Scheme 1. 55: Aminations of diols with Marichev's complex

Non-noble or first row transition metals have also recently proved efficient in different borrowing hydrogen alkylation reactions.[136] In this regard Fe-based Knölker- type piano stool complex **1-96** (Scheme 1. 56) was shown excellent for the α-alkylation of ketones and for the N-alkylation of amines with primary or secondary alcohols, for the cyclization of amines with diols *etc*.[137]

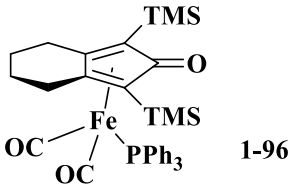

Scheme 1. 56: General Structure of Fe-based Knölker- type piano stool complex

Beller *et al*. reported Mn-based PNP and NNN pincer complexes as catalysts for the N-alkylation of aromatic amines with primary alcohols (Scheme 1. 57). The PNP-type pincer complex **1-97** gave the best results. A large number of substrates with different alcohol and amine groups were efficiently converted.[138]

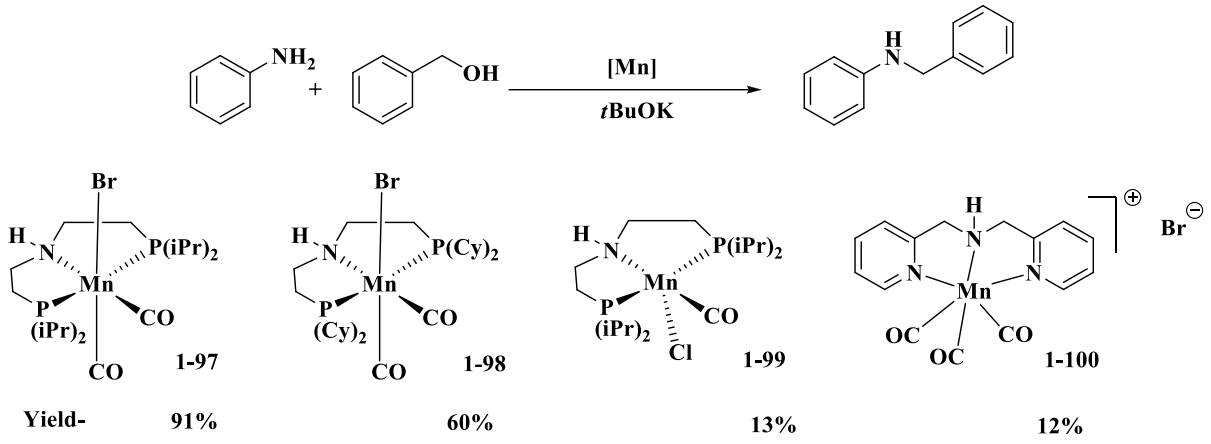

Scheme 1. 57 : BH N-alkylations with Pincer-based Mn Complexes

Zheng *et al*. reported the Co(II)-complex- **1-101,** stabilized by a simple PNP pincer ligand and used them for the N-alkylation of amines with primary alcohols under base-free conditions (Scheme-1.51). Later on, they developed a complex **1-102** stabilized by a PNP pincer ligand based on a triazine backbone (Scheme 1. 58), which worked efficiently for similar kinds of N-alkylation reactions with a broader substrate scope.[139]

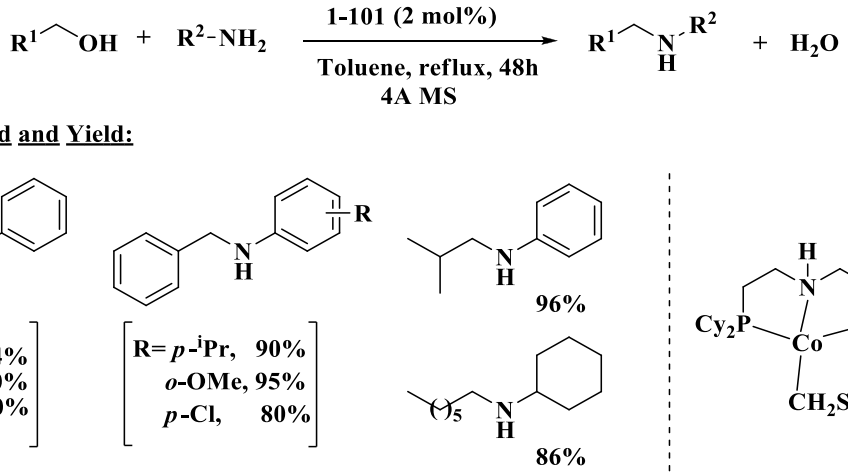

Scheme 1. 58: Co- complex with a PNP pincer ligand used for BH-alkylations

The greater efficiency of complex- **1-102** was proven through its superior performance in the alkylation of primary alcohols with inactivated esters and amides via the Knovenagel reaction as intermediate condensation process (Scheme 1. 59).[140]

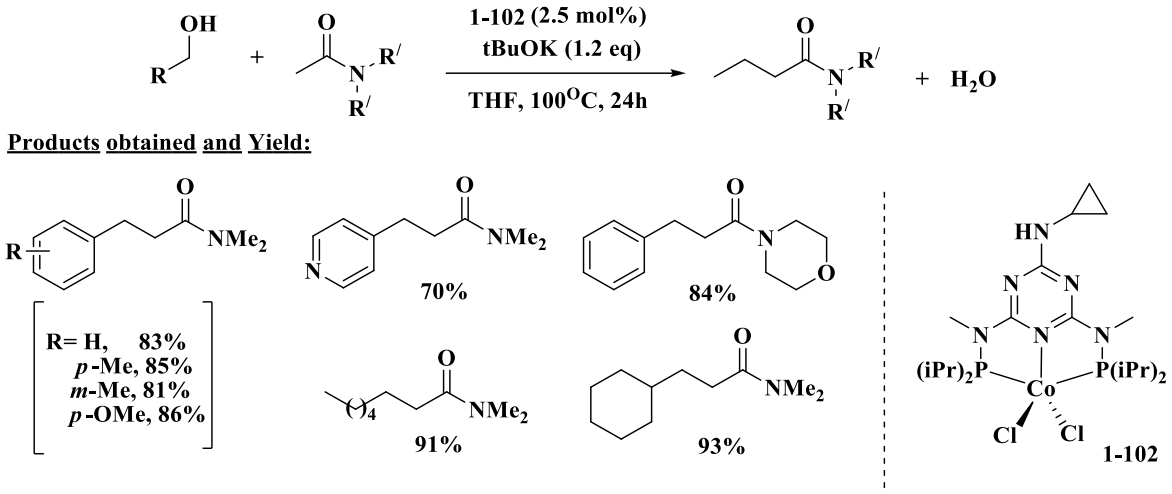

Scheme 1. 59 : Co complex with a triazine-based PNP pincer ligand used for BH alkylations

The 8-hydroxyquinoline-based high-valent Cp*Co(III)-Complex- **1-103** and the Mn(I) complex- **1-104,** which is stabilized by 2-picolylamine containing a thiophene-functionalized side arm, were reported very recently by Sundararaju *et al.*[141] and Maji *et al.*[142] respectively. Both complexes showed moderate to excellent catalytic activities towards the α-alkylation of acetophenone derivatives with different secondary alcohols at high temperatures (Scheme 1. 60).

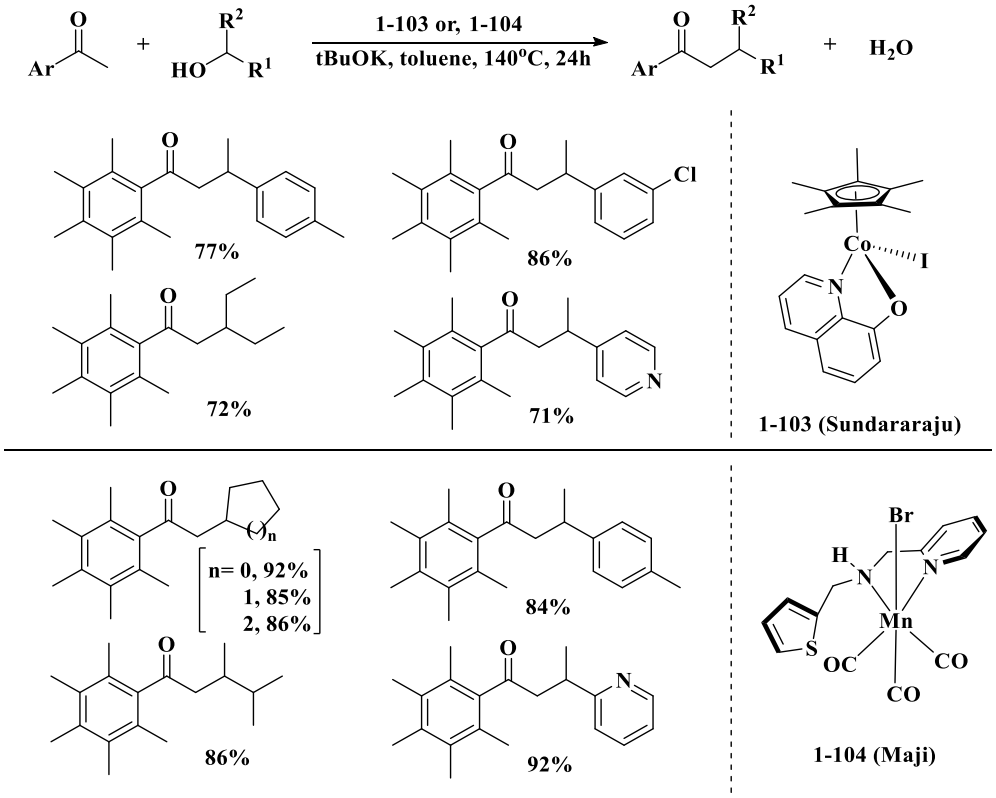

Scheme 1. 60: Sundararaju's and Maji's catalysts for the α-alkylation of acetophenone derivatives

1. 4) Asymmetric Borrowing Hydrogen Methodology

Asymmetric versions of BH catalysis are of great interest and are rapidly emerging as powerful tools in the field of asymmetric catalysis. The extent of asymmetry induced during the transfer hydrogenation step where hydrogen atoms return to the achiral unsaturated intermediate, is considered as the key factor of stereocontrol. One of the traditional ways is to use enantiopure substrates (chiral amine or alcohol) prepared beforehand or substrates with attached chiral auxiliaries (*e.g.* chiral sulfinimide).[143] The stereogenic center that is present in the substrate controls the stereoselectivity of the metal-catalyzed transfer hydrogenation and thus enantiospecific products are obtained.

However, a more sustainable way to perform asymmetric alkylation of achiral substrates, along with opening access to a broader substrate scopes, is to develop chiral catalyst systems fitting the usual requirements of the BH methodology with the additional capability of catalytic asymmetric reduction.

Earlier report by Nishibayashi *et al.* (2006), depicted asymmetric α-alkylation of acetophenones with primary alcohols in the presence of combined catalytic system of $[Ir(COD)Cl]_2$ and chiral FOXAP based Ru-complex- **1-105**. The working principle was propsed as Ir- catalyst is associated with the usual BH- sequence (*i.e.*- dehydrogenation of primary alcohol, aldol condensation with ketone, hydrogenation affording α-alkylated ketone) at the beginning. The subsequent addition of chiral Ru-complex into the reaction mixture affords the asymmetric transfer hydrogenation of the newly formed α-alkylated ketone to produce the chiral alcohol (Scheme 1. 61). Good yield (up to 79%) and excellent enantioselectivities (98% ee) could be attained with a limited number of substrates.[144]

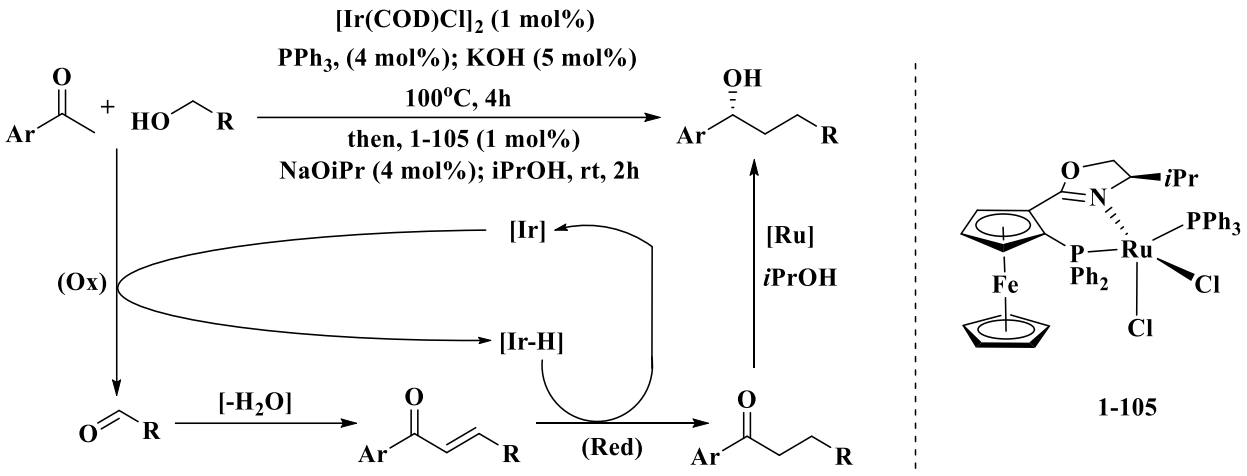

Scheme 1. 61: BH- alkylation followed by ATH in presence of two catalyst

Suzuki *et al*. reported the BH-alkylation between a *meso* diol and benzaldehyde catalyzed by the *(R,R)*-Tsdpen based Cp*Ir complex- **1-106**. It follows oxidative desymmetrization of the di-ol, followed by condensation with benzaldehyde and diastereoselective enone reduction (Scheme 1. 62). Enantioselectivities up to 94% were achieved with good yield (88%).[145]

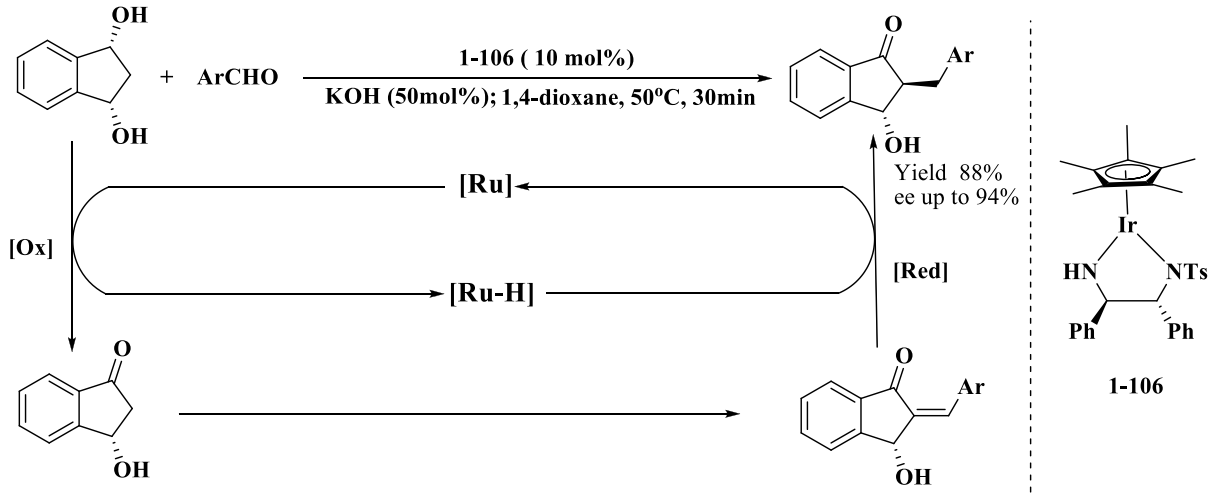

Scheme 1. 62: Preparation of α-Benzyl-β-hydroxyindan-1-one by the BH methodology

Adolfson *et al*. reported a single Ru-catalyst comprised of $[Ru(Cl)_2(p\text{-cymene})]_2$ and the amino acid hydroxyamide- **1-107** as ligand (Scheme 1. 63), which promoted both the BH-alkylation and the asymmetric reduction step with good yields and enantioselectivities for a few number of substrates. The alcohol partner was used in excess amount (3 equiv.) and it played the role of terminal reductant for the transfer hydrogenation step.[146]

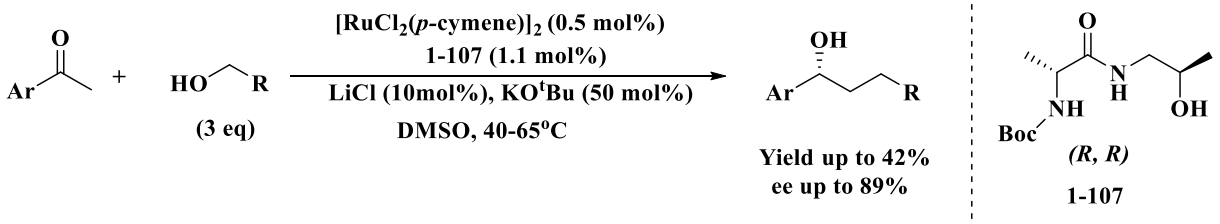

Scheme 1. 63: BH alkylation of acetophenone using amino acid hydroxyamide ligand and a Ru-precursor

The synthesis of chiral amines and amino alcohols through BH-alkylation is one of the emerging areas of research in the field of asymmetric BH methodology. Chiral amines can be prepared either by stereoselective C-N bond formation or by generating stereocentre in the adjacent side chain of the resulting amine. A few recent examples of chiral ligand based asymmetric BH-alkylations followed either way.

Ohta *et al*. synthesized β-amino alcohols from racemic 1,2-diols by a Ru-catalyzed BH-methodology in the presence of the chiral Josiphos ligand- **1-52a** (Scheme 1. 64). They were able to obtain moderate enantioselectivities with good yields.[147] Subsequent work of Zhao *et al.* with the introduction of a Brønsted acid into the catalytic reaction scheme significantly boosted the enantioselectivity. Mechanistically, they proposed the existence of an acid-catalyzed isomerization by a protonation/deprotonation equilibrium of the iminium intermediate formed after the condensation reaction. Benzoic acid was the most efficient Brønsted acid. The authors proposed that a chiral Ru-hydride subsequently reduces preferentially one of the enantiomers of the hydroxy-iminium intermediate (Scheme 1. 64).[148]

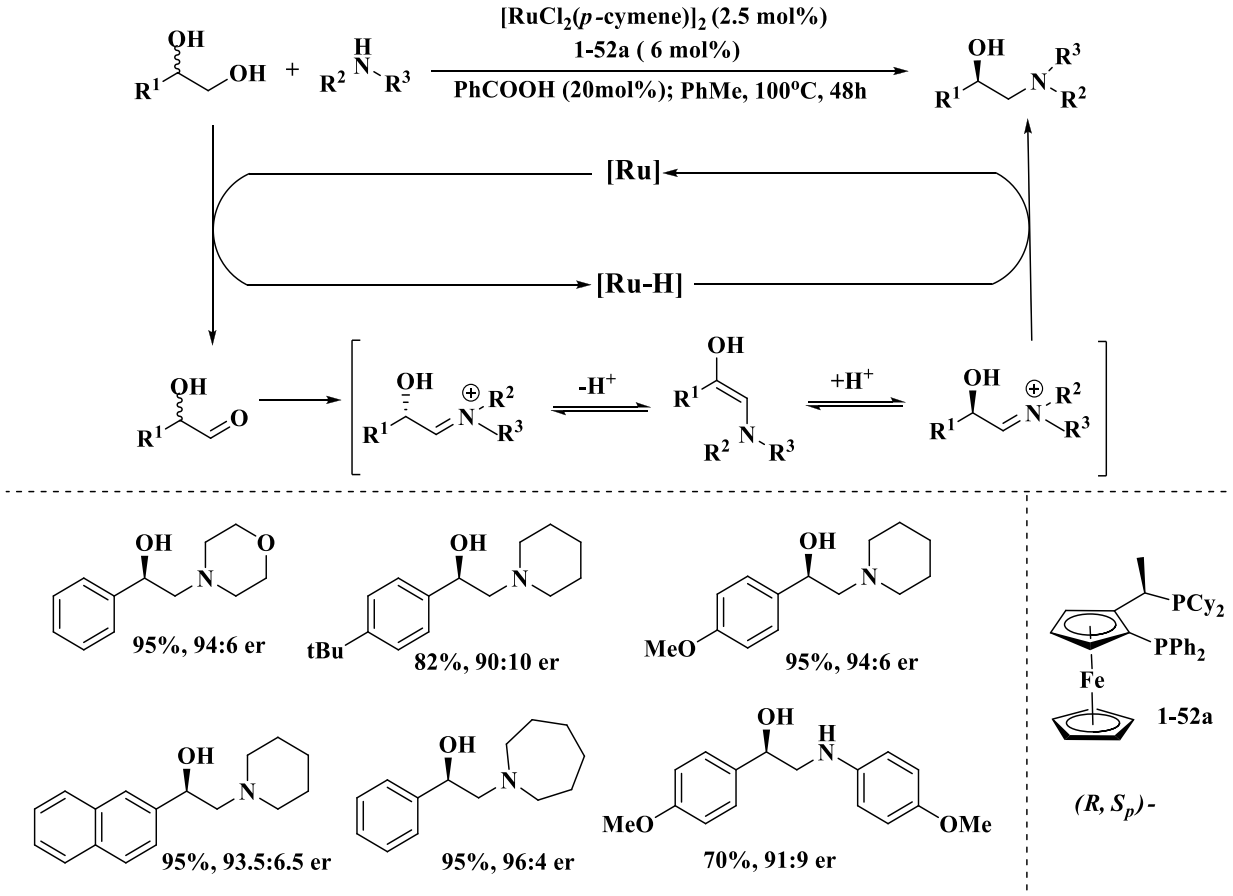

Scheme 1. 64: Ru- Josiphos- mediated BH alkylation of amines (mechanism and substrate scope)

The same group reported another important example of asymmetric C-N bond formation using a co-operative dual catalytic system. The combination of chiral Ir-catalyst- **1-109** and phosphoric acid- cocatalyst **1-110** afforded excellent yields and enantioselectivities for the asymmetric coupling of secondary alcohols and *p*-anisidine to produce chiral secondary amines (Scheme 1. 65). Interestingly, no conversion was observed in absence of the acid.[149] They proposed a cycle on the basis of a few control experiments. They also proposed that, apart from the Brønsted acidity of the chiral phosphoric acid, which activates the amine-based Ir-complex, the chiral conjugate anion of the acid has significant influence on the asymmetric induction during the enantioselective reduction step of the iminium intermediate.[150]

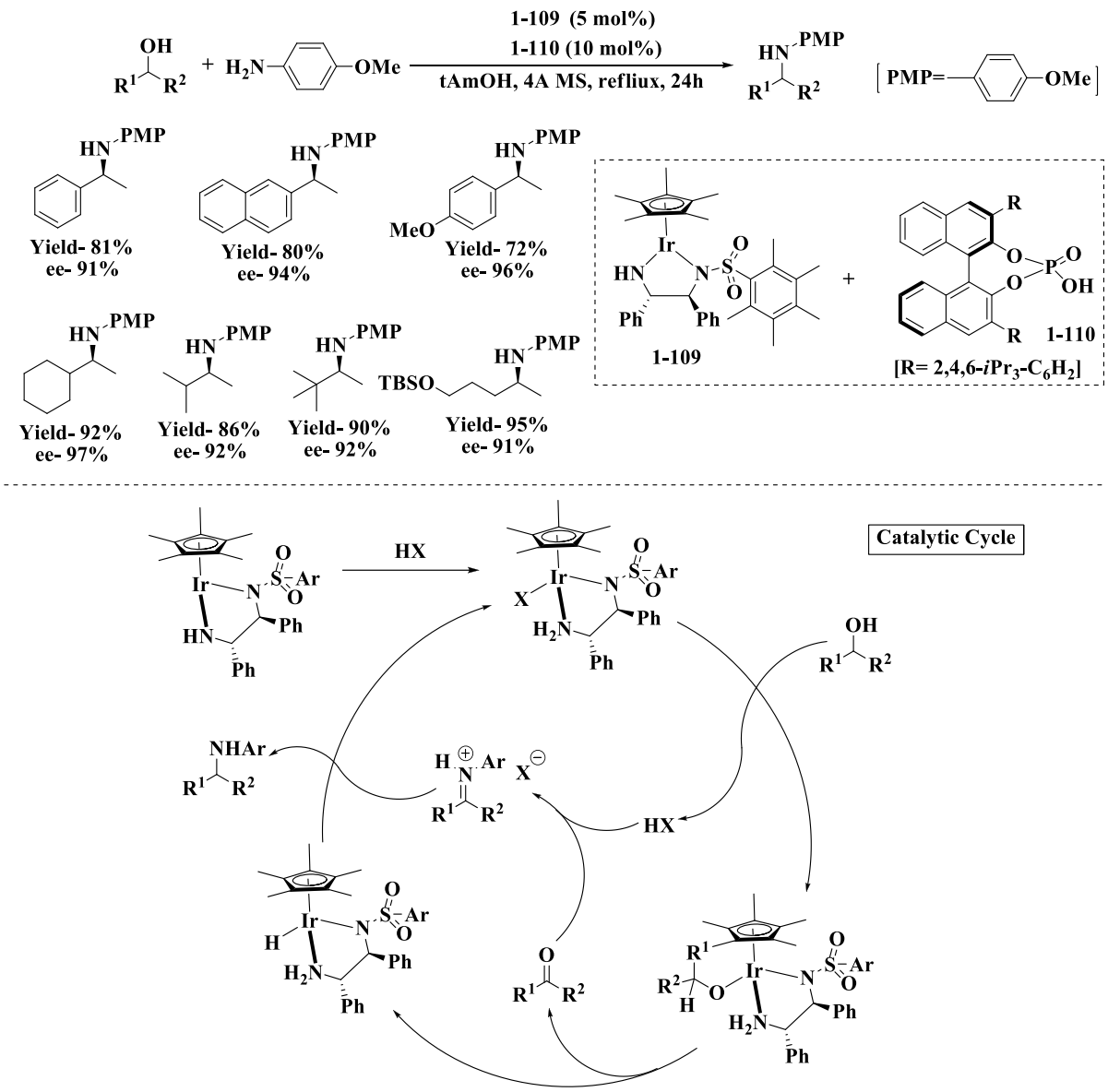

Scheme 1. 65: Dual catalytic system and catalytic cycle for the alkylation of *p*-anisidine by secondary alcohols

The Zhao group reported an intriguing result involving the stereo-control of multiple stereocenters to obtain a diastereomerically and enantiomerically pure single product. Racemic alcohols were transformed to α, β-branched amines using a dual catalytic system comprising the Ir-complex- **1-109** and the spiro phosphoric acid **1-111.** The transformation was proposed to rely on a 'dynamic kinetic asymmetric amination'-mechanism. Inspite of very long reaction times, good yields and high level of diastereoselectivities and enantioselectivities were achieved for the different amines formed (Scheme 1. 66).[151]

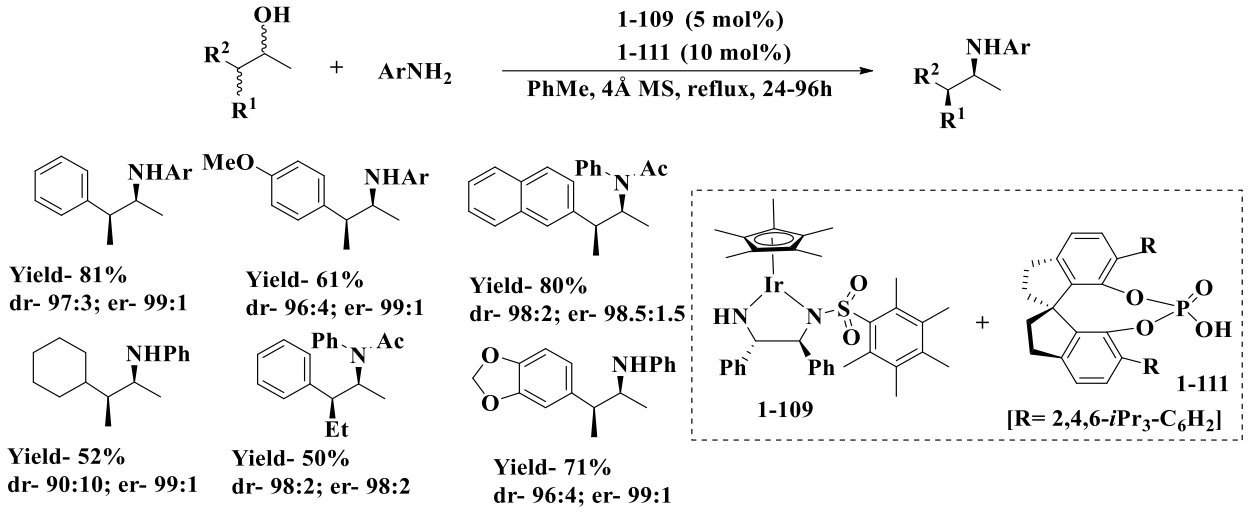

Scheme 1. 66: Stereocontrol of multiple stereocentres

The same authors also applied this particular concept to control the adjacent axis of chirality. Using an Ir(III)-catalyst **1-112** and penta-fluoro benzoic acid **1-113** as co-catalyst they reported atroposelective amination of biaryl alcohols with *p*-morpholine-substituted aniline (yield up to 88%, ee up to 98%, see Scheme 1. 67).[152]

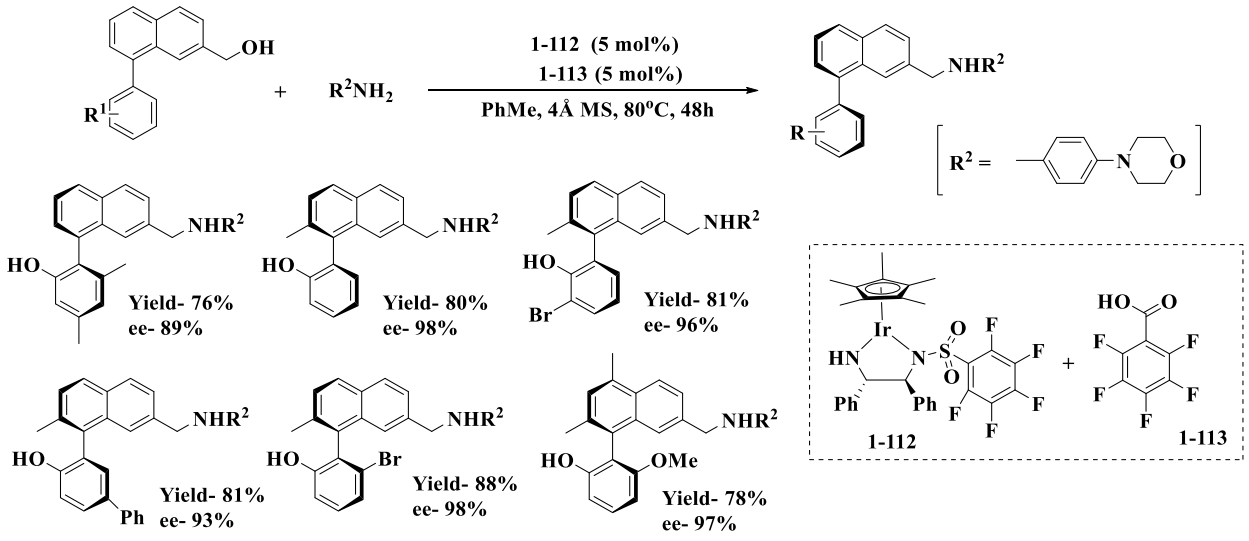

Scheme 1. 67: Atropselective amination of biaryl alcohols reported by Zhang *et al.*

Later on, they discovered a rather interesting example case where the chiral phosphoric acid alone is be responsible for the asymmetric induction. An achiral Ir-catalyst- **1-113** in combination with the chiral phosphoric acid **1-114,** provided high levels of enatioselectivity for intramolecular BH alkylation reactions to prepare several tetrahydroquinolines (Scheme 1. 68).[153]

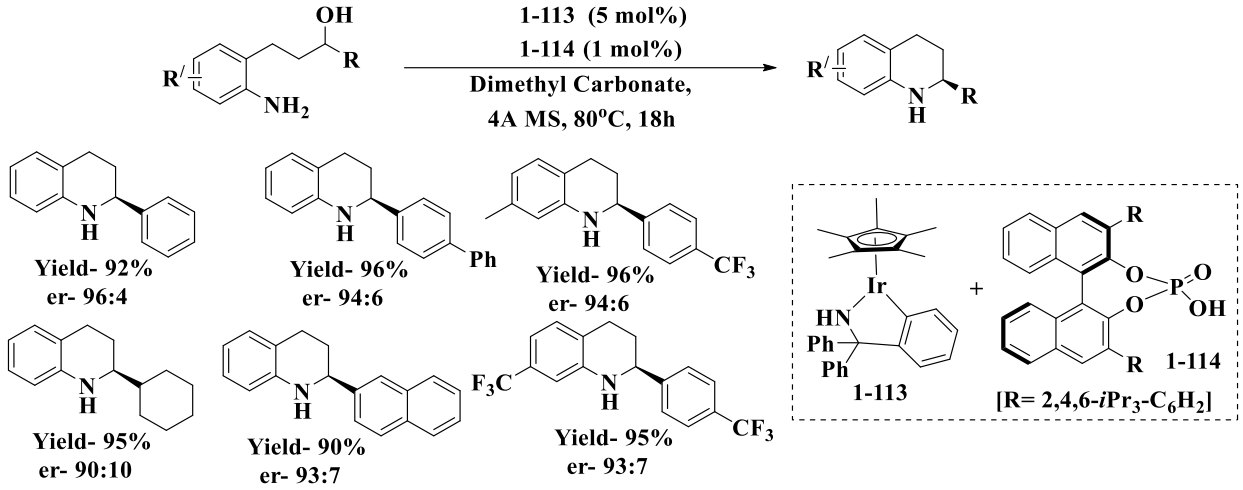

Scheme 1. 68: Chiral tetrahydroquinolines obtained by intramolecular BH alkylation with an achiral Ir catalyst and a chiral phosphoric acid cocatalyst

These selected examples are pioneering contributions reported to date with chiral ligand-mediated asymmetric BH-alkylation. There are other approaches like bio catalysis, conjugate addition *etc*.[154] These are not directly related to the objectives of this thesis, but can also be useful.

1. 5) Conclusion and Objectives

I have presented several families of phosphine containing ligand families (ferrocenyl and non ferrocenyl) and their applications in transition metal-catalyzed hydrogenation reactions with various unsaturated substrates. In addition to that, recent advances of the BH methodology were briefly highlighted. The key points of the entire discussion are:

a) Efficiency of phosphine-containing chiral ligands in the asymmetric hydrogenation reaction in combination with transition metals

b) Significance of phosphine-containing bidentate, tridentate ferrocenyl ligands and their extensive applications in the asymmetric hydrogenation and a few latest instances in the BH methodology

c) Rapid involvement of first row transition metals in both the field of hydrogenation and BH methodology, to address the scarcity of noble metals and prevent an environmental crisis

In our group, various bidentate phosphine-containing ferrocenyl ligands have been applied over the past two decades in different asymmetric catalytic reactions (hydrogenation, Suzuki-Miyaura reaction *etc*.) in combination with late transition or non-noble metal (Ru, Rh, Ir, Pd, Pt) precursors.

Motivated by these former attainments, the main objective of my thesis is development of new families of ferrocenyl phosphine- containing tridentate ligands. The synthetic protocols and the detailed procedures that have been developed in this thesis to synthesize new tridentate phosphine-containing ferrocenyl ligands (PNP, PNN, PSP *etc.*) will be described in the coming chapters.

The ultimate aim of the ligand development is associated with further catalytic application in asymmetric BH methodology in presence of non-noble metal precursors. A brief perspective is given later (see general conclusion).

.

Chapter-2: New Tridentate Phosphine-Containing Tertiary Ferrocenyl Amine Ligands

2. 1) Introduction

Heterodentate ligands containing phosphorus and nitrogen as ligating atoms are one of the widely used ligands in the field of asymmetric catalysis. The softness of P atom, which is determined by its π-accepting nature (depending on nature of substituents), provides stability towards metal centers with low oxidation states. On the other hand, the sp^3 or sp^2 nature of the N atom and the electronic, steric effects of the substituents (alkyl, aryl) modulate the hardness and the σ-donor ability of the N atom. Depending on the nature of the metal center, hard donor groups are generally more labile than soft ones and dissociate more readily. Thus, hemi-lability is incorporated in the metal center by using heterofunctional soft-hard ligands to reversibly open the coordination sphere during the steps of catalytic cycles.[155] Hence, increasing the number of donor or ligating atoms in a ligand system opens a wide window to play with the electronic asymmetry to be generated at the metal center and therefore, influences the outcome of the catalytic activities towards a given organic substrates.

Phosphine containing chiral ferrocenyl ligand systems are well-known as several research groups have contributed towards the evolution of numerous homodentate (P,P; P,P,P) and heterodentate (P,N; P,S *etc*.) ligands. These ligands were subjected to metal complexation with metals all across the periodic table. In addition, different kinds of asymmetric organic catalytic reactions were screened with the presence of either the metal complex synthesized beforehand or the mixture of ligand and metal precursor (exposed to *in situ* complexation during the course of catalysis); in order to generate or improve the stereoselectivity of the reaction. Most often the catalytic system comprised of the combination of metal precursor and ligand has proved efficient to bring significant stereoselectivities for asymmetric catalytic reactions.

The design of phosphine-containing ferrocenyl ligands with more than two different coordination centers (PNN, PNP, PSP *etc*.) is one of the emerging fields of the last decade. The facile incorporation of planar chirality through the 1,2- substituted ferocenyl backbone, coupled with the success of chiral tridentate ligands throughout the last decade for asymmetric hydrogenation-dehydrogenation and other fields of catalysis[156] works as the ultimate source of motivation for ligand design.

The main focus of this thesis is the synthesis of different tridentate phosphine-containing ferrocenyl ligands. The very first ligand family that has been identified as an interested target is **2-1** (Scheme 2. 1).

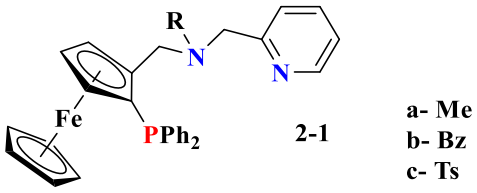

Scheme 2. 1: General molecular structure of designed ligand **2-1**

Ligand **2-1** is a planar chiral tridentate ligand, comprising one P- based coordinating group directly attached to the ferrocene backbone and two N-based coordinating groups situated on the side chain linked to the ferrocene scaffold at the C2 position. The detailed synthesis of the family of ligand **2-1** is the main objective of this chapter. Before describing the synthetic details of the target ligands, the synthetic strategies that have been developed so far for similar phosphine-containing bidentate and tridentate ligands will be described in a short literature overview.

2. 2) Overview of Homoentate (P,P or, P,P,P) and Heterodentate (P,N) Planar Chiral 1,2-Substituted Phosphine-containing Ferrocenyl Ligands

Ligands based on planar chiral 1,2-disubtituted ferrocenyl scaffold are a privileged family for asymmetric catalysis. Pioneering work of Ugi *et al*. in the early1970s played a pivotal role for the foundation of planar chiral ferrocenyl ligand systems by introducing a simple methodology- for the synthesis of N,N-dimethyl-1-ferrocenylethylamine in its enantiomerically pure form (Scheme-2.1). This compound, known as Ugi's Amine,[157] possesses a stereogenic center in the α-position of the side chain which controls the diastereoselectivity of the Cp ring substitution and thus provides specific planar chirality in the ferrocenyl moieties.[158] Following this simple methodology, Hayashi and Kumada developed 2-(1-(dimethylamino)ethyl)-1-(diphenylphosphino)ferrocene or PPFA (Scheme 2.2)[159] by diastereoselective lithiation in the 2 position of Ugi's Amine, followed by electrophilic trapping (*e.g.* PPh_2Cl). This was considered as the first ever example of a chiral ferrocenyl phosphine. A further S_N1 reaction at the C2 carbon, which occurs with retention of configuration substitutes the dimethylamino moiety with different other species (*e.g* Ac_2O, R_2PH, pyrazoles *etc*.). Thus, a library of ligands with a large variety of

homo and heteroatomic coordinating groups were developed by several research groups. Examples comprise: Pigiphos[160], ferrocenyl pyrazole,[161] Josiphos[88] ligands developed by Togni *et al.*; Bophoz developed by Boaz *et al.*;[82] Walphos developed Spindler *et al.*; [162] (See Scheme 2. 2); ligands with chiral phosphines attached at C1 position of Cp ring of ferrocenyl backbone by Whittall *et al.*[163] *etc*. The commercial availability of both [*(R)* and *(S)*-] enantiomers of Ugi's Amine has given further impulse to the development of chiral ligands.

All the ligands described in Scheme 2. 2 have been used for diverse asymmetric catalytic applications. The Josiphos ligands **2-8**, probably the most effective ones of this ligand family, were described briefly in chapter-1 for their application in hydrogenation and very recent advances in BH-reactions (see chapter 1, sections 1.2.3 and 1.4). Josiphos ligands were also efficient for the Pd-catalyzed asymmetric hydrophosphorylation of norbornene,[164] the asymmetric nucleophilic addition of conjugate dienes,[165] the alkylative desymmetrization of meso-succinic anhydrides,[166] the Rh- catalyzed enantioselective ring opening of heterobicyclic alkenes,[167] the Cu-catalyzed asymmetric conjugate addition to α,β- unsaturated carbonyl compounds,[168] the Rh-catalyzed asymmetric hydroboration of vinyl arenes, [88] *etc*.

The Pigiphos ligand **2-6** was utilized for the Ni-catalyzed hydroamination of α,β- unsaturated nitriles.[169] Higher level of enantioselectivities were obtained for the asymmetric amination and hydrophosphination of methacrylonitrile using the same Ni-based catalyst.[170] The ferrocenyl pyrazole ligands **2-7** were used for the Pd-catalyzed enantioselective allylic amination of unsaturated esters[171] and for the Rh-catalyzed hydroboration of styrenes.[172]

The Bophoz ligands **2-9**, similar to Josiphos, have shown efficiency in a few catalytic hydrogenation reactions, *e.g.* the Rh- catalyzed asymmetric hydrogenation of (Z)- dehydroamino acid derivatives (ee up to 95%),[173] hydrogenation of α- keto esters (ee up to 95.8%).[174] The Walphos ligands **2-10** were useful for the Rh and Ru- catalyzed hydrogenation of α,β- unsaturated acid derivatives, of carbonyl compounds, *etc*. (ee up to 95%),[162] the Rh- catalyzed asymmetric hydrogenation of vinyl boronates (ee up to 93%), [175] *etc.* The Walphos ligands have also shown good performance in the Rh-catalyzed asymmetric [4+2] annulation of 4-alkynals with N,N-dialkyl acrylamides[176] and in the reductive coupling of enynes with α- ketoesters.[177]

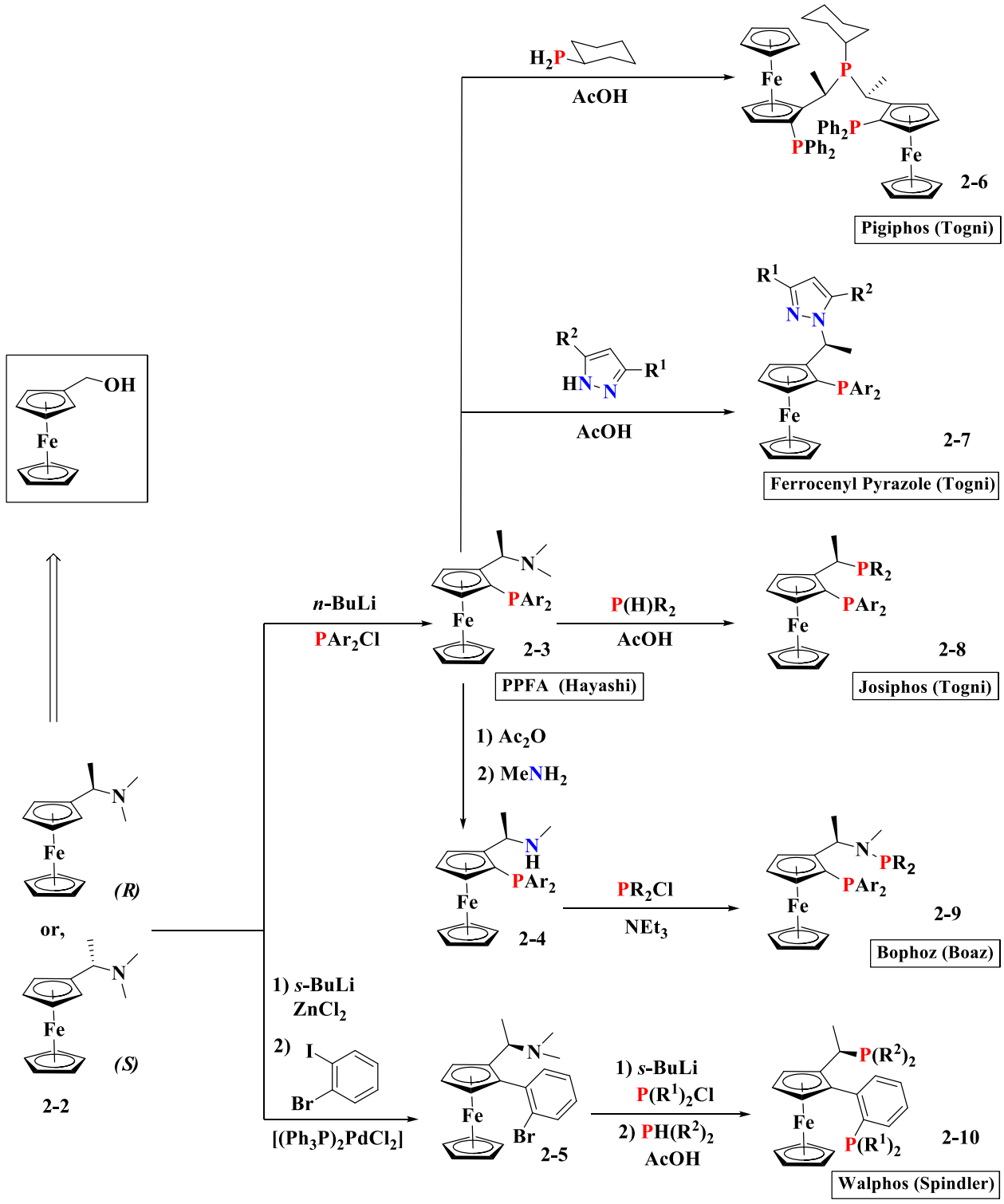

Scheme 2. 2: Ferrocenyl Bidentate Ligands from Ugi Amine

Among the several other approaches of chiral *ortho*-directing group (sulfoxides, oxazolines, acetals, azepines, pyrrolidines, hydrazones, sulfoximines, O-methyl ephedrine derivatives,

imidazolines *etc*.) to mediate the substitution at the ferrocene ring,[178] those making use of chiral oxazolines[179] and sulphoxides[180] were widely used next to the Ugi's Amine approach in order to synthesize other phosphine-containing chiral ferrocenyl ligands. **F**errocenyl**oxa**zolinyl**p**hosphines (FOXAP ligands), a significant type of P,N ligands, were synthesized following the same technique. The lithiation in the 2 position of 2-ferrocenyl oxazolines **2-11** (with a stereogenic center on the oxazoline ring C4 atom) at the cyclopentadienyl C2 atom and *in situ* trapping with PPh_2Cl resulted in enantiopure *(S, S_p)*- phosphino-substituted 2-ferrocenyl oxazoline derivatives (Scheme 2. 3). The synthesis of the corresponding *(S, R_p)*-diastereomer starting from the same 2-ferroenyl oxazoline enantiomer was carried out sequentially by introduction of a trimethylsilyl (TMS) blocking group, lithiation with *n*-BuLi and electrophilic trapping with PPh_2Cl and final deprotection by TMS removal with tetrabutylammonium fluoride (TBAF) (Scheme 2. 3).[181]

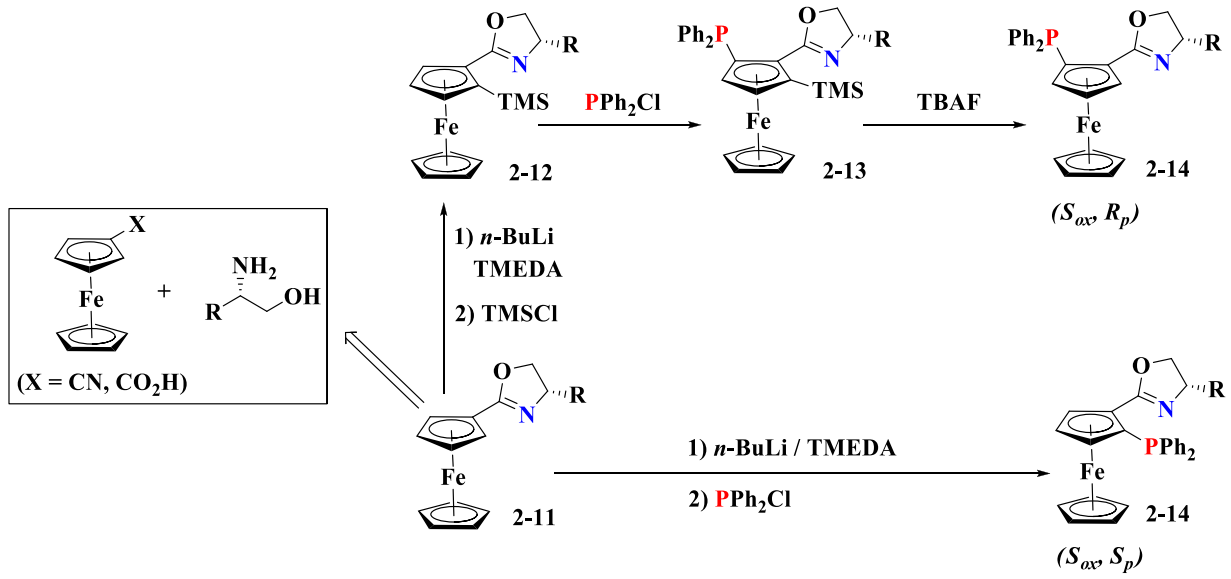

Scheme 2. 3: Ferrocene oxazoline approach

The FOXAP ligands **2-14** were utilized for the asymmetric hydrogenation and transfer hydrogenation reactions with various metals (see chapter-1), for the Pd- catalyzed asymmetric allylic substitution of cycloalkenyl acetates with dimethyl sodiomalonate,[182] for the asymmetric inter-[183] and intramolecular-[184] Heck reaction, for the Ag- and Cu- catalyzed 1,3-dipolar cycloaddition of azomethine ylides [185] *etc*.

Knochel *et al.* reported a new class of Ferrocenyl di-Phosphine ligands **2-17**, named Taniaphos (Scheme 2. 3). Starting from a ferrocenyl ketone (Friedel-Crafts adduct of ferrocene and 2-bromobenzoyl chloride), a Corey-Baksi-Shibata (CBS) reduction [186] to the corresponding enantiopure alcohol **2-16a** followed by subsequent acetylation and nucleophilic substitution by amines yielded an enantiopure amine intermediates **2-16b**. Final ligands- **2-17** were obtained by diastereoselective di-lithiation and trapping with chlorophosphines (Scheme 2. 4).[103-104]

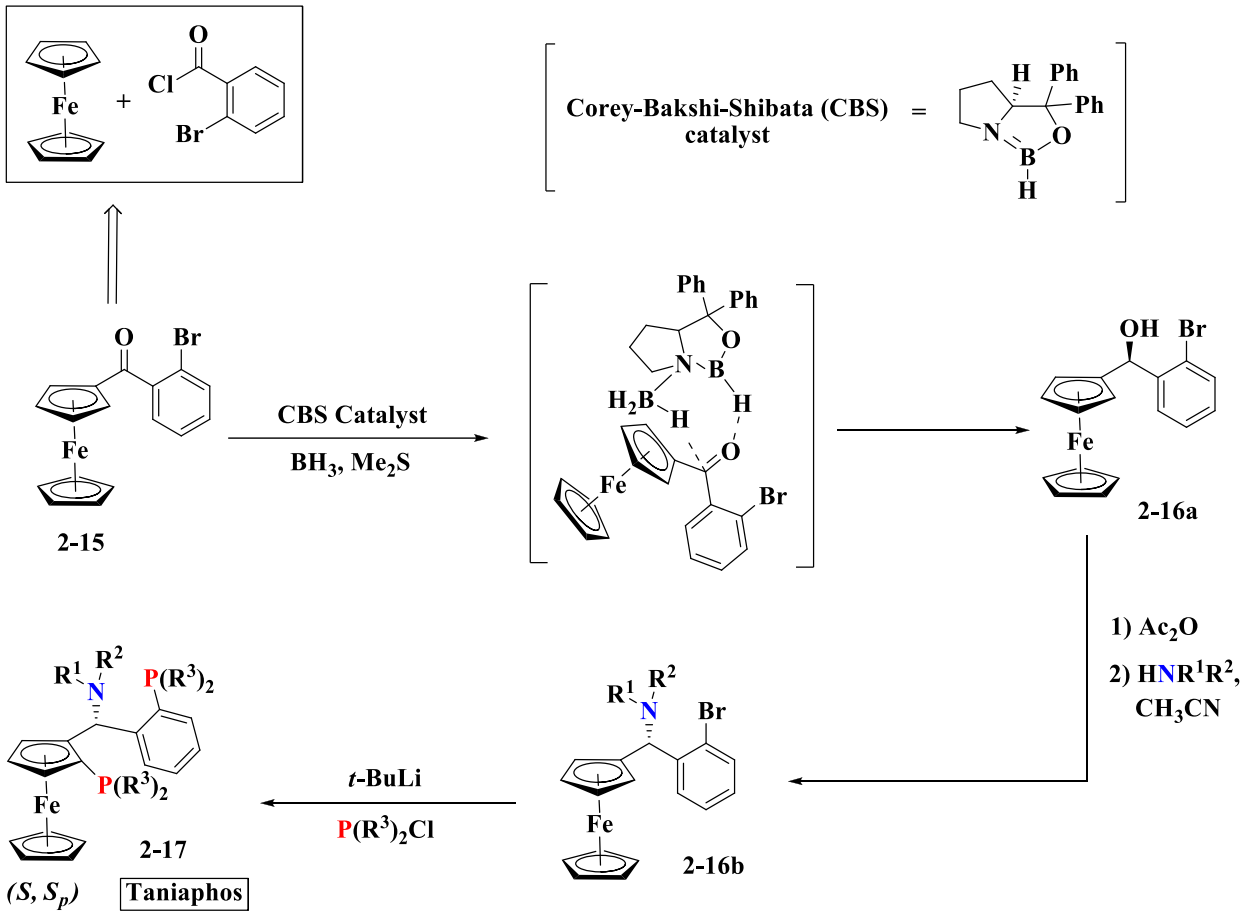

Scheme 2. 4: Synthesis of Taniaphos **2-17**

Later on, considering the few limitations associated with the Taniaphos ligand (*i.e.*- the equivalence of the two phosphine substituents) new and modified ligands were designed. The synthetic strategy was changed in favor of the sulphoxide approach. According to the new strategy, diastereoselective *ortho*- metalation in the 2 position /functionalization of chiral ferrocenyl sulphoxide and subsequent substitution of the sulphoxide group with PR_2Cl led to new ligands **2-20** with different phosphine substituents variable to each other. On the other hand, substitution of

the sulphoxide **2-21** group with 2-pyridine carboxaldehyde followed by alkylation, phosphine deprotection led to another type of new ligand-**2-23** (Scheme 2. 5).[105, 187]

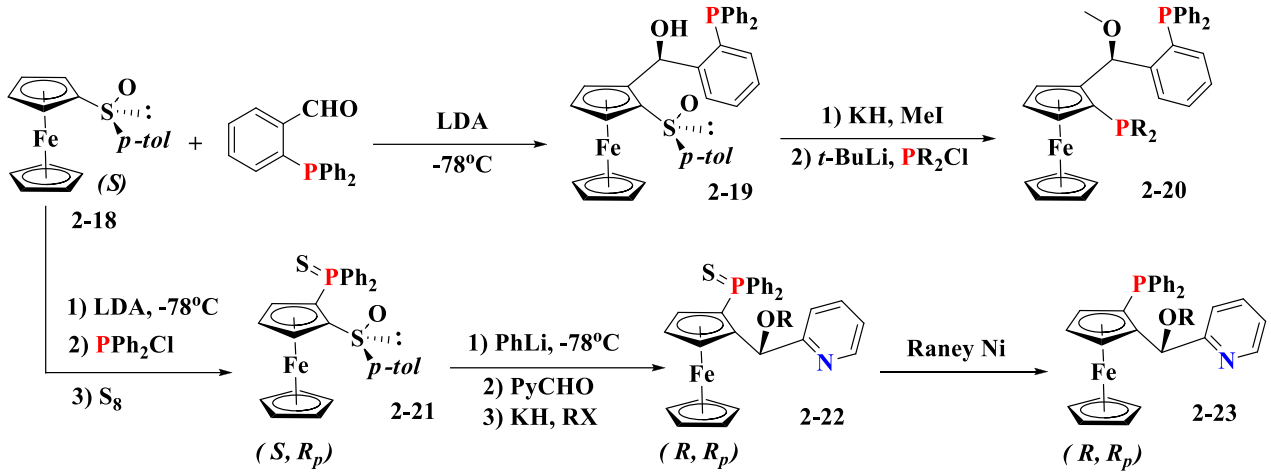

Scheme 2. 5: Modified Taniaphos ligand

In addition to their application in asymmetric hydrogenation (see chapter-1), taniaphos ligands **2-17** have been applied to the Cu-catalyzed asymmetric reductive aldol reaction between methyl acrylate and aryl methyl ketones,[188] to the asymmetric aldol addition of silyl ketene acetals to ketones,[189] to the asymmetric allylic alkylation of allyl bromides with Grignard reagents [190] *etc.*

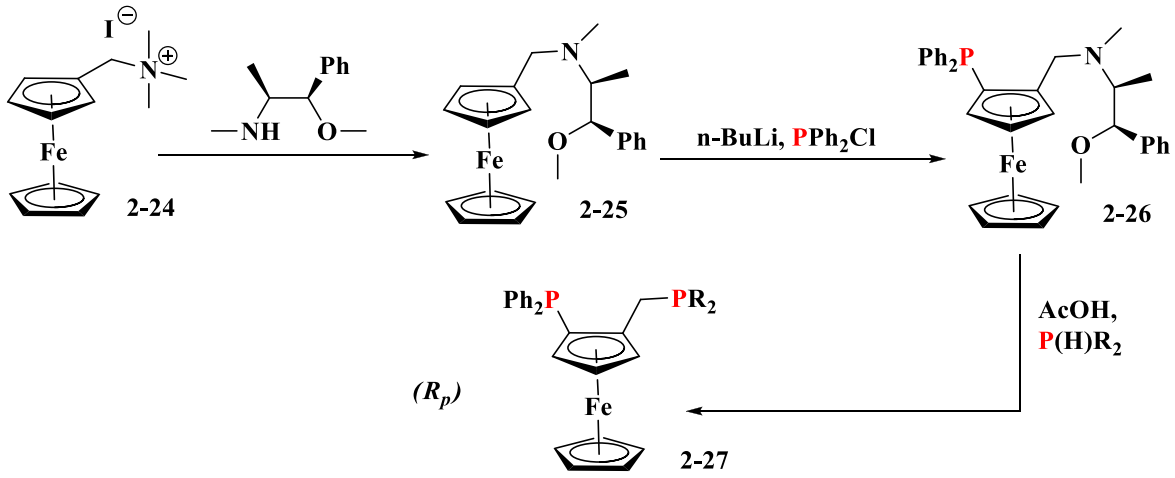

Scheme 2. 6: Ephedrine method to synthesize Josiphos ligand analogs with only planar chirality

The vast majority of chiral ferrocene- based phosphines feature a central chirality from the stereogenic carbon atom of the side chain along with planner chirality of the ferrocene backbone. Similar ligands exhibiting only the planar chirality, *i.e.*- without an additional central chirality on

the side chain, have received less attention. Weissensteiner *et al.* developed a method allowing the introduction of planar chirality without assistance by a permanent chiral ferrocene substituent. Enantiopure *O*- Methylephedrine, temporarily attached to the ferrocenyl side chain, was exploited as a chiral auxiliary and directing group for the metalation/electrophilic trapping process. Subsequent substitution of the ephedrine moiety led to the diphosphine ligand **2-27**, analogous to the Josiphos family (Scheme 2. 6).[178c, 191]

2. 3) Retrosynthetic analysis of the designed ligands

The retrosynthetic approach for the designed PNN ligands **2-1** is depicted below (Scheme 2. 7).

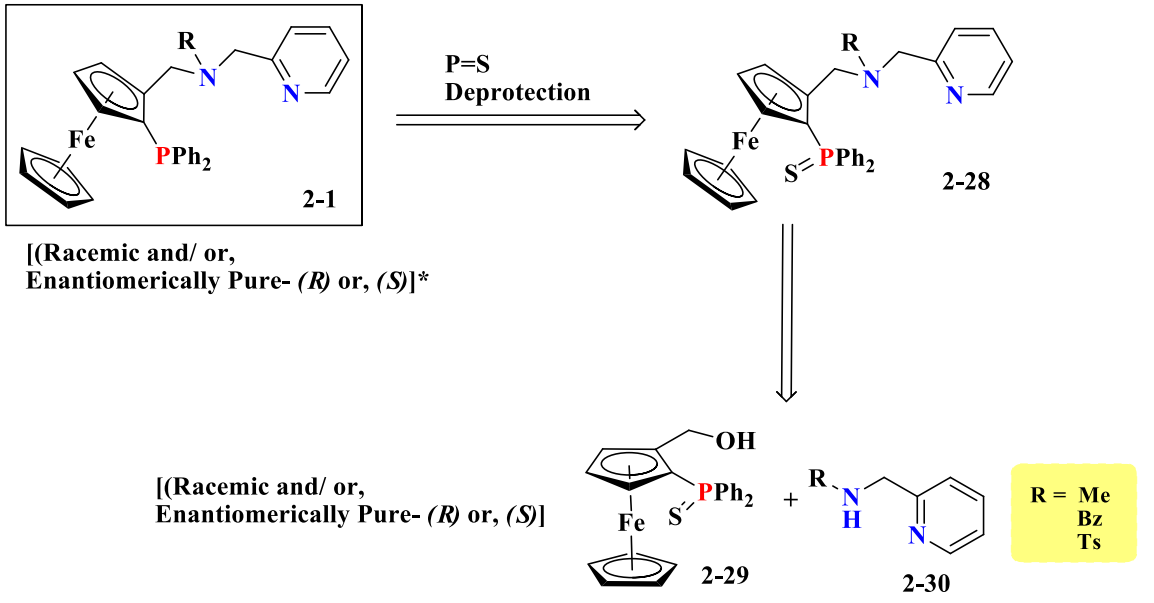

Scheme 2. 7: Retrosynthetic analysis of ligand **2-1**

The phosphine containing ferrocenyl alcohol **2-29** shown in the retrosynthetic scheme can be synthesized following a well-optimized protocol developed in our group (see next section). In order to obtain the expected ligand, we subsequently need 2-picolylamine and its N-alkylated derivatives (**2-30**) beforehand.

*(R) or, (S)= Absolute configuration of planar chirality of ferrocene backbone; in case of other chirality (*e.g.* central chirality) present in the system the planar chirality is depicted as (R_p) or, (S_p)

2. 4) Synthesis of (2-diphenylthiophosphinoferrocenyl)methanol: Most Useful Synthetic Intermediate

2-Thiodiphenylphosphino-(hydroxymethyl)ferrocene or (2-diphenylthiophosphinoferrocenyl) methanol **2-29** has been one of the most versatile chiral ferrocenyl synthetic intermediates in our group for several years because of its stability, particular stereo-electronic property and most importantly facile introduction of planar chirality in the earlier stage of the synthesis allowing to access both enantiomers in an enantiomerically pure form.

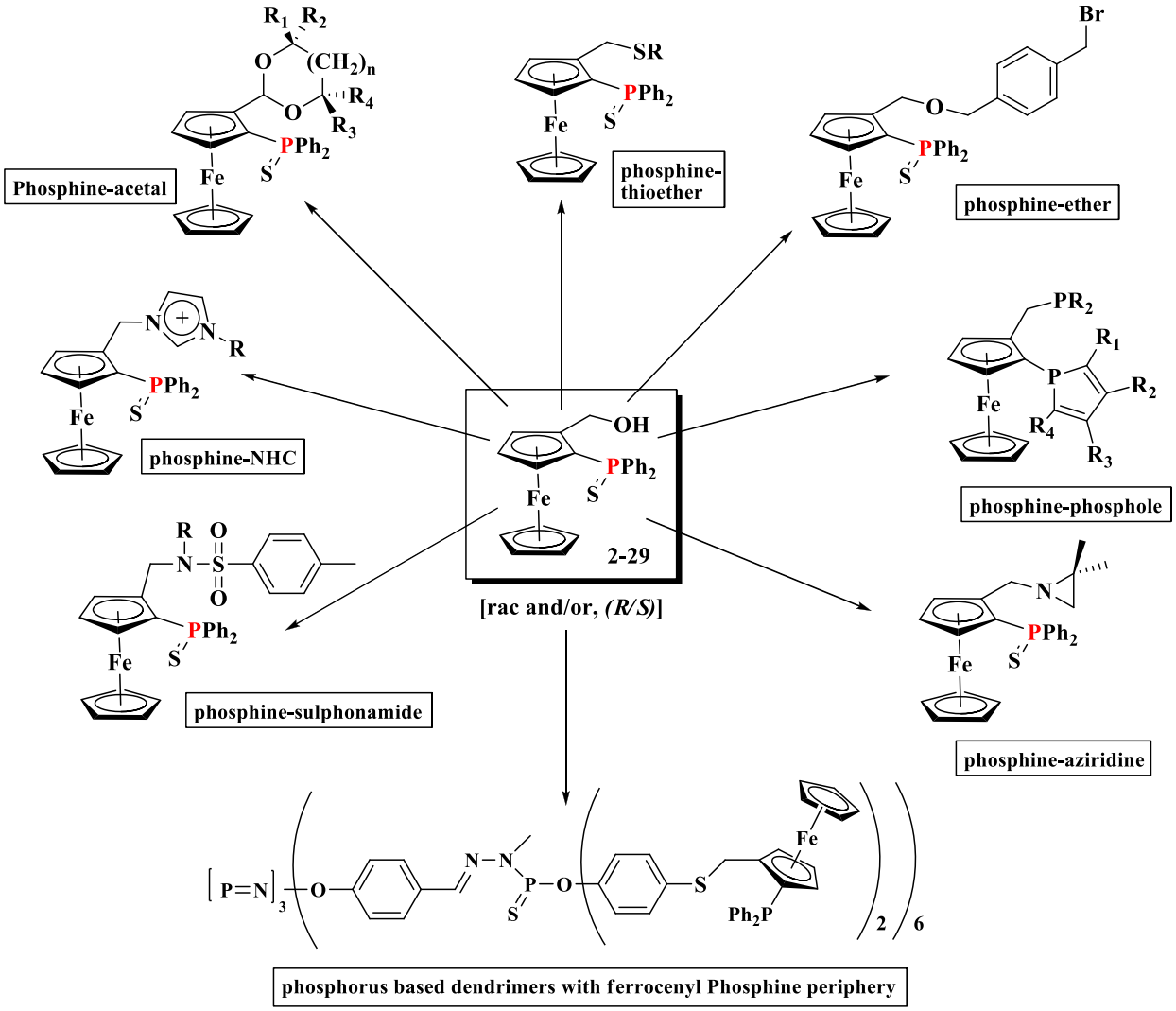

Scheme 2. 8: Different varieties of ligands developed from alcohol **2-29**

A series of ligands with different variants has been developed till now from this phosphine containing alcohol (**2-29**) and they have been intensively studied for synthetic and catalytic

purposes. Among them, phosphine-acetals,[192] phosphine-ethers, thioethers and aziridines,[106b, 106c, 107, 193] phosphine-phospholes,[194] phosphine- N- hetereocyclic Carbenes,[195] phosphine-sulphonamides,[196] phosphorus-based dendrimers with ferrocenyl phosphine periphery [197] (Scheme 2. 8) are noteworthy. Our group published a book chapter dedicated to review the synthesis, the coordination chemistry with different late transition metal salts and the catalytic activity of these ligands.[198]

After this short literature overview, a conclusive remark can be drawn about the high possibility to obtain the newly designed ligands from the ferrocenyl alcohol **2-29**. The synthesis is described below.

The racemic version of the alcohol **2-29** was synthesized in high yields by a method published by our group [192a] optimizing a classical procedure developed by Hayashi *et al*.[199] The first step is a one pot *ortho*-lithiation of ferrocenyl amine **2-30** followed by an electrophilic trapping by PPh_2Cl and then protection of the phosphine group by sulfur to yield the thiophosphine-amine **2-31** efficiently (91% yield). The compound was then transformed to corresponding acetate **2-32** through nucleophilic substitution by action of acetic anhydride and into the alcohol **2-29** by the final saponification step using basic conditions. The overall yield was typically around 80-90% from N,N-dimethylamino-methylferrocene (Scheme 2. 9).

The *(S_p)*- enantiomer of the alcohol **2-29** can be synthesized by a method developed by Kagan *et al*.[200] However, in order to obtain both enantiomerically pure forms of the alcohol, the method developed by Weissensteiner *et al.* to resolve 2-bromodimethylaminomethylferrocene and 2-iododimethylaminomethyl ferrocene with ephedrine as a chiral auxiliary[201] was revisited and published by our group.[192a] The same method has been followed in this thesis (Scheme 2.8). The reaction of iodomethane with **2-31** quantitatively yielded the ammonium salt **2-33**. Then nucleophilic substitution of trimethylamine by enantiomerically pure *(1R, 2R)*-ephedrine was performed yielding two planar chiral ferrocenyl diastereomers **2-34** with opposite planar chirality which were separated by flash chromatography on silica gel. Each enantiomerically pure diastereoisomer was individually acetylated followed by saponification to yield the enantiomerically pure form of alcohol **2-29** *(R_p* and *S_p)* with an overall yield of 70% from N,N-dimethylamino-methylferrocene (Scheme 2. 9).

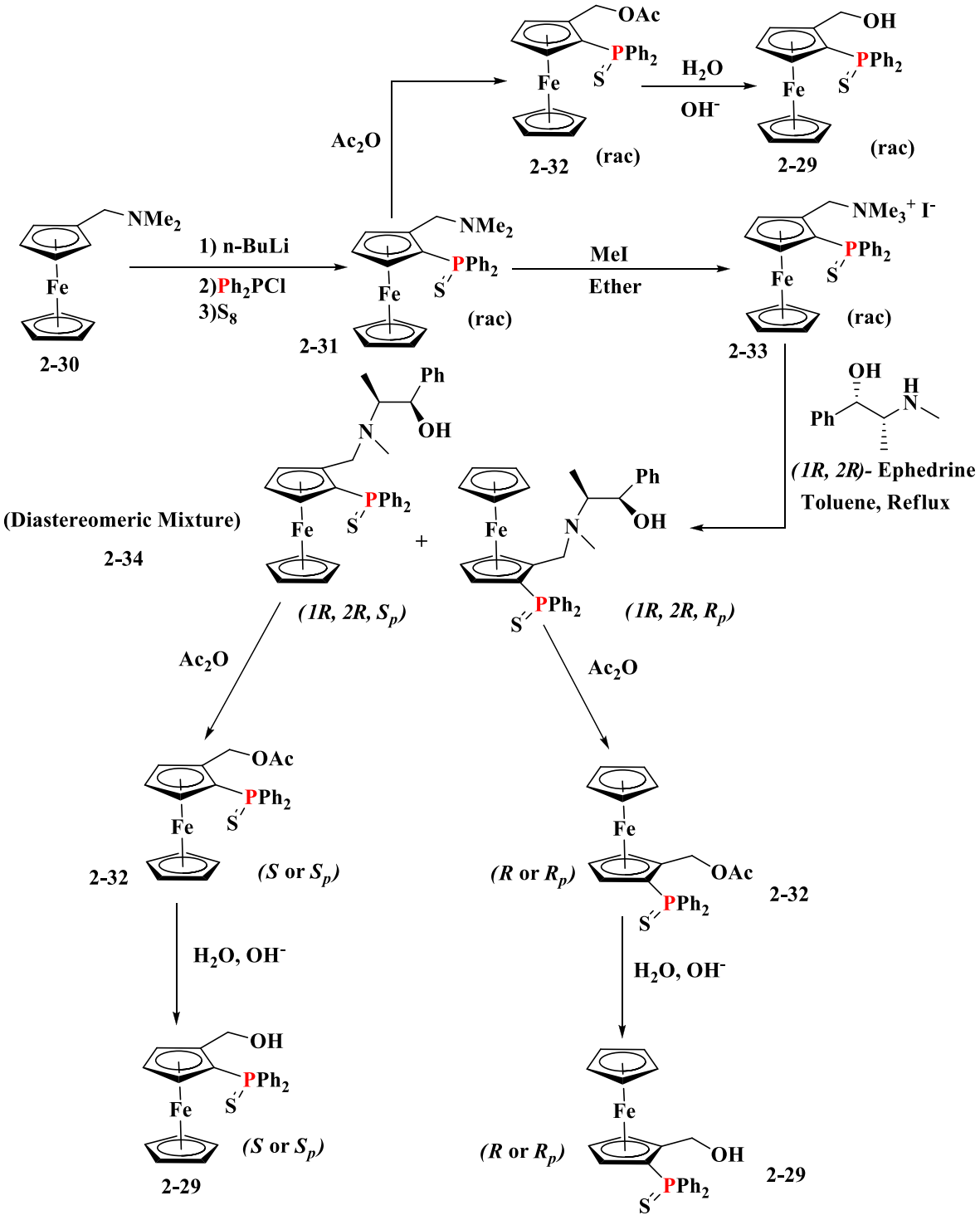

Scheme 2. 9: Synthesis of racemic and enantiomerically pure alcohol **2-29**

2. 5) Preparation of relevant 2- substituted pyridyl derivatives

2-Pyridylmethylamine (or 2-Picolylamine) **2-30** and N-Methyl-N-2-Pyridylmethylamine **2-30a** are readily available starting materials. Other derivatives (*e.g.* benzyl, tosyl) were synthesized from 2-Picolylamine following appropriate procedures.

N-Benzyl-N-2-pyridylmethylamine **2-30b** was synthesized by reductive amination of 2-picolylamine with benzaldehyde using $NaBH_4$ as the reducing agent.[202] On the other hand, 4-methyl-N-(2-pyridinylmethyl)-benzenesulfonamide **2-30c** was prepared following standard tosylation method using TsCl and NEt_3 as the base (Scheme 2. 10).[203]

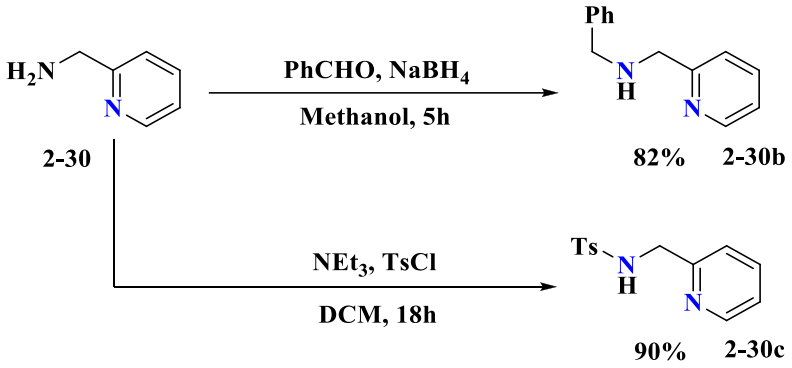

Scheme 2. 10: Synthesis of 2-Picolylamine derivatives

2. 6) Ligand Synthesis: Final Step

In order to find out good conditions for the coupling reaction between the ferrocenyl alcohol and picolylamine derivatives, the reaction was first tested with different (*ortho*- unsubstitued) ferrocenyl alcohols **2-35**. Jiang and Xu *et al*. developed a nucleophilic substitution method using catalytic amount of cerium ammonium nitrate or CAN $\{(NH_4)_2[Ce(NO_3)_6]\}$ and synthesized a series of ferrocene derivatives with alkyl, thioether, ether and also arylamine groups (**2-36**, Scheme 2. 11), presumably by S_N1 through a carbocation intermediate starting from different **2-35** derivatives.[204] In general, CAN has very rich involvement in versatile organic transformations as a single electron oxidant because of its high reduction potential value (1.61 V vs NHE) and other advantages, such as- low toxicity, solubility in several organic solvents, convenient experimental condition and easy handling.[205] However, the catalytic nature of CAN was pointed out by the same research group in their former work, where indole-based alcohols were substituted by other

indole derivatives as nucleophile, in presence of catalytic amount of CAN (10 mol%) and ultrasonic irradiation.[206]

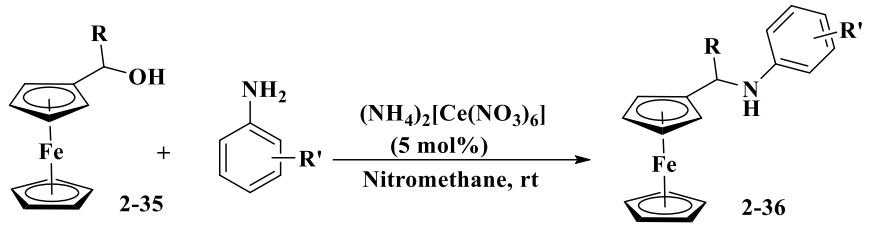

Scheme 2. 11: Nucleophilic substitution by amine nucleophile in presence of catalytic amount of Cerium Ammonium Nitrate (CAN) by Jiang and Xu *et al.*

Unfortunately, in our case, compound **2-29** was not activated and remained unchanged after 72 h of room temperature stirring or refluxing (100 ^{o}C) in the presence of CAN (5 mol%) and N-methyl picolylamine (**2-30a**) as the nucleophile (Scheme 2. 12).

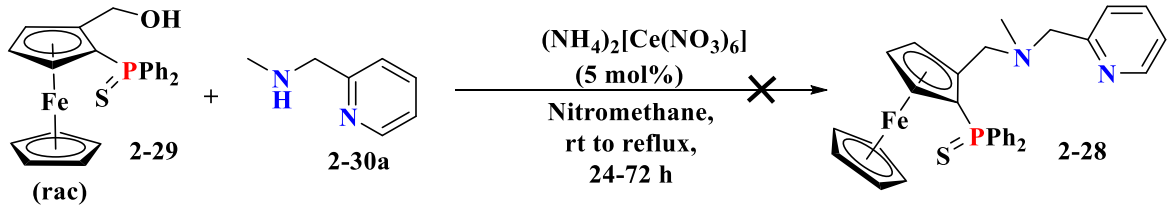

Scheme 2. 12: Failed attempt with CAN

The Mitsunobu reaction since its discovery by Mitsunobu *et al.* (1967),[207] has been one of the classical methods for converting alcohols to a broad range of other type of functional groups (*e.g.* amines, ethers, thioethers, azides, thioesters, cyanides, thiocyanides *etc.*). The reaction gained immense interest in the field of organic synthesis and medicinal chemistry; not only because of its broad substitution range of alcohol, but also due to its stereospecificity and mild conditions. The reaction has also been employed frequently as a key step in the synthesis of several natural products. [208]

In this reaction condition, a primary or secondary alcohol is substituted by an activated nucleophile in the presence of triphenylphosphine (PPh_3) and Diethyl azodicarboxylate (DEAD) or diisopropyl azodicarboxylate (DIAD), at ambient temperature. In case of a chiral secondary alcohol, the product is formed with an inversion of configuration after the nucleophilic substitution. DEAD or DIAD is reduced to its corresponding aza species (*e.g.* diethyl 1,2-hydrazinedicarboxylate in case

of DEAD) and PPh_3 is oxidized to triphenylphosphine oxide (PPh_3O), during the course of alcohol substitution (Scheme 2. 13). [208b]

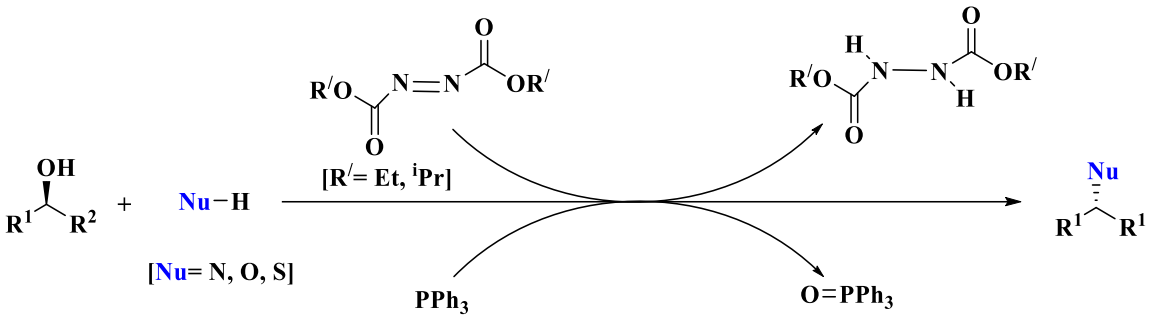

Scheme 2. 13: General Scheme of the Mitsunobu reaction

In the team, the same reaction conditions (depicted in Scheme 2. 13) were previously applied to synthesize enantiomerically pure phosphinoferrocenyl-alixarenes **2-38** by alkylation of 4-*tert*-butylcalix[4]arene **2-37** with *(S)*-**2-29** (Scheme 2. 14).[209]

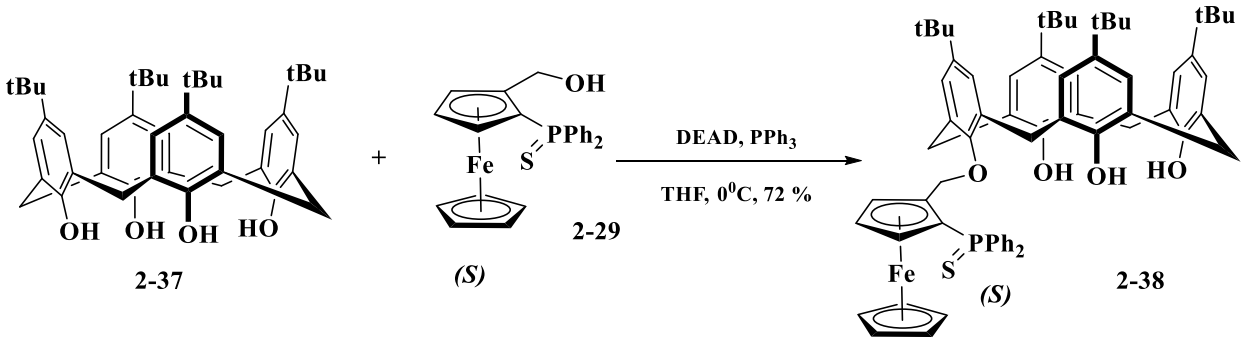

Scheme 2. 14: Mitsunobu reaction for the synthesis *o* Phosphinoferrocenyl-Calixarenes **2-38**

Having the same ferrocenyl alcohol in racemic and/or enantiopure form, as starting material in our case, we devised the equivalent procedure with previously synthesized 2-picolylamine derivatives (**2-30a, b, c**) as nucleophile. The expected ligands were obtained with variable yields (Scheme 2. 15).

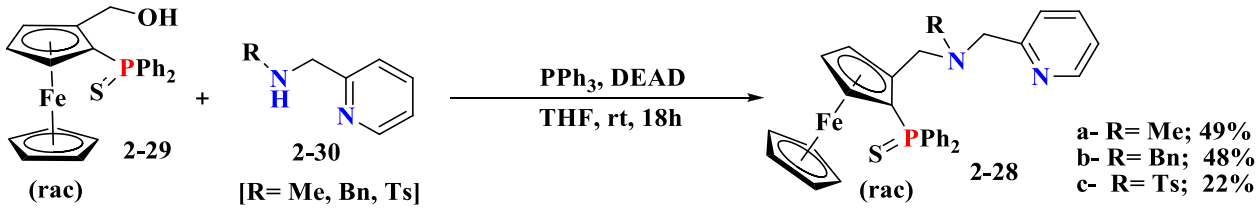

Scheme 2. 15: Synthesis of Different PNN Ligands by Mitsunobu Condition

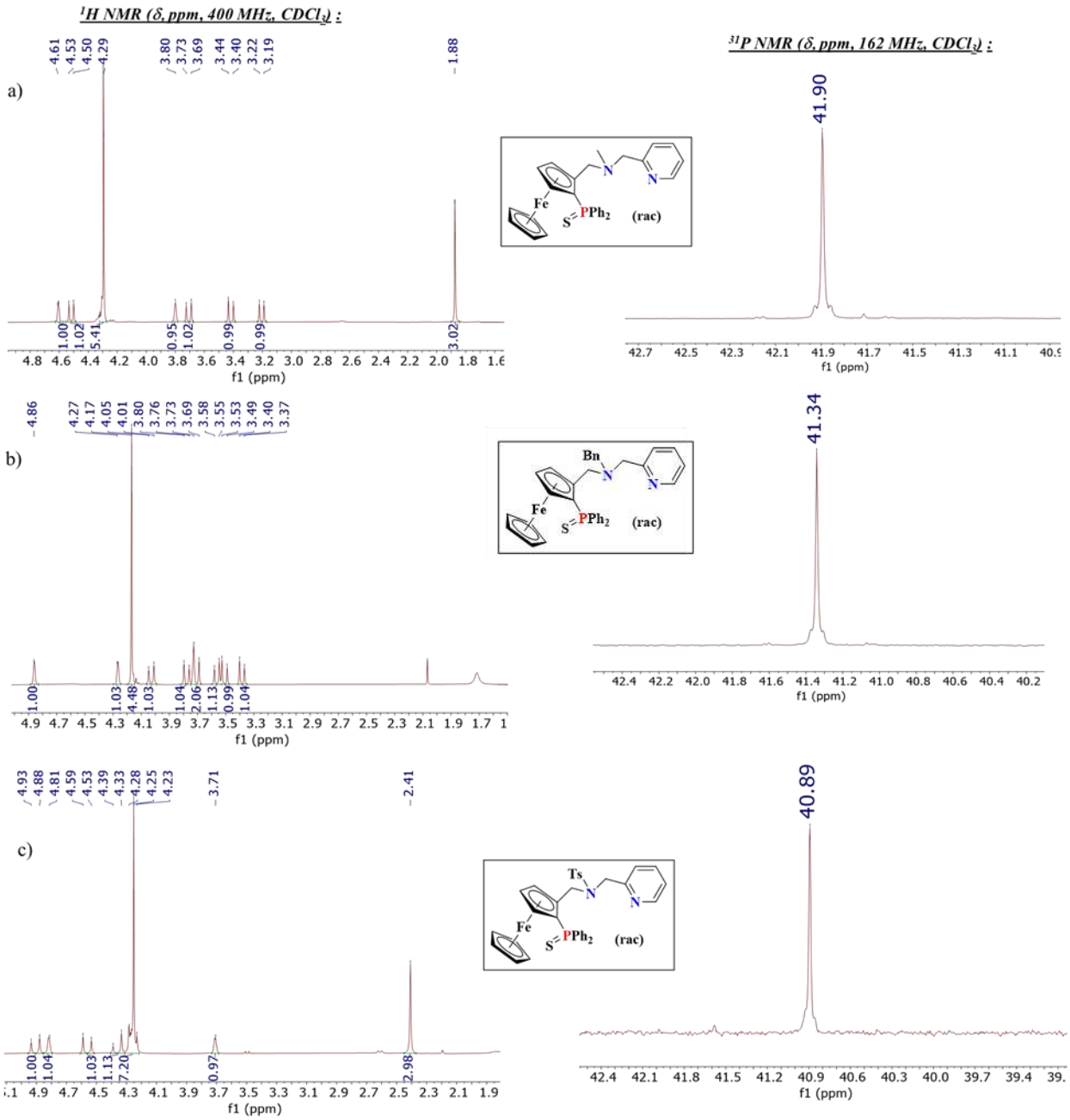

Figure 2. 1: ^{1}H (Cp and aliphatic region) ($CDCl_3$, 400 MHz) and ^{31}P NMR ($CDCl_3$, 162 MHz) Spectra of **2-28a**, **2-28b** and **2-28c**

All the three new synthesized compounds in the Scheme 2. 15 were characterized by multinuclear (^{1}H, ^{31}P, ^{13}C) NMR and High-Resolution Mass Spectrometry (HRMS). In case of **2-28a**, the ^{1}H NMR spectrum shows four AB-type doublet resonances, which indicates -CH_2 groups containing two sets of non-equivalent, diastereotopic, mutually coupled (confirmed by COSY) protons (δ = 4.51, 3.20 and 3.70, 3.41). One CH_2 group is directly attached to the Cp ring and the other one to

the pyridyl ring. The planar chirality of the ferrocenyl backbone differentiates the electronic environment around each proton of both CH_2 groups and thus induces diastereotopicity. A similar pattern was observed in the ^{1}H NMR spectrum of **2-28c** (δ = 4.90, 4.55 and 4.35, 4.25). In case of **2-28b**, since a third -CH_2 moiety was introduced from the benzyl part, three sets of AB-type resonances were recognized (δ = 4.02, 3.77; 3.70, 3.38 and 3.55, 3.50). The five chemically equivalent protons of the unsubstituted Cp ring gave a singlet peak at δ = 4.29 for **2-28a**, 4.17 for **2-28b**, 4.23 for **2-28c**. The three non-identical protons of the substituted Cp ring gave three multiplets at similar regions for all the three compounds (δ = 4.61, 4.29, 3.80 for **2-28a**; δ = 4.86, 4.26, 3.73 for **2-28b**; δ= 4.86, 4.81, 4.28, 3.71 for **2-28c**). The peak at δ = 1.88 for **2-28a** and δ = 2.41 for **2-28c** correspond to the N-C$\underline{H_3}$ and tosyl-C$\underline{H_3}$, respectively. The ^{31}P NMR spectrum gave peaks in similar regions for all three compounds (δ = 41.89 for **2-28a**; δ = 41.34 for **2-28b**; δ= 40.89 for **2-28c**). The ^{1}H (Cp and aliphatic region) and ^{31}P NMR spectra of these three compounds are shown in Figure 2. 1 [a) for **2-28a**, b) for **2-28b**, c) for **2-28c**].

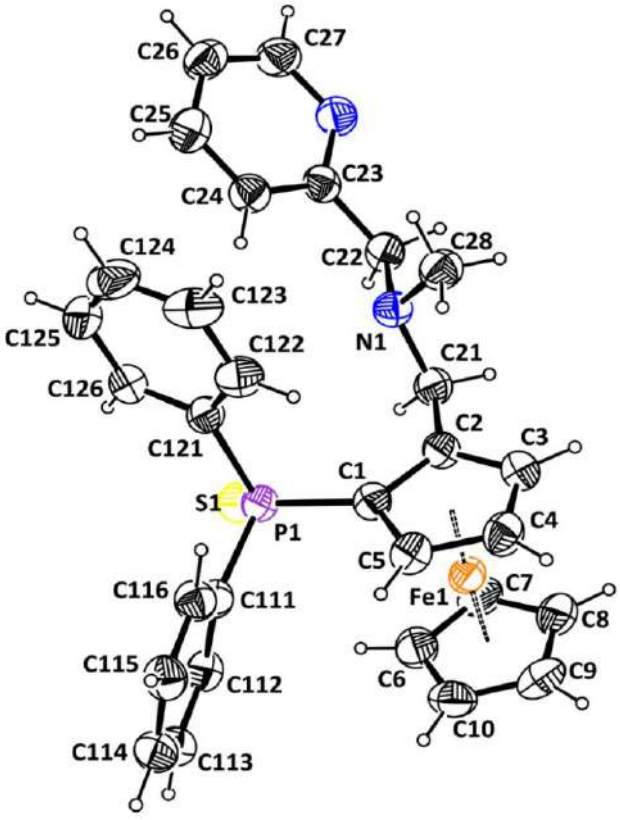

Figure 2. 2: Molecular view of ligand **2-28a** (R= Me) showing 50% probability displacement ellipsoids and the atom numbering scheme. H atoms are shown as small spheres of arbitrary radii.

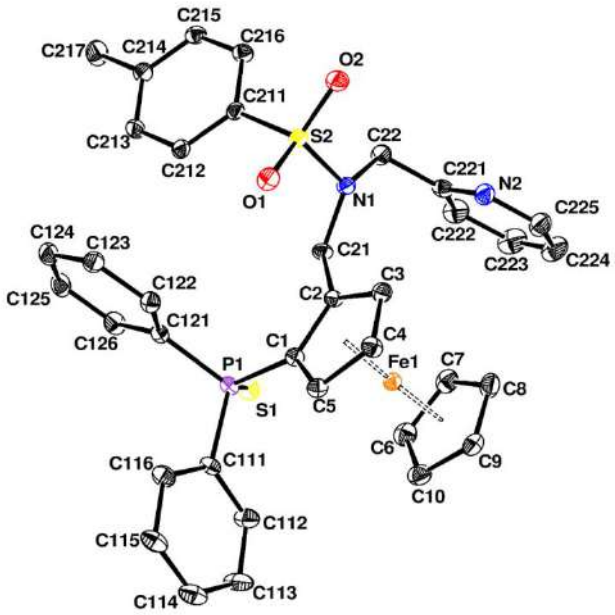

Figure 2. 3: Molecular view of compound ligand 2-28c (R= Ts) showing 30% probability displacement ellipsoids and the atom numbering scheme. H atoms have been omitted for clarity

Recrystallization of these synthesized racemic proligands was subsequently attempted. Pentane vapor, obtained by slow evaporation, was diffused into concentrated solutions of these compounds in dichloromethane (DCM). Thus, single crystals of two of these protected ligands **2-28** (R = Me, Ts) were obtained. The structures of the molecules, obtained from X-ray diffraction (XRD) analyses, are shown in Figure 2. 2 for **2-28a** (R = Me) and Figure 2. 3 for **2-28c** (R = Ts).

In the **2-28a** structure (Figure 2. 2), Cp rings are roughly eclipsed, the P1 atom is nearly in the mean plane of the Cp ring with a deviation of -0.021(6) Å, whereas the S1 atom is located at -1.226(7) Å below the Cp mean plane. The N1 atom is 1.402(6) Å above the Cp plane. In the **2-28c** structure (Figure 2. 3), the Cp rings are also roughly eclipsed. As usual in this kind of protected disubstituted ferrocene, the P1 atom is nearly in the mean plane of the Cp ring with a deviation from the plane being 0.033(6) Å, *i.e.* in the opposite direction relative to that of **2-28a**, whereas the S1 is -1.236(7) Å below the Cp mean plane. The N1 amine is above this mean plane by 0.731(4) Å.

The sulphur protection of the phosphine function in **2-28a** (R=Me) was removed by an exchange reaction with $P(NMe_2)_3$ at elevated temperatures. Thus, the activated free phosphine containing ligand **2-1** (R= Me) was obtained (Scheme 2. 16).

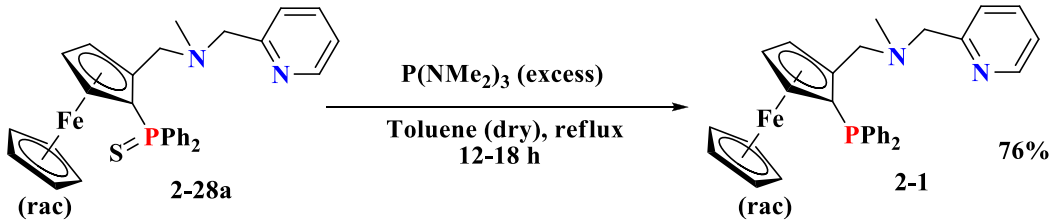

Scheme 2. 16: Phosphine deprotection of ligand **2-28a** (R= Me)

Ligand **2-1** (R = Me) was characterized by multinuclear (^{1}H, ^{31}P, ^{13}C) NMR. In the ^{31}P NMR spectrum the peak at δ = -23.85 confirms the presence of a free phosphine. In the ^{1}H NMR spectrum two sets of AB-type doublet resonances were found (δ = 3.76, 3.03 and 3.24, 3.35) for the two different types of diastereotopic, mutually coupled C$\underline{H_2}$ protons along with usual aromatic, cyclopentadienyl (Cp) and aliphatic proton peaks (Figure 2. 4).

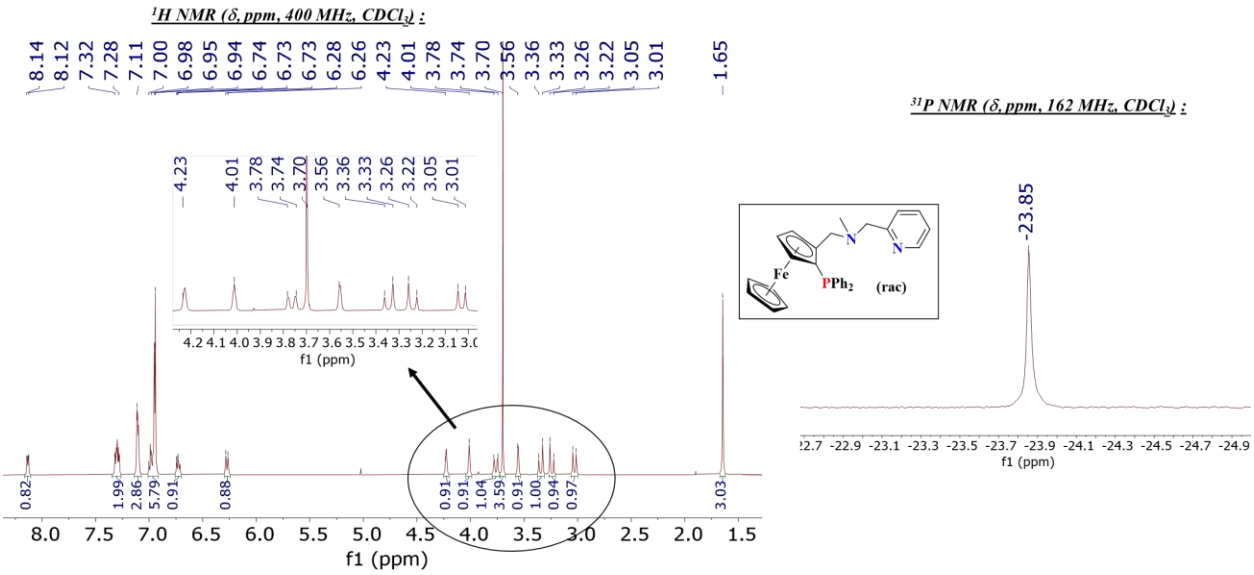

Figure 2. 4: ^{1}H ($CDCl_3$, 400 MHz) and ^{31}P ($CDCl_3$, 162 MHz) NMR Spectra of **2-1** (R= Me)

The phosphine deprotection of the other two variants (**2-28b and 2-28c**) are not yet performed and are in progress.

2. 7) Switching to PNN ligands with hydroxyl substituted pyridine ring

The new PNN compounds described above (**2-28** and **2-1**) can't provide a proton during the catalytic cycles because the central N donor atom is a teriary amine. In the next chapter, I will discuss the synthesis of a few similar ligands with a central secondary amine and highlight the

importance of having an NH center for improved efficiency in hydrogenation-dehydrogenation catalysis.

2-Hydroxy pyridines exhibit tautomeric equilibria with 2- pyridines (Scheme 2. 17) [210] and the ratio of NH containing lactam tautomer increases upon increasing the solvent polarity.[211]

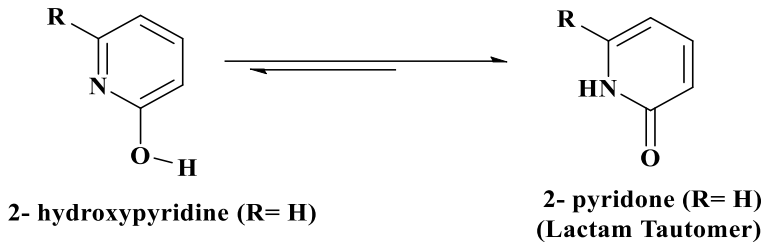

Scheme 2. 17: Tautomeric structure of hydroxyl pyridine

The pK_a value of 2-hydroxypyridine being low (0.75), 2-hydroxy pyridines and its substituted derivatives can be easily deprotonated. This give rise to the ambident nucleophilicity in 2-hydroxy pyridine systems.[212] The corresponding anions generated after deprotonation have also been used for metal complexations (*e.g.* Zr, Pd, Fe, Cu, Ti, Sm *etc*.) and the resulting complexes have been utilized as precatalysts or catalysts in a variety of transformations.[213] In this context, it is relevant to mention recent work of Schafar *et al.* where a number of substituted 2-pyridonate ligated tantulum complexes (Scheme 2. 18) were synthesized and studied as catalysts for the hydroamination of alkenes with several secondary amines.[214]

Scheme 2. 18: 2- pyridonate-based Ta complexes reported by Schafer *et al.*

Szymczak *et al.* reported 6,6/ -dihydroxy terpyridine-based ruthenium complexes (Scheme 2. 19), which acted as bi-functional catalysts for the transfer hydrogenation of ketone, because of the assistance of the pendant hydroxyl groups.[215]

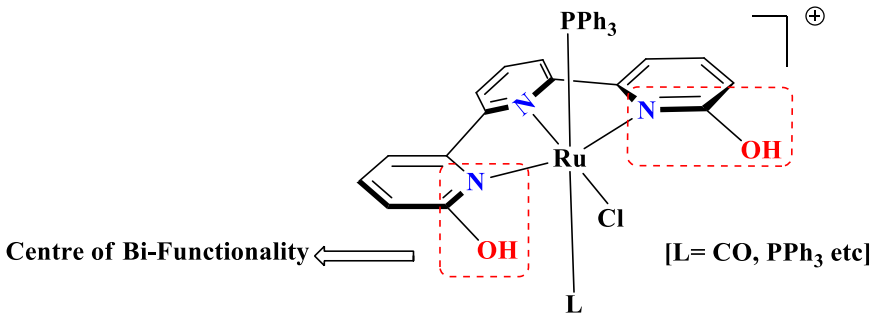

Scheme 2. 19: 6,6′ -dihydroxy terpyridine-based Ru complexes developed by 6,6′ -dihydroxy terpyridine-based ruthenium complexes

However, there are no such ferrocenyl ligands reported to date. Hence, by combining the planar chirality of substituted ferrocenes and the acidic property of 2-hydroxypyridines, we designed the following tridentate ferrocenyl ligand **2-39** with modified pyridine moiety (Scheme 2. 20). The synthesis will be described in the following sections.

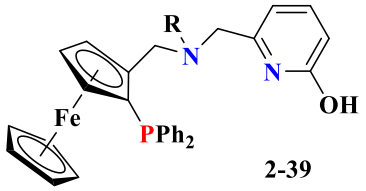

Scheme 2. 20: General molecular structure of the designed ligand **2-39**

2. 8) Retrosynthetic Analysis of Ligand- 2-39

To synthesize the PNN ligands **2-39**, a molecule with protected phosphine and hydroxyl functions (**2-40**) must first be assembled from commercially available starting materials (Scheme 2. 21). According to the retrosynthetic analysis depicted in Scheme 2. 21, It is possible to envisage two different ways to access the protected precursor **2-40**. Path-A is the same strategy already used for the synthesis of PNN proligands **2-28** (see section- 2.5). In this case, the required coupling partner is a 6-methoxy 2-pyridylamine **2-41.** Path-B, on the other hand, involves formation of the other N-C bond from a ferrocenyl amines **2-42** and a 6-methoxy pyridine functionalized with a suitable CH_2X arm at the 2 position (X= leaving group), **2-43**. Both the pathways require **2-43** as a common starting reagent. The synthesis of this intermediate, which is not commercially available, is described in the next section.

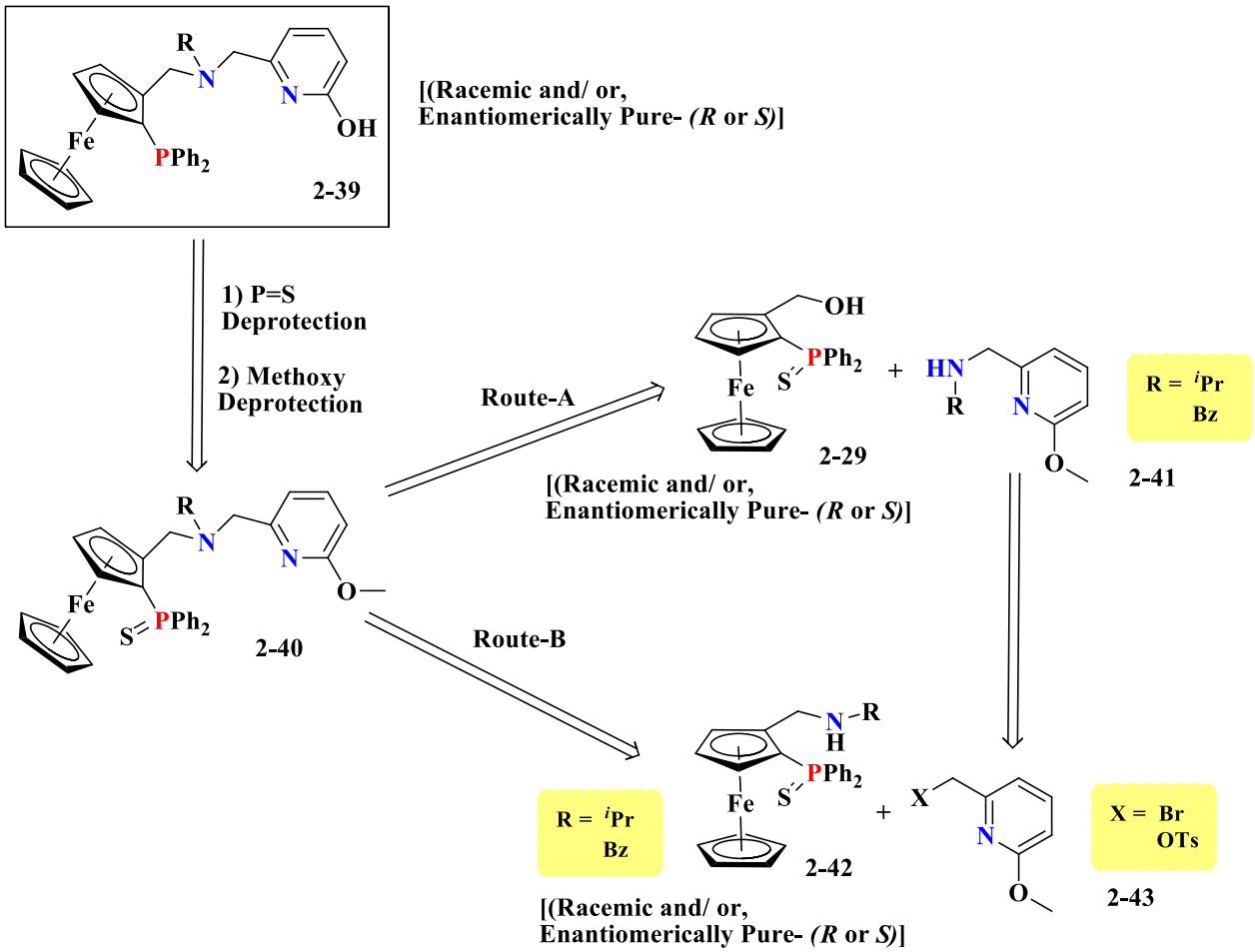

Scheme 2. 21: Retrosynthetic Analysis of the ligand **2-39**

2. 9) Synthesis of 2-(bromomethyl)-6-methoxypyridine and 2-(tosylmethyl)-6-methoxypyridine

The bromo and tosylate functions have been selected as suitable leaving groups. The synthesis of the target molecules **2-43** (X= Br, Ts) was carried out starting from commercially available 6-hydroxy-2-pyridinecarboxylic acid, **2-44**. The first step is a methylation reaction to protect the hydroxyl group, by using silver oxide and MeI as methylating agent. At first, Ag complexes are formed by deprotonation of the two hydroxyl functions followed by nucleophilic substitution on MeI. After purification, the ester product **2-45** in the form of a white solid is obtained with a yield of 76%. The formation of the expected species **2-44** was confirmed after comparing its NMR spectra (^{1}H, ^{13}C) with the reported spectral data.[216] Then, $LiAlH_4$ is chosen as the most effective agent for the ester reduction. However, product decomposition was observed during column

chromatographic separation in spite of careful work up. The pure product could not be obtained under these conditions (Scheme 2. 22). It was predicted that, $LiAlH_4$ being highly moisture sensitive and intolerable in presence of the other reducible functional groups [217] (here, methoxy) is most probably responsible for the decomposition.

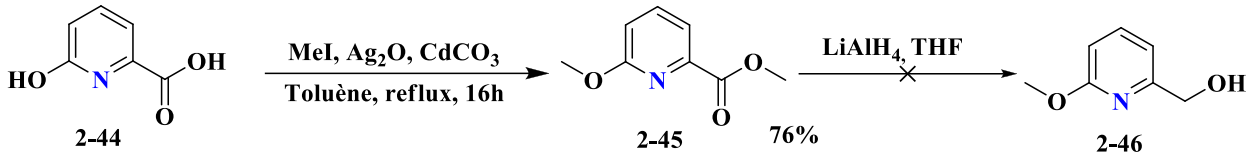

Scheme 2. 22: Preparation of ester **2-45** and decomposition towards reduction using $LiAlH_4$

Usually, $NaBH_4$ is less efficient than $LiAlH_4$ for the reduction of esters, yielding suitable results in special cases, such as elevated temperatures or with activated esters.[218] Singaram *et al.* reported a new and efficient method to reduce a number of esters by $NaBH_4$ in the presence of catalytic amount of NaOMe. The success of this strategy relies on the stabilizing ability of NaOMe towards $NaBH_4$ in MeOH. According to these authors, the resulting $NaBH_3OMe$ intermediate is most likely responsible for the ester reduction at room temperature.[219] Therefore, we adapted this procedure to reduce **2-45** and eventually succeeded to obtain the corresponding alcohol **2-46** in moderate yields (56%). Later on, it was observed that introducing a delay between the NaOMe and $NaBH_4$ addition to the reaction mixture significantly improved the yields (Table 2. **1**).

Table 2. 1:Optimization of the reduction of **2-45** by $NaBH_4$

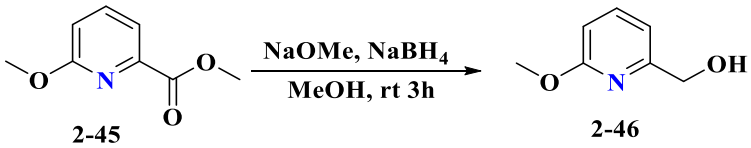

Entry	Delay between the NaOMe and $NaBH_4$ addition at 0 °C (min)	NaOMe (mol %)	Yield (%)
1	0	5	56
2	0	7.5	63
3	30	7.5	72
4	60	7.5	89

[a] Standard Reaction Conditions- ester (1 equiv.), $NaBH_4$(2.5 equiv.), NaOMe (varied accordingly) in MeOH (0 °C to rt)

2-(bromomethyl)-6-methoxy-pyridine **2-43a,** was then prepared from the alcohol **2-46** by using PBr_3 as a brominating agent.[220] Tosylation of the alcohol using tosylchloride to yield **2-43b**, was

carried out under strong basic conditions (KOH),[221] while using the weaker base, NEt_3, [222] no activation of alcohol was observed and therefore, no conversion took place (Scheme 2. 23).

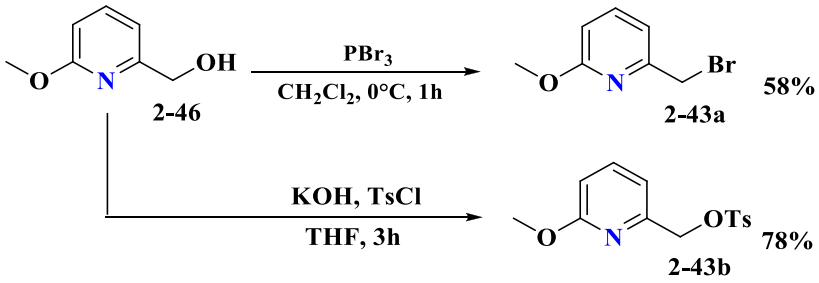

Scheme 2. 23: Preparation of Bromo and Tosyl intermediate

The bromo intermediate, **2-43a**, is a reported compound;[223] whereas the tosyl intermediate **2-43b** is unprecedented. Figure 2. 5 shows the ^{1}H NMR spectra of these two compounds. For **2-43a,** one triplet (δ = 7.55) and two doublet resonances (δ = 6.99, 6.67) in the aromatic region represent 3 pyridyl protons. The peak at δ = 4.47 and δ = 3.95 corresponds to the –C$\underline{H_2}$ and -OC$\underline{H_3}$ group, respectively [Figure 2. 5, a)]. Similarly, one triplet (δ = 7.55) and two doublets (δ = 6.95, 6.66) in the same aromatic region were found for **2-43b**, indicating 3 pyridyl protons. Two other doublets (δ = 7.85, 7.35) represent four aromatic tosyl protons. The CH_2 is slightly more deshielded for **2-43b** (relative to **2-43a**) as the peak found at δ = 5.05. The peaks at δ = 5.05, δ = 3.85 and δ = 2.93 correspond to the C$\underline{H_2}$ and OC$\underline{H_3}$ and tosyl-C$\underline{H_3}$ group, respectively [Figure 2. 5, b)].

Single crystals of the tosyl derivative, **2-43b**, were grown by layering hexane onto a dichloromethane solution, followed by slow evaporation. The crystal structure is shown in Figure 2. 6. The tosyl and the pyridyl rings make a dihedral angle of 46.88(5)°.

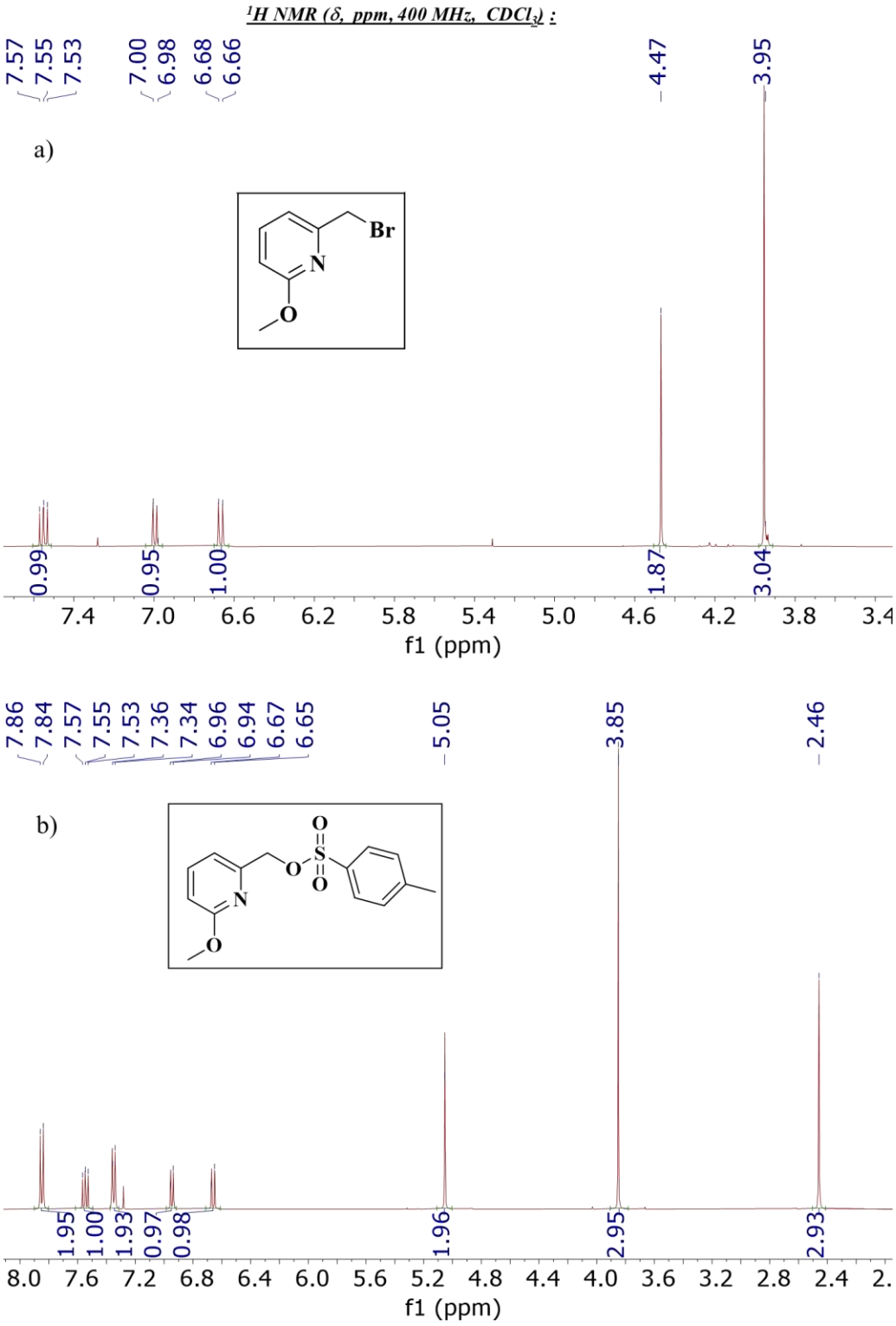

Figure 2. 5: ^{1}H NMR spectra ($CDCl_3$, 400 MHz) of **2-43a** and **2-43b**

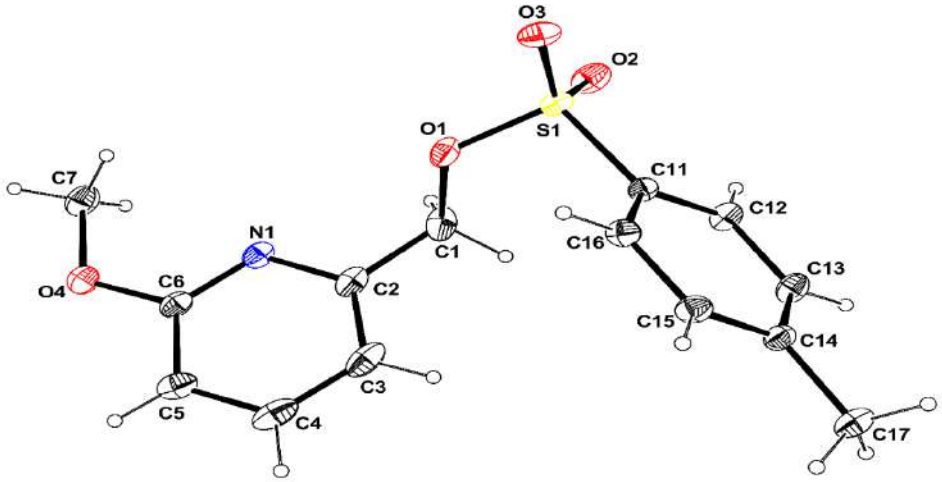

Figure 2. 6: Molecular view of compound **2-43b** showing 30% probability displacement ellipsoids and the atom numbering scheme. H atoms are represented as small sphere of arbitrary radii.

Initial attempts were directed toward the synthesis of pyridylamines, which are needed for Path-A (Scheme 2.16). However, the reaction of **2-43b** with methylamine in the presence of triethylamine (NEt_3) resulted in the corresponding disubstituted tertiary amine **2-48**, even when using 1 equivalent of amine reagent (Scheme 2. 24). The same result was obtained using K_2CO_3 as a base. Consequently, this pathway was abandoned.

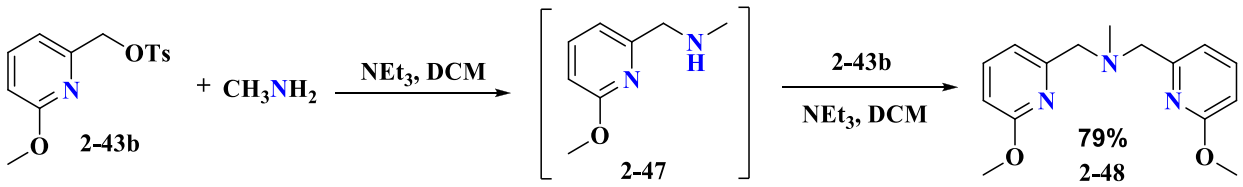

Scheme 2. 24: Tertiary Amine **2-48** formation

The amine **2-48** was characterized by multinuclear NMR (^1H, ^{13}C) and HRMS. Figure 2. 7 shows the ^1H NMR spectrum of the compound. The aromatic region is comprised of three resonances: one triplet (δ = 7.56) and two doublets (δ = 7.13, 6.63), which indicate two identical sets of three pyridyl protons. The peaks at δ = 3.95, 3.78, and 2.43 represent two identical O$\underline{CH_3}$, $\underline{CH_2}$ and one N-$\underline{CH_3}$ group, respectively.

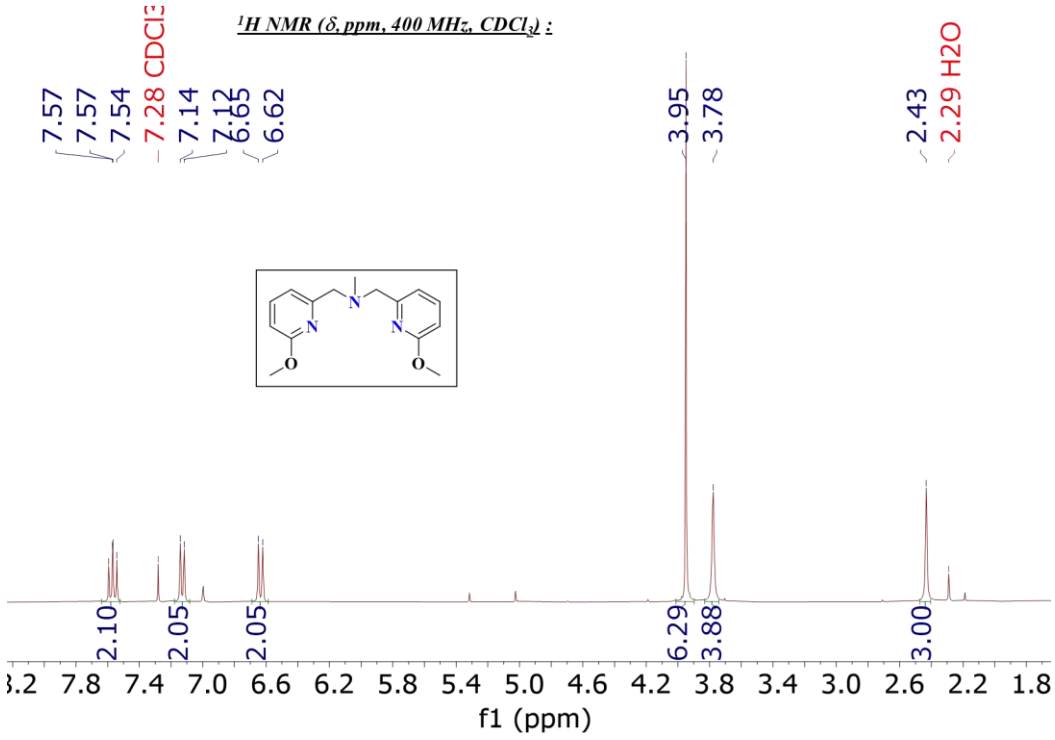

Figure 2. 7: ^{1}H NMR Spectrum ($CDCl_3$, 400 MHz) of **2-48**

Interestingly this kind of tertiary amines may be useful as tridentate ligands after methoxy deprotection in view of the possible assistance of the 6-hydroxyl groups through H-bonding.

2. 10) Synthesis of secondary Ferrocenylamine Intermediates: Approach via Path-B

The needed ferrocenylamine **2-42** could be conveniently accessed by the HBF_4 method according to the procedure developed by Dr. Lucie Routaboul in our the team for the synthesis of different phosphine containing ferrocenylamines.[224] The same procedure was followed here to synthesize two varieties of **2-42** (R= Bn, ^{i}Pr; Scheme 2. 25).

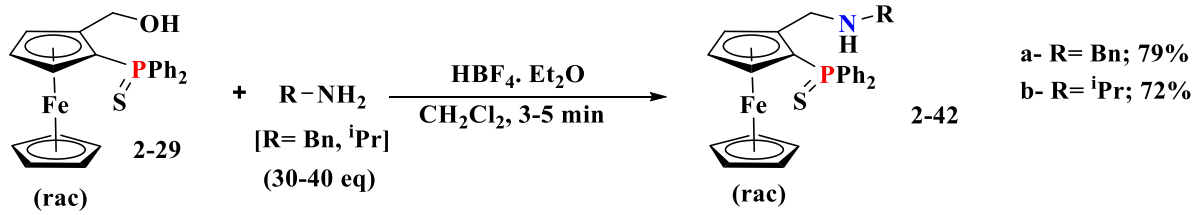

Scheme 2. 25: Synthesis of different ferrocenylamines by HBF_4 method

Figure 2. 8 shows selected regions of the ^{1}H and ^{31}P NMR spectra of these amines. In the ^{1}H NMR spectrum of **2-42a**, along with the usual singlet of the unsubstituted Cp ring protons (δ = 4.31) and three multiplets of the non-identical protons of the substituted Cp ring (δ = 4.59, 4.31, 3.79), four AB-type doublet resonances are found. These peaks indicate two CH_2 groups (attached to the Cp and phenyl rings) with two non- equivalent, diastereotopic, mutually coupled (confirmed by COSY in each case) protons. The resonance at δ = 4.51 represents one of them. The other three resonances are merged in the region δ = 3.59- 3.49 [Figure 2. 8, a)]. Similarly, in the ^{1}H NMR spectrum of **2-42b**, along with the usual unsubstituted Cp singlet (δ = 4.33) and three multiplets of the non-identical substituted Cp ring protons (δ = 4.59, 4.30, 3.75), two AB-type doublet resonances are recognized (δ = 4.30, 3.54) indicating the CH_2 group attached to the Cp ring [Figure 2. 8, b)]. The ^{31}P NMR spectrum gave peaks in similar regions for the two compounds (δ = 41.22 for **2-42a**; δ = 41.05 for **2-42b**, see Figure 2. 8).

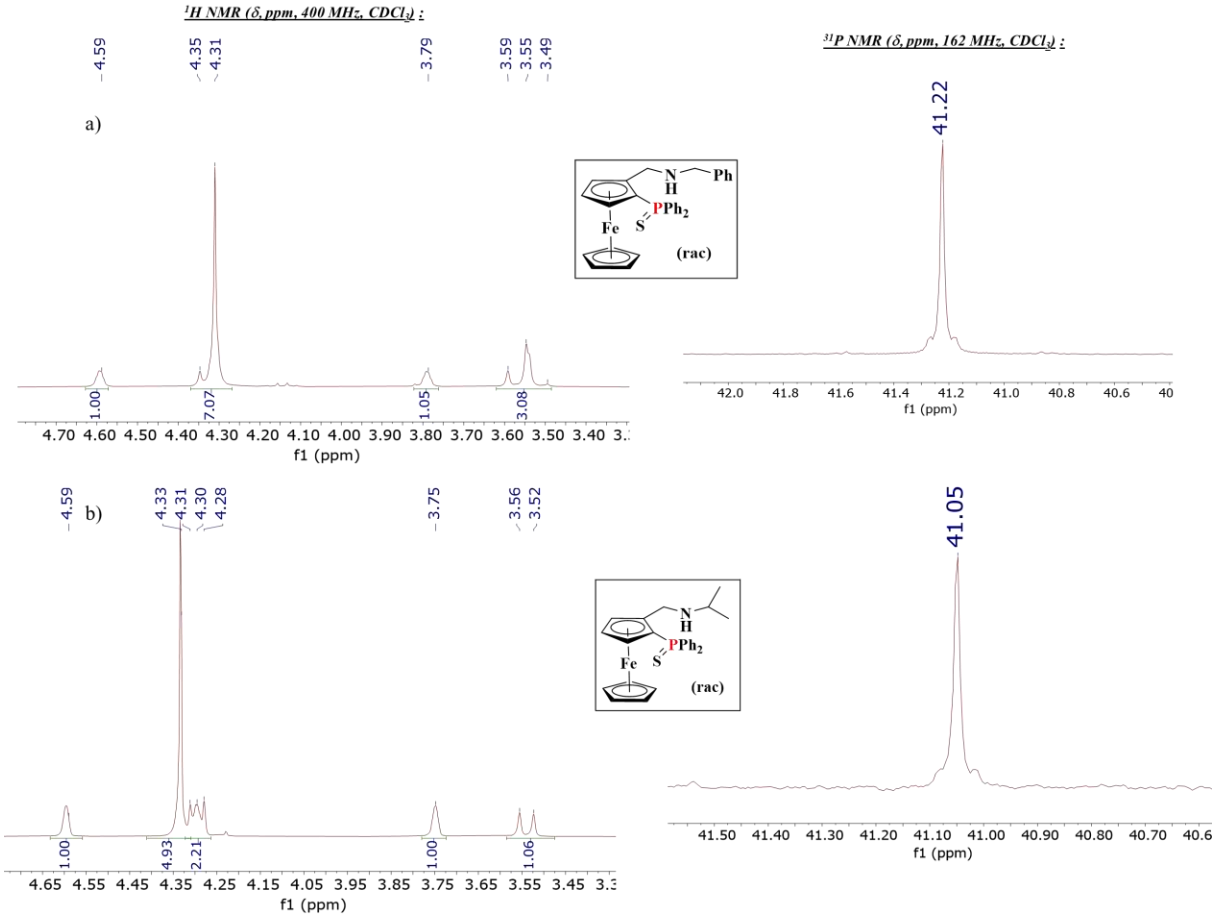

Figure 2. 8: ^{1}H ($CDCl_3$, 400 MHz) (Cp region) and ^{31}P NMR Spectra ($CDCl_3$, 162 MHz) of **2-42a** and **2-42b**

Although, the benzyl (**2-42a**) derivative have been previously described by Dr. Lucie Routaboul in her thesis,[224] the isopropyl derivative (**2-42b**) is a new member of the family. Hence, **2-42b** was characterized by multinuclear NMR (^{1}H, ^{13}C, ^{31}P) and HRMS. Moreover, a good-quality single crystal for and X- ray diffraction investigation of **2-42b** was obtained by slow evaporation of a DCM solution. The structure is shown in Figure 2. 9.

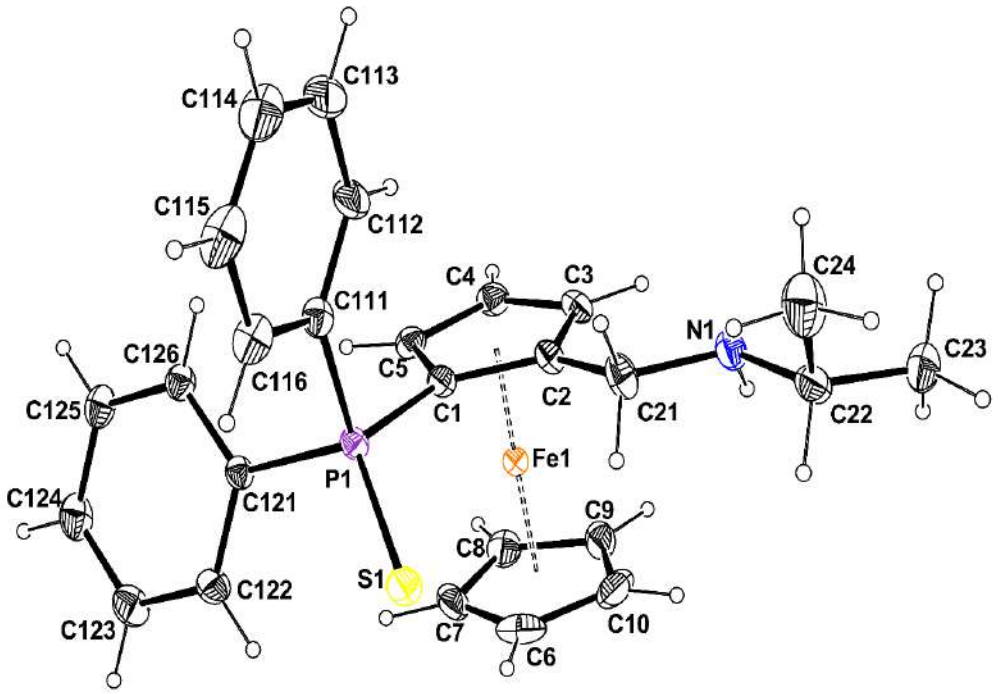

Figure 2. 9: Molecular view of compound **2-42b** showing 30% probability displacement ellipsoids and the atom numbering scheme. H atoms are represented as small sphere of arbitrary radii.

In this molecule, the two Cp rings are staggered with a twist angle of 23°. As observed in all the other ferrocenyl diphenylthiophosphine derivatives, the S atom is placed below the mean plane of the Cp ring, with a distance of -1.069(4) Å, whereas the P atom is roughly coplanar with the in the Cp ring, -0.064(3) Å. The N atom is also roughly coplanar with the Cp ring, being slightly below the plane by -0.055(4)Å. The C2-C21-N1-C22 torsion angle is 172.02(2)°.

Mitsunobu conditions have also been investigated for the synthesis, since they are milder. However, this reaction led to the formation of diethyl 1,2-hydrazinedicarboxylate as one of the expected byproducts,[225] together with the target secondary amine. Generally, this byproduct forms after the reduction of the DEAD reagent in the reaction medium (see Scheme 2. 13). However, in certain cases of our targeted reaction, the polarity of this byproduct is very close to

that of amine (*e.g.* for R=Bn), rendering a chromatographic separation to be difficult. The HBF_4 method eliminates this constraint and results in relatively better yields.

These secondary ferrocenylamines **2-42a, b** were then utilized for the subsequent step, which is the alkylation of ferrocenyl amines with the previously synthesized pyridyl intermediate **2-43** to obtain the final (protected) structure **2-40** of the designed ligand (see next section).

It is important to mention that Dr. Lucie Routaboul has previously synthesized a few enantiomerically pure PNP type ferrocenyl proligands **2-51**, which are also described in her thesis.[224] These compounds contain two identical *ortho*-(thiodiphenylphosphino)-ferrocenylmethyl units joined by a tertiary amine unit. The synthesis was carried out by nucleophilic substitution of the pyridinium salt of alcohol **2-29** (**2-50**) under refluxing condition either by simple amine (benzyl amine) or by amines **2-42** (Scheme 2. 26). Subsequent phosphorus deprotection by $P(NMe_2)_3$ resulted the active PNP form of proligands **2-51**. To study the coordination chemistry, Ru(II) and Ag(I)-complexes of the active form of **2-51** were synthesized and characterized by multinuclear NMR spectroscopy.

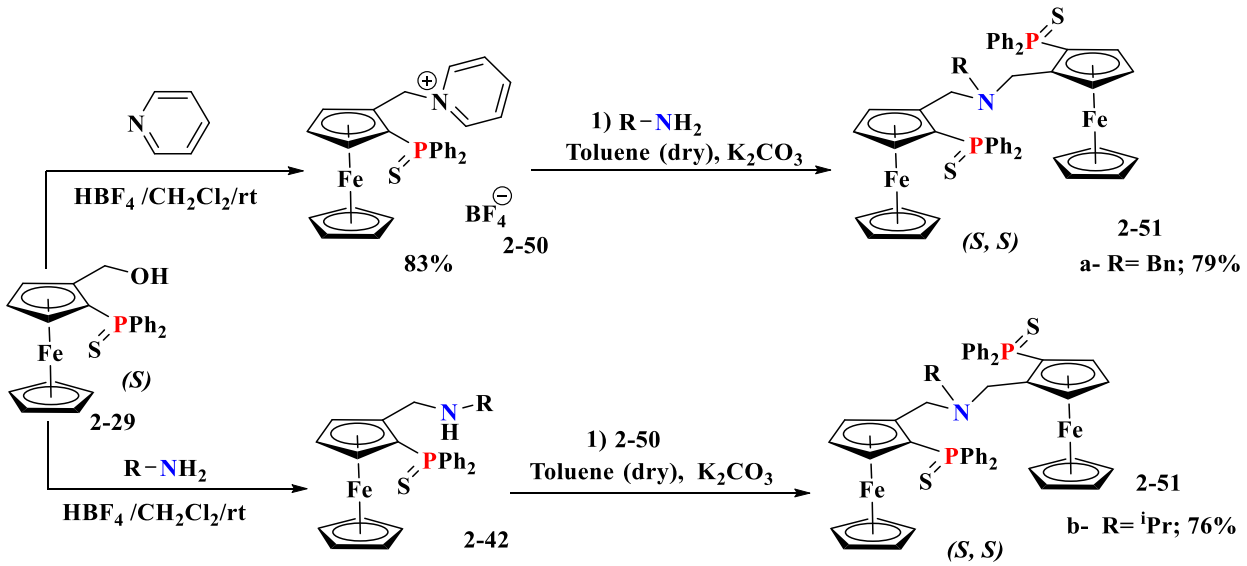

Scheme 2. 26: PNP ligands developed previously in our Team by Dr. Lucie Routaboul

These ligands remain unexplored to date for any kind catalytic applications. Hence, to involve these PNP-type chiral ligands in our desired catalytic applications with non-noble metal precursors, the synthesis of **2-51** was repeated following the Scheme 2. 26.

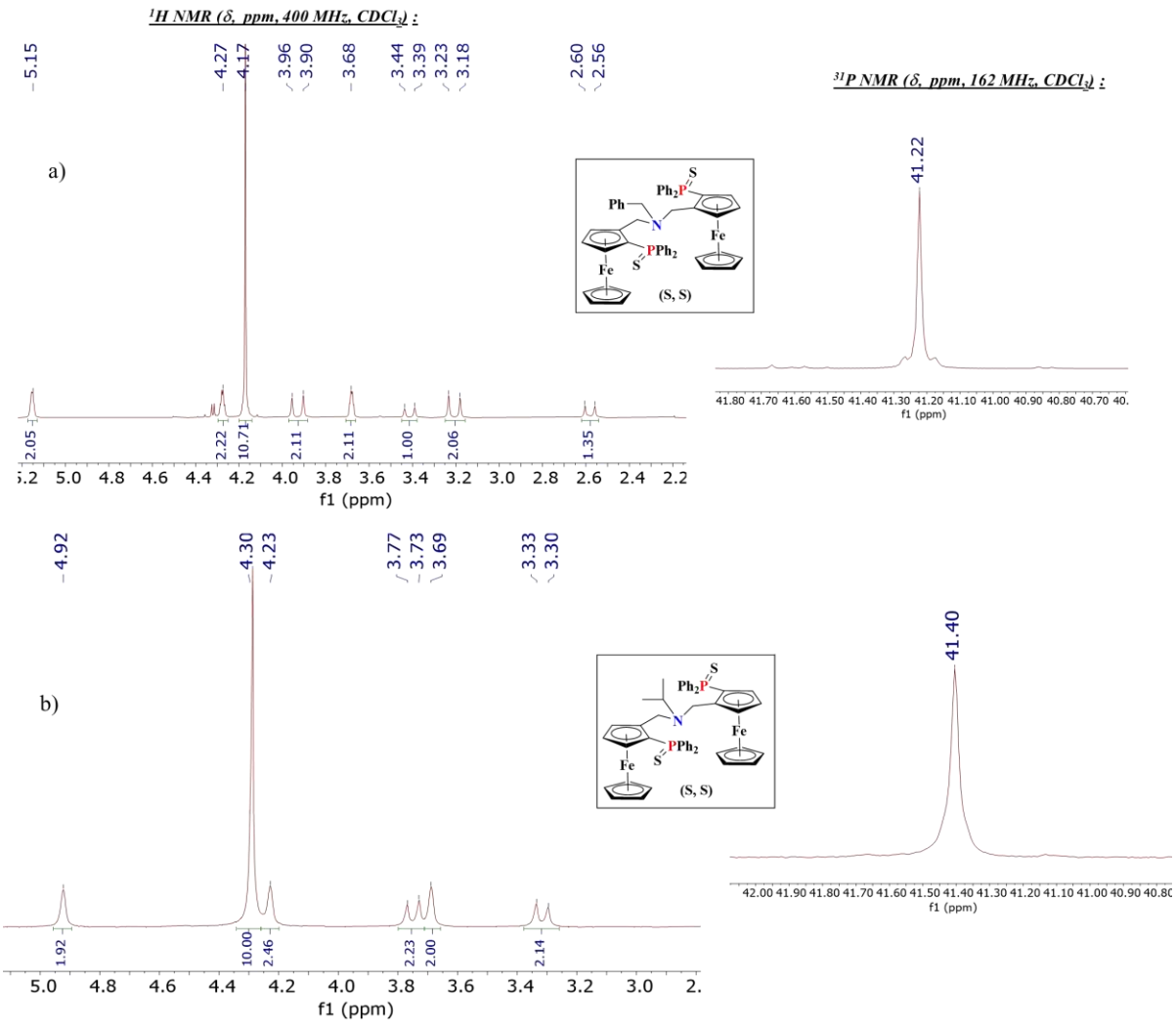

Figure 2. 10: ^{1}H ($CDCl_3$, 400 MHz) (Cp region) and ^{31}P NMR Spectra ($CDCl_3$, 162 MHz) of **2-50a** and **2-50b**

Figure 2. 10 shows the ^{1}H (Cp region) and ^{31}P NMR spectra of **2-51a** and **2-51b**. In case of **2-51a**, two sets of AB doublets were found in the ^{1}H NMR spectra. The peak intensity of one set of doublets (δ = 3.93, 3.21) is higher than that of the other set (δ = 3.43, 2.58) and thus represents the diastereotopic protons of the two identical C$\underline{H_2}$ groups attached to the Cp ring. The set of doublets with lower intensity corresponds the one C$\underline{H_2}$ group from the N-benzyl part. This was further confirmed by the integration value (~2 for δ = 3.93, 3.21 and ~1 for δ = 3.43, 2.58) [Figure 2. 10, a)]. In case of **2-51b**, AB doublets at δ = 3.75, 3.31 represent the C$\underline{H_2}$Cp protons. The multiplet at δ = 2.72 corresponds to the proton of the -C$\underline{H}$ group of the isopropyl (^{i}Pr) moiety [Figure 2. 10, b)]. The ^{31}P NMR spectra show peaks in similar regions for the two compounds (δ = 41.22 for **2-51a**; δ = 41.40 for **2-51b,** see Figure 2. 10).

Additionally, crystal structure of one of the proligands (**2-51b**) which was not obtained before, was established after the XRD- analysis of the orange single crystals grown by diffusion method in pentane-DCM (Figure 2. 11).

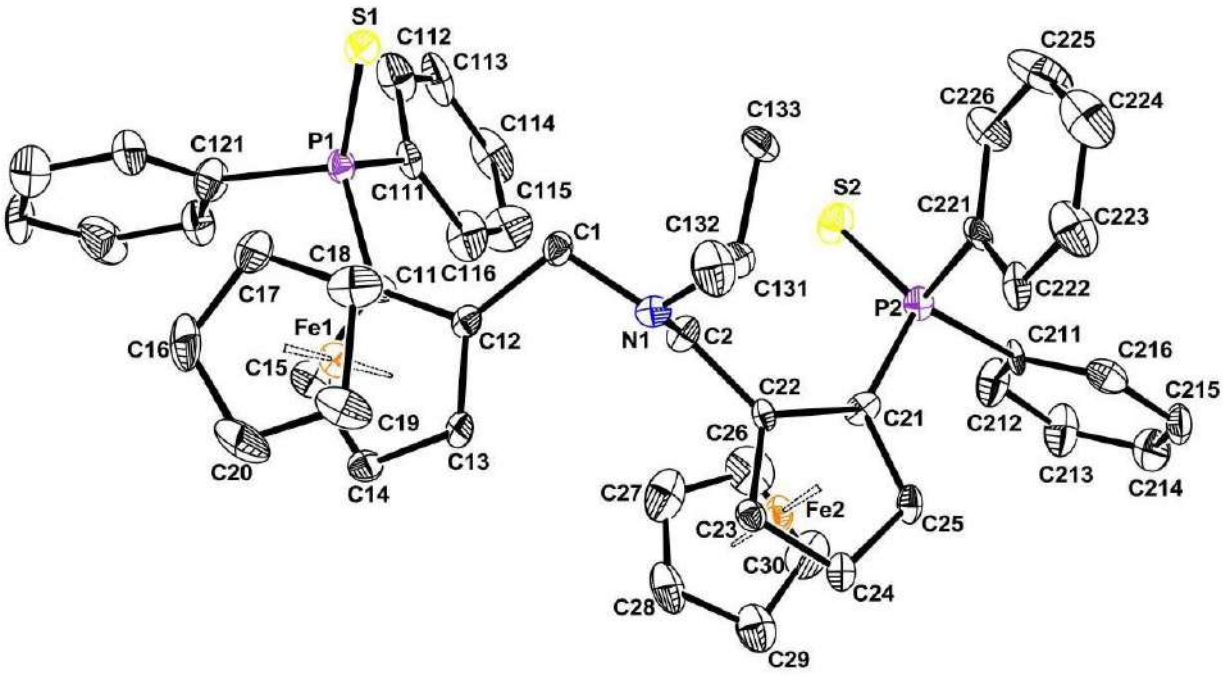

Figure 2. 11: Molecular view of compound **2-51b** showing 30% probability displacement ellipsoids and the atom numbering scheme. H atoms have been omitted for clarity

2. 11) Ligand Synthesis: Final Step

In general, the alkylation of secondary amines is comparatively easier considering the increasing nucleophilicity of amines (tertiary> secondary> primary). Alkyl halides are widely used as alkylating agents in this regard. Therefore, a simple protocol to couple benzyl ferrocenylamine and pyridylmethyl bromide in the presence of NEt_3 as base at room temperature was initially followed.[226] The desired tertiary amine was obtained, but only in low yields (10-20%). The plausible reason that can be anticipated for low yield in such reaction condition is most likely to be a side reaction between NEt_3 and the bromide. Although, the corresponding product has never been isolated in our case, there are several reports where ammonium ylides have been synthesized from benzyl halides using different trialkylamines (NEt_3, NMe_3, DABCO, Quincidine *etc*.).[227] A

typical example is given in Scheme 2. 27, where 4-chloromethyl-*N*,*N*-diethylbenzamide **2-52** is converted to its corresponding benzyltriethylammonium chloride **2-53** in presence of NEt_3.[227b]

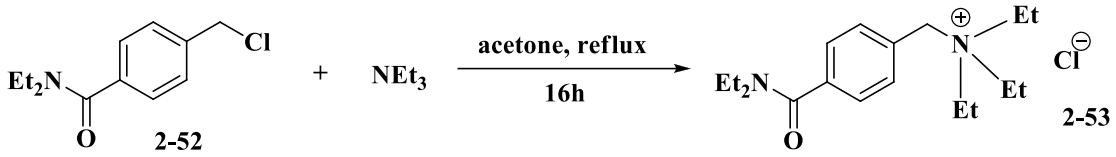

Scheme 2. 27: Preparation of ammonium chloride **2-53** reported by Kimachi *et al.*

In order to circumvent this obstacle, we found inspiration from the work of Liu *et al.* which reported that the tosylate of 5-nitro-1,3-bishydroxymehylbenzene **2-54** was cleanly substituted by dipicolylamine in the presence of Na_2CO_3 and KI (Scheme 2. 28).[228]

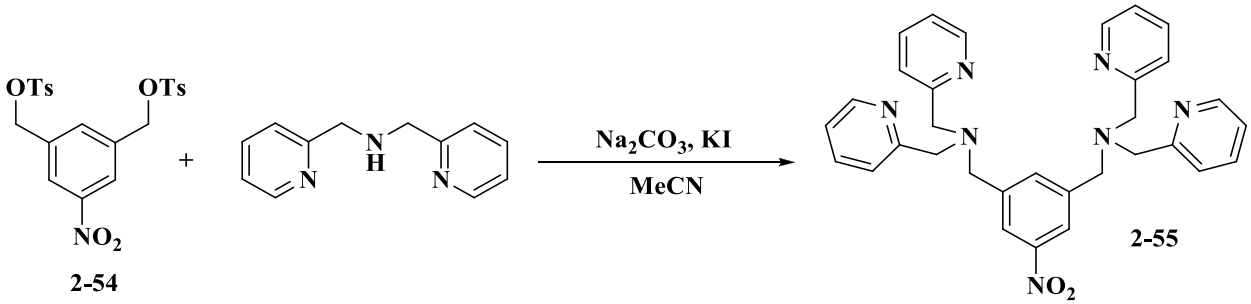

Scheme 2. 28: Substitution of **2-54** by dipicolylamine

Hence, we used pyridyl bromide or tosylate (**2-43a** or **b**) and ferrocenylamines **2-42** in the presence of K_2CO_3 in DCM (instead of the Na analogue in MeCN, used by Liu *et al.*). Two variants of **2-40** (R= Bn, ^{i}Pr) were synthesized (Scheme 2. 29).

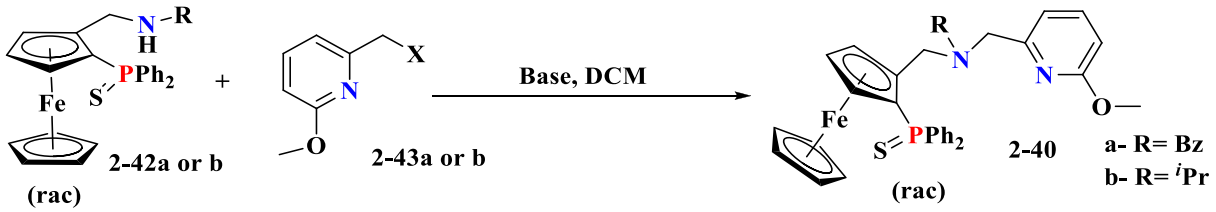

Scheme 2. 29: Synthesis of modified PNN proligand 2-40 in methoxy protected form

After a few optimizations, we could obtain the desired tertiary amines **2-40** in relatively good yields (Table 2. 2). In the presence of 2 equiv. pyridyl tosylate **2-43b** and 3 equiv. K_2CO_3 as base, the best yield (75%) so far was obtained for **2-40a** (R= Bn) (Table 2.2, Entry 3). Later on, **2-40b**

(R= ^{i}Pr) was synthsized with good yield (71%) by using 1.2 equiv. of **2-43b** and same equivalence of K_2CO_3 (3 equiv.) (Table 2. 2, Entry 5).

Table 2. 2: Optimization table for synthesis of the modified PNN ligand in methoxy protected form

Entry	-R	-X (equiv.)	Base (equiv.)	Reaction Time (h)	Yield (%)
1	-Bn (**a**)	-Br (1.5)	NEt_3 (2)	18	28
2	-Bn (**a**)	- OTs (1.5)	NEt_3 (1.5)	4-5	62
3	-Bn (**a**)	-OTs (2)	K_2CO_3 (3)	18	75
4	-Bn (**a**)	-OTs (1.2)	K_2CO_3 (3)	18	71
5	-*i*Pr (**b**)	-OTs (1.2)	K_2CO_3 (3)	18	70

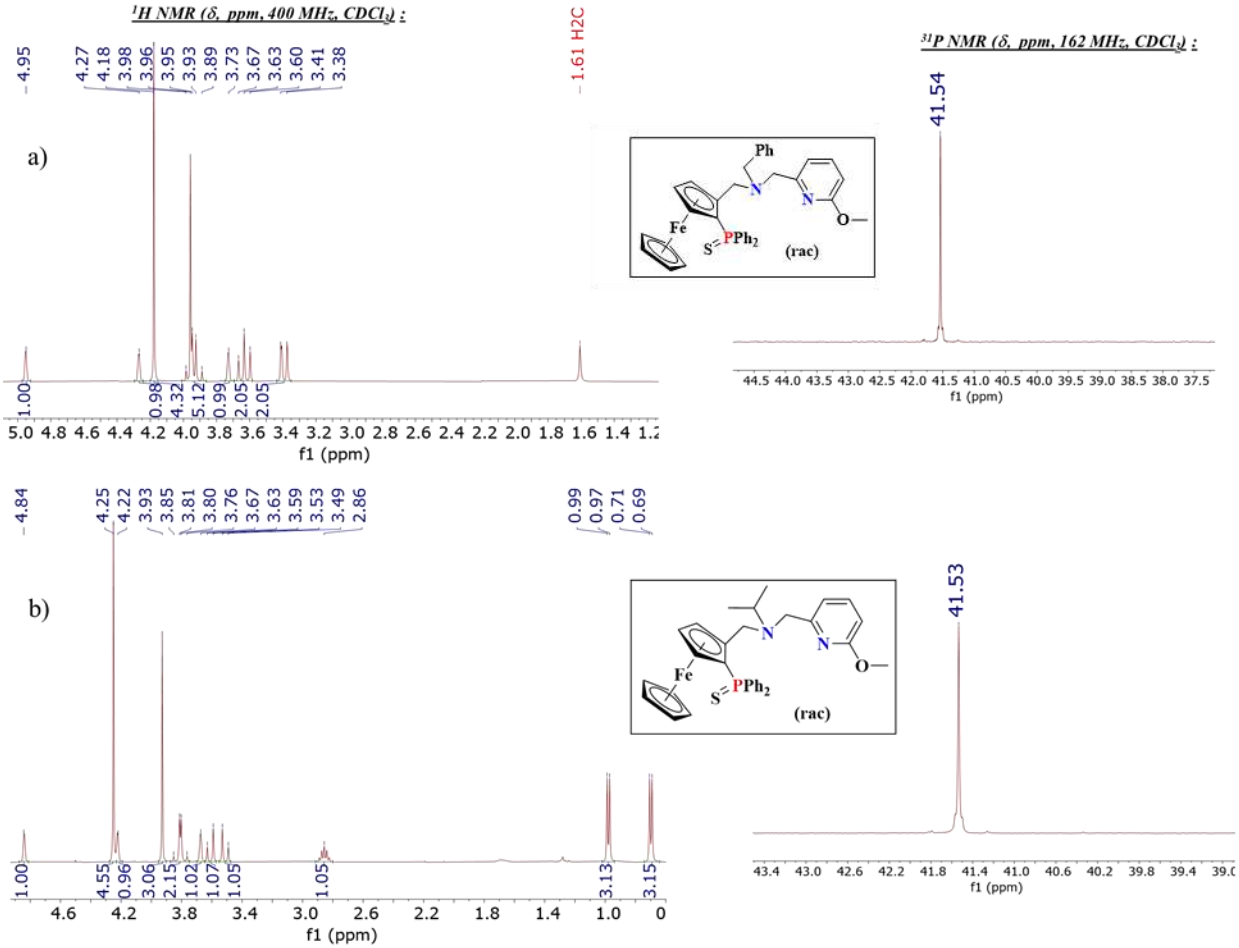

Figure 2. 12: ^{1}H ($CDCl_3$, 400 MHz) (Cp and aliphatic region) and ^{31}P NMR Spectra ($CDCl_3$, 162 MHz) of **2-40a** and **2-40b**

2-40a and **2-40b** were characterized by multinuclear NMR (^{1}H, ^{31}P, ^{13}C) spectroscopy and HRMS.

In case of **2-40a**, as expected, three distinct sets of AB-type doublets (δ = 3.97, 3.91; δ = 3.65, 3.394 and δ = 3.62, 3.391) were found in its ^{1}H NMR spectrum [Figure 2.12, a)]. Two distinct sets of AB-type doublets were also observed for **2-40b** (δ = 3.83, 3.78 and δ = 3.61, 3.51). The protons of the two inequivalent isopropyl methyl groups in **2-40b** appeared as non-identical doublets (δ = 0.98 and 0.70); the C<u>H</u> proton was identified as a multiplet at δ = 2.86 [Figure 2.12, b)]. The pyridyl OCH_3 group gives a singlet at δ = 3.96 and δ = 3.93 for **2-40a** and **2-40b**, respectively. The ^{31}P NMR spectra show peaks in similar region for the two compounds (δ = 41.54 for **2-40a**; δ = 41.53 for **2-40b,** see Figure 2.12).

The molecular structure of the benzyl variant **2-40a** was established by X-ray diffraction from the grown monocrystals (Figure 2. 13).

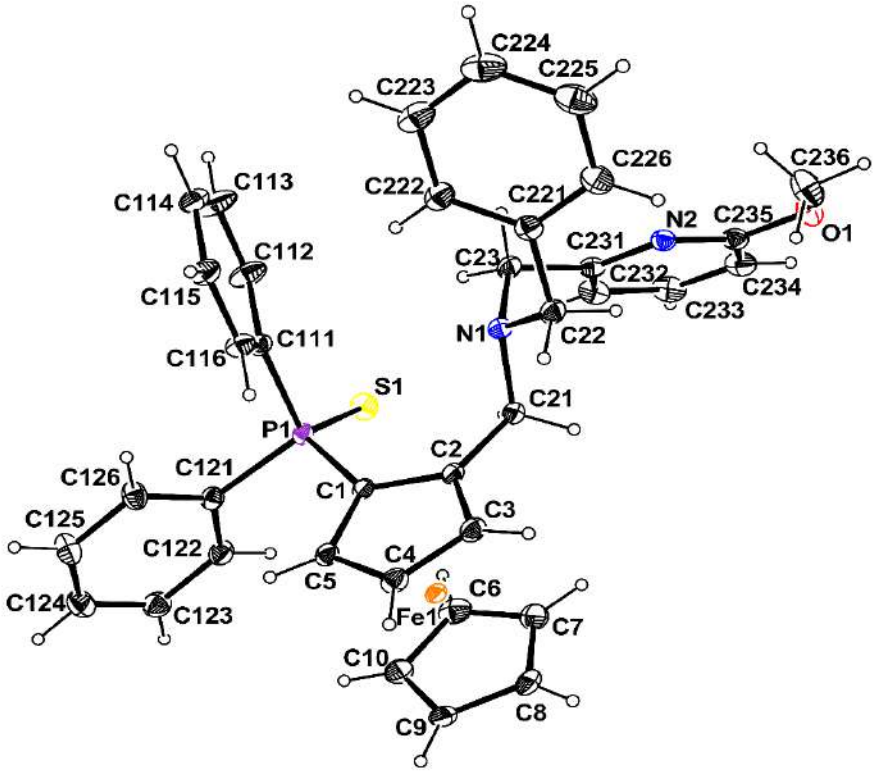

Figure 2. 13: Molecular view of **2-40a** showing 30% probability displacement ellipsoids and the atom numbering scheme. H atoms are represented as small sphere of arbitrary radii.

This structure is related to that of the analogue with a pyridylaminomethyl substituent (**2-28c**, Figure 2.2) with a N-benzyl in place of the N-tosyl substituent and the addition of the pyridine *ortho* substituent. The C2-C21-N1-C22 and C2-C21-N1-C23 torsion angles chains are respectively 85.2(1)° and -143.32(7) °. The S1 atom is as usual -0.884(2) Å from the Cp ring plane

whereas, the P1 atom is slightly above the plane by 0.145(1) Å. The N1 and pyridine N2 atoms are 1.312(2) Å and 0.868(3) The presence of the benzyl substituent on the N1 atom forces the pyridine to rotate to minimize the steric interactions. The benzyl phenyl and the pyridine rings make a dihedral angle of 56.20(3)°. The orientation of the benzyl group is influenced by the occurrence of a C-H...π interaction involving the benzyl C222 atom and the C111-C116 phenyl ring centroid (C---centroid = 2.95 Å; C-H---centroid = 161°). The two Cp rings are slightly staggered with a twist angle of 18.5°. Owing to the centrosymmetry of the space group, the unit cell contains the two enantiomers.

The OMe deprotection was tried with two different reagents, namely BBr_3[229] and the relatively mild L-selectride.[230] Unfortunately, the BBr_3 treatment led to product decomposition, whereas, L-selectride did not result in any reaction even after keeping at higher temperatures and for longer reaction times relative to the reported procedure (Scheme 2. 30).

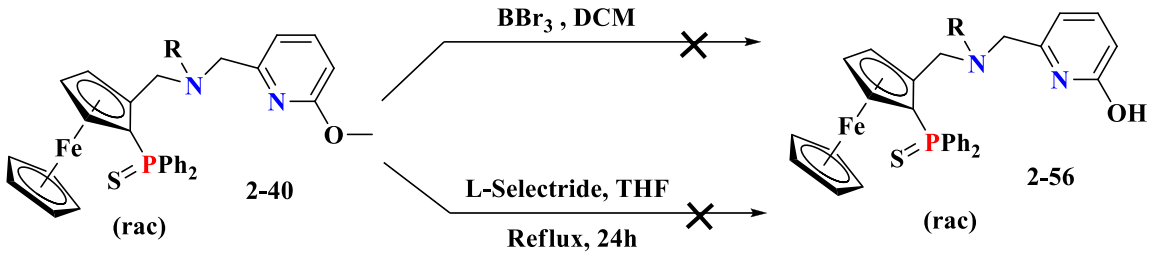

Scheme 2. 30: Failed attempts of methoxy deprotection

Further work on to the hydroxide deprotection is ongoing. Once compound **2-39** will be in hand, the synthesis of the target ligand **2-39** will be completed by the phosphine deprotection.

2. 12) Conclusion

Two similar types of phosphine containing tridentate tertiary ferrocenyl amine ligands in their protected form (phosphine and hydroxy) have been synthesized and fully characterized (NMR, mass spectrometry and X-ray crystallography). These ligands are the final products resulting from the coupling of a phosphine-containing ferrocenyl alcohol or amine and different substituted pyridine derivatives. The synthetic intermediates and unexpected byproducts that formed during the course of the various reactions were thoroughly characterized by NMR, mass spectrometry and X-ray crystallography (in a few cases). The Mitsunobu condition was screened for the synthesis of the phosphine-protected form (**2-2**) of ligand **2-1**. The free phosphine form was also obtained

in one case (**2-1a**) by phosphorus deprotection with $P(NMe_2)_3$. Compounds **2-40 (a** and **b)** which are the hydroxyl and phosphine protected form of ligands **2-39**, were prepared by base-mediated coupling of a ferrocenyl amine and a substituted pyridyl tosylate. However, the methoxy deprotection still need to be achieved using other techniques along with the optimization of the existing ones (BBr_3, L-seletride). We believe that once this obstacle will be removed, the ligand-**2-39** will be accessible by further phosphorus deprotection (which worked well to prepare ligand-**2-1a**; see Scheme 2. 16) to be screened for catalysis.

Chapter-3: New Tridentate Phosphine-Containing Secondary Ferrocenyl Amine Ligands

3. 1) Introduction

The activation of bonds by metal complexes where both metal and ligand play synergistic roles is known as metal-ligand bifunctionality or co-operativity. This interesting phenomenon adds great impact in organometallic chemistry by intensifying the further quest for ligand development and their applicability in transition metal-based catalysis.[231]

Noyori originated the 'Metal-Ligand Bifunctional Catalysis' terminology.[232] Either hydrogenation or transfer hydrogenation of C=N and C=O bonds, following an outer-sphere and/or inner-sphere mechanism, can be influenced significantly depending upon the ancillary ligand framework and the ability to provide bi-functionality.[19]

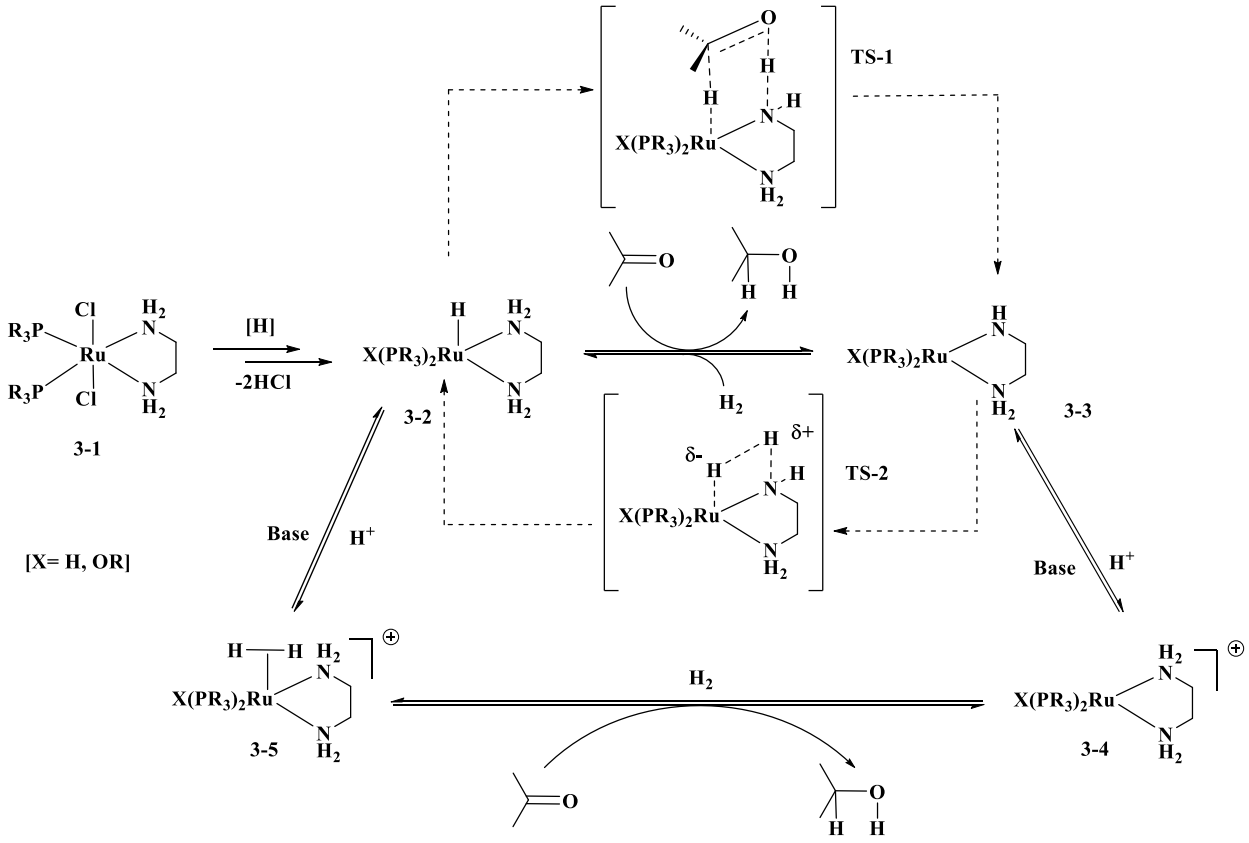

Scheme 3. 1: Mechanistic model of M-L Bifuntionality proposed by Noyori *et al.*

A mechanistic model was proposed earlier by Noyori *et al.* (2001), where a pathway for ketone transfer hydrogenation catalyzed by $[RuCl_2(PR_3)_2(NH_2CH_2CH_2NH_2)]$ complex **3-1** was outlined (Scheme 3. 1).[233] It involves a metal hydride species **3-2**, typically formed by β-H elimination from an alkoxide after Cl/alkoxide exchange. The NH_2 proton and the hydride from the metal

center are transferred to the ketone via **TS-1** to yield **3-3**, which can then be transformed back to **3-2** by H_2 addition via **TS-2**. The ligand geometry and the electrostatic attraction between the hydridic Ru-H atom and the protonic N-H atom allows these two bonds to be aligned during the course of hydrogen transfer in **TS-1**.[19] It is also possible in principle to envisage the same transformation via the corresponding protonated species **3-4** and **3-5**, but the catalyst in more active in the presence of base, leading the authors to propose that the transformation proceeds preferentially through a cycle involving **3-2** and **3-3**. The assisting ligand being a primary diamine in this case, the bifunctional activity can also be seen as the 'N-H effect'.[19]

Milstein *et al.* highlighted two major modes of H_2 bond activations (activation through M-L bonds; aromatization/dearomatization) by means of metal-ligand cooperativity or bifunctionality; as a primary step necessary for the catalytic hydrogenation of unsaturated substrates containing a polar bond. The bond activation mode mostly depends upon the type of metal-ligand bond (M-N, M-S, M-B, M-O, *etc.*) and ligand framework, for instance lutidine- or picoline-based tridentate pincer ligands- (PNN, PNP, NNN), amino-pyridine based ligands, fused N-heterocyclic ligands, imidazole- and pyridine-based NHC ligands- *etc.*[234]

A number of bifunctional catalytic systems with the additional effect of ligand chirality have been developed till now and they have been effective for the asymmetric hydrofunctionalization of unsaturated polar bonds with good to excellent enantioselectivities. A few typical examples, worth mentioning, are- *(S)*-BINAP-$RuCl_2$-*(S)*-DPEN (**3-6**) developed by Noyori *et al.*,[235] Ir-SpiroPAP systems (**3-7**) developed by Zhou *et al.*,[73c] ferrocene-based PNN ligands and their corresponding metal complexes (**3-8**) developed independently by Zhang[236] and Clarke[110] (Scheme 3. 2).

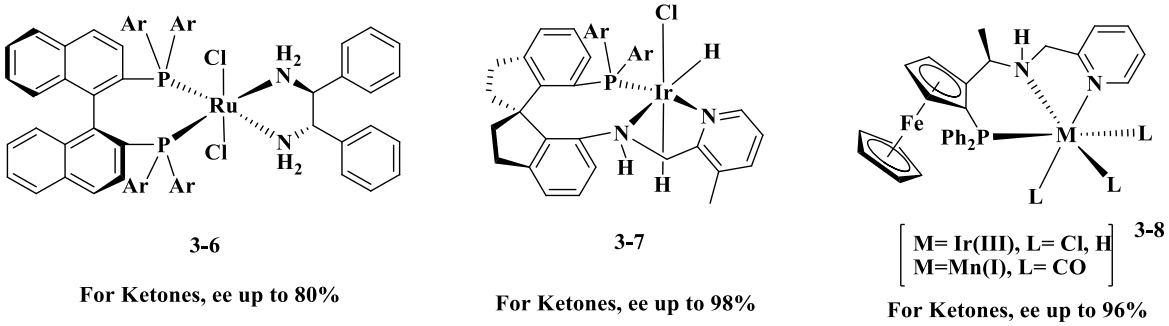

Scheme 3. 2: A few Chiral Bi-functional Catalyst Systems

Inspired by the achievements of these bifunctional catalyst systems, we designed two new tridentate phosphine-containing ferrocenyl ligands bearing an N-H group as the potential source of metal-ligand bifunctionality (Scheme 3. 3). Ligand **3-9** contains one phosphine heteroatom center and two nitrogen heteroatom centers (P, N, N coordination pattern). The other ligand **3-10** comprises one nitrogen heteroatom center flanked by two phosphine heteroatom centers (P, N, P coordination pattern).

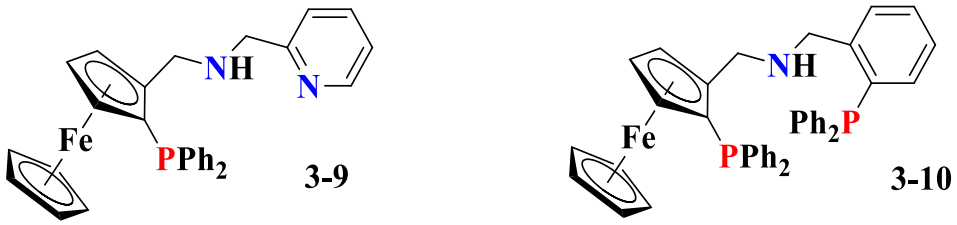

Scheme 3. 3: Molecular formula of the two designed ligands

A short literature review of a few reported tridentate phosphine containing ferrocenyl ligands will be presented in the next section (3.2), followed by the synthesis of the two ligands depicted above.

3. 2) Synthetic methods of different amine-containing (NH and non-NH) tridentate ferrocenyl phosphine ligands

In Chapter 1, a few recently developed phosphine-based ferrocenyl tridentate ligands were discussed in terms of their utilization in asymmetric hydrogenation of various substrates. The synthetic protocols to prepare those ligands (both NH and non-NH) are the main focus for this chapter. The commercially available Ugi's amine, once again, has been the most convenient, chiral, ferrocene-containing starting material for most of the tridentate ligands. In this regard, Zhang *et al.* developed f-Amphox, f-Amphol and f-Ampha, which are similar kinds of amine-containing ferrocenyl phosphine ligands.

Tridentate ferrocenyl aminophosphoxazoline or f-Amphox ligands involve various chiral oxazoline and ferrocenyl amino phosphine motifs and were synthesized as shown in Scheme 3. 4. At first, PPFA (**2-3**) was prepared as the synthetic intermediate as previously discussed (see Scheme 2. 2) by diastereoselective *ortho*-lithiation of Ugi's *(S)*-amine, followed by treatment with $ClPAr_2$. After reaction of PPFA with Ac_2O at 100 ^oC and subsequent treatment with excess ammonia in a water-methanol-THF mixture, the dimethyl amino group was substituted by an NH_2 group to form **3-11**. The intermediate **3-11** was subsequently reacted with various 2-

chloromethyloxazoline in the presence of K_2CO_3 as hydrogen chloride scavenger, generating various f-Amphox ligands **3-12** in good yields. One of the planar chiral diastereomers, **3-12a**, was synthesized separately starting from Ugi's *(R)*-amine, using the same synthetic route.[116b]

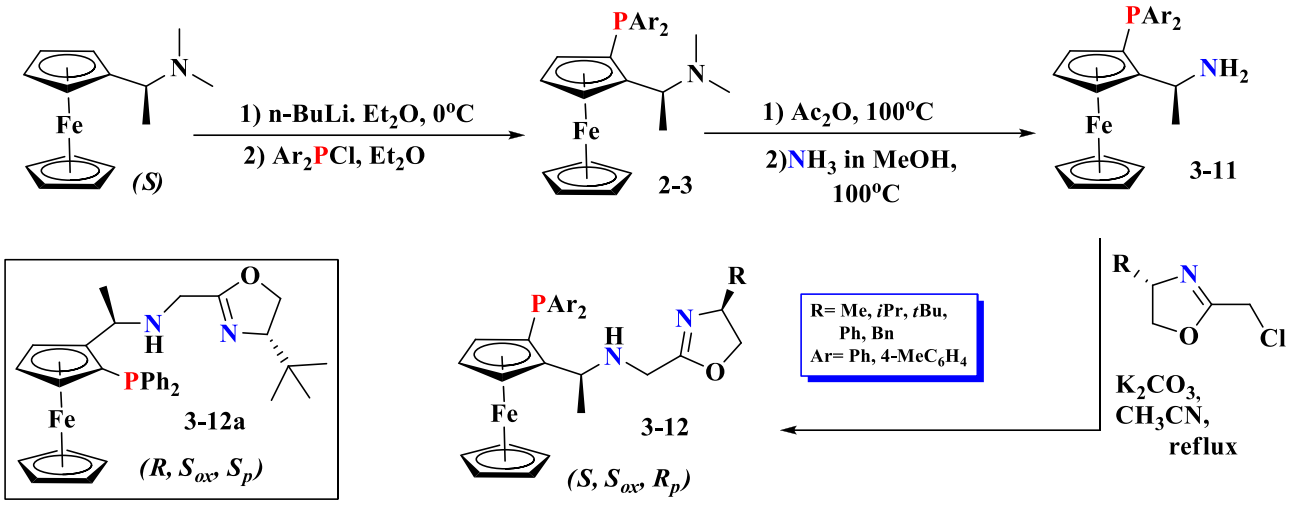

Scheme 3. 4: Synthesis of f-Amphox ligands

f-Ampha ligands are tridentate ferrocene-based amino phosphine acids. This kind of ligands with high air stability were easily prepared via a simple synthetic route (Scheme 3. 5)[116c, 237] by introducing a chiral amino acid on the ferrocenyl phosphine motif. Starting from Ugi's *(S)*-Amine, the PPFA intermediate was obtained by a slightly different procedure in this case (use of PCl_3 and a Grignard reagent instead of Ar_2PCl). PPFA was then converted to its acetate analogue **3-13** by treatment with acetic anhydride at elevated temperatures. **3-13** was then reacted with amino acid *(S)*-2-amino-3,3-dimethylbutanoic acid via condensation in MeOH, generating various f-Ampha ligands, **3-14**. The other planar diastereomer **3-14a** was also produced for one specific ligand to investigate the relationship between the stereoselectivity and the ligand configuration.

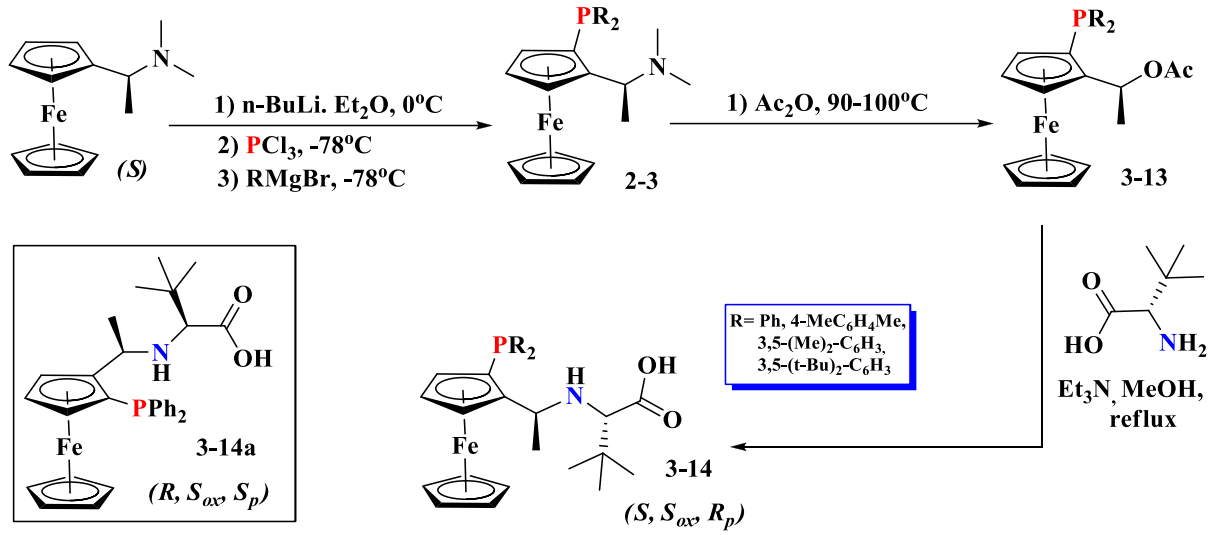

Scheme 3. 5: Synthesis of f-Ampha

Ferrocene-based aminophosphine alcohols **3-15** and **3-16**, known as f-Amphol ligands, were obtained through the condensation of the acetates **3-13** with inexpensive and easily available chiral amino alcohols (Scheme 3. 6).[116a]

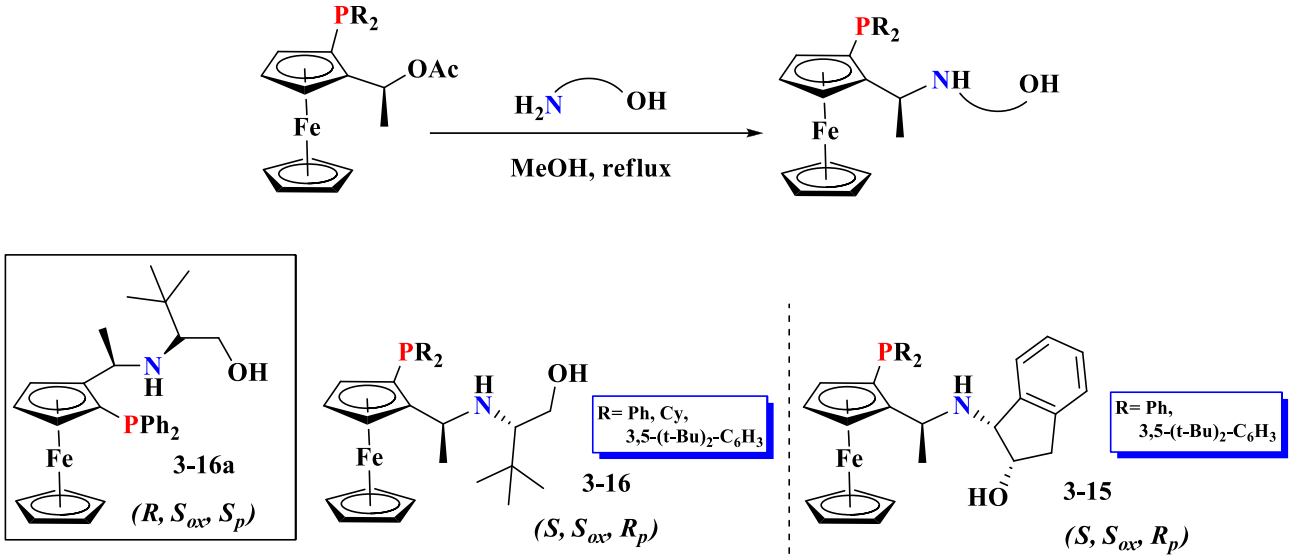

Scheme 3. 6: Synthesis of f-Amphol ligands

The catalytic applications of these three analogous ligands in asymmetric hydrogenation have already been briefly discussed in chapter 1. There are a few other unsaturated substrates that were successfully hydrogenated with good enantioselectivities exploiting these chiral ligands. For example, f-Amphox ligands were further utilized for the Ir-catalyzed asymmetric hydrogenation of α-haloketones (ee > 99%),[238] β-ketoamines (dr > 99/1, ee > 99%),[239] styrylglyoxylamides (ee

up to 98%).[240] f-Amphol was proven excellent for the Ir-catalyzed asymmetric hydrogenation of benzo-fused 5-7 membered cyclic ketones (ee > 99%).[241] Finally, f-Ampha is particularly useful for the Ir-catalyzed asymmetric hydrogenation of cyclic 1,3-diketones to disymmetric monohydroxy ketones (dr up to 50/1, ee up to > 99%).[242]

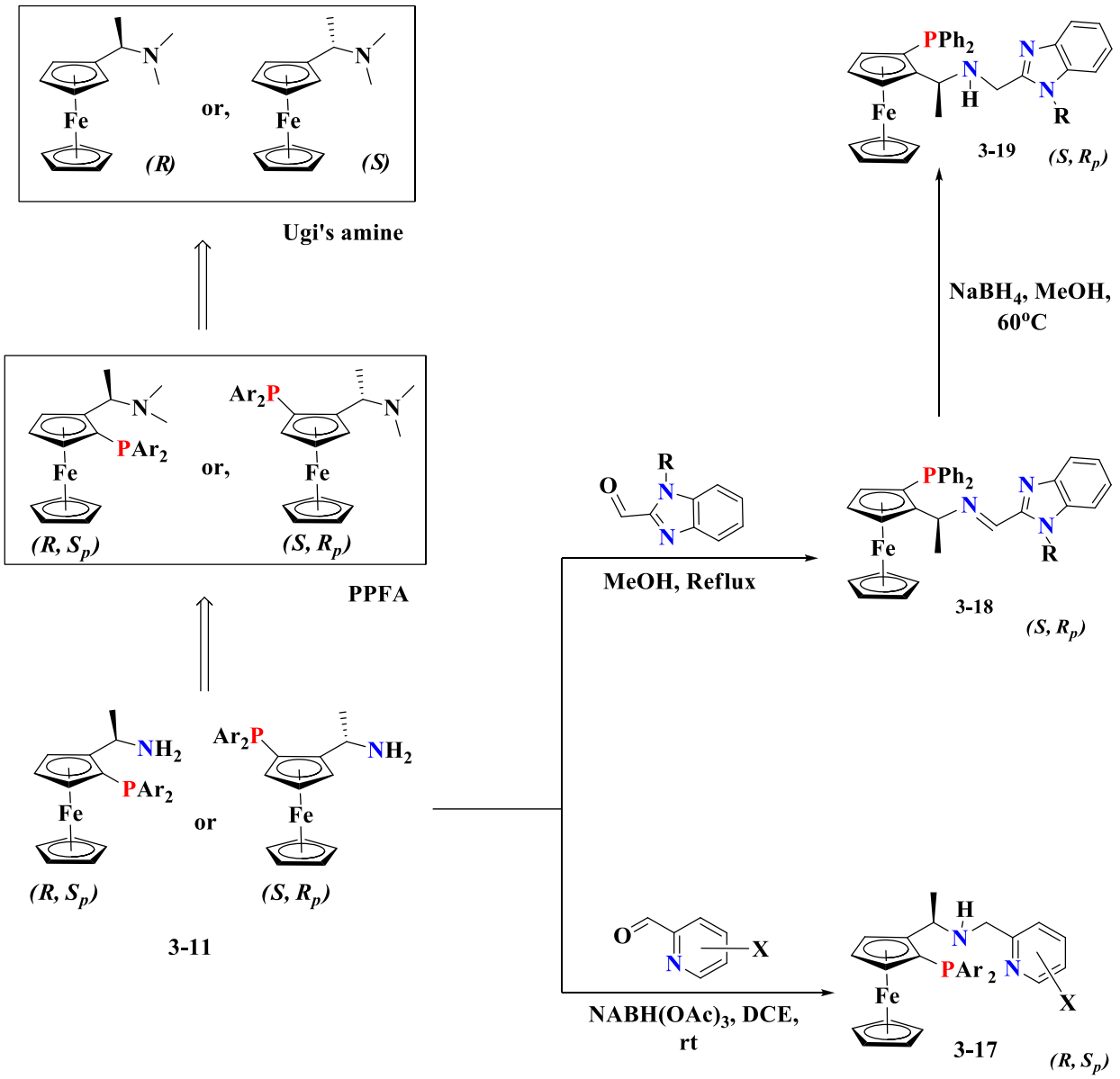

Scheme 3. 7: Synthesis of ferrocenyl PNN ligands

Zhong and Zhang *et al*. independently, developed PNN type phosphine-based ferrocenyl tridentate ligands in a similar way. Ligands **3-17** [109] and **3-19**[111-112] were prepared by condensation of

amine **3-11** with substituted pyridinecarboxaldehyde and imidazolinecarboxaldehyde, respectively, followed by subsequent reduction of the imine intermediate **3-18** (Scheme 3. 7).

Hu *et al*. prepared ligands **3-21**, similar to **3-17** but with an additional stereogenic center. The condensation step was carried out using a pyridyl ketone rather than the corresponding aldehyde. Subsequent reduction by H_2 on Pd/C of the intermediate imine **3-20** resulted in the ligand **3-21** (Scheme 3. 8). Ligands **3-21** were utilized for the Ir-catalyzed diastereo- and enantioselective hydrogenation of α-alkyl-β-ketoesters via dynamic kinetic resolution (dr up to 95/5; ee up to 95%).[243]

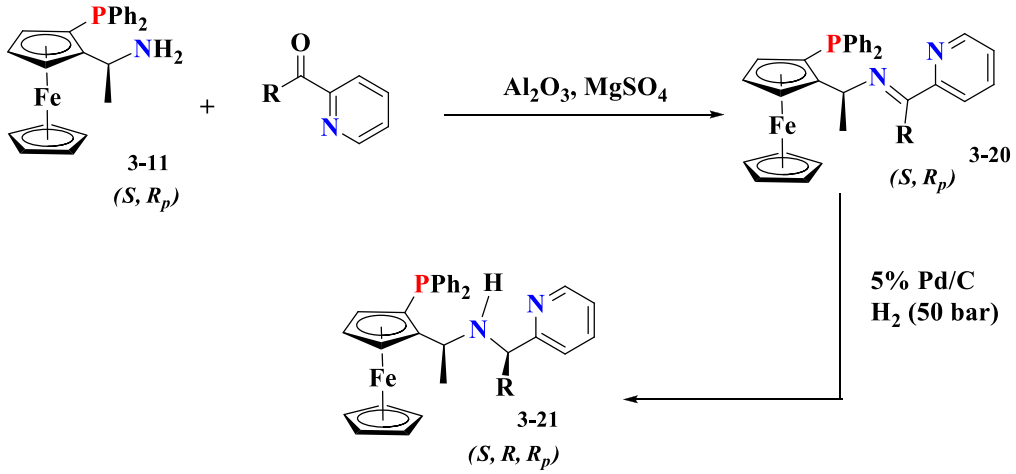

Scheme 3. 8: Synthesis of ligands **3-21** reported by Hu *et al.*

Most of the above-described ligands were utilized in various asymmetric hydrogenation and transfer hydrogenation reactions (see chapter 1). In addition, ligand **3-21** with R = H was used for the Ru-catalyzed asymmetric cyclopropanation of styrene with ethyl diazoacetate,[244] the Pd-catalyzed allylic substitution,[245] the Cu-catalyzed [3+3] cycloaddition of racemic propargylic esters with cyclic enamines[246] and 5-pyrazolones,[247] and for the Cu-catalyzed asymmetric substitution or alkylation of racemic propargylic esters with primary and secondary amines,[248] β-keto esters,[249] acyclic enamines,[250] oxindoles,[251] *etc*.

Another variety of ferrocenyl PNP ligands where Ugi's amine was used in a slightly different approach (**3-25**), was reported by Zhang *et al*. Ligands **3-25** contain two different phosphine groups, both linked to side chains rather than to the ferrocene ring. The synthesis involves a few steps (Scheme 3. 9): *ortho*-halogenation of Ugi's amine, substitution of the dimethylamino group

by a phosphine moiety followed by phosphine protection, formylation of the cyclopentadienyl ring, condensation of the phosphine-protected ferrocenecarboxaldehyde **3-24** and imine formation with chiral phosphino amines followed by reduction.[115]

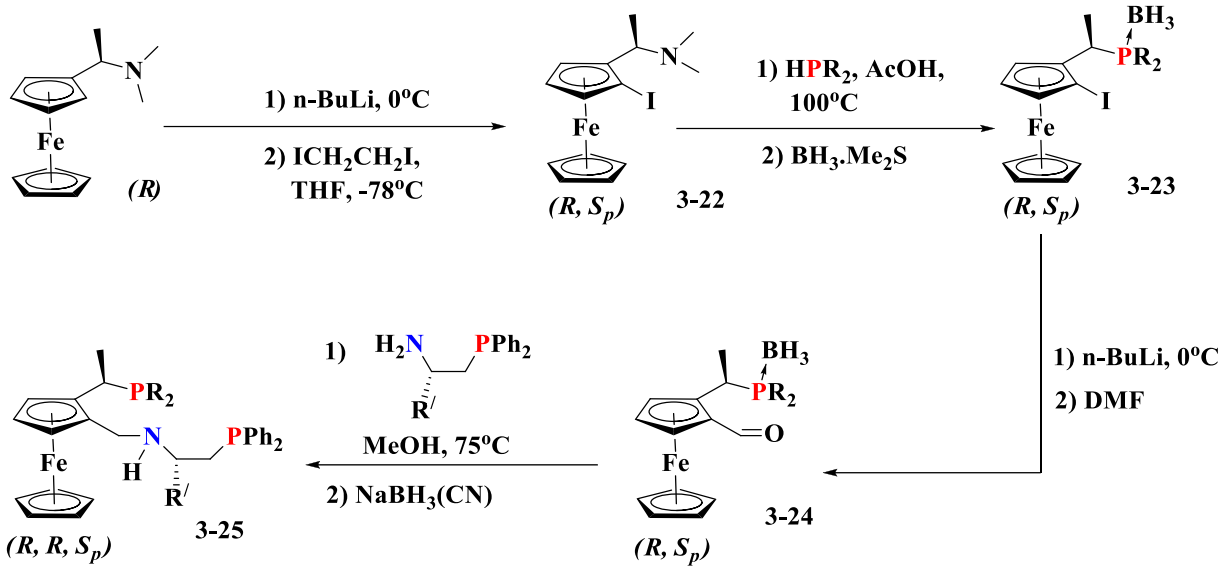

Scheme 3. 9: Synthesis of ligand **3-25** reported by Zhang *et al.*

Zikarzadeh *et al.* synthesized a series of PNP-type ferrocenyl tridentate ligands starting from either Ugi's amine or other ferrocene-containing starting materials. Ligand **3-26**, obtained by reaction between the amine and the corresponding acetate species (Scheme 3. 10), features two identical phosphine-containing ferrocenyl species.[252]

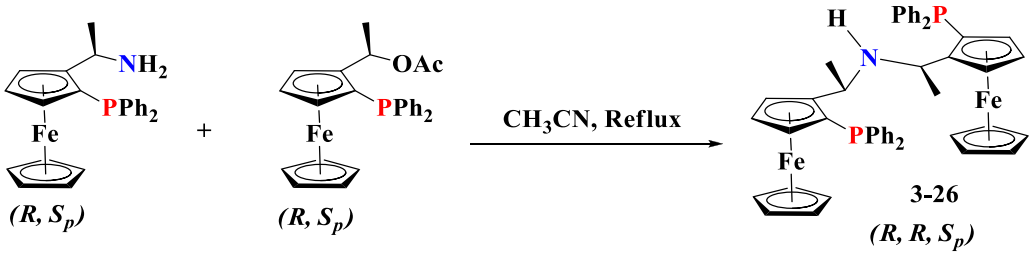

Scheme 3. 10: Synthesis of Ligand **3-26** Zikarzadeh *et al.*

The analogous PNP ligand **3-30**, without the α-C stereocenter, was also developed by the same authors. In this case, the ligand was prepared by reductive amination of the aldehyde **3-27** by the amine **3-28** (Scheme 3. 11). The starting materials were obtained by the Kagan methodology.[200a]

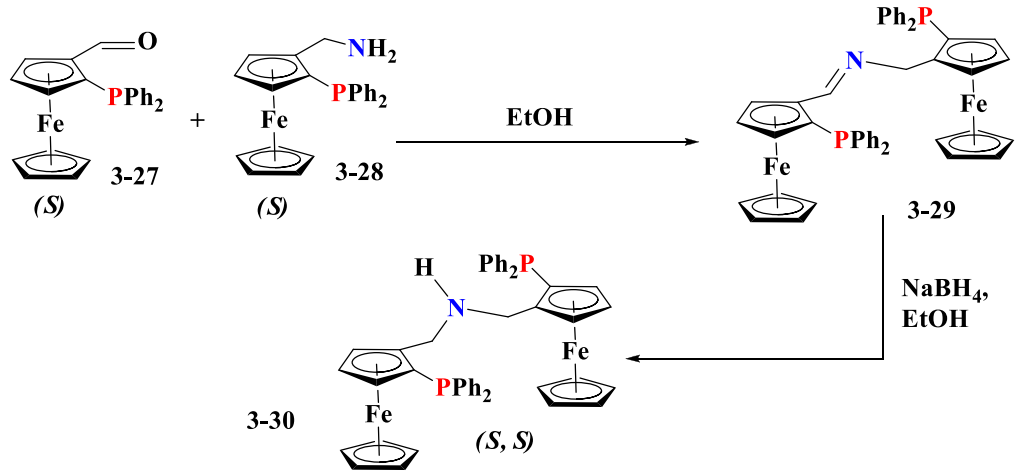

Scheme 3. 11: Synthesis of ligands **3-30**

They also prepared PNP ligands **3-31a** and **b** with phosphine-containing chiral side chains by condensation between ferrocene aldehyde and the corresponding aminophosphine species (Scheme 3. 12).[113]

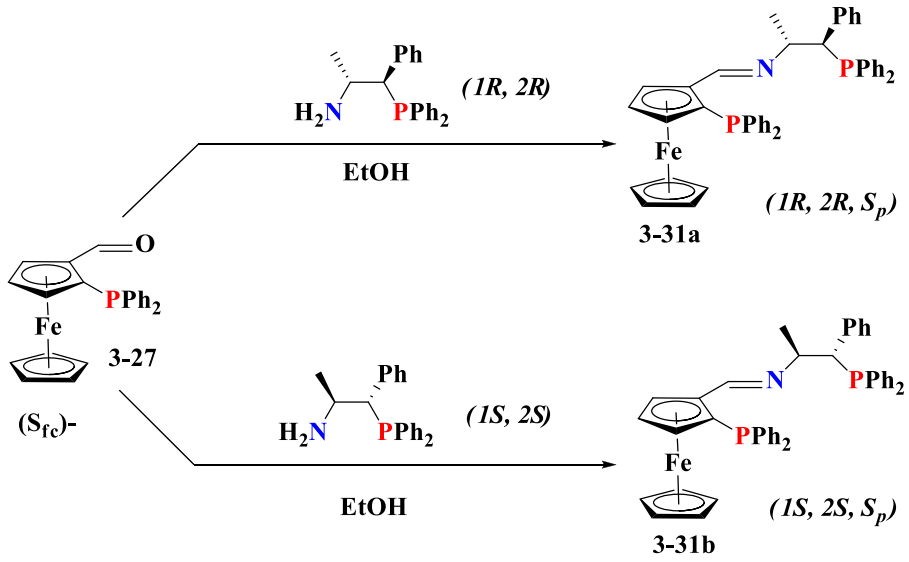

Scheme 3. 12: Synthesis of ligands **3-31**

The ligands shown in Scheme 3. 10, Scheme 3. 11, Scheme 3. 12 were utilized for complexation with Fe^{II} salts ($FeBr_2$). A few of the resulting complexes were proved excellent in asymmetric hydrogenation (see chapter 1).

3. 3) Synthesis of Pro-ligand 3-32

The sulphur-protected form **3-32**, of the target ligand **3-9** was obtained by the HBF_4 method from the ferrocenyl alcohol **2-29** and a large excess of commercially available 2-picolylamine (Scheme 3. 13). Although the desired product was indeed formed, the yield was moderate (48%) and several byproducts were formed, indicating probable product decomposition.

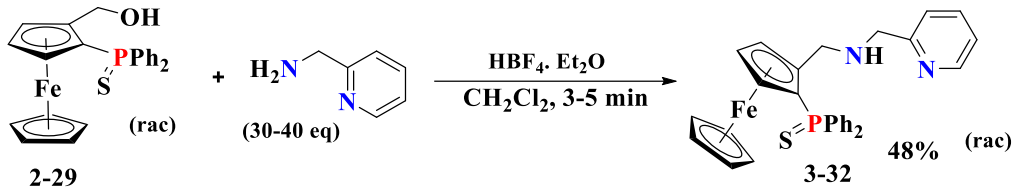

Scheme 3. 13: Preparation of 3-32 by HBF_4 method

The new compound **3-32** was characterized by multinuclear NMR spectroscopy and mass spectrometry (HRMS). In the ^1H NMR spectrum of **3-32**, 14 aromatic protons were found as multiplets in the aromatic region (pyridyl protons: δ = 8.48, 7.09, 7.04; PPh_2 protons: δ = 7.87-7.79, 7.72-7.63, 7.57-7.47, 7.40-7.32). The multiplets at δ = 4.62, 4.31, 3.78 and the singlet at δ = 4.33 are due to the three non-identical protons of the substituted Cp ring and the five equivalent protons of the unsubstituted Cp ring, respectively. Two AB-type doublets assigned to the two different CH_2 groups are found at δ = 4.28, 3.63 and δ = 3.73, 3,65. The ^{31}P NMR spectrum showed a single peak at δ = 41.36 (Figure 3. 1).

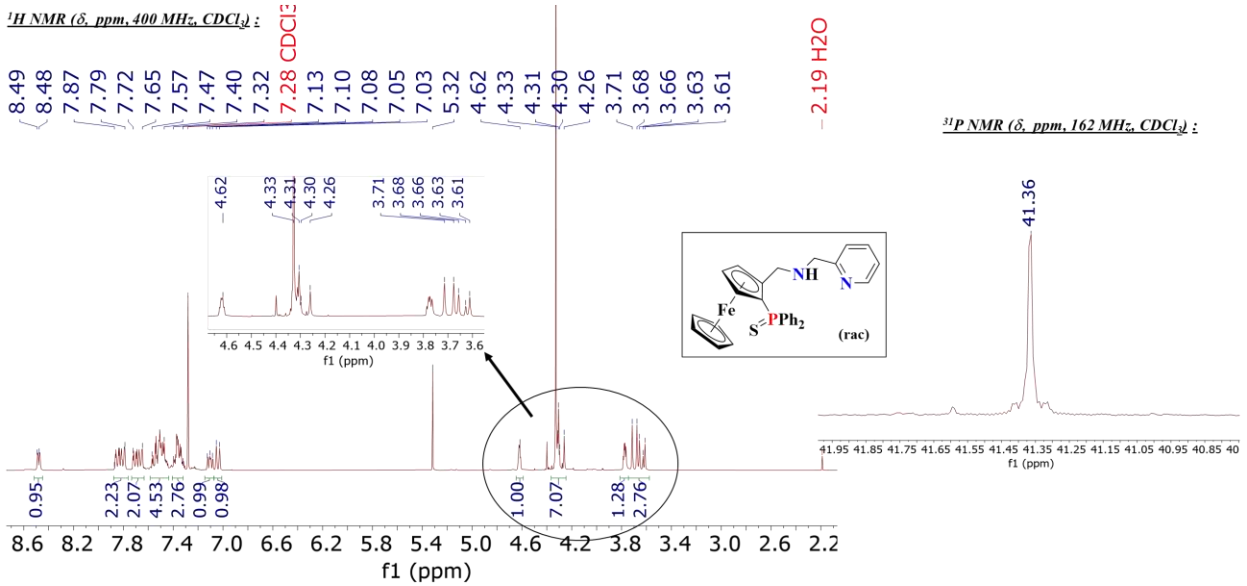

Figure 3. 1: ^1H and ^{31}P NMR Spectrum ($CDCl_3$, 400 MHz) of **3-32**

Single crystals of **3-32** could be grown by the slow diffusion of pentane-DCM solution. The molecular view is shown in Figure 3. 2.

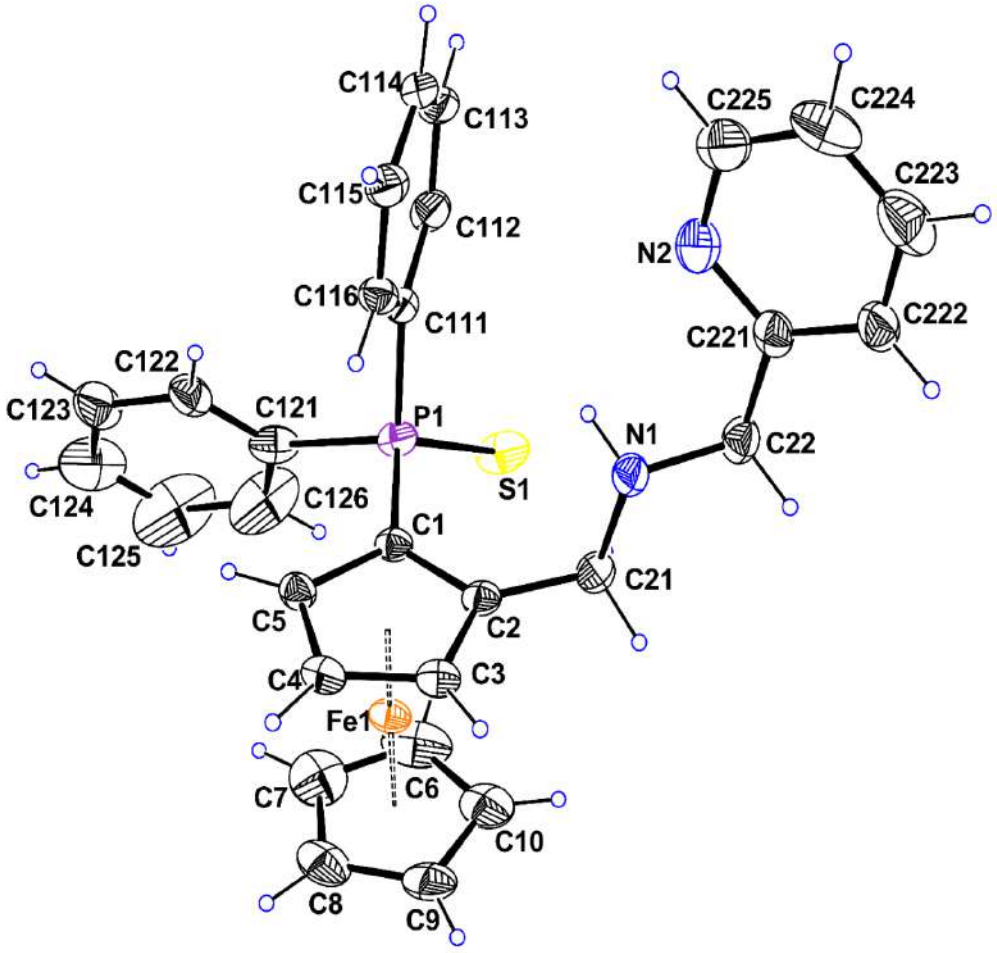

Figure 3. 2: Molecular view of compound **3-32** showing 50% probability displacement ellipsoids and the atom numbering scheme. H atoms are represented as small sphere of arbitrary radii.

The C2-C21-N1-C22 torsion angle is 177.5(2)°, *i.e.*- the four atoms are nearly coplanar. The S1 atom is as usual -0.92(4) Å from the Cp ring plane, whereas the P1 atom is slightly above the plane by 0.097(3) Å. The N1 atom and pyridine N atom are 1.479(4) Å and 3.883(5) Å above the Cp ring plane, respectively. The pyridine and the Cp ring make a dihedral angle of 81.80(8)°. The two Cp rings are slightly staggered with a twist angle of 10.1°.

To improve the yield, other synthetic methods were considered. The Mitsunobu conditions turned out yet again unsuccessful for the same reasons mentioned earlier (see section 2.5) with the additional generation of decomposed byproducts. Reductive amination[253] was then examined as

an alternative possibility. In this regard, the previously mentioned ferrocenylaldehyde **3-27** was prepared beforehand by oxidation of the alcohol **2-29** (Scheme 3. 14) following a previously reported procedure,[192a] which uses N-morpholine oxide (NMO) as the oxidizing agent and $[Ru(Cl)_2(PPh_3)_3]$ as catalyst.

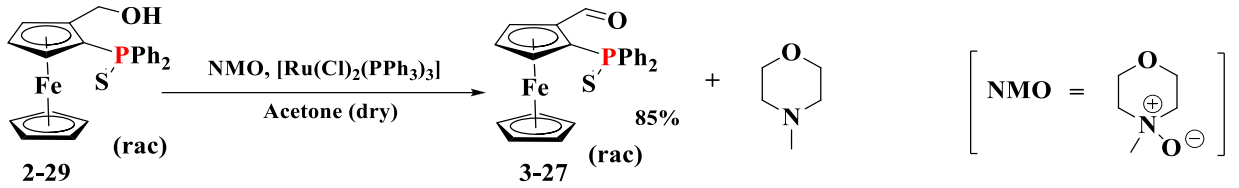

Scheme 3. 14: Oxidation of ferrocenyl alcohol **2-29**

2-Picolylamine was added to a solution of the aldehyde **3-27** in methanol, followed by *in situ* addition of $NaBH_4$.[202] Unfortunately, the desired imine product did not form. Rather, reduction of **3-27** to yield the precursor alcohol **2-29** was observed. No indication of imine formation (before adding the reducing agent) could be obtained, even after changing the reaction solvent (DCM, Et_2O, THF) or increasing reaction time and temperature.

Only when acetone was used as solvent under refluxing conditions, a reaction took place to yield species **3-33** (Scheme 3. 15), which is the aldol adduct of the ferrocenecarboxaldehyde **3-27** and acetone, as the major product. This shows the role 2-picolylamine as a base rather than as a reactant- in this particular case.

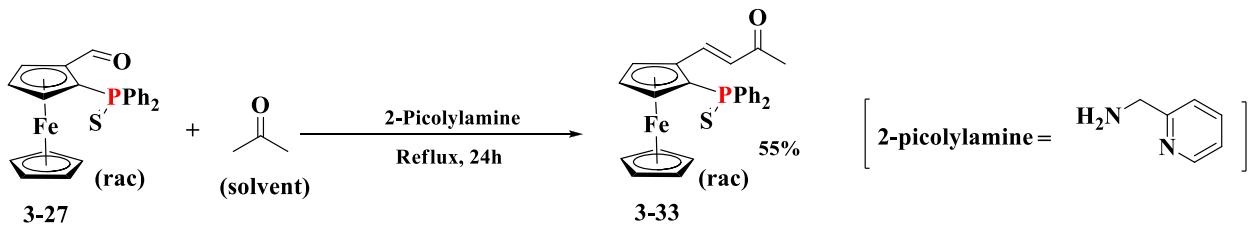

Scheme 3. 15: Synthesis of aldol adduct **3-33**

Compound **3-33** was characterized by multinuclear (^1H, ^{31}P, ^{13}C) NMR spectroscopy (Figure 3. 3) and HRMS. In the ^1H NMR spectrum, the signals for the two *trans* vinylic protons are found as mutually coupled doublets at $\delta = 8.44$ and $\delta = 6.28$ ($J = 16.3$ Hz). The aromatic region shows peak for the 10 PPh_2 protons. Multiplets at $\delta = 5.01$, 4.65, 4.08 and a singlet at $\delta = 4.39$ are observed for the three non-identical protons of the substituted Cp ring and for the five equivalent protons of the

unsubstituted Cp ring, respectively. The singlet at δ = 2.20 represents the C<u>H$_3$</u> group directly attached to the carbonyl carbon. The ^{31}P NMR spectrum show a peak at δ = 41.01. The carbonyl carbon signal was found at δ = 198.16 in the ^{13}C NMR spectrum (Figure 3. 3).

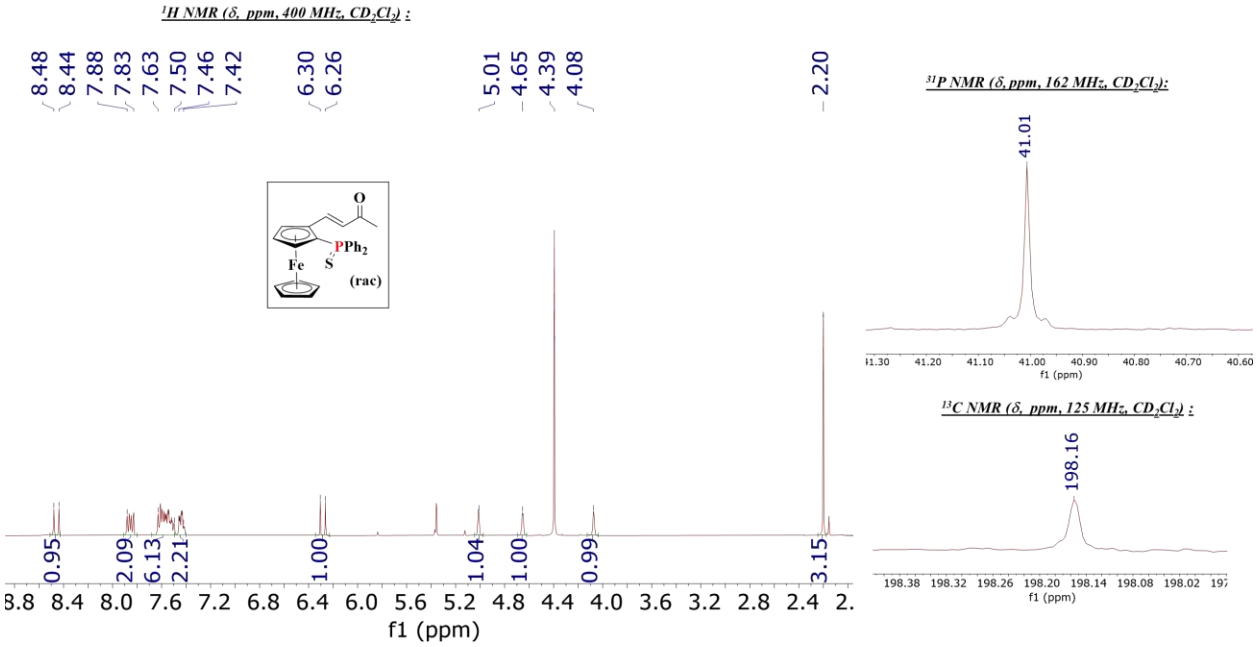

Figure 3. 3: ^{1}H, ^{31}P and ^{13}C (specific region) NMR spectra (CD_2Cl_2, 400 MHz) of **3-33**

Also, a single crystal of **3-33** was obtained by slow diffusion of pentane-DCM solution and the structure was determined by X-ray diffraction (see Figure 3. 4). In this structure, the two Cp ring form a twist angle of 37.1°. The C=C double bond has an E-configuration which again supports the NMR evidence for predicting a *trans* H-coupling. The C2- C21-C22-C23 torsion angle is 172.4(4)° and the plane containing the double bond is twisted with respect to the Cp ring by 22.8(2)°. As the space group is centrosymmetric, the two enantiomers are present within the crystal.

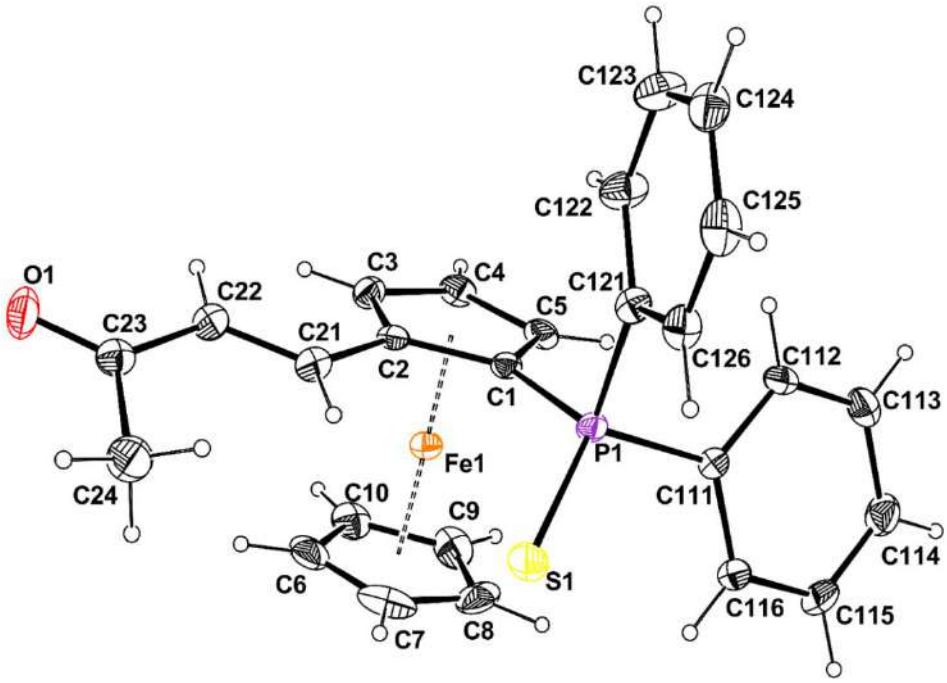

Figure 3. 4: Molecular view of compound 3-33 showing 30% probability displacement ellipsoids and the atom numbering scheme. H atoms are represented as small sphere of arbitrary radii

To the best of our knowledge, there is only one report on the synthesis of a similar kind of α,β-ferrocenyl carbonyls, to date. Císařová *et al.* synthesized an enantiopure and free phosphine-containing version of this compound (**3-33**) by a Horner–Wadsworth–Emmons alkenylation[254] of enantionpure ferrocene carboxaldehyde with diethyl (2-oxopropyl)phosphonate[255] for utilization in the Pd-catalyzed asymmetric allylic alkylation. Nevertheless, our procedure via aldol condensation is effective and easier. Thus, this procedure could be extended to the preparation of other similar compounds.

3. 4) Retrosynthetic Analysis of Ligand-3-10

The retrosynthetic analysis for the ligand **3-10** is shown in Scheme 3. 16.

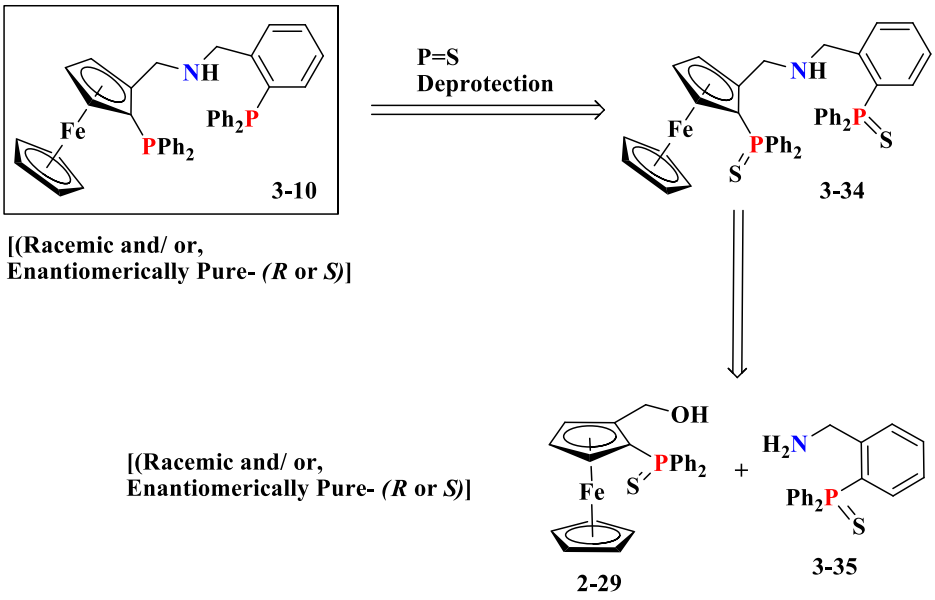

Scheme 3. 16: Retrosynthetic analysis of the PNP ligand **3-10**

The primary requirement to carry out the synthesis is *o*-(thiodiphenylphosphino)-benzylamine **3-34.** This compound should be prepared in good amounts (5-10 g) in order to use a large excess to couple with the ferrocenyl alcohol according to the HBF_4 method. A further retrosynthetic analysis for this amine is shown in Scheme 3. 17, identifying the needed starting materials as the commercially available benzylamine and *o*-halo (chloro, bromo)benzonitrile.

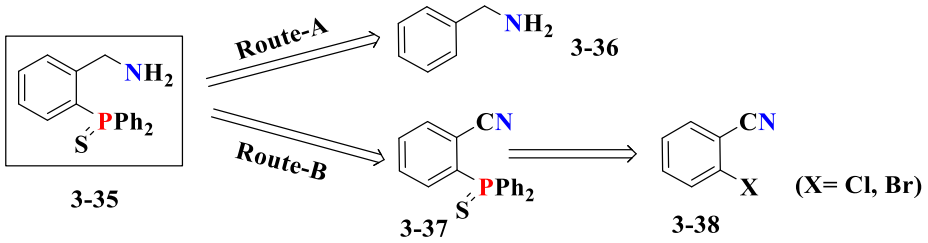

Scheme 3. 17: Retrosynthetic Analysis of the amine **3-34**

3. 5) Synthesis of *ortho*-(thiodiphenylphosphino)-benzylamine 3-35

The direct *ortho*-phosphorylation of benzylamine (Route-A) does not appear promising as there is only one valid procedure in the literature (discussed later). The other pathway (Route-B) was preferred because of several previous reports about the synthesis of *ortho*-diphenylphsphino nitrile as a synthetic intermediate[256] or as a bidentate (N,P) ligand,[257] starting from *ortho* halobenzonitriles. Hence, we synthesized this compound by conventional transmetallation under

strong basic condition (*n*-BuLi), followed by electrophilic trapping (PPh_2Cl), following the procedure reported by Blum *et al*.[258] The phosphine was *in situ* protected by sulphur and the final compound 2-thiodiphenylphosphino-benzonitrile was obtained after purification in good yield as expected. The reduction of the substituted benzonitrlie **3-36** was carried out by using the highly reactive reducing agent $LiAlH_4$ under refluxing condition in THF according to the procedure reported by Karlin *et al*.[259] Expected amine **3-35** was obtained in moderate yields. The synthetic scheme is shown in Scheme 3. 18.

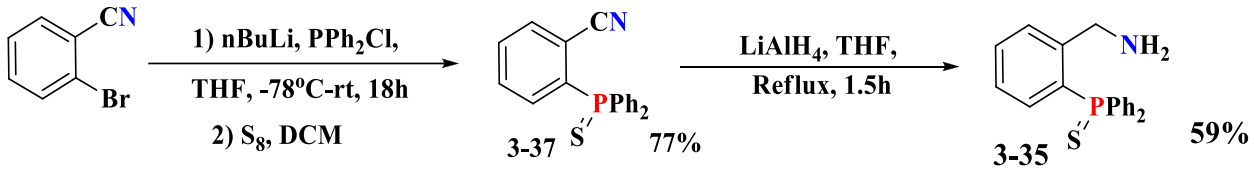

Scheme 3. 18: Synthesis of *o*-(thiodiphenylphosphino)-benzylamine **3-35**

Although the free phosphine versions of both **3-37** and **3-35** are previously reported, these two sulphur-protected species (**3-37** and **3-35**) are unprecedented. Therefore, they were characterized by multinuclear NMR (^1H, ^{13}C, ^{31}P) spectroscopy and mass spectrometry (HRMS). In the ^1H NMR spectrum of **3-37**, multiplets at slightly different positions in the aromatic region (7-8 ppm) represent 14 aromatic protons [Figure 3. 5, a)]. The ^1H NMR spectrum of **3-35** shows similar multiplets in the aromatic region, although the pattern is slightly different from that of **3-37**. The singlet at $\delta = 3.96$ represents the $C\underline{H_2}$ protons and a broad singlet at $\delta = 2.05$ represents the $-N\underline{H_2}$ group [Figure 3. 5, b)]. The ^{31}P NMR spectrum shows a peak in the same region for the two compounds ($\delta = 41.35$ for **3-37** and 41.51 for **3-35,** see Figure 3. 5).

The crystal structure of the compound **3-37** was also established from a single crystal grown by slow evaporation technique using hexane-dichloromethne solution. The structure is shown in Figure 3.6.

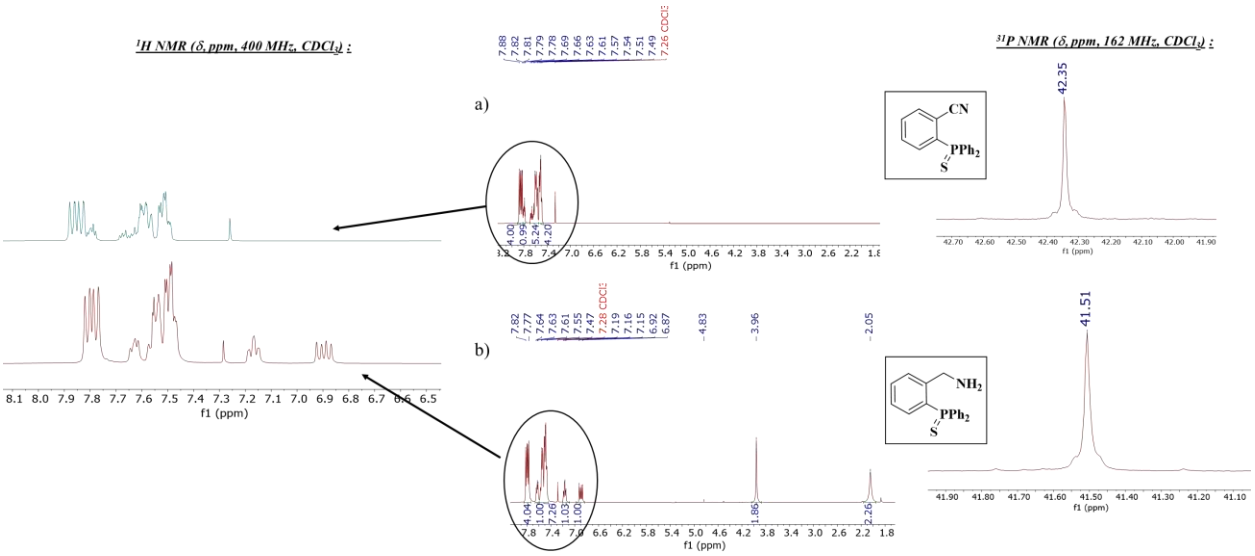

Figure 3. 5: ^{1}H ($CDCl_3$, 400 MHz) and ^{31}P NMR ($CDCl_3$, 162 MHz) of **3-37** and **3-35**

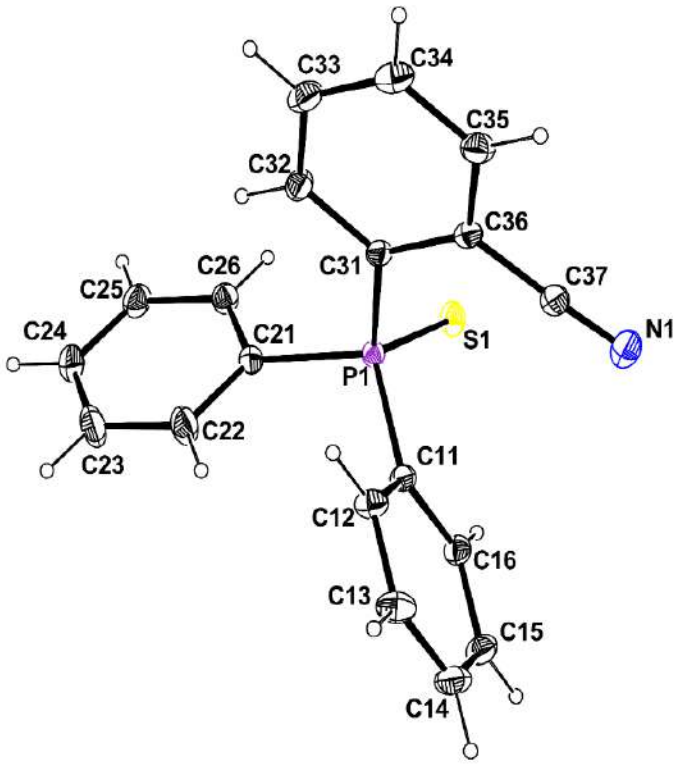

Figure 3.6: Molecular view of compound **3-37** showing 30% probability displacement ellipsoids and the atom numbering scheme. H atoms are represented as small sphere of arbitrary radii.

In an attempt to improve the yield as well as prepare the compound on a larger scale (4-5 g), direct *ortho*-phosphorylation of the less expensive and more readily available was also tested (Route A in Scheme 3. 17). Hu *et al.* prepared 2-diphenylphosphino-benzylamines directly from simple or

α-substituted benzylamines **3-36** as the synthetic intermediate needed for the subsequent transformation to 2-picolylimine-based tridentate (P,N,N) ligand **3-42** (Scheme 3. 19), which were then used for the Pd-catalyzed asymmetric allylic substitution[260] and for the Cu-catalyzed [3+2] cycloaddition reaction between propargylic esters and β-enamino esters.[261] According to their protocol, benzylamine was treated with n-BuLi and TMSCl at -35 ^{o}C to give a silyl-protected benzylamine **3-39** as a reactive intermediate in the initial step. Then the resulting silylamine intermediate **3-39** was further dilithiated with excess (3equiv.) *n*-BuLi treatment at -35 ^{o}C.[262a] The *ortho*-phosphinated amine **3-41** was obtained in moderate yields (40%) by subsequent treatment with PPh_2Cl (-35 ^{o}C- rt) followed by acidic work up [1(M) HCl] to remove the silyl protection.

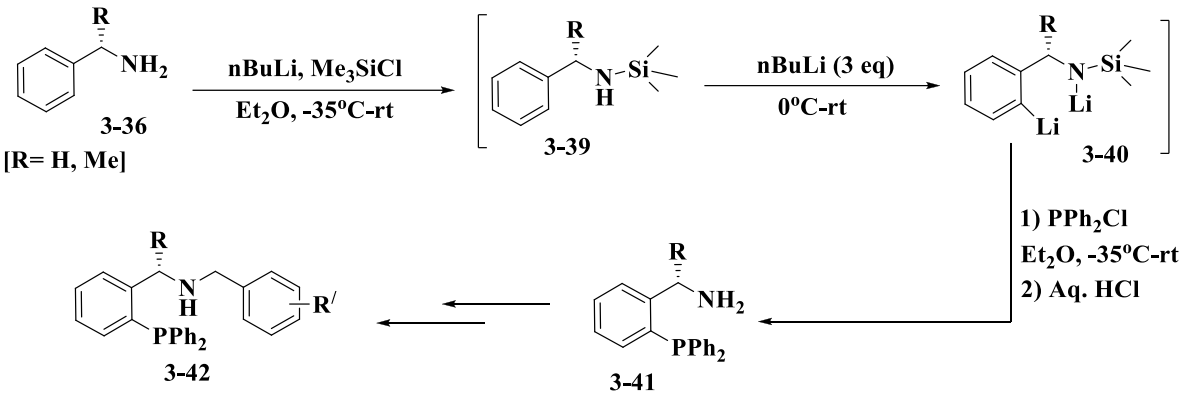

Scheme 3. 19: Preparation of amine reported by Hu *et al.*

The same procedure was thoroughly followed in our case, with the usual inclusion of sulphur addition step after work up stage to protect the free phosphine. Unfortunately, the desired amine was not isolated. Multiple spots with similar spot intensity were observed from the TLC of the crude reaction mixture, indicating partial decomposition. No predominant species could be isolated even after purification by column chromatography. However, one of isolated low yield (11%) byproducts, was further analyzed. The ^{1}H NMR spectrum showed the TMS resonance as a strong singlet at δ = 0.24 and two multiplets at δ= 5.07 and 4.1, indicating two non-identical, mutually coupled (confirmed by COSY) C-H protons. In the ^{31}P NMR spectrum, two resonance were observed at δ= 65.59 and 39.90 (Figure 3. 7). On the basis of these NMR data and on the mass spectrum, the product could be identified as the new tertiary aminophosphine **3-43** (Scheme 3.20). Therefore, this result indicates that phosphorylation occurs both at the aromatic ring and at the N

atom. In addition, the silyl protecting group was not removed from the amine, probably because of an inefficient work up. The yield of this particular compound increased to 28% when the reaction was carried out at 0 ^{o}C (Scheme 3. 20).

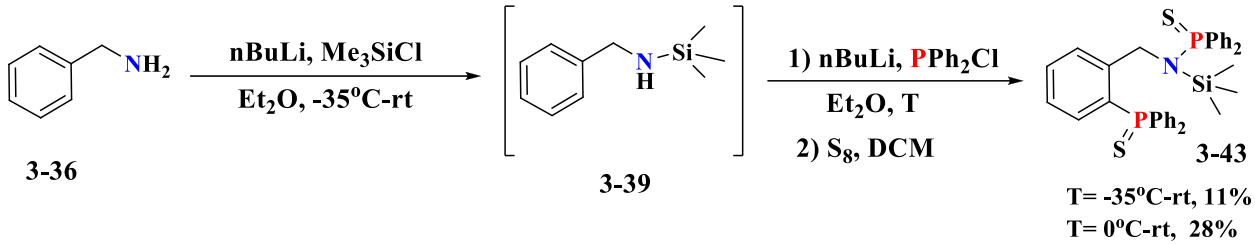

Scheme 3. 20: Formation of amino-phosphine **3-43**

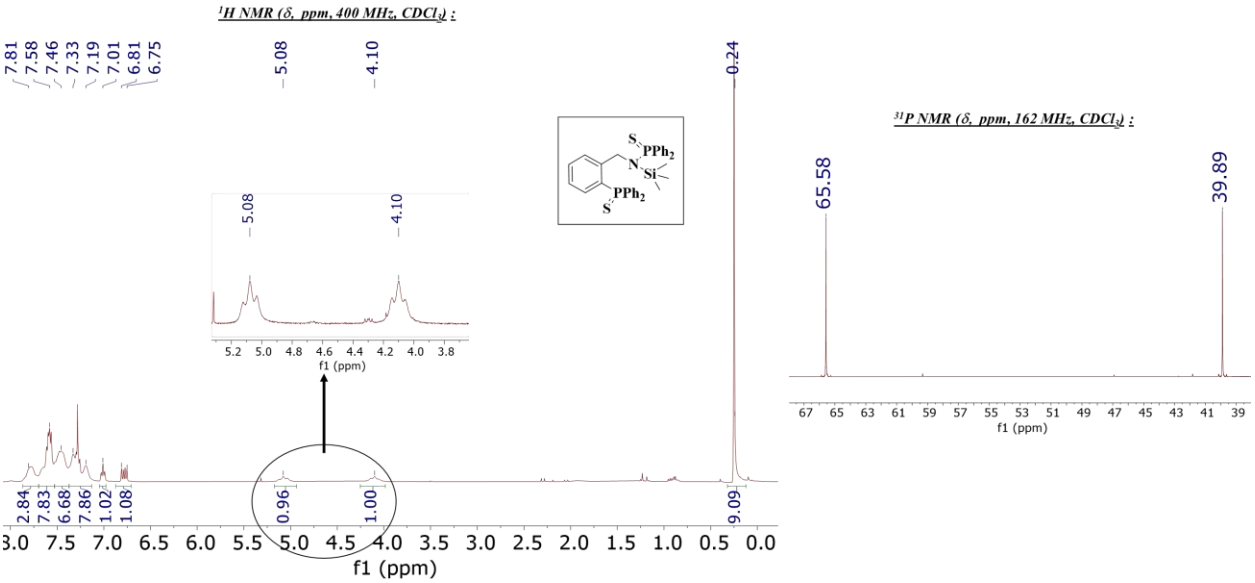

Figure 3. 7: ^{1}H and ^{31}P NMR Spectra of **3-43**

For further confirmation, single crystal of the detected species **3-43**, grown from a DCM solution by slow diffusion of hexane, was investigated by X-ray diffraction. The structure was found to be the same, as predicted**.** The structure features two crystallographically independent and identical molecules within the asymmetric unit. One of them is shown in Figure 3. 8 and a molecular fitting of the two molecules is shown in Figure 3. 9. In both molecules the N atom is planar with a deviation from the mean plane of 0.108(4) Å and 0.026(5) Å, respectively. The sum of the angles around the nitrogen atom (357.6° and 359.9°, respectively) confirms the N group planarity.

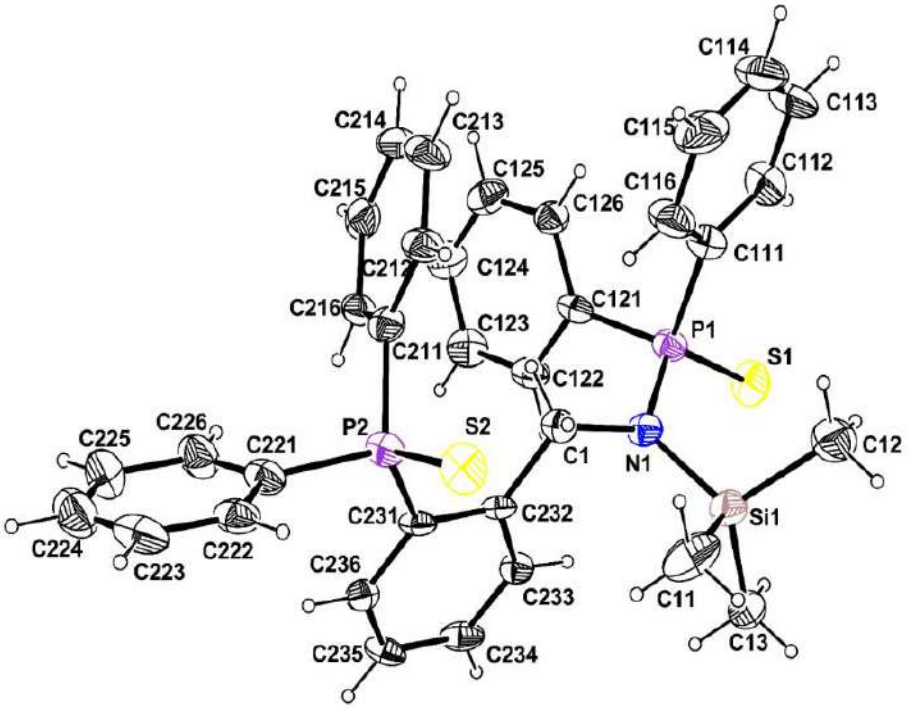

Figure 3. 8: Molecular view of compound **3-43** showing 50% probability displacement ellipsoids and the atom numbering scheme. H atoms are represented as small sphere of arbitrary radii.

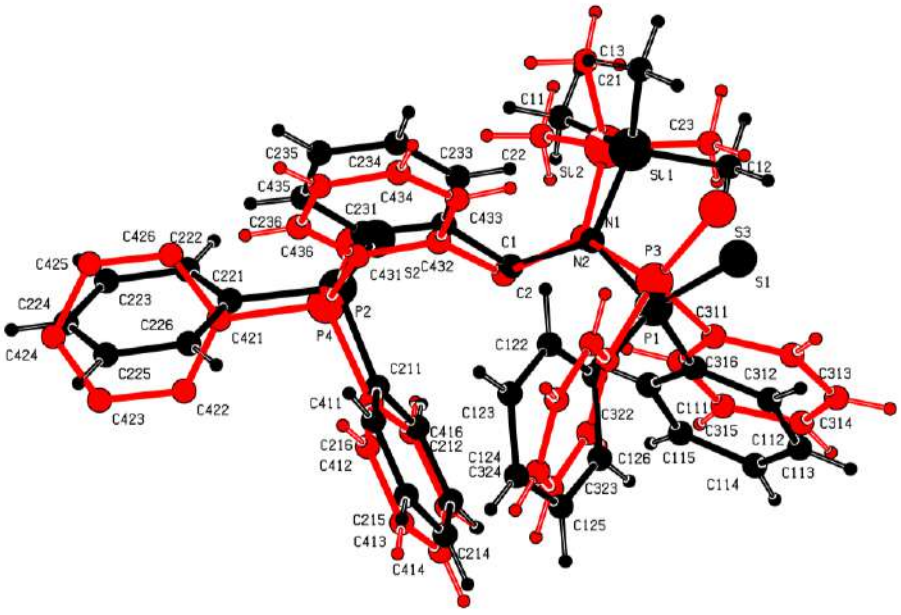

Figure 3. 9: Molecular fitting of the two molecules of **3-43** represented as balls red or black

^{1}H and ^{31}P decoupled ^{1}H NMR spectra at low temperature (253K) were recorded for the aminophosphine **3-43**. The multiplets at δ= 5.07 and 4.1 (shown in Figure 3. 7) were found as

triplets at slightly shifted positions at δ= 5.42 and 4.42 in the hydrogen NMR [Figure 3. 10, a)] and similar sets of doublets were found at δ= 5.42 and 4.42 in the ^{31}P decoupled hydrogen NMR [Figure 3. 10, b)], at 253K. These observations indicate the mutual coupling of the two geminal CH_2 protons and thus identify those two protons to be diastereotopic. These two diastereotopic protons, individually, is further coupled with the N- bonded Phosphorous nucleus, exhibiting two triplets (or, a merged doublet of doublet) in simple hydrogen NMR at low temperature.

The most probable explaination of having diastereotopicity in the molecule **3-43** can be due to the existance of planar chirality along the phenyl backbone. The N- atom that contains three different sterically hindered substituents [-P(S)Ph_2, -$SiMe_3$ and -CH_2Ar] restrict the subsequent C-C bond rotation and therefore, planar chirality is generated. Thus, diastereotopicity is introduced into the -CH_2 protons adjacent to the N-center. A few subsequent studies with **3-43**, (*e.g.* variable temperature NMR experiments, calculation of rotational barrier *etc.*) are ongoing in order to prove our predictions.

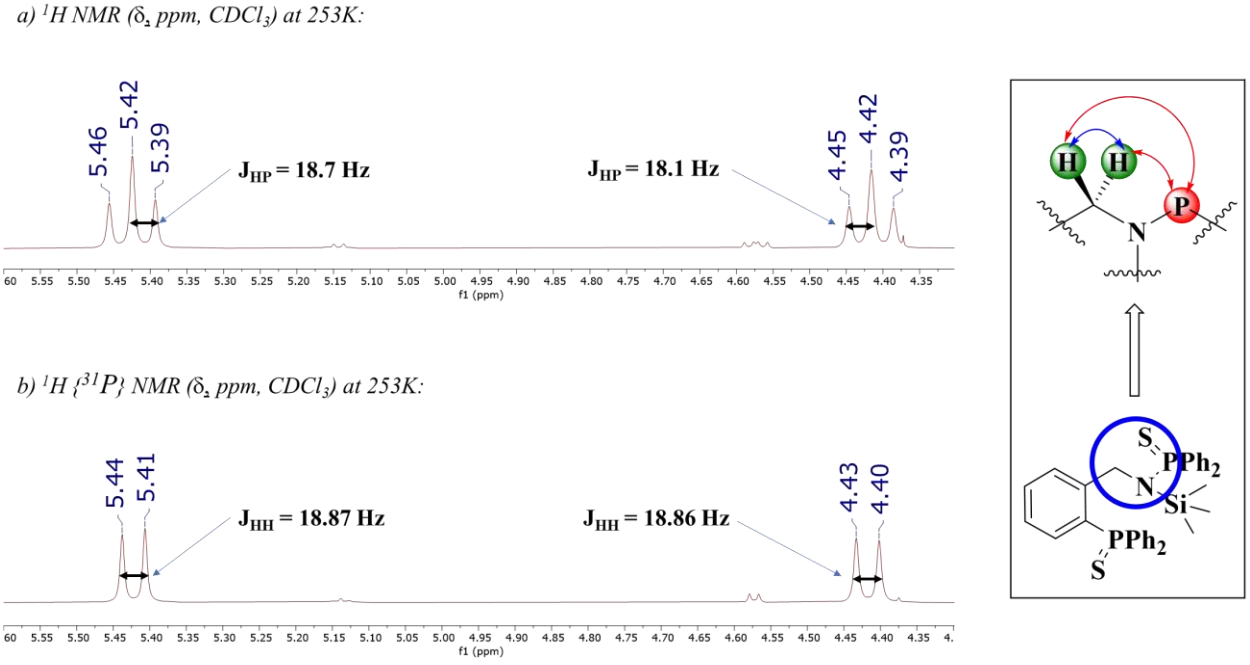

Figure 3. 10: Selected region of ^1H and ^1H {^{31}P} ($CDCl_3$, 400 MHz) NMR spectra of **3-43** at 253K

As a conclusive remark, the targeted *ortho*-phosphinated benzylamine **3-35** (Scheme 3. 18) was successfully obtained, albeit in moderate yields, via the Route-B approach of the retrosynthesis (via *ortho*-phosphino benzonitrile).

3. 6) Synthesis of Proligand 3-34: Final Step

With the freshly prepared amine **3-35** in hand and by using the HBF_4 method, the designed (protected) ligand **3-34** could be successfully prepared (Scheme 3. 21). Keeping atom economy (amine synthesis) into consideration, a compromise was sought to improve the product yield with a minimal amine/alcohol ratio through a preliminary investigation. After a few attempts the proligand **3-34** could be obtained in moderate yields (53%) by using 6 equivalents of the amine **3-35** in the presence of 3 equivalents of acid (Table 3. 1, Entry-3).

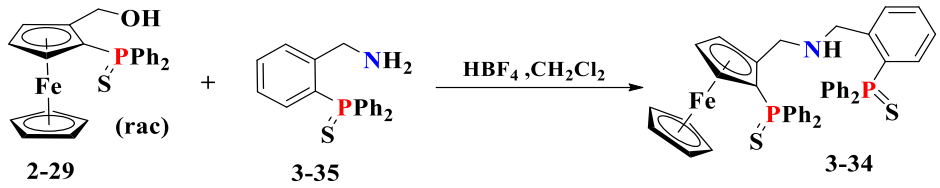

Scheme 3. 21: Synthesis of new PNP proligand **3-34**

Table 3. 1: Optimization of reaction depicted in Scheme 3. 21

Entry	HBF_4 (equiv.)	Amine (equiv.)	Reaction Time (min)	Yield (%)	Conversion of alcohol 2-29
1	2.2	7	5	31	Incomplete
2	1.5	2.5	30	19	Incomplete
3	3.0	6	15	53	Complete

The proligand **3-34** was completely characterized by multinuclear NMR (^1H, ^{31}P, ^{13}C) spectroscopy and mass spectrometry (HRMS). From the ^1H NMR spectrum of **3-34**, 14 aromatic protons were recognized from multiplets at slightly different positions in the aromatic region (δ = 7.83-6.82). Multiplets at δ = 4.45, 4.24, 3.72 and a singlet at δ = 4.27 represent the three non-identical protons of the substituted Cp ring and the five equivalent protons of the unsubstituted Cp ring, respectively. Two AB-type doublets assigned to the two different $C\underline{H_2}$ groups are observed at δ = 3.94, 3.42 and δ = 3.83, 3,67. The ^{31}P NMR spectrum shows two distinct peaks at δ = 41.74 and 41.42, indicating two different thiophosphines (Figure 3. 11).

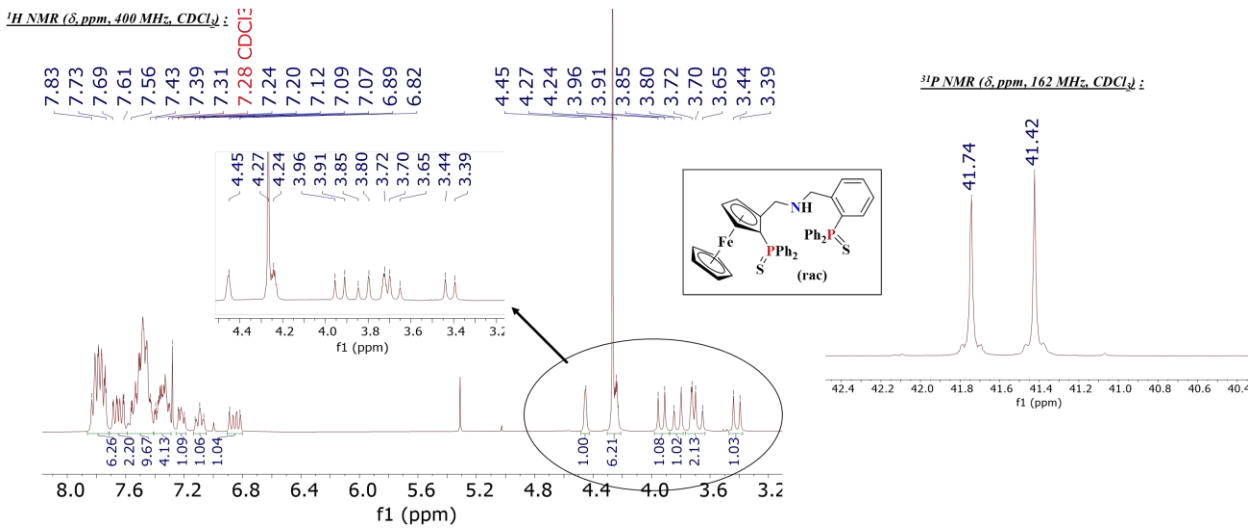

Figure 3. 11: ^{1}H ($CDCl_3$, 400 MHz) and ^{31}P NMR ($CDCl_3$, 162 MHz) spectra of **3-34**

Orange single crystal of **3-34** were obtained by slow diffusion of hexane into the solution of ligand in dichloromethane. The crystal structure was established by X-ray diffraction (Figure 3. 12).

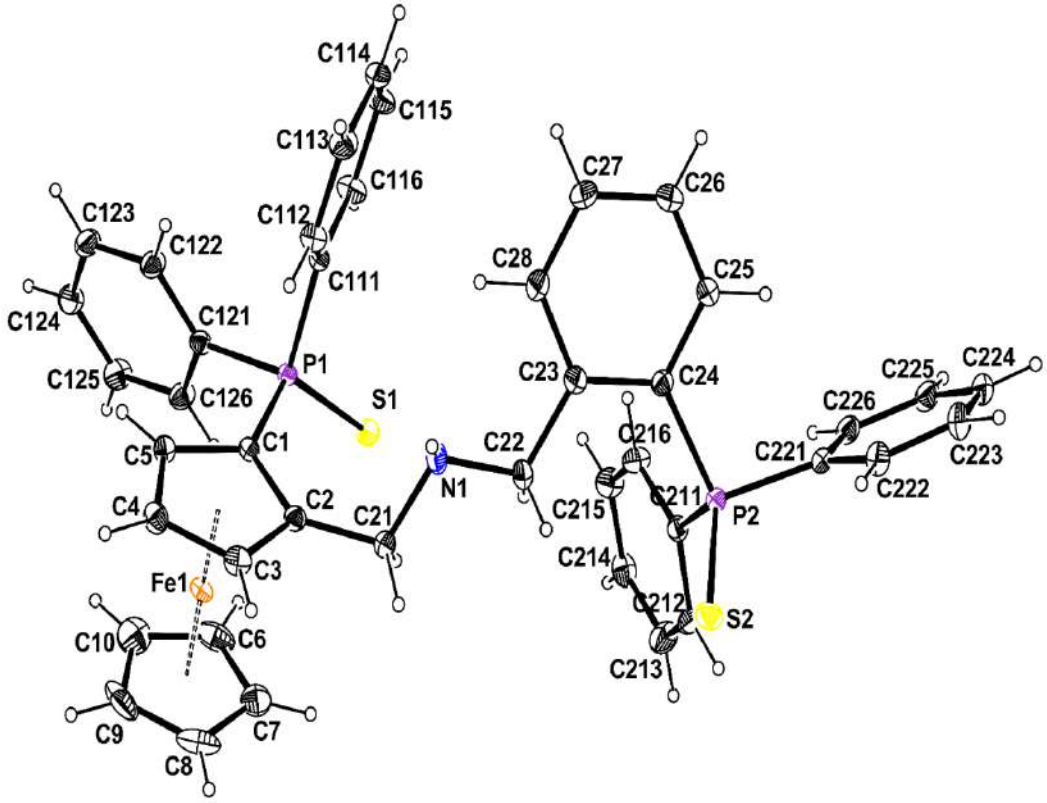

Figure 3. 12: Molecular view of compound **3-34** showing 30% probability displacement ellipsoids and the atom numbering scheme. H atoms are represented as small sphere of arbitrary radii

The C2-C21-N1-C22 torsion angle is 171.9(2)°, meaning that the four atoms are roughly coplanar. The mean plane of these four atoms and the Cp ring plane make a dihedral of 72.0(2)°. The S1

atom is placed at -0.914(5) Å from the Cp ring plane, whereas the P1 atom is 0.083(4) slightly above. The two ferrocene Cp rings are eclipsed.

3. 7) Conclusion

Two similar types of phosphine-containing tridentate secondary ferrocenyl amine ligands in their phosphine protected form, **3-32** and **3-34,** have been synthesized and fully characterized (NMR. mass spectrometry and X-ray crystallography). The synthetic intermediates and a few unexpected byproducts that formed during the course of the syntheses have also been thoroughly characterized. Protected ligands in both racemic and enantoimerically pure forms have been transferred to the research group of Prof. Basker Sundararaju, at the IIT Kanpur, India. The phosphine deprotection and the catalytic applications are currently ongoing.

Chapter-4: New Tridentate Phosphine-Containing Ferrocenyl Thioether Ligands

4. 1) Introduction

Bidentate or tridentate ligands containing sulphur as one of the heteroatoms have a rich coordination chemistry.[263] On the other hand, planar chiral phosphine-containing ferrocenyl ligands with a 1,2-disubstitution of a Cp ring are among the most successful ligands in asymmetric catalysis.[264] Therefore, the combination of thioether and phosphine moieties brings very interesting coordinating systems due to:[265]

1) A significant electronic differentiation due to the P and S heteroatoms

2) The implementation of central chirality at the S atom upon metal coordination, enforcing an asymmetric environment in close proximity to the reactive metal center

Two tridentate ferrocenyl phosphine thioether ligands have been designed for this thesis work (Scheme 4. 1). Ligand **4-1** contains two phosphine and one thioether donor groups (P,S,P coordination pattern). The other ligand **4-2** features three different heteroatom donors (P,S,N): a phosphine, a thioether and a pyridine, bringing greater diversity in terms of stereoelectronic properties. The *ortho* hydroxyl group on the pyridine ring is chosen purposefully to potentially deliver metal-ligand cooperativity through tautomerism and thus may prove interesting during complexation and catalysis.

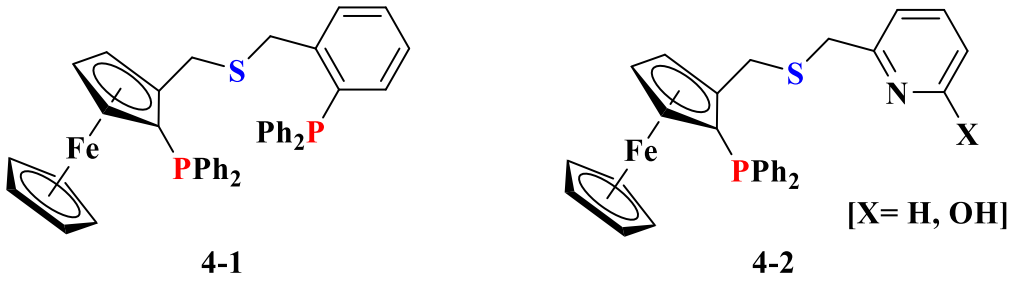

Scheme 4. 1: Molecular formula of the two phosphine thioether ligands

In this chapter, the synthetic protocols that have been used to synthesize previously reported 1,2-disubstituted ferrocenyl bidentate and tridentate ligands with different thioether and phosphine groups, where the thioether moiety is either directly attached to the ferrocene ring or is located on a side chain, will first be summarized in section 4.2. Subsequently, the synthetic protocols chosen for the assembly of the target ligands will be presented.

4. 2) Synthetic methods of different thioether containing 1,2-substituted ferrocenyl bidentate and tridentate ligands

We already discussed how Togni utilized the Ugi amine approach to synthesize various chiral phosphine-containing ferrocenyl derivatives (see chapter 2). This approach also served to access several ferrocenyl ligands containing thioether and phosphine donor groups. A relevant one in this context, reported in 1992, is chiral [(diphenylphosphino)ferrocenyl]ethyl mercaptan, **4-4** (Scheme 4. 2). This ligand was synthesized from *(R, S_p)*- [(diphenylphosphino)ferrocenyl]ethyl acetate (which was obtained from Ugi's amine)[160, 266] by treatment with KSAc in acetic acid followed by reduction. The coordination chemistry of this ligand with Cu(I) was reported.[267]

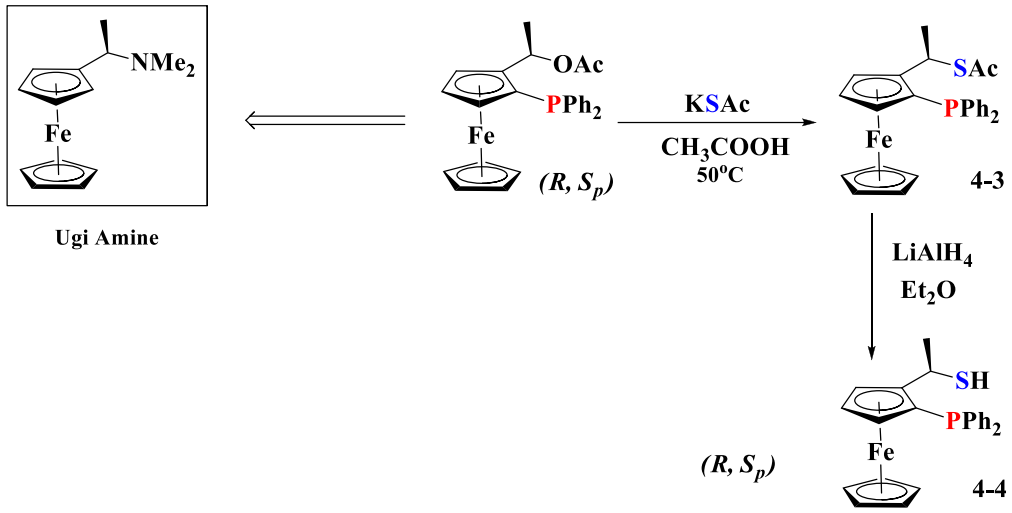

Scheme 4. 2: Synthesis of chiral [(diphenylphosphino)ferrocenyl]ethyl mercaptan **4-4** reported by Togni *et al.*

Several other ligands were synthesized by further substitution at the S center. One such ligand is the sulphur derived version of Pigiphos, namely S-pigiphos **4-5** (S- stands for sulphur particularly in this case, see Scheme 4. 3).[268] It was synthesized by the substitution reaction of *(R)*-1-[*(R)*-(diphenylphosphino)ferrocenyl]ethyl acetate with either *(R)*-1-[*(R)*-(diphenylphosphino)ferrocenyl]ethyl mercaptan in hot acetic acid or its sodium salt in dry methanol. These reactions proceed with retention of configuration on the side chains stereocenters. The S-Pigiphos coordination to Ru(II) was reported. However, the resulting complexes were only moderately successful for the asymmetric transfer hydrogenation of acetophenone (ee up to 71.7%).

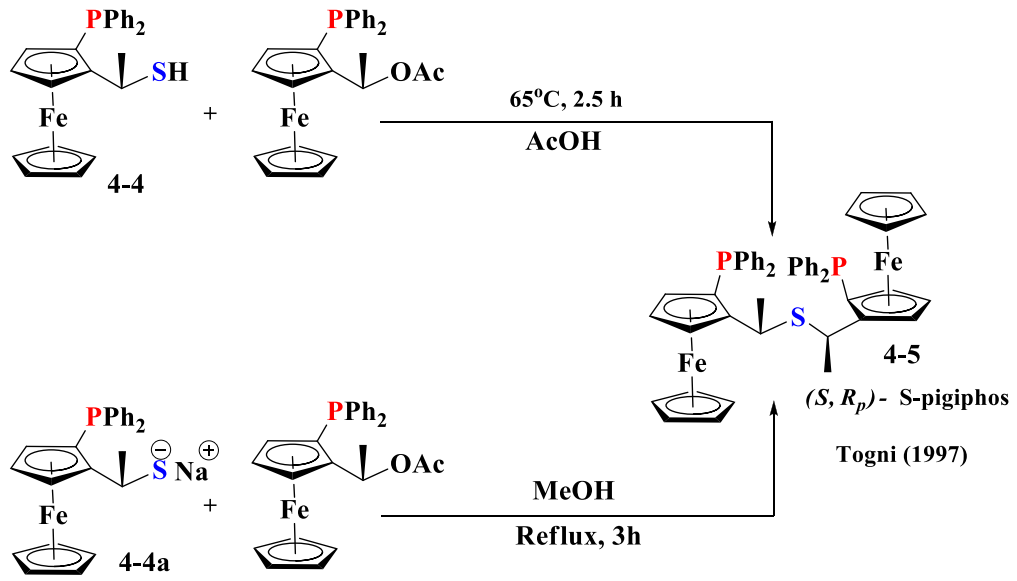

Scheme 4. 3: Synthesis of *(S, R_p)*-S-pigiphos

One P,S,O-ferrocenyl derivative (**4-6**, Scheme 4. 4) was developed using **4-4** and racemic *cis*-indene epoxide as starting materials under epoxide ring opening condition.[269] The resulting diastereomeric mixture was separable by column chromatography. Pd(II)- allyl complexes were synthesized using this ligand, but the catalytic activities in hydroboration and alkylation processes proved unexceptional in terms of enantioselectivity.

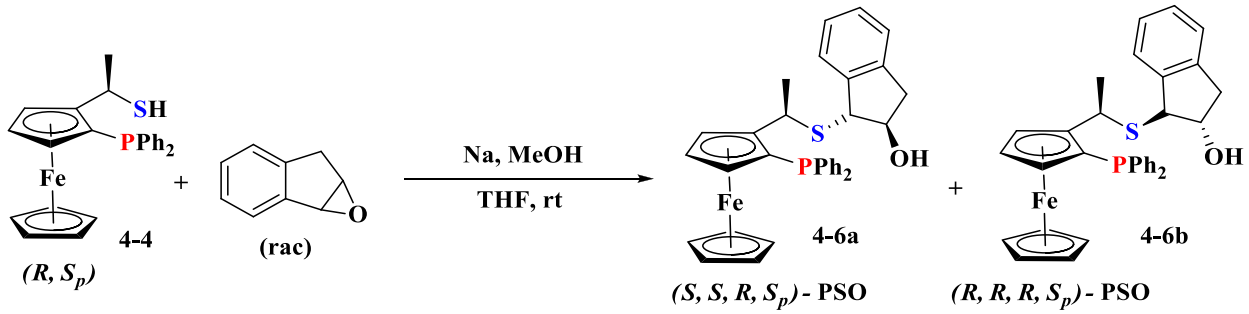

Scheme 4. 4: Synthesis of the P,S,O ligands **4-6**

Tu *et al.* (2003) utilizing the diastereoselective *ortho*-metallation of the enantiopure Ugi's amine, synthesized two phosphine-containing ferrocenyl thioether ligands **4-9** and **4-10** (Scheme 4. 5), which are structural isomers. They resulted from the inverted order of addition of the trapping electrophile (Ph_2S_2 or PPh_2Cl) for the lithiated ring quenching and the nucleophile (Ph_2PH or

Ph_2S_2) for the NMe_2 substitution. These ligands were tested for the Pd-catalyzed allylic substitution of 1,3-diphenyl-2-propenyl acetate with diethyl Malonate (ee up to 93.8%).[270]

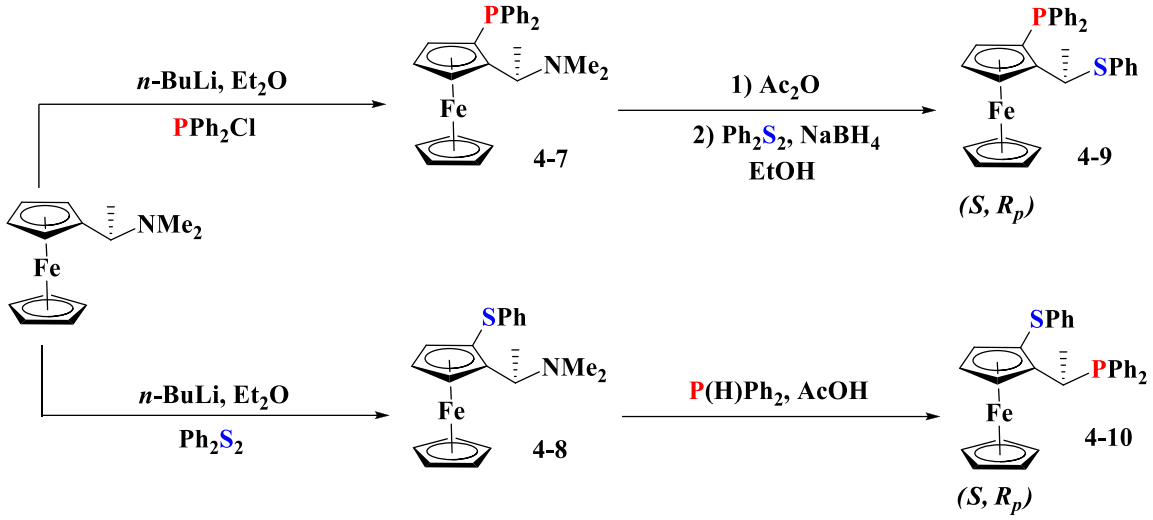

Scheme 4. 5: Synthesis of ligands **4-9** and **4-10**

Similar syntheses were reported by Chan *et al.* leading to the new N-phosphine-thioether (FerroNPS) ligand family (**4-11 – 4-14**, Scheme 4. 6). Nucleophilic substitution of the NMe_2 group in the amino-thioether with methyl amine or with other nitrogen-containing heterocycles (imidazole, benzimidazole, 1,2,4-triazole), followed by further diphenylphosphine substitution at the side chain, afforded the ligands.[271] These ligands were extensively utilized for the Pd-catalyzed allylic substitution of (rac)- 1,3-diphenyl-2-propenyl acetate with diethyl malonate (DEM), different amines, indoles, ethers, *etc*. Good to excellent enantioselectivities were obtained by varying the reaction conditions and nucleophiles (ee 33-97%).[272]

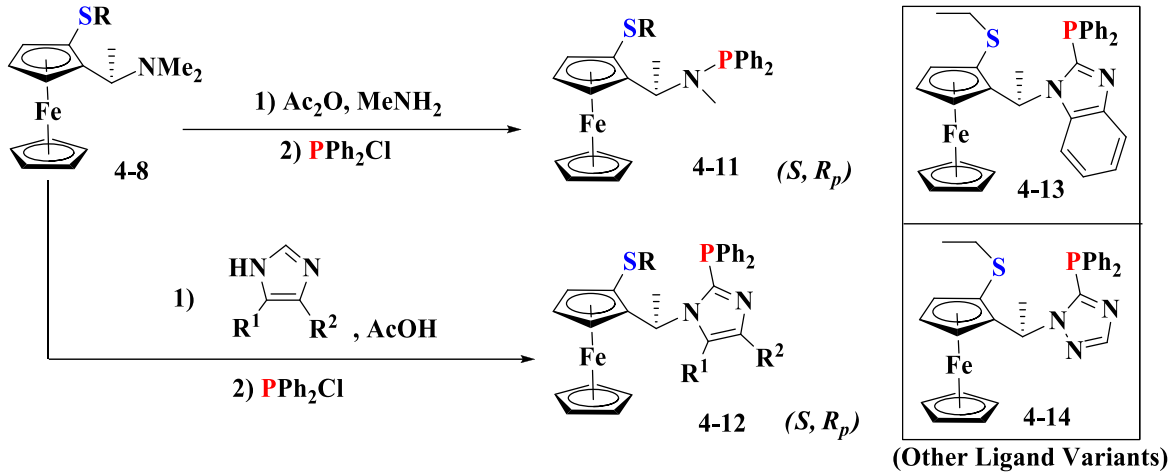

Scheme 4. 6: Ferro-NPS Ligands

Recently, Fukuzawa *et al.* (2009) utilizing the newly developed convenient click chemistry methodology,[273] synthesized a new class of thioether-containing ferrocenyl ligands, namely Thioclickferrophos (**4-19** and **4-20**, Scheme 4. 7). A click reaction between *(S,R_p)-ortho*-bromo-(1-azidoethyl)ferrocene **4-15** and substituted alkynes generated the triazole backbone at the C1 position of the substituted Cp ring (**4-16**). Subsequent lithium-halogen exchange followed by electrophilic trapping by either a disulphide or a chlorophosphine derivative at the C2 position resulted in the two differently 2-*ortho*-functionalized ferroenes **4-17** and **4-18**, respectively. Then, by further lithiation of **4-17** at the triazole ring and trapping by PPh_2Cl Thioclickferrophos ligands of the Type-I (**4-19**) were achieved. Type-II ligands (**4-20**) were obtained from **4-18** by the same triazole lithiation followed by trapping by a disulfide (Scheme 4. 7).[274]

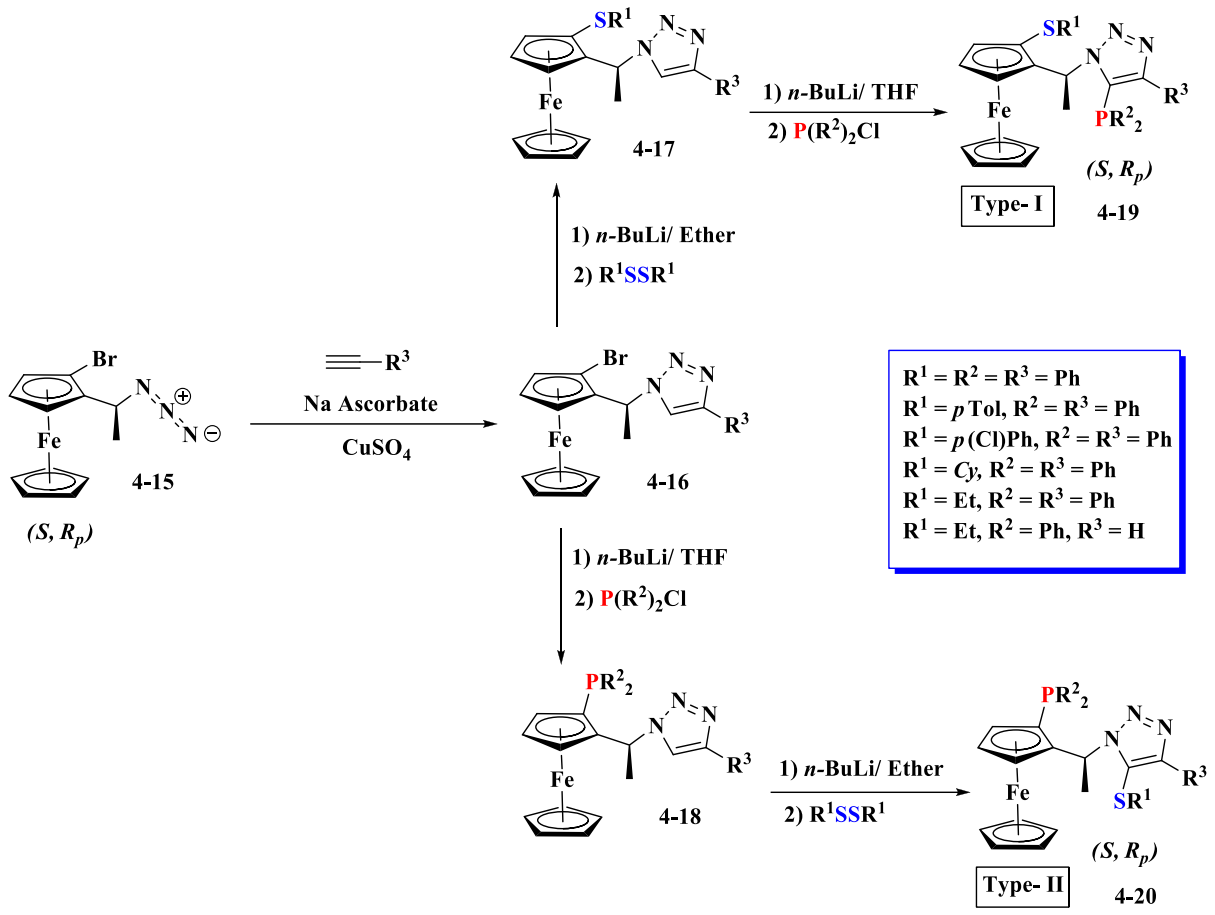

Scheme 4. 7: Thioclickferrophos Ligands

The type-II ligands (**4-20**) were proven better than the type-I (**4-19**) in the Pd-catalyzed allylic substitution, leading to moderate enatioselectivities (ee 66-90%).[275] They were also successful for the Ag- catalyzed 1,3- dipolar cycloaddition of azomethane ylides with α-enones,[276] activated alkenes[277] and nitro alkenes[278] and the conjugate additions of imino esters with nitroalkanes,[279] unsaturated malonates and α-enones,[280] as well as for the Ag-catalyzed enantioselective Mannich reaction of glycine Schiff bases.[281]

Besides the use of Ugi's amine method, there have been a few instances where alternative diastereoselective approaches were made to develop new phosphine-thioether ligands. Enders *et al.* (2000) reported an asymmetric synthesis of planar chiral ferrocenyl ligands (**4-26**, Scheme 4. 8) bearing a stereogenic center at the β-position of the side chain, starting from ferrocenyl ketones with α-acidic protons.[282] The key step of the multistep synthesis is the introduction of asymmetry in the ferrocenyl system. This was achieved using the *(S)*-1-amino-2-methoxymethylpyrrolidine

(SAMP) hydrazone method,[283] which induces a very high diastereoselectivity for the α-alkylation of the functionalized hydrazone[284] and for the subsequent electrophilic *ortho*-substitution of the ferrocenyl backbone with different electrophiles.[285] These ligands were applied to the Pd-catalyzed asymmetric allylic substitution reactions with moderate to excellent enatioselectivities (ee up to 97%).[286]

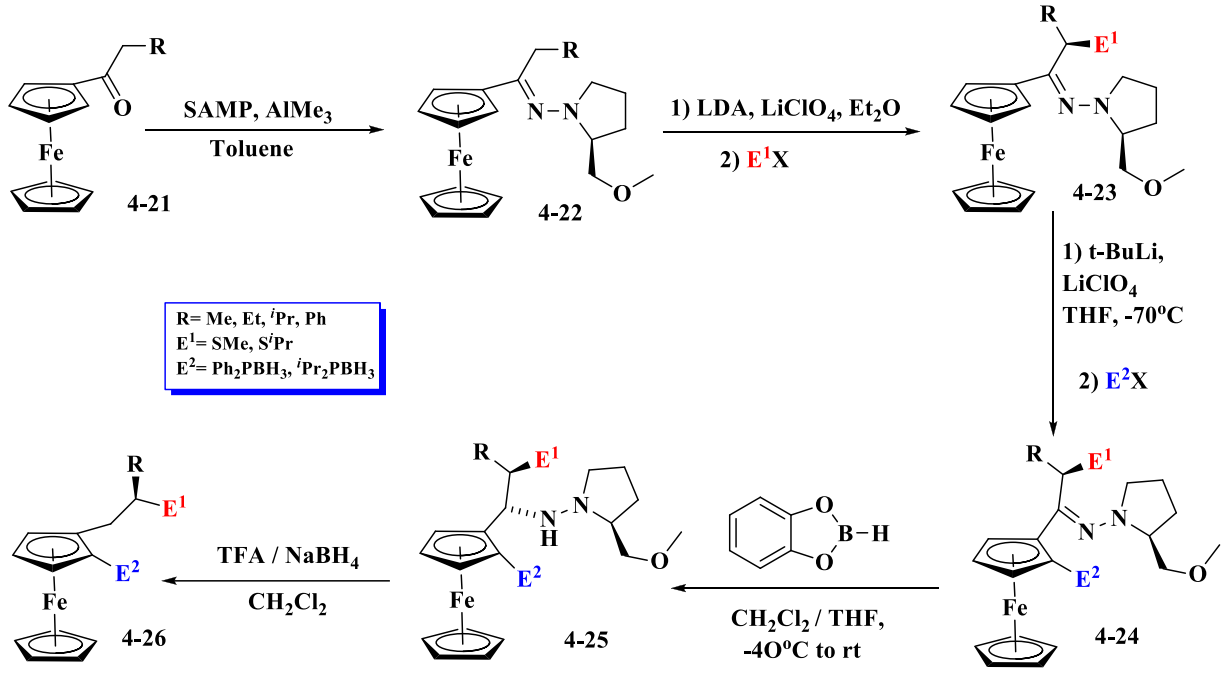

Scheme 4. 8: Synthesis of thioether ligands with a stereogenic center at the β-position

Carretero *et al.* (2003) introduced the Fesulphos ligands, which are 1-phosphino-2-sulfenyl ferrocenes, where the thioeher moiety is directly attached to the ferrocene ring (**4-29a** and **b**, see Scheme 4. 9).[287] The sulphoxide approach for the diastreoselective *ortho* phosphorylation (see Chapter 2) was followed. Either *(R)-tert*-butylsulfenylferrocene (**4-27a**) or *(S)-p*-tolylsulfenylferrocene (**4-27b**) was used as starting material. Kagan *et al*. synthesized these starting materials by sulfinylation of ferrocenyl lithium with enantiopure *tert*-butylsulfinates and by asymmetric oxidation of *tert*-butylsulfenyl ferrocene.[288] The synthetic route of enantiomerically pure Fesulphos ligands comprised two steps: ortho-lithiation/phosphination and sulphoxide to sulphide reduction. The *ortho*-lithiation step occurs with complete diastereocontrol.[265]

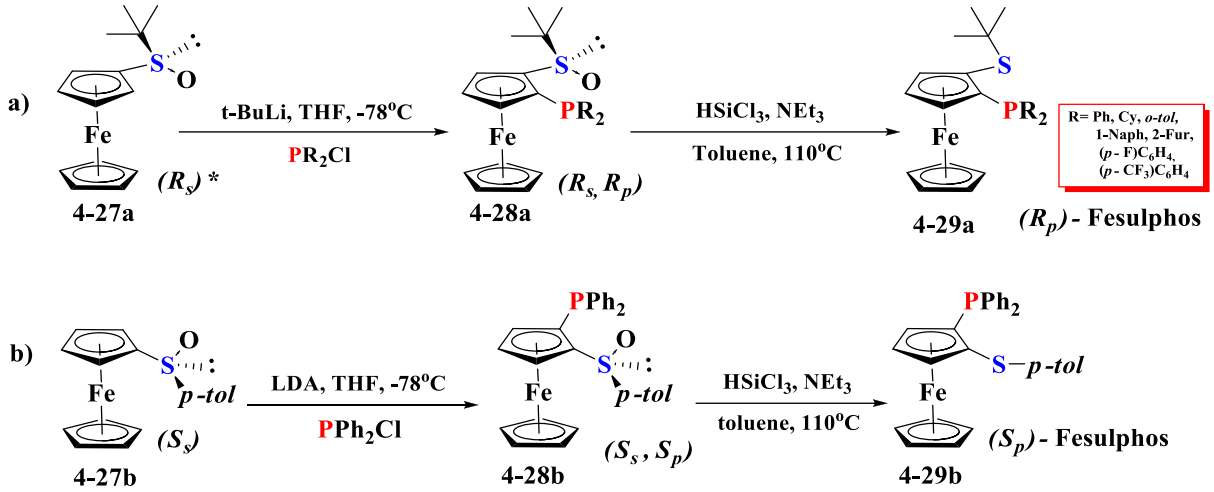

Scheme 4. 9: Synthesis of *(R_p)*-Fesulphos ligands and one *(S_p)*-Fesulphos*

The same authors also synthesized a few aminophosphine ferrocene ligands **4-32** to understand the size effect during metal chelation (Scheme 4. 10).[287]

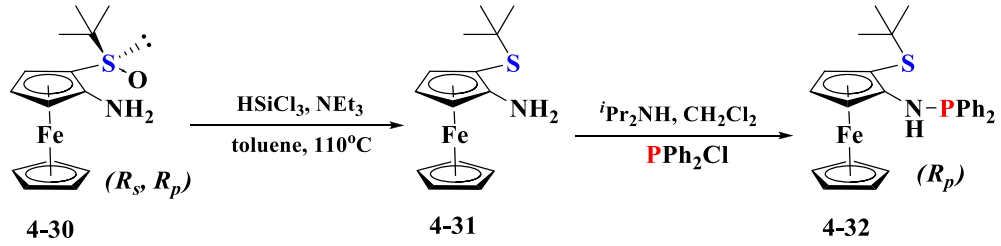

Scheme 4. 10: Synthesis of an aminophosphine analog of the fesulphos ligand

The analogue with a CH_2 spacer of the ligand (**4-35**) was also synthesized starting from 2-hydroxymethyl sulfinylferrocene **4-33** (Scheme 4. 11).[287]

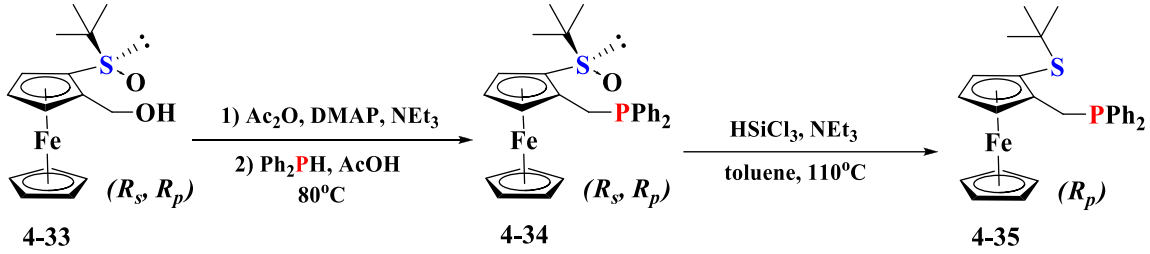

Scheme 4. 11: Synthesis of a phosphinomethyl analog of the Fesulphos ligand

* *(R_S/ S_s)*= Absolute configuration of chiral sulphur atom; the planar chirality of ferrocene backbone is indicated by *(R_p/ S_p)*, in these cases.

Fesulphos ligands, have been the most versatile P,S ligands among the different types of chiral ferrocenyl phosphine-thioether ligands for relevant asymmetric C-C bond forming reactions. The most possible reason is that the planar chirality imposes a diastereoselective coordination of the sulphur atom, which therefore becomes stereogenic and enforces a strongly asymmetric environment in close proximity of the reactive metal center and therefore allows higher enatioselectivities.[289] It is not easy to single out the most significant catalytic achievements of fesulphos ligands. They have been distinctly effective, for instance, in Pd-catalyzed allylic substitution,[287, 290] desymmetrization of bicyclic alkenes,[291] Cu-catalyzed asymmetric Diels-Alder reaction of cyclpentadiene with N-acryloyl oxazolidinone,[289] aza Diels-Alder reactions of substituted dienes and aldimines,[292] Cu- and Ag-catalyzed 1,3-dipolar cycloadditions of azomethine ylides with activated alkenes[293] and α,β-unsaturated ketones,[294] Cu-catalyzed asymmetric Mannich reaction of N-sulfonyl imines with silyl enol ethers,[295] *etc*.

New bidentate ferrocenyl phosphine thioether (P,S) **4-37** and thiophosphine thioether (S,S) **4-36** ligands have also been reported by our group (Scheme 4. 12).[107b] These ligands, like Fesulphos, contain only planar chirality. The starting material in this case was again the alcohol **2-29** in its enantiomerically pure form. Upon strong acidic condition, the alcohol generates a ferrocenyl carbocation,[296] which is then coupled with a rapidly added thiol nucleophile yielding enantiomerically pure **4-36**. Subsequent desulfuration of the P=S group provided the free phosphine-containing P,S ligands **4-37**. The latter afforded good yield (93-97%) and enatioselectivities (ee 78-93%) in the Pd-catalyzed asymmetric allylic substitution of 1,3-diphenylprop-2-enylacetate with the anion of dimethyl malonate. These ligands were also utilized for asymmetric hydrogenations (see chapter 1, section 1.2).

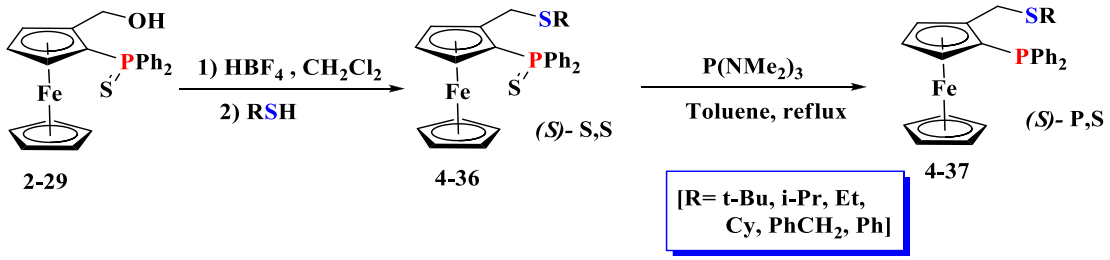

Scheme 4. 12: Synthesis of ferrocenyl phosphine thioether bidentate ligands

4. 3) Retrosynthetic Analysis of the P.S.P Ligand 4-1

One possible retrosynthetic scheme for the target ligand **4-1**, is presented in Scheme 4. 13.

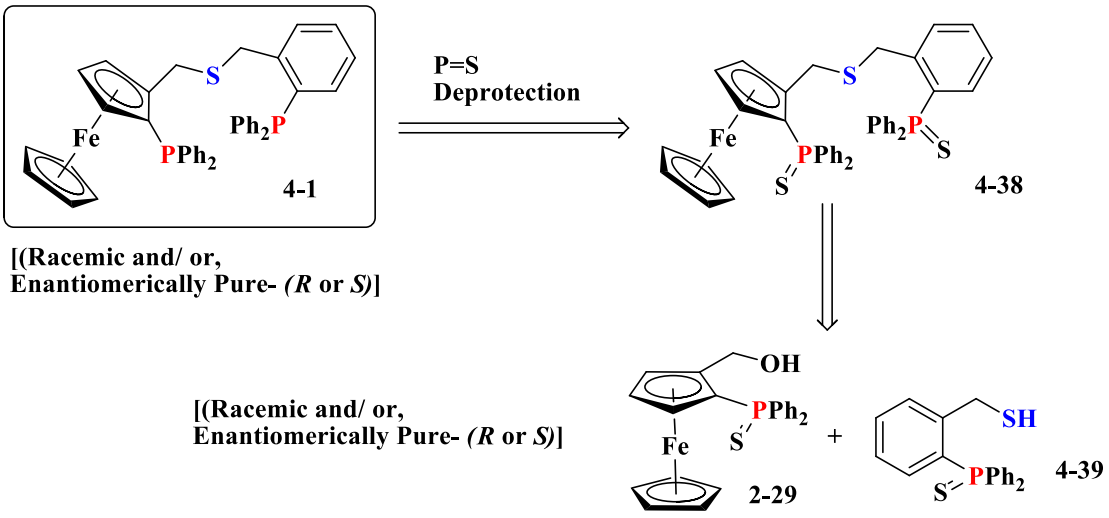

Scheme 4. 13: Retrosynthetic Analysis of the corresponding P,S,P ligand

Since free phosphines, even the triaryl ones, are relatively unstable and susceptible of oxidation in air,[297] we found it is necessary to carry out the molecular assembly with sulphur-protected phosphine groups, **4-38**. The assembly relies, once again, on the starting alcohol **2-29,** which has to be enantiomerically pure. The method utilizing ephedrine as a chiral auxiliary easily leads to the enantiomerically pure alcohol,[107b] as already discussed earlier (see chapter 2). The *ortho*-substituted benzyl mercaptan derivative **4-39**, needed for the coupling with the ferrocenyl alcohol **2-29**, can be accessible from commercially available *ortho*-halobenzyl alcohol (**4-41**) as starting material, shown in Scheme 4. 14.

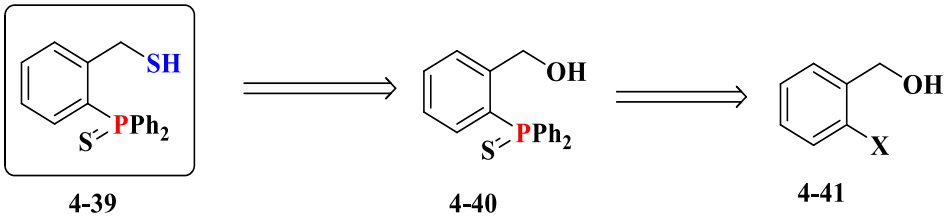

Scheme 4. 14: Retrosynthetic Analysis of the benzyl mercaptan derivative

The phosphorylation must be carried out with the protected form of the alcohol to prevent the reactivity of the hydroxyl group. Then the phosphorus containing alcohol should be converted to corresponding thiol.

4. 4) Synthesis of 2-(diphenylthiophosphino) benzylmercaptan

The synthetic investigation started with the inexpensive *ortho*- bromobenzyl alcohol. The first step was the alcohol protection using (Scheme 4. 15).[298]

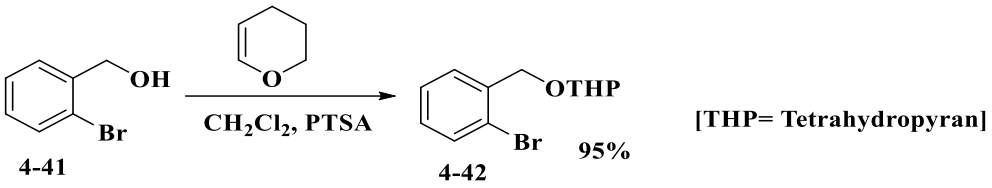

Scheme 4. 15: De-protection of *ortho*- bromobenzyl alcohol

Keskar *et al.* (2008) reported a standard technique for the phosphorylation of **4-42** by PPh_2Cl.[299] The procedure involves treatment with an organolithium compound (*e.g.* BuLi) for transmetallation followed by addition of PPh_2Cl as a electrophile and finally deprotection of alcohol by *p*-toluenesulphonic acid (PTSA). Schmalz *et al.* earlier synthesized (2002) analogous *ortho*-diphenyl phosphenyl phenol and β- diphenyl phosphenyl napthol using the same protection, phosphorylation, deprotection scheme.[300]

An identical phosphorylation procedure, followed by *in situ* sulphur protection of the free phosphine using elemental sulphur, yielded a mixture of thiophosphorylated species (Scheme 4.16) before the deprotection step, as shown by the observation of two distinct resonances in the ^{31}P NMR spectrum for the crude material at δ= 41.67 and 41.42. One of them corresponds to the expected product **4-43** and the other one is the product **4-40** with the alcohol group already de-protected. Since chromatographic purification at this stage is unnecessary, the crude mixture was treated under acidic condition for the *in situ* alcohol de-protection and the expected alcohol was obtained in low yields (Scheme 4. 16).

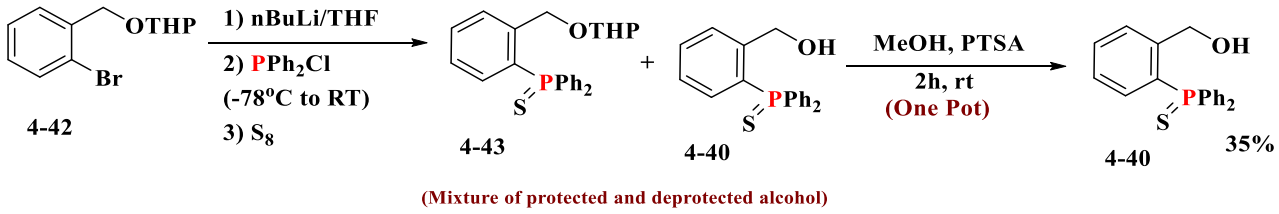

Scheme 4. 16: Synthesis of 2-diphenylthiophosphinobenzyl alcohol **4-40**

Two possible choices were available at this stage: either optimize the existing scheme or introduce a different procedure. Initial optimization attempts, which inclined like changing the equivalents

of the reagents or changing the solvents of the *ortho* substitution step did not significantly help to improve the yield (see Table 4. 1).

Table 4. 1: Few attempts of optimization of the reaction Scheme 4. 16

Entry	Solvent	*n*-BuLi (equiv.)	PPh_2Cl (equiv.)	Yield (%)[a]
1	THF (dry)	1	1	28
2	THF (dry)	1.2	1.5	39
3	THF (dry)	2	2.5	19
4	CH_2Cl_2 (dry)	1.5	2.5	36

[a] yield calculated for the alcohol after *in situ* deprotection

Since this procedure led to the formation of several other byproducts and impurities (difficult to characterize), chromatographic separation to obtain the pure alcohol was not very convenient. Therefore, it was decided to search for a new procedure.

Rachwalski *et al.* (2019) obtained the same free phosphine-containing alcohol (without sulphur protection) from commercially available 2-(diphenylphosphanyl)benzoic acid by reduction, using $LiAlH_4$.[301] kesker *et al.*(2012) also reported the same reduction.[302] In the same contribution, they reported the methyl ester analogue, namely methyl-2-(diphenylphosphanyl)benzoate. However, this compound was synthesized differently, starting from methyl-2-bromo-benzoate. The phosphorylation was carried out by diphenylphosphine in the presence of a mild base (Cs_2CO_3) and catalytic amounts of CuI under refluxing condition.

Inspired by these reports, phosphorylation was carried out on methyl-2-bromo-benzoate under the specific conditions mentioned above, followed by *in situ* sulphur protection, to yield the expected product **4-44** was obtained in good yields and without any separation difficulties (Scheme 4. 17).

Subsequently, rather than ester saponification, preparing for the final reduction of the free acid according to the procedure of Rachwalski *et al.*[301] the reduction process was investigated directly on the methyl ester **4-44**. A first attempt was based on the use of excess sodium borohydride ($NaBH_4$) in methanol with moderate heating. De Souza *et al.* (2004), reported these specific conditions for the reduction of different substituted aromatic methyl esters.[303] Unfortunately, these conditions did not prove strong enough for the reduction of **4-44**. Indeed, the reduction of esters and other similar kind of functional groups using sodium borohydride is relatively difficult

in general.[218b] Therefore, we turned to the stronger reducing agent lithium aluminium hydride ($LiAlH_4$) as a solution in THF, [304] which led to the formation of the alcohol **4-41** in relatively good yields (Scheme 4. 17).

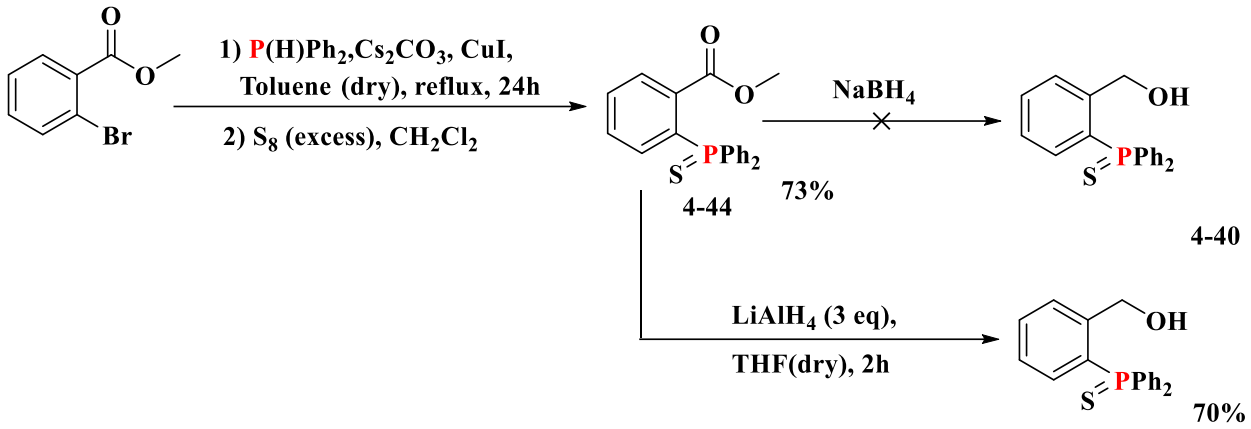

Scheme 4. 17: Synthesis of alcohol **4-41** starting from *ortho*-bromo ester

The alcohol **4-40**, its protected form **4-43** and the ester **4-44** were thoroughly characterized by multinuclear NMR (^1H, ^{31}P, ^{13}C) spectroscopy and HRMS. In the ^1H NMR spectrum of **4-43**, along with the usual aromatic resonances, the singlet at δ = 4.87 corresponds to the C$\underline{H}_2$ protons and the triplet at δ = 4.39 corresponds to the C$\underline{H}$ proton of the pyran ring. The protons of the C$\underline{H}_2$ group adjacent to the pyran CH group become diastereotopic because of the CH-group asymmetry and thus provide multiplets that are mutually coupled (confirmed by COSY) and further coupled with the CH- proton, at slightly different region (δ = 3.64 and 3.35). The six protons of the other three pyran ring C$\underline{H}_2$ groups were found as multiplet at δ = 1.59-1.43 [Figure 4. 1, a)]. In the ^1H NMR spectrum of **4-40**, alongside the aromatic protons, a doublet at δ = 4.65 and a triplet δ = 3.98 correspond to the two C$\underline{H}_2$ group protons and the alcoholic O$\underline{H}$, respectively [Figure 4. 1, b)]. They are coupled to each other (J_{HH} = 7.64 Hz). The ^1H NMR spectrum of **4-44** shows a singlet at δ = 3.44 for the OC$\underline{H}_3$ protons along with the usual aromatic protons [Figure 4. 1, c)]. The presence of the C=O group was confirmed by the peak at δ = 168.03 in the ^{13}C NMR spectrum. The ^{31}P NMR spectra gave peaks in similar regions for the three compounds (δ = 41.42 for **4-43**; δ = 41.67 for **4-40**; δ= 46.16 for **4-44**, see Figure 4. 1).

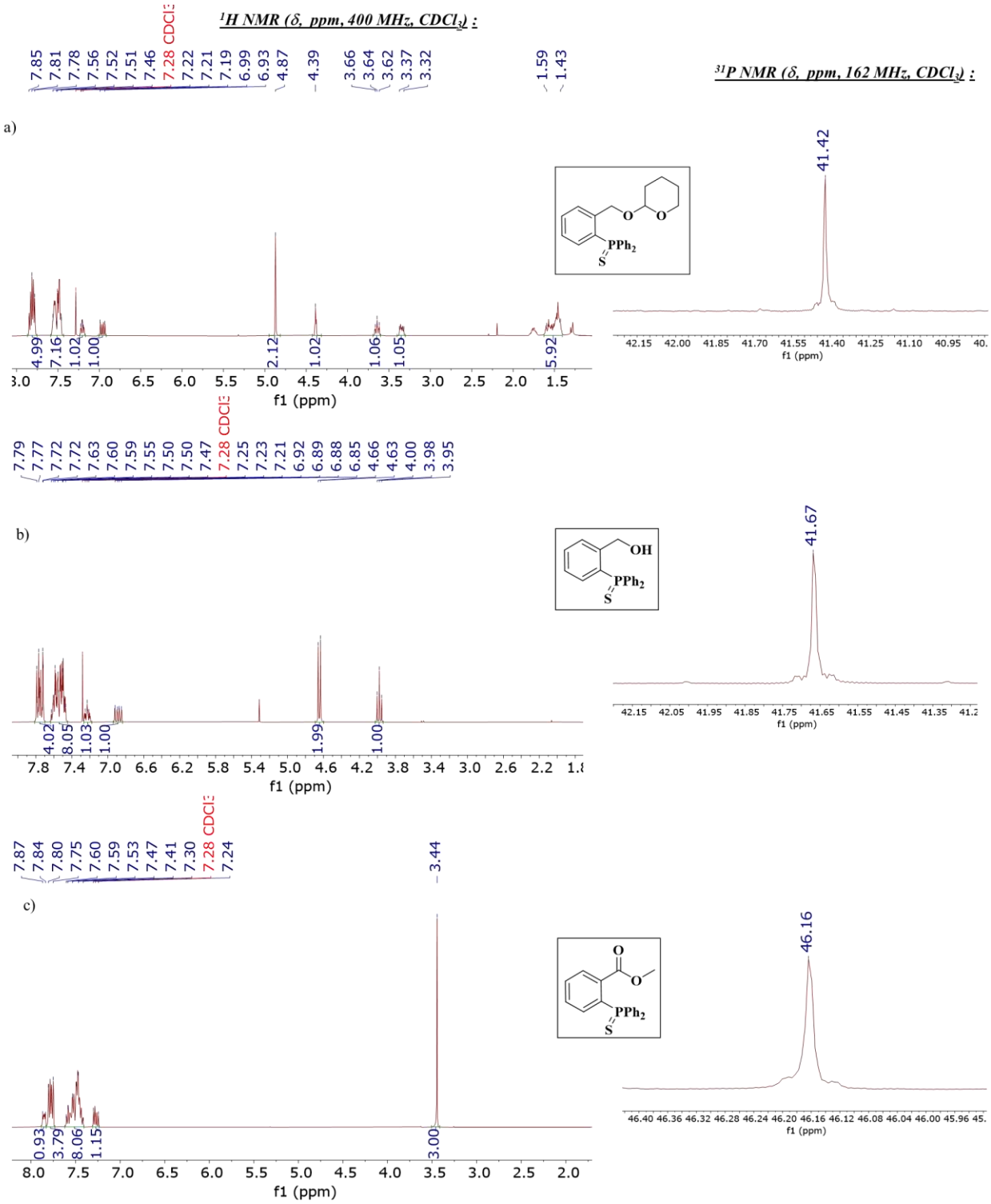

Figure 4. 1: ^{1}H ($CDCl_3$, 400 MHz), ^{31}P ($CDCl_3$, 162 MHz) NMR spectra of **4-43, 4-40** and **4-44**

White crystals of **4-43** were grown from the concentrated crude mixture in dichloromethane and the crystallographic structure was established by X-ray diffraction (Figure 4. 2), confirming the

presence of the tetrahydropyran ring in its chair conformation with puckering amplitude.[305] Single crystal of **4-44** were also grown by slow diffusion technique using hexane-DCM solvent combination and the molecular view obtained after X-ray diffraction has shown below (Figure 4. 3).

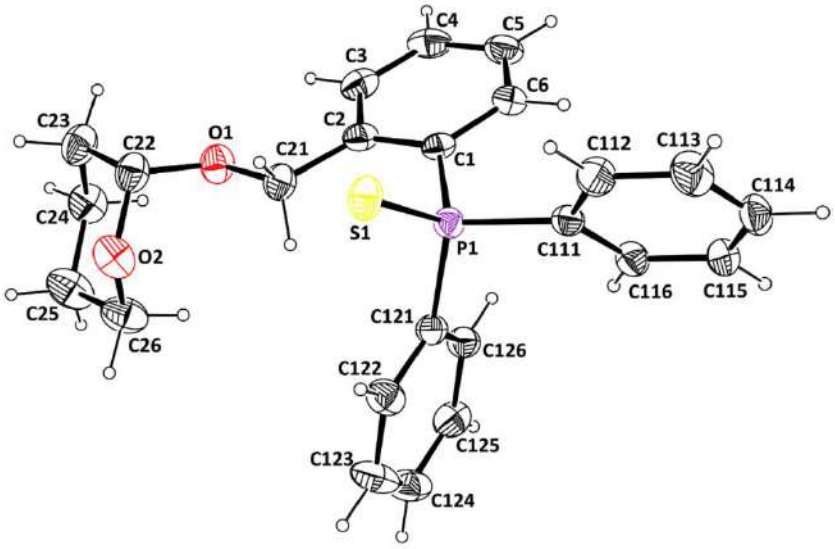

Figure 4. 2: Molecular view of compound **4-43** showing 50% probability displacement ellipsoids and the atom numbering scheme. H atoms are shown as small spheres of arbitrary radii.

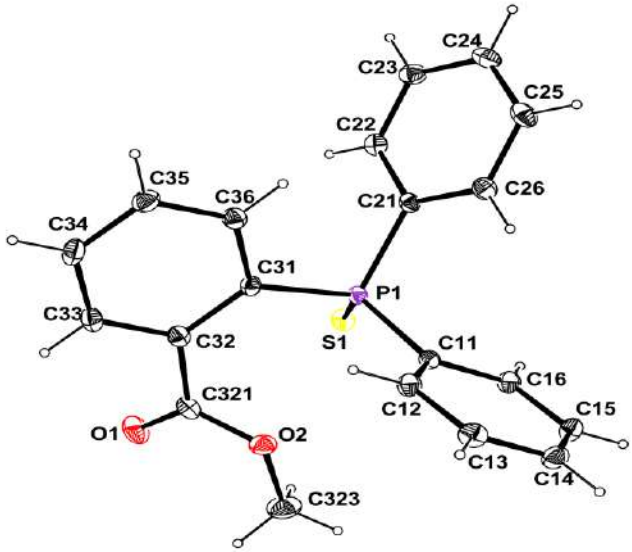

Figure 4. 3**:** Molecular view of **4-44** showing 50% probability displacement ellipsoids and the atom numbering scheme. H atoms are represented as small sphere of arbitrary radii.

The next objective was the OH/SH exchange on **4-40** There are several methods to synthesize thiols from alcohols. A few of the favorable ones are based on the use of thiourea,[306] Lawesson's reagent,[307] thioacetic acid or potassium thioacetate [308] *etc.*, followed by hydrolysis or deacetylation as appropriate.[309]

Bandgar *et al*. (2000) reported a direct one-pot synthesis of thiols from alcohols via the corresponding trifluoroacetates using trifluoroacetic anhydride (TFAA) and polymer-supported hydrosulphide [Amberlite IRA-400(SH^-)] (Scheme 4. 18).[310] This procedure yielded thiols in good yields in a very short time and under mild condition. This is because the polymer supported hydrosulfide is more nucleophilic than other sulphur-containing nucleophiles (*e.g.* NaSH). Therefore, activated alcohols are believed to react with the hydrosulfide exchange resin much faster.[310-311]

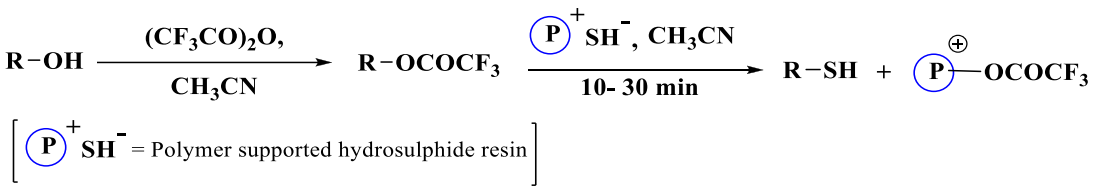

Scheme 4. 18: Thiol synthesis using polymer supported hydrosulphide resin

The procedure appeared to be convenient to perform. At first the hydrosulfide exchange resin was prepared by ion exchange from available Amberlite IRA- 400 ($C1^-$).[312] However, except partial activation of the alcohol **4-41** to the trifluoroacetate **4-45** upon addition of TFAA, detected by the crude ^1H and ^{31}P NMR (see Figure 4. 4), no significant further change took place after addition of resin or, other nucleophiles (*e.g.* NaSH, CH_3COSH); even after long reaction times (Scheme 4. 19).

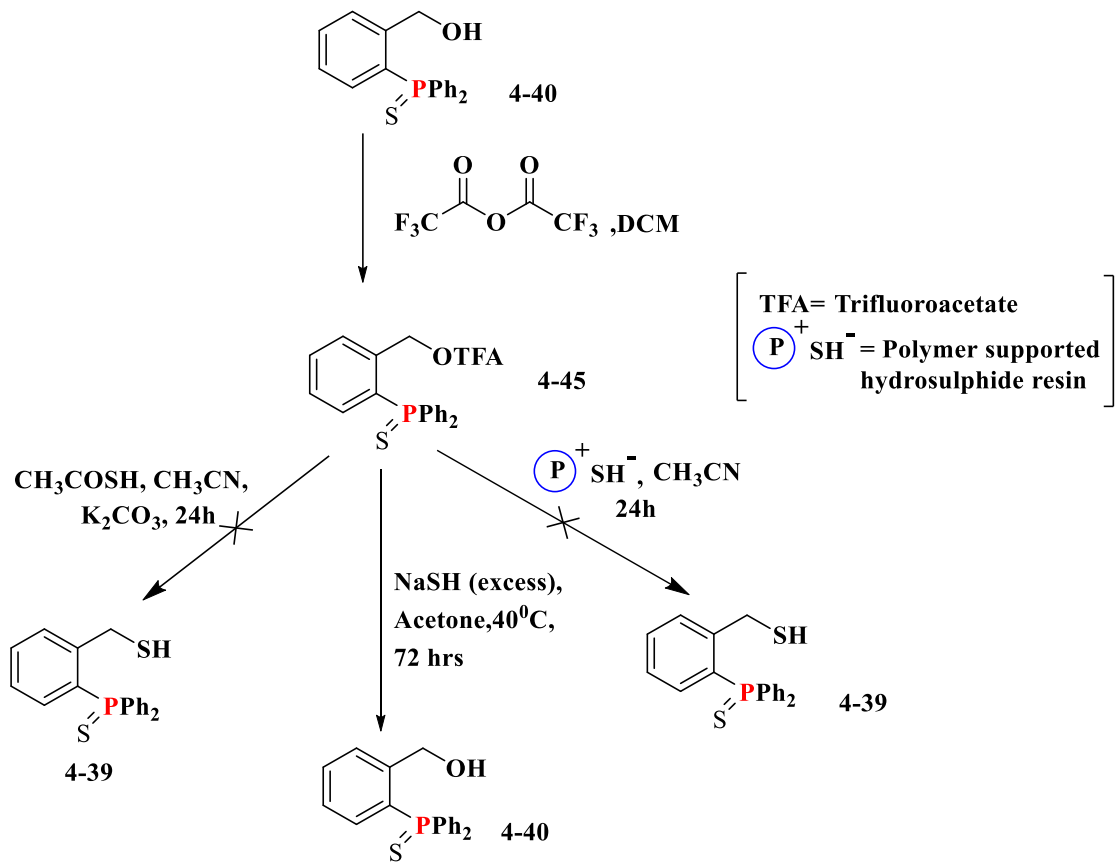

Scheme 4. 19: Initial attempts to synthesize thiol using polymer supported hydrosulphide resins and others

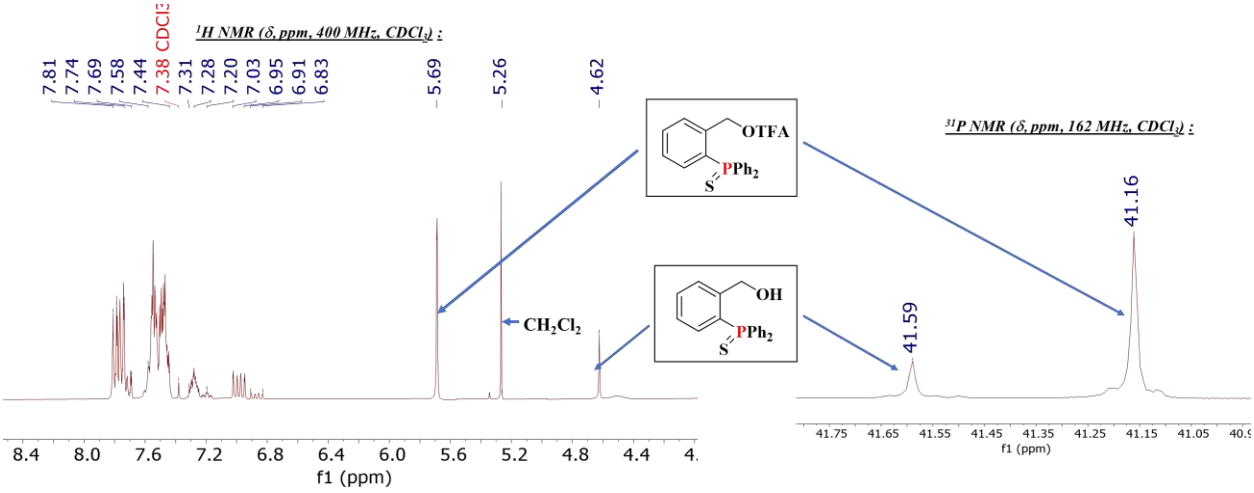

Figure 4. 4: Crude ^{1}H ($CDCl_3$, 400 MHz), ^{31}P ($CDCl_3$, 162 MHz) NMR spectra after the activation of **4-40** using trifluoroacetic anhydride

Certain modifications of the reaction condition could have been effective to produce the target molecule. As we were at the trial phase in pursuit of an optimum procedure of thiol synthesis, we kept on trying several other conventional procedures simultaneously. Among them, two different

are worth mentioning for the preparation of corresponding thioacetate. These are- the classical Mitsunobu reaction conditions, [313] which have already been used to synthesize thioacetates from alcohols[308a, 309a, 314] and the method developed in our team with the use of HBF_4 as a strong acid. In both cases thioacetic acid was utilized as the source of thioacetate part in the resulting product.

In regard to the Mitsunobu approach, we followed the procedure described by Rozwadowska *et al.* (1997)[314] which led to thioesterifcation of the enantiomerically pure 2-amino-l-phenyl-l,3-propanediol. Under these conditions, **4-40** led to thioacetate **4-46** in moderate yields (49%). However, a change of solvent (from THF to DCM) resulted in a yield enhancement (up to 15%) (Scheme 4. 20).

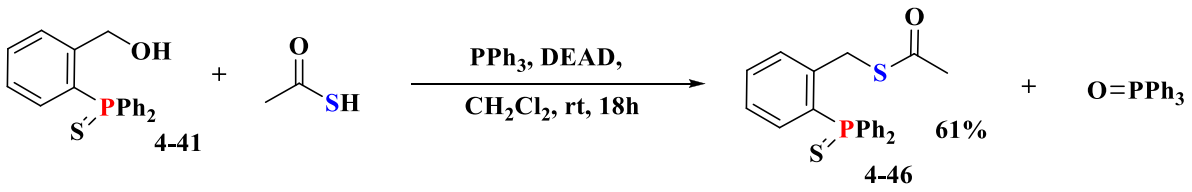

Scheme 4. 20: Synthesis of Thioacetate **4-46**

Alternatively, our previous experiences allowed us to recognize HBF_4 as a very strong acid to activate the ferrocenyl alcohols and assist the further substitution by amine (see Chapter-2) and thiol nucleophiles.[107b] Hence, this methodology was extended towards the alcohol **4-40** with thioacetic acid as the nucleophile. However, in presence of catalytic amount of HBF_4 (0.15 equiv.), surprisingly, instead of obtaining the desired thioacetate **4-46**; analogues thionoacetate **4-47** species was found as the major product (Scheme 4. 21).

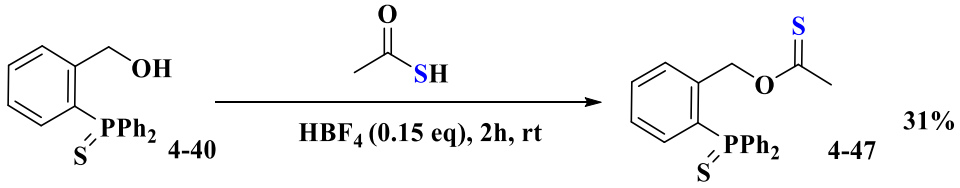

Scheme 4. 21: Formation of thionoacetate species **4-47** under catalytic HBF_4 condition

Thiocarboxylic acids, in general, exist in two different tautomeric forms- thiol and thione from (Scheme 4. 22); with the thiol form being the predominant one.[315]

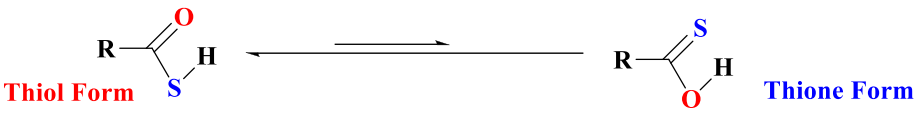

Scheme 4. 22:Tautomeric forms of simple thioacerboxylic acids

The preliminary observation with our system depicted in Scheme 4. 21, thus becomes intriguing as it reflects an O-centered nucleophilic attack and indicates reactivity of less stable thion tautomeric form of thioacetic acid. This phenomenon, therefore, requires further explorations directed towards kinetic and thermodynamic control of the reaction condition. The further investigations were subsequently carried out by another student (Abdelhak Lachguar) in our group. The aim, at the initial stage, is to carry out the esterification (thio or thiono) of simple benzyl alcohols by varying the equivalence of thioacetic acid; in order to establish a set of standard optimized conditions for obtaining either thio- or thiono- species as product. The work is ongoing at present.

The thioacetate **4-46** and thionoacetate **4-47**, were characterized by multinuclear NMR (^{1}H, ^{31}P, ^{13}C) spectroscopy and high-resolution mass spectrometry. The singlets at δ = 4.45 and 2.29, in the ^{1}H NMR spectrum of **4-46**, corresponds to the C$\underline{H}_2$ and C$\underline{H}_3$ protons, respectively [Figure 4. 5, a)]. The singlets at δ = 5.77 and 2.37 in corresponds to the C$\underline{H}_2$ and C$\underline{H}_3$ protons of **4-47**, respectively, in its ^{1}H NMR spectrum [Figure 4. 5, b)]. The ^{31}P NMR spectrum shows a peak at δ = 41.77 for the thioacetate **4-46** [Figure 4. 5, a)] and at δ = 41.46 for thionoacetate **4-47** [Figure 4. 5, b)]. From the ^{13}C NMR spectra, the presence of the CO group is confirmed by the peak at δ = 195.74 in case of **4-46**, whereas, the peak at δ = 218.61 represents the CS group for thionoacetate **4-47** (Figure 4. 6).

Single crystals of both the forms (**4-46** and **4-47**) were obtained by slow evaporation of the corresponding concentrated solutions in DCM and crystal structures were determined. The molecular views are shown in Figure 4. 7 for thioacetate **4-46** and in Figure 4. 8 for thionoacetate **4-47**. Both **4-46** and **4-47** molecules are built by an S-protected triphenylphosphine in which one of the phenyl rings is substituted at the β position by a methylthioacetate fragment either via the S- or the O-atom. For the thioacetate **4-46**, the C33-S2-C34-C35 torsion angle is 179.8(4)° and the dihedral angle of this average plane with the phenyl ring is 75.2(2)°.

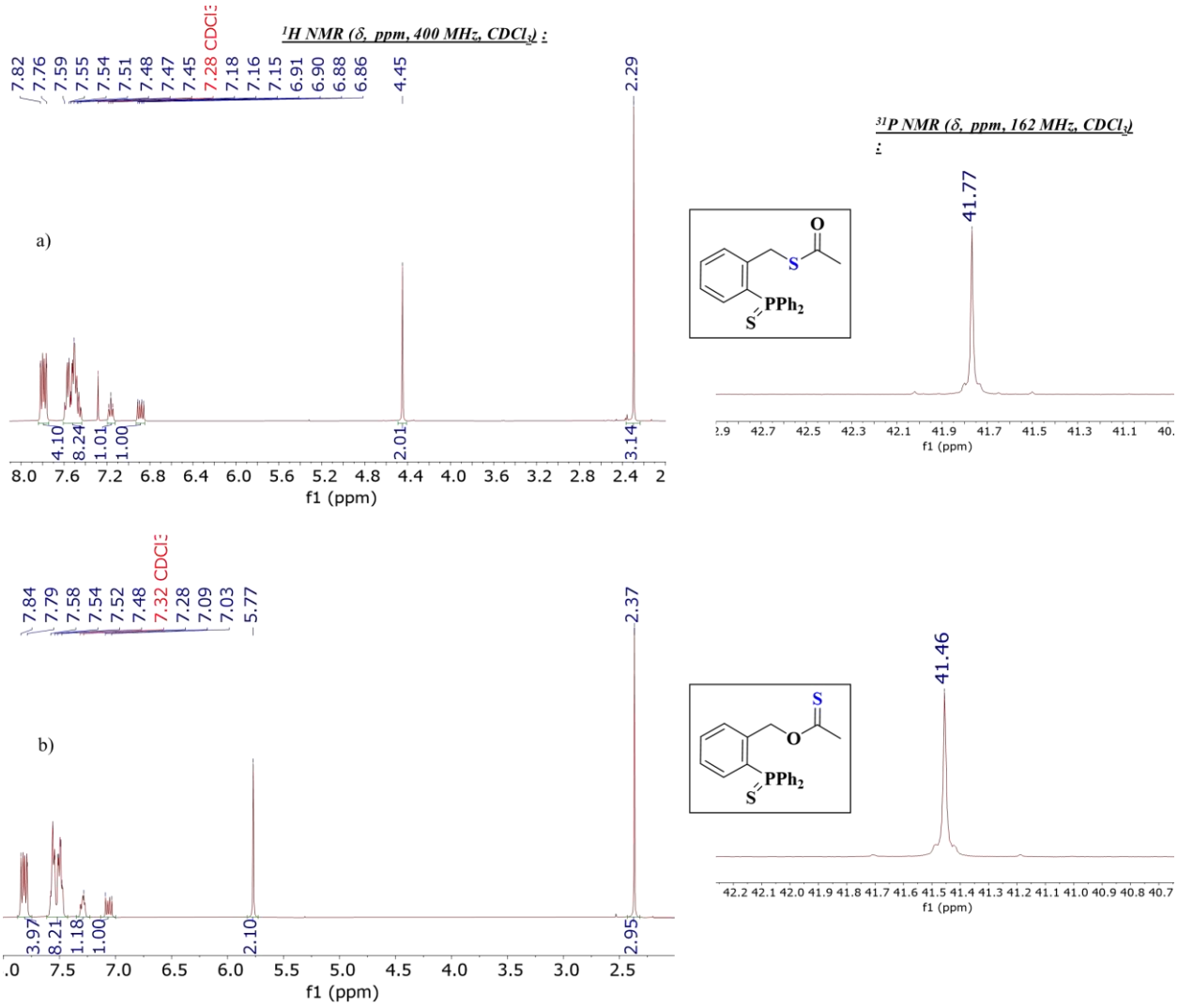

Figure 4. 5: ^{1}H ($CDCl_3$, 400 MHz) and ^{31}P ($CDCl_3$, 162 MHz) NMR of **4-46** and **4-47**

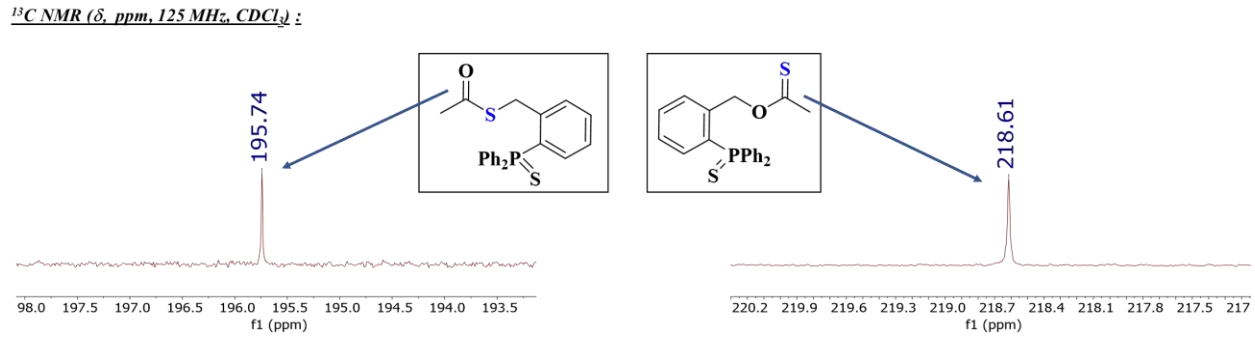

Figure 4. 6: ^{13}C ($CDCl_3$, 125 MHz) NMR spectra (selected region) of **4-46** and **4-47**

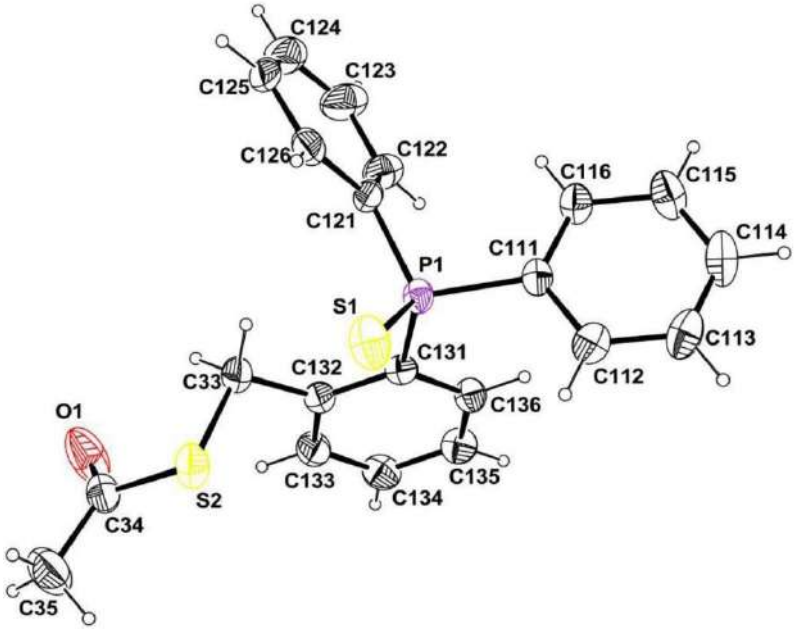

Figure 4. 7: Molecular view of compound **4-46** showing 50% probability displacement ellipsoids and the atom numbering scheme. H atoms are represented as small sphere of arbitrary radii

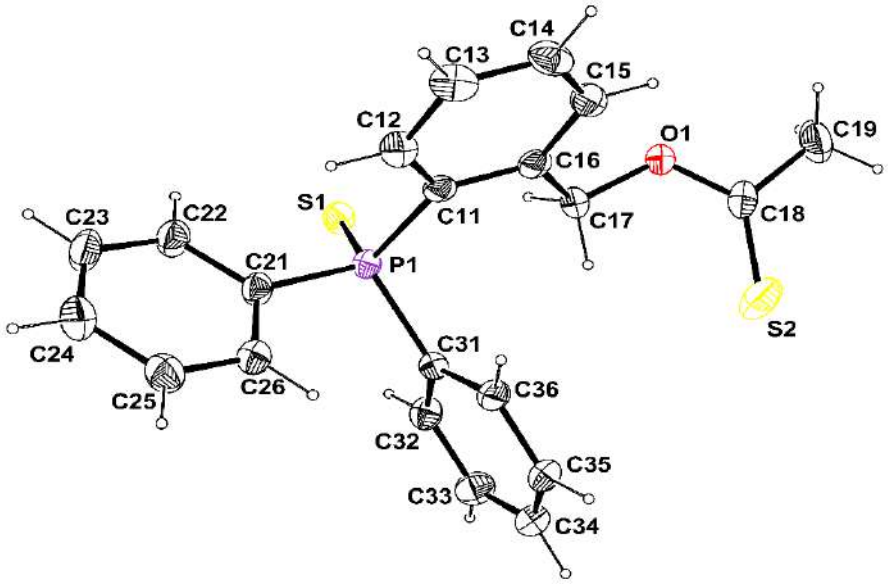

Figure 4. 8: Molecular view of compound **4-47** showing 50% probability displacement ellipsoids and the atom numbering scheme. H atoms are represented as small sphere of arbitrary radii.

With the suitable protocol of the Mitsunobu condition to synthesize the thioacetate **4-46** in hand, the next focus was on the deacetylation process to yield the thiol. Normally, the deacetylation reaction requires rather harsh reaction conditions, for instance strong bases (*e.g.* NaOH, KOH, NaOMe) at elevated temperatures. As a matter of fact, the thiol yield was reported as very low in

certain cases.[316] One of the factors responsible for these low yields is the thiol oxidation to disulfide, as commented in a survey by Balakumar *et al.* (2006).[309b] These authors optimized the base/solvent combination for the deacetylation of benzyl thioacetate, finding that the K_2CO_3/ methanol combination yielded no disulphide byproduct. The outcome of this brief survey reflects the fact that obtaining thiols in good yield and without disulphide byproduct is a challenging task. The thioacetate **4-46** yielded mostly the disulphide **4-48** (Scheme 4. 23) in relatively poor yields whenever basic hydrolytic conditions (aq. NaOH or NaOMe, MeOH) were used, even working under an argon atmosphere. It was obtained along with several impurities hard to analyze and purify. The thiol **4-39,** on the other hand, was formed as the major product when the K_2CO_3/ MeOH combination was used, as suggested by Balakumar *et al.* However, the yields were not very good (40%) and disulphide impurities formed as well. Next, reducing condition were tested using $LiAlH_4$ according to the protocol of Volante *et al.* (1981).[309a] To our delight, these conditions provided only the thiol **4-39,** without any significant impurities and in good yields (Scheme 4. 23). Hence, a completed, well-optimized scheme to synthesize the thiol **4-39** was established.

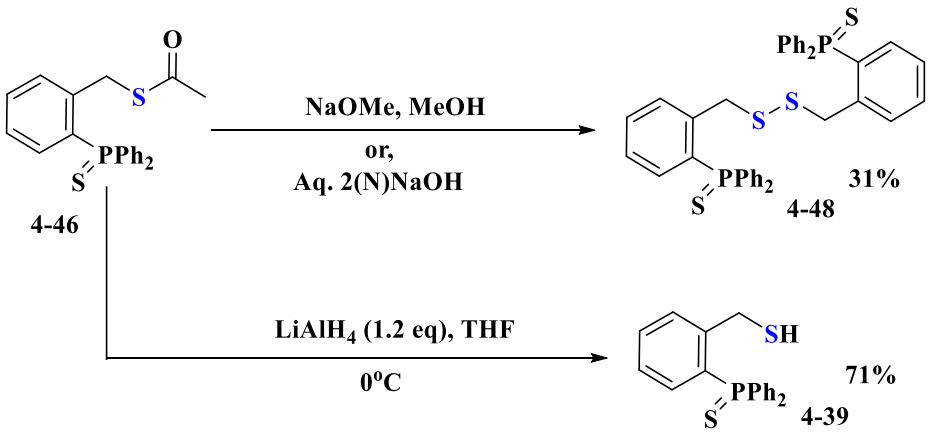

Scheme 4. 23: Formation of **4-50** or **4-39** depending upon reaction condition

The disulphide **4-48** and thiol **4-39** are recognizable after the comparison of their respective ^1H NMR spectra. In the ^1H NMR spectrum of **4-48**, a singlet at δ = 4.12 indicates the $C\underline{H}_2$ protons [Figure 4. 9, a)]. On the other hand, the same protons in **4-39** appeared as a doublet at δ = 3.92 due to the coupling (J= 8.5 Hz) with the SH proton. Correspondingly, a triplet resonance at δ = 2.42 was observed for the S$\underline{H}$ proton of **4-39** [Figure 4. 9, b)]. The ^{31}P NMR spectrum shows a peak in a similar region for the two compounds (δ = 41.69 for **4-48** and 41.50 for **4-39**, see Figure 4. 9).

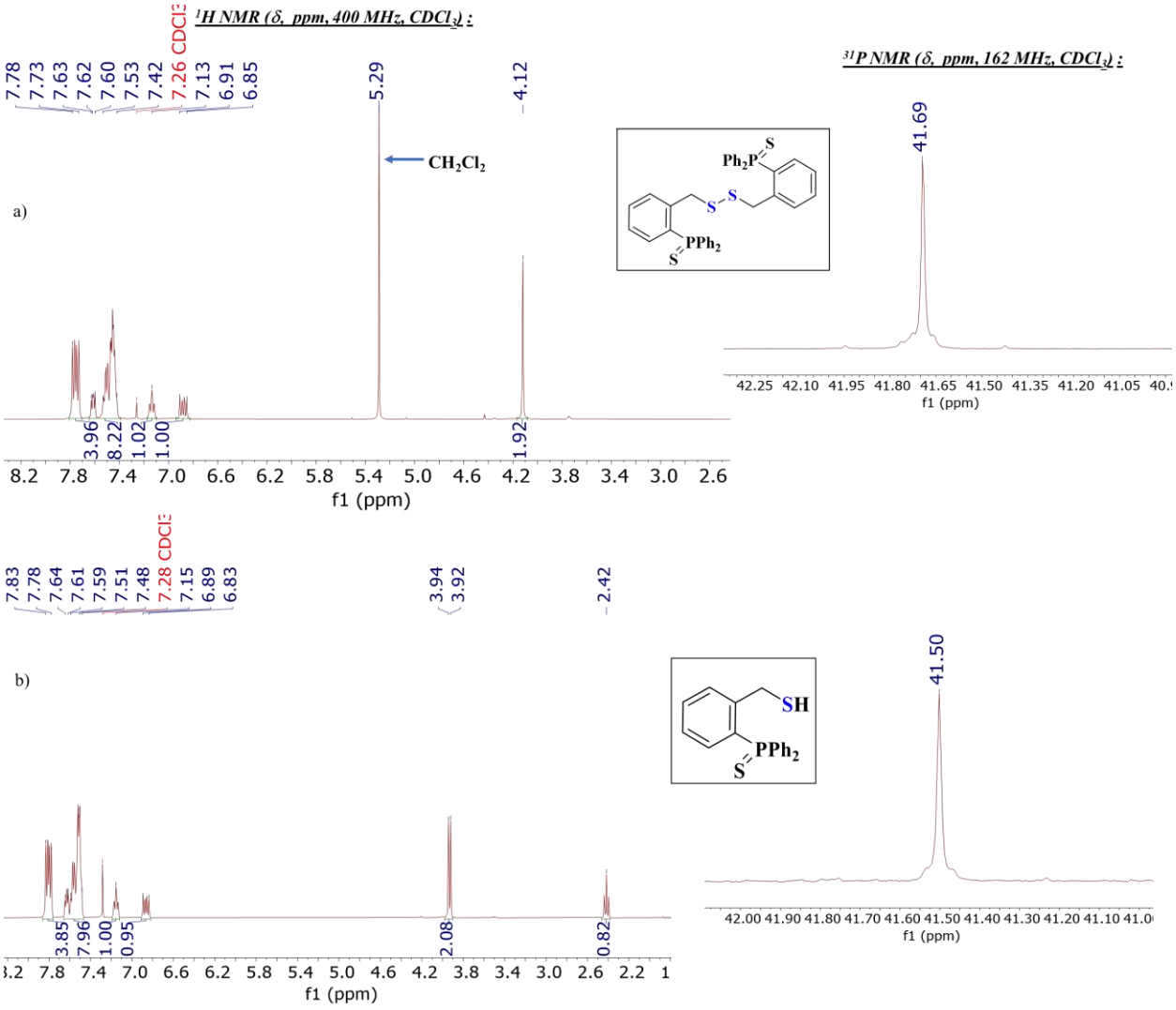

Figure 4. 9: ^{1}H ($CDCl_3$, 400 MHz) and ^{31}P ($CDCl_3$, 162 MHz) NMR spectra of **4-48** and **4-39**

Single crystals of the disulphide compound **4-48** were grown by slow diffusion of hexane in concentrated dichloromethane. Single crystals of the thiol **4-39,** on the other hand, were obtained by slow evaporation of a concentrated DCM solution. The molecular views of these structures are shown in Figure 4. 10 and Figure 4. 11, respectively.

Although the crystal of the disulphide compound **4-48** was twinned and poorly diffracting, the structure could be solved. One of the phenyl rings attached to the P2 atom and the disulphide fragment are statistically disordered over two positions as shown in the Figure 4.4. The disordered model was refined using restraints on the C-C and C-S distances as well as on the anisotropic thermal parameters to maintain a chemically reasonable model.

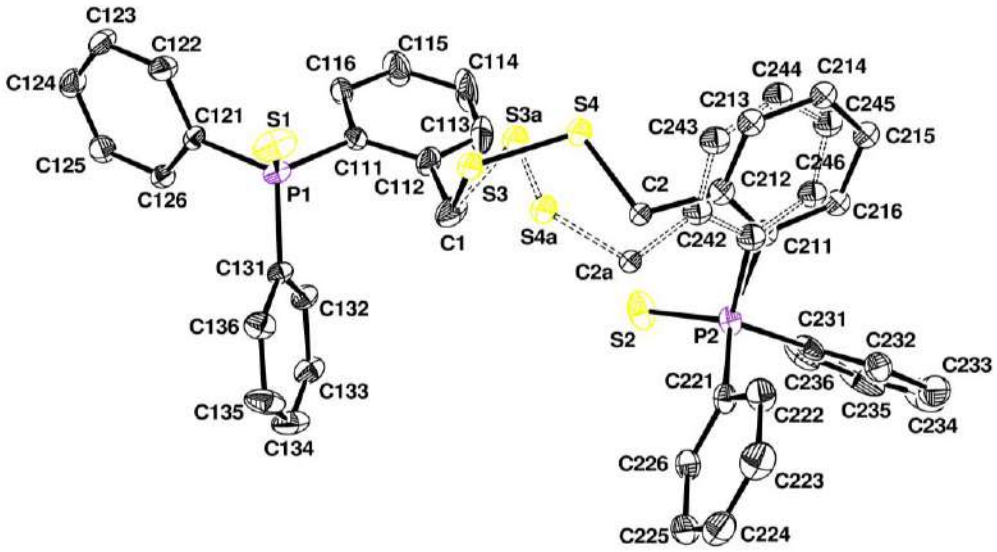

Figure 4. 10: Molecular view of compound **4-48** showing 30% probability displacement ellipsoids and the atom numbering scheme. H atoms have been omitted for clarity. The bonds for the disordered part are shown as dashed lines.

For the thiol compound **4-39**, two independent and essentially identical molecules are present in the asymmetric unit as shown on the molecular fitting (Figure 4. 12). Each molecule is isolated and exhibits only intramolecular C-H···S and S-H···S weak interactions.

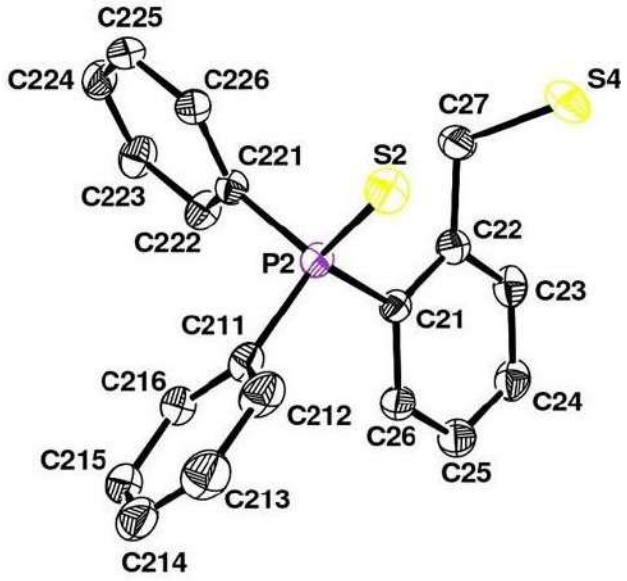

Figure 4. 11: Molecular view of compound **4-39** showing 50% probability displacement ellipsoids and the atom numbering scheme. H atoms are represented as small sphere of arbitrary radii.

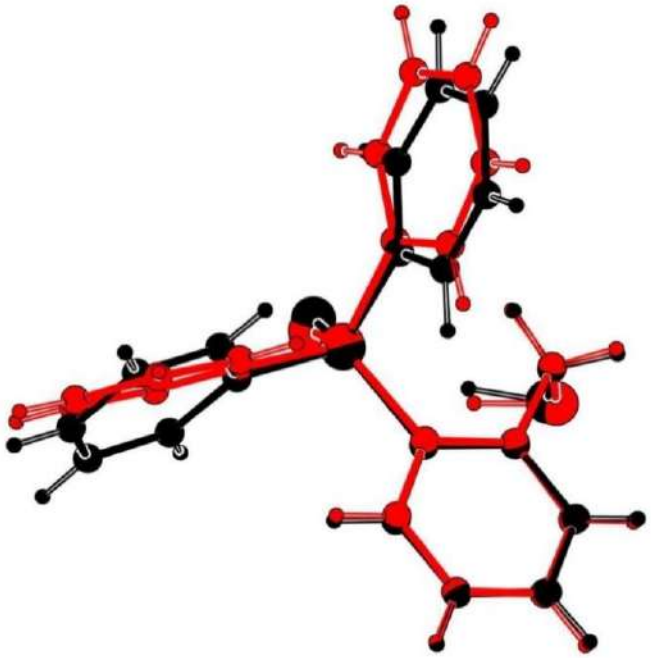

Figure 4. 12: Molecular fitting of the two molecules of **4-39** represented as balls red or black

4. 5) Ligand Synthesis: Final Step

Having in hand both coupling partners (the phosphine-containing mercaptan intermediate **4-39** and the enantiopure ferrocenyl alcohol **2-29**), we proceeded with the HBF_4 approach, a methodology largely used in the team to synthesize thioether containing ferrocenyl phosphine ligands (see Scheme 4. 24).[107b] The reaction entails treatment of the alcohol reagent with a concentrated (54%) solution of tetrafluoroboric acid (HBF_4) in Et_2O, followed by rapid addition of the coupling thiol partner. The reaction proceeds via the relatively stable α- ferrocenyl carbocation generated upon these strongly acidic conditions, which is then attacked by the nucleophilic thiol. We then succeeded to synthesize the protected form of the P,S,P ligand, **4-38** (Scheme 4.24). The reaction optimization revealed that 2 equivalents of thiol are sufficient for an efficient coupling reaction, whereas the original procedure with simpler thiols required a larger excess (20-30 equiv.) of the thiol nucleophile.

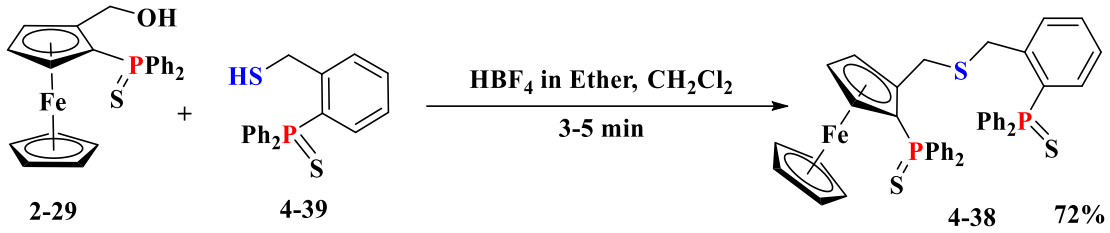

Scheme 4. 24: Synthesis of P,S,P proligand **4-38**

The proligand **4-38** was completely characterized by multinuclear NMR (^{1}H, ^{31}P, ^{13}C) spectroscopy and HRMS. From the ^{1}H NMR spectrum, 14 aromatic protons were recognized from multiplets at slightly different positions in the aromatic region (δ = 7.85-6.83). Multiplets at δ = 4.44, 4.24, 3.80 and a singlet at δ = 4.28 represent the three non-identical protons of the substituted Cp ring and the five equivalent protons of the unsubstituted Cp ring, respectively. Two AB-type doublets, indicating the two different C<u>H$_2$</u> groups, are observed at δ = 4.04, 3.82 and δ = 3.96, 3,51. The ^{31}P NMR spectrum shows two distinct peaks at δ = 41.77 and δ = 41.51 indicating two different thiophosphines (Figure 4. 13).

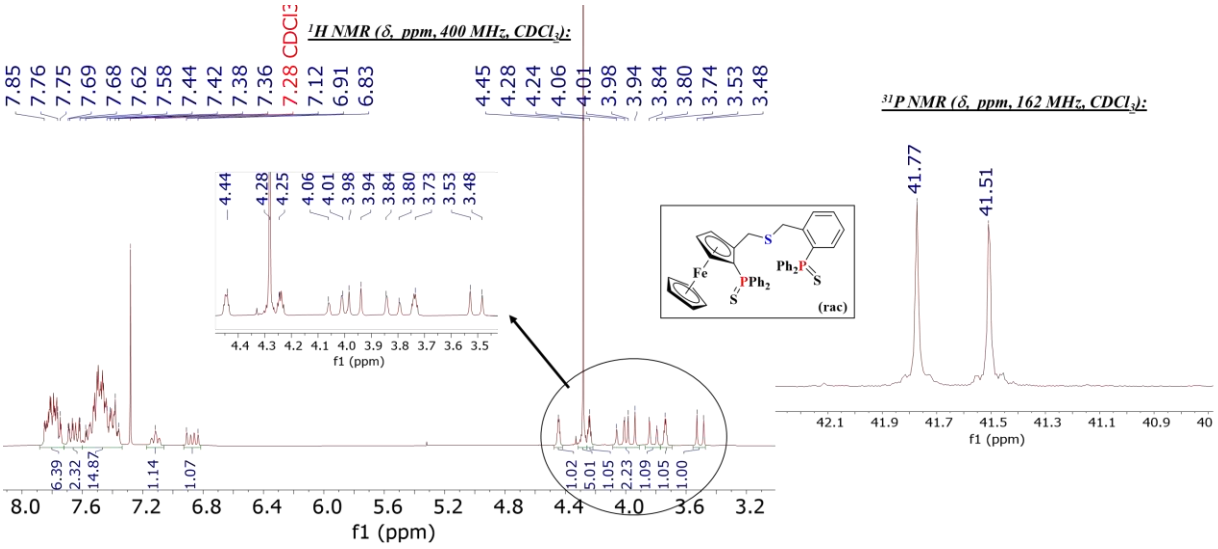

Figure 4. 13: ^{1}H ($CDCl_3$, 400 MHz) and ^{31}P ($CDCl_3$, 162 MHz) NMR Spectra of **4-38**

Single crystals of racemic **4-38** were grown by slow diffusion of hexane into a concentrated THF solution. The structure was determined accordingly by X-ray diffraction (see Figure 4. 14). The compound crystallizes in the centrosymmetric space group P-1, thus both R/S enantiomers are present in the crystal.

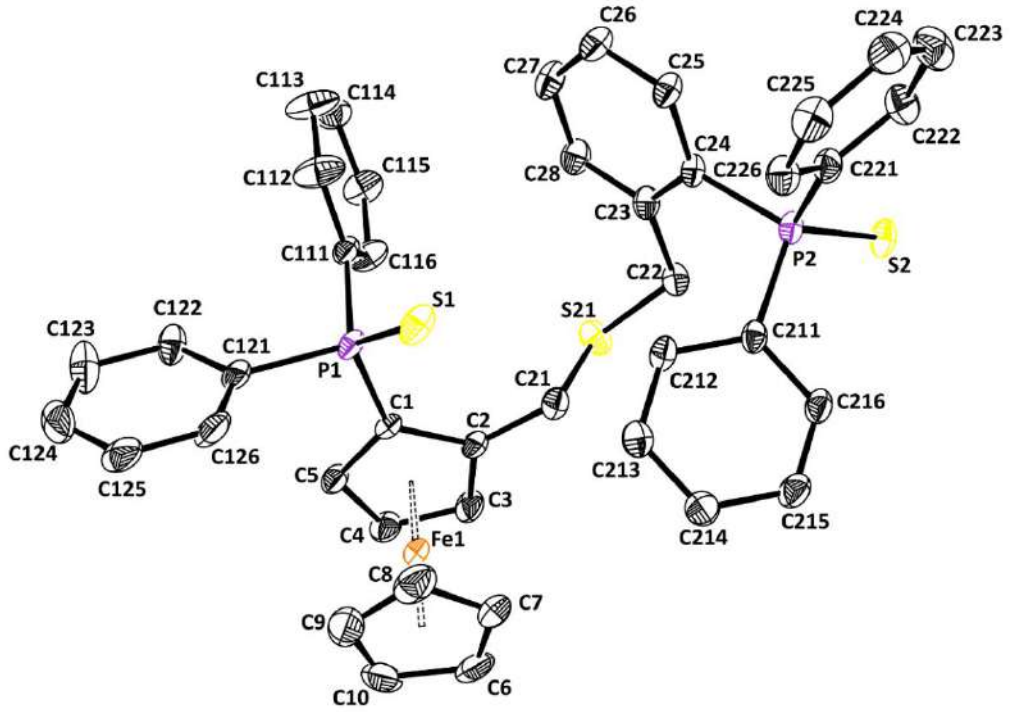

Figure 4. 14: Molecular view of compound **4-38** showing 30% probability displacement ellipsoids and the atom numbering scheme. H atoms have been omitted for clarity.

The two Cp rings are roughly eclipsed. The P1 atom is nearly in the Cp ring mean plane (deviation of 0.106(6) Å) whereas, the S1 atom is -0.939(7) Å from this plane. The S2 atom is above the plane by 0.619 Å. There are weak intramolecular C-H···S interactions within the molecule.

The desulfuration of the ligand was carried out using excess (10-12 equiv.) of tris(dimethylamino)phosphine in dry toluene under refluxing condition, yielding the free P,S,P ligand **4-1** (yield 77%, see Scheme 4. 25).

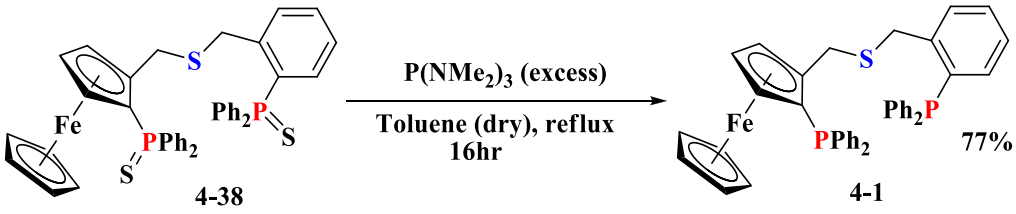

Scheme 4. 25: Desulphuration of the protected P,S,P ligand **4-38**

Ligand **4-1** was characterized by multinuclear (^{1}H, ^{31}P, ^{13}C) NMR spectroscopy. In the ^{31}P NMR spectrum, peaks at δ = -23.76 and δ = -16.63 confirms the free phosphines in the molecule. In the ^{1}H NMR spectrum, two sets of AB-type doublets were found (δ = 4.00, 3.81 and 3.68, 3.64) for

the two different type of diastereotopic, mutually coupled CH_2 protons along with the usual aromatic, cyclopentadienyl (Cp) and aliphatic proton resonances (Figure 4. 15).

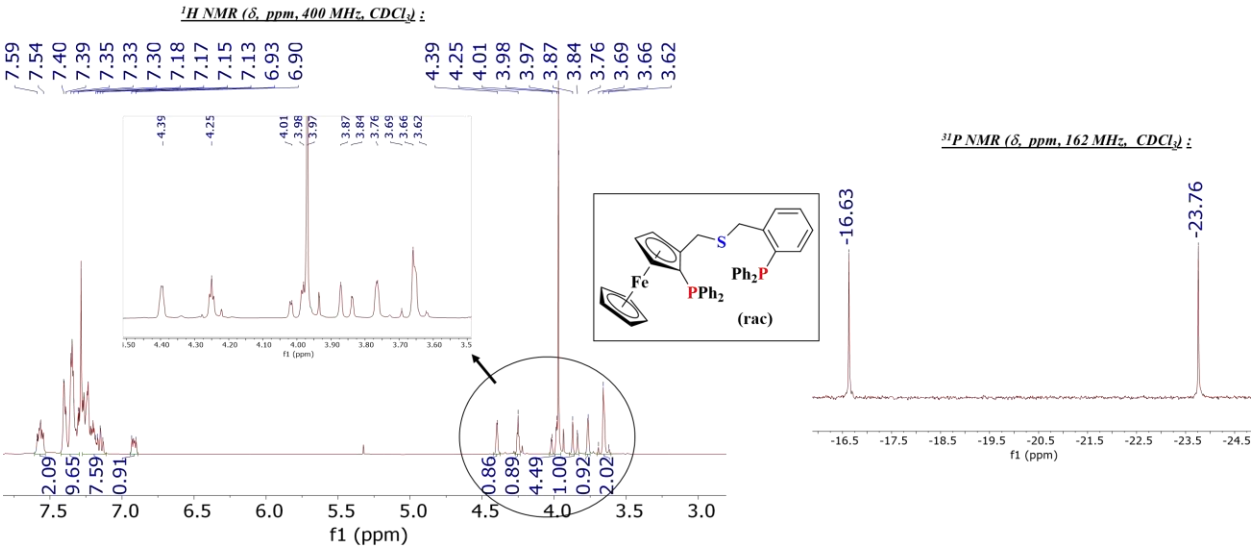

Figure 4. 15: ^{1}H ($CDCl_3$, 400 MHz) and ^{31}P ($CDCl_3$, 162 MHz) NMR spectra of **4-1**

4. 6) Retrosynthetic Analysis of the P,S,N ligand 4-2

The retrosynthetic analysis scheme for the P,S,N ligand **4-2** is given below in Scheme 4. 26.

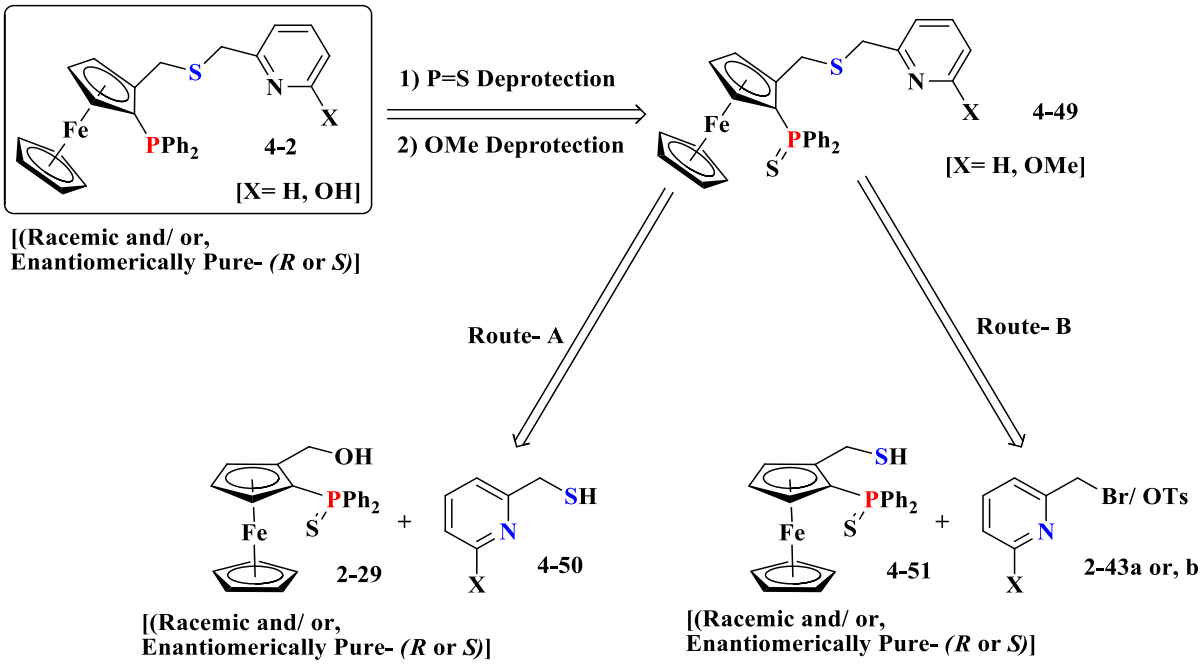

Scheme 4. 26: Retrosynthetic Analysis of the corresponding P,S,N ligand

Two possibilities have been considered: either the same pathway already established for the P,S,P ligand **4-1** (Route-A) from the alcohol **2-29** and a suitably thiol-functionalized pyridine, or an alternative pathway (Route-B) resulting in the assembly of the same C-S bond with exchanged functional groups (thiol on the ferrocene side chain and a leaving group on the pyridine side chain).

4. 7) Selection of Synthetic Route: Comparison between Route-A and Route-B

Route A requires the synthesis of a picolylthiol **4-50** as an intermediate. On the other hand, a phosphine-containing ferrocenyl thiol **4-51** should be synthesized and coupled with the previously synthesized 2-(bromomethyl)-6-methoxypyridine **2-43a** or 2-(tosylmethyl)-6-methoxypyridine **2-43b** (see Chapter 2) if Route B has to be followed. Taking into account of the points raised during the previous synthesis of the P,S,P ligand **4-1** and the literature overview, it was realized that the formation of a certain amount of disulphide is inevitable when synthesizing a thiol. Thus, Route A features a few limitations. Notably:

1) For every newly designed thioether-containing ligand, the corresponding thiol has to be independently synthesized, bringing the possibility of substantial dimerization. Thus, this synthetic route becomes entangled at the thiol intermediate preparation stage.

2) For the pyridyl species, even if the thiol, can be efficiently obtained, it will be necessary to find a new procedure to couple it with the ferrocenyl alcohol. The reason behind that is under strong acidic condition (HBF_4), the pyridine nitrogen atom will be readily protonated. The question then is whether the resulting mercaptomethyl-substituted pyridinium cation remains sufficiently reactive to quench the carbocation produced from the alcohol **2-29** in the presence of excess HBF_4.

Our first assumption was validated during the synthetic attempts to prepare the pyridyl thiol **4-50**. The corresponding pyridyl disulphide **4-53** was obtained as the major product, even under strong reducing ($LiAlH_4$) condition (Scheme 4. 27).

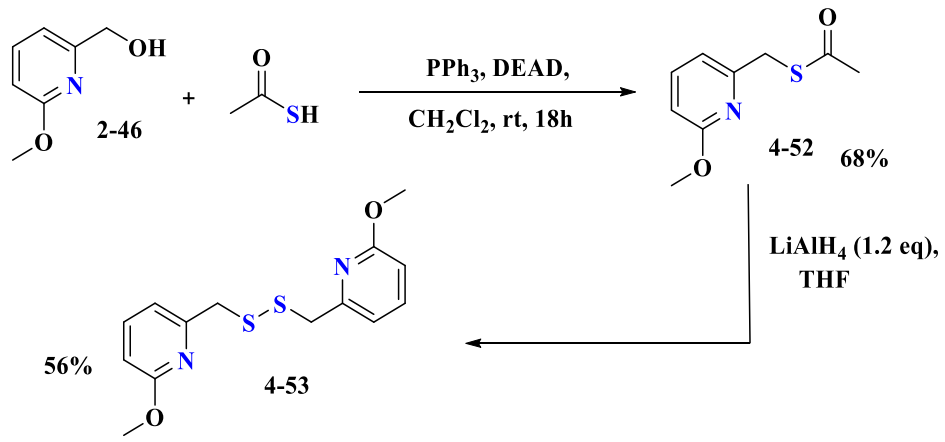

Scheme 4. 27: Formation of pyridyl disulphide **4-53**

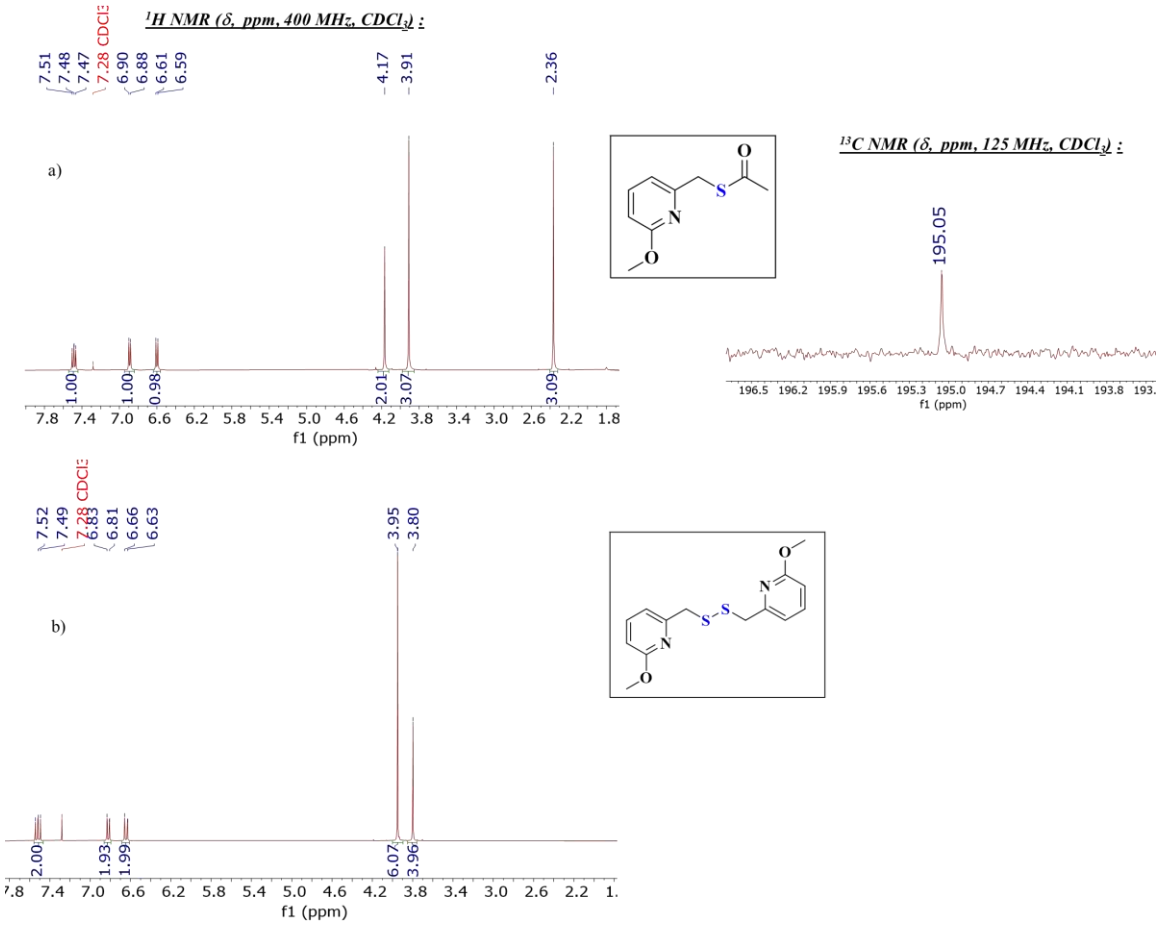

Figure 4. 16: ^{1}H ($CDCl_3$, 400 MHz) NMR spectra of **4-52, 4-53** and ^{13}C ($CDCl_3$, 125 MHz) NMR spectrum (selected region) of **4-52**

The thioacetate **4-52** and the disulphide **4-53** were characterized by multinuclear NMR (^{1}H, ^{31}P, ^{13}C) spectroscopy and HRMS. In the ^{1}H NMR spectrum of **4-52**, the singlets at δ = 4.17, 3.91 and

2.36 correspond to the C$\underline{H}_2$, OC$\underline{H}_3$ and C$\underline{H}_3$ protons, respectively. The presence of the CO group is confirmed by the peak at δ = 195.05 in the ^{13}C NMR spectrum of **4-52** [Figure 4. 16, a)]. In case of **4-53**, the corresponding OC$\underline{H}_3$ and C$\underline{H}_2$ proton resonances were observed at δ = 3.95 and δ = 3.80, respectively [Figure 4. 16, b)]. However, the existence of **4-53** was confirmed by its high resolution mass spectrum ([M-H]$^+$ at 309.0728, see Figure 4. 17).

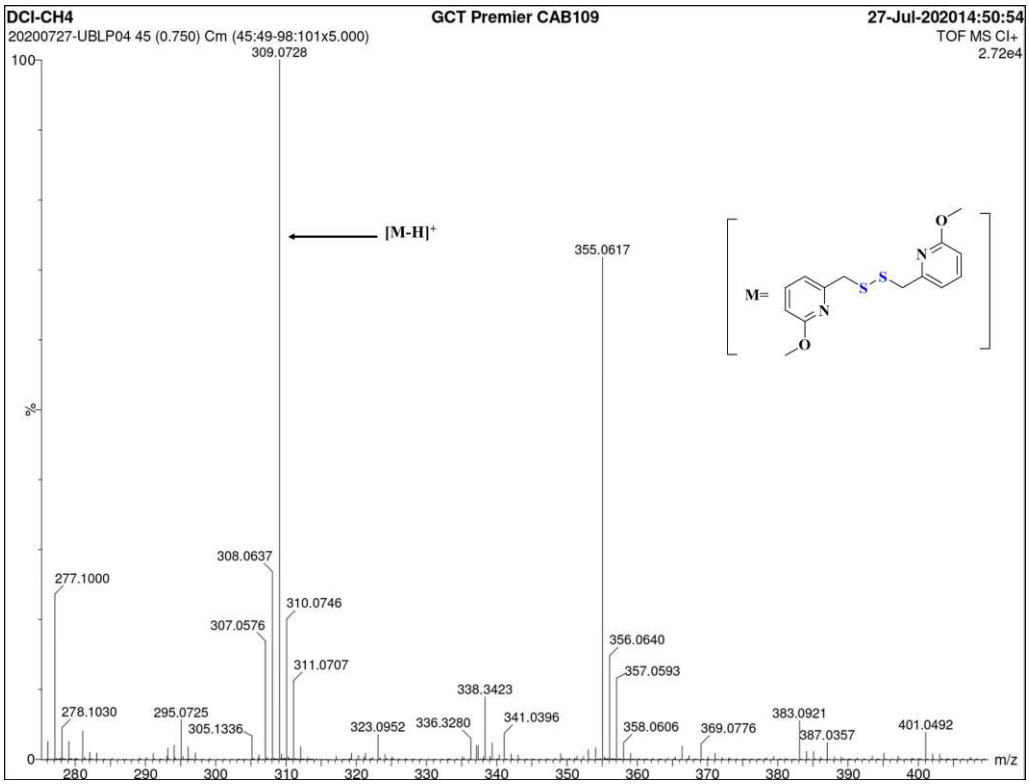

Figure 4. 17: High resolution mass spectrometry of **4-53**

When considering Route B, there is again the possibility of ferrocenyl disulphide formation. However, if a good protocol can be developed in terms of thiol stabilization, the subsequent activation of the thiol to the needed thiolate for the coupling process must be easy. Thus, the desired ligand synthesis would become easier. In addition, the procedure can easily be extended to the formation of other yet unknown ferrocenyl thioethers. Interestingly, Togni *et al*. previously reported a procedure to synthesize enantiomerically pure 1-[(diphenylphosphino)ferrocenyl]ethyl mercaptan (**4-4)**, which was already discussed earlier in this chapter (see Scheme 4. 2).[267] Therefore, although not free of challenges, Route B was chosen for the ligand synthesis.

4. 8) Synthesis of (2-diphenylthiophosphinoferrocenyl)methylmercaptan 4-51

To synthesize the ferrocenyl thiol, the corresponding thioacetate **4-54** of alcohol **2-29** was prepared by the HBF_4 method, using thioacetic acid as nucleophile. In the presence of 2 equivalents of HBF_4 and an excess of thioacetic acid, the expected thioacetate **4-54** was found to be formed with good yield. (Scheme 4. 28).

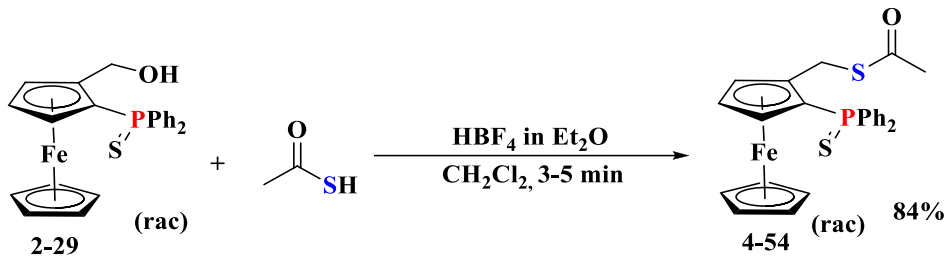

Scheme 4. 28: Synthesis of ferrocenyl thioacetate **4-54**

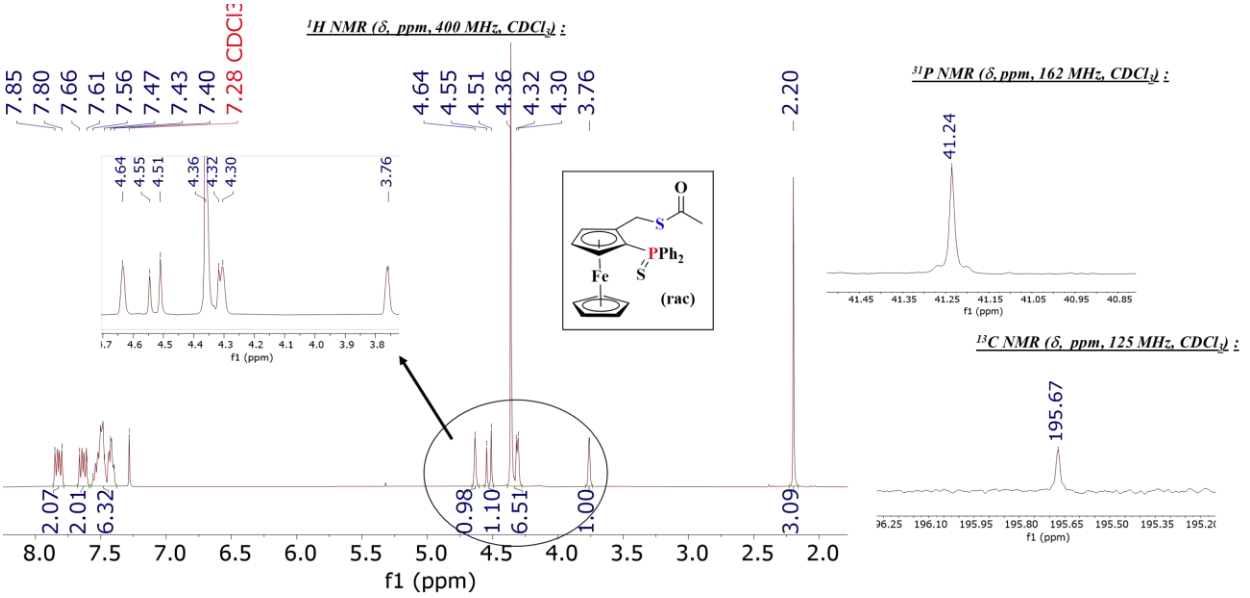

Figure 4. 18: ^{1}H ($CDCl_3$, 400 MHz), ^{31}P ($CDCl_3$, 162 MHz) and ^{13}C ($CDCl_3$, 125 MHz) (selected region) NMR Spectra of **4-54**

In the ^{1}H NMR spectra of **4-54,** along with the usual singlet of the unsubstituted Cp ring protons (δ = 4.36) and the three multiplets of the non-identical Cp ring protons (δ = 4.64, 4.30, 3.76), two AB-type doublets are observed (δ = 4.53, 4.34) and assigned to the CH_2 group attached to the Cp ring. The singlet at δ = 2.20 corresponds to the $C\underline{H_3}$ protons. The ^{31}P NMR spectrum shows a peak at δ = 41.24. The presence of the CO group is confirmed by the peak at δ = 195.66 in the ^{13}C NMR

spectrum (Figure 4. 18). Compound **4-54** was also characterized by HRMS (see supporting information).

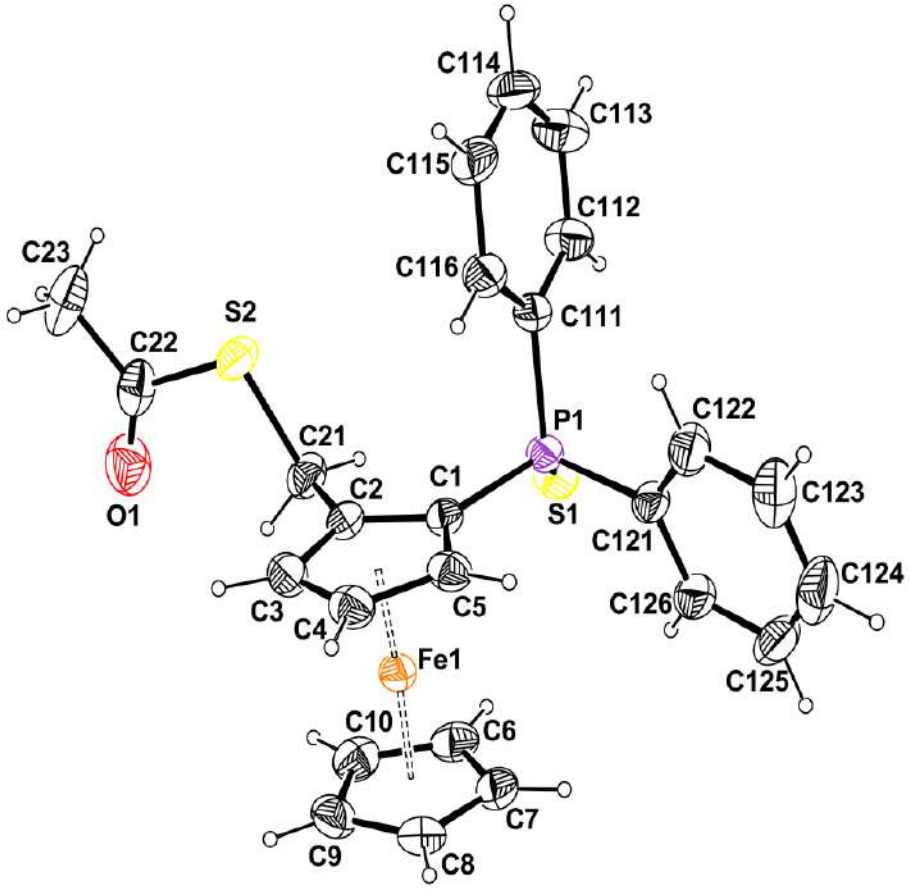

Figure 4. 19: Molecular view of compound **4-54** showing 50% probability displacement ellipsoids and the atom numbering scheme. H atoms are represented as small sphere of arbitrary radii.

Orange single crystals of **4-54** were formed by slow evaporation from a concentrated dichloromethane solution and the crystal structure was established by X-ray diffraction (Figure 4. 19). The two Cp rings are slightly staggered with a twist angle of 21.4°. The C21-S1-C22-C23 torsion angle is 179.5(4)°, thus the four atoms are essentially coplanar. This plane has a dihedral angle with the Cp plane of 87.7(2)°.

The phosphine-containing ferrocenyl thiol **4-51** was formed under reducing conditions at elevated temperatures ($LiAlH_4$ in refluxing THF), although the disulfide species **4-55** was also obtained in significant amounts (Scheme 4. 29).

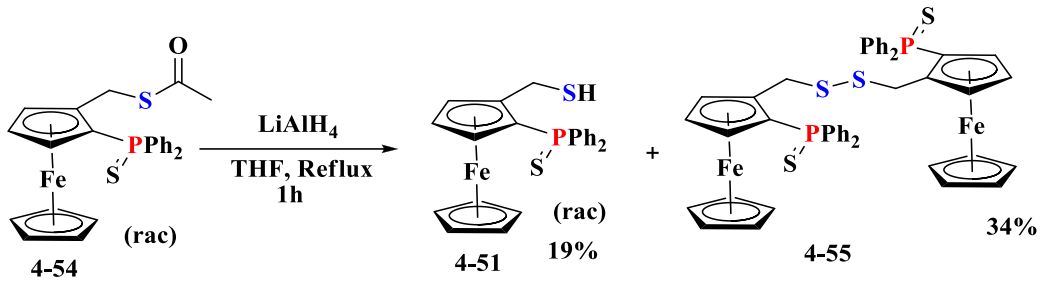

Scheme 4. 29: Synthesis of thiol by reducing the thioacetate

However, the two species could be separated, isolated and fully characterized (NMR and HRMS). The air stability of **4-53** was found poor. Upon storage in air for few days, partial dimerization was observed (See Figure 4. 23).

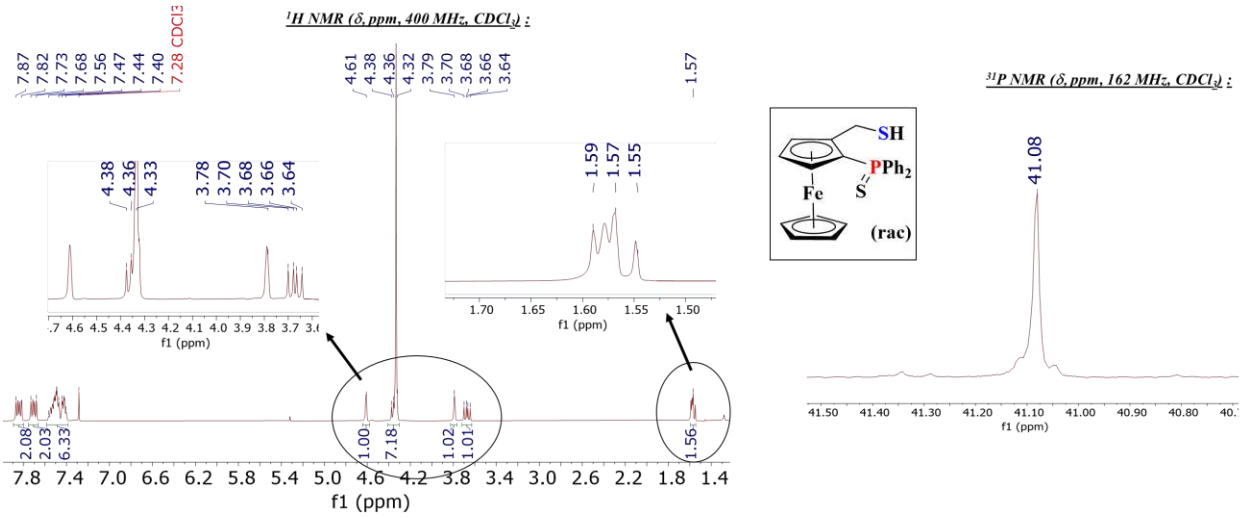

Figure 4. 20: ^{1}H ($CDCl_3$, 400 MHz) and ^{31}P ($CDCl_3$, 162 MHz) NMR Spectra of **4-51**

In the ^{1}H NMR spectrum of **4-51,** the singlet of the unsubstituted Cp ring protons is found at δ = 4.36. The three multiplets assigned to the non-identical Cp ring protons are found at δ = 4.61, 4.32, 3.78. The diastereotopic, mutually coupled C<u>H</u>$_2$-protons appeared as doublets of doublet at δ = 4.35 and δ = 3.67, due to further coupling with the S<u>H</u> proton, which is in turn characterized by a triplet at δ = 1.57. The ^{31}P NMR spectrum shows the thiophosphine resonance at δ = 41.24 (Figure 4. 20).

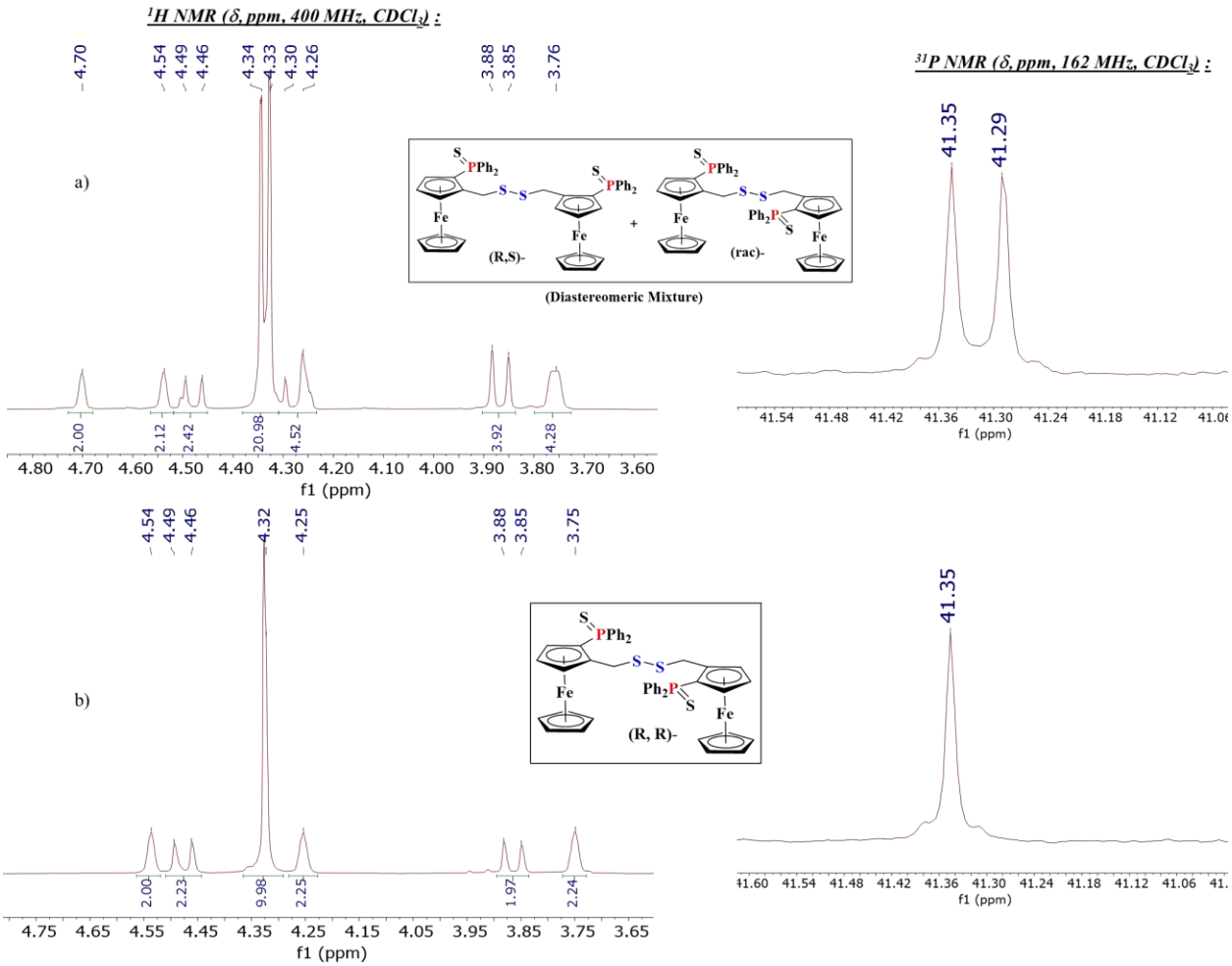

Figure 4. 21: ^{1}H ($CDCl_3$, 400 MHz) (Cp region) and ^{31}P ($CDCl_3$, 162 MHz) NMR Spectra of diastereomeric mixture of **4-55** and *(R,R)*- **4-55**

Dimerization of the racemic **4-51** resulted in a diastereomeric mixture of the disulphides **4-55** *(R,R/S,S* and *R,S)*, which could not be separated by traditional column chromatographic techniques. The enantiomerically pure disulphide *(R,R)* was obtained from the dimerization of the enantiomerically pure *(R)* **4-51** and thoroughly characterized by NMR. By comparison of the NMR spectra of the pure enantiomer and diastereomeric mixture, the resonances of the *meso* isomer (R,S) could be assigned. To describe the assignment the Cp region of the ^{1}H and the ^{31}P NMR spectra of diastereomeric mixture of **4-55** [Figure 4. 21**,** a)] and *(R,R)*- **4-55** [Figure 4. 21, b)] were chosen. From the ^{1}H NMR spectrum (Cp region) of the **4-55** diastereomeric mixture, the singlet at δ = 4.33 could be assigned to the unsubstituted Cp of the chiral *(R,R* or *S,S)* **4-55**, thus the peak at δ = 4.34 [Figure 4. 21, a)] is assigned to the unsubstituted Cp of the *meso (R,S)* **4-55**, by exclusion.

Through the same procedure, the multiplets at δ = 4.70, 4.26, 3.75 could be assigned to the unsubstituted Cp protons of *meso* **4-55**, while those at δ = 4.54, 4.26, 3.75 belong to chiral *(R,R* or *S,S)* **4-55**. The AB-type doublets for *meso* **4-55** and *(R,R* or *S,S)* **4-55** are at δ = 4.28, 3.86 and δ = 4.47, 3.86, respectively. Finally, the ^{31}P NMR spectra give peaks at δ = 41.29 for *meso* **4-55** and at δ = 41.35 for chiral *(R,R* or *S,S)* **4-55** (Figure 4. 21).

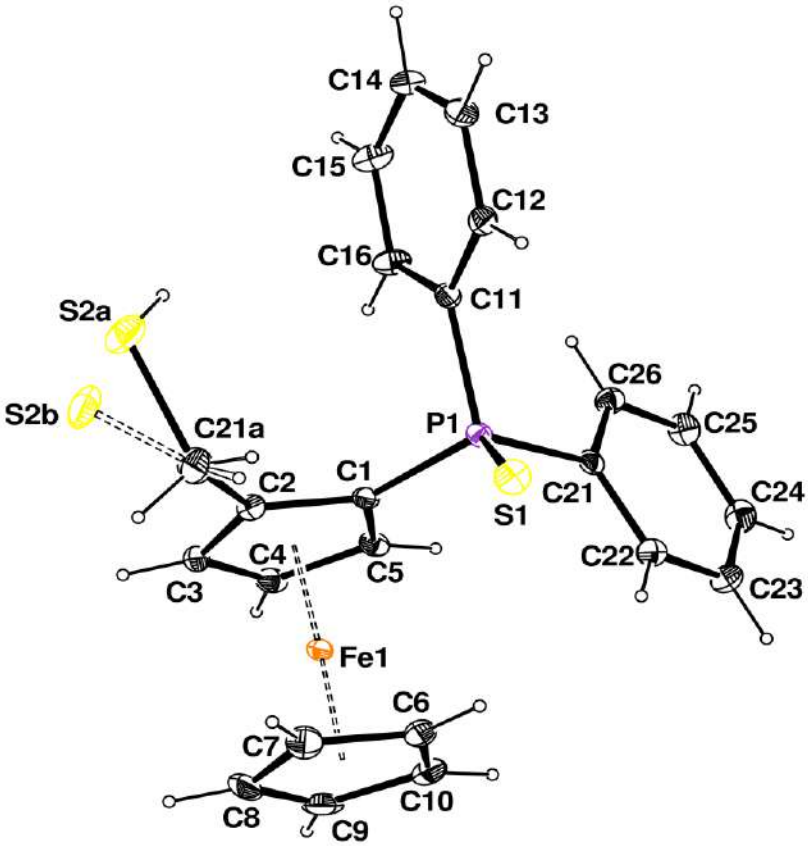

Figure 4. 22: Molecular view of compound **4-51** showing 30% probability displacement ellipsoids and the atom numbering scheme. H atoms have been omitted for clarity. The bonds for the disordered CHS part are shown as dashed lines.

Unfortunately, single crystals of any isomeric form of **4-55** could not be obtained to date, in spite of several attempts with different techniques (slow evaporation, diffusion, layering etc.). Nevertheless, a single crystal of the thiol derivative **4-51** could be obtained by slow diffusion of hexane into DCM solution and the crystal structures was determined (Figure 4. 22).

From the structure, shown in Figure-4. 22, two rather large electron densities in proximity of the 2-substituted CH_2 group were observed at distances of 1.8 and 1.6 Å from the C atom, respectively.

Free refinement of these densities as partial occupancy S atoms, with the only constraint of a full total occupancy, gave well-behaved thermal parameters for S2a and S2b in a refined occupancy ratio of 0.84/0.16 (Figure 4. 22), with C21a-S2a = 1.871 Å and C21a-S2b = 1.516Å. This suggests that the crystal is a solid solution of two compounds where methylthiol (mercaptan) being one of them.

The air stability of the thiol species **4-53** was determined by NMR spectra of the crude reaction mixture (after a précised basic work up) exposed to aerial oxidation, recorded at different times (Figure 4. 23). After 8 days, the monomeric thiol was partially converted to its disulphide [Figure 4. 23, b)]. It is therefore quite clear that the thiol compound is stable only under an inert atmosphere or probably, in its crystalized form.

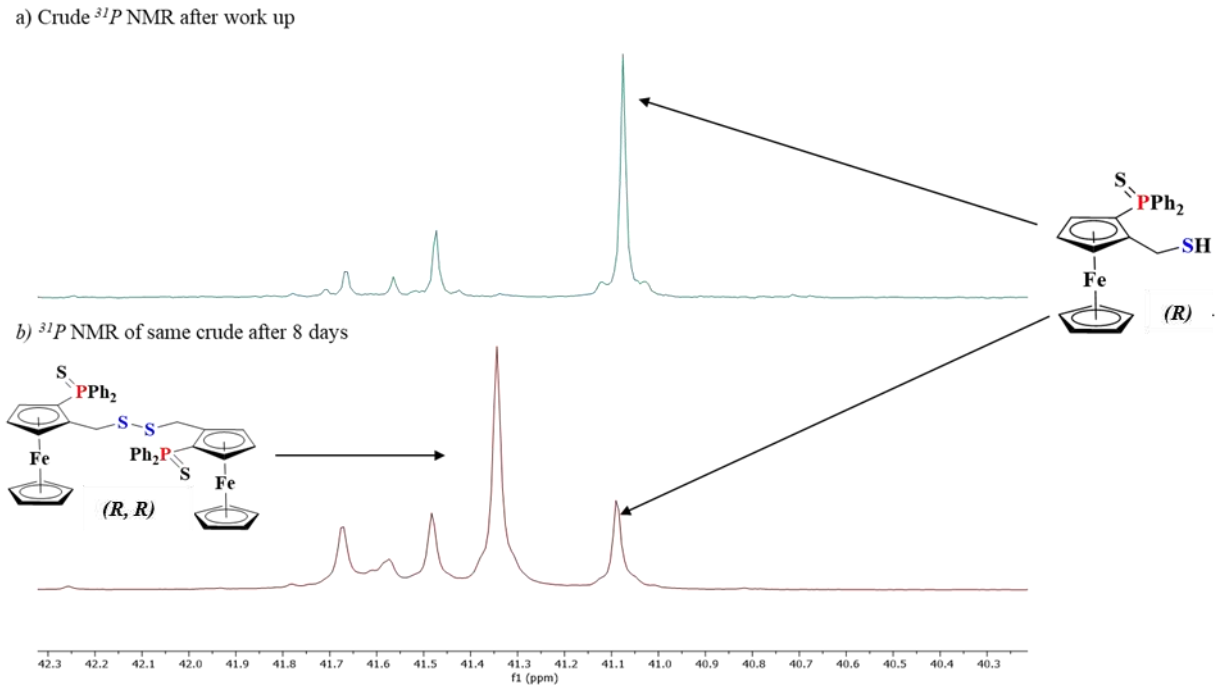

Figure 4. 23: ^{31}P ($CDCl_3$, 162 MHz) NMR spectra at different times of crude of reaction depicted in Scheme 4.29

4. 9) Ligand Synthesis: Final Step

Given the air sensitivity, the thiol **4-51** obtained after reduction of the thioacetate precursor shown in Figure 4. 23, it was not isolated but rather deprotonated *in situ* to the thiolate, followed by alkylation. An efficient procedure reported by Zhang *et al.*[317] where benzyl mercaptan was coupled with benzyl bromide in the presence of NaH, was thoroughly followed. The presence of

NaH ensures that any residual (or adventitiously generated) disulfide, is converted back to thiolate. Subsequent addition of pyridyl tosylate (2-3 equiv.) resulted in the expected alkylation of the thiolate and the desired S-protected ligands **4-49** were obtained in pure form after chromatographic purification (Scheme 4. 30).

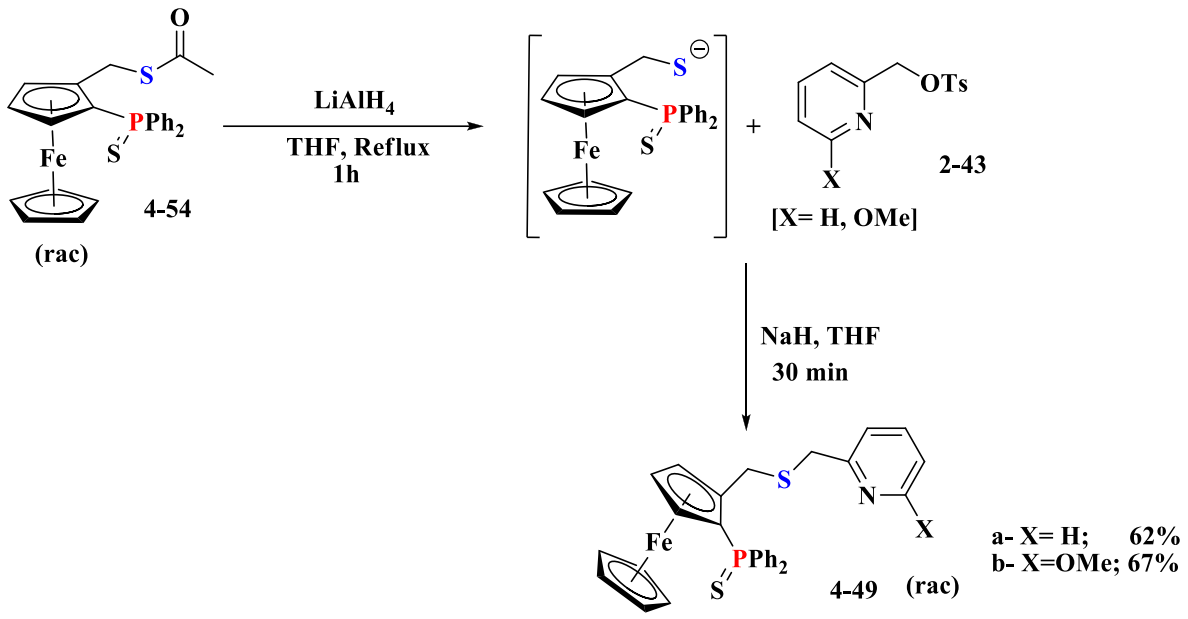

Scheme 4. 30: Synthesis of Protected PSN Ligands **4-49** (yields are calculated wrt **4-54**)

Compounds **4-49a** and **b** were characterized by multinuclear NMR (^{1}H, ^{31}P, ^{13}C) spectroscopy and HRMS. In case of **4-49a**, two sets of AB-type doublets were recognized at δ = 4.16, 3.78 and 3.71, 3.65 in the ^{1}H NMR spectrum [Figure 4. 24, a)]. Similar resonances (δ = 4.13, 3.91 and δ = 3.60, 3.53) were found in the ^{1}H NMR of **4-49b** [Figure 4. 24, b)]. Multiplets at δ = 4.60, 4.30, 3.79 [Figure 4. 24, a)] and δ = 4.64, 4.30, 3.78 [Figure 4. 24, b)] correspond to the three substituted Cp ring protons of **4-49a** and **4-49b**, respectively. The unsubstituted Cp ring protons yield a singlet at δ = 4.30 for both **4-49a** and **4-49b**. In case of **4-49b**, the O$C\underline{H_3}$ peak appeared at δ = 3.89. The ^{31}P NMR spectrum shows a peak in a similar region for the two compounds (δ = 41.50 for **4-49a**; δ = 41.56 for **4-49b,** see Figure 4. 24).

So far, single crystals of these compounds have not been obtained. The phosphine deprotection to produce the final target ligands **4-2** is also currently in progress.

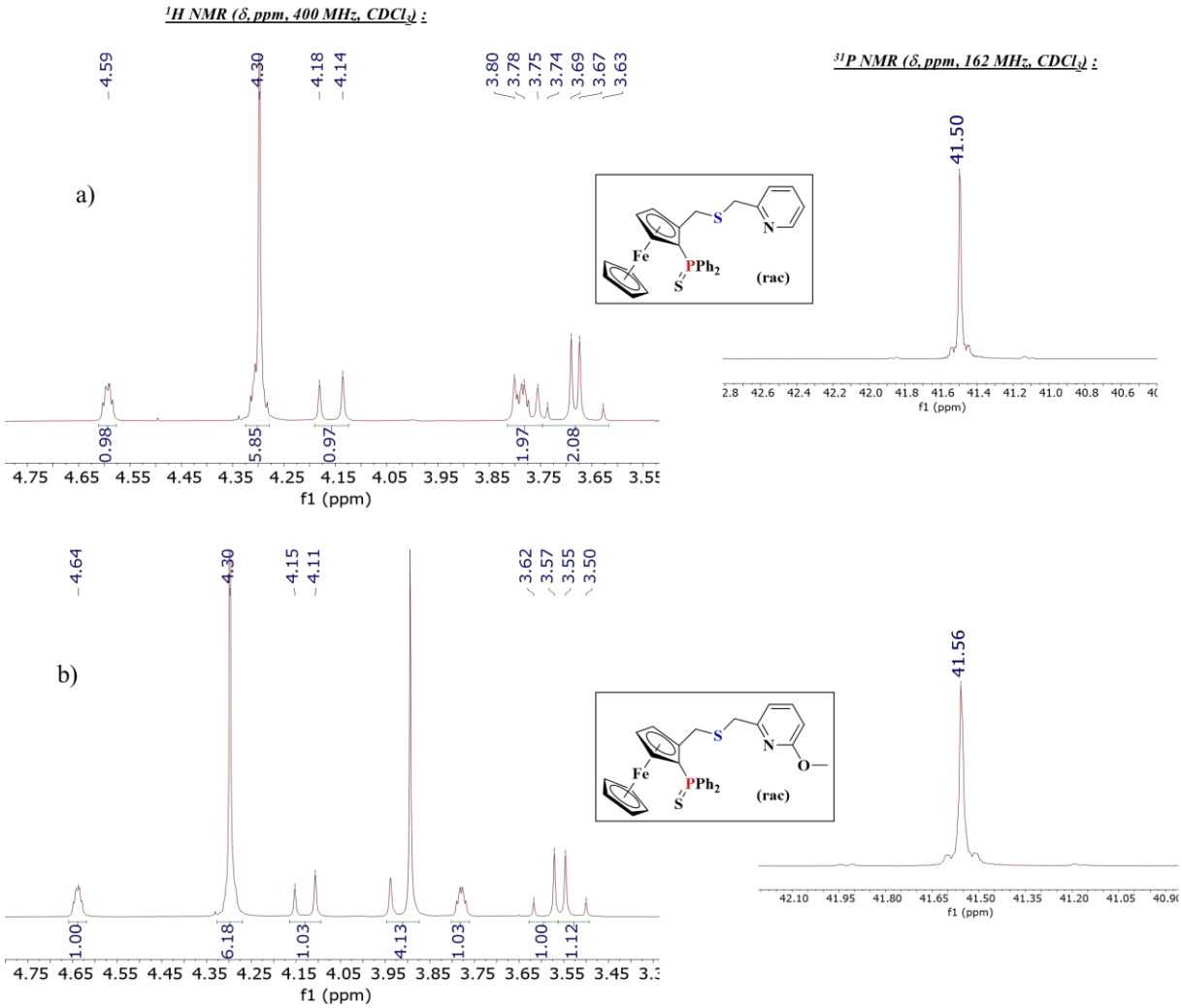

Figure 4. 24: ^{1}H ($CDCl_3$, 400 MHz) (Cp and aliphatic region) and ^{31}P ($CDCl_3$, 162 MHz) NMR Spectra of **4-49a** and **4-49b**

4. 10) Generalization of the Procedure

The just-established pathway to the (protected) PSN ligands **4-49** via activation of the S center of an *in situ*-generated thiol can be extended as a general synthetic tool to prepare other ferrocenyl thioethers that are hitherto synthetically inaccessible, because of the non-existence of corresponding alkyl mercaptan analogue. In addition, since the ferrocenyl thiol intermediate does not to be isolated, the procedure can be viewed as a one-pot and relatively rapid (2-3 h) transformation of ferrocenyl thioacetates to various ferrocenyl thioethers. Hence, we believe that it will be a valuable addition to the already established HBF_4 method. The procedure can be adapted to the type of substrate.

In order to prove this principle, this method has been tested for the synthesis of two additional new ferrocenyl thioethers from the corresponding alkyl halides. The methyl thioether **4-56** would be difficult to access through the HBF_4/thiol method as the required methanethiol species is a dangerous gas. On the other hand, the one-pot reductive alkylation method may be accomplished with the easy-to-handle and safer iodomethane. The reaction (Scheme 4. 31) has indeed allowed the generation of the desired thioether **4-56** with an isolated yield of 58% from **4-54**.

Another very interesting compound **4-57** was obtained by reaction with CH_2Cl_2, where both Cl atoms were replaced by the *in situ*-formed thiolate, even when using an excess amount of the chlorinated molecule.

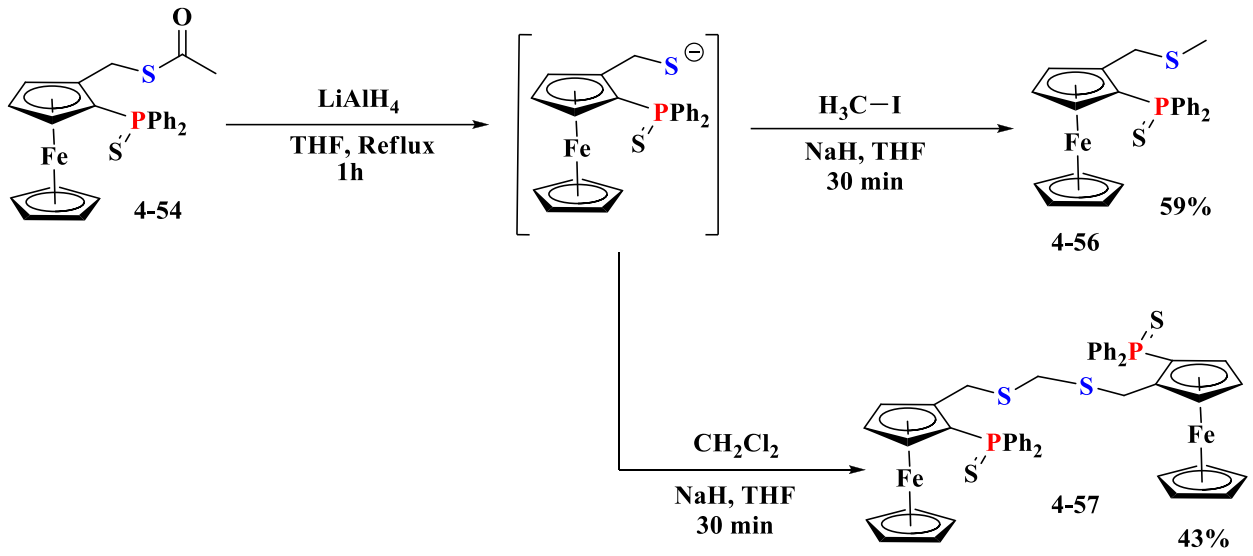

Scheme 4. 31: Synthesis of two different Thioethers

The mono-substituted analogue, **4-58**, of thioether **4-57**, has never been isolated during the course of reaction. This perhaps, indicates the higher extent of electrophilicity in **4-58** (than CH_2Cl_2). Hence, it is predicted that the reaction rather follows further substitution of the Cl atom in **4-58** by another thiolate and thus, thioether **4-57** is formed as the final product (Scheme 4. 32). However, more insights about the reaction mechanism are getting investigated by a few control experiments (*e.g.* change of electrophile- dichloromethane to dichloroethane *etc.*) and theoretical aspects.

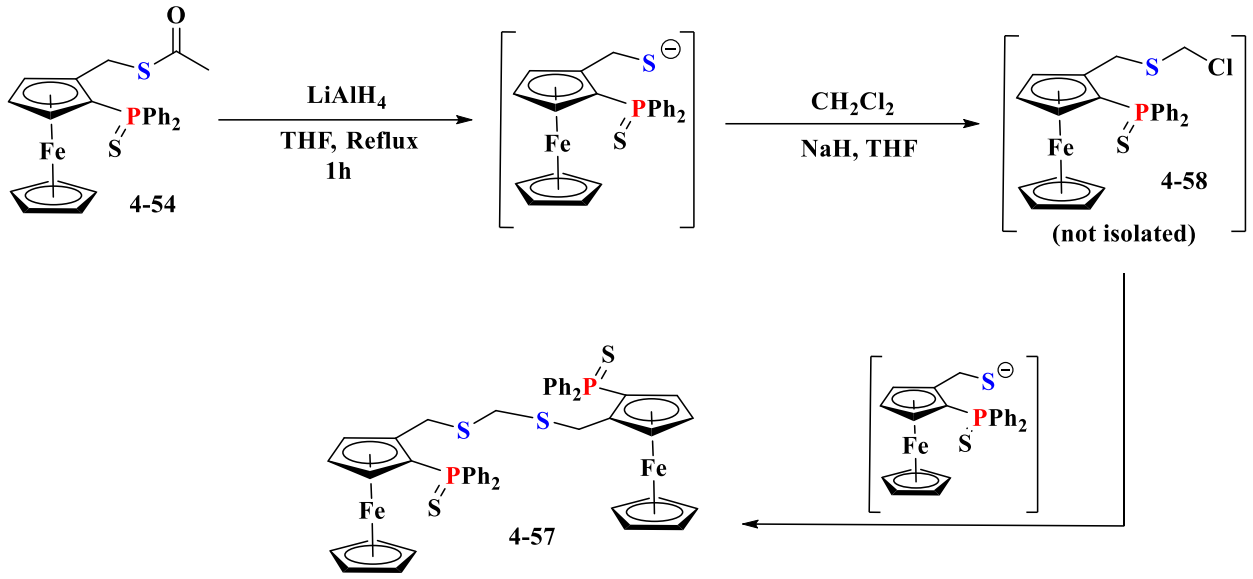

Scheme 4. 32: Probable mechanism for formation of thioether **4-57**

Both products **4-56** and **4-57** were fully characterized by multinuclear NMR and HRMS analyses. In the ^{1}H NMR spectrum of **4-56,** along with the usual unsubstituted Cp singlet (δ = 4.32) and three multiplets of the non-identical substituted Cp ring protons (δ = 4.60, 4.30, 3.79), two AB-type doublets are recognized (δ = 4.08, 3.77) and attributed to the CH_2 group attached to the Cp ring. The singlet at δ = 2.20 corresponds to the C<u>H</u>$_3$ protons. The ^{31}P NMR shows a peak at δ = 41.57 (Figure 4. 25).

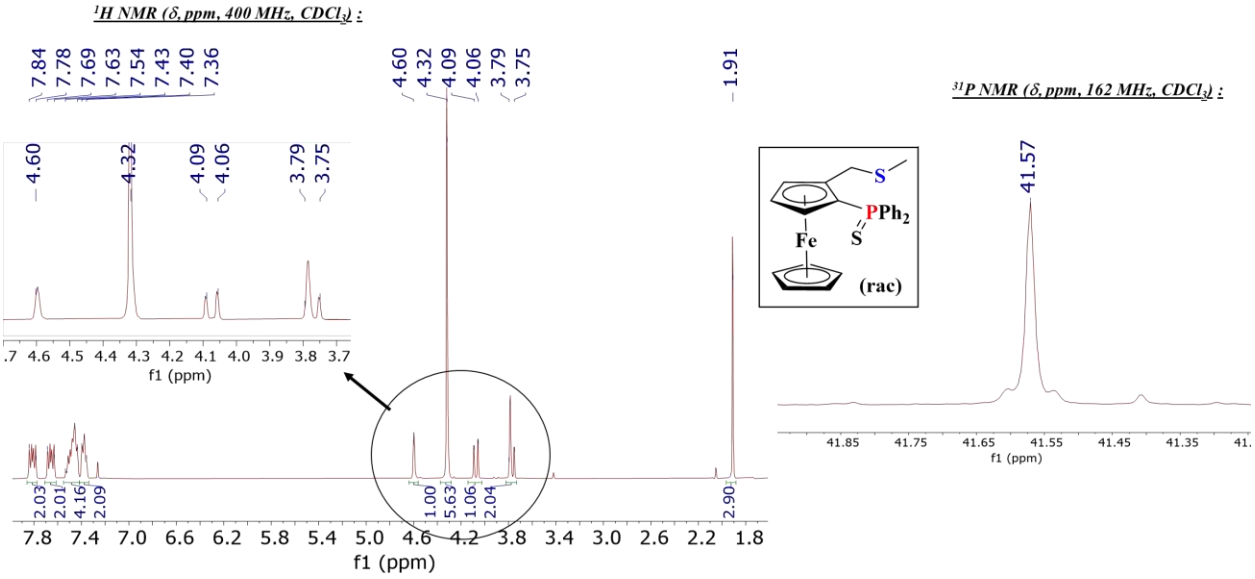

Figure 4. 25: ^{1}H ($CDCl_3$, 400 MHz) and ^{31}P ($CDCl_3$, 162 MHz) NMR Spectra of **4-56**

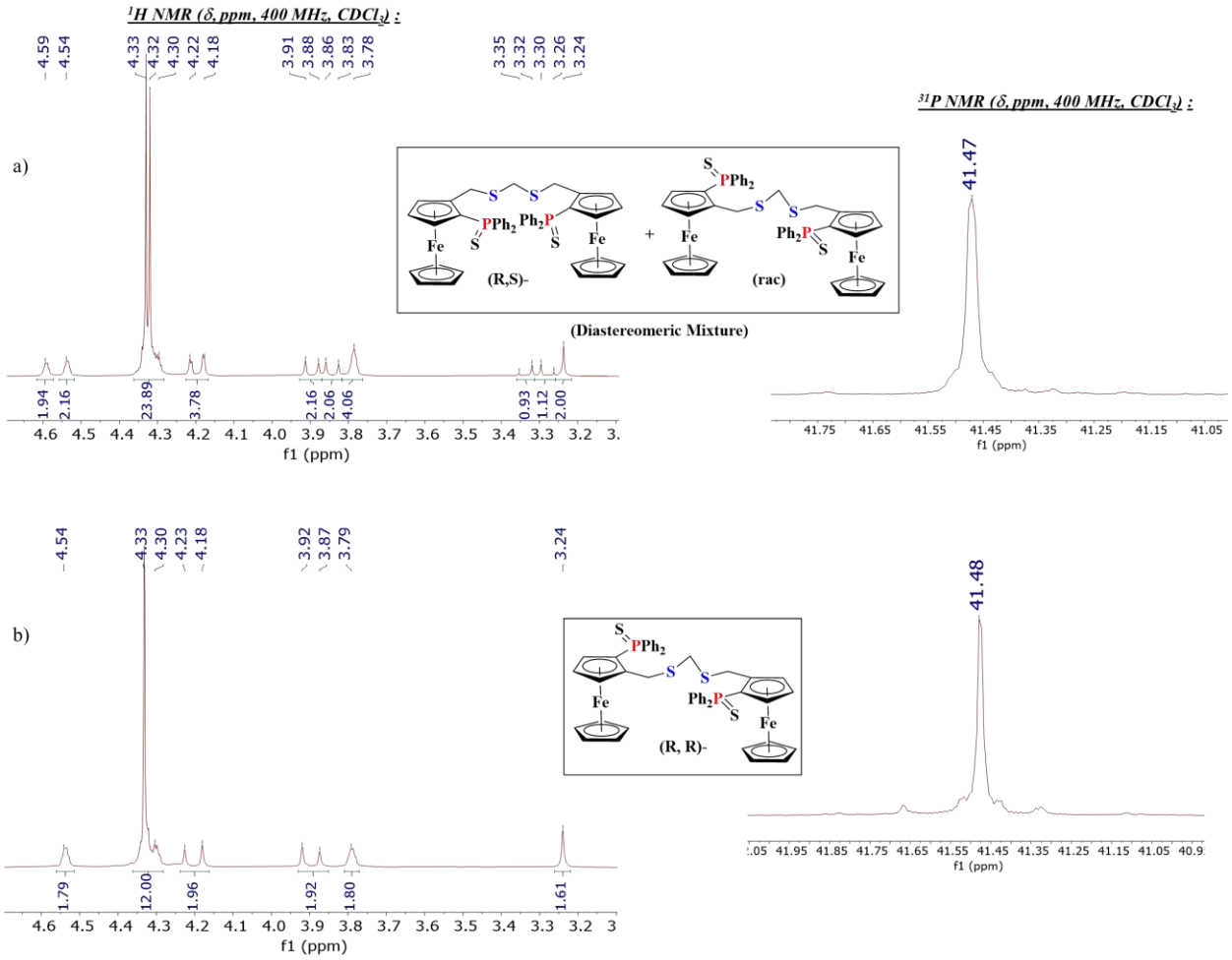

Figure 4. 26: ^{1}H ($CDCl_3$, 400 MHz) (Cp region) and ^{31}P ($CDCl_3$, 162 MHz) NMR Spectra of diastereomeric mixture of **4-57** and *(R,R)*- **4-57**

The compound **4-57** was characterized by multinuclear NMR spectroscopy in both its diastereomer mixture and in the enantiomerically pure *(R,R)* form. By comparison, the chiral *(R,R/S,S)* and *meso (R,S)* diastereoisomer resonances could be assigned as already described above for compound **4-55** (see Figure 4. 21). Thus, the singlets at δ = 4.33 and 4.32 correspond to the to the unsubstituted Cp protons of the *meso (R,R)* isomers, respectively**.** The three inequivalent protons of the substituted Cp ring are characterized by multiplets at δ = 4.59, 4.30, 3.78 for the *meso* isomer and at δ = 4.54, 4.30, 3.78 for the chiral one *(R,R* and *S,S)*. The AB-type doublets for *meso* **4-57** and *(R,R/S,S)* **4-57** could be assigned to the resonances at δ = 4.20, 3.76 and δ = 4.20, 3.90, respectively (Figure 4. 26). For the C$\underline{H_2}$ protons flanked between the two planar ferrocene units, the magnetic behavior is the opposite because these protons respond to the central chirality of the C atom and

not to the ferrocene planar chirality. Therefore, the chiral *(R,R/S,S)* diastereoisomer with two equivalent ferrocenyl groups at the central C atom has chemically equivalent protons because of the overall C_2 symmetry and exhibit a singlet at δ = 3.24 [Figure 4. 26, a)]; whereas, the meso *(R,S)* isomer, has ferrocenyl groups of opposite chirality, rendering the $C\underline{H_2}$ protons diastereotopic and yielding two AB-type doublets at δ = 3.34 and δ = 3.28 [Figure 4. 26, b)]. The ^{31}P NMR gives peak at same region (δ = 41.48) in both cases (Figure 4. 26).

A single crystal of both **4-56** and **4-57** (from its diastereomeric mixture) was obtained by slow evaporation of concentrated pentane-ether solution. The resulting structure obtained after X-ray diffraction is shown in Figure 4. 27 and Figure 4. 28, respectively.

In compound **4-56**, the C2-C21-S2-C22 torsion angle is 95.8(2)°. The S1 atom is as usual 0.927(4) Å below the Cp ring plane, whereas the P1 atom is slightly above the plane by 0.103(3) Å. The S2 atom is located 1.587(3) Å above the Cp ring plane. The two Cp rings are nearly eclipsed with a twist angle of 6.1°. Owing to the centrosymmetric space group, the unit cell contains the two enantiomers. In the structure of compound **4-57**, the two crystallographic ally independent ferrocenes have the same absolute configuration *(S,S)* as indicated by the value, 0.02(7), of the Flack parameters. In each ferrocene unit the Cp display an eclipsed conformation.

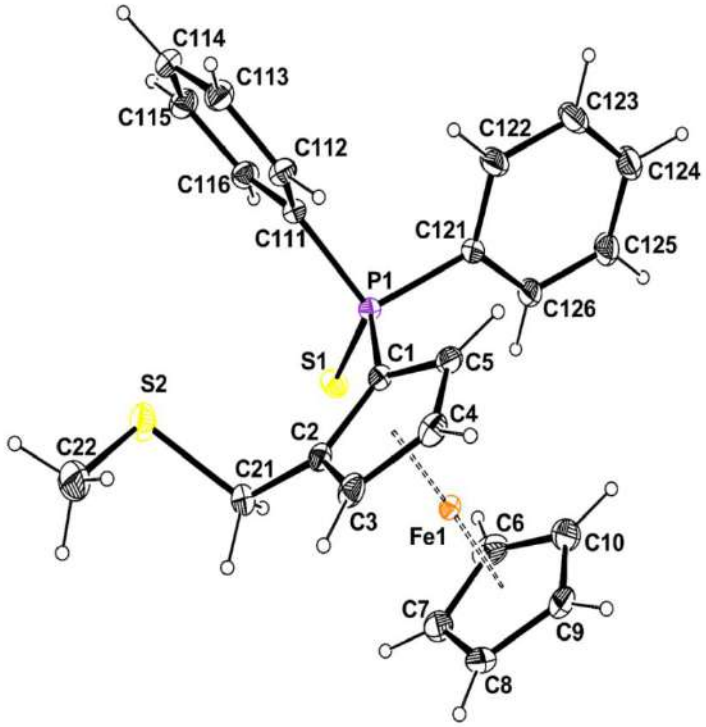

Figure 4. 27: Molecular view of compound **4-56** showing 30% probability displacement ellipsoids and the atom numbering scheme. H atoms are represented as small sphere of arbitrary radii.

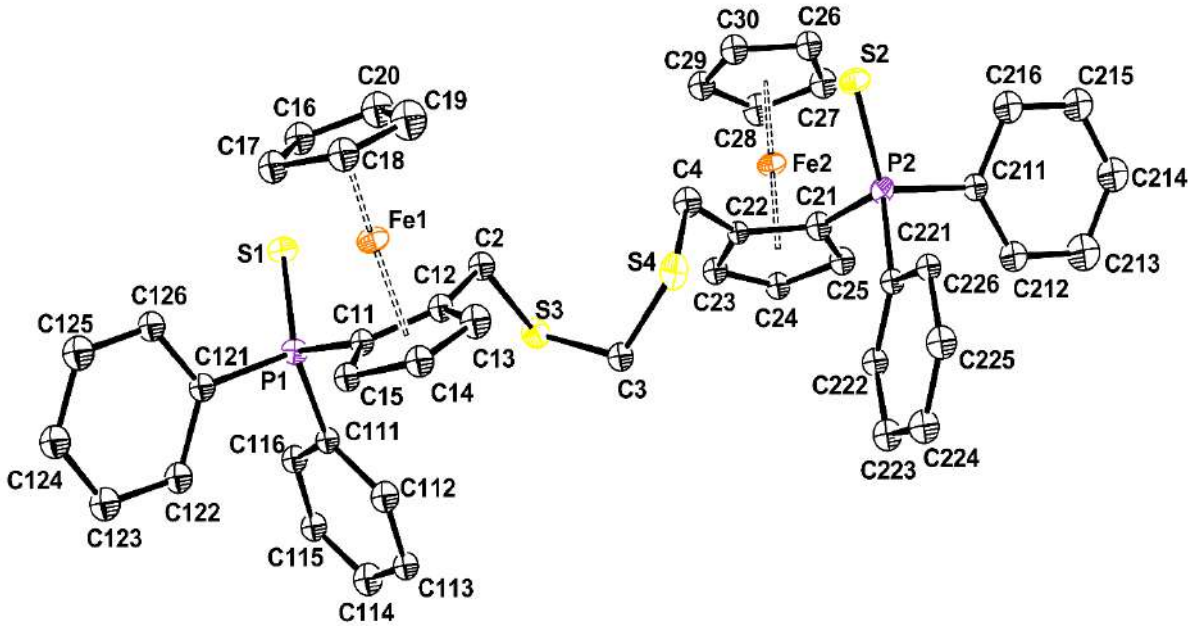

Figure 4. 28: Molecular view of compound **4-57** showing 30% probability displacement ellipsoids and the atom numbering scheme. H atoms are represented as small sphere of arbitrary radii.

4. 11) Conclusion

Two new planar chiral thioether-containing ferrocenyl phosphine ligands (PSP and PSN) have been synthesized. These syntheses have been optimized and the crystallographical structures of several synthetic intermediates and of the final (S-protected) ligands were determined by X-ray diffraction. Different thiolation reaction procedures were screened and the thioacetylation/$LiAlH_4$ reduction sequence has been identified as the best solution to prepare the benzyl thiol intermediates. The nucleophilic addition to the ferrocenyl carbocation generated *in situ* by strong acid treatment (HBF_4) proved again to be a very efficient method for side chain substitution in ferrocene systems. As an added bonus, we could develop a new method to access ferrocenyl thioethers directly from ferrocenyl thioacetate. Extending the same strategy proved successful for the PSN (pro)ligand synthesis. This new protocol can be considered a competitive procedure to the HBF_4/RSH method for the synthesis of different ferrocenyl thioethers.

Catalytic tests with the ligand **4-1,** phosphine deprotection of proligands **4-49** (**a** and **b**), and optimization (base, solvent, substrate scope screening *etc.*) of the reductive alkylation process (see section 4.10) are ongoing.

General Conclusions and Perspectives

New families of phosphine-containing planar chiral tridentate ligands in their PS-protected form were synthesized and are described in this thesis. The families are summarized in Scheme 1.

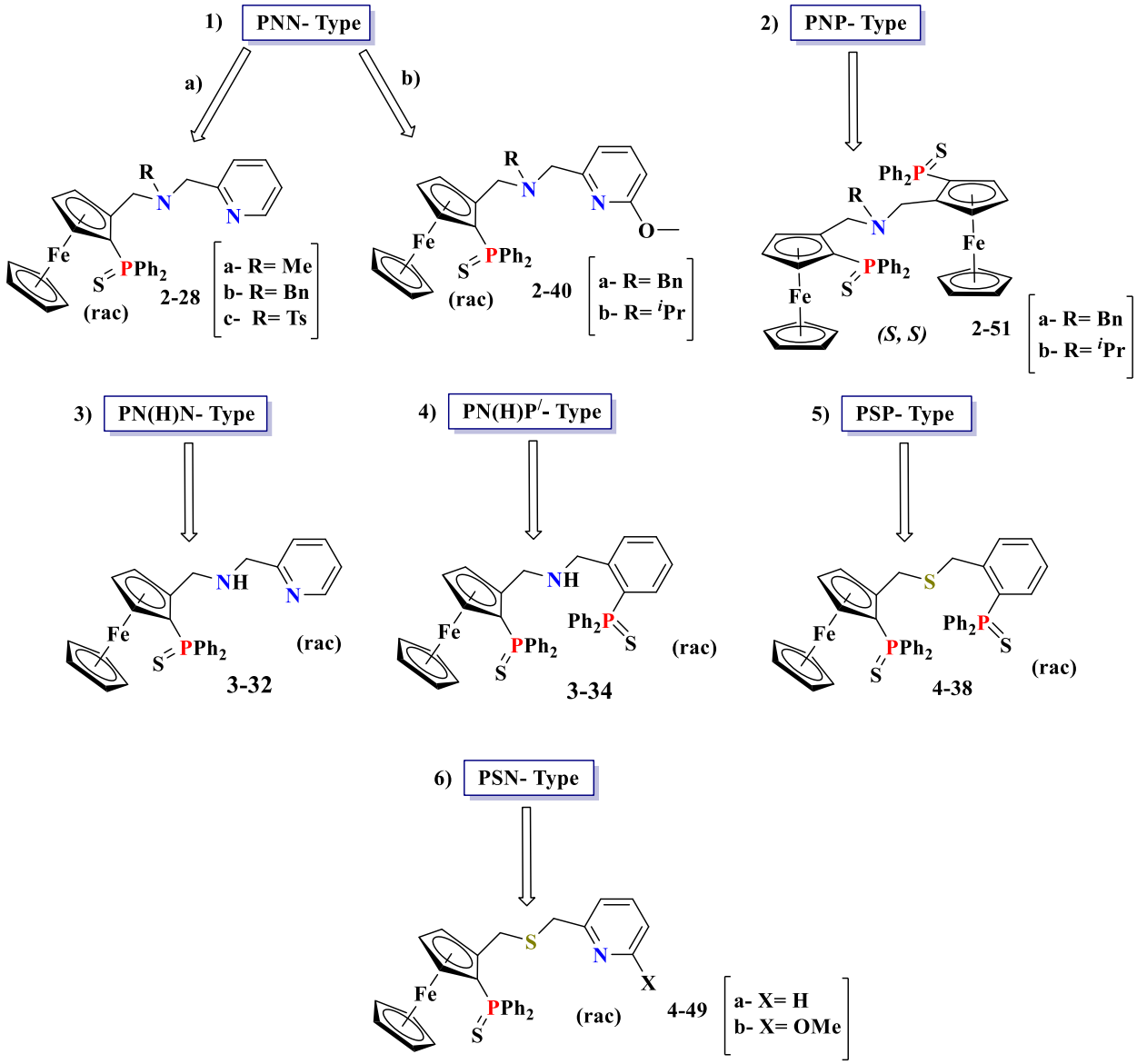

Scheme 1: Tridentate phosphine-containing ligand families

The PNP family of proligands **2-51**, unexplored to date for catalytic applications, were produced following the method developed by Dr. Lucie Routaboul. Apart from that, all the proligands have not been previously described. They were characterized by multinuclear NMR and HRMS. In addition, at least one member of each family was structurally characterized by X-ray diffraction,

except for the PSN family, for which single crystals have not yet been obtained. A short-term perspective of this work is the optimization and upscaling of the various ligand syntheses, for the subsequent exploration of their catalytic potential.

The synthesis of these phosphine-containing ligands requires a number of organic as well as ferrocenyl synthetic intermediates. Several of these intermediates were prepared following standard procedures, not requiring extensive optimizations. The previously unreported intermediates (both organic and ferrocenyl) were thoroughly characterized by NMR, mass spectrometry and in most cases also by XRD. Various organic reactions (the Mitsunobu reaction, reduction, tosylation, the HBF_4 method, *etc*.) were screened for optimization purposes. A few of them did not work while others led to the formation of unexpected byproducts. A few of these could be isolated and fully characterized.

However, appropriate solutions for a few synthetic problems associated with the targeted proligands have not yet been found. The deprotection of the *ortho*-methoxy function in the pyridine ring of the PNN proligands **2-40** has not yet been successful. Because of the limited time, the P=S deprotection of a few of the ligands (*e.g.* **2-28b, c, 3-32, 3-34, 4-49**) is yet to be carried out. Efforts in these directions are ongoing and we are confident in the eventual success.

The new protocol for ferrocenyl thioether preparation (see Chapter 4, section 4-10), *i.e.*- alkylation of *in situ*-generated ferrocenyl thiolate (from ferrocenyl thioacetate) by NaH, eliminates the use of corresponding thiol species as nucleophiles for substitution since ferrocenyl thiolate acts as nucleophile and substitutes another electrophilic species present in the medium (*e.g.* CH_3I, CH_2Cl_2 *etc.*). This new procedure has advantages with respect to the competitive and well-established HBF_4 method (which inevitably requires a thiol species as nucleophile), potentially leading to the generation of a large family of structurally diverse ferrocenyl thioethers, but is also associated with a few limitations such as lower yields. Optimizations and substrate scope investigations are among the short-term perspectives.

Preliminary complexation attempts for a few of these ligands have yielded promising results. For an example, the PSP ligand **4-1** was found to displace CO in $MnBr(CO)_5$ and yield a tricarbonyl product, according to the infrared spectrum (Scheme 2). However, further characterization (NMR, Mass, XRD) of any of the proposed species is needed. Hence, due to lack of conclusive evidence,

these complexes were not described in the main chapters. Optimization of the complexation reactions and product characterization are ongoing.

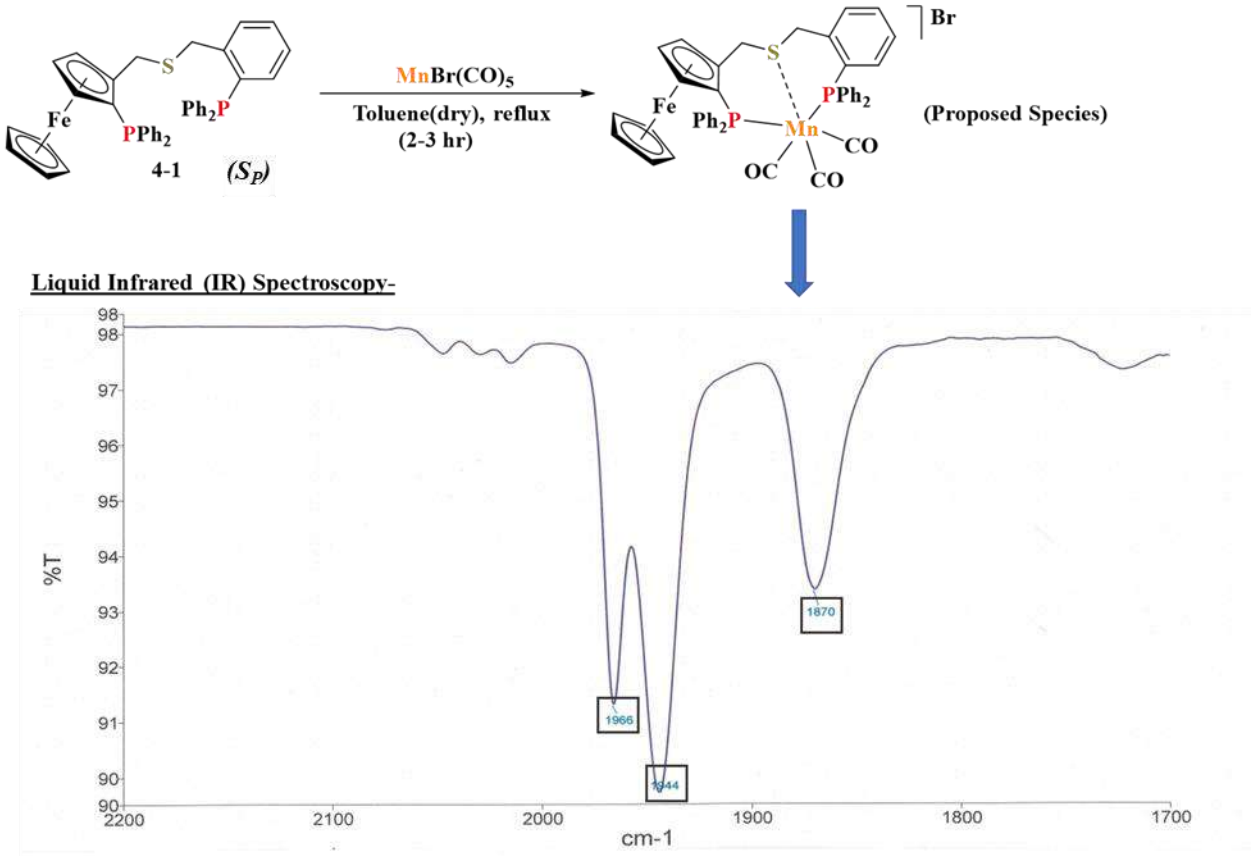

Scheme 2: Detection of a metal-tricarbonyl species by IR spectroscopy

A few protected ligands in their racemic and enantiomerically pure forms have been sent to the laboratory of our Indian collaborator (Prof. Basker Sundararaju, IIT Kanpur, India) to test the catalytic activities in the presence of non-noble metal precursors. The overall aim is to attain high enantioselectivities in asymmetric C-C and C-N bond-forming reactions starting from alcohols following the pathway of the borrowing hydrogen methodology, in the presence of metal complexes as precatalysts (Scheme 3).

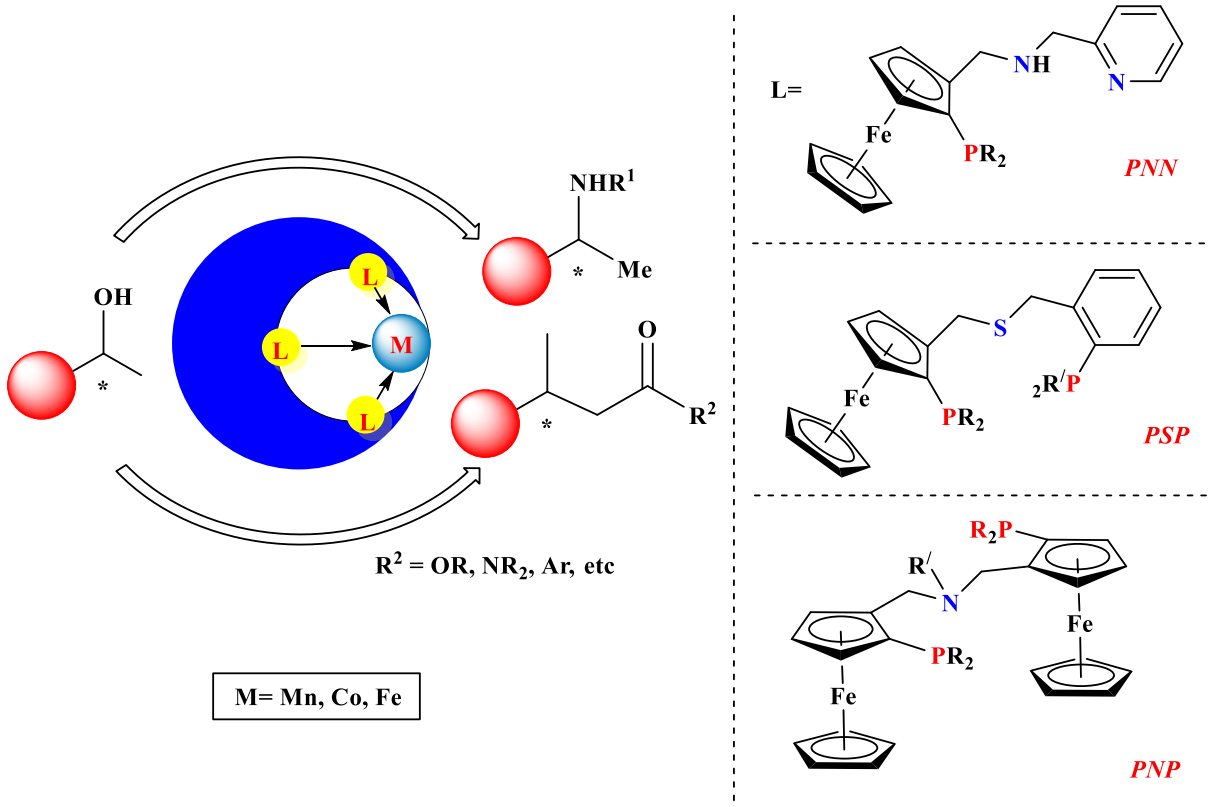

Scheme 3:General overview of our target reactions and catalyst development

Initial catalytic studies will be carried out with *in situ* generation of the active species from the ligands and the appropriate metal precursors, starting with the racemic version for the optimization of the reaction conditions. The investigations will then be extended to the asymmetric versions for the best catalytic systems.

The strategy of our project is to combine the expertise of our group in ferrocenyl-based ligand synthesis and the group of our Indian collaborator in catalysis with base metals. We are looking forward to achieve these realistic yet challenging targets with good success in our designed catalytic reactions in the near future.

Experimental Section

General conditions

All reactions were carried out using conventional Schlenk techniques under either an inert atmosphere of argon or normal aerial condition depending on the reaction. Necessary starting materials were bought from well-known international chemical companies. (Dimethylaminomethyl)ferrocene was purchased from Strerm Chemicals. 2-(methylamino)methylpyridine was bought from Sigma- Aldrich. 2-picolylamine and Methyl 2-bromobenzoate were purchased from TCI Chemicals. 2-bromobenzonitrile and 6-hydroxypyridine-2-carboxylic acid were bought from Acros Organics. 2-Bromobenzyl alcohol was purchased from Fluorochem. Other common reagents (*n*-BuLi, HBF_4, DEAD *etc.*) were purchased from either any of the above-mentioned companies or a few other companies (*e.g.* Alfa Aesar). Thin-layer chromatography (TLC) and column chromatography were carried out on Merck Kiselgel 60F254 recoated aluminium plates and Merck Kiselgel 60, respectively. Dry Solvents (THF, Toluene, Pentane, DCM and Diethyl ether) and regular solvents for column chromatography (Hexane, Ethyl Acetate, Diethyl ether *etc.*) were purchased from Carlo Erba Reagents, as per need. Dry solvents were used for reactions and solvent other than above mentioned ones (*e.g.* Acet^{o}ne) were dried by distillation method (if needed). NMR analyses were performed on Bruker AV400pas, AV300pas, AV400hd, AV400liq instruments. The spectra were referenced internally using the signal from the residual solvent for ^1H and ^{13}C, and externally using 85% H_3PO_4 for ^{31}P. Chemical shifts (δ) and coupling constants are given in ppm and Hertz, respectively. Mass spectra analyses [GCT 1er Waters for DCI, CH_4; UPLC Xevo G2 Q TOF (waters) for ES^+] were performed by the 'Service de Spectrometre de masse' of the Universite Paul-Sabatier, Toulouse (France).

X-ray structural analyses

All the X-ray structures described in this thesis were determined by **Dr. Jean-Claude Daran** at LCC. Single crystal of all the compounds were mounted under inert perfluoropolyether at the tip of a glass fibre and cooled in a nitrogen ccryostream. Of the 22 structures reported in this thesis, 8 data sets were recorded on a Rigaku Oxford Diffraction GEMINI EOS[318] equipped with Cu-Kα radiation, 2 data sets were collected on a Nonius-Bruker fitted with a CCD Apex2 detector and equipped with Mo-Kα radiation whereas the remaining 12 single crystals were mounted on a Bruker Apex2[319] equipped with Mo-Kα radiation using a micro source. The structures were

solved by the Integrated Space-Group method using the SHELXt software[320] and refined by least-squares procedures on F^2 using SHELXL-2015.[321] All H atoms attached to C were fixed geometrically and treated as riding with C-H = 0.95Å(aromatic), C-H = 1.0 Å(Cp) or 0.97 Å (methylene) with U_{iso}(H) = 1.2Ueq(C) and C-H = 0.96 Å (C_{methyl}) with U_{iso}(H) = 1.2Ueq(C). The H atom attached to nitrogen were located on difference Fourier synthesis and its coordinates were freely refined with restrained isotropic thermal parameter U_{iso}(H) = 1.2Ueq(N). In the case of non centrosymmetric space group, the absolute structure or absolute configuration have been determined by refining the Flack's parameter.[322] The drawing of the molecules was realized with the help of ORTEP32.[323] Crystal data and refinement parameters, bond distances, bond angles and hydrogen bond parameters are provided in the appendix section at the end.

Experimental Procedure and Characterization of Synthesized Compounds of Chapter-2

2-30b

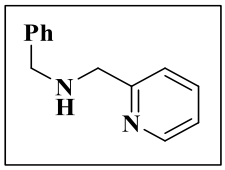

Procedure. Benzaldehyde (1.7 ml, 16.31 mmol) was added to a solution of 2-picolylamine (1.6 ml, 15.53 mmol) in methanol. The reaction mixture was stirred for 30 min at room temperature. $NaBH_4$ (0.47g, 12.42 mmol) was added slowly to the reaction mixture at 0 ^oC. The reaction mixture was allowed to warm to r.t. and stirred for 4h and then quenched with 2 (M) HCl. The residue after solvent evaporation was extracted with water-DCM. The water layer was further extracted with DCM after consecutive addition of Na_2CO_3 and brine. The combined organic layers were dried over Na_2SO_4 and concentrated under reduced pressure. The resulting orange oil was purified by column chromatography (methanol: DCM = 1:1). The expected product **2-30b** was obtained as a form of pale-yellow liquid (yield- 2.4g, 81%).

^{1}H NMR (δ, ppm, 400 MHz, $CDCl_3$): 8.55 (1H, d, J = 4.9 Hz, Py), 7.64-7.59 (1H, m, Py), 7.37-7.28 (5H, m, Ph), 7.28-7.22 (1H, m, Py), 7.15-7.12 (1H, m, Py), 3.93 (1H, s, CH_2), 3.85 (1H, s, CH_2), 3.05 (1H, s, NH).

$^{13}C\{^1H\}$ NMR (δ, ppm, 125 MHz, $CDCl_3$): 159.32 (s, *quat*. Ar), 149.28 (s, Ar), 139.69 (s, *quat*. Ar), 136.46 (s, Ar), 128.42 (s, Ar), 128.34 (s, Ar), 127.08 (s, Ar), 122.40 (s, Ar), 122.01 (s, Ar), 54.23 (s, CH_2), 53.32 (s, CH_2).

HRMS (DCI-CH_4): 199.1228 (100%, calcd. for $C_{13}H_{15}N_2$ [$(M+H)^+$] 199.1235).

2-30c

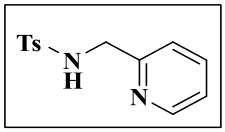

Procedure. In a 500 ml round bottom flask with a magnetic rod, 2-picolylamine (10 ml, 97.1 mmol) was dissolved in DCM (120 ml) and NEt_3 (32 ml, 233 mmol) was added to it. The solution was stirred at 0 ^oC for 20 min and solid tosyl chloride (27 g, 146 mmol) was added portion wise for 30 min to prevent over alkylation. The resulting reaction mixture was then stirred at r.t. for 16h. The reaction was quenched with a saturated aqueous NH_4Cl solution and then extracted with DCM (3x 100 ml). The combined organic layers were dried by solvent evaporation. The dry crude product was purified by column chromatography (hexane: EtOAc= 1:1) to obtain the desired product as a fade white solid (Yield- 22.5g, 90%)

^1H NMR (δ, ppm, 400 MHz, $CDCl_3$): 8.47 (1H, d, J = 4.77 Hz, Py), 7.77 (2H, d, J = 8.4 Hz, TsPh), 7.62 (1H, dt, J = 7.67 Hz, J = 1.76 Hz, Ph), 7.27 (2H, d, J = 7.88 Hz, TsPh), 7.18 (1H, m, Py), 5.90 (1H, t, J = 5.18 Hz, NH), 4.26 (d, J = 5.49 Hz, CH_2Py), 2.41 (3H, s, TsCH_3).

$^{13}C\{^1H\}$ NMR (δ, ppm, 125 MHz, $CDCl_3$): 154.82 (s, *quat*. Ar), 148.94 (s, Ar), 143.36 (s, *quat*. Ar), 136.80 (s, Ar), 129.61 (s, Ar), 127.22 (s, Ar), 127.1 (s, Ar), 122.61 (s, Ar), 121.95 (s, Ar), 47.40 (s, CH_2), 21.48 (s, Ts$\underline{C}H_3$).

HRMS (DCI-CH_4): 263.09 (100%, calcd. for $C_{13}H_{15}N_2O_2S$ [$(M+H)^+$] 263.0851)

2-28a

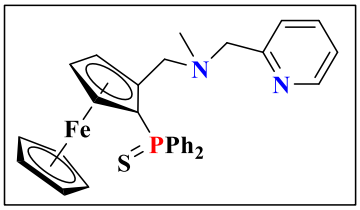

Procedure: A solution of racemic 2-(diphenylthiophosphinoferrocenyl)methanol **2-29** (0.5g, 1.16 mmol) in 30 ml dry THF was introduced into a Schlenk tube, followed by the addition of triphenylphosphine (0.46 mg, 1.74 mmol) under an argon atmosphere. Then, 2-(N-methylaminomethyl)pyridine (0.29 ml, 2.32 mmol) was added, followed by the slow addition of a commercially available diethylazadicarboxylate (DEAD) solution in hexane (0.66 ml, 1.45 mmol). The reaction mixture was stirred for 18h under argon at room temperature. Then, after solvent evaporation, the crude reddish-orange oil was purified by flash chromatography on silica using 50% EtOAc-hexane (1:1) (with 1% triethylamine) as eluent. 0.3g, (yield- 49%) of racemic (*N*-2-diphenylthiophosphinoferrocenyl-*N*-methyl)aminomethylpyridine **2-28a** were obtained in pure form as a yellow-orange solid.

^{1}H NMR (δ,(ppm) 400 MHz, $CDCl_3$): 8.40 (1H, d, J = 4.0 Hz, Py), 7.88-7.80 (2H, m, Ph), 7.72-7.65 (2H, m, Ph), 7.53-7.42 (4H, m, Ph), 7.36-7.32 (2H, m, Ph), 7.28-7.24 (1H, m, Py), 6.99 (1H, m, Py), 6.48 (1H, d, J = 7.8 Hz, Py), 4.60 (1H, m, *subst*. Cp), 4.52 (1H, d(AB system), J = 12.8 Hz, C$\underline{H}_2$Cp), 4.30 (5H, s, Cp), 4.28 (1H, m, *subst*. Cp), 3.80 (1H, m, *subst*. Cp), 3.70 (1H, d(AB system), J = 13.9 Hz, C$\underline{H}_2$Py), 3.42 (1H, d(AB system), J = 13.9 Hz, C$\underline{H}_2$Py), 3.21 (1H, d(AB system), J = 12.8 Hz, C$\underline{H}_2$Cp), 1.88 (s, 3H, N-C$\underline{H}_3$).

^{13}C {^{1}H} NMR (δ, (ppm), 125 MHz, $CDCl_3$): 159.9 (s, *quat.* Py), 148.30 (s, Py), 136.09 (s, Py), 135.30 (d, J_{CP} = 87.9 Hz, *quat.* Ph), 134.11 (d, J_{CP} = 85.3 Hz, *quat.* Ph), 132.20 (d, J_{CP} = 10.7 Hz, Ph), 132.06 (d, J_{CP} = 10.7 Hz, Ph), 131.09 (d, J_{CP} = 3.0 Hz, Ph), 130.82 (d, J_{CP} = 3.0 Hz, Ph), 127.91 (d, J_{CP} = 12.4 Hz, 2C, Ph), 122.86 (s, Py), 121.44 (s, Py), 89.70 (d, J_{CP} = 11.8 Hz, *quat.* Cp), 75.48 (d, J_{CP} = 9.8 Hz, *subst.* Cp), 75.15 (d, J_{CP} = 12.9 Hz, *subst.* Cp), 73.88 (d, J_{CP} = 95.8 Hz, *quat.* Cp), 70.70 (s, Cp), 68.83 (d, J_{CP} = 10.6 Hz, *subst.* Cp), 63.66 (s, $\underline{C}H_2$Py), 56.41 (s, $\underline{C}H_2$Cp), 40.84 (s, N-$\underline{C}H_3$).

^{31}P NMR (δ (ppm), 162MHz, $CDCl_3$): 41.89 (s, PPh_2).

HRMS (DCI-CH_4): 537.1205 (100%, calcd. for $C_{30}H_{30}N_2PSFe$ $[(M+H)^+]$ 537.1217).

2-28b

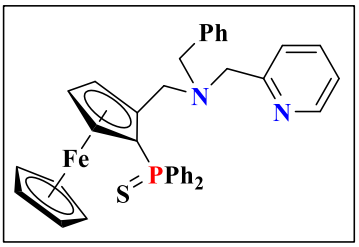

Procedure: Followed same as **2-28a.** Stoichiometry of starting material, corresponding reagents and yield of product as follows-

2-29- 0.1g, 0.23 mmol

PPh_3- 134 mg, 0.51 mmol Yield of racemic **2-28b**- 0.067g, 48%

DEAD- 0.23 ml, 0.51 mmol

2-30b- 0.1g, 0.51 mmol

^{1}H NMR (δ, (ppm), 400 MHz, $CDCl_3$): 8.50 (1H, d, J = 4.0 Hz, Py), 7.85-7.80 (2H, m, Ph), 7.74-7.69 (2H, m, Ph), 7.58-7.44 (5H, m, 4H, Ph + 1H, Py), 7.42-7.38 (2H, m, Ph), 7.29-7.19 (6H, m, (5H, Ar + 1H, Py), 7.13-7.10 (1H, m, Py), 4.86 (1H, m, *subst* .Cp), 4.27 (1H, m, *subst*. Cp), 4.17 (5H, s, Cp), 4.03 (1H, d(AB system), J = 14.8 Hz, CH_2Ar), 3.78 (1H, d(AB system), J = 14.8 Hz, CH_2Ar), 3.73 (1H, m, *subst.* Cp), 3.71 (1H, d(AB system), J = 14.9 Hz, CH_2Py), 3.57 (1H, d(AB system), J = 13.8 Hz, CH_2Cp), 3.51 (1H, d(AB system), J = 14.7 Hz, CH_2Py), 3.39 (1H, d(AB system), J = 13.8 Hz, CH_2C$_P$).

^{13}C {^{1}H} NMR (δ, (ppm), 125 MHz, $CDCl_3$): 160.07 (s, *quat*. Py), 148.75 (s, Py); 139.01 (s, *quat*. CH_2Ph), 136.16 (s, Py), 134.61 (d, J_{CP} = 86.3 Hz, *quat*. Ph), 133.74 (d, J_{CP} = 87.0 Hz, *quat*. Ph), 132.05 (d, J_{CP} = 11.1 Hz, 2C, Ph), 132.02 (d, J_{CP} = 10.6 Hz, 2C, Ph), 131.14 (s, Ph), 128.99 (s, 2C, Ar), 128.26 (d, J_{CP} = 12.7 Hz, 2C, Ph), 128.06 (s, 2C, Ar), 127.99 (d, J_{CP} = 11.9 Hz, 2C, Ph), 126.78 (s, Ar), 122.82 (s, Py), 121.67 (s, Py), 90.58 (d, J_{CP} = 12.3 Hz, *quat*. Cp), 74.65 (d, J_{CP} = 10.0 Hz, *subst.* Cp), 74.42 (d, J_{CP} = 12.7 Hz, *subst.* Cp), 73.99 (d, J_{CP} = 95 Hz, *quat*. Cp), 70.79 (s, Cp), 68.58 (d, J_{CP} = 10.3 Hz, *subst.* Cp), 59.25 (s, CH_2Py), 57.88 (s, CH_2Cp), 52.69 (s, CH_2Ar).

^{31}P NMR (δ (ppm), 162MHz, $CDCl_3$): 41.34 (s, PPh_2)

HRMS (DCI-CH_4): 613.1500 (100%, calcd. for $C_{36}H_{35}N_2PSFe$ $[(M+H)^+]$ 613.1530).

2-28c

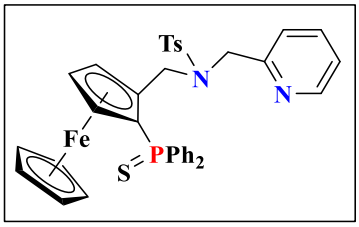

Procedure: Followed same as **2-28a.** Stoichiometry of starting material, corresponding reagents and yield of product as follows-

2-29- 0.45g, 1.04 mmol

PPh_3- 0.6g, 2.3 mmol Yield of racemic **2-28c**- 0.15g, 22%

DEAD- 1 ml, 2.3 mmol

2-30c- 0.6g, 2.3 mmol

^{1}H NMR (δ, (ppm), 400 MHz, $CDCl_3$): 8.37 (1H, d, J = 4.8 Hz, Py), 7.83-7.75 (2H, m, Ph), 7.60-7.41 (8H, m, Ph + TsPh), 7.40-7.36 (1H, m, Py), 7.30-7.24 (2H, m, Ph), 7.19 (2H, d, J = 8.0 Hz, Ph), 7.13 (1H, d, J = 6.8 Hz, Py), 7.09 (1H, m, Py), 4.90 (1H, d(AB system), J = 16.3 Hz, C$\underline{H}_2$Cp), 4.81 (m, 1H, *subst*. Cp), 4.57 (1H, d(AB system), J = 17.1 Hz, C$\underline{H}_2$Cp), 4.36 (1H, d(AB system), J = 16.8 Hz, C$\underline{H}_2$Py), 4.27-4.24 (1H, m, *subst*. Cp), 4.26 (1H, d(AB system), J = 16.6 Hz, C$\underline{H}_2$Py), 4.25 (5H, s, Cp), 2.42 (s, 3H, Ts-C$\underline{H}_3$).

^{13}C {^{1}H} NMR (δ, (ppm), 125 MHz, $CDCl_3$): 157.04 (s, *quat.* Py), 148.79 (s, Py), 143.17 (s, *quat*. TsPh), 136.39 (s, Py), 134.14 (d, J_{CP} = 86.3 Hz, *quat*. Ph), 133.05 (d, J_{CP} = 86.2 Hz, *quat*. Ph), 132.00 (d, J = 10.8 Hz, Ph), 131.80 (d, J_{CP} = 10.6 Hz, Ph), 131.36 (d, J_{CP} = 3.0 Hz, Ph), 131.25 (d, J_{CP} = 3.0 Hz, Ph), 129.52 (s, TsPh), 128.29 (d, J_{CP} = 12.2 Hz, Ph), 128.05 (d, J_{CP} = 12.4 Hz, Ph), 127.42 (s,TsPh), 122.04 (s, Py), 121.95 (s, Py), 88.74 (d, J_{CP} = 12.1 Hz, *quat*. Cp), 74.62 (d, J_{CP} = 9.5 Hz, *subst*. Cp), 74.27 (d, J_{CP} = 12.2 Hz, *subst*. Cp), 73.44 (d, J_{CP} = 95.8 Hz, *quat.* Cp), 71.14 (s, Cp), 69.04 (d, J_{CP} = 10.2 Hz, *subst*. Cp), 53.70 (s, $\underline{C}H_2$Py), 48.00 (s, $\underline{C}H_2$Cp), 21.52 (s, Ts-$\underline{C}H_3$).

^{31}P NMR (δ (ppm), 162MHz, $CDCl_3$): 40.89 (s, PPh_2).

HRMS (DCI-CH_4): 676.1060 (100%, calcd. for $C_{36}H_{33}N_2O_2S_2PFe$ [M] 676.1070).

2-1

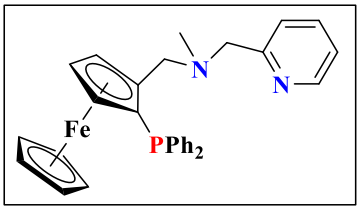

Procedure. In a dry Schlenk tube, under an argon atmosphere, racemic **2-28a** (0.100g, 0.19 mmol) were dissolved in 7 ml of dry and degassed toluene. Degassed tris-(dimethylamino)phosphine (0.17 ml, 0.93 mmol) was added to the solution. The reaction mixture was heated to reflux overnight. Then, after cooling to room temperature, the solvent was evaporated by vacuum. The resulting orange residue was purified by flash column chromatography under argon using degassed 90% pentane-

dichloromethane (with 0.5% NEt_3) as eluent. The pure compound was obtained as a yellow solid (yield 0.70 g, 80%).

^{1}H NMR (δ, (ppm), 400 MHz, $CDCl_3$): 8.13 (1H, d, J = 4.95 Hz, Py), 7.30 (2H, m, Ph), 7.11 (3H, m, Ph), 7.00-6.92 (6H, m, 5H Ph + 1H Py), 6.73 (1H, m, Py), 6.27 (1H, d, J = 7.85 Hz, Py), 4.23 (1H, m, *subst.* Cp), 4.01 (1H, m, *subst.* Cp), 3.76 (1H, d, J = 12.7 Hz, C$\underline{H}_2$Py), 3.70 (5H, s, Cp), 3.55 (1H, m, *subst.* Cp), 3.35 (1H, d, J = 14.4 Hz, C$\underline{H}_2$Cp), 3.24 (1H, d, J = 14.5 Hz, C$\underline{H}_2$Cp), 3.03 (1H, d, J = 12.7 Hz, C$\underline{H}_2$Py), 1.64 (3H, s, N-CH_3).

^{13}C {^{1}H} NMR (δ, (ppm), 125 MHz, $CDCl_3$): 160.06 (s, *quat*. Py), 148.39 (s, Py), 140.60 (d, J_{CP} = 9.1 Hz, *quat*. Ph), 138.06 (d, J_{CP} = 8.4 Hz, *quat*. Ph), 136.18 (s, Py), 135.21 (d, J_{CP} = 21.4 Hz, Ph), 132.47 (d, J_{CP} = 18.0 Hz, Ph), 129.01 (s, Ph), 128.03 (d, J_{CP} = 8.0 Hz, Ph), 127.81 (d, J_{CP} = 6.1 Hz, Ph), 127.47 (s, Ph), 122.70 (s, Py), 121.45 (s, Py), 90.58 (d, J_{CP} = 25.9 Hz, *quat*. Cp), 76.54 (d, J_{CP} = 8.3 Hz, *quat*. Cp), 73.59 (d, J_{CP} = 3.9 Hz, *subst*. Cp), 71.90 (d, J_{CP} = 4.7 Hz, *subst*. Cp), 69.62 (s, Cp), 69.26 (s, *subst*. Cp), 63.75 (s, $\underline{C}H_2$Py), 57.29 (d, J_{CP} = 8.4 Hz, $\underline{C}H_2$Cp), 41.21 (s, $\underline{C}H_3$).

^{31}P NMR (δ (ppm), 162MHz, $CDCl_3$): -28.9 (s, PPh_2).

2-45

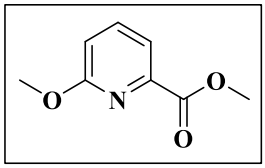

Procedure. To a 250 mL flask fitted with a magnetic rod and containing a solution of 6-hydroxy-2-picolinic acid (4.00 g, 29 mmol) in toluene (100 ml) was added silver oxide (Ag_2O) (7.00 g, 30 mmol). Iodomethane (4 ml, 60 mmol) was then added and the reaction mixture was refluxed overnight. The resulting dark orange mixture was filtered, the solvent was evaporated *in vacuo* and the residue was then extracted with CH_2Cl_2 (3x 60ml). The combined organic phases were dried over Na_2SO_4 and evaporated to dryness. The resulting orange oily crude was purified by column chromatography (90/10 pentane/ether) to obtain the desired product (yield 7 g, 86%) as a white crystalline solid.

^{1}H NMR (δ, (ppm), 400 MHz, $CDCl_3$): 7.71 (2H, m, Py), 6.94 (1H, dd, J = 6.2 Hz, J = 1.5 Hz, Py), 4.04 (s, 3H, O-C$\underline{H}_3$), 3.97 (s, 3H, O-C$\underline{H}_3$).

$^{13}C\ \{^1H\}$ NMR (δ, (ppm), 125 MHz, $CDCl_3$): 165.73 (s, CO), 163.92 (s, *quat.* Py), 145.43 (s, *quat*. Py), 139.00 (s, Py), 118.63 (s, Py), 115.26 (s, Py), 53.64 (s, O-$\underline{C}H_3$), 52.64 (s, O-$\underline{C}H_3$).

***HRMS (DCI-CH_4)*:** 168.0664 (100%, calcd. for $C_8H_{10}NO_3$ $[(M+H)^+]$ 168.0661).

2-46

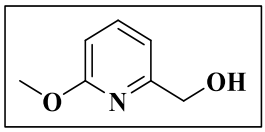

Procedure. In a 50 ml Schlenk tube fitted with a magnetic rod under an argon atmosphere, product **2-45** (3 g, 18 mmol) was dissolved in 20 ml of methanol. After further addition of solid NaOMe (1.7 g; 1.4 mmol; 7.5 mol%) at 0°C, the mixture was stirred for 40 min at same temperature. Solid $NaBH_4$ (7.27 g, 45 mmol) was then added portion wise, also at 0°C, followed by stirring for another 30 min. The ice bath was then removed and the reaction mixture was further stirred at r.t. for 3h. The remaining $NaBH_4$ in the reaction mixture was quenched by addition of excess methanol (30 ml) followed by 2 (M) HCl (until pH= 3) into the reaction medium. After converting the pH of the crude medium to basic (pH = 8-9) by adding a saturated $NaHCO_3$ solution, the solvent was evaporated and the residue was extracted with CH_2Cl_2 (3 x 60 ml). The combined DCM layers dried over Na_2SO_4 and evaporated to dryness. The crude was purified by column chromatography (pentane:ether = 80:20) to yield the product **2-46** as a colorless oil (yield 2.6 g, 80%).

^1H NMR (δ, (ppm), 300 MHz, $CDCl_3$): 7.57 (1H, t, J = 7.8 Hz, Py), 6.82 (1H, d, J = 7.2 Hz, Py), 6.65 (1H, d, J = 8.2 Hz, Py), 4.68 (2H, s, CH_2), 3.96 (s, 3H, O-$C\underline{H}_3$).

$^{13}C\ \{^1H\}$ NMR (δ, (ppm), 75 MHz, $CDCl_3$): 163.66 (s, *quat.* Py), 156.75 (s, *quat.* Py), 139.31 (s, Py), 112.71 (s, Py), 109.08 (s, Py), 63.87 (s, *C*H_2), 53.40 (s, O-$\underline{C}H_3$).

***HRMS (DCI-CH_4)*:** 140.0707 (100%, calcd. for $C_7H_{10}NO_2$ $[(M+H)^+]$ 140.0712)

2-43a

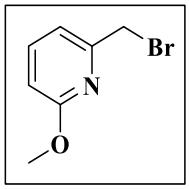

Procedure: To a stirred solution of 6-methoxypicolyl alcohol **2-46** (0.5 g, 3.5 mmol) in dry dichloromethane (10 ml) was added phosphorus tribromide (0.5 ml, 5.4 mmol) drop wise at 0 ^{o}C and the reaction mixture was stirred at room temperature for 1.5 h. After complete alcohol consumption (TLC monitoring), the reaction was quenched using a saturated $Na_2S_2O_3$ solution at 0 ^{o}C. The aqueous phase was extracted with dichloromethane (2x 20ml). The combined organic layers were washed with a saturated $NaHCO_3$ solution, followed by brine. The crude mixture found after drying over Na_2SO_4 and solvent evaporation under reduced pressure was purified by silica gel column chromatography (petroleum ether/ether: 4:1). The desired pyridyl bromide **2-43a** was obtained as a colorless liquid (yield- 0.45g, 62%).

^{1}H NMR (δ, (ppm), 400 MHz, $CDCl_3$): 7.57-7.53 (1H, m, Py), 7.00 (1H, d, J = 7.3 Hz, Py), 6.67 (1H, d, J = 8.3 Hz, Py), 4.47 (2H, s, -CH_2), 3.95 (3H, s, CH_3).

^{13}C {^{1}H} NMR (δ, (ppm), 125 MHz, $CDCl_3$): 163.79 (s, *quat.* Py), 154.20 (s, *quat.* Py), 139.23 (s, Py), 133.08 (s, *quat.* Ph), 115.95 (s, Py), 110.41 (s, Py), 53.46 (s, O-$\underline{C}H_3$), 34.08 (s, $\underline{C}H_2$Py).

HRMS (DCI-CH_4): 201.9868 (100%, calcd. for C_7H_9NOBr [$(M+H)^+$] 201.9868).

2-43b

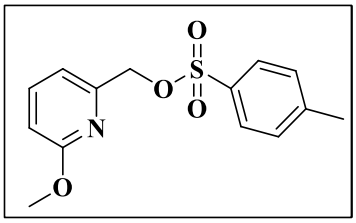

Procedure: To a solution of pyridyl alcohol (1 g, 7.2 mmol) in THF (20 ml), solid KOH beads (2 g, 36 mmol) were added, followed by stirring for 30 min. Tosyl chloride (4 g, 21 mmol) was added portion wise to the resulting suspension and the reaction mixture was stirred overnight at room temperature. The reaction mixture was extracted with water-dichloromethane (1:3 volume ratio). The combined organic phase was dried over Na_2SO_4 and then evaporated under reduced pressure. The resulting yellow crude was purified by column chromatography to obtain the pure tosylate product **2-43b** (Yield- 1.7g, 84%) as a white crystalline solid.

^{1}H NMR (δ, (ppm), 400 MHz, $CDCl_3$): 7.85 (2H, d, J = 8.4 Hz, Ph), 7.55 (1H, t, J = 7.78 Hz, Py), 7.35 (2H, d, J = 8.71 Hz, Ph), 6.94 (1H, d, J = 7.3 Hz, Py), 6.66 (1H, d, J = 8.4 Hz, Py), 5.05 (2H, s, -CH_2), 3.85 (3H, s, CH_3), 2.46 (3H, s, CH_3).

$^{13}C\{^1H\}$ NMR (δ, (ppm), 125 MHz, $CDCl_3$): 163.65 (s, *quat.* Py), 151.0 (s, *quat.* Py), 144.88 (s, quat Ph), 139.14 (s, Py), 133.08 (s, *quat.* Ph); 129.83 (s, 2C, Ph); 128.04 (s, 2C, Ph); 114.51 (s, 2C, Py); 110.63 (s, 2C, Py); 71.61 (s, $\underline{C}H_2Py$); 53.35 (s, O-$\underline{C}H_3$), 21.63 (s, Ts$\underline{C}H_3$).

HRMS (DCI-CH_4): 294.0796 (100%, calcd. for $C_{14}H_{16}NO_4S$ $[(M+H)^+]$ 294.0800).

2-42b

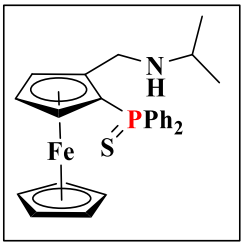

Procedure: In a dry schlenk tube, under argon atmosphere, racemic **2-29** (0.8g, 1.85 mmol) was dissolved in 5 ml of dry dichloromethane. 54% solution of HBF_4 in ether (0.5 ml, 5.55 mmol) was added and stirred for 1 min. Then isopropylamine (4 ml, 46.3 mmol) was added rapidly. Immediately after 2 min. of stirring, the resulting dark orange crude solution was filtered on silica gel using ether. The yellow filtrate that came out was evaporated and further purified by column chromatography (30% EtOAc-hexane) to yield pure racemic **2-42b** (0.64g, 72%).

^1H NMR (δ (ppm), 400MHz, $CDCl_3$): 7.84 (2H, m, Ph), 7.74 (2H, m, Ph), 7.57-7.38 (6H, m, Ph), 4.60 (1H, m, *subst*. Cp), 4.33 (5H, s, Cp), 4.296 (1H, m, *subst*. Cp), 4.294 (1H, d(AB system), J= 12.9 Hz, $C\underline{H}_2Cp$), 3.75 (1H, m, *subst*. Cp), 3.54 (1H, d(AB system), J= 12.9 Hz, $C\underline{H}_2Cp$), 2.56 (1H, hept, J = 6.2Hz, $C\underline{H}^iPr$) 1.62 (s, 1H, br, NH), 0.75 (H, d= 6.2 Hz, $C\underline{H}_3$), 0.73 (H, d= 6.2 Hz, $C\underline{H}_3$).

$^{13}C\{^1H\}$ NMR (δ (ppm), 125 MHz, $CDCl_3$): 134.86 (d, J_{CP} = 85.7 Hz, *quat.* Ph), 133.43 (d, J_{CP} = 85.9 Hz, *quat.* Ph), 131.96 (d, J_{CP} = 10.4 Hz, Ph), 131.94 (d, J_{CP} = 10.8 Hz, Ph), 131.41 (d, J_{CP} = 3.0 Hz, Ph), 131.27 (d, J_{CP} = 3.1 Hz, Ph), 128.40 (d, J_{CP} = 12.3 Hz, Ph), 128.07 (d, J_{CP} = 12.5 Hz, Ph), 91.02 (d, J_{CP} = 13.4 Hz, *quat.subst.* Cp), 74.68 (d, J_{CP} = 12.3 Hz, *subst.* Cp), 74.60 (d, J_{CP} = 10.0 Hz, *subst.* Cp), 74.38 (d, J_{CP} = 95.1 Hz, *quat.subst.* Cp), 70.58 (s, Cp), 68.85 (d, J_{CP} = 10.4 Hz, *subst.* Cp), 47.41 (s, $\underline{C}H$), 44.89 (s, $\underline{C}H_2$), 22.55 (s, $\underline{C}H_3$), 22.22 (s, $\underline{C}H_3$).

^{31}P NMR (δ (ppm), 162MHz, $CDCl_3$): 41.05 (s, PPh_2).

HRMS (DCI-CH_4): 473.1030 (100%, calcd. for $C_{26}H_{28}FeNPS$ [M+H] 473.1029).

2-48

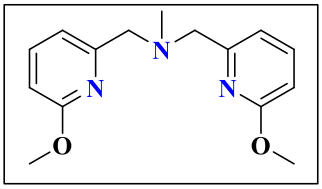

Procedure. A solution of methylamine (0.07 ml, 0.17 mmol) in THF (10 ml) was treated with solid K_2CO_3 (0.09 g, 0.68 mmol) at 0 ^oC. The resulting suspension was stirred at 0 ^oC for 30 min. A solution of pyridyl tosylate **2-43b** (0.1 g, 0.34 mmol) in THF was added to it drop wise and then the reaction mixture was kept for overnight stirring at r.t. After the complete consumption of **2-43b**, the reaction mixture was extracted with water-DCM (3 x 25ml). The combined organic layers were dried and then evaporated. After purification of the dry crude by column chromatography (Hexane: Ether= 4:1). The expected product was obtained as colourless oil (yield 0.04 g, 84%).

^{1}H NMR (δ (ppm), 400MHz, $CDCl_3$): 7.55 (2H, t, J = 7.23 Hz, Py), 7.13 (2H, d, J = 7.25 Hz, Py), 6.64 (2H, d, J = 8.23 Hz, Py), 3.94 (s, 6H, O-CH_3), 3.71 (4H, CH_2Py), 2.38 (3H, N-CH_3).

^{13}C {^{1}H} NMR (δ (ppm), 125 MHz, $CDCl_3$): 163.58 (s, 2C, *quat.* Py), 157.27 (s, 2C, *quat.* Py), 138.78 (s, 2C, Py), 115.34 (s, 2C, Py), 108.41 (s, 2C, Py), 63.06 (s, 2C, O-CH_3), 53.24 (s, 2C, CH_2Py), 42.86 (s, N-CH_3).

HRMS (DCI-CH_4): 274.1550 (100%, calcd. for $C_{15}H_{20}N_3O_2$ [$(M+H)^+$] 274.1550).

2-40a

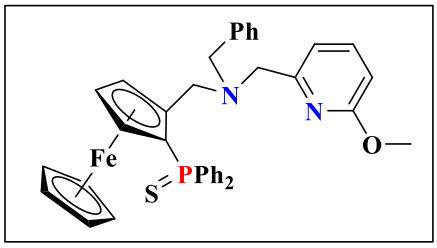

Procedure. Solid K_2CO_3 (0.074g, 0.54 mmol) was added to a solution of ferrocenylamine **2-42a** (0.1g, 0.19 mmol) in 5 ml of DCM and the resulting mixture was stirred for 30 min. Then to the resulting suspension a solution of pyridyl tosylate **2-43b** (0.11g, 0.38 mmol) in 4 ml DCM was added drop wise. The reaction mixture was stirred overnight at room temperature. The orange suspension was extracted with water (2x25 ml). The organic phase was dried over Na_2SO_4 and then evaporated *in vacuum* The orange crude was purified by column chromatography (petroleum ether:ether = 4:1). The pure ligand was obtained in the form of an orange solid (yield- 0.092g, 75%).

^{1}H NMR (δ (ppm), 400MHz, $CDCl_3$): 7.86-7.80 (2H, m, Ph), 7.72-7.67 (2H, m, Ph), 7.55-7.44 (5H, m, 4H, Ph + 1H, Py), 7.41-7.35 (2H, m, Ph), 7.27-7.18 (5H, m, Ph), 6.84 (1H, d, J = 7.2 Hz, Py), 6.59 (1H, d, J = 8.2 Hz, Py), 4.95 (m, 1H, *subst*. Cp), 4.27 (m, 1H, *subst.* Cp), 4.18 (5H, s, Cp), 3.97 (1H, d(AB system), J = 14.8 Hz, CH_2Cp), 3.96 (3H, s, O-CH_3), 3.91 (1H, d(AB system), J = 14.8 Hz, CH_2Cp), 3.73 (m, 1H, *subst.* Cp), 3.65 (1H, d(AB system), J = 13.0 Hz, CH_2Cp), 3.62 (1H, d(AB system), J = 15.0 Hz, CH_2Py), 3.394 (1H, d(AB system), J = 15.0 Hz, CH_2Py), 3.391 (1H, d(AB system), J = 13.0 Hz, CH_2Ph).

^{13}C{^{1}H} NMR (δ (ppm), 125 MHz, $CDCl_3$): 163.41 (s, *quat.* Py {C-OMe}), 157.61 (s, *quat.* Py CCH_2), 139.51 (s, quat Ph), 138.53 (s, Py), 134.66 (d, J_{CP} = 86.8 Hz, *quat.* Ph), 133.77 (d, J_{CP} = 85.9 Hz, *quat.* Ph), 132.07 (d, J = 10.7 Hz, Ph); 132.01 (d, J = 10.3 Hz, Ph), 131.14 (d, J_{PC} = 3.4 Hz, Ph), 131.10 (d, J_{CP} = 3.3 Hz, Ph), 128.86 (s, Ph), 128.21 (d, J_{CP} = 12.2 Hz, Ph), 128.01 (s, Ph), 127.98 (d, J = 12.4 Hz, Ph), 126.67 (s, Ph), 115.49 (s, Py), 108.26 (s, Py), 91.03 (d, J = 12.0 Hz, *quat.* Cp), 74.54 (d, J = 10.0 Hz, *subst.* Cp), 74.34 (d, J = 13.0 Hz, *subst.* Cp), 73.85 (d, J = 95.5 Hz, *quat.* Cp), 70.80 (s, Cp), 68.50 (d, J = 10.4 Hz, *subst.* Cp), 57.92 (s, CH_2), 57.72 (s, CH_2), 53.34 (s, O-CH_3), 52.40 (s, CH_2).

^{31}P NMR (δ (ppm), 162MHz, $CDCl_3$): 41.54 (s, PPh_2).

HRMS (DCI-CH_4): 643.1647 (100%, calcd. for $C_{37}H_{36}N_2OPSFe$ [MH^+] 643.1635).

2-40b

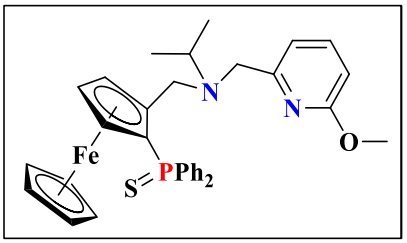

Procedure: Followed same as **2-40a.** Stoichiometry of starting material, corresponding reagents and yield of product as follows-

2-42b - 0.5g, 1.05 mmol

2-43b - 0.4g, 1.38 mmol Yield of racemic **2-40b**- 0.4g, 71%

K_2CO_3- 0,43g, 3.15 mmol

^{1}H NMR (δ (ppm), 400MHz, $CDCl_3$): 7.84 (2H, m, Ph), 7.80 (2H, m, Ph), 7.72-7.42 (5H, m, 4H, Ph + 1H, Py), 7.37 (2H, m, Ph), 7.0 (1H, d, J = 7.3 Hz, Py), 6.57 (1H, d, J = 8.1 Hz, Py), 4.84 (m, 1H,

subst. Cp), 4.25 (5H, s, Cp), 4.22 (m, 1H, *subst*. Cp), 3.93 (3H, s, O-C$\underline{H}_3$), 3.82 (1H, d(AB system), J = 154 Hz, C$\underline{H}_2$Cp), 3.78 (1H, d(AB system), J = 15.4 Hz, C$\underline{H}_2$Cp), 3.68 (1H, m, *subst.* Cp), 3.61 (1H, d(AB system), J = 15.8 Hz, C$\underline{H}_2$Py), 3.51 (1H, d(AB system), J = 15.8 Hz, C$\underline{H}_2$Py), 2.86 (1H, hept, J = 6.6 Hz, -C$\underline{H}$-), 0.98 (3H, d, J = 6.6 Hz, -C$\underline{H}_3$), 0.70 (3H, d, J = 6.6 Hz, -C$\underline{H}_3$).

$^{13}C\{^1H\}$ NMR (δ (ppm), 125 MHz, $CDCl_3$): 163.35 (s, *quat.* Py {$\underline{C}$-OMe}), 159.81 (s, *quat.* Py $\underline{C}CH_2$), 138.54 (s, Py), 134.41 (d, J_{CP} = 86.5 Hz, *quat.* Ph), 133.7 (d, J_{CP} = 85.7 Hz, *quat.* Ph), 132.03 (d, J_{CP} = 10.7 Hz, 4C, Ph), 131.13 (d, J_{CP} = 2.6 Hz, 1C, Ph), 131.11 (d, J_{CP} = 2.7 Hz, 1C, Ph), 128.16 (d, J_{CP} = 12.3 Hz, 2C, Ph), 127.99 (d, J = 12.3 Hz, 2C, Ph), 114.6 (s, Py), 107.79 (s, Py), 92.25 (d, J = 12.1 Hz, *quat.* Cp), 74.24 (d, J = 9.9 Hz, *subst.* Cp), 74.13 (d, J = 12.7 Hz, *subst.* Cp), 71.91 (d, J = 95.5 Hz, *quat.* Cp), 70.78 (s, Cp), 68.26 (d, J = 10.5 Hz, *subst.* Cp), 54.92 (s, $\underline{C}H_2$Py), 53.23 (s, O-$\underline{C}H_3$), 49.85 (s, -$\underline{C}$H-), 48.87 (s, $\underline{C}H_2$Cp), 19.2 (s, -$\underline{C}H_3$), 16.41 (s, -$\underline{C}H_3$).

^{31}P NMR (δ (ppm), 162MHz, $CDCl_3$): 41.53 (s, PPh_2).

HRMS (DCI-CH_4): 594.1537 (100%, calcd. for $C_{33}H_{35}N_2PSFe$ [M^+] 594.1557).

Experimental Procedure and Characterization of Synthesized Compounds of Chapter-3

3-32

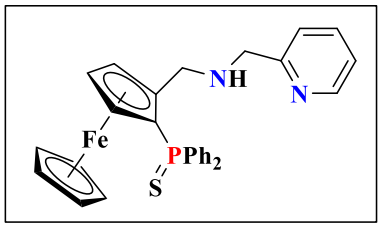

Procedure: In a dry schlenk tube, under argon atmosphere, racemic **2-29** (200 mg, 0.46 mmol) was dissolved in 2 mL of dry dichloromethane. 54% solution of HBF_4 in ether (0.2 ml, 1.38 mmol) was added and stirred for 1 min. Then 2-picolylamine (1.4ml, 14 mmol) was added rapidly. Immediately after 2 min. of stirring, the resulting dark orange crude solution was filtered on silica gel using ether. The yellow filtrate that came out was evaporated and further purified by column chromatography (50% Et_2O-hexane) to yield pure racemic **3-32** (0.08g, 32%).

^1H NMR (δ (ppm), 400MHz, $CDCl_3$): 8.48 (1H, d, J= 4.1 Hz, Py), 7.9-7.75 (2H, m, Ph), 7.75-7.6 (2H, m, Ph), 7.6-7.45 (4H, m, Ph), 7.45-7.3 (3H, m, 2H, Ph + 1H Py); 7.12 (1H, dd, J= 7.2Hz, J= 5.2Hz, Py), 7.06 (1H, d, J= 7.8 Hz, Py), 4.68 (m, 1H, *subst*. Cp), 4.32 (s, 5H, Cp), 4.35-4.25

(2H, m; 1H C$\underline{H}_2$Cp + 1H, *subst.* Cp), 3.80 (1H, d(AB system), J=14.6Hz, C$\underline{H}_2$Py), 3.79 (s, 1H, subst Cp), 3.70 (1H, d(AB system), J=14.6Hz, C$\underline{H}_2$Py), 3.67 (1H, d(AB system), J=13.4Hz, C$\underline{H}_2$Cp).

$^{13}C\{^1H\}$ NMR (δ (ppm), 125 MHz, $CDCl_3$): 159.91 (s, *quat.* Py), 148.94 (s, Py), 136.26 (s, Py), 134.89 (d, J=86Hz, *quat*. Ph), 133.45 (d, J=86Hz, *quat.* Ph), 131.99 (d, J=10.7Hz, Ph), 131.83 (d, J=10.7Hz, Ph), 131.28 (d, J=3.0Hz, Ph), 131.19 (d, J=3.0Hz, Ph), 128.30 (d, J=12.3Hz, Ph), 128.05 (d, J=12.3Hz, Ph), 121.67 (s, Py), 121.61 (s, Py), 90.89 (d, J=12.3Hz, *quat.* Cp), 74.64 (d, J=12.7Hz, *subst.* Cp), 74.40 (d, J=10.0Hz, *subst.* Cp), 74.16 (d, J=95.1Hz, *quat.* Cp), 70.58 (s, Cp); 68.90 (d, J=13.3Hz, *subst.* Cp), 53.08 (s, $\underline{C}H_2$Py), 46.69 (s, $\underline{C}H_2$Cp).

^{31}P NMR (δ (ppm), 162MHz, $CDCl_3$): 41.3 (s, PPh_2).

***HRMS (DCI-CH_4)*:** 522.0956 (100%, calcd. for $C_{29}H_{27}FeN_2PS$ [M] 522.0979).

3-33

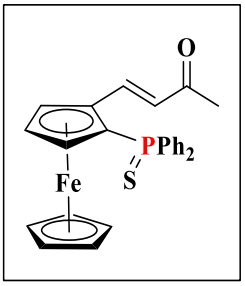

Procedure: To a solution of Ferrocenyl carboxaldehyde **3-27** (0.22g, 0.51 mmol) in acetone (40 ml), 2-picolylamine (0.2 mL, 1.53 mmol) was added. The reaction mixture was refluxed 24h along with the TLC monitoring for the consumption of aldehyde. After the complete consumption, the reaction mixture was evaporated *in vacuum* and extracted with water-DCM. Combined organic layer was dried over Na_2SO_4 and evaporated to dryness. Crude was purified by silica gel column chromatography with hexane-ether (1:1) to obtain product **3-33** as a red solid (0.13 g, 55%).

^1H NMR (δ (ppm), 400MHz, CD_2Cl_2): 8.46 (1H, d, J=16.3Hz, vinyl), 7.90-7.80 (1H, m, Ph), 7.65-7.15 (9H, m, Ph), 6.28 (1H, d, J=16.3Hz, vinyl), 5.01 (1H, m, *subst*. Cp), 4.65 (1H, m, *subst.* Cp), 4.39 (5H, s, *subst.* Cp), 4.07 (1H, m, *subst.* Cp), 3.87 (3H, s, $C\underline{H}_3$).

$^{13}C\{^{1}H\}$ NMR (δ (ppm), 125 MHz, CD_2Cl_2): 198. 16 (s, C=O), 143.46 (s, vinyl), 134.93 (d, J_{CP}=87.4Hz , *quat*. Ph), 133.01 (d, J_{CP}=86.6Hz , *quat*. Ph), 132.03 (d, J_{CP}=11.0Hz, Ph), 131.69 (d, J_{CP}=10.7Hz, Ph), 131.54 (d, J_{CP}=3.0Hz, Ph), 131.39 (d, J_{CP}=3.0Hz, Ph), 128.40 (d, J_{CP}=12.5Hz, Ph), 128.19 (d, J_{CP}=12.4Hz, Ph), 126.89 (s, vinyl), 83.06 (d, J_{CP}=10.7Hz, *quat*. Cp), 77.44 (d, J_{CP}=11.9Hz, *subst*. Cp), 77.00 (d, J_{CP}=93.2Hz, *quat*. Cp), 71.87 (s, Cp), 71.85 (d, J_{CP}=10.3Hz, *subst*. Cp), 69.90 (d, J_{CP}=8.4Hz, *subst*. Cp), 25.87 (s, CH_2).

^{31}P NMR (δ (ppm), 162MHz, CD_2Cl_2): 41.01 (s, PPh_2).

HRMS (DCI-CH_4): 471.0638 (100%, calcd. for $C_{26}H_{24}FeOPS$ [M] 471.0635)

3-36

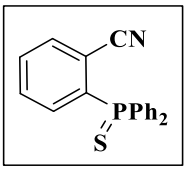

Procedure: 2-bromobenzonitrile (0.5 g, 2.74 mmol) was dissolved in 20 mL of dry and degassed THF in argon atmosphere and the solution was cooled down to -78 °C. *n*-butyl lithium [1.1 mL, 2.74 mmol; 2.5 (M) in hexane] was slowly added to it at -78 °C over a period of 10 min. The reaction mixture was stirred for 2h at -78 °C. Chlorodiphenylphosphine (0.5 mL, 2.74 mmol) was added in a drop wise manner using Teflon cannula at -78 °C; over a period of 40 min. The final reaction mixture was slowly warmed-up to room temperature and kept for another 16 h. Degassed saturated $NaHCO_3$ solution was added to quench the reaction. The organic phase was extracted with degassed DCM (3 times) under argon atmosphere. Combined organic phases were dried over Na_2SO_4. Solid sulphur was added to the organic phase and stirred for 2 h. Solvents were removed under reduced pressure. The crude was purified by column chromatography (Ether: Hexane= 1:4) on silica to obtain the pure product **3-36** (yield- 0.47g, 55%).

^{1}H NMR (δ (ppm), 400MHz, $CDCl_3$): 7.95- 7.85 (4H, m, Ar), 7.85- 7.79 (1H, m, Ar), 7.72- 7.50 (9H, m, Ar).

$^{13}C\{^{1}H\}$ NMR (δ (ppm), 125 MHz, $CDCl_3$): 137.68 (d, J_{CP} = 79.3 Hz, *quat.* Ar), 135.80 (d, J_{CP} = 7.9 Hz, Ar), 133.81 (d, J_{CP} = 9.8 Hz, Ar), 132.47 (d, J_{CP} = 10.9 Hz, Ph), 132.27 (s, Ph), 132.20 (d, J_{CP} =

13.4 Hz, *quat.* Ar), 131.54 (d, J_{CP} = 2.6 Hz, Ar), 130.77 (d, J_{CP} = 86.9 Hz, *quat.* Ph), 128.83 (d, J_{CP} = 12.9 Hz, Ph), 116.53 (d, J_{CP} = 5 Hz, CN or, Ar), 115.34 (d, J_{CP} = 5.9 Hz, CN or, Ar).

^{31}P NMR (δ (ppm), 162MHz, $CDCl_3$): 42.34 (s, PPh_2).

HRMS (DCI-CH_4): 320.0658 (100%, calcd. for $C_{19}H_{15}NPS$ [M+H] 320.0663).

3-35

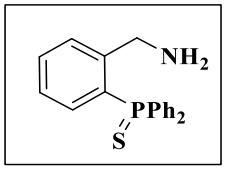

Procedure: **3-37** (0.5g, 1.57 mmol) was dissolved in 20 ml dry THF and cooled to 0 ^{o}C. 1(M) solution of $LiAlH_4$ in THF (2.5 ml, 2.4 mmol) was added drop wise into that. The reaction was slowly shifted to room temperature and then refluxed for 1.5h. After that the reaction mixture was again cooled down to 0 ^{o}C and quenched by 2(M) aq. NaOH (up to pH= 12). The resulting suspension was filtered off by Teflon cannula. The filtrate after drying *in vacuo* extracted with water-dichloromethane (3x 40 ml). Combined organic layers were dried over Na_2SO_4, filtered and concentrated. The dry crude was purified by column chromatography on silica gel (60% EtOAc/n-hexane) to afford 2-diphenylthiophosphinobenzylamine **3-35** as pale-yellow solid (yield- 0.3g, 59%).

^{1}H NMR (δ (ppm), 400MHz, $CDCl_3$): 7.85-7.70 (4H, m, Ar), 7.70-7.40 (8H, m, Ar), 7.20-7.10 (1H, m, Ar), 6.90 (1H, dd, J=7.8Hz, J_{HP}=14.7Hz, Ar), 3.96 (2H, s, CH_2Ar), 2.05 (2H,br, NH_2).

$^{13}C\{^{1}H\}$ NMR (δ (ppm), 125 MHz, $CDCl_3$): 147.23 (d, J_{CP} = 9.5 Hz, *quat.* Ar), 132.68 (d, J_{CP} = 11.6 Hz, Ph), 132.57 (d, J_{CP} = 84.1 Hz, *quat.* Ph), 132.43 (d, J_{CP} = 2.7 Hz, Ar), 132.26 (d, J_{CP} = 10.6 Hz, Ph), 131.73 (d, J_{CP} = 2.9 Hz, Ph), 131.60 (d, J_{CP} = 84.9 Hz, *quat.* Ar), 131.29 (d, J_{CP} = 10.2 Hz, Ar), 128.66 (d, J_{CP} = 12.6 Hz, Ph), 126.54 (d, J_{CP} = 12.5 Hz, Ar), 44.60 (d, J_{CP} = 6.3 Hz, CH_2).

^{31}P NMR (δ (ppm), 162MHz, $CDCl_3$): 41.51 (s, PPh_2)

HRMS (DCI-CH_4): 324.0967 (100%, calcd. for $C_{19}H_{19}NPS$ [MH+] 324.0976).

3-43

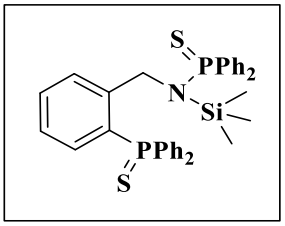

Procedure: To an oven dried Schlenk tube benzylamine (2.14 g, 20.0 mmol) was dissolved in dry ether (30 mL) under argon. The solution was cooled to 0℃ and *n*-BuLi (8.0 mL, 2.5 M in hexane, 20.0 mmol) was added drop wise. The resulting solution was stirred at 0℃ for 30 minutes and TMSCl (2.8 mL, 22.0 mmol) was added slowly at the same temperature. The reaction mixture was stirred for 1 hour and again *n*-BuLi (24 mL, 2.5 M in hexane, 60.0 mmol) was added drop wise. After the addition was completed, the reaction mixture was stirred at 0℃ for 3h, then slowly warmed to room temperature and stirred overnight. The reaction mixture was cooled at 0 ^{o}C again, and a solution of chlorodiphenylphosphine (8 mL, 44.0 mmol) was added drop wise. The reaction mixture was kept for 3-4 h at the same temperature, then stirred for another overnight after warming up to room temperature. After the complete consumption of benzylamine monitored by TLC, reaction was quenched by addition of degassed aq. $NaHCO_3$ (40-50 mL) and the turbid aqueous phase was extracted with degassed dichloromethane (3-4 times). Combined organic solution was washed with degassed brine, dried over Na_2SO_4. S_8 was added to the dried solution and after 2-3 hours of stirring at room temperature excess S_8 was filtered off. After the solvent evaporation the crude filtrate was purified by silica gel column chromatography (20% ethyl acetate-hexane) to obtain the product as a white solid (yield- 3.4g, 28%).

^{1}H NMR (δ (ppm), 400MHz, $CDCl_3$): 7.86-7.19 (23H, m, Ph + Ar), 7.00 (1H, m, Ar), 6.79 (1H, m, Ar), 5.08 (1H, m, CH_2Ar), 4.10 (1H, m, CH_2Ar), 0.26 (9H, s, $Si(CH_3)_3$)

^{31}P NMR (δ (ppm), 162MHz, $CDCl_3$): 65.58 (s, PPh_2), 39.86 (s, PPh_2).

HRMS (DCI-CH_4): 612.1530 (100%, calcd. for $C_{34}H_{36}NP_2S_2Si$ [MH+] 612.1500)

3-33

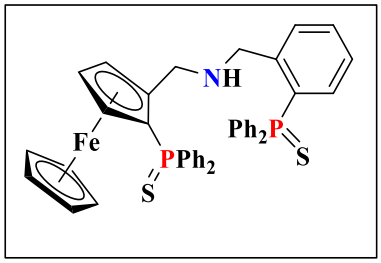

Procedure: In a dry schlenk tube, under argon atmosphere, racemic **2-29** (0.2g, 0.46 mmol) was dissolved in 2 mL of dry dichloromethane. 54% solution of HBF_4 in ether (0.2 ml, 1.38 mmol) was added and stirred for 6 min. Then a solution of amine **3-35** (0.9g, 2.78 mmol) in DCM (4 ml) was added rapidly. Immediately after 15 min of stirring (monitored by TLC to detect the complete consumption of **2-29**), the resulting dark orange crude solution was filtered on silica gel using ether. The yellow filtrate that came out was evaporated and further purified by column chromatography (25% EtOAc-hexane) to yield pure racemic **3-33** (yield- 0.18g, 53%).

^{1}H NMR (δ (ppm), 400MHz, $CDCl_3$): 7.90-7.70 (6H, m, Ph), 7.70-7.60 (2H, dd, J = 7.4 Hz, J_{HP} = 13.4 Hz, Ph), 7.60-7.28 (13H, m, 12H, Ph + 1H, Ar), 7.23 (1H, m, Ar), 7.10 (1H, t, J=7.6 Hz, Ar), 6.86 (1H, dd, J = 7.7 Hz, J_{HP} = 14.9 Hz, Ar), 4.46 (1H, m, *subst.* Cp), 4.27 (5H, s, Cp), 4.24 (1H, m, *subst.* Cp), 3.94 (1H, d (AB system), J=13.5Hz, CH_2Cp), 3.82 (1H, d (AB system), J=14.5Hz, CH_2Ar), 3.73 (1H, m, subst Cp), 3.68 (1H, d (AB system), J=14.5Hz, CH_2Ar), 3.43 (1H, d (AB system), J=13.5Hz, CH_2Cp).

^{13}C{^{1}H} NMR (δ (ppm), 125 MHz, $CDCl_3$): 144.71 (br, *quat.* Ar), 133.05 (d, J_{CP} = 86.6 Hz, *quat.* Ph), 133.70 (d, J_{CP} = 85.5 Hz, *quat.* Ph), 132.87 (d, J_{CP} = 84.0 Hz, *quat.* Ph), 132.61 (d, J_{CP} = 84.0 Hz, *quat.* Ph), 132.61 (d, J_{CP} = 11.5 Hz, Ph), 132.35 (d, J_{CP} = 10.4 Hz, Ph), 132.13 (d, J_{CP} = 10.7 Hz, Ph), 132.08 (d, J_{CP} = 10.7 Hz, Ph), 131.97 (d, J_{CP} = 11.1 Hz, Ph), 131.75 (d, J_{CP} = 2.9 Hz, Ph), 131.61 (d, J_{CP} = 3.0 Hz, Ph), 131.52 (d, J_{CP} = 10.7 Hz, Ph), 131.16 (d, J_{CP} = 3.0 Hz, Ph), 131.06 (d, J_{CP} = 2.9 Hz, Ph), 131.0 (d, J_{CP} = 83.5 Hz, *quat*. Ar), 130.65 (d, J_{CP} = 11.0 Hz, Ph), 128.63 (d, J_{CP} = 12.5 Hz, Ph), 128.54 (d, J_{CP} = 12.5 Hz, Ph), 128.25 (d, J_{CP} = 12.4 Hz, Ph), 127.97 (d, J_{CP} = 12.3 Hz, Ph), 126.13 (d, J_{CP} = 12.6 Hz, Ph), 91.13 (d, J_{CP} = 14.0 Hz, *quat.subst.* Cp), 74.58 (d, J_{CP} = 15.8 Hz, *subst.* Cp), 74.03 (d, J_{CP} = 9.6 Hz, *subst* Cp), 73.62 (d, J_{CP} = 95.5 Hz, *quat.subst.* Cp), 70.56 (s, Cp), 68.44 (d, J_{CP} = 10.5 Hz, *subst.* Cp), 51.00 (d, J_{CP} = 6.2 Hz, CH_2Ar), 46.71 (s, CH_2Cp).

^{31}P NMR (δ (ppm), 162MHz, $CDCl_3$): 41.74 (s, PPh_2), 41.43 (s, PPh_2).

***HRMS (DCI-CH_4)*:** 522.0956 (100%, calcd. for $C_{29}H_{27}FeN_2PS$ [M] 522.0979).

Experimental Procedure and Characterization of Synthesized Compounds of Chapter-4

4-44

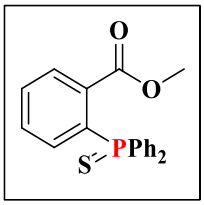

Procedure: In a 250-mL round bottom Schlenk flask under Argon, Cs_2CO_3 (1.90 g, 5.9 mmol) and CuI (10 mol-% wrt diphenyl phosphine) were charged and dissolved in dry toluene (50 mL). The flask was sealed with a rubber septum and then methyl-2-bromobenzoate (1 g, 4.7 mmol), diphenylphosphine (0.72 g, 3.8 mmol) were injected to the turbid solution, consecutively. After replacing the rubber septum with a dry argon flushed reflux condenser, the reaction mixture was refluxed at 110 °C for next 24 h. The mixture was cooled to room temperature. Insoluble residues were filtered through Celite bed. Combined filtrate was concentrated *in vacuo* and degassed dichloromethane (150 ml) followed by solid Sulphur (3-4 eq) was added to it (to protect the free phosphorus from aerial oxidation). The mixture was stirred for 2-3 h under Argon. Then after solvent evaporation the yellow crude was purified by silica gel column chromatography (10% ether-pentane) to obtain pure methyl-2-diphenylthiophosphinobenzoate **4-44** as a white crystalline solid (yield- 0.88g, 73%).

^{1}H NMR (δ (ppm), 400MHz, $CDCl_3$): 7.90-7.83 (1H, m, Ar), 7.83-7.73 (4H, m, Ar), 7.61-7.40 (8H, m, Ar), 7.31-7.23 (vm, Ar), 3.44 (3H, s, C*H*$_3$).

^{13}C{^{1}H} NMR (δ (ppm), 125 MHz, $CDCl_3$): 168.03 (d, J_{CP} = 3.4 Hz, *C*=O), 136.33 (d, J_{CP} = 7.7 Hz, *quat.* Ar (*C*-C=O), 134.01 (d, J_{CP} = 10.5 Hz, Ar), 133.39 (d, J_{CP} = 87.4 Hz, *quat.* Ph), 133.29 (d, J_{CP} = 91.7 Hz, *quat.* Ph), 132.03 (d, J_{CP} = 10.7 Hz, Ph), 131.46 (d, J_{CP} = 2.8 Hz, Ar), 131.45 (d, J_{CP} = 3.0 Hz, Ph), 131.09 (d, J_{CP} = 8.8 Hz, Ar), 130.50 (d, J_{CP} = 11.8 Hz, Ar), 128.41 (d, J_{CP} = 12.8 Hz, Ph), 52.03 (s, O-CH_3).

^{31}P NMR (δ (ppm), 162MHz, $CDCl_3$): 46.16 (s, PPh_2)

HRMS (DCI-CH_4): 353.0758 (100%, calcd. for $C_{20}H_{18}O_2PS$ [$(M+H)^+$] 383.0765)

4-40

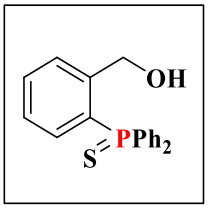

Procedure:1(M) solution of $LiAlH_4$ in THF (1 mL, 1.32 mmol) was added drop wise into the dry THF (7 mL) solution of methyl-2-diphenylthiophosphinobenzoate (0.1g, 0.28 mmol) under argon atmosphere with steady magnetic stirring at 0 °C. The reaction was slowly shifted to room temperature after the complete addition of reducing agent and was monitored by TLC to determine the consumption of the benzoate. When the starting material was consumed completely, the reaction mixture was quenched at 0 ºC with 2(M) HCl and filtered by Teflon cannula. The filtrate after drying *in vacuo* extracted with dichloromethane (3x 25 mL). Combined organic layers were dried over Na_2SO_4, filtered and concentrated. The dry crude was purified by column chromatography on silica gel (20% EtOAc/n-hexane) to afford 2-diphenylthiophosphinobenzylalcohol as white solid (0.11g, 70%).

^{1}H NMR (δ (ppm), 400MHz, $CDCl_3$): 7.80-7.70 (4H, m, Ar), 7.65-7.45 (8H, m, Ar), 7.22 (1H, m, Ph), 6.88 (1H, m, Ph), 4.64 (2H, s, CH_2Ar), 4.03 (1H, br, O*H*).

^{13}C{^{1}H} NMR (δ (ppm), 125 MHz, $CDCl_3$): 145.0 (d, J_{CP} = 9.3 Hz, *quat.* Ar), 132.9 (d, J_{CP} = 11.2 Hz, Ar), 132.66 (d, J_{CP} = 4.5 Hz, Ar), 132.64 (d, J_{CP} = 8.5 Hz, Ar), 132.3 (d, J_{CP} = 10.7 Hz, Ph), 132.13(d, J_{CP} = 83.5 Hz, *quat*. Ar), 132.05(d, J_{CP} = 85.0 Hz, *quat*. Ar), 128.8(d, J_{CP} = 12.8 Hz, Ph), 131.98 (s, Ph), 127.4 (d, J_{CP} = 12.3 Hz, Ar), 63.1 (d, J_{CP} = 6.2 Hz, *C*H_2Ar).

^{31}P NMR (δ (ppm), 162MHz, $CDCl_3$): 41.6 (s, PPh_2)

***HRMS (DCI-CH_4)*:** 325.0813 (100%, calcd. for $C_{19}H_{18}OPS$ [$(M+H)^+$] 325.0816)

4-43

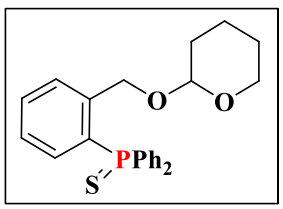

Procedure: Alcohol **4-40** (0.1g, 0.3 mmol) was added with dry DCM, dihydropyran (DHP) (0.025g, 0.3 mmol) and a catalytic amount of *p*-toluenesulphonic acid (0.01g). The reaction mixture was stirred at 0 ^{o}C for 1h. Then the mixture was extracted with saturated aq. $NaHCO_3$-DCM. The combined organic layers were dried over Na_2SO_4, concentrated. The residual crude oil was purified by column chromatography (20% EtOAc-Hexane). The product **4-43** was obtained as a crystalline white solid (0.11g, 92%) for NMR and mass spectrometric characterization.

^{1}H NMR (δ (ppm), 400MHz, $CDCl_3$): 7.85-7.75 (5H, m, Ar), 7.59-7.44 (7H, m, Ar), 7.21 (1H, m, Ar), 6.96 (1H, dd, J=7.9Hz, J_{HP}=14.9Hz Ar), 4.87 (2H, s, CH_2Ar), 4.39 (1H, t, J=3.6Hz, OCHO), 3.64 (1H, m, CH_2O), 3.35 (1H, m, CH_2O), 1.85-1.70 (1H, m, CH_2), 1.65-1.40 (m, 5H, CH_2).

^{13}C{^{1}H} NMR (δ, ppm, 125 MHz, $CDCl_3$): 143.09 (d, J_{CP} = 8.6 Hz, *quat.* Ar (C-CH_2), 132.51 (d, J_{CP} = 11.3 Hz, Ar), 132.51 (d, J_{CP} = 84.3 Hz, *quat.* Ar), 132.47 (d, J_{CP} = 84.3 Hz, *quat.* Ar), 132.36 (d, J_{CP} = 10.7 Hz, Ar), 132.32 (d, J_{CP} = 10.7 Hz, Ar), 131.86 (d, J_{CP} = 2.7 Hz, Ph), 131.59 (d, J_{CP} = 3.2 Hz, Ph), 130.76 (d, J_{CP} = 83.8 Hz, *quat.* Ph), 129.75 (d, J_{CP} = 10.1 Hz, Ph), 128.60 (d, J_{CP} = 12.6 Hz, Ph), 128.52 (d, J_{CP} = 12.6 Hz, Ph), 126.79 (d, J_{CP} = 12.5 Hz, Ph), 98.53 (s, OCHO), 66.74 (d, J_{CP} = 6.1 Hz, Ar*C*H_2O), 62.13 (s, O*C*H_2CH_2), 30.37 (s, CH_2), 25.34 (s, CH_2), 19.44 (s, CH_2).

^{31}P NMR (δ (ppm), 162MHz, $CDCl_3$): 41.42.

HRMS (DCI-CH_4): 437.1690 (25%, calcd. for $C_{26}H_{31}O_2PS$ [$(M+C_2H_5)^+$] 437.1704)

4-46

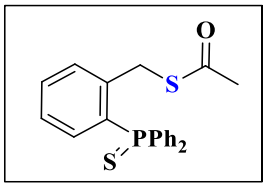

Procedure: A reaction mixture of PPh_3 (2.14g, 8.14 mmol) and diethylazadicarboxylate solution (in toluene) (3.7 mL, 8.14 mmol) in 30 mL dry THF or DCM was prepared and stirred at 0 ^{o}C under argon for 30-40 min. Then into that resulting dark orange solution, another dry THF or DCM solution (20 ml) of 2-diphenylthiophosphinobenzylalcohol **4-41** (1.2g, 3.7 mmol) and thioaceticacid (0.57ml, 8.14 mmol) in was added drop wise. The reaction mixture was stirred at rt for next 16h. Then after solvent evaporation the crude orange oil was purified by silica gel column chromatography with hexane-dichloromethane (1:1) to achieve of pure 2-diphenylthiophosphinobenzylthioacetate **4-47** (0.80g, yield-63%).

^{1}H NMR (δ (ppm), 400MHz, $CDCl_3$): 7.84-7.74 (4H, m, Ph), 7.59-7.44 (8H; m, 6H, Ph + 2H, CH_2Ph), 7.16 (1H, br t, J= 7.5 Hz, CH_2Ph), 7.06 (1H, dd, J = 7.8 Hz, J_{HP} = 14.6 Hz, CH_2Ph), 4.45 (2H, s, C*H*$_2$), 2.29 (3H, s, CH_3).

$^{13}C\{^{1}H\}$ NMR (δ (ppm), 125 MHz, $CDCl_3$): 195.76 (s, CO), 142.90 (d, J_{CP} = 8.5 Hz, *quat.*Ar), 132.55 (d, J_{CP} = 9.2 Hz, Ar), 132.50 (d, J_{CP} =11.5 Hz, Ar), 132.42 (d, J_{CP} = 11.0 Hz, Ph), 132.35 (d, J_{CP} = 3.8 Hz, Ar), 132.15 (d, J_{CP} = 85.1 Hz, *quat.* Ph), 131.84 (d, J_{CP} = 3.1 Hz, Ph), 131.84 (d, J_{CP} = 84.0 Hz, *quat.* Ar), 128.73 (d, J_{CP} = 12.5 Hz, Ph), 126.84 (d, J_{CP} = 12.2 Hz, Ar), 31.43 (d, J_{CP} = 6.5 Hz, CH_2), 30.08 (s, CH_3).

^{31}P NMR (δ (ppm), 162MHz, $CDCl_3$): 41.77 (s, PPh_2)

***HRMS (DCI-CH_4)*:** 383.0701 (100%, calcd. for $C_{21}H_{20}OPS_2$ [$(M+H)^+$] 383.0693)

4-47

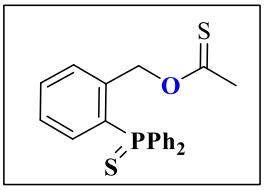

Procedure: 0.15equivalents of (54%) $HBF_4.Et_2O$ (0.03 ml, 0.23 mmol) is added to alcohol **4-40** (0.5g, 1.54 mmol) dissolved in 3ml thioacetic acid, at room temperature. After 30 min the thioacetic acid is removed under vacuum, and the crude is purified by column chromatography on silica gel (Eluent- 20% DCM in Hexane) to obtain the thionoacetate **4-46** (Yield 0.26g, 47%).

^{1}H NMR (δ (ppm), 400MHz, $CDCl_3$): 7.85-7.75 (4H, m, Ph), 7.60-7.45 (8H; m, 6H, Ph + 2H, Ar), 7.29 (1H, m, Ar), 7.06 (1H, dd, J = 7.7 Hz, J_{HP} = 14.7 Hz, CH_2PhH), 5.77 (2H, s, C*H*$_2$), 2.37 (3H, s, CH_3).

$^{13}C\{^{1}H\}$ NMR (δ (ppm), 125 MHz, $CDCl_3$): 218.61 (s, C=S), 139.09 (d, J_{CP} = 8.4 Hz, *quat.* Ar), 132.99 (d, J_{CP} = 10.8 Hz, Ar), 132.43 (d, J_{CP} = 10.7 Hz, Ph), 132.30 (d, J_{CP} = 84.3 Hz, quat. Ar), 132.01 (d, J_{CP} = 84.7 Hz, *quat.* Ph), 131.91 (d, J_{CP} = 2.7 Hz, Ar), 131.83 (d, J_{CP} = 3.1 Hz, Ph), 130.77 (d, J_{CP} = 9.8 Hz, Ar), 128.67 (d, J_{CP} = 12.6 Hz, Ph), 127.89 (d, J_{CP} = 12.2 Hz, Ar), 71.58 (d, J_{CP} = 5.9 Hz, *C*H_2), 33.94 (s, CH_3).

^{31}P NMR (δ (ppm), 162MHz, $CDCl_3$): 41.46 (s, PPh_2)

***HRMS (DCI-CH_4)*:** 383.0702 (27%, calcd. for $C_{21}H_{20}OPS_2$ [$(M+H)^+$] 383.0693)

4-48

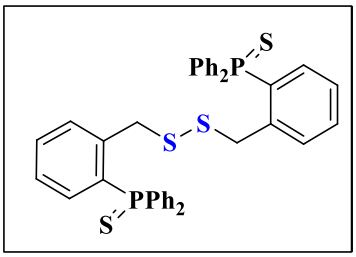

Procedure: 2-diphenylthiophosphinobenzylthioacetate **4-47** (0.12g, 0.314 mmol) was dissolved in 10 ml of degassed methanol and stirred under argon for 20 min. Then solid sodium methoxide (0.05g, 0.941mmol) was added to it. The reaction mixture kept on stirring under argon overnight. After completion of reaction the mixture was quenched with 2(M) HCl and extracted with dichloromethane. Then after drying under Na_2SO_4 followed by solvent evaporation the faint yellow oil was purified by silica gel column chromatography (hexane-dichloromethane- 1:1) as eluant (0.03g, 31%) pure product **4-48** has been achieved after purification.

^{1}H NMR (δ (ppm), 400MHz, $CDCl_3$): 7.75-7.81 (4H, m, Ph), 7.64 (1H, m, Ar), 7.44-7.56 (7H; m, 6H, Ph + 1H, Ar), 7.16 (1H, m, Ar), 6.91 (1H, m, Ar), 4.14 (2H, s, C*H*$_2$).

^{13}C{^{1}H} NMR (δ (ppm), 125 MHz, $CDCl_3$): 142.11 (d, J_{CP} = 8.6 Hz, *quat.* Ar), 132.85 (d, J_{CP} = 11.4 Hz, Ar), 132.67 (d, J_{CP} = 3.0 Hz, Ph), 132.47 (s, Ar), 132.42 (d, J_{CP} = 9.3 Hz, Ph), 132.28 (d, J_{CP} = 75.3 Hz, *quat.* Ph), 131.99 (d, J_{CP} = 12.3 Hz, Ar), 131.78 (d, J_{CP} = 3.1 Hz, Ph), 131.54 (d, J_{CP} = 83.9 Hz, *quat.* Ar), 128.66 (d, J_{CP} = 12.5 Hz, Ph), 126.84 (d, J_{CP} = 12.3 Hz, Ar), 42.52 (d, J_{CP} = 6.1 Hz, *C*H_2).

^{31}P NMR (δ (ppm), 162MHz, $CDCl_3$): 41.69 (s, PPh_2).

***HRMS (DCI-CH_4)*:** 341.0585 (75%, calcd. for $C_{19}H_{17}PS_2$ [(1/2M+H)$^+$] 341.0588).

4-39

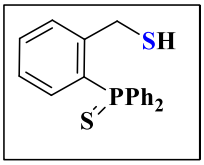

Procedure: Thioacetate **4-47** (0.75g, 1.96 mmol) was dissolved in 10 ml dry THF and cooled to 0 ^{o}C. 1(M) solution of $LiAlH_4$ in THF (2.4 mL, 2.4 mmol) was added drop wise into that. The reaction was slowly shifted to room temperature and was monitored by TLC to determine the consumption of the benzoate. Then, 2(M) Aq. HCl was added to quench the reaction at 0 ^{o}C. The

resulting white suspension was filtered off by Teflon cannula. The filtrate after drying *in vacuo* extracted with dichloromethane (3x 20 mL). Combined organic layers were dried over Na_2SO_4, filtered and concentrated. The dry crude was purified by column chromatography on silica gel (15% Et_2O/n-hexane) to afford 2-diphenylthiophosphinobenzylmercaptan **4-39** as white crystalline solid (0.44g, 71%).

^{1}H NMR (δ (ppm), 400MHz, $CDCl_3$): 7.83-7.78 (4H, m, Ph), 7.62 (1H, m, Ar), 7.60-7.47 (7H, m, 6H, Ph + 1H, Ar), 7.15 (1H, m, Ar), 6.86 (1H, m, Ar), 3.93 (2H, d, J= 8.6 Hz, C*H*$_2$), 2.42 (1H, t, J = 8.6 Hz, SH).

^{13}C{^{1}H} NMR (δ (ppm), 125 MHz, $CDCl_3$): 146.16 (d, J_{CP} = 8.8 Hz, *quat.*Ar), 132.59 (d, J_{CP} = 9.6 Hz, Ar), 132.44 (d, J_{CP} = 11.5 Hz, Ar), 132.37 (d, J_{CP} = 10.6 Hz, Ph), 132.34 (s, Ar), 132.31 (d, J_{CP} = 84.7 Hz, *quat.* Ph), 131.83 (d, J_{CP} = 3.0 Hz, Ph), 131.15 (d, J_{CP} = 85.0 Hz, *quat.* Ar), 128.72 (d, J_{CP} = 12.5 Hz, Ph), 126.47 (d, J_{CP} = 12.3 Hz, Ar), 27.46 (d, J_{CP} = 6.7 Hz, *C*H$_2$).

^{31}P NMR (δ (ppm), 162MHz, $CDCl_3$): 41.50(s, PPh_2)

***HRMS (DCI-CH_4)*:** 341.0585 (75%, calcd. for $C_{19}H_{17}PS_2$ [(1/2M+H)$^+$] 341.0588)

4-38

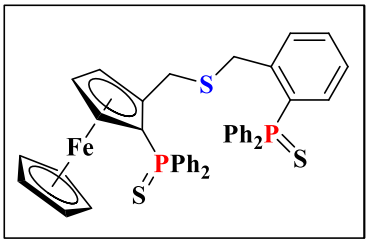

Procedure: In a dry schlenk tube, under argon atmosphere, of racemic **2-29** (100 mg, 0.23 mmol) was dissolved in 2 ml of dry dichloromethane. 54% solution of HBF_4 in ether (0.1 ml, 0.724 mmol) was added and stirred for 1 min. Then a solution of 2-diphenylthiophosphinobenzylmercaptan **4-39** (158 mg, 0.46 mmol) in dry dichloromethane (3 ml) was added rapidly. Immediately after 2 min. of stirring, the resulting dark orange crude solution was filtered on silica gel using ether. The yellow filtrate that came out was evaporated and further purified by column chromatography (30% Et_2O-hexane) to yield pure racemic **4-38** (0.13g, 76%).

^{1}H NMR (δ (ppm), 400MHz, $CDCl_3$): 7.85-7.75 (6H, m, Ph), 7.70-7.55 (2H, m, Ph), 7.55-7.35 (14H, m, 12H, Ph+ 2H, Ar), 7.12 (1H, br t, J=7.6Hz, Ar), 6.87 (1H, dd, J=7.8Hz, J_{HP}=14.8Hz, Ar), 4.45

(1H, m, *subst.* Cp), 4.28 (5H, s, Cp), 4.24 (1H, m, *subst.* Cp), 4.03 (1H, d (AB system), J=14.7Hz, C*H*$_2$Ar), 3.96 (1H, d (AB system), J=13.5Hz, C*H*$_2$Cp), 3.82 (1H, d (AB system), J=14.7Hz, C*H*$_2$Ar), 3.74 (1H, m, subst Cp), 3.51 (1H, d (AB system), J=13.5Hz, C*H*$_2$Cp).

^{13}C{^{1}H} NMR (δ (ppm), 125 MHz, CDCl$_3$): 142.71 (d, J_{CP} = 8.5 Hz, *quat.*Ar), 134.71 (d, J_{CP} = 87.2 Hz, *quat.* Ph), 133.69 (d, J_{CP} = 84.8 Hz, *quat.* Ph), 132.59 (d, J_{CP} = 11.7 Hz, Ar), 132.41 (d, J_{CP} = 84.3 Hz, *quat.* Ar), 132.34 (d, J_{CP} = 84.0 Hz, *quat.* Ar), 132.33 (d, J_{CP} = 10.7 Hz, Ph), 132.12 (d, J_{CP} = 10.7 Hz, Ph), 131.90 (d, J_{CP} = 2.7 Hz, Ar), 131.70 (d, J_{CP} = 3.0 Hz, Ph), 131.62 (d, J_{CP} = 3.0 Hz, Ph), 131.48 (d, J_{CP} = 9.5 Hz, Ar), 131.45 (d, J_{CP} = 85.9 Hz, *quat.*Ar), 131.18 (d, J_{CP} = 3.0 Hz, Ph), 131.12 (d, J_{CP} = 2.9 Hz, Ph), 128.66 (d, J_{CP} = 12.7 Hz, Ph), 128.59 (d, J_{CP} = 12.3 Hz, Ph), 128.11 (d, J_{CP} = 12.4 Hz, Ph), 127.96 (d, J_{CP} = 12.7 Hz, Ph), 126.29 (d, J_{CP} = 12.3 Hz, Ph), 89.62 (d, J_{CP} = 11.8 Hz, *quat.subst.* Cp), 74.46 (d, J_{CP} = 12.7 Hz, *subst.* Cp), 73.96 (d, J_{CP} = 9.3 Hz, Cp), 73.38 (d, J_{CP} = 95.5 Hz, *quat.subst.* Cp), 70.83 (s, Cp), 69.16 (d, J_{CP} = 10.3 Hz,.*subst.* Cp), 35.77 (d, J_{CP} = 6.2 Hz, S*C*H$_2$Ar), 31.13 (s, *C*H$_2$Cp).

^{31}P NMR (δ (ppm), 162MHz, CDCl$_3$): 41.77(s, PPh$_2$), 41.51 (s, PPh$_2$).

HRMS (DCI-CH$_4$): 755.0900 (6%, calcd. for $C_{42}H_{36}P_2S_3Fe$ [$(M+H)^+$] 755.0928)

4-1

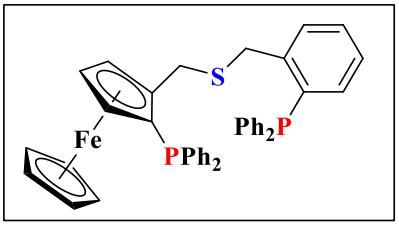

Procedure: In a dry schlenk tube, under Argon atmosphere, (0.1g, 0.19 mmol) of **4-38** was dissolved in 7 mL of dry and degassed toluene. (0.17 ml, 0.93 mmol) degassed tris-(dimethylamino)phosphine [P(NMe$_2$)$_3$] was added to the solution. The reaction mixture was heated to reflux overnight. Then after cooling to room temperature, the solvent was evaporated *in vacuum*. Orange crude obtained was purified by flash column chromatography under argon using degassed eluent (5 % Et$_2$O-pentane) to obtain pure racemic **4-1** (0.07g, 77%) as yellow solid.

^{1}H NMR (δ (ppm), 400MHz, CDCl$_3$): 7.57 (2H, m, Ph), 7.40-7.13 (21H, m, 18H, Ph+ 3H, Ar), 6.92 (1H, m, Ar), 4.40 (1H, m, *subst*. Cp), 4.25 (1H, t, J=2.4Hz, *subst*. Cp), 4.00 (1H, d (ABX system), J=13.5Hz, J_{HP}=2Hz, C*H*$_2$Ar), 3.97 (s, 5H, Cp), 3.85 (1H, d, AB system, J=13.5Hz,

C*H*$_2$Ar), 3.77 (1H, m, *subst*. Cp), 3.68 (1H, d, AB system, J=13.3Hz, C*H*$_2$Cp), 3.64 (1H, d, AB system), J=13.3Hz, J_{HP}=1.8Hz, C*H*$_2$Cp).

^{13}C{^{1}H} NMR (δ (ppm), 125MHz, CDCl$_3$): 142.96 (d, J_{CP} = 25.2 Hz, *quat.* Ph), 139.88 (d, J_{CP} = 9.2 Hz, *quat.* Ph), 137.71 (d, J_{CP} = 10.7 Hz, *quat.* Ph), 136.90 (d, J_{CP} = 11.7 Hz, *quat.* Ph), 136.86 (d, J_{CP} = 10.4 Hz, *quat.* Ph), 136.07 (d, J_{CP} = 13.4 Hz, *quat.* Ph), 135.11 (d, J_{CP} = 21 Hz, Ph), 134.01 (s, Ph), 133.91 (d, J_{CP} = 19.9 Hz, Ph), 133.71 (d, J_{CP} = 19.8 Hz, Ph), 132.40 (d, J_{CP} = 17.7 Hz, Ph), 129.53 (d, J_{CP} = 5.1 Hz, Ph), 129.06 (s, Ph), 128.62 (d, J_{CP} = 8.6 Hz, Ph), 128.48 (d, J_{CP} = 12.4 Hz, Ph), 128.11 (d, J_{CP} = 12.7 Hz, Ph), 127.93 (d, J_{CP} = 12.3 Hz, Ph), 127.70 (s, Ph), 127.14 (s, Ph), 90.74 (d, J_{CP} = 25.5 Hz, *quat.* Cp), 75.62 (d, J_{CP} = 8.1Hz, *quat.* Cp), 71.58 (d, J_{CP} = 3.4 Hz, CH subst. Cp), 71.25 (d, J_{CP} = 3.8 Hz, *subst.* Cp), 69.77 (s, Cp), 69.33 (s, *subst.* Cp), 35.94 (d, J_{CP} = 25.4 Hz, S*C*H$_2$Ar), 31.25 (d, J_{CP} = 11.6 Hz *C*H$_2$Cp).

^{31}P NMR (δ (ppm), 162MHz, CDCl$_3$): -16.6 (s, PPh$_2$), -23.8 (s, PPh$_2$).

4-52

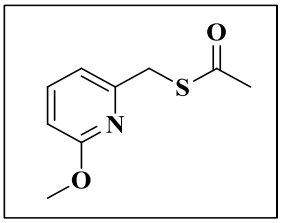

Procedure: A reaction mixture of PPh_3 (2.4g, 9.4 mmol) and diethylazadicarboxylate solution (in toluene) (4.3 mL, 8.14 mmol) in 15 mL dry THF was prepared and stirred at 0 ^oC under argon for 30-40 min. Then into that resulting dark orange solution, another dry THF solution (10 ml) of 6-methoxy-2-pyridinemethanol **2-46** (0.6g, 4.3 mmol) and thioaceticacid (0.65ml, 9.4 mmol) in was added drop wise. The reaction mixture was stirred at rt for next 16h. Then after solvent evaporation the crude orange oil was purified by silica gel column chromatography with hexane-dichloromethane (1:1) to achieve pure 6-methoxy-2-pyridinemethylthioacetate **4-52** (0.59g, 70%).

^{1}H NMR (δ (ppm), 400MHz, CDCl$_3$): 7.48 (1H, t, J = 7.15 Hz, Py), 6.89 (1H; d, J = 7.15 Hz, Py), 6.60 (1H, d, J = 8.29 Hz, Py), 4.17 (2H, s, C*H*$_2$), 3.91 (3H, s, OCH_3), 2.36 (3H, s, CH_3).

^{13}C NMR (δ (ppm), 125MHz, CDCl$_3$): 195.05 (s, CO), 163.74 (s, *quat.*Py), 154.70 (s, *quat.*Py), 139.06 (s, Py), 115.48 (s, Py), 109.13 (s, Py), 53.31 (s, O<u>C</u>H$_3$); 35.25 (s, CH_2Py), 30.22 (s, CH_3).

HRMS (DCI-CH$_4$): 198.0600 (100%, calcd. for $C_9H_{12}NO_2S$ [$(M+H)^+$] 198.0589)

4-53

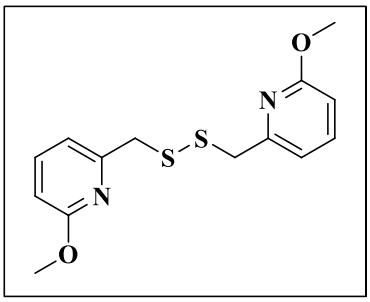

Procedure: **4-52** (0.1g, 0.51 mmol) was dissolved in 10 ml dry THF at inert atmosphere. 1(M) $LiAlH_4$ solution (suspended) in THF (0.36ml, 0.36 mmol) was drop wise added at 0 ^oC. After the addition the reaction mixture was slowly brought back to rt and stirred for 30 min. Reaction was quenched by degassed 2(M) HCl and followed by addition of sat. $NaHCO_3$ (up to pH= 8). Then after a cannula filtration, the filtrate obtained was evaporated to dryness, extracted with water-DCM (2x 20 mL) and dried over Na_2SO_4. Combined organic layers after further solvent evaporation gives colorless oily crude which was purified by column chromatography (10% DCM-Hexane). The pure disulphide **4-53** was obtained in moderate yield (0.056g, 56%).

^{1}H NMR (δ (ppm), 400MHz, $CDCl_3$): 7.52 (t, 2H, J= 7.7 Hz), 6.82 (2H; d, J = 7.2 Hz, Py), 6.65 (2H; d, J = 7.5 Hz, Py), 3.95 (6H, s, O-CH_3), 3.80 (4H, s, CH_2).

$^{13}C\{^1H\}$ NMR (δ (ppm), 125 MHz, $CDCl_3$): 163.54 (s, *quat.*Py), 154.79 (s, *quat.*Py), 138.77 (s, Py), 116.18 (s, Py), 109.30 (s, Py), 53.37 (s, O$\underline{C}H_3$); 45.29 (s, CH_2Py).

HRMS (DCI-CH_4): 309.0728 (100%, calcd. for $C_{14}H_{17}N_2O_2S_2$ [$(M+H)^+$] 309.0731)

4-54

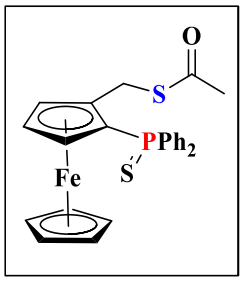

Procedure: Followed same as **4-38.** Stoichiometry of starting material, corresponding reagents and yield of product as follows-

2-29- 0.5g, 1.16 mmol

(54%) HBF_4 in Et_2O - 0.5 ml, 3.5 mmol Yield of racemic **4-54**- 0.44g, 79%

Thioacetic Acid- 0.45 ml, 6 mmol

^{1}H NMR (δ (ppm), 400MHz, $CDCl_3$): 7.86-7.79 (2H, m, Ph), 7.67-7.60 (2H, m, Ph), 7.60-7.38 (6H, m, Ph), 4.63 (1H, m, *subst*. Cp), 4.53 (1H, d(AB system), J= 14.1 Hz, C$\underline{H_2}$Cp), 4.36 (5H, s, Cp), 4.34 (1H, d(AB system), J= 14.0 Hz, C$\underline{H_2}$Cp), 4.30 (1H, m, *subst*. Cp), 3.76 (1H, m, *subst.* Cp), 2.20 (s, 3H, s, $\underline{CH_3}$).

^{13}C{^{1}H} NMR (δ (ppm), 125 MHz, $CDCl_3$): 195.64 (s, CO), 134.52 (d, J_{CP} = 86.7 Hz, *quat.* Ph), 133.28 (d, J_{CP} = 86.5 Hz, *quat.* Ph), 132.11 (d, J_{CP} = 8.4 Hz, Ph), 132.03 (d, J_{CP} = 10.7 Hz, Ph), 131.33 (d, J_{CP} = 3.0 Hz, Ph), 128.24 (d, J_{CP} = 12.4 Hz, Ph), 128.06 (d, J_{CP} = 12.3 Hz, Ph), 89.09 (d, J_{CP} = 12.2 Hz, *quat.subst.* Cp), 74.43 (d, J_{CP} = 12.3 Hz, *subst.* Cp), 74.17 (d, J_{CP} = 94.6 Hz, *quat.subst.* Cp), 73.98 (d, J_{CP} = 9.2 Hz, *subst.* Cp), 70.94 (s, Cp), 69.36 (d, J_{CP} = 10.1 Hz, *subst.* Cp), 30.23 (s, *C*H_3).

^{31}P NMR (δ (ppm), 162MHz, $CDCl_3$): 41.23 (s, PPh_2)

***HRMS (DCI-CH_4)*:** 491.0344 (100%, calcd. for $C_{25}H_{24}FeOPS_2$ $[(M+H)^+]$ 491.0322)

4-51

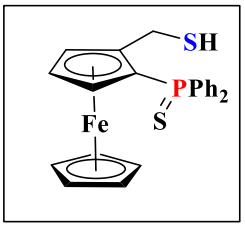

Procedure: 1(M) solution of $LiAlH_4$ in THF (1.2 mL, 1.22 mmol) was added drop wise into the dry THF (7 mL) solution of **4-54** (0.5g, 0.28 mmol) under argon atmosphere with steady magnetic stirring at 0 °C. The reaction mixture was refluxed at 80 °C for 30 min. Then it was again shifted to 0 °C and was quenched with degassed 2(M) HCl, resulting an orange suspension. The suspension was filtered off by Teflon cannula and dried over Na_2SO_4. The filtrate after removing Na_2SO_4 was concentrated *in vacuo* and was purified by column chromatography on silica gel (10% Et_2O/n-hexane). Monomeric **4-51** (yield- 0.08g, 19%) and disulphide **4-55** are collected as successive fractions for characterization.

^{1}H NMR (δ (ppm), 400MHz, $CDCl_3$): 7.90-7.80 (2H, m, Ph), 7.75-7.65 (2H, m, Ph), 7.60-7.37 (6H, m, Ph), 4.61 (1H, m, *subst*. Cp), 4.38- 4.31 (2H, m, 1H *subst.* Cp + 1H C$\underline{H_2}$Cp), 4.33 (5H, s, Cp), 3.79 (1H, m, *subst.* Cp), 3.67 (dd, J = 14.2 Hz, J = 8.5 Hz, C$\underline{H_2}$Cp), 1.57 (t, J = 8.5 Hz, SH).

$^{13}C\{^1H\}$ NMR (δ (ppm), 125 MHz, $CDCl_3$): 134.60 (d, J_{CP} = 86.7 Hz, *quat.* Ph), 133.27 (d, J_{CP} = 86.2 Hz, *quat.* Ph), 132.16 (d, J_{CP} = 10.8 Hz, Ph), 132.05 (d, J_{CP} = 11.1 Hz, Ph), 131.42 (d, J_{CP} = 3.1 Hz, Ph), 131.36 (d, J_{CP} = 3.0 Hz, Ph), 128.34 (d, J_{CP} = 12.6 Hz, Ph), 128.08 (d, J_{CP} = 12.3 Hz, Ph), 92.93 (d, J_{CP} = 12.1 Hz, *quat.subst.* Cp), 74.52 (d, J_{CP} = 12.3 Hz, *subst.* Cp), 73.49 (d, J_{CP} = 95.1 Hz, *quat.subst.* Cp), 73.20 (d, J_{CP} = 9.4 Hz, *subst.* Cp), 70.82 (s, Cp), 69.20 (d, J_{CP} = 10.3 Hz, *subst.* Cp), 22.82 (s, CH_2Cp).

^{31}P NMR (δ (ppm), 162MHz, $CDCl_3$): 41.08 (s, PPh_2)

HRMS (DCI-CH_4): 448.0151 (100%, calcd. for $C_{23}H_{21}FePS_2$ [M^+] 448.0172)

4-55

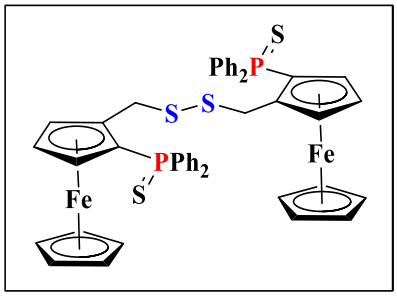

Yield of diastereomeric mixture of **4-55-** 0.14g, 31%

Yield of (R,R)- **4-55-** 0.12g, 26%

Chiral diastereoisomer (R,R)

^1H NMR (δ (ppm), 400MHz, $CDCl_3$): 7.90-7.75 (2H, m, Ph), 7.65-7.30 (8H, m, Ph), 4.54 (1H, m, *subst.* Cp), 4.48 (1H, d (AB system), J = 13.1Hz, C$\underline{H}_2$Cp), 4.34 (5H, s, *subst.* Cp), 4.25 (1H, m, *subst.* Cp), 3.87 (1H, d (AB system), J = 13.1Hz, C$\underline{H}_2$Cp), 3.75 (1H, m, *subst.* Cp).

$^{13}C\{^1H\}$ NMR (δ (ppm), 125 MHz, $CDCl_3$): 134.74 (d, J_{CP}=87.4Hz , *quat*. Ph), 133.57 (d, J_{CP}=85.9Hz , *quat*. Ph), 132.18 (d, J_{CP}=10.7Hz, Ph), 132.13 (d, J_{CP}=10.8Hz, Ph), 131.26 (d, J_{CP}=2.6Hz, Ph), 131.14 (d, J_{CP}=2.6Hz, Ph), 128.13 (d, J_{CP}=13.0Hz, Ph), 128.00 (d, J_{CP}=12.9Hz, Ph), 88.53 (d, J_{CP}=11.9Hz, *quat*. Cp), 74.56 (d, J_{CP}=12.7Hz, *subst*. Cp), 74.33 (d, J_{CP}=9.2Hz, *subst*. Cp), 73.19 (d, J_{CP}=95.1Hz, *quat*. Cp), 70.89 (s, Cp), 69.51 (d, J_{CP}=10.5Hz, *subst*. Cp). 33.57 (s, CH_2).

^{31}P NMR (δ (ppm), 162MHz, $CDCl_3$): 41.35 (s, PPh_2).

Meso diastereoisomer (R,S)

^{1}H NMR (δ (ppm), 400MHz, $CDCl_3$): 7.90-7.75 (2H, m, Ph), 7.65-7.30 (8H, m, Ph), 4.71 (1H, m, *subst.* Cp), 4.33 (s, 5H, *subst.* Cp), 4.31-4.24 (2H, m, 1H *subst.* Cp + 1H C$\underline{H}_2$), 3.87 (1H, d (AB system), J = 13.1Hz, C$\underline{H}_2$Cp), 3.76 (1H, m, *subst.* Cp).

^{13}C{^{1}H} NMR (δ (ppm), 125 MHz, $CDCl_3$): 134.43 (d, J_{CP}=87.0Hz , *quat*. Ph), 133.46 (d, J_{CP}=85.9Hz, *quat*. Ph), 132.15 (d, J_{CP}=10.7Hz, Ph), 132.08 (d, J_{CP}=10.7Hz, Ph), 131.32 (d, J_{CP}=3Hz, Ph), 131.28 (d, J_{CP}=3Hz, Ph), 128.26 (d, J_{CP}=12.7Hz, Ph), 128.03 (d, J_{CP}=12.6Hz, Ph), 88.43 (d, J_{CP}=11.9Hz, *quat*. Cp), 74.68 (d, J_{CP}=12.5Hz, *subst*. Cp), 74.15 (d, J_{CP}=9.2Hz, *subst.* Cp), 73.87 (d, J_{CP}=95.1Hz, *quat*. Cp), 70.92 (s, Cp), 69.46 (d, J_{CP}=10.4Hz, *subst*. Cp), 37.70 (s, CH_2).

^{31}P NMR (δ (ppm), 162MHz, $CDCl_3$): 41.29 (s, PPh_2)..

HRMS (DCI-CH_4): 917.0087 (100%, calcd. for $C_{46}H_{40}Fe_2P_2S_4Na$ [$(M+Na)^+$] 917.01)

4-49a

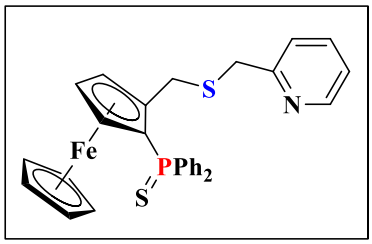

Procedure: 1(M) solution of $LiAlH_4$ in THF (0.66 ml, 1.22 mmol) was added drop wise into the dry THF (5 mL) solution of **4-54** (0.27g, 0.55 mmol) under argon atmosphere with steady magnetic stirring at 0 °C. The reaction mixture was refluxed at 80 ^{o}C for 30 min. Then it was again shifted to 0 ^{o}C and was quenched with degassed 2(M) aq. NaOH up to pH= 11=12, resulting an orange suspension. The suspension was further stirred with Na_2SO_4 for 15 min and then filtered off by Teflon cannula. The orange filtrate was then again shifted to 0 ^{o}C, NaH (0.6g, 2.5 mmol) and 2 pyridinemethyltosylate (0.3g, 1.1 mmol) were added, successively. The reaction mixture was stirred at rt monitoring by TLC to detect the complete consumption of newly formed **4-51** species. When, it is completely consumed NEt_3 (2 ml) was added to quench the excess tosylate and stirred 1 hr at rt. Then, the mixture was concentrated *in vacuo* and extracted with water-DCM. The combined organic layer was further dried over Na_2SO_4 and concentrated. The crude residue was purified by column

chromatography on silica gel (20% Et_2O/n-hexane) to afford racemic **4-49a** (0.19 g, yield- 62%) as an orange solid.

^{1}H NMR (δ (ppm), 400MHz, $CDCl_3$): 8.52 (1H, d, J= 4.7 Hz, Py), 7.83 (2H, m, Ph), 7.68 (2H, m, Ph), 7.6-7.45 (4H, m, Ph), 7.12 (1H, td, J= 7.7 Hz, J= 1.9 Hz, Py); 7.55 (6H, m, Ph); 7.24 (1H, d, J= 7.7Hz, Py); 7.14 (1H, m, Py); 4.60 (1H, m, *subst*. Cp), 4.32-4.29 (1H, m, *subst*. Cp), 4.30 (5H, s, Cp); 4.16 (1H, d(AB system), J=13.6Hz, CH_2Cp), 3.79 (1H, m, *subst*. Cp), 3.78 (1H, d(AB system), J=13.6Hz, CH_2Cp), 3.71 (1H, d(AB system), J=13.8Hz, CH_2Py), 3.65 (1H, d(AB system), J=13.8Hz, CH_2Py).

^{13}C{^{1}H} NMR (δ (ppm), 125 MHz, $CDCl_3$): 158.80 (s, *quat.* Py), 149.12 (s, Py), 136.59 (s, Py), 134.68 (d, J=87.3Hz, *quat*. Ph), 133.58 (d, J=85.9Hz, *quat.* Ph), 132.12 (d, J=10.8Hz, Ph), 132.09 (d, J=10.7Hz, Ph), 131.24 (d, J=3.1 Hz, Ph), 131.09 (d, J=3.0 Hz, Ph), 128.71 (d, J=11.8Hz, Ph), 127.99 (d, J=11.8 Hz, Ph), 123.06 (s, Py), 121.76 (s, Py), 89.49 (d, J=11.9Hz, *quat.* Cp), 74.63 (d, J=95.2 Hz, *quat.* Cp), 74.55 (d, J=12.6Hz, 2 C *subst.* Cp), 71.91 (d, J=9.2 Hz, *subst.* Cp), 70.89 (s, Cp), 69.14 (d, J=10.4Hz, *subst.* Cp), 38.60 (s, CH_2Py), 30.03 (s, CH_2Cp).

^{31}P NMR (δ (ppm), 162MHz, $CDCl_3$): 41.50 (s, PPh_2).

HRMS (DCI-CH_4): 540.0688 (100%, calcd. for $C_{29}H_{27}NPS_2Fe$ [$(M+H)^+$] 540.0672)

4-49b

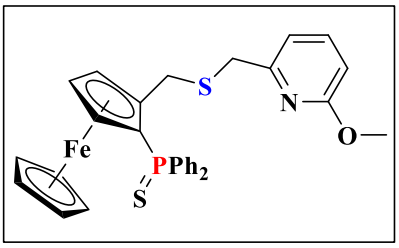

Procedure: Followed same as **4-49a.** Stoichiometry of starting material, corresponding reagents and yield of product as follows-

4-54- 0.3g, 0.61 mmol

1(M) $LiAlH_4$ in THF- 0.75 ml, 0.73 mmol

NaH- 0.72g, 3 mmol

2-43b- 0.27g, 0.92 mmol

Yield of racemic **4-49b-** 0.2g, 67%

^{1}H NMR (δ (ppm), 400MHz, $CDCl_3$): 7.90-7.77 (2H, m, PPh_2), 7.74-7.64 (2H, m, PPh_2), 7.60-7.35 (7H, m, 6H, PPh_2 + 1H, Py), 6.78 (1H, d, J = 7.25 Hz, , Py), 6.60 (1H, d, J = 8.3 Hz, Py), 4.66 (m, 1H, *subst*. Cp), 4.40- 4.30 (6H, m, 5H, Cp {4.32 ppm} + 1H, *subst*. Cp), 4.15 (1H, d(AB system), J = 13.7 Hz, C$\underline{H}_2$Cp), 3.94 (1H, d(AB system), J = 13.7 Hz, C$\underline{H}_2$Cp), 3.92 (3H, s, O-C$\underline{H}_3$), 3.82 (1H, d(AB system), J = 154 Hz, C$\underline{H}_2$Cp), 3.78 (1H, d(AB system), J = 15.4 Hz, C$\underline{H}_2$Cp), 3.80 (1H, m, *subst.* Cp), 3.61 (1H, d(AB system), J = 13.8 Hz, C$\underline{H}_2$Py), 3.55 (1H, d(AB system), J = 13.8 Hz, C$\underline{H}_2$Py).

^{13}C{^{1}H} NMR (δ (ppm), 125 MHz, $CDCl_3$): 163.53 (s, *quat.* Py {$\underline{C}$-OMe}), 156.84 (s, *quat.* Py), 139.0 (s, Py), 134.63 (d, J_{CP} = 87.3 Hz, *quat.* Ph), 133.63 (d, J_{CP} = 86.1 Hz, *quat.* Ph), 132.13 (d, J_{CP} = 10.8 Hz, 2C, Ph), 132.10 (d, J_{CP} = 10.8 Hz, 2C, Ph), 131.25 (d, J_{CP} = 2.9 Hz, Ph), 131.18 (d, J_{CP} = 3.0 Hz, Ph), 128.11 (d, J_{CP} = 12.7 Hz, 2C, Ph), 128.01 (d, J = 12.2 Hz, 2C, Ph), 115.35 (s, Py), 108.57 (s, Py), 89.72 (d, J = 11.9 Hz, *quat.* Cp), 74.59 (d, J = 12.5 Hz, *subst.* Cp), 73.78 (d, J = 9.3 Hz, *subst.* Cp), 73.76 (d, J = 95.1 Hz, *quat.* Cp), 70.88 (s, Cp), 69.07 (d, J = 10.4 Hz, *subst.* Cp), 53.36 (s, O-$\underline{C}H_3$), 37.95 (s, $\underline{C}H_2$Py), 30.05 (s, $\underline{C}H_2$Cp).

^{31}P NMR (δ (ppm), 162MHz, $CDCl_3$): 41.57 (s, PPh_2).

HRMS (DCI-CH_4): 570.0752 (100%, calcd. for $C_{30}H_{29}NOPS_2Fe$ $[(M+H)^+]$ 570.0744)

4-56

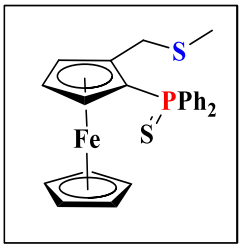

Procedure: Followed same as **4-49a.** Stoichiometry of starting material, corresponding reagents and yield of product as follows-

4-56- 0.11g, 0.22 mmol

1(M) $LiAlH_4$ in THF - 0.27 ml, 0.27 mmol

NaH- 0.36g, 1.5 mmol

Iodomethane (CH_3I)- 0.5 ml (excess)

Yield of racemic **4-56-** 0.06g, 59%

^{1}H NMR (δ (ppm), 400MHz, $CDCl_3$): 7.83 (2H, m, Ph), 7.68 (2H, m, Ph), 7.56-7.35 (6H, m, Ph), 7.60-7.37 (6H, m, Ph), 4.62 (1H, m, *subst.* Cp), 4.34 (5H, s, Cp), 4.35- 4.32 (1H, m, *subst.* Cp), 4.10 (d, J = 13.6 Hz, C$\underline{H_2}$Cp), 3.81 (1H, m, *subst.* Cp), 3.79 (d, J = 13.6 Hz, C$\underline{H_2}$Cp), 1.93 (3H, s, C$\underline{H_3}$).

^{13}C{^{1}H} NMR (δ (ppm), 125 MHz, $CDCl_3$): 134.64 (d, J_{CP} = 87.0 Hz, *quat.* Ph), 133.58 (d, J_{CP} = 85.9 Hz, *quat.* Ph), 132.12 (d, J_{CP} = 10.7 Hz, Ph), 132.02 (d, J_{CP} = 10.0 Hz, Ph), 131.25 (d, J_{CP} = 3.0 Hz, Ph), 131.22 (d, J_{CP} = 2.9 Hz, Ph), 128.11 (d, J_{CP} = 12.2 Hz, Ph), 128.0 (d, J_{CP} = 12.0 Hz, Ph), 89.80 (d, J_{CP} = 12.0 Hz, *quat.subst.* Cp), 74.52 (d, J_{CP} = 12.7 Hz, *subst.* Cp), 73.69 (d, J_{CP} = 95.1 Hz, *quat.subst.* Cp), 73.62 (d, J_{CP} = 9.2 Hz, *subst.* Cp), 70.92 (s, Cp), 68.09 (d, J_{CP} = 10.4 Hz,.*subst.* Cp), 32.51 (s, CH_2Cp), 16.25 (s, CH_3).

^{31}P NMR (δ (ppm), 162MHz, $CDCl_3$): 41.57 (s, PPh_2)

HRMS (DCI-CH_4): 462.00 (100%, calcd. for $C_{24}H_{23}FePS_2$ [M^+] 462.03)

4-57

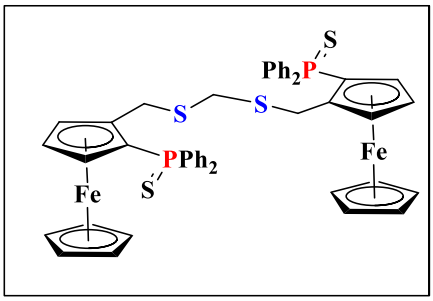

Procedure: Followed same as **4-49a.** Stoichiometry of starting material, corresponding reagents and yield of product as follows-

4-56- 0.17g, 0.34 mmol

1(M) $LiAlH_4$ in THF - 0.41 ml, 0.4 mmol

NaH- 0.76g, 2.1 mmol

Iodomethane (CH_2Cl_2)- 1-2 ml (excess)

Yield of diastereomeric mixture of **4-57-** 0.13g, 43%

Yield of (R,R)- **4-57-** 0.12g, 39%

Chiral diastereoisomer (R,R)

^{1}H NMR (δ (ppm), 400MHz, $CDCl_3$): 7.90-7.75 (4H, m, Ph), 7.70-7.60 (4H, m, Ph), 7.55-7.30 (4H, m, Ph), 4.54 (2H, m, subst. Cp), 4.33 (10H, s, subst. Cp), 4.30 (2H, m, subst. Cp), 4.20 (2H, d (AB system), J= 13.6Hz, C$\underline{H_2}$Cp), 3.90 (2H, d (AB system), J= 13.6Hz, C$\underline{H_2}$Cp), 3.79 (2H, m, subst. Cp), 3.24 (2H, m, SC$\underline{H_2}$S).

$^{13}C\{^{1}H\}$ NMR (δ (ppm), 125 MHz, $CDCl_3$): 134.75 (d, J_{CP}=87.4Hz , *quat.* Ph), 133.63 (d, J_{CP}=86.1Hz, *quat.* Ph), 132.14 (d, J_{CP}=10.7Hz, Ph), 132.02 (d, J_{CP}=10.6Hz, Ph), 131.24 (d, J_{CP}=3.0Hz, Ph), 131.16 (d, J_{CP}=3.0Hz, Ph), 128.07 (d, J_{CP}=12.6Hz, Ph), 127.98 (d, J_{CP}=12.4Hz, Ph), 89.2 (d, J_{CP}=12.0Hz, *quat.* Cp), 74.57 (d, J_{CP}=12.4Hz, subst Cp), 74.03 (d, J_{CP}=9.1Hz, *subst*. Cp), 73.45 (d, J_{CP}=95.5Hz, *quat*. Cp), 70.92 (s, Cp), 69.12 (d, J_{CP}=10.3Hz, *subst*. Cp), 34.90 (s, S<u>C</u>H_2S), 28.46 (s, CH_2Cp).

^{31}P NMR (δ (ppm), 162MHz, $CDCl_3$): 41.48 (s, PPh_2)

Meso diastereoisomer (R,S)

^{1}H NMR (δ (ppm), 400MHz, $CDCl_3$): 7.90-7.75 (4H, m, Ph), 7.70-7.60 (4H, m, Ph), 7.55-7.30 (4H, m, Ph), 4.59 (2H, m, subst. Cp), 4.32 (10H, s, subst. Cp), 4.34-4.29 (2H, m, subst. Cp), 4.19 (2H, d (AB system), J= 13.4Hz, C<u>H</u>$_2$Cp), 3.84 (2H, d (AB system), J= 13.6Hz, C<u>H</u>$_2$Cp), 3.79 (2H, m, subst. Cp), 3.43 (1H, d (AB system), J= 13.6Hz, SC<u>H</u>$_2$S), 3.28 (1H, d (AB system), J= 13.6Hz, SC<u>H</u>$_2$S).

$^{13}C\{^{1}H\}$ NMR (δ (ppm), 125 MHz, $CDCl_3$): 134.71 (d, J_{CP}=86.7Hz , *quat.* Ph), 133.63 (d, J_{CP}=86.0Hz, *quat.* Ph), 132.14 (d, J_{CP}=10.7Hz, Ph), 132.02 (d, J_{CP}=10.6Hz, Ph), 131.24 (d, J_{CP}=3.0Hz, Ph), 131.16 (d, J_{CP}=3.0Hz, Ph), 127.93 (d, J_{CP}=12.8Hz, Ph), 89.18 (d, J_{CP}=11.7Hz, *quat.* Cp), 74.61 (d, J_{CP}=12.6Hz, subst Cp), 74.07 (d, J_{CP}=9.2Hz, *subst*. Cp), 73.69 (d, J_{CP}=93Hz, *quat*. Cp), 70.92 (s, Cp), 69.2 (d, J_{CP}=10.3Hz, *subst*. Cp), 36.336 (s, S<u>C</u>H_2S), 29.32 (s, CH_2Cp).

^{31}P NMR (δ (ppm), 162MHz, $CDCl_3$): 41.48 (s, PPh_2)

HRMS (DCI-CH_4): 909.0413 (100%, calcd. for $C_{47}H_{43}Fe_2P_2S_4$ $[(M+H)^+]$ 909.0422)

References

References

1. a) J. R. Ludwig, J. R. ; Schindler, C. S. ; *Chem*, 2017, **2**, 313-316; b) Wei, D. and Darcel, C., *Chem. Rev.*, 2019, **119**, 2550-2610; c) Bauer, I. and Knölker, H.-J., *Chem. Rev.*, 2015, **115**, 3170-3387; d) Bolm, C. ; Legros, J. ; Le Paih, J. and Zani, L., *Chem. Rev.*, 2004, **104**, 6217-6254.
2. a) Kallmeier, F. and Kempe, R., *Angew. Chem. Int. Ed.*, 2018, **57**, 46-60; b) Valyaev, D. A. ; Lavigne, G. and Lugan, N., *Coord. Chem. Rev.*, 2016, **308**, 191-235; c) Liu, W. and Ackermann, L., *ACS. Catal.*, 2016, **6**, 3743-3752.
3. a) Alig, L. ; Fritz, M. and Schneider, S., *Chem. Rev.*, 2019, **119**, 2681-2751; b) Pototschnig, G. ; Maulide, N. and Schnürch, M., *Chemistry – A European Journal*, 2017, **23**, 9206-9232; c) Ackermann, L., *J. Org. Chem.*, 2014, **79**, 8948-8954.
4. Tasker, S. Z. ; Standley, E. A. and Jamison, T. F., *Nature*, 2014, **509**, 299-309.
5. a) Wu, L. ; Moteki, T. ; Gokhale, Amit A. ; Flaherty, David W. and Toste, F. D., *Chem*, 2016, **1**, 32-58; b) Sun, D. ; Sato, S. ; Ueda, W. ; Primo, A. ; Garcia, H. and Corma, A., *Green Chemistry*, 2016, **18**, 2579-2597.
6. a) Risi, C. ; Calamante, M. ; Cini, E. ; Faltoni, V. ; Petricci, E. ; Rosati, F. and Taddei, M., *Green Chemistry*, 2020, **22**, 327-331; b) Wang, Q. ; Wu, K. and Yu, Z., *Organometallics*, 2016, **35**, 1251-1256.
7. a) Alonso, F. ; Foubelo, F. ; González-Gómez, J. C. ; Martínez, R. ; Ramón, D. J. ; Riente, P. and Yus, M., *Mol. Divers.*, 2010, **14**, 411-424; b) Huang, F. ; Liu, Z. and Yu, Z., *Angew. Chem. Int. Ed.*, 2016, **55**, 862-875.
8. a) Suzuki, T., *Chem. Rev.*, 2011, **111**, 1825-1845; b) Sheldon, R. A. ; Arends, I. W. C. E. ; ten Brink, G.-J. and Dijksman, A., *Acc. Chem. Res.*, 2002, **35**, 774-781.
9. a) Carlini, C. ; Macinai, A. ; Marchionna, M. ; Noviello, M. ; Galletti, A. M. R. and Sbrana, G., *J. Mol. Catal. A: Chem.*, 2003, **206**, 409-418; b) Carlini, C. ; Di Girolamo, M. ; Macinai, A. ; Marchionna, M. ; Noviello, M. ; Raspolli Galletti, A. M. and Sbrana, G., *J. Mol. Catal. A: Chem.*, 2003, **200**, 137-146; c) Carlini, C. ; Girolamo, M. D. ; Marchionna, M. ; Noviello, M. ; Galletti, A. M. R. and Sbrana, G., *J. Mol. Catal. A: Chem.*, 2002, **184**, 273-280.
10. a) Ogawa, S. and Obora, Y., *Chem. Commun.*, 2014, **50**, 2491-2493; b) Chan, L. K. M. ; Poole, D. L. ; Shen, D. ; Healy, M. P. and Donohoe, T. J., *Angew. Chem. Int. Ed.*, 2014, **53**, 761-765; c) Yamamoto, N. ; Obora, Y. and Ishii, Y., *J. Org. Chem.*, 2011, **76**, 2937-2941; d) Moran, J. ; Preetz, A. ; Mesch, R. A. and Krische, M. J., *Nat. Chem.*, 2011, **3**, 287.
11. Lawrence, S. A., *Amines: synthesis, properties and applications*, Cambridge University Press, 2005.
12. Salvatore, R. N. ; Yoon, C. H. and Jung, K. W., *Tetrahedron*, 2001, **57**, 7785-7812.
13. a) Hughes, G. ; Devine, P. N. ; Naber, J. R. ; O'Shea, P. D. ; Foster, B. S. ; McKay, D. J. and Volante, R. P., *Angew. Chem. Int. Ed.*, 2007, **46**, 1839-1842; b) Brunet, J.-J. ; Chu, N.-C. and Rodriguez-Zubiri, M., *Eur. J. Inorg. Chem.*, 2007, **2007**, 4711-4722; c) Kwong, F. Y. and Buchwald, S. L., *Org. Lett.*, 2003, **5**, 793-796; d) Old, D. W. ; Wolfe, J. P. and Buchwald, S. L., *J. Am. Chem. Soc.*, 1998, **120**, 9722-9723.
14. Magano, J. and Dunetz, J. R., *Chem. Rev.*, 2011, **111**, 2177-2250.
15. Nugent, T. C. and El-Shazly, M., *Adv. Synth. Catal.*, 2010, **352**, 753-819.
16. a) Goudriaan, P. E. ; van Leeuwen, P. W. N. M. ; Birkholz, M.-N. and Reek, J. N. H., *Eur. J. Inorg. Chem.*, 2008, **2008**, 2939-2958; b) Blaser, H.-U. ; Malan, C. ; Pugin, B. ; Spindler, F. ; Steiner, H. and Studer, M., *Adv. Synth. Catal.*, 2003, **345**, 103-151; c) Tolman, C. A., *Chem. Rev.*, 1977, **77**, 313-348; d) Tang, W. and Zhang, X., *Chem. Rev.*, 2003, **103**, 3029-3070.
17. Rideal, E. K., *Biorg. Mem. R. Soc.*, 1942, **4**, 63-66.
18. a) Sedgwick, D. M. and Hammond, G. B., *J. Fluorine Chem.*, 2018, **207**, 45-58; b) Taylor, H., *J. Am. Chem. Soc.*, 1944, **66**, 1615-1617.
19. Clapham, S. E. ; Hadzovic, A. and Morris, R. H., *Coord. Chem. Rev.*, 2004, **248**, 2201-2237.
20. a) Ikariya, T. and Blacker, A. J., *Acc. Chem. Res.*, 2007, **40**, 1300-1308; b) Mestroni, G. ; Gladiali, S. and Zassinovich, G., *Chem. Rev.*, 1992, **92**, 1051-1069.
21. Samec, J. S. M. ; Bäckvall, J.-E. ; Andersson, P. G. and Brandt, P., *Chem. Soc. Rev.*, 2006, **35**, 237-248.
22. de Graauw, C. F. ; Peters, J. A. ; van Bekkum, H. and Huskens, J., *Synthesis*, 1994, **1994**, 1007-1017.
23. Oppenauer, R. V., *Recl. Trav. Chim. Pays-Bas*, 1937, **56**, 137-144.
24. a) Ooi, T. ; Miura, T. and Maruoka, K., *Angew. Chem. Int. Ed.*, 1998, **37**, 2347-2349; b) Ponndorf, W., *Angew. Chem.*,, 1926, **39**; c) Verley, A., *Bull. Soc. Chim. Fr.*, 1925, **37**, 537; d) Meerwein, H. and Schmidt, R., *Justus Liebigs Ann Chem*, 1925, **444**, 221-238.
25. Bäckvall, J.-E., *J. Organomet. Chem.*, 2002, **652**, 105-111.
26. Gladiali, S. and Alberico, E., *Chem. Soc. Rev.*, 2006, **35**, 226-236.

27. Osborn, J. A. ; Jardine, F. H. ; Young, J. F. and Wilkinson, G., *J, Chem, Soc. Inorg, Phys. Theor*, 1966, 1711-1732.
28. Knowles, W. S. and Sabacky, M. J., *Chem. Commun. Lond.*, 1968, 1445-1446.
29. a) Kagan, H. B. ; Langlois, N. and Phat Dang, T., *J. Organomet. Chem.*, 1975, **90**, 353-365; b) Kagan, H. B. and Dang, T.-P., *J. Am. Chem. Soc.*, 1972, **94**, 6429-6433; c) Dang, T. P. and Kagan, H. B., *J. Chem. Soc. Chem. Commun.*, 1971, 481-481.
30. a) Knowles, W. S., *Acc. Chem. Res.*, 1983, **16**, 106-112; b) Vineyard, B. D. ; Knowles, W. S. ; Sabacky, M. J. ; Bachman, G. L. and Weinkauff, D. J., *J. Am. Chem. Soc.*, 1977, **99**, 5946-5952. c) Knowles, W.S. (2003). Asymmetric Hydrogenations – The Monsanto L-Dopa Process. In Asymmetric Catalysis on Industrial Scale (eds H.-U. Blaser and E. Schmidt).
31. a) Burk, M. J., *Acc. Chem. Res.*, 2000, **33**, 363-372; b) Burk, M. J. and Harlow, R. L., *Angew. Chem. Int. Ed.*, 1990, **29**, 1462-1464; c) Burk, M. J. ; Feaster, J. E. and Harlow, R. L., *Organometallics*, 1990, **9**, 2653-2655.
32. a) Noyori, R., *Tetrahedron*, 1994, **50**, 4259-4292; b) Noyori, R. and Takaya, H., *Acc. Chem. Res.*, 1990, **23**, 345-350; c) Noyori, R., *Science*, 1990, **248**, 1194; d) Noyori, R., *Chem. Soc. Rev.*, 1989, **18**, 187-208.
33. a) Gridnev, I. D. and Imamoto, T., *Chem. Commun.*, 2009, 7447-7464; b) Knowles, W. S. and Noyori, R., *Acc. Chem. Res.*, 2007, **40**, 1238-1239.
34. a) Chiba, T. ; Miyashita, A. ; Nohira, H. and Takaya, H., *Tetrahedron Lett.*, 1993, **34**, 2351-2354; b) Chiba, T. ; Miyashita, A. ; Nohira, H. and Takaya, H., *Tetrahedron Lett.*, 1991, **32**, 4745-4748; c) Miyashita, A. ; Karino, H. ; Shimamura, J.-i. ; Chiba, T. ; Nagano, K. ; Nohira, H. and Takaya, H., *Chem. Lett.*, 1989, **18**, 1849-1852.
35. Schmid, R. ; Cereghetti, M. ; Heiser, B. ; Schönholzer, P. and Hansen, H.-J., *Helv. Chim. Acta*, 1988, **71**, 897-929.
36. Schmid, R. ; Foricher, J. ; Cereghetti, M. and Schönholzer, P., *Helv. Chim. Acta*, 1991, **74**, 370-389.
37. a) Zhang, X. ; Mashima, K. ; Koyano, K. ; Sayo, N. ; Kumobayashi, H. ; Akutagawa, S. and Takaya, H., *J. Chem. Soc., Perkin Trans. 1*, 1994, 2309-2322; b) Zhang, X. ; Mashima, K. ; Koyano, K. ; Sayo, N. ; Kumobayashi, H. ; Akutagawa, S. and Takaya, H., *Tetrahedron Lett.*, 1991, **32**, 7283-7286.
38. Sollewijn Gelpke, A. E. ; Kooijman, H. ; Spek, A. L. and Hiemstra, H., *Chem. Eur. J.*, 1999, **5**, 2472-2482.
39. Saito, T. ; Yokozawa, T. ; Ishizaki, T. ; Moroi, T. ; Sayo, N. ; Miura, T. and Kumobayashi, H., *Adv. Synth. Catal.*, 2001, **343**, 264-267.
40. Zhang, Z. ; Qian, H. ; Longmire, J. and Zhang, X., *J. Org. Chem.*, 2000, **65**, 6223-6226.
41. Wu, S. ; Wang, W. ; Tang, W. ; Lin, M. and Zhang, X., *Org. Lett.*, 2002, **4**, 4495-4497.
42. a) Benincori, T. ; Brenna, E. ; Sannicolò, F. ; Trimarco, L. ; Antognazza, P. ; Cesarotti, E. ; Demartin, F. and Pilati, T., *J. Org. Chem.*, 1996, **61**, 6244-6251; b) Benincori, T. ; Brenna, E. ; Sannicolò, F. ; Trimarco, L. ; Antognazza, P. and Cesarotti, E., *J. Chem. Soc. Chem. Commun.*, 1995, 685-686.
43. a) Wu, J. ; Chen, X. ; Guo, R. ; Yeung, C.-h. and Chan, A. S. C., *J. Org. Chem.*, 2003, **68**, 2490-2493; b) Wu, J. ; Chen, H. ; Kwok, W. H. ; Lam, K. H. ; Zhou, Z. Y. ; Yeung, C. H. and Chan, A. S. C., *Tetrahedron Lett.*, 2002, **43**, 1539-1543; c) Pai, C.-C. ; Lin, C.-W. ; Lin, C.-C. ; Chen, C.-C. ; Chan, A. S. C. and Wong, W. T., *J. Am. Chem. Soc.*, 2000, **122**, 11513-11514.
44. Schnider, P. ; Koch, G. ; Prétôt, R. ; Wang, G. ; Bohnen, F. M. ; Krüger, C. and Pfaltz, A., *Chem. Eur. J.*, 1997, **3**, 887-892.
45. Crabtree, R., *Acc. Chem. Res.*, 1979, **12**, 331-337.
46. Lightfoot, A. ; Schnider, P. and Pfaltz, A., *Angew. Chem. Int. Ed.*, 1998, **37**, 2897-2899.
47. Cozzi, Pier G. ; Zimmermann, N. ; Hilgraf, R. ; Schaffner, S. and Pfaltz, A., *Adv. Synth. Catal.*, 2001, **343**, 450-454.
48. Blankenstein, J. and Pfaltz, A., *Angew. Chem. Int. Ed.*, 2001, **40**, 4445-4447.
49. Menges, F. ; Neuburger, M. and Pfaltz, A., *Org. Lett.*, 2002, **4**, 4713-4716.
50. Menges, F. and Pfaltz, A., *Adv. Synth. Catal.*, 2002, **344**, 40-44.
51. Hou, D.-R. ; Reibenspies, J. ; Colacot, T. J. and Burgess, K., *Chemistry- A European Journal*, 2001, **7**, 5391-5400.
52. Diéguez, M. ; Mazuela, J. ; Pàmies, O. ; Verendel, J. J. and Andersson, P. G., *J. Am. Chem. Soc.*, 2008, **130**, 7208-7209.
53. Mazuela, J. ; Norrby, P.-O. ; Andersson, P. G. ; Pàmies, O. and Diéguez, M., *J. Am. Chem. Soc.*, 2011, **133**, 13634-13645.
54. Mazuela, J. ; Pàmies, O. and Diéguez, M., *ChemCatChem*, 2013, **5**, 2410-2417.
55. a) Phillips, S. D. ; Andersson, K. H. O. ; Kann, N. ; Kuntz, M. T. ; France, M. B. ; Wawrzyniak, P. and Clarke, M. L., *Catalysis Science & Technology*, 2011, **1**, 1336-1339; b) Díaz-Valenzuela, M. B. ; Phillips, S.

D. ; France, M. B. ; Gunn, M. E. and Clarke, M. L., *Chemistry- A European Journal*, 2009, **15**, 1227-1232; c) Clarke, M. L. ; Díaz-Valenzuela, M. B. and Slawin, A. M. Z., *Organometallics*, 2007, **26**, 16-19.
56. Fuentes, J. A. ; Phillips, S. D. and Clarke, M. L., *Chemistry Central Journal*, 2012, **6**, 151.
57. Fuentes, J. A. ; Carpenter, I. ; Kann, N. and Clarke, M. L., *Chem. Commun.*, 2013, **49**, 10245-10247.
58. a) Sonnenberg, J. F. ; Lough, A. J. and Morris, R. H., *Organometallics*, 2014, **33**, 6452-6465; b) Lagaditis, P. O. ; Sues, P. E. ; Sonnenberg, J. F. ; Wan, K. Y. ; Lough, A. J. and Morris, R. H., *J. Am. Chem. Soc.*, 2014, **136**, 1367-1380.
59. Sonnenberg, J. F. ; Wan, K. Y. ; Sues, P. E. and Morris, R. H., *ACS. Catal.*, 2017, **7**, 316-326.
60. Smith, S. A. M. ; Lagaditis, P. O. ; Lüpke, A. ; Lough, A. J. and Morris, R. H., *Chemistry – A European Journal*, 2017, **23**, 7212-7216.
61. Seo, C. S. G. ; Tannoux, T. ; Smith, S. A. M. ; Lough, A. J. and Morris, R. H., *J. Org. Chem.*, 2019, **84**, 12040-12049.
62. Burk, M. J. ; Feaster, J. E. and Harlow, R. L., *Tetrahedron: Asymmetry*, 1991, **2**, 569-592.
63. a) Garbe, M. ; Junge, K. ; Walker, S. ; Wei, Z. ; Jiao, H. ; Spannenberg, A. ; Bachmann, S. ; Scalone, M. and Beller, M., *Angew. Chem. Int. Ed.*, 2017, **56**, 11237-11241; b) Garbe, M. ; Wei, Z. ; Tannert, B. ; Spannenberg, A. ; Jiao, H. ; Bachmann, S. ; Scalone, M. ; Junge, K. and Beller, M., *Adv. Synth. Catal.*, 2019, **361**, 1913-1920.
64. a) Gladiali, S. ; Medici, S. ; Pirri, G. ; Pulacchini, S. and Fabbri, D., *Can. J. Chem.*, 2001, **79**, 670-678; b) Gladiali, S. ; Antonio, D. and Davide, F., *Tetrahedron: Asymmetry*, 1994, **5**, 1143-1146.
65. Gladiali, S. ; Grepioni, F. ; Medici, S. ; Zucca, A. ; Berente, Z. and Kollár, L., *Eur. J. Inorg. Chem.*, 2003, **2003**, 556-561.
66. Evans, D. A. ; Michael, F. E. ; Tedrow, J. S. and Campos, K. R., *J. Am. Chem. Soc.*, 2003, **125**, 3534-3543.
67. Borràs, C. ; Biosca, M. ; Pàmies, O. and Diéguez, M., *Organometallics*, 2015, **34**, 5321-5334.
68. Margalef, J. ; Pàmies, O. ; Pericàs, M. A. and Diéguez, M., *Chem. Commun.*, 2020, **56**, 10795-10808.
69. a) Margalef, J. ; Caldentey, X. ; Karlsson, E. A. ; Coll, M. ; Mazuela, J. ; Pàmies, O. ; Diéguez, M. and Pericàs, M. A., *Chemistry – A European Journal*, 2014, **20**, 12201-12214; b) Caldentey, X. ; Cambeiro, X. C. and Pericàs, M. A., *Tetrahedron*, 2011, **67**, 4161-4168.
70. a) Coll, M. ; Pàmies, O. and Diéguez, M., *Adv. Synth. Catal.*, 2013, **355**, 143-160; b) Coll, M. ; Pàmies, O. and Diéguez, M., *Chem. Commun.*, 2011, **47**, 9215-9217.
71. a) Margalef, J. ; Borràs, C. ; Alegre, S. ; Alberico, E. ; Pàmies, O. and Diéguez, M., *ChemCatChem*, 2019, **11**, 2142-2168; b) Margalef, J. ; Pàmies, O. and Diéguez, M., *Chemistry – A European Journal*, 2017, **23**, 813-822.
72. Xie, J.-B. ; Xie, J.-H. ; Liu, X.-Y. ; Kong, W.-L. ; Li, S. and Zhou, Q.-L., *J. Am. Chem. Soc.*, 2010, **132**, 4538-4539.
73. a) Chen, G.-Q. ; Lin, B.-J. ; Huang, J.-M. ; Zhao, L.-Y. ; Chen, Q.-S. ; Jia, S.-P. ; Yin, Q. and Zhang, X., *J. Am. Chem. Soc.*, 2018, **140**, 8064-8068; b) Bao, D.-H. ; Wu, H.-L. ; Liu, C.-L. ; Xie, J.-H. and Zhou, Q.-L., *Angew. Chem. Int. Ed.*, 2015, **54**, 8791-8794; c) Xie, J.-H. ; Liu, X.-Y. ; Xie, J.-B. ; Wang, L.-X. and Zhou, Q.-L., *Angew. Chem. Int. Ed.*, 2011, **50**, 7329-7332.
74. Yan, P.-C. ; Zhu, G.-L. ; Xie, J.-H. ; Zhang, X.-D. ; Zhou, Q.-L. ; Li, Y.-Q. ; Shen, W.-H. and Che, D.-Q., *Org. Process Res. Dev.*, 2013, **17**, 307-312.
75. Xie, J.-H. ; Liu, X.-Y. ; Yang, X.-H. ; Xie, J.-B. ; Wang, L.-X. and Zhou, Q.-L., *Angew. Chem. Int. Ed.*, 2012, **51**, 201-203.
76. Yang, X.-H. ; Xie, J.-H. ; Liu, W.-P. and Zhou, Q.-L., *Angew. Chem. Int. Ed.*, 2013, **52**, 7833-7836.
77. Yan, P.-C. ; Xie, J.-H. ; Zhang, X.-D. ; Chen, K. ; Li, Y.-Q. ; Zhou, Q.-L. and Che, D.-Q., *Chem. Commun.*, 2014, **50**, 15987-15990.
78. Yang, X.-H. ; Yue, H.-T. ; Yu, N. ; Li, Y.-P. ; Xie, J.-H. and Zhou, Q.-L., *Chem. Sci.*, 2017, **8**, 1811-1814.
79. Liu, W.-P. ; Yuan, M.-L. ; Yang, X.-H. ; Li, K. ; Xie, J.-H. and Zhou, Q.-L., *Chem. Commun.*, 2015, **51**, 6123-6125.
80. Bao, D.-H. ; Gu, X.-S. ; Xie, J.-H. and Zhou, Q.-L., *Org. Lett.*, 2017, **19**, 118-121.
81. Hayashi, T. ; Kawamura, N. and Ito, Y., *J. Am. Chem. Soc.*, 1987, **109**, 7876-7878.
82. Boaz, N. W. ; Debenham, S. D. ; Mackenzie, E. B. and Large, S. E., *Org. Lett.*, 2002, **4**, 2421-2424.
83. Togni, A., *Chim. Int. J. Chem*, 1996, **50**, 86-93.
84. Blaser, H.-U. ; Brieden, W. ; Pugin, B. ; Spindler, F. ; Studer, M. and Togni, A., *Top. Catal.*, 2002, **19**, 3-16.
85. Bader, R. R. and Blaser, H.-U., in *Stud. Surf. Sci. Catal.*, 1997, vol. 108, pp. 17-29.
86. Imwinkelried, R., *Chim. Int. J. Chem*, 1997, **51**, 300-302.

87. Dobbs, D. A. ; Vanhessche, K. P. M. ; Brazi, E. ; Rautenstrauch, V. ; Lenoir, J.-Y. ; Genêt, J.-P. ; Wiles, J. and Bergens, S. H., *Angew. Chem. Int. Ed.*, 2000, **39**, 1992-1995.
88. Togni, A. ; Breutel, C. ; Schnyder, A. ; Spindler, F. ; Landert, H. and Tijani, A., *J. Am. Chem. Soc.*, 1994, **116**, 4062-4066.
89. a) Spindler, F. and Blaser, H.-U., *Adv. Synth. Catal.*, 2001, **343**, 68-70; b) Blaser, H. U. ; Buser, H. P. ; Hausel, R. ; Jalett, H. P. and Spindler, F., *J. Organomet. Chem.*, 2001, **621**, 34-38.
90. Baratta, W. ; Benedetti, F. ; Del Zotto, A. ; Fanfoni, L. ; Felluga, F. ; Magnolia, S. ; Putignano, E. and Rigo, P., *Organometallics*, 2010, **29**, 3563-3570.
91. Calvin, J. R. ; Frederick, M. O. ; Laird, D. L. T. ; Remacle, J. R. and May, S. A., *Org. Lett.*, 2012, **14**, 1038-1041.
92. Yoshikawa, N. ; Tan, L. ; McWilliams, J. C. ; Ramasamy, D. and Sheppard, R., *Org. Lett.*, 2010, **12**, 276-279.
93. Nie, H. ; Zhu, Y. ; Hu, X. ; Wei, Z. ; Yao, L. ; Zhou, G. ; Wang, P. ; Jiang, R. and Zhang, S., *Org. Lett.*, 2019, **21**, 8641-8645.
94. Abbas, Z. ; Hu, X.-H. ; Ali, A. ; Xu, Y.-W. and Hu, X.-P., *Tetrahedron Lett.*, 2020, **61**, 151860.
95. a) Richards, C. J. ; Hibbs, D. E. and Hursthouse, M. B., *Tetrahedron Lett.*, 1995, **36**, 3745-3748; b) Nishibayashi, Y. ; Segawa, K. ; Ohe, K. and Uemura, S., *Organometallics*, 1995, **14**, 5486-5487.
96. Lu, S.-M. ; Han, X.-W. and Zhou, Y.-G., *Adv. Synth. Catal.*, 2004, **346**, 909-912.
97. a) Nishibayashi, Y. ; Takei, I. ; Uemura, S. and Hidai, M., *Organometallics*, 1999, **18**, 2291-2293; b) Nishibayashi, Y. ; Takei, I. ; Uemura, S. and Hidai, M., *Organometallics*, 1998, **17**, 3420-3422.
98. Naud, F. ; Malan, C. ; Spindler, F. ; Rüggeberg, C. ; Schmidt, A. T. and Blaser, H.-U., *Adv. Synth. Catal.*, 2006, **348**, 47-50.
99. a) Fürstner, A. ; Bindl, M. and Jean, L., *Angew. Chem. Int. Ed.*, 2007, **46**, 9275-9278; b) Oppolzer, W. ; Darcel, C. ; Rochet, P. ; Rosset, S. and De Brabander, J., *Helv. Chim. Acta*, 1997, **80**, 1319-1337; c) Evans, D. ; Ennis, M. and Mathre, D., *J. Am. Chem. Soc.*, 1982, **104**, 1737-1739.
100. Lu, W.-J. and Hou, X.-L., *Adv. Synth. Catal.*, 2009, **351**, 1224-1228.
101. Lu, S.-M. ; Han, X.-W. and Zhou, Y.-G., *Adv. Synth. Catal.*, 2004, **346**, 909-912.
102. a) Zirakzadeh, A. ; Schuecker, R. ; Gorgas, N. ; Mereiter, K. ; Spindler, F. and Weissensteiner, W., *Organometallics*, 2012, **31**, 4241-4250; b) Schuecker, R. ; Zirakzadeh, A. ; Mereiter, K. ; Spindler, F. and Weissensteiner, W., *Organometallics*, 2011, **30**, 4711-4719.
103. Ireland, T. ; Grossheimann, G. ; Wieser-Jeunesse, C. and Knochel, P., *Angew. Chem. Int. Ed.*, 1999, **38**, 3212-3215.
104. Ireland, T. ; Tappe, K. ; Grossheimann, G. and Knochel, P., *Chemistry- A European Journal* 2002, **8**, 843-852.
105. Cheemala, M. N. and Knochel, P., *Org. Lett.*, 2007, **9**, 3089-3092.
106. a) Malacea, R. ; Routaboul, L. ; Manoury, E. ; Daran, J.-C. and Poli, R., *J. Organomet. Chem.*, 2008, **693**, 1469-1477; b) Malacea, R. ; Manoury, E. ; Routaboul, L. ; Daran, J.-C. ; Poli, R. ; Dunne, J. P. ; Withwood, A. C. ; Godard, C. and Duckett, S. B., *Eur. J. Inorg. Chem.*, 2006, **2006**, 1803-1816; c) Malacea, R. ; Daran, J.-C. ; Duckett, S. B. ; Dunne, J. P. ; Godard, C. ; Manoury, E. ; Poli, R. and Whitwood, A. C., *Dalton Transactions*, 2006, 3350-3359.
107. a) Le Roux, E. ; Malacea, R. ; Manoury, E. ; Poli, R. ; Gonsalvi, L. and Peruzzini, M., *Adv. Synth. Catal.*, 2007, **349**, 309-313; b) Routaboul, L. ; Vincendeau, S. ; Daran, J.-C. and Manoury, E., *Tetrahedron: Asymmetry*, 2005, **16**, 2685-2690.
108. Biosca, M. ; Coll, M. ; Lagarde, F. ; Brémond, E. ; Routaboul, L. ; Manoury, E. ; Pàmies, O. ; Poli, R. and Diéguez, M., *Tetrahedron*, 2016, **72**, 2623-2631.
109. Nie, H. ; Zhou, G. ; Wang, Q. ; Chen, W. and Zhang, S., *Tetrahedron: Asymmetry*, 2013, **24**, 1567-1571.
110. Widegren, M. B. ; Harkness, G. J. ; Slawin, A. M. Z. ; Cordes, D. B. and Clarke, M. L., *Angew. Chem. Int. Ed.*, 2017, **56**, 5825-5828.
111. Ling, F. ; Chen, J. ; Nian, S. ; Hou, H. ; Yi, X. ; Wu, F. ; Xu, M. and Zhong, W., *Synlett*, 2020, **31**, 285-289.
112. Ling, F. ; Hou, H. ; Chen, J. ; Nian, S. ; Yi, X. ; Wang, Z. ; Song, D. and Zhong, W., *Org. Lett.*, 2019, **21**, 3937-3941.
113. Zirakzadeh, A. ; Kirchner, K. ; Roller, A. ; Stöger, B. ; Widhalm, M. and Morris, R. H., *Organometallics*, 2016, **35**, 3781-3787.
114. Zirakzadeh, A. ; de Aguiar, S. R. M. M. ; Stöger, B. ; Widhalm, M. and Kirchner, K., *ChemCatChem*, 2017, **9**, 1744-1748.

115. Zeng, L. ; Yang, H. ; Zhao, M. ; Wen, J. ; Tucker, J. H. R. and Zhang, X., *ACS. Catal.*, 2020, **10**, 13794-13799.
116. a) Yu, J. ; Duan, M. ; Wu, W. ; Qi, X. ; Xue, P. ; Lan, Y. ; Dong, X.-Q. and Zhang, X., *Chem. - Eur. J.*, 2017, **23**, 970-975; b) Wu, W. ; Tan, X. ; Chen, C. ; Xie, Y. ; Dong, X.-Q. ; Zhang, X. ; Liu, S. ; Zhang, X. ; Duan, M. and Lan, Y., *Org. Lett.*, 2016, **18**, 2938-2941; c) Yu, J. ; Long, J. ; Yang, Y. ; Wu, W. ; Xue, P. ; Chung, L. W. ; Dong, X.-Q. and Zhang, X., *Org. Lett.*, 2017, **19**, 690-693; d) Ling, F. ; Nian, S. ; Chen, J. ; Luo, W. ; Wang, Z. ; Lv, Y. and Zhong, W., *The Journal of Organic Chemistry*, 2018, **83**, 10749-10761.
117. Wu, W. ; Xie, Y. ; Li, P. ; Li, X. ; Liu, Y. ; Dong, X.-Q. and Zhang, X., *Org. Chem. Front.*, 2017, **4**, 555-559.
118. Nian, S. ; Ling, F. ; Chen, J. ; Wang, Z. ; Shen, H. ; Yi, X. ; Yang, Y.-F. ; She, Y. and Zhong, W., *Org. Lett.*, 2019, **21**, 5392-5396.
119. Hu, Y. ; Wu, W. ; Dong, X.-Q. and Zhang, X., *Org. Chem. Front.*, 2017, **4**, 1499-1502.
120. Tao, L. ; Yin, C. ; Dong, X.-Q. and Zhang, X., *Org Biomol Chem*, 2019, **17**, 785-788.
121. Gu, G. ; Yang, T. ; Lu, J. ; Wen, J. ; Dang, L. and Zhang, X., *Org. Chem. Front.*, 2018, **5**, 1209-1212.
122. a) Qin, C. ; Chen, X.-S. ; Hou, C.-J. ; Liu, H. ; Liu, Y.-J. ; Huang, D.-Z. and Hu, X.-P., *Synth. Commun.*, 2018, **48**, 672-676; b) Gu, G. ; Lu, J. ; Yu, O. ; Wen, J. ; Yin, Q. and Zhang, X., *Org. Lett.*, 2018, **20**, 1888-1892.
123. Grigg, R. ; Mitchell, T. R. B. ; Sutthivaiyakit, S. and Tongpenyai, N., *Journal of the Chemical Society, Chemical Communications*, 1981, 611-612.
124. Watanabe, Y. ; Tsuji, Y. and Ohsugi, Y., *Tetrahedron Lett.*, 1981, **22**, 2667-2670.
125. Gunanathan, C. and Milstein, D., *Science*, 2013, **341**, 1229712.
126. Shimizu, K.-i., *Catalysis Science & Technology*, 2015, **5**, 1412-1427.
127. a) Corma, A. ; Navas, J. and Sabater, M. J., *Chem. Rev.*, 2018, **118**, 1410-1459; b) Obora, Y., *Top. Curr. Chem.*, 2016, **374**, 11; c) Ma, X. ; Su, C. and Xu, Q., *Top. Curr. Chem.*, 2016, **374**, 27; d) Yang, Q. ; Wang, Q. and Yu, Z., *Chem. Soc. Rev.*, 2015, **44**, 2305-2329; e) Muzart, J., *Eur. J. Org. Chem.*, 2015, **2015**, 5693-5707; f) Hamid, M. H. S. A. ; Slatford, P. A. and Williams, J. M. J., *Adv. Synth. Catal.*, 2007, **349**, 1555-1575.
128. Guillena, G. ; Ramón, D. J. and Yus, M., *Angew. Chem. Int. Ed.*, 2007, **46**, 2358-2364.
129. Li, Y. ; Li, H. ; Junge, H. and Beller, M., *Chem. Commun.*, 2014, **50**, 14991-14994.
130. Bähn, S. ; Imm, S. ; Neubert, L. ; Zhang, M. ; Neumann, H. and Beller, M., *ChemCatChem*, 2011, **3**, 1853-1864.
131. Michlik, S. and Kempe, R., *Chemistry- A European Journal*, 2010, **16**, 13193-13198.
132. Gunanathan, C. and Milstein, D., *Acc. Chem. Res.*, 2011, **44**, 588-602.
133. a) Pingen, D. ; Müller, C. and Vogt, D., *Angew. Chem. Int. Ed.*, 2010, **49**, 8130-8133; b) Imm, S. ; Bähn, S. ; Neubert, L. ; Neumann, H. and Beller, M., *Angew. Chem. Int. Ed.*, 2010, **49**, 8126-8129.
134. Pingen, D. ; Diebolt, O. and Vogt, D., *ChemCatChem*, 2013, **5**, 2905-2912.
135. Marichev, K. O. and Takacs, J. M., *ACS. Catal.*, 2016, **6**, 2205-2210.
136. Irrgang, T. and Kempe, R., *Chem. Rev.*, 2019, **119**, 2524-2549.
137. a) Elangovan, S. ; Sortais, J.-B. ; Beller, M. and Darcel, C., *Angew. Chem. Int. Ed.*, 2015, **54**, 14483-14486; b) Yan, T. ; Feringa, B. L. and Barta, K., *Nature Communications*, 2014, **5**, 5602.
138. Elangovan, S. ; Neumann, J. ; Sortais, J.-B. ; Junge, K. ; Darcel, C. and Beller, M., *Nature Communications*, 2016, **7**, 12641.
139. a) Zhang, G. ; Yin, Z. and Zheng, S., *Org. Lett.*, 2016, **18**, 300-303; b) Rösler, S. ; Ertl, M. ; Irrgang, T. and Kempe, R., *Angew. Chem. Int. Ed.*, 2015, **54**, 15046-15050.
140. Deibl, N. and Kempe, R., *J. Am. Chem. Soc.*, 2016, **138**, 10786-10789.
141. Chakraborty, P. ; Gangwar, M. K. ; Emayavaramban, B. ; Manoury, E. ; Poli, R. and Sundararaju, B., *ChemSusChem*, 2019, **12**, 3463-3467.
142. a) Waiba, S. ; Jana, S. K. ; Jati, A. ; Jana, A. and Maji, B., *Chem. Commun.*, 2020, **56**, 8376-8379; b) Jana, A. ; Das, K. ; Kundu, A. ; Thorve, P. R. ; Adhikari, D. and Maji, B., *ACS. Catal.*, 2020, **10**, 2615-2626.
143. a) Xi, X. ; Li, Y. ; Wang, G. ; Xu, G. ; Shang, L. ; Zhang, Y. and Xia, L., *Org. Biomol. Chem,*, 2019, **17**, 7651-7654; b) Homberg, L. ; Roller, A. and Hultzsch, K. C., *Org. Lett.*, 2019, **21**, 3142-3147; c) Oldenhuis, N. J. ; Dong, V. M. and Guan, Z., *J. Am. Chem. Soc.*, 2014, **136**, 12548-12551; d) Hamid, M. H. S. A. ; Allen, C. L. ; Lamb, G. W. ; Maxwell, A. C. ; Maytum, H. C. ; Watson, A. J. A. and Williams, J. M. J., *J. Am. Chem. Soc.*, 2009, **131**, 1766-1774.
144. Onodera, G. ; Nishibayashi, Y. and Uemura, S., *Angew. Chem. Int. Ed.*, 2006, **45**, 3819-3822.

145. Suzuki, T. ; Ishizaka, Y. ; Ghozati, K. ; Zhou, D.-Y. ; Asano, K. and Sasai, H., *Synthesis*, 2013, **45**, 2134-2136.
146. Kovalenko, O. O. ; Lundberg, H. ; Hübner, D. and Adolfsson, H., *Eur. J. Org. Chem.*, 2014, **2014**, 6639-6642.
147. Eka Putra, A. ; Oe, Y. and Ohta, T., *Eur. J. Org. Chem.*, 2013, **2013**, 6146-6151.
148. Yang, L.-C. ; Wang, Y.-N. ; Zhang, Y. and Zhao, Y., *ACS. Catal.*, 2017, **7**, 93-97.
149. Zhang, Y. ; Lim, C.-S. ; Sim, D. S. B. ; Pan, H.-J. and Zhao, Y., *Angew. Chem. Int. Ed.*, 2014, **53**, 1399-1403.
150. Phipps, R. J. ; Hamilton, G. L. and Toste, F. D., *Nat. Chem.*, 2012, **4**, 603-614.
151. Rong, Z.-Q. ; Zhang, Y. ; Chua, R. H. B. ; Pan, H.-J. and Zhao, Y., *J. Am. Chem. Soc.*, 2015, **137**, 4944-4947.
152. Zhang, J. and Wang, J., *Angew. Chem. Int. Ed.*, 2018, **57**, 465-469.
153. Lim, C. S. ; Quach, T. T. and Zhao, Y., *Angew. Chem. Int. Ed.*, 2017, **56**, 7176-7180.
154. Kwok, T. ; Hoff, O. ; Armstrong, R. J. and Donohoe, T. J., *Chemistry – A European Journal*, 2020, **26**, 1-16.
155. Guiry, P. J. and Saunders, C. P., *Adv. Synth. Catal.*, 2004, **346**, 497-537.
156. Bandyopadhyay, U. ; Sundararaju, B. ; Poli, R. and Manoury, E., *" Chiral tridentate based ligands ", in "Chiral Ligands: Evolution of Ligand Libraries for Asymmetric Catalysis: Evolution of Ligand Libraries for Asymmetric Catalysis" , M Dieguez, Editor, CRC Press, Boca Raton, USA, 2021* 2021, 167-194.
157. a) Marquarding, D. ; Klusacek, H. ; Gokel, G. ; Hoffmann, P. and Ugi, I., *J. Am. Chem. Soc.*, 1970, **92**, 5389-5393; b) Marquarding, D. ; Hoffmann, P. ; Heitzer, H. and Ugi, I., *J. Am. Chem. Soc.*, 1970, **92**, 1969-1971.
158. Togni, A., *Angew. Chem. Int. Ed.*, 1996, **35**, 1475-1477.
159. Hayashi, T. ; Yamamoto, K. and Kumada, M., *Tetrahedron Lett.*, 1974, **15**, 4405-4408.
160. Barbaro, P. and Togni, A., *Organometallics*, 1995, **14**, 3570-3573.
161. Burckhardt, U. ; Hintermann, L. ; Schnyder, A. and Togni, A., *Organometallics*, 1995, **14**, 5415-5425.
162. Sturm, T. ; Weissensteiner, W. and Spindler, F., *Adv. Synth. Catal.*, 2003, **345**, 160-164.
163. Chen, W. ; Mbafor, W. ; Roberts, S. M. and Whittall, J., *J. Am. Chem. Soc.*, 2006, **128**, 3922-3923.
164. Xu, Q. and Han, L.-B., *Org. Lett.*, 2006, **8**, 2099-2101.
165. Leitner, A. ; Larsen, J. ; Steffens, C. and Hartwig, J. F., *J. Org. Chem.*, 2004, **69**, 7552-7557.
166. Bercot, E. A. and Rovis, T., *J. Am. Chem. Soc.*, 2004, **126**, 10248-10249.
167. Lautens, M. ; Fagnou, K. and Rovis, T., *J. Am. Chem. Soc.*, 2000, **122**, 5650-5651.
168. a) López, F. ; Harutyunyan, S. R. ; Meetsma, A. ; Minnaard, A. J. and Feringa, B. L., *Angew. Chem. Int. Ed.*, 2005, **44**, 2752-2756; b) Des Mazery, R. ; Pullez, M. ; López, F. ; Harutyunyan, S. R. ; Minnaard, A. J. and Feringa, B. L., *J. Am. Chem. Soc.*, 2005, **127**, 9966-9967.
169. Fadini, L. and Togni, A., *Chem. Commun.*, 2003, 30-31.
170. Sadow, A. D. and Togni, A., *J. Am. Chem. Soc.*, 2005, **127**, 17012-17024.
171. Togni, A. ; Burckhardt, U. ; Gramlich, V. ; Pregosin, P. S. and Salzmann, R., *J. Am. Chem. Soc.*, 1996, **118**, 1031-1037.
172. Schnyder, A. ; Hintermann, L. and Togni, A., *Angew. Chem. Int. Ed.*, 1995, **34**, 931-933.
173. a) Boaz, N. W. ; Mackenzie, E. B. ; Debenham, S. D. ; Large, S. E. and Ponasik, J. A., *J. Org. Chem.*, 2005, **70**, 1872-1880; b) Boaz, N. W. ; Ponasik, J. A. and Large, S. E., *Tetrahedron: Asymmetry*, 2005, **16**, 2063-2066.
174. Boaz, N. W. ; Ponasik, J. A. and Large, S. E., *Tetrahedron Lett.*, 2006, **47**, 4033-4035.
175. Moran, W. J. and Morken, J. P., *Org. Lett.*, 2006, **8**, 2413-2415.
176. Tanaka, K. ; Hagiwara, Y. and Noguchi, K., *Angew. Chem. Int. Ed.*, 2005, **44**, 7260-7263.
177. Kong, J.-R. ; Ngai, M.-Y. and Krische, M. J., *J. Am. Chem. Soc.*, 2006, **128**, 718-719.
178. a) Peters, R. and Fischer, D. F., *Org. Lett.*, 2005, **7**, 4137-4140; b) Farrell, A. ; Goddard, R. and Guiry, P. J., *J. Org. Chem.*, 2002, **67**, 4209-4217; c) Xiao, L. ; Kitzler, R. and Weissensteiner, W., *J. Org. Chem.*, 2001, **66**, 8912-8919; d) Bolm, C. ; Kesselgruber, M. ; Muñiz, K. and Raabe, G., *Organometallics*, 2000, **19**, 1648-1651; e) Widhalm, M. ; Mereiter, K. and Bourghida, M., *Tetrahedron: Asymmetry*, 1998, **9**, 2983-2986.
179. a) Sammakia, T. ; Latham, H. A. and Schaad, D. R., *J. Org. Chem.*, 1995, **60**, 10-11; b) Richards, C. J. ; Damalidis, T. ; Hibbs, D. E. and Hursthouse, M. B., *Synlett*, 1995, **1995**, 74-76; c) Nishibayashi, Y. and Uemura, S., *Synlett*, 1995, **1995**, 79-81.
180. a) Lotz, M. ; Kramer, G. and Knochel, P., *Chem. Commun.*, 2002, 2546-2547; b) Lagneau, N. M. ; Chen, Y. ; Robben, P. M. ; Sin, H.-S. ; Takasu, K. ; Chen, J.-S. ; Robinson, P. D. and Hua, D. H., *Tetrahedron*, 1998, **54**, 7301-7334; c) Rebière, F. ; Riant, O. ; Ricard, L. and Kagan, H. B., *Angewandte Chemie International Edition Engl*, 1993, **32**, 568-570.
181. a) Miyake, Y. ; Nishibayashi, Y. and Uemura, S., *Synlett*, 2008, **2008**, 1747-1758; b) Sutcliffe, O. B. and Bryce, M. R., *Tetrahedron: Asymmetry*, 2003, **14**, 2297-2325.

182. Geisler, F. M. and Helmchen, G., *J. Org. Chem.*, 2006, **71**, 2486-2492.
183. Kilroy, T. G. ; Hennessy, A. J. ; Connolly, D. J. ; Malone, Y. M. ; Farrell, A. and Guiry, P. J., *J. Mol. Catal. A: Chem.*, 2003, **196**, 65-81.
184. a) Kiely, D. and Guiry, P. J., *Tetrahedron Lett.*, 2003, **44**, 7377-7380; b) Kiely, D. and Guiry, P. J., *J. Organomet. Chem.*, 2003, **687**, 545-561.
185. a) Zeng, W. and Zhou, Y.-G., *Org. Lett.*, 2005, **7**, 5055-5058; b) Gao, W. ; Zhang, X. and Raghunath, M., *Org. Lett.*, 2005, **7**, 4241-4244.
186. a) Wright, J. ; Frambes, L. and Reeves, P., *J. Organomet. Chem.*, 1994, **476**, 215-217; b) Corey, E. ; Bakshi, R. K. and Shibata, S., *J. Am. Chem. Soc.*, 1987, **109**, 5551-5553.
187. Lotz, M. ; Polborn, K. and Knochel, P., *Angew. Chem. Int. Ed.*, 2002, **41**, 4708-4711.
188. Deschamp, J. ; Chuzel, O. ; Hannedouche, J. and Riant, O., *Angew. Chem. Int. Ed.*, 2006, **45**, 1292-1297.
189. Oisaki, K. ; Zhao, D. ; Kanai, M. and Shibasaki, M., *J. Am. Chem. Soc.*, 2006, **128**, 7164-7165.
190. López, F. ; van Zijl, A. W. ; Minnaard, A. J. and Feringa, B. L., *Chem. Commun.*, 2006, 409-411.
191. Kitzler, R. ; Xiao, L. and Weissensteiner, W., *Tetrahedron: Asymmetry*, 2000, **11**, 3459-3462.
192. a) Mateus, N. ; Routaboul, L. ; Daran, J.-C. and Manoury, E., *J. Organomet. Chem.*, 2006, **691**, 2297-2310; b) Daran, J.-C. ; Manoury, E. ; Routaboul, L. and Rivals, F., *Acta Crystallographica Section C*, 2006, **62**, m378-m380.
193. a) Bayda, S. ; Cassen, A. ; Daran, J.-C. ; Audin, C. ; Poli, R. ; Manoury, E. and Deydier, E., *J. Organomet. Chem.*, 2014, **772-773**, 258-264; b) Kozinets, E. M. ; Koniev, O. ; Filippov, O. A. ; Daran, J.-C. ; Poli, R. ; Shubina, E. S. ; Belkova, N. V. and Manoury, E., *Dalton Transactions*, 2012, **41**, 11849-11859; c) Audin, C. ; Daran, J.-C. ; Deydier, É. ; Manoury, É. and Poli, R., *Comptes Rendus Chimie*, 2010, **13**, 890-899.
194. Guadalupe Lopez Cortes, J. ; Ramon, O. ; Vincendeau, S. ; Serra, D. ; Lamy, F. ; Daran, J.-C. ; Manoury, E. and Gouygou, M., *Eur. J. Inorg. Chem.*, 2006, **2006**, 5148-5157.
195. a) Debono, N. ; Labande, A. ; Manoury, E. ; Daran, J.-C. and Poli, R., *Organometallics*, 2010, **29**, 1879-1882; b) Labande, A. ; Daran, J.-C. ; Manoury, E. and Poli, R., *Eur. J. Inorg. Chem.*, 2007, **2007**, 1205-1209.
196. Wei, M.-M. ; García-Melchor, M. ; Daran, J.-C. ; Audin, C. ; Lledós, A. ; Poli, R. ; Deydier, E. and Manoury, E., *Organometallics*, 2012, **31**, 6669-6680.
197. a) Routaboul, L. ; Vincendeau, S. ; Turrin, C.-O. ; Caminade, A.-M. ; Majoral, J.-P. ; Daran, J.-C. and Manoury, E., *J. Organomet. Chem.*, 2007, **692**, 1064-1073; b) Turrin, C.-O. ; Chiffre, J. ; de Montauzon, D. ; Daran, J.-C. ; Caminade, A.-M. ; Manoury, E. ; Balavoine, G. and Majoral, J.-P., *Macromolecules*, 2000, **33**, 7328-7336.
198. Manoury, E. and Poli, R., in *Phosphorus Compounds: Catalysis by Metal Complexes*, Springer, 2011, vol. 37, pp. 121-149.
199. Hayashi, T. ; Mise, T. ; Fukushima, M. ; Kagotani, M. ; Nagashima, N. ; Hamada, Y. ; Matsumoto, A. ; Kawakami, S. ; Konishi, M. ; Yamamoto, K. and Kumada, M., *Bull. Chem. Soc. Jpn.*, 1980, **53**, 1138-1151.
200. a) Riant, O. ; Samuel, O. ; Flessner, T. ; Taudien, S. and Kagan, H. B., *The Journal of Organic Chemistry*, 1997, **62**, 6733-6745; b) Riant, O. ; Samuel, O. and Kagan, H. B., *J. Am. Chem. Soc.*, 1993, **115**, 5835-5836.
201. Xiao, L. ; Mereiter, K. ; Weissensteiner, W. and Widhalm, M., *Synthesis*, 1999, **08**, 1354-1362.
202. Yajima, T. ; Okajima, M. ; Odani, A. and Yamauchi, O., *Inorg. Chim. Acta*, 2002, **339**, 445-454.
203. Yudasaka, M. ; Shimbo, D. ; Maruyama, T. ; Tada, N. and Itoh, A., *Org. Lett.*, 2019, **21**, 1098-1102.
204. a) Jiang, R. ; Zhang, Y. ; Shen, Y.-C. ; Zhu, X. ; Xu, X.-P. and Ji, S.-J., *Tetrahedron*, 2010, **66**, 4073-4078; b) Xu, X. ; Jiang, R. ; Zhou, X. ; Liu, Y. ; Ji, S. and Zhang, Y., *Tetrahedron*, 2009, **65**, 877-882.
205. a) Nair, V. and Deepthi, A., *Chem. Rev.*, 2007, **107**, 1862-1891; b) Heiba, E.-A. I. and Dessau, R. M., *J. Am. Chem. Soc.*, 1971, **93**, 524-527; c) Iranpoor, N. and Mothaghineghad, E., *Tetrahedron*, 1994, **50**, 1859-1870.
206. Zeng, X.-F. ; Ji, S.-J. and Wang, S.-Y., *Tetrahedron*, 2005, **61**, 10235-10241.
207. a) Mitsunobu, O. ; Yamada, M. and Mukaiyama, T., *Bull. Chem. Soc. Jpn.*, 1967, **40**, 935-939; b) Mitsunobu, O. and Yamada, M., *Bull. Chem. Soc. Jpn.*, 1967, **40**, 2380-2382.
208. a) Swamy, K. C. K. ; Kumar, N. N. B. ; Balaraman, E. and Kumar, K. V. P. P., *Chem. Rev.*, 2009, **109**, 2551-2651; b) Fletcher, S., *Org. Chem. Front.*, 2015, **2**, 739-752.
209. Karpus, A. ; Yesypenko, O. ; Boiko, V. ; Poli, R. ; Daran, J.-C. ; Voitenko, Z. ; Kalchenko, V. and Manoury, E., *Eur. J. Org. Chem.*, 2016, **2016**, 3386-3394.
210. a) Stokes, S. T. ; Vlk, A. ; Wang, Y. ; Martinez-Martinez, C. ; Zhang, X. and Bowen, K. H., *Chem. Phys. Lett.*, 2019, **730**, 634-637; b) Galstyan, G. and Knapp, E.-W., *J. Phys. Chem. A*, 2012, **116**, 6885-6893.
211. Wong, M. W. ; Wiberg, K. B. and Frisch, M. J., *J. Am. Chem. Soc.*, 1992, **114**, 1645-1652.
212. Breugst, M. and Mayr, H., *J. Am. Chem. Soc.*, 2010, **132**, 15380-15389.

213. a) Bexrud, J. A. ; Eisenberger, P. ; Leitch, D. C. ; Payne, P. R. and Schafer, L. L., *J. Am. Chem. Soc.*, 2009, **131**, 2116-2118; b) Chong, E. and Schafer, L. L., *Org. Lett.*, 2013, **15**, 6002-6005; c) Djakovitch, L. and Rouge, P., *J. Mol. Catal. A: Chem.*, 2007, **273**, 230-239; d) Chen, D. ; Ahrens-Botzong, A. ; Schünemann, V. ; Scopelliti, R. and Hu, X., *Inorg. Chem.*, 2011, **50**, 5249-5257; e) Lopes, I. ; Hillier, A. C. ; Liu, S. Y. ; Domingos, Â. ; Ascenso, J. ; Galvão, A. ; Sella, A. and Marques, N., *Inorg. Chem.*, 2001, **40**, 1116-1125.
214. a) Brandt, J. W. ; Chong, E. and Schafer, L. L., *ACS. Catal.*, 2017, **7**, 6323-6330; b) Chong, E. ; Brandt, J. W. and Schafer, L. L., *J. Am. Chem. Soc.*, 2014, **136**, 10898-10901.
215. a) Moore, C. M. ; Bark, B. and Szymczak, N. K., *ACS. Catal.*, 2016, **6**, 1981-1990; b) Moore, C. M. and Szymczak, N. K., *Chem. Commun.*, 2013, **49**, 400-402.
216. Donohoe, T. J. ; Johnson, D. J. ; Mace, L. H. ; Thomas, R. E. ; Chiu, J. Y. K. ; Rodrigues, J. S. ; Compton, R. G. ; Banks, C. E. ; Tomcik, P. ; Bamford, M. J. and Ichihara, O., *Org. Biomol. Chem,*, 2006, **4**, 1071-1084.
217. Soai, K. ; Oyamada, H. ; Takase, M. and Ookawa, A., *Bull. Chem. Soc. Jpn.*, 1984, **57**, 1948-1953.
218. a) Kasturi, T. R. and Pragnacharyulu, P. V. P., *Tetrahedron*, 1992, **48**, 4431-4438; b) Brown, H. C. ; Narasimhan, S. and Choi, Y. M., *The Journal of Organic Chemistry*, 1982, **47**, 4702-4708.
219. C. P, P. ; Joseph, E. ; A, A. ; D. S, N. ; Ibnusaud, I. ; Raskatov, J. and Singaram, B., *The Journal of Organic Chemistry*, 2018, **83**, 1431-1440.
220. Sri Ramya, P. V. ; Angapelly, S. ; Guntuku, L. ; Singh Digwal, C. ; Nagendra Babu, B. ; Naidu, V. G. M. and Kamal, A., *European Journal of Medicinal Chemistry*, 2017, **127**, 100-114.
221. Ackroyd, N. C. and Katzenellenbogen, J. A., *Organometallics*, 2010, **29**, 3669-3671.
222. Liu, Y. ; Yu, H. ; Zhao, L. and Zhang, H., *Nuclear Medicine and Biology*, 2013, **40**, 126-134.
223. Gray, M. A. ; Konopski, L. and Langlois, Y., *Synth. Commun.*, 1994, **24**, 1367-1379.
224. Routaboul, L., *'Synthèse de Ligands Ferroceniques Polysubstitues Enatiomeriquement Purs. Etude de Leur Chimie de Coordination et Utilisation en Catalyse Asymétrique', doctoral dissertation, Université Paul Sabatier de Toulouse- III, Toulouse, France.*, 2003.
225. Mitsunobu, O., *Synthesis*, 1981, **1981**, 1-28.
226. Zishiri, V. K. ; Hunter, R. ; Smith, P. J. ; Taylor, D. ; Summers, R. ; Kirk, K. ; Martin, R. E. and Egan, T. J., *European Journal of Medicinal Chemistry*, 2011, **46**, 1729-1742.
227. a) Roiser, L. ; Robiette, R. and Waser, M., *Synlett*, 2016, **27**, 1963-1968; b) Kimachi, T. ; Kinoshita, H. ; Kusaka, K. ; Takeuchi, Y. ; Aoe, M. and Ju-ichi, M., *Synlett*, 2005, **2005**, 842-844; c) Kinoshita, H. ; Ihoriya, A. ; Ju-ichi, M. and Kimachi, T., *Synlett*, 2010, **2010**, 2330-2334; d) Robiette, R. ; Conza, M. and Aggarwal, V. K., *Org. Biomol. Chem,*, 2006, **4**, 621-623.
228. Liu, D. J. ; Credo, G. M. ; Su, X. ; Wu, K. ; Lim, H. C. ; Elibol, O. H. ; Bashir, R. and Varma, M., *Chem. Commun.*, 2011, **47**, 8310-8312.
229. Turrin, C.-O. ; Chiffre, J. ; Daran, J.-C. ; de Montauzon, D. ; Balavoine, G. ; Manoury, É. ; Caminade, A.-M. and Majoral, J.-P., *Comptes Rendus Chimie*, 2002, **5**, 309-318.
230. Makino, K. ; Hasegawa, Y. ; Inoue, T. ; Araki, K. ; Tabata, H. ; Oshitari, T. ; Ito, K. ; Natsugari, H. and Takahashi, H., *Synlett*, 2019, **30**, 951-954.
231. a) Ben-Ari, E. ; Leitus, G. ; Shimon, L. J. W. and Milstein, D., *J. Am. Chem. Soc.*, 2006, **128**, 15390-15391; b) Casey, C. P. ; Bikzhanova, G. A. ; Cui, Q. and Guzei, I. A., *J. Am. Chem. Soc.*, 2005, **127**, 14062-14071; c) Abbel, R. ; Abdur-Rashid, K. ; Faatz, M. ; Hadzovic, A. ; Lough, A. J. and Morris, R. H., *J. Am. Chem. Soc.*, 2005, **127**, 1870-1882; d) Yamakawa, M. ; Ito, H. and Noyori, R., *J. Am. Chem. Soc.*, 2000, **122**, 1466-1478.
232. Haack, K.-J. ; Hashiguchi, S. ; Fujii, A. ; Ikariya, T. and Noyori, R., *Angew. Chem. Int. Ed. Engl.*, 1997, **36**, 285-288.
233. Noyori, R. ; Koizumi, M. ; Ishii, D. and Ohkuma, T., *Pure Appl. Chem.*, 2001, **73**, 227-232.
234. Khusnutdinova, J. R. and Milstein, D., *Angew. Chem. Int. Ed.*, 2015, **54**, 12236-12273.
235. Doucet, H. ; Ohkuma, T. ; Murata, K. ; Yokozawa, T. ; Kozawa, M. ; Katayama, E. ; England, A. F. ; Ikariya, T. and Noyori, R., *Angew. Chem. Int. Ed.*, 1998, **37**, 1703-1707.
236. Nie, H. ; Zhou, G. ; Wang, Q. ; Chen, W. and Zhang, S., *Tetrahedron: Asymmetry*, 2013, **24**, 1567-1571.
237. Nie, H. ; Yao, L. ; Li, B. ; Zhang, S. and Chen, W., *Organometallics*, 2014, **33**, 2109-2114.
238. Yin, C. ; Wu, W. ; Hu, Y. ; Tan, X. ; You, C. ; Liu, Y. ; Chen, Z. ; Dong, X.-Q. and Zhang, X., *Adv. Synth. Catal.*, 2018, **360**, 2119-2124.
239. Wu, W. ; You, C. ; Yin, C. ; Liu, Y. ; Dong, X.-Q. ; Zhang, X. and Zhang, X., *Org. Lett.*, 2017, **19**, 2548-2551.
240. Wang, S. ; Yu, Y. ; Wen, J. and Zhang, X., *Synlett*, 2018, **29**, 2203-2207.
241. Yin, C. ; Dong, X.-Q. and Zhang, X., *Adv. Synth. Catal.*, 2018, **360**, 4319-4324.

242. Gong, Q. ; Wen, J. and Zhang, X., *Chem. Sci.*, 2019, **10**, 6350-6353.
243. Hou, C.-J. and Hu, X.-P., *Org. Lett.*, 2016, **18**, 5592-5595.
244. Dai, H. ; Hu, X. ; Chen, H. ; Bai, C. and Zheng, Z., *J. Mol. Catal. A: Chem.*, 2004, **211**, 17-21.
245. Hu, X. ; Dai, H. ; Bai, C. ; Chen, H. and Zheng, Z., *Tetrahedron: Asymmetry*, 2004, **15**, 1065-1068.
246. Zhang, C. ; Hu, X.-H. ; Wang, Y.-H. ; Zheng, Z. ; Xu, J. and Hu, X.-P., *J. Am. Chem. Soc.*, 2012, **134**, 9585-9588.
247. Li, L. ; Liu, Z.-T. and Hu, X.-P., *Chem. Commun.*, 2018, **54**, 12033-12036.
248. Zhang, C. ; Wang, Y.-H. ; Hu, X.-H. ; Zheng, Z. ; Xu, J. and Hu, X.-P., *Adv. Synth. Catal.*, 2012, **354**, 2854-2858.
249. Zhu, F.-L. ; Wang, Y.-H. ; Zhang, D.-Y. ; Xu, J. and Hu, X.-P., *Angew. Chem. Int. Ed.*, 2014, **53**, 10223-10227.
250. Wang, B. ; Liu, C. and Guo, H., *RSC Adv.*, 2014, **4**, 53216-53219.
251. Xia, J.-T. and Hu, X.-P., *Org. Lett.*, 2020, **22**, 1102-1107.
252. Zirakzadeh, A. ; Kirchner, K. ; Roller, A. ; Stöger, B. ; Carvalho, M. D. and Ferreira, L. P., *RSC Adv.*, 2016, **6**, 11840-11847.
253. Afanasyev, O. I. ; Kuchuk, E. ; Usanov, D. L. and Chusov, D., *Chem. Rev.*, 2019, **119**, 11857-11911.
254. Maryanoff, B. E. and Reitz, A. B., *Chem. Rev.*, 1989, **89**, 863-927.
255. Štěpnička, P. ; Lamač, M. and Císařová, I., *J. Organomet. Chem.*, 2008, **693**, 446-456.
256. a) Ren, W. ; Zuo, Q.-M. and Yang, S.-D., *Synlett*, 2019, **30**, 1719-1724; b) Zhang, L. ; Yang, F. ; Tao, G. ; Qiu, L. ; Duan, Z. and Mathey, F., *Eur. J. Inorg. Chem.*, 2017, **2017**, 2355-2362; c) Zhang, L. ; Liu, C. ; Duan, Z. and Mathey, F., *Eur. J. Inorg. Chem.*, 2017, **2017**, 2504-2509; d) Zhao, Y.-L. ; Wu, G.-J. ; Li, Y. ; Gao, L.-X. and Han, F.-S., *Chemistry – A European Journal*, 2012, **18**, 9622-9627.
257. Fischer, M. ; Barbul, D. ; Schmidtmann, M. and Beckhaus, R., *Organometallics*, 2018, **37**, 1979-1991.
258. Ravindar, V. ; Hemling, H. ; Schumann, H. and Blum, J., *Synth. Commun.*, 1992, **22**, 1453-1459.
259. Kim, S. ; Ginsbach, J. W. ; Lee, J. Y. ; Peterson, R. L. ; Liu, J. J. ; Siegler, M. A. ; Sarjeant, A. A. ; Solomon, E. I. and Karlin, K. D., *J. Am. Chem. Soc.*, 2015, **137**, 2867-2874.
260. Huang, J.-D. ; Hu, X.-P. ; Yu, S.-B. ; Deng, J. ; Wang, D.-Y. ; Duan, Z.-C. and Zheng, Z., *J. Mol. Catal. A: Chem.*, 2007, **270**, 127-131.
261. Li, Q. ; Hou, C.-J. ; Hui, Y.-Z. ; Liu, Y.-J. ; Yang, R.-F. and Hu, X.-P., *RSC Advances*, 2015, **5**, 85879-85883.
262. a) Burns, S. A. ; Corriu, R. J. P. ; Huynh, V. and Moreau, J. J. E., *J. Organomet. Chem.*, 1987, **333**, 281-290; b) Rauk, A., Allen, L.C. and Mislow, K., *Angew. Chem. Int. Ed. Engl*., 1970, **9**, 400-414; c) Ghosh, D.C., Jana, J. and Biswas, R., (2000) *Int. J. Quantum Chem.*, 2000, **80**, 1-26.
263. a) Murray, S. G. and Hartley, F. R., *Chem. Rev.*, 1981, **81**, 365-414; b) Dilworth, J. R. and Wheatley, N., *Coord. Chem. Rev.*, 2000, **199**, 89-158.
264. a) Atkinson, R. C. J. ; Gibson, V. C. and Long, N. J., *Chem. Soc. Rev.*, 2004, **33**, 313-328; b) Colacot, T. J., *Chem. Rev.*, 2003, **103**, 3101-3118.
265. Silvia, C. ; Olga García, M. ; Ramón Gómez, A. ; Inés, A. ; Pablo, M. and Juan, C. C., *Pure Appl. Chem.*, 2006, **78**, 257-265.
266. Gischig, S. and Togni, A., *Organometallics*, 2004, **23**, 2479-2487.
267. a) Togni, A. ; Rihs, G. and Blumer, R. E., *Organometallics*, 1992, **11**, 613-621; b) Togni, A. and Häusel, R., *Synlett*, 1990, **1990**, 633-635.
268. Barbaro, P. ; Bianchini, C. and Togni, A., *Organometallics*, 1997, **16**, 3004-3014.
269. Spencer, J. ; Gramlich, V. ; Häusel, R. and Togni, A., *Tetrahedron: Asymmetry*, 1996, **7**, 41-44.
270. Tu, T. ; Zhou, Y.-G. ; Hou, X.-L. ; Dai, L.-X. ; Dong, X.-C. ; Yu, Y.-H. and Sun, J., *Organometallics*, 2003, **22**, 1255-1265.
271. a) Cheung, H. Y. ; Yu, W.-Y. ; Au-Yeung, T. T. L. ; Zhou, Z. and Chan, A. S. C., *Adv. Synth. Catal.*, 2009, **351**, 1412-1422; b) Lam, F. L. ; Au-Yeung, T. T. L. ; Cheung, H. Y. ; Kok, S. H. L. ; Lam, W. S. ; Wong, K. Y. and Chan, A. S. C., *Tetrahedron: Asymmetry*, 2006, **17**, 497-499.
272. Lam, F. L. ; Kwong, F. Y. and Chan, A. S. C., *Chem. Commun.*, 2010, **46**, 4649-4667.
273. a) Gil, M. V. ; Arevalo, M. J. and Lopez, O., *Synthesis*, 2007, **11**, 1589-1620; b) Kolb, H. C. ; Finn, M. G. and Sharpless, K. B., *Angew. Chem. Int. Ed.*, 2001, **40**, 2004-2021.
274. Fukuzawa, S.-i. ; Oki, H. ; Hosaka, M. ; Sugasawa, J. and Kikuchi, S., *Org. Lett.*, 2007, **9**, 5557-5560.
275. Kato, M. ; Nakamura, T. ; Ogata, K. and Fukuzawa, S.-i., *Eur. J. Org. Chem.*, 2009, **2009**, 5232-5238.
276. Oura, I. ; Shimizu, K. ; Ogata, K. and Fukuzawa, S.-i., *Org. Lett.*, 2010, **12**, 1752-1755.
277. a) Watanabe, S. ; Tada, A. ; Tokoro, Y. and Fukuzawa, S.-i., *Tetrahedron Lett.*, 2014, **55**, 1306-1309; b) Shimizu, K. ; Ogata, K. and Fukuzawa, S.-i., *Tetrahedron Lett.*, 2010, **51**, 5068-5070.

278. Kimura, M. ; Matsuda, Y. ; Koizumi, A. ; Tokumitsu, C. ; Tokoro, Y. and Fukuzawa, S.-i., *Tetrahedron*, 2016, **72**, 2666-2670.
279. Imae, K. ; Konno, T. ; Ogata, K. and Fukuzawa, S.-i., *Org. Lett.*, 2012, **14**, 4410-4413.
280. a) Koizumi, A. ; Harada, M. ; Haraguchi, R. and Fukuzawa, S.-i., *J. Org. Chem.*, 2017, **82**, 8927-8932; b) Konno, T. ; Watanabe, S. ; Takahashi, T. ; Tokoro, Y. and Fukuzawa, S.-i., *Org. Lett.*, 2013, **15**, 4418-4421.
281. Imae, K. ; Shimizu, K. ; Ogata, K. and Fukuzawa, S.-i., *J. Org. Chem.*, 2011, **76**, 3604-3608.
282. Enders, D. ; Peters, R. ; Lochtman, R. ; Raabe, G. ; Runsink, J. and Bats, Jan W., *European Journal of Organic Chemistry*, 2000, **2000**, 3399-3426.
283. a) Enders, D. ; Schäfer, T. and Mies, W., *Tetrahedron*, 1998, **54**, 10239-10252; b) Enders, D. ; Joseph, R. and Poiesz, C., *Tetrahedron*, 1998, **54**, 10069-10078.
284. Enders, D. ; Peters, R. ; Lochtman, R. and Raabe, G., *Angew. Chem. Int. Ed.*, 1999, **38**, 2421-2423.
285. Enders, D. ; Peters, R. ; Lochtman, R. and Runsink, J., *Synlett*, 1997, **12**, 1462-1464.
286. a) Enders, D. ; Peters, R. ; Lochtman, R. ; Raabe, G. ; Runsink, J. and Bats, Jan W., *Eur. J. Org. Chem.*, 2000, 3399-3426; b) Enders, D. ; Peters, R. ; Runsink, J. and Bats, J. W., *Org. Lett.*, 1999, **1**, 1863-1866.
287. Mancheño, O. G. ; Priego, J. ; Cabrera, S. ; Arrayás, R. G. ; Llamas, T. and Carretero, J. C., *J. Org. Chem.*, 2003, **68**, 3679-3686.
288. a) Diter, P. ; Samuel, O. ; Taudien, S. and Kagan, H. B., *Tetrahedron: Asymmetry*, 1994, **5**, 549-552; b) Rebière, F. ; Riant, O. ; Ricard, L. and Kagan, H. B., *Angewandte Chemie International Edition in English*, 1993, **32**, 568-570.
289. Cabrera, S. ; García Mancheño, O. ; Gómez Arrayás, R. ; Alonso, I. ; Mauleón, P. and Carretero, J. C., *Pure Appl. Chem.*, 2006, **78**, 257-265.
290. Priego, J. ; Mancheño, O. G. ; Cabrera, S. ; Arrayás, R. G. ; Llamas, T. and Carretero, J. C., *Chem. Commun.*, 2002, 2512-2513.
291. a) Cabrera, S. ; Arrayás, R. G. ; Alonso, I. and Carretero, J. C., *J. Am. Chem. Soc.*, 2005, **127**, 17938-17947; b) Cabrera, S. ; Gómez Arrayás, R. and Carretero, J. C., *Angew. Chem. Int. Ed.*, 2004, **43**, 3944-3947.
292. Mancheño, O. G. ; Arrayás, R. G. and Carretero, J. C., *J. Am. Chem. Soc.*, 2004, **126**, 456-457.
293. a) Molina, A. ; Pascual-Escudero, A. ; Adrio, J. and Carretero, J. C., *J. Org. Chem.*, 2017, **82**, 11238-11246; b) Pascual-Escudero, A. ; de Cózar, A. ; Cossío, F. P. ; Adrio, J. and Carretero, J. C., *Angew. Chem. Int. Ed.*, 2016, **55**, 15334-15338; c) López-Pérez, A. ; Adrio, J. and Carretero, J. C., *J. Am. Chem. Soc.*, 2008, **130**, 10084-10085; d) Cabrera, S. ; Arrayás, R. G. and Carretero, J. C., *J. Am. Chem. Soc.*, 2005, **127**, 16394-16395.
294. a) Corpas, J. ; Ponce, A. ; Adrio, J. and Carretero, J. C., *Org. Lett.*, 2018, **20**, 3179-3182; b) Hernández-Toribio, J. ; Arrayás, R. G. ; Martín-Matute, B. and Carretero, J. C., *Org. Lett.*, 2009, **11**, 393-396.
295. a) Salvador González, A. ; Gómez Arrayás, R. ; Rodríguez Rivero, M. and Carretero, J. C., *Org. Lett.*, 2008, **10**, 4335-4337; b) González, A. S. ; Arrayás, R. G. and Carretero, J. C., *Org. Lett.*, 2006, **8**, 2977-2980.
296. a) Kreindlin, A. Z. ; Dolgushin, F. M. ; Yanovsky, A. I. ; Kerzina, Z. A. ; Petrovskii, P. V. and Rybinskaya, M. I., *Journal of Organometallic Chemistry*, 2000, **616**, 106-111; b) Brunner, A. ; Taudien, S. ; Riant, O. and Kagan, H. B., *Chirality*, 1997, **9**, 478-486; c) Richards, C. J. ; Hibbs, D. and Hursthouse, M. B., *Tetrahedron Letters*, 1994, **35**, 4215-4218.
297. Stewart, B. ; Harriman, A. and Higham, L. J., *Organometallics*, 2011, **30**, 5338-5343.
298. Curran, D. P. ; Yang, F. and Cheong, J.-h., *Journal of the American Chemical Society*, 2002, **124**, 14993-15000.
299. McNulty, J. and Keskar, K., *Tetrahedron Letters*, 2008, **49**, 7054-7057.
300. Blume, F. ; Zemolka, S. ; Fey, T. ; Kranich, R. and Schmalz, H.-G., *Advanced Synthesis & Catalysis*, 2002, **344**, 868-883.
301. Wujkowska, Z. ; Zawisza, A. ; Leśniak, S. and Rachwalski, M., *Tetrahedron*, 2019, **75**, 230-235.
302. McNulty, J. and Keskar, K., *European Journal of Organic Chemistry*, 2012, **2012**, 5462-5470.
303. Boechat, N. ; da Costa, J. C. S. ; de Souza Mendonça, J. ; de Oliveira, P. S. M. and Vinícius Nora De Souza, M., *Tetrahedron Letters*, 2004, **45**, 6021-6022.
304. Neuvonen, A. J. ; Földes, T. ; Madarász, Á. ; Pápai, I. and Pihko, P. M., *ACS. Catal.*, 2017, **7**, 3284-3294.
305. Cremer, D. and Pople, J. A., *J. Am. Chem. Soc.*, 1975, **97**, 1354-1358.
306. a) Aparna, E. ; Rai, K. M. L. ; Sureshbabu, M. ; Jagadish, R. L. ; Gaonkar, S. L. and Byrappa, K., *Journal of Materials Science*, 2006, **41**, 1391-1393; b) Kellogg, R. M. ; Nieuwenhuijzen, J. W. ; Pouwer, K. ; Vries, T. R. ; Broxterman, Q. B. ; Grimbergen, R. F. P. ; Kaptein, B. ; Crois, R. M. L. ; de Wever, E. ; Zwaagstra, K. and van der Laan, A. C., *Synthesis*, 2003, **2003**, 1626-1638; c) Frank, R. L. and Smith, P. V., *Journal of the American Chemical Society*, 1946, **68**, 2103-2104.

307. a) Nishio, T., *J. Chem. Soc., Perkin Trans. 1*, 1993, 1113-1117; b) Cava, M. P. and Levinson, M. I., *Tetrahedron*, 1985, **41**, 5061-5087.
308. a) in *Organic Reactions*, pp. 335-656; b) Amorati, R. ; Lynett, P. T. ; Valgimigli, L. and Pratt, D. A., *Chemistry – A European Journal*, 2012, **18**, 6370-6379; c) Gauthier, J. Y. ; Bourdon, F. and Young, R. N., *Tetrahedron Letters*, 1986, **27**, 15-18.
309. a) Volante, R. P., *Tetrahedron Lett.*, 1981, **22**, 3119-3122; b) Han, C.-C. and Balakumar, R., *Tetrahedron Letters*, 2006, **47**, 8255-8258; c) Tewari, N. ; Nizar, H. ; Mane, A. ; George, V. and Prasad, M., *Synthetic Communications*, 2006, **36**, 1911-1914.
310. Bandgar, B. P. ; Sadavarte, V. S. and Uppalla, L. S., *Chemistry Letters*, 2000, **29**, 1304-1305.
311. Bandgar, B. P. and Sadavarte, V. S., *Synlett*, 2000, **2000**, 0908-0910.
312. P. Bandgar, B. and B. Pawar, S., *Journal of Chemical Research, Synopses*, 1998, 212-213.
313. a) Mitsunobu, O. ; Wada, M. and Sano, T., *Journal of the American Chemical Society*, 1972, **94**, 679-680; b) Mitsunobu, O. and Eguchi, M., *Bulletin of the Chemical Society of Japan*, 1971, **44**, 3427-3430.
314. Rozwadowska, M. D., *Tetrahedron*, 1997, **53**, 10615-10622.
315. Fausto, R. ; De Carvalho, L. A. E. B. and Teixeira-Dias, J. J. C., *J. Mol. Struct. (Theochem.)*, 1990, **207**, 67-83.
316. a) Zheng, T.-C. ; Burkart, M. and Richardson, D. E., *Tetrahedron Letters*, 1999, **40**, 603-606; b) Ohlsson, J. and Magnusson, G., *Tetrahedron Letters*, 1999, **40**, 2011-2014; c) Yeager, L. J. ; Amirsakis, D. G. ; Newman, E. and Garrell, R. L., *Tetrahedron Letters*, 1998, **39**, 8409-8412; d) Li, W. ; Lynch, V. ; Thompson, H. and Fox, M. A., *Journal of the American Chemical Society*, 1997, **119**, 7211-7217.
317. Yu, M. ; Xie, Y. ; Xie, C. and Zhang, Y., *Org. Lett.*, 2012, **14**, 2164-2167.
318. *Rigaku Oxford Diffraction (2015). CrysAlis PRO. Rigaku Oxford Diffraction Ltd, Yarnton, England*.
319. *Bruker (2015). APEX2 and SAINT. Bruker Nano Inc., Madison, Wisconsin, USA.*
320. Sheldrick, G., *Acta Crystallogr., A71*, 2015, 3-8.
321. Sheldrick, G., *Acta Crystallogr., C71*, 2015, **71**, 3-8.
322. a) Flack, H. D. and Bernardinelli, G., *Acta Crystallogr., A55*, 1999, 908-915; b) Parsons, S., *Tetrahedron: Asymmetry*, 2017, **28**, 1304-1313.
323. a) Farrugia, L., *J. Appl. Crystallogr.*, 1997, **30**, 565; b) Burnett, M. N., Johnson, C.K., *ORTEPIII. Report ORNL-6895, 1996, Oak Ridge National Laboratory, Tennessee, USA.*

Annexes

A- 1) Planar Chirality of di-Substituted Ferrocenes- Nomenclature

Ferrocene derivatives having at least two different substituents, **A** and **B**, attached to the same cyclopentadienyl ring on the 1,2- or, 1,3- position to each other; are chiral. This means, such a compound can exist as two enantiomers, one being mirror-image to the other (Scheme A-1. 1).

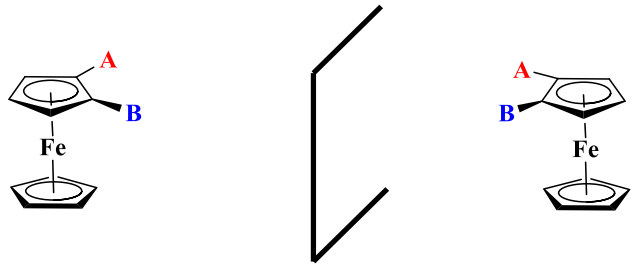

Scheme A-1. 1: General chemical structure of enantiomers of 1,2-disubstituted ferrocene compounds

The chirality associated with these kinds of compounds appears due to the presence of the complex Fe (C_5H_5)- group on the disubstituted cyclopentadienyl ring; resulting the disappearance of the plane of symmetry. This type of asymmetry is known as **'Planar Chirality'.** For the notation of the absolute configuration of planar chirality, the method proposed by Schlögl[a] is usually followed.

The priority order of the substituents attached to a Cp ring is mainly determined by the standard C.I.P. rule.[b] Now, for the determination of absolute configuration of a Cp ring, the molecule is looked at along the axis passing through the Fe atom. The part of the ring to be studied (which contains the 1,2- disubstitution) is placed in the front and thus the rest of the molecular backbone positioned in the back automatically. We then follow what the rotation along the axis sounds considering the decreasing order of the priority of the substituents. A clockwise sequence determines the *(R)*-configuration and a counter-clockwise sequence determines the *(S)*-configuration.

As an illustration (given below in Scheme A-1. 2), we have chosen a tetra-substituted ferrocene with two substituents **A** and **B** (**A**> **B**) in position 1 and 2. There are rather three stereoisomers that fit this structure than one single compound. The first two *(R, R′)* and *(S, S′)* constitute a pair of enantiomers. They have C2 symmetry and they are chiral.

References-

[a] Schlögl, K. In Topics in Stereochemistry; Allinger, N.L.; Eliel, E.L., Eds,; John Wiley & Sons, Inc., 2007; 39-91.
[b] Cahn, R.S.; Ingold, C.; Prelog, V. *Angew. Chem. Int. Ed. Engl.* **1966**, 5, 385-415.

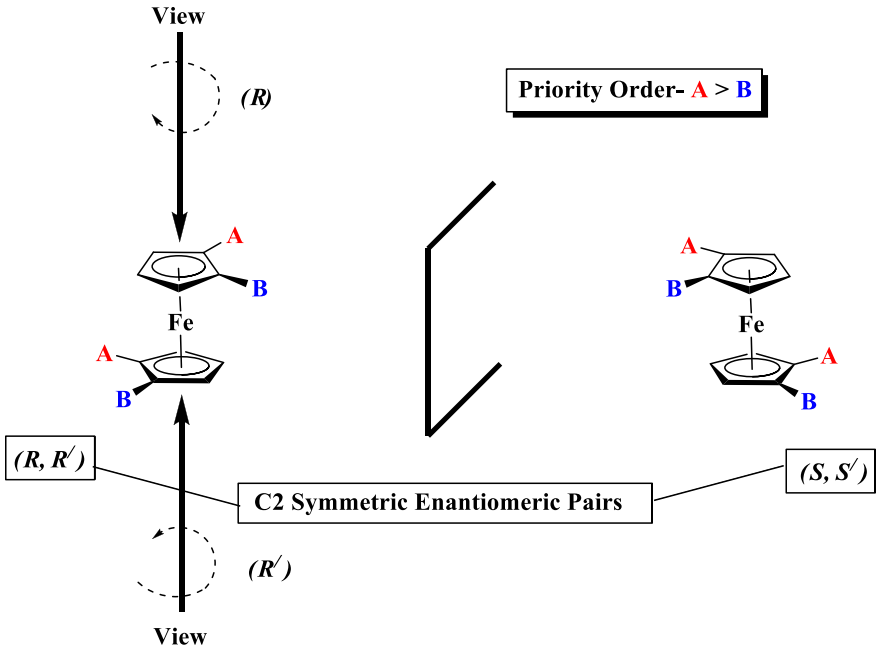

Scheme A-1. 2: Illustration of chirality nomencleature in substituted ferrocenes

The third one- *(R, S′)* and *(S, R′)* is not chiral because they are superimposable mirror images to each other. Hence, this is the *meso*- isomer (Scheme A-1. 3).

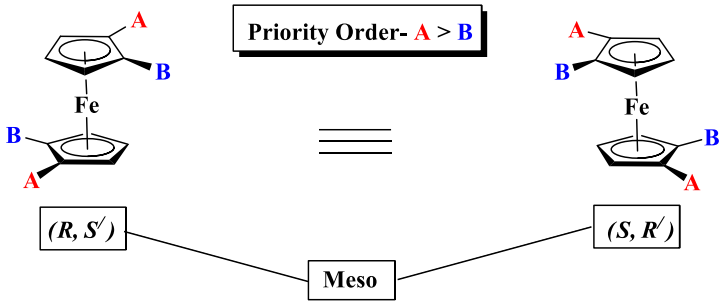

Scheme A-1. 3: Two identical forms of meso isomer of substituted ferrocenes

For the ferrocenyl compounds which contain several types chirality elements (Planar Chirality, Central Chirality, Axial Chirality), the order that to be respected for the writing of the configurations is as follows:

Central Chirality> Axial Chirality> Planar Chirality

Thus, a derivative having an *(S)*-configuration on the asymmetric carbon atom and a planar chirality of *(R)*-configuration will be denoted *(S, R)*.[c]

[c] Marquarding, D.; Klusacek, H.; Gokel, G.; Hoffmann, P. and Ugi, I., *J. Am. Chem. Soc.*, 1970, **92**, 5389-5393.

A- 2) Table of X-ray Data

Table of X- ray Data: Chapter-2

Crystal data and structure refinement for 2-28a

Identification code	**2-28a**
Empirical formula	C_{30} H_{29} Fe N_2 P S
Formula weight	536.43
Temperature, K	173(2)
Wavelength, Å	1.54184
Crystal system	Orthorhombic
Space group	P $2_12_12_1$
a, Å	10.50290(10)
b, Å	14.2573(2)
c, Å	17.1197(3)
α, °	90.0
β, °	90.0
γ, °	90.0
Volume, $Å^3$	2563.56(6)
Z	4
Density (calc), Mg/m^3	1.390
Abs. coefficient, mm^{-1}	6.228
F(000)	1120
Crystal size, mm^3	0.25, 0.28, 0.28
Theta range, °	4.035 - 61.531.
Reflections collected	11452
Indpt reflections (R_{int})	3918 (0.0287)
Absorption correction	Sphere
Max. / min. transmission	0.14457 / 0.06312
Refinement method	F^2
Data /restraints/parameters	3918 / 0 / 317
Goodness-of-fit on F^2	1.028
R1, wR2 [I>2σ(I)]	0.0265, 0.0654
R1, wR2 (all data)	0.0282, 0.0666
Absolute configuration parameter	-0.013(2)

Residual density, e.Å^{-3}	0.285 / -0.144

Bond lengths [Å] and angles [°] for **2-28a**

Fe(1)-Cg(1)	1.638(2)	Fe(1)- Cg (2)	1.659(2)
P(1)-C(111)	1.831(3)	P(1)-C(121)	1.820(3)
P(1)-S(1)	1.9567(12)	P(1)-C(1)	1.800(3)
N(1)-C(28)	1.463(4)		
N(1)-C(21)	1.470(4)	N(1)-C(22)	1.459(4)
N(2)-C(23)	1.342(4)	N(2)-C(27)	1.336(5)
C(2)-C(21)	1.486(5)	C(24)-C(25)	1.375(5)
C(22)-C(23)	1.510(5)	C(25)-C(26)	1.379(6)
C(23)-C(24)	1.381(5)	C(26)-C(27)	1.369(6)
C(111)-C(112)	1.389(5)	C(121)-C(122)	1.388(5)
C(111)-C(116)	1.393(5)	C(121)-C(126)	1.389(5)
C(112)-C(113)	1.382(5)	C(122)-C(123)	1.386(5)
C(113)-C(114)	1.386(5)	C(123)-C(124)	1.379(7)
C(114)-C(115)	1.380(5)	C(124)-C(125)	1.374(7)
C(115)-C(116)	1.376(5)	C(125)-C(126)	1.383(6)

C(1)-P(1)-S(1)	116.93(12)	Cg(1)-Fe(1)-Cg(2)	177.50(9)
C(121)-P(1)-S(1)	112.16(12)	C(1)-P(1)-C(121)	106.17(15)
C(111)-P(1)-S(1)	112.97(11)	C(1)-P(1)-C(111)	103.04(15)
C(22)-N(1)-C(28)	110.4(3)	C(121)-P(1)-C(111)	104.40(15)
C(22)-N(1)-C(21)	110.6(3)	C(28)-N(1)-C(21)	111.8(3)
C(2)-C(1)-P(1)	127.3(2)	C(27)-N(2)-C(23)	116.6(3)
C(1)-C(2)-C(21)	128.1(3)	C(5)-C(1)-P(1)	125.3(3)
N(1)-C(21)-C(2)	112.1(3)	C(3)-C(2)-C(21)	125.0(3)
N(2)-C(23)-C(22)	115.4(3)	N(1)-C(22)-C(23)	113.7(3)
N(2)-C(27)-C(26)	124.5(3)	N(2)-C(23)-C(24)	122.6(3)
C(25)-C(24)-C(23)	119.3(3)	C(24)-C(23)-C(22)	121.9(3)
C(27)-C(26)-C(25)	118.1(3)	C(24)-C(25)-C(26)	118.8(4)
C(112)-C(111)-C(116)	119.5(3)	C(122)-C(121)-C(126)	119.2(3)
C(112)-C(111)-P(1)	119.6(3)	C(122)-C(121)-P(1)	121.4(3)
C(116)-C(111)-P(1)	120.9(2)	C(126)-C(121)-P(1)	119.4(3)

C(113)-C(112)-C(111)	120.0(3)	C(123)-C(122)-C(121)	120.2(4)
C(112)-C(113)-C(114)	120.1(3)	C(124)-C(123)-C(122)	120.0(4)
C(115)-C(114)-C(113)	120.1(3)	C(125)-C(124)-C(123)	120.2(4)
C(116)-C(115)-C(114)	120.2(3)	C(124)-C(125)-C(126)	120.1(4)
C(115)-C(116)-C(111)	120.2(3)	C(125)-C(126)-C(121)	120.3(4)

Hydrogen bonds for **2-28a** [Å and °].

D-H...A	d(D-H)	d(H...A)	d(D...A)	<(DHA)
C(21)-H(21B)...S(1)	0.97	2.97	3.679(3)	131.1
C(112)-H(112)...S(1)	0.93	2.92	3.391(4)	113.0
C(126)-H(126)...S(1)	0.93	2.94	3.388(4)	111.1

Symmetry transformations used to generate equivalent atoms:

Crystal data and structure refinement for 2-28c

Identification code	**2-28c**
Empirical formula	C_{36} H_{33} Fe N_2 O_2 P S_2
Formula weight	676.58
Temperature, K	100(2)
Wavelength, Å	0.71073
Crystal system	Monoclinic
Space group	$P2_1$
a, Å	9.8327(3)
b, Å	13.4161(5)
c, Å	12.3211(4)
α, °	90.0
β, °	97.364(3)
γ, °	90.0
Volume, $Å^3$	1611.95(9)
Z	2
Density (calc), Mg/m^3	1.394

Abs. coefficient, mm^{-1}	0.683
F(000)	704
Crystal size, mm^3	0.500 x 0.350 x 0.090
Theta range, °	1.667 to 31.264
Reflections collected	36932
Indpt reflections (R_{int})	10445 (0.050)
Absorption correction	Multiscan
Max. / min. transmission	0.7462 / 0.6581
Refinement method	F^2
Data /restraints/parameters	10445 / 0 / 398
Goodness-of-fit on F^2	1.069
R1, wR2 [I>2σ(I)]	0.0349, 0.0793
R1, wR2 (all data)	0.0476, 0.1024
Absolute configuration parameter	-0.004(6)
Residual density, $e.Å^{-3}$	0.573 / -0.502

Bond lengths [Å] and angles [°] for **2-28c**

Ct(1)-Fe(1)	1.666(8)	Ct(2)-Fe(1)	1.675(9)
P(1)-C(1)	1.807(3)	P(1)-S(1)	1.9757(9)
P(1)-C(111)	1.829(3)	P(1)-C(121)	1.835(3)
S(2)-O(1)	1.447(2)	S(2)-N(1)	1.659(2)
S(2)-O(2)	1.448(2)	S(2)-C(211)	1.782(3)
N(1)-C(21)	1.497(3)	N(1)-C(22)	1.473(3)
N(2)-C(221)	1.354(4)	N(2)-C(225)	1.355(4)
C(2)-C(21)	1.524(3)	C(22)-C(221)	1.526(4)
C(111)-C(112)	1.405(4)	C(121)-C(122)	1.410(4)
C(111)-C(116)	1.407(4)	C(121)-C(126)	1.417(4)
C(112)-C(113)	1.407(4)	C(122)-C(123)	1.411(4)
C(113)-C(114)	1.395(5)	C(123)-C(124)	1.400(4)
C(114)-C(115)	1.400(5)	C(124)-C(125)	1.408(5)
C(115)-C(116)	1.409(4)	C(125)-C(126)	1.394(5)
C(211)-C(212)	1.403(4)	C(214)-C(217)	1.517(4)
C(211)-C(216)	1.407(4)	C(221)-C(222)	1.407(4)
C(212)-C(213)	1.405(4)	C(222)-C(223)	1.405(5)

C(213)-C(214)	1.411(4)	C(223)-C(224)	1.396(6)
C(214)-C(215)	1.411(4)	C(224)-C(225)	1.397(5)
C(215)-C(216)	1.401(4)		

C(1)-P(1)-C(111)	102.34(12)	C(1)-P(1)-S(1)	116.72(9)
C(1)-P(1)-C(121)	105.10(12)	C(111)-P(1)-S(1)	113.53(9)
C(111)-P(1)-C(121)	106.64(12)	C(121)-P(1)-S(1)	111.53(9)
O(1)-S(2)-O(2)	120.47(13)	O(1)-S(2)-C(211)	107.77(12)
O(1)-S(2)-N(1)	106.48(12)	O(2)-S(2)-C(211)	107.37(13)
O(2)-S(2)-N(1)	106.41(13)	N(1)-S(2)-C(211)	107.77(12)
C(22)-N(1)-C(21)	115.5(2)	C(22)-N(1)-S(2)	116.78(18)
C(21)-N(1)-S(2)	117.23(18)	C(221)-N(2)-C(225)	117.2(3)
C(2)-C(1)-P(1)	126.95(18)	C(5)-C(1)-P(1)	125.6(2)
C(1)-C(2)-C(21)	125.5(2)	C(3)-C(2)-C(21)	126.5(2)
N(1)-C(21)-C(2)	112.1(2)	N(1)-C(22)-C(221)	110.4(2)
C(112)-C(111)-C(116)	119.1(2)	C(122)-C(121)-C(126)	119.2(3)
C(112)-C(111)-P(1)	118.2(2)	C(122)-C(121)-P(1)	121.1(2)
C(116)-C(111)-P(1)	122.5(2)	C(126)-C(121)-P(1)	119.8(2)
C(111)-C(112)-C(113)	120.4(3)	C(121)-C(122)-C(123)	120.2(3)
C(114)-C(113)-C(112)	120.1(3)	C(124)-C(123)-C(122)	120.1(3)
C(113)-C(114)-C(115)	120.1(3)	C(123)-C(124)-C(125)	119.8(3)
C(114)-C(115)-C(116)	119.9(3)	C(126)-C(125)-C(124)	120.5(3)
C(111)-C(116)-C(115)	120.3(3)	C(125)-C(126)-C(121)	120.3(3)
C(212)-C(211)-C(216)	120.9(3)	C(215)-C(216)-C(211)	119.1(3)
C(212)-C(211)-S(2)	119.50(19)	N(2)-C(221)-C(222)	123.0(3)
C(216)-C(211)-S(2)	119.6(2)	N(2)-C(221)-C(22)	115.9(2)
C(211)-C(212)-C(213)	119.3(2)	C(222)-C(221)-C(22)	121.1(3)
C(212)-C(213)-C(214)	120.9(3)	C(223)-C(222)-C(221)	118.8(3)
C(215)-C(214)-C(213)	118.6(3)	C(224)-C(223)-C(222)	118.5(3)
C(215)-C(214)-C(217)	120.2(2)	C(225)-C(224)-C(223)	118.8(3)
C(213)-C(214)-C(217)	121.2(3)	N(2)-C(225)-C(224)	123.7(3)
C(216)-C(215)-C(214)	121.2(2)	Ct(1)-Fe(1)-Ct(2)	177.1(4)

Hydrogen bonds for **2-28c** [Å and °].

D-H...A	d(D-H)	d(H...A)	d(D...A)	<(DHA)
C(126)-H(126)...S(1)	0.95	2.91	3.381(3)	112.1
C(225)-H(225)...O(1)#1	0.95	2.59	3.416(4)	145.3
C(217)-H(21C)...O(2)#2	0.98	2.55	3.369(4)	141.0
C(4)-H(4)...CT1#1	0.95	2.76	3.670(6)	159.6
C(212)-H(212)...CT2	0.95	2.68	3.538(3)	151.1

Symmetry transformations used to generate equivalent atoms:

#1 -x+1,y-1/2,-z+1 #2 -x+2,y+1/2,-z+1

Crystal data and structure refinement for 2-43b

Identification code	**2-43b**
Empirical formula	C_{14} H_{15} N O_4 S
Formula weight	293.33
Temperature, K	107(2)
Wavelength, Å	0.71073
Crystal system	Monoclinic
Space group	$P2_1/n$
a, Å	10.9829(17)
b, Å	6.9149(11)
c, Å	18.064(3)
α, °	90.0
β, °	91.615(5)
γ, °	90.0
Volume, Å3	1371.3(4)
Z	4
Density (calc), Mg/m^3	1.421
Abs. coefficient, mm^{-1}	0.249
F(000)	616
Crystal size, mm^3	0.12 x 0.09 x 0.07
Theta range, °	2.144 to 26.369
Reflections collected	27549

Indpt reflections (R_{int})	2813 (0.0563)
Absorption correction	Multi-scan
Max. / min. transmission	0.7473 / 0.6941
Refinement method	F^2
Data /restraints/parameters	2813 / 0 / 182
Goodness-of-fit on F^2	1.029
R1, wR2 [I>2σ(I)]	0.0303, 0.0769
R1, wR2 (all data)	0.0377, 0.0804
Residual density, e.$Å^{-3}$	n/a
Identification code	0.371 / -0.394

Bond lengths [Å] and angles [°] for **2-43b**

S(1)-O(3)	1.4271(11)	S(1)-O(1)	1.5784(11)
S(1)-O(2)	1.4313(11)	S(1)-C(11)	1.7571(14)
O(4)-C(6)	1.3572(18)	O(4)-C(7)	1.4400(19)
N(1)-C(2)	1.3557(19)	N(1)-C(6)	1.321(2)
C(1)-C(2)	1.499(2)	O(1)-C(1)	1.4789(18)
C(2)-C(3)	1.385(2)	C(4)-C(5)	1.379(2)
C(3)-C(4)	1.396(2)	C(5)-C(6)	1.405(2)
C(11)-C(12)	1.389(2)	C(14)-C(15)	1.400(2)
C(11)-C(16)	1.391(2)	C(14)-C(17)	1.504(2)
C(12)-C(13)	1.388(2)	C(15)-C(16)	1.383(2)
C(13)-C(14)	1.393(2)		

O(3)-S(1)-O(2)	119.68(7)	O(3)-S(1)-C(11)	110.25(7)
O(3)-S(1)-O(1)	103.80(6)	O(2)-S(1)-C(11)	108.93(7)
O(2)-S(1)-O(1)	109.68(6)	O(1)-S(1)-C(11)	103.17(6)
C(1)-O(1)-S(1)	117.02(9)	C(6)-N(1)-C(2)	117.03(13)
C(6)-O(4)-C(7)	116.56(12)	O(1)-C(1)-C(2)	106.41(12)
N(1)-C(2)-C(1)	115.43(14)	N(1)-C(2)-C(3)	123.22(15)
C(3)-C(2)-C(1)	121.35(14)	C(5)-C(4)-C(3)	119.64(15)
C(2)-C(3)-C(4)	118.25(14)	C(4)-C(5)-C(6)	117.37(15)
N(1)-C(6)-O(4)	119.50(13)	C(12)-C(11)-S(1)	119.66(11)
N(1)-C(6)-C(5)	124.47(14)	C(16)-C(11)-S(1)	118.84(11)

O(4)-C(6)-C(5)	116.03(14)	C(13)-C(12)-C(11)	118.81(13)
C(12)-C(11)-C(16)	121.47(13)	C(15)-C(14)-C(17)	120.80(13)
C(12)-C(13)-C(14)	121.03(14)	C(16)-C(15)-C(14)	121.00(13)
C(13)-C(14)-C(15)	118.83(13)	C(15)-C(16)-C(11)	118.84(13)
C(13)-C(14)-C(17)	120.36(13)		

Hydrogen bonds for **2-43b** [Å and °].

D-H...A	d(D-H)	d(H...A)	d(D...A)	<(DHA)
C(1)-H(1A)...O(2)#1	0.99	2.53	3.1197(19)	117.9

Symmetry transformations used to generate equivalent atoms:

#1 -x+1/2,y-1/2,-z+1/2

Crystal data and structure refinement for 2-42b

Identification code	**2-42b**
Empirical formula	C_{26} H_{28} Fe N P S
Formula weight	473.37
Temperature, K	110(2)
Wavelength, Å	0.71073
Crystal system	Orthorhombic
Space group	$P2_12_12_1$
a, Å	9.284(2)
b, Å	14.364(3)
c, Å	17.128(4)
α, °	90.0
β, °	90.0

γ, °	90.0
Volume, $Å^3$	2284.1(8)
Z	4
Density (calc), Mg/m^3	1.377
Abs. coefficient, mm^{-1}	0.835
F(000)	992
Crystal size, mm^3	0.200 x 0.200 x 0.180
Theta range, °	1.850 to 35.224
Reflections collected	131041
Indpt reflections (R_{int})	9852 (0.0399)
Absorption correction	Multi-scan
Max. / min. transmission	0.7469 / 0.6982
Refinement method	F^2
Data /restraints/parameters	9852 / 0 / 276
Goodness-of-fit on F^2	1.180
R1, wR2 [I>2σ(I)]	0.0294, 0.0841
R1, wR2 (all data)	0.0312, 0.0867
Absolute configuration parameter	-0.002(4)
Residual density, $e.Å^{-3}$	0.714 and -0.457

Bond lengths [Å] and angles [°] for **2-42b**

Ct(1)-Fe(1)	1.649(1)	Ct(2)-Fe(1)	1.655(1)

S(1)-P(1)	1.9606(6)	P(1)-C(1)	1.7892(16)
P(1)-C(111)	1.8181(17)	P(1)-C(121)	1.8173(15)
N(1)-C(21)	1.468(2)	N(1)-C(22)	1.468(2)
C(2)-C(21)	1.498(2)		
C(22)-C(23)	1.523(3)	C(22)-C(24)	1.528(3)
C(111)-C(112)	1.402(3)	C(121)-C(122)	1.402(2)
C(111)-C(116)	1.405(3)	C(121)-C(126)	1.402(2)
C(112)-C(113)	1.401(3)	C(122)-C(123)	1.398(3)
C(113)-C(114)	1.393(4)	C(123)-C(124)	1.388(3)
C(114)-C(115)	1.392(4)	C(124)-C(125)	1.397(3)
C(115)-C(116)	1.397(3)	C(125)-C(126)	1.393(2)

C(1)-P(1)-S(1)	117.33(5)	C(1)-P(1)-C(121)	104.55(7)
C(121)-P(1)-S(1)	112.60(6)	C(1)-P(1)-C(111)	104.51(8)
C(111)-P(1)-S(1)	111.61(6)	C(121)-P(1)-C(111)	105.19(7)
C(21)-N(1)-C(22)	113.23(15)	Ct(1)-Fe(1)-Ct(2)	178.59(5)
C(2)-C(1)-P(1)	128.76(12)	C(5)-C(1)-P(1)	123.94(11)
C(1)-C(2)-C(21)	126.81(15)	C(3)-C(2)-C(21)	125.75(15)
N(1)-C(21)-C(2)	111.54(15)	N(1)-C(22)-C(23)	108.86(16)
C(23)-C(22)-C(24)	110.76(18)	N(1)-C(22)-C(24)	110.61(18)
C(112)-C(111)-C(116)	119.59(16)	C(122)-C(121)-C(126)	119.80(14)
C(112)-C(111)-P(1)	121.65(14)	C(122)-C(121)-P(1)	119.57(12)
C(116)-C(111)-P(1)	118.75(14)	C(126)-C(121)-P(1)	120.63(12)

C(113)-C(112)-C(111)	120.2(2)	C(123)-C(122)-C(121)	119.72(17)
C(114)-C(113)-C(112)	119.6(2)	C(124)-C(123)-C(122)	120.25(17)
C(115)-C(114)-C(113)	120.69(19)	C(123)-C(124)-C(125)	120.26(16)
C(114)-C(115)-C(116)	120.0(2)	C(126)-C(125)-C(124)	119.96(17)
C(115)-C(116)-C(111)	119.9(2)	C(125)-C(126)-C(121)	120.01(16)

Hydrogen bonds for **2-42b** [Å and °].

D-H...A	d(D-H)	d(H...A)	d(D...A)	<(DHA)
C(122)-H(122)...S(1)	0.95	2.86	3.3504(19)	113.3

Symmetry transformations used to generate equivalent atoms:

Crystal data and structure refinement for 2-51b

Identification code	**2-51b**
Empirical formula	$(C_{49}H_{46}Fe_2NP_2S_2)_2$, CH_2Cl_2
Formula weight	1858.18
Temperature, K	150(2)
Wavelength, Å	1.54184
Crystal system	Monoclinic
Space group	P 2_1
a, Å	8.7681(3)
b, Å	35.9828(11)
c, Å	14.2050(6) Å
α, °	90.0
β, °	92.436(4)
γ, °	90.0
Volume, $Å^3$	4477.6(3)
Z	2
Density (calc), Mg/m^3	1.378

Abs. coefficient, mm^{-1}	7.557
F(000)	1928
Crystal size, mm^3	0.250 x 0.030 x 0.020
Theta range, °	3.114 to 71.572
Reflections collected	16795
Indpt reflections (R_{int})	11457 (0.0653)
Absorption correction	Multi-scan
Max. / min. transmission	1.0 / 0.41383
Refinement method	F^2
Data /restraints/parameters	11457 / 1 / 1016
Goodness-of-fit on F^2	0.969
R1, wR2 [I>2σ(I)]	0.0641, 0.1173
R1, wR2 (all data)	0.0926, 0.1414
Absolute structure parameter	-0.013(6)
Residual density, $e.Å^{-3}$	0.628 / -0.529

Bond lengths [Å] and angles [°] for **2-51b**

Molecule A		**Molecule B**	
S(1)-P(1)	1.953(4)	S(3)-P(3)	1.945(4)
S(2)-P(2)	1.952(4)	S(4)-P(4)	1.953(4)
P(1)-C(11)	1.776(10)	P(3)-C(31)	1.786(10)
P(1)-C(121)	1.824(12)	P(3)-C(311)	1.809(12)
P(1)-C(111)	1.835(11)	P(3)-C(321)	1.826(13)
P(2)-C(21)	1.794(10)	P(4)-C(41)	1.795(10)
P(2)-C(211)	1.807(10)	P(4)-C(411)	1.797(12)
P(2)-C(221)	1.823(12)	P(4)-C(421)	1.822(10)
N(1)-C(1)	1.449(12)	N(2)-C(3)	1.465(12)
N(1)-C(2)	1.463(12)	N(2)-C(4)	1.482(12)
N(1)-C(131)	1.473(12)	N(2)-C(231)	1.478(13)
C(1)-C(12)	1.526(14)	C(3)-C(32)	1.484(13)
C(2)-C(22)	1.512(12)	C(4)-C(42)	1.501(13)
C(111)-C(116)	1.366(16)	C(311)-C(316)	1.348(19)
C(111)-C(112)	1.374(16)	C(311)-C(312)	1.398(18)

C(112)-C(113)	1.418(18)	C(312)-C(313)	1.391(19)
C(113)-C(114)	1.372(19)	C(313)-C(314)	1.36(2)
C(114)-C(115)	1.359(19)	C(314)-C(315)	1.37(3)
C(115)-C(116)	1.400(17)	C(315)-C(316)	1.41(2)
C(121)-C(122)	1.372(18)	C(321)-C(326)	1.373(18)
C(121)-C(126)	1.398(17)	C(321)-C(322)	1.385(19)
C(122)-C(123)	1.40(2)	C(322)-C(323)	1.417(18)
C(123)-C(124)	1.35(2)	C(323)-C(324)	1.39(2)
C(124)-C(125)	1.35(2)	C(324)-C(325)	1.35(2)
C(125)-C(126)	1.420(17)	C(325)-C(326)	1.34(2)
C(211)-C(212)	1.372(16)	C(411)-C(416)	1.381(16)
C(211)-C(216)	1.398(15)	C(411)-C(412)	1.406(17)
C(212)-C(213)	1.391(16)	C(412)-C(413)	1.40(2)
C(213)-C(214)	1.380(18)	C(413)-C(414)	1.35(2)
C(214)-C(215)	1.398(17)	C(414)-C(415)	1.373(18)
C(215)-C(216)	1.398(14)	C(415)-C(416)	1.379(16)
C(221)-C(226)	1.374(15)	C(421)-C(426)	1.381(14)
C(221)-C(222)	1.390(16)	C(421)-C(422)	1.397(15)
C(222)-C(223)	1.407(15)	C(422)-C(423)	1.381(17)
C(223)-C(224)	1.373(19)	C(423)-C(424)	1.372(18)
C(224)-C(225)	1.36(2)	C(424)-C(425)	1.380(17)
C(225)-C(226)	1.397(17)	C(425)-C(426)	1.393(15)
C(131)-C(133)	1.532(15)	C(231)-C(232)	1.507(15)
C(131)-C(132)	1.533(17)	C(231)-C(233)	1.515(15)
C(5)-Cl(1)	1.800(14)	C(5)-Cl(2)	1.794(17)

C(11)-P(1)-C(121)	103.7(6)	C(31)-P(3)-C(311)	102.0(6)
C(11)-P(1)-C(111)	103.8(5)	C(31)-P(3)-C(321)	106.2(6)
C(121)-P(1)-C(111)	103.8(5)	C(311)-P(3)-C(321)	105.6(6)
C(11)-P(1)-S(1)	116.9(3)	C(31)-P(3)-S(3)	117.7(4)
C(121)-P(1)-S(1)	113.5(4)	C(311)-P(3)-S(3)	113.6(5)
C(111)-P(1)-S(1)	113.7(4)	C(321)-P(3)-S(3)	110.7(5)
C(21)-P(2)-C(211)	103.3(4)	C(41)-P(4)-C(411)	100.7(5)
C(21)-P(2)-C(221)	104.3(4)	C(41)-P(4)-C(421)	103.8(5)
C(211)-P(2)-C(221)	105.9(5)	C(411)-P(4)-C(421)	106.9(5)

C(21)-P(2)-S(2)	116.6(4)	C(41)-P(4)-S(4)	116.7(3)
C(211)-P(2)-S(2)	113.0(4)	C(411)-P(4)-S(4)	114.1(4)
C(221)-P(2)-S(2)	112.7(4)	C(421)-P(4)-S(4)	113.2(4)
C(1)-N(1)-C(2)	108.4(8)	C(3)-N(2)-C(231)	114.5(8)
C(1)-N(1)-C(131)	111.9(8)	C(3)-N(2)-C(4)	109.1(8)
C(2)-N(1)-C(131)	113.8(9)	C(231)-N(2)-C(4)	113.3(8)
N(1)-C(1)-C(12)	110.1(8)	N(2)-C(3)-C(32)	110.7(8)
N(1)-C(2)-C(22)	111.6(8)	N(2)-C(4)-C(42)	110.0(9)
C(12)-C(11)-P(1)	128.5(8)	C(35)-C(31)-P(3)	124.5(8)
C(15)-C(11)-P(1)	125.0(8)	C(32)-C(31)-P(3)	125.7(8)
C(13)-C(12)-C(1)	127.9(9)	C(33)-C(32)-C(3)	127.3(9)
C(11)-C(12)-C(1)	125.0(8)	C(31)-C(32)-C(3)	129.3(9)
C(25)-C(21)-P(2)	123.5(8)	C(45)-C(41)-P(4)	125.2(7)
C(22)-C(21)-P(2)	128.5(7)	C(42)-C(41)-P(4)	127.6(8)
C(23)-C(22)-C(2)	124.1(9)	C(43)-C(42)-C(4)	125.8(9)
C(21)-C(22)-C(2)	128.5(8)	C(41)-C(42)-C(4)	127.6(10)
C(116)-C(111)-C(112)	122.2(12)	C(316)-C(311)-C(312)	118.4(14)
C(116)-C(111)-P(1)	120.3(9)	C(316)-C(311)-P(3)	120.2(12)
C(112)-C(111)-P(1)	117.5(10)	C(312)-C(311)-P(3)	121.3(11)
C(111)-C(112)-C(113)	118.6(14)	C(313)-C(312)-C(311)	120.1(16)
C(114)-C(113)-C(112)	118.7(14)	C(314)-C(313)-C(312)	120.7(18)
C(115)-C(114)-C(113)	121.6(13)	C(313)-C(314)-C(315)	119.6(16)
C(114)-C(115)-C(116)	120.2(15)	C(314)-C(315)-C(316)	119.5(19)
C(111)-C(116)-C(115)	118.4(14)	C(311)-C(316)-C(315)	121.5(18)
C(122)-C(121)-C(126)	122.3(12)	C(326)-C(321)-C(322)	120.8(14)
C(122)-C(121)-P(1)	119.1(10)	C(326)-C(321)-P(3)	119.4(13)
C(126)-C(121)-P(1)	118.5(10)	C(322)-C(321)-P(3)	119.7(11)
C(121)-C(122)-C(123)	117.0(16)	C(321)-C(322)-C(323)	118.7(17)
C(124)-C(123)-C(122)	122.2(17)	C(324)-C(323)-C(322)	118.2(19)
C(125)-C(124)-C(123)	121.0(15)	C(325)-C(324)-C(323)	120.6(17)
C(124)-C(125)-C(126)	119.5(15)	C(326)-C(325)-C(324)	121.8(18)
C(121)-C(126)-C(125)	117.9(13)	C(325)-C(326)-C(321)	119.7(18)
C(212)-C(211)-C(216)	119.8(10)	C(416)-C(411)-C(412)	116.6(12)
C(212)-C(211)-P(2)	118.2(9)	C(416)-C(411)-P(4)	124.1(9)
C(216)-C(211)-P(2)	121.9(8)	C(412)-C(411)-P(4)	118.4(10)

C(211)-C(212)-C(213)	119.6(12)	C(411)-C(412)-C(413)	120.8(14)
C(214)-C(213)-C(212)	121.4(13)	C(414)-C(413)-C(412)	118.1(14)
C(213)-C(214)-C(215)	119.5(11)	C(413)-C(414)-C(415)	123.6(15)
C(214)-C(215)-C(216)	118.9(11)	C(414)-C(415)-C(416)	116.9(13)
C(211)-C(216)-C(215)	120.7(10)	C(415)-C(416)-C(411)	123.5(12)
C(226)-C(221)-C(222)	119.0(11)	C(426)-C(421)-C(422)	118.7(10)
C(226)-C(221)-P(2)	120.7(10)	C(426)-C(421)-P(4)	122.0(8)
C(222)-C(221)-P(2)	120.3(8)	C(422)-C(421)-P(4)	119.3(9)
C(221)-C(222)-C(223)	120.1(12)	C(423)-C(422)-C(421)	119.7(12)
C(224)-C(223)-C(222)	120.3(15)	C(424)-C(423)-C(422)	121.7(12)
C(225)-C(224)-C(223)	118.8(14)	C(423)-C(424)-C(425)	118.9(12)
C(224)-C(225)-C(226)	122.1(14)	C(424)-C(425)-C(426)	120.3(12)
C(221)-C(226)-C(225)	119.6(13)	C(421)-C(426)-C(425)	120.7(11)
N(1)-C(131)-C(133)	115.4(10)	N(2)-C(231)-C(232)	115.5(10)
N(1)-C(131)-C(132)	111.2(10)	N(2)-C(231)-C(233)	110.1(9)
C(133)-C(131)-C(132)	112.1(10)	C(232)-C(231)-C(233)	110.8(11)
Cl(2)-C(5)-Cl(1)	107.5(10)		

Crystal data and structure refinement for 2-40a

Identification code	**2-40a**
Empirical formula	C_{37} H_{35} Fe N_2 O P S
Formula weight	642.55
Temperature, K	103(2)
Wavelength, Å	0.71073
Crystal system	Triclinic
Space group	P -1
a, Å	9.2854(5)
b, Å	11.2952(6)
c, Å	15.1349(7)
α, °	96.145(3)
β, °	91.933(3)
γ, °	103.600(3)
Volume, Å^3	1531.13(14)
Z	2

Density (calc), Mg/m^3	1.394
Abs. coefficient, mm^{-1}	0.647
F(000)	672
Crystal size, mm^3	0.200 x 0.080 x 0.050
Theta range, °	1.356 to 42.839
Reflections collected	118903
Indpt reflections (R_{int})	15996 (0.0474)
Absorption correction	Multi-scan
Max. / min. transmission	0.7484 / 0.7200
Refinement method	F^2
Data /restraints/parameters	15996 / 0 / 389
Goodness-of-fit on F^2	1.108
R1, wR2 [I>2σ(I)]	0.0336, 0.0891
R1, wR2 (all data)	0.0479, 0.0983
Residual density, $e.Å^{-3}$	0.621 / -0.691

Bond lengths [Å] and angles [°] for **2-40a**

Fe(1)-Ct(1)	1.6408(5)	Fe(1)-Ct(2)	1.6560(5)
S(1)-P(1)	1.9636(3)	P(1)-C(1)	1.7957(8)
P(1)-C(111)	1.8179(9)	P(1)-C(121)	1.8155(9)
O(1)-C(235)	1.3498(12)	O(1)-C(236)	1.4351(13)
N(1)-C(21)	1.4681(11)	N(1)-C(22)	1.4641(12)
N(1)-C(23)	1.4706(11)	N(2)-C(231)	1.3528(11)
N(2)-C(235)	1.3216(11)	C(2)-C(21)	1.5016(11)
C(22)-C(221)	1.5070(13)	C(23)-C(231)	1.5108(12)
C(111)-C(112)	1.3903(12)	C(121)-C(126)	1.3961(12)
C(111)-C(116)	1.3958(12)	C(121)-C(122)	1.3998(12)
C(112)-C(113)	1.3930(15)	C(122)-C(123)	1.3888(14)
C(113)-C(114)	1.3846(16)	C(123)-C(124)	1.3925(15)
C(114)-C(115)	1.3851(13)	C(124)-C(125)	1.3875(15)
C(115)-C(116)	1.3963(13)	C(125)-C(126)	1.3961(13)
C(221)-C(226)	1.3934(14)	C(225)-C(226)	1.3905(15)
C(221)-C(222)	1.3952(13)	C(231)-C(232)	1.3904(13)
C(222)-C(223)	1.3968(14)	C(232)-C(233)	1.3991(15)

C(223)-C(224)	1.3856(18)	C(233)-C(234)	1.3784(15)
C(224)-C(225)	1.3918(18)	C(234)-C(235)	1.4046(13)

Ct(1)-Fe(1)-Ct(2)	178.47(3)		
C(1)-P(1)-C(121)	104.27(4)	C(1)-P(1)-S(1)	116.64(3)
C(1)-P(1)-C(111)	103.70(4)	C(121)-P(1)-S(1)	111.75(3)
C(121)-P(1)-C(111)	106.59(4)	C(111)-P(1)-S(1)	112.95(3)
C(22)-N(1)-C(21)	110.62(7)	C(22)-N(1)-C(23)	115.52(7)
C(21)-N(1)-C(23)	113.26(7)	C(235)-N(2)-C(231)	117.70(8)
C(1)-C(2)-C(21)	125.91(7)	C(3)-C(2)-C(21)	126.97(8)
N(1)-C(21)-C(2)	111.27(7)	C(235)-O(1)-C(236)	116.42(8)
N(1)-C(22)-C(221)	113.54(7)	N(1)-C(23)-C(231)	117.16(7)
C(112)-C(111)-C(116)	119.45(8)	C(126)-C(121)-C(122)	119.61(8)
C(112)-C(111)-P(1)	119.28(7)	C(126)-C(121)-P(1)	122.08(7)
C(116)-C(111)-P(1)	121.26(6)	C(122)-C(121)-P(1)	118.29(7)
C(111)-C(112)-C(113)	119.90(9)	C(123)-C(122)-C(121)	120.18(9)
C(114)-C(113)-C(112)	120.58(9)	C(122)-C(123)-C(124)	120.00(9)
C(113)-C(114)-C(115)	119.89(9)	C(125)-C(124)-C(123)	120.13(9)
C(114)-C(115)-C(116)	119.89(9)	C(124)-C(125)-C(126)	120.16(9)
C(111)-C(116)-C(115)	120.28(8)	C(125)-C(126)-C(121)	119.88(9)
C(226)-C(221)-C(222)	119.07(9)	N(2)-C(231)-C(232)	122.25(8)
C(226)-C(221)-C(22)	119.82(8)	N(2)-C(231)-C(23)	116.08(7)
C(222)-C(221)-C(22)	121.08(8)	C(232)-C(231)-C(23)	121.67(8)
C(221)-C(222)-C(223)	120.40(10)	C(231)-C(232)-C(233)	118.81(9)
C(224)-C(223)-C(222)	120.09(10)	C(234)-C(233)-C(232)	119.48(9)
C(223)-C(224)-C(225)	119.77(10)	C(233)-C(234)-C(235)	117.19(9)
C(226)-C(225)-C(224)	120.19(11)	N(2)-C(235)-O(1)	119.33(8)
C(225)-C(226)-C(221)	120.49(10)	N(2)-C(235)-C(234)	124.56(9)
O(1)-C(235)-C(234)	116.11(8)		

Hydrogen bonds for **2-40a** [Å and °].

D-H...A	d(D-H)	d(H...A)	d(D...A)	<(DHA)
C(21)-H(21B)...S(1)	0.99	2.77	3.5345(9)	134.8

C(22)-H(22A)...N(2)	0.99	2.55	3.1709(11)	120.4
C(112)-H(112)...S(1)	0.95	2.89	3.3700(10)	112.2
C(122)-H(122)...S(1)	0.95	2.94	3.3834(10)	110.2
C(236)-H(23D)...S(1)#1	0.98	2.90	3.5464(11)	124.5

Symmetry transformations used to generate equivalent atoms:

#1 x,y-1,z

Table of X- ray Data: Chapter-3

Crystal data and structure refinement for 3-32

Identification code	**3-32**
Empirical formula	C_{30} H_{28} Fe N P S
Formula weight	521.41
Temperature, K	103(2)
Wavelength, Å	0.71073
Crystal system	Monoclinic
Space group	$P2_1/c$
a, Å	14.3654(6)
b, Å	8.9688(4)
c, Å	19.0757(8)
α, °	90.0
β, °	102.416
γ, °	90.0
Volume, $Å^3$	2400.24(18)
Z	4
Density (calc), Mg/m^3	1.443
Abs. coefficient, mm^{-1}	0.802
F(000)	1088
Crystal size, mm^3	0.200 x 0.200 x 0.020
Theta range, °	2.186 to 26.371
Reflections collected	58282
Indpt reflections (R_{int})	4851 (0.0525)
Absorption correction	Multi-scan
Max. / min. transmission	0.7473 / 0.6941

Refinement method	F^2
Data /restraints/parameters	4851 / 0 / 310
Goodness-of-fit on F^2	1.129
R1, wR2 [I>2σ(I)]	0.0357, 0.0846
R1, wR2 (all data)	0.0402, 0.0871
Residual density, e.Å^{-3}	0.379 / -0.359

Table 2. Bond lengths [Å] and angles [°] for **3-32**

Fe(1)-Ct(1)	1.640(1)	Fe(1)-Ct(2)	1.651(1)
S(1)-P(1)	1.9566(7)	P(1)-C(1)	1.790(2)
P(1)-C(111)	1.816(2)	P(1)-C(121)	1.820(2)
N(1)-C(21)	1.469(3)	N(1)-C(22)	1.445(3)
C(2)-C(21)	1.490(3)	C(22)-C(221)	1.500(3)
C(111)-C(116)	1.389(3)	C(121)-C(122)	1.374(3)
C(111)-C(112)	1.394(3)	C(121)-C(126)	1.384(3)
C(112)-C(113)	1.390(3)	C(122)-C(123)	1.400(3)
C(113)-C(114)	1.376(3)	C(123)-C(124)	1.353(4)
C(114)-C(115)	1.381(3)	C(124)-C(125)	1.372(6)
C(115)-C(116)	1.393(3)	C(125)-C(126)	1.385(5)
C(221)-N(2)	1.344(3)	C(225)-N(2)	1.342(3)
C(221)-C(222)	1.382(3)	C(223)-C(224)	1.389(4)
C(222)-C(223)	1.373(4)	C(224)-C(225)	1.372(4)

Ct(1)-Fe(1)-Ct(2)	177.86(6)	C(22)-N(1)-C(21)	113.40(16)
C(1)-P(1)-C(111)	103.94(9)	C(1)-P(1)-S(1)	116.51(7)
C(1)-P(1)-C(121)	104.29(10)	C(111)-P(1)-S(1)	112.88(7)
C(111)-P(1)-C(121)	105.73(9)	C(121)-P(1)-S(1)	112.45(8)
C(2)-C(1)-P(1)	128.40(15)	C(5)-C(1)-P(1)	123.92(15)
C(1)-C(2)-C(21)	127.22(18)	C(3)-C(2)-C(21)	125.55(18)
N(1)-C(21)-C(2)	109.43(16)	N(1)-C(22)-C(221)	110.47(17)
C(116)-C(111)-C(112)	119.41(19)	C(122)-C(121)-C(126)	118.9(2)
C(116)-C(111)-P(1)	121.35(15)	C(122)-C(121)-P(1)	121.63(16)
C(112)-C(111)-P(1)	119.23(16)	C(126)-C(121)-P(1)	119.4(2)
C(113)-C(112)-C(111)	120.0(2)	C(121)-C(122)-C(123)	120.7(2)

C(114)-C(113)-C(112)	120.2(2)	C(124)-C(123)-C(122)	120.0(3)
C(113)-C(114)-C(115)	120.4(2)	C(123)-C(124)-C(125)	119.4(3)
C(114)-C(115)-C(116)	119.9(2)	C(124)-C(125)-C(126)	121.4(3)
C(111)-C(116)-C(115)	120.11(19)	C(121)-C(126)-C(125)	119.4(3)
N(2)-C(221)-C(22)	116.34(19)	N(2)-C(221)-C(222)	122.9(2)
C(222)-C(221)-C(22)	120.8(2)	C(225)-C(224)-C(223)	118.0(2)
C(223)-C(222)-C(221)	118.2(2)	N(2)-C(225)-C(224)	123.3(2)
C(222)-C(223)-C(224)	119.8(2)	C(225)-N(2)-C(221)	117.6(2)

Hydrogen bonds for **3-32** [Å and °].

D-H...A	d(D-H)	d(H...A)	d(D...A)	<(DHA)
C(21)-H(21B)...S(1)	0.99	2.78	3.596(2)	139.7
C(126)-H(126)...S(1)	0.95	2.91	3.380(4)	111.5

Symmetry transformations used to generate equivalent atoms:

Crystal data and structure refinement for 3-33

Identification code	**3-33**
Empirical formula	C_{26} H_{23} Fe O P S
Formula weight	470.32
Temperature, K	110(2)
Wavelength, Å	0.71073 Å
Crystal system	Monoclinic
Space group	$P2_1/c$
a, Å	7.364
b, Å	17.90210(10)
c, Å	16.70380(10)
α, °	90.0
β, °	95.216(4)
γ, °	90.0
Volume, $Å^3$	2192.90(2)

Z	4
Density (calc), Mg/m^3	1.425
Abs. coefficient, mm^{-1}	0.872
F(000)	976
Crystal size, mm^3	0.1 x 0.07 x 0.01
Theta range, °	2.584 to 26.366
Reflections collected	39661
Indpt reflections (R_{int})	4462 (0.1085)
Absorption correction	Multi-scan
Max. / min. transmission	0.7300 / 0.6725
Refinement method	F^2
Data /restraints/parameters	4462 / 0 / 272
Goodness-of-fit on F^2	1.072
R1, wR2 [I>2σ(I)]	0.0472, 0.1326
R1, wR2 (all data)	0.0685, 0.1476
Residual density, $e.Å^{-3}$	1.498 / -0.481

Table 2. Bond lengths [Å] and angles [°] for **3-33**

Ct(1)-Fe(1)	1.642 (2)	Ct(2)-Fe(1)	1.662(2)
S(1)-P(1)	1.9561(11)	P(1)-C(1)	1.792(3)
P(1)-C(111)	1.817(3)	P(1)-C(121)	1.810(3)
O(1)-C(23)	1.205(4)	C(22)-C(23)	1.468(5)
C(2)-C(21)	1.460(4)	C(23)-C(24)	1.512(5)
C(21)-C(22)	1.339(5)		
C(111)-C(116)	1.387(5)	C(121)-C(122)	1.387(5)
C(111)-C(112)	1.391(4)	C(121)-C(126)	1.397(5)
C(112)-C(113)	1.381(5)	C(122)-C(123)	1.398(5)
C(113)-C(114)	1.388(5)	C(123)-C(124)	1.388(5)
C(114)-C(115)	1.384(5)	C(124)-C(125)	1.372(5)
C(115)-C(116)	1.391(5)	C(125)-C(126)	1.377(5)

Ct(1)-Fe(1)-Ct(2)	178.26(9)		
C(1)-P(1)-S(1)	115.63(11)	C(1)-P(1)-C(121)	105.07(15)
C(121)-P(1)-S(1)	112.85(11)	C(1)-P(1)-C(111)	104.47(15)

C(111)-P(1)-S(1)	113.06(11)	C(121)-P(1)-C(111)	104.73(15)
C(2)-C(1)-P(1)	128.2(2)	C(5)-C(1)-P(1)	125.0(2)
C(3)-C(2)-C(21)	125.0(3)	C(22)-C(21)-C(2)	123.1(3)
C(21)-C(22)-C(23)	125.3(3)	C(22)-C(23)-C(24)	119.9(3)
O(1)-C(23)-C(22)	121.5(3)	O(1)-C(23)-C(24)	118.6(3)
C(116)-C(111)-C(112)	119.3(3)	C(122)-C(121)-C(126)	119.4(3)
C(116)-C(111)-P(1)	120.0(2)	C(122)-C(121)-P(1)	121.6(3)
C(112)-C(111)-P(1)	120.6(2)	C(126)-C(121)-P(1)	119.0(3)
C(113)-C(112)-C(111)	120.6(3)	C(121)-C(122)-C(123)	120.2(3)
C(112)-C(113)-C(114)	120.3(3)	C(124)-C(123)-C(122)	119.6(3)
C(115)-C(114)-C(113)	119.3(3)	C(125)-C(124)-C(123)	119.9(3)
C(114)-C(115)-C(116)	120.7(3)	C(124)-C(125)-C(126)	121.1(3)
C(111)-C(116)-C(115)	119.9(3)	C(125)-C(126)-C(121)	119.8(3)

Table 3. Hydrogen bonds for **3-33** [Å and °].

D-H...A	d(D-H)	d(H...A)	d(D...A)	<(DHA)
C(22)-H(22)...O(1)#1	0.95	2.63	3.549(4)	163.7
C(112)-H(112)...S(1)#2	0.95	2.83	3.577(3)	136.3
C(116)-H(116)...S(1)	0.95	2.88	3.372(4)	113.0

Symmetry transformations used to generate equivalent atoms:

#1 -x+1,-y+2,-z+1 #2 x-1,y,z

Crystal data and structure refinement for 3-37

Identification code	**3-37**
Empirical formula	C_{19} H_{14} N P S
Formula weight	319.34
Temperature, K	107(2)
Wavelength, Å	0.71073
Crystal system	Orthorhombic
Space group	$P2_12_12_1$
a, Å	7.630
b, Å	12.725

c, Å	16.4513(1)
α, °	90.0
β, °	90.0
γ, °	90.0
Volume, $Å^3$	1597.231(10)
Z	4
Density (calc), Mg/m^3	1.328
Abs. coefficient, mm^{-1}	0.298
F(000)	664
Crystal size, mm^3	0.200 x 0.150 x 0.040
Theta range, °	2.023 to 35.381
Reflections collected	112228
Indpt reflections (R_{int})	7104 (0.0615)
Absorption correction	Multi-scan
Max. / min. transmission	0.7470 / 0.6909
Refinement method	F^2
Data /restraints/parameters	7104 / 0 / 199
Goodness-of-fit on F^2	1.105
R1, wR2 [I>2σ(I)]	0.0301, 0.0714
R1, wR2 (all data)	0.0379, 0.0752
Absolute configuration parameter	0.020(17)
Residual density, $e.Å^{-3}$	0.383 / -0.242

Table 2. Bond lengths [Å] and angles [°] for **3-37**

S(1)-P(1)	1.9542(5)	N(1)-C(37)	1.148(2)
P(1)-C(11)	1.8086(13)	P(1)-C(21)	1.8190(14)
C(11)-C(16)	1.3947(18)	C(21)-C(22)	1.393(2)
C(11)-C(12)	1.3997(18)	C(21)-C(26)	1.3952(18)
C(12)-C(13)	1.391(2)	C(22)-C(23)	1.393(2)
C(13)-C(14)	1.393(2)	C(23)-C(24)	1.390(2)
C(14)-C(15)	1.387(2)	C(24)-C(25)	1.384(2)
C(15)-C(16)	1.3913(19)	C(25)-C(26)	1.392(2)
P(1)-C(31)	1.8210(13)	C(31)-C(32)	1.3969(18)
C(31)-C(36)	1.4079(19)	C(34)-C(35)	1.390(2)

C(32)-C(33)	1.396(2)	C(35)-C(36)	1.3975(19)
C(33)-C(34)	1.384(2)	C(36)-C(37)	1.4426(19)

C(11)-P(1)-S(1)	114.45(5)	C(11)-P(1)-C(21)	107.57(6)
C(21)-P(1)-S(1)	112.59(5)	C(11)-P(1)-C(31)	104.57(6)
C(31)-P(1)-S(1)	111.81(4)	C(21)-P(1)-C(31)	105.13(6)
C(16)-C(11)-C(12)	120.09(12)	C(22)-C(21)-C(26)	119.68(13)
C(16)-C(11)-P(1)	119.49(10)	C(22)-C(21)-P(1)	122.48(10)
C(12)-C(11)-P(1)	120.41(10)	C(26)-C(21)-P(1)	117.84(10)
C(13)-C(12)-C(11)	119.60(13)	C(21)-C(22)-C(23)	119.81(14)
C(12)-C(13)-C(14)	120.18(14)	C(24)-C(23)-C(22)	120.24(15)
C(15)-C(14)-C(13)	120.11(13)	C(25)-C(24)-C(23)	120.11(14)
C(14)-C(15)-C(16)	120.21(13)	C(24)-C(25)-C(26)	119.93(14)
C(15)-C(16)-C(11)	119.81(12)	C(25)-C(26)-C(21)	120.23(13)
C(32)-C(31)-C(36)	118.07(12)	C(34)-C(35)-C(36)	119.68(14)
C(32)-C(31)-P(1)	121.51(11)	C(35)-C(36)-C(31)	121.05(12)
C(36)-C(31)-P(1)	120.31(10)	C(35)-C(36)-C(37)	117.07(13)
C(33)-C(32)-C(31)	120.73(14)	C(31)-C(36)-C(37)	121.88(12)
C(34)-C(33)-C(32)	120.48(13)	N(1)-C(37)-C(36)	176.49(16)
C(33)-C(34)-C(35)	119.97(14)		

Table 3. Hydrogen bonds for **3-37** [Å and °].

D-H...A	d(D-H)	d(H...A)	d(D...A)	<(DHA)
C(12)-H(12)...S(1)#1	0.95	2.91	3.7931(14)	155.6
C(16)-H(16)...S(1)	0.95	2.91	3.3903(14)	112.7
C(26)-H(26)...S(1)	0.95	2.89	3.3553(14)	111.5

Symmetry transformations used to generate equivalent atoms:

#1 -x+1,y-1/2,-z+1/2

Crystal data and structure refinement for 3-43

Identification code	**3-43**

Empirical formula	C_{68} H_{70} N_2 P_4 S_4 Si_2
Formula weight	1223.56
Temperature, K	120(2)
Wavelength, Å	0.71073
Crystal system	Orthorhombic
Space group	$P2_12$ 2_1
a, Å	9.0473(8)
b, Å	25.277(3)
c, Å	27.797(4)
α, °	90.0
β, °	90.0
γ, °	90.0
Volume, $Å^3$	6356.8(13)
Z	4
Density (calc), Mg/m^3	1.278
Abs. coefficient, mm^{-1}	0.331
F(000)	2576
Theta range, °	1.089 to 25.022
Reflections collected	127620
Indpt reflections (R_{int})	11209 (0.157)
Absorption correction	Multi-scan
Max. / min. transmission	0.7458 and 0.6412

Refinement method	F^2
Data /restraints/parameters	11209 / 0 / 727
Goodness-of-fit on F^2	1.045
R1, wR2 [I>2σ(I)]	0.0643, 0.1232
R1, wR2 (all data)	0.0951, 0.1353
Absolute configuration parameter	0.03(4)
Residual density, e.Å^{-3}	0.417 / -0.395

Bond lengths [Å] and angles [°] for **3-43**

Molecule A		**Molecule B**	
P(1)-N(1)	1.659(6)	P(3)-N(2)	1.662(7)
P(1)-C(121)	1.815(7)	P(3)-C(311)	1.800(8)
P(1)-C(111)	1.817(7)	P(3)-C(321)	1.843(8)
P(1)-S(1)	1.946(3)	P(3)-S(3)	1.955(3)
P(2)-C(211)	1.808(7)	P(4)-C(421)	1.816(7)
P(2)-C(231)	1.815(7)	P(4)-C(431)	1.821(7)
P(2)-C(221)	1.818(7)	P(4)-C(411)	1.828(7)
P(2)-S(2)	1.965(3)	P(4)-S(4)	1.950(3)
Si(1)-N(1)	1.797(6)	Si(2)-N(2)	1.783(7)
Si(1)-C(11)	1.843(9)	Si(2)-C(22)	1.828(12)
Si(1)-C(13)	1.870(7)	Si(2)-C(23)	1.846(9)
Si(1)-C(12)	1.871(8)	Si(2)-C(21)	1.864(12)

N(1)-C(1)	1.484(8)	N(2)-C(2)	1.481(9)
C(1)-C(232)	1.516(9)	C(2)-C(432)	1.516(10)
C(111)-C(112)	1.366(10)	C(311)-C(312)	1.390(11)
C(111)-C(116)	1.395(11)	C(311)-C(316)	1.392(11)
C(112)-C(113)	1.374(12)	C(312)-C(313)	1.380(11)
C(113)-C(114)	1.360(14)	C(313)-C(314)	1.361(12)
C(114)-C(115)	1.382(13)	C(314)-C(315)	1.383(12)
C(115)-C(116)	1.383(11)	C(315)-C(316)	1.384(11)
C(121)-C(122)	1.396(10)	C(321)-C(322)	1.365(11)
C(121)-C(126)	1.399(10)	C(321)-C(326)	1.388(11)
C(122)-C(123)	1.390(10)	C(322)-C(323)	1.383(13)
C(123)-C(124)	1.387(10)	C(323)-C(324)	1.370(14)
C(124)-C(125)	1.348(11)	C(324)-C(325)	1.353(14)
C(125)-C(126)	1.390(10)	C(325)-C(326)	1.371(13)
C(211)-C(212)	1.387(10)	C(411)-C(416)	1.376(11)
C(211)-C(216)	1.388(10)	C(411)-C(412)	1.381(11)
C(212)-C(213)	1.385(10)	C(412)-C(413)	1.412(11)
C(212)-H(212)	0.9500	C(412)-H(412)	0.9500
C(213)-C(214)	1.389(11)	C(413)-C(414)	1.347(14)
C(214)-C(215)	1.362(11)	C(414)-C(415)	1.375(14)
C(215)-C(216)	1.395(10)	C(415)-C(416)	1.396(13)
C(221)-C(226)	1.389(11)	C(421)-C(422)	1.380(9)

C(221)-C(222)	1.390(10)	C(421)-C(426)	1.405(9)
C(222)-C(223)	1.385(11)	C(422)-C(423)	1.412(10)
C(223)-C(224)	1.380(12)	C(423)-C(424)	1.381(10)
C(224)-C(225)	1.371(12)	C(424)-C(425)	1.375(11)
C(225)-C(226)	1.411(11)	C(425)-C(426)	1.372(10)
C(231)-C(236)	1.381(9)	C(431)-C(436)	1.391(10)
C(231)-C(232)	1.422(9)	C(431)-C(432)	1.414(9)
C(232)-C(233)	1.398(9)	C(432)-C(433)	1.392(10)
C(233)-C(234)	1.370(10)	C(433)-C(434)	1.387(10)
C(234)-C(235)	1.366(10)	C(434)-C(435)	1.382(10)
C(235)-C(236)	1.393(10)	C(435)-C(436)	1.385(10)

N(1)-P(1)-C(121)	107.9(3)	N(2)-P(3)-C(311)	105.6(4)
N(1)-P(1)-C(111)	108.6(3)	N(2)-P(3)-C(321)	107.6(3)
C(121)-P(1)-C(111)	104.8(3)	C(311)-P(3)-C(321)	104.4(4)
N(1)-P(1)-S(1)	113.0(2)	N(2)-P(3)-S(3)	114.1(3)
C(121)-P(1)-S(1)	111.0(2)	C(311)-P(3)-S(3)	112.8(3)
C(111)-P(1)-S(1)	111.2(3)	C(321)-P(3)-S(3)	111.7(3)
C(211)-P(2)-C(231)	104.1(3)	C(421)-P(4)-C(431)	108.4(3)
C(211)-P(2)-C(221)	105.3(3)	C(421)-P(4)-C(411)	106.7(3)
C(231)-P(2)-C(221)	107.1(3)	C(431)-P(4)-C(411)	104.8(3)
C(211)-P(2)-S(2)	113.7(3)	C(421)-P(4)-S(4)	109.7(2)
C(231)-P(2)-S(2)	114.2(2)	C(431)-P(4)-S(4)	113.5(2)

C(221)-P(2)-S(2)	111.8(3)	C(411)-P(4)-S(4)	113.3(3)
N(1)-Si(1)-C(11)	107.0(3)	N(2)-Si(2)-C(22)	110.0(5)
N(1)-Si(1)-C(13)	112.1(3)	N(2)-Si(2)-C(23)	111.9(4)
C(11)-Si(1)-C(13)	109.1(4)	C(22)-Si(2)-C(23)	107.5(6)
N(1)-Si(1)-C(12)	111.0(3)	N(2)-Si(2)-C(21)	109.1(5)
C(11)-Si(1)-C(12)	107.0(5)	C(22)-Si(2)-C(21)	107.5(7)
C(13)-Si(1)-C(12)	110.4(4)	C(23)-Si(2)-C(21)	110.7(6)
C(1)-N(1)-P(1)	118.6(4)	C(2)-N(2)-P(3)	122.0(5)
C(1)-N(1)-Si(1)	118.7(4)	C(2)-N(2)-Si(2)	118.9(5)
P(1)-N(1)-Si(1)	120.3(3)	P(3)-N(2)-Si(2)	119.0(4)
N(1)-C(1)-C(232)	115.5(6)	N(2)-C(2)-C(432)	115.7(6)
C(112)-C(111)-C(116)	119.4(7)	C(312)-C(311)-C(316)	118.4(7)
C(112)-C(111)-P(1)	120.7(6)	C(312)-C(311)-P(3)	121.7(6)
C(116)-C(111)-P(1)	119.9(6)	C(316)-C(311)-P(3)	119.9(6)
C(111)-C(112)-C(113)	121.1(9)	C(313)-C(312)-C(311)	121.3(8)
C(114)-C(113)-C(112)	120.0(9)	C(314)-C(313)-C(312)	119.0(8)
C(113)-C(114)-C(115)	120.0(9)	C(313)-C(314)-C(315)	121.8(8)
C(114)-C(115)-C(116)	120.3(9)	C(314)-C(315)-C(316)	118.8(9)
C(115)-C(116)-C(111)	119.2(8)	C(315)-C(316)-C(311)	120.6(8)
C(122)-C(121)-C(126)	117.8(7)	C(322)-C(321)-C(326)	119.5(9)
C(122)-C(121)-P(1)	118.6(5)	C(322)-C(321)-P(3)	121.9(7)
C(126)-C(121)-P(1)	123.2(5)	C(326)-C(321)-P(3)	118.5(6)

C(123)-C(122)-C(121)	121.4(7)	C(321)-C(322)-C(323)	118.8(9)
C(124)-C(123)-C(122)	119.3(7)	C(324)-C(323)-C(322)	121.1(10)
C(125)-C(124)-C(123)	119.9(8)	C(325)-C(324)-C(323)	120.0(10)
C(124)-C(125)-C(126)	121.8(7)	C(324)-C(325)-C(326)	119.7(10)
C(125)-C(126)-C(121)	119.8(7)	C(325)-C(326)-C(321)	120.7(9)
C(212)-C(211)-C(216)	119.2(7)	C(416)-C(411)-C(412)	121.9(8)
C(212)-C(211)-P(2)	120.2(6)	C(416)-C(411)-P(4)	119.0(7)
C(216)-C(211)-P(2)	120.5(6)	C(412)-C(411)-P(4)	119.1(6)
C(213)-C(212)-C(211)	120.5(7)	C(411)-C(412)-C(413)	118.7(9)
C(212)-C(213)-C(214)	119.4(7)	C(414)-C(413)-C(412)	119.8(9)
C(215)-C(214)-C(213)	120.9(7)	C(413)-C(414)-C(415)	120.8(9)
C(214)-C(215)-C(216)	119.7(8)	C(414)-C(415)-C(416)	121.2(9)
C(211)-C(216)-C(215)	120.3(7)	C(411)-C(416)-C(415)	117.5(9)
C(226)-C(221)-C(222)	117.9(7)	C(422)-C(421)-C(426)	118.3(7)
C(226)-C(221)-P(2)	123.6(6)	C(422)-C(421)-P(4)	123.7(5)
C(222)-C(221)-P(2)	118.4(6)	C(426)-C(421)-P(4)	117.7(5)
C(223)-C(222)-C(221)	121.0(8)	C(421)-C(422)-C(423)	120.4(7)
C(224)-C(223)-C(222)	120.6(8)	C(424)-C(423)-C(422)	119.9(7)
C(225)-C(224)-C(223)	119.9(8)	C(425)-C(424)-C(423)	119.5(7)
C(224)-C(225)-C(226)	119.5(9)	C(426)-C(425)-C(424)	121.0(7)
C(221)-C(226)-C(225)	121.1(8)	C(425)-C(426)-C(421)	120.8(7)
C(236)-C(231)-C(232)	120.4(6)	C(436)-C(431)-C(432)	120.5(7)

C(236)-C(231)-P(2)	118.7(5)	C(436)-C(431)-P(4)	118.3(5)
C(232)-C(231)-P(2)	120.8(5)	C(432)-C(431)-P(4)	121.0(5)
C(233)-C(232)-C(231)	116.6(6)	C(433)-C(432)-C(431)	117.6(7)
C(233)-C(232)-C(1)	122.0(6)	C(433)-C(432)-C(2)	120.7(7)
C(231)-C(232)-C(1)	121.4(6)	C(431)-C(432)-C(2)	121.7(7)
C(234)-C(233)-C(232)	122.1(7)	C(434)-C(433)-C(432)	121.3(7)
C(235)-C(234)-C(233)	120.9(7)	C(435)-C(434)-C(433)	120.5(7)
C(234)-C(235)-C(236)	119.0(7)	C(434)-C(435)-C(436)	119.4(7)
C(231)-C(236)-C(235)	120.9(7)	C(435)-C(436)-C(431)	120.5(7)

Table 3. Hydrogen bonds for **3-43** [Å and °].

D-H...A	d(D-H)	d(H...A)	d(D...A)	<(DHA)
C(1)-H(1B)...S(2)	0.99	2.85	3.650(7)	138.5
C(112)-H(112)...S(1)	0.95	2.85	3.335(9)	112.5
C(212)-H(212)...S(2)	0.95	2.87	3.365(8)	113.8
C(222)-H(222)...S(2)	0.95	2.72	3.267(8)	117.2
C(2)-H(2B)...S(4)	0.99	2.76	3.589(8)	142.0
C(326)-H(326)...S(3)	0.95	2.87	3.350(11)	112.5
C(416)-H(416)...S(4)	0.95	2.82	3.324(10)	114.4

Symmetry transformations used to generate equivalent atoms:

Crystal data and structure refinement for 3-34

Identification code	**3-34**
Empirical formula	C_{42} H_{37} Fe N P_2 S_2

Formula weight	737.63
Temperature, K	106(2)
Wavelength, Å	0.71073
Crystal system	Triclinic
Space group	P -1
a, Å	9.5336(3)
b, Å	11.6915(3)
c, Å	17.1705(4)
α, °	107.914(2)
β, °	96.837(2)
γ, °	103.382(2)
Volume, Å^3	1733.81(8)
Z	2
Density (calc), Mg/m^3	1.413
Abs. coefficient, mm^{-1}	0.681
F(000)	768
Crystal size, mm^3	0.160 x 0.120 x 0.120
Theta range, °	1.892 to 26.372
Reflections collected	76984
Indpt reflections (R_{int})	7087 (0.5257)
Absorption correction	Multi-scan
Max. / min. transmission	0.7384 / 0.6907

Refinement method	F^2
Data /restraints/parameters	7087 / 1 / 436
Goodness-of-fit on F^2	1.061
R1, wR2 [I>2σ(I)]	0.0581, 0.1344
R1, wR2 (all data)	0.0603, 0.1370
Residual density, e.Å^{-3}	1.348 / -0.454

Bond lengths [Å] and angles [°] for **3-34**

Fe(1)-Ct(1)	1.629(1)	Fe(1)-Ct(2)	1.642(1)
S(1)-P(1)	1.9475(8)	S(2)-P(2)	1.9481(8)
P(1)-C(1)	1.784(2)	P(2)-C(211)	1.804(2)
P(1)-C(121)	1.806(2)	P(2)-C(221)	1.806(2)
P(1)-C(111)	1.807(2)	P(2)-C(24)	1.818(2)
N(1)-C(21)	1.453(3)	N(1)-C(22)	1.445(3)
C(2)-C(21)	1.490(3)	C(24)-C(25)	1.390(3)
C(22)-C(23)	1.508(3)	C(25)-C(26)	1.388(3)
C(23)-C(28)	1.386(3)	C(26)-C(27)	1.370(4)
C(23)-C(24)	1.410(3)	C(27)-C(28)	1.384(4)
C(111)-C(112)	1.382(3)	C(121)-C(126)	1.380(4)
C(111)-C(116)	1.390(3)	C(121)-C(122)	1.391(3)
C(112)-C(113)	1.384(4)	C(122)-C(123)	1.386(3)
C(113)-C(114)	1.382(4)	C(123)-C(124)	1.372(4)

C(114)-C(115)	1.378(4)	C(124)-C(125)	1.385(4)
C(115)-C(116)	1.383(4)	C(125)-C(126)	1.385(3)
C(211)-C(212)	1.385(3)	C(221)-C(226)	1.392(3)
C(211)-C(216)	1.386(3)	C(221)-C(222)	1.391(4)
C(212)-C(213)	1.376(4)	C(222)-C(223)	1.378(4)
C(213)-C(214)	1.379(4)	C(223)-C(224)	1.391(4)
C(214)-C(215)	1.372(4)	C(224)-C(225)	1.377(4)
C(215)-C(216)	1.380(4)	C(225)-C(226)	1.388(4)

Ct(1)-Fe(1)-Ct(2)	176.83(7)	C(22)-N(1)-C(21)	111.8(2)
C(1)-P(1)-S(1)	116.67(8)	C(1)-P(1)-C(121)	104.04(10)
C(121)-P(1)-S(1)	112.61(8)	C(1)-P(1)-C(111)	105.02(10)
C(111)-P(1)-S(1)	113.10(8)	C(121)-P(1)-C(111)	104.21(10)
C(211)-P(2)-S(2)	113.50(8)	C(211)-P(2)-C(221)	105.95(11)
C(221)-P(2)-S(2)	111.24(7)	C(211)-P(2)-C(24)	104.75(10)
C(24)-P(2)-S(2)	116.47(8)	C(221)-P(2)-C(24)	103.95(10)
C(2)-C(1)-P(1)	127.75(17)	C(5)-C(1)-P(1)	124.90(16)
C(1)-C(2)-C(21)	126.8(2)	C(3)-C(2)-C(21)	125.7(2)
N(1)-C(21)-C(2)	110.46(19)	N(1)-C(22)-C(23)	112.5(2)
C(23)-C(24)-P(2)	121.95(18)	C(25)-C(24)-P(2)	118.90(17)
C(26)-C(25)-C(24)	121.3(2)	C(28)-C(23)-C(24)	118.2(2)
C(27)-C(26)-C(25)	119.6(2)	C(28)-C(23)-C(22)	119.9(2)
C(26)-C(27)-C(28)	119.7(2)	C(24)-C(23)-C(22)	121.9(2)

C(27)-C(28)-C(23)	122.1(2)	C(25)-C(24)-C(23)	119.1(2)
C(112)-C(111)-C(116)	119.6(2)	C(126)-C(121)-C(122)	119.8(2)
C(112)-C(111)-P(1)	122.51(17)	C(126)-C(121)-P(1)	119.71(18)
C(116)-C(111)-P(1)	117.84(19)	C(122)-C(121)-P(1)	120.45(19)
C(111)-C(112)-C(113)	119.7(2)	C(123)-C(122)-C(121)	119.6(2)
C(114)-C(113)-C(112)	120.6(2)	C(124)-C(123)-C(122)	120.3(2)
C(115)-C(114)-C(113)	119.7(2)	C(123)-C(124)-C(125)	120.3(2)
C(114)-C(115)-C(116)	120.0(2)	C(124)-C(125)-C(126)	119.7(2)
C(115)-C(116)-C(111)	120.3(2)	C(121)-C(126)-C(125)	120.3(2)
C(212)-C(211)-C(216)	119.3(2)	C(226)-C(221)-C(222)	119.4(2)
C(212)-C(211)-P(2)	119.91(18)	C(226)-C(221)-P(2)	122.52(19)
C(216)-C(211)-P(2)	120.81(18)	C(222)-C(221)-P(2)	118.05(18)
C(213)-C(212)-C(211)	119.9(2)	C(223)-C(222)-C(221)	120.2(2)
C(212)-C(213)-C(214)	120.4(2)	C(222)-C(223)-C(224)	120.4(2)
C(215)-C(214)-C(213)	120.2(2)	C(225)-C(224)-C(223)	119.5(2)
C(214)-C(215)-C(216)	119.6(2)	C(224)-C(225)-C(226)	120.5(2)
C(215)-C(216)-C(211)	120.6(2)	C(225)-C(226)-C(221)	119.9(2)

Hydrogen bonds for **3-34** [Å and °].

D-H...A	d(D-H)	d(H...A)	d(D...A)	<(DHA)
C(21)-H(21A)...S(2)#1	0.99	2.92	3.739(2)	140.9
C(21)-H(21B)...S(1)	0.99	2.85	3.510(2)	124.4
C(22)-H(22B)...S(2)	0.99	2.80	3.562(3)	134.3
C(126)-H(126)...S(1)	0.95	2.93	3.382(3)	110.4

Symmetry transformations used to generate equivalent atoms:

#1 -x,-y,-z+1

Table of X- ray Data: Chapter-4

Crystal data and structure refinement for 4-43

Identification code	**4-43**
Empirical formula	C_{24} H_{24} O_2 P S
Formula weight	407.46
Temperature, K	180.05(10)
Wavelength, Å	1.54184
Crystal system	Orthorhombic
Space group	$Pna2_1$
a, Å	10.1151(3)
b, Å	23.4091(6)
c, Å	8.9847(2)
α, °	90.0
β, °	90.0
γ, °	90.0
Volume, $Å^3$	2127.45(10)
Z	4
Density (calc), Mg/m^3	1.272
Abs. coefficient, mm^{-1}	2.187
F(000)	860
Crystal size, mm^3	? x ? x ?
Theta range, °	3.777 - 61.577
Reflections collected	9246
Indpt reflections (R_{int})	3008 (0.0283)
Absorption correction	Multiscan
Max. / min. transmission	1.0 / 0.47315
Refinement method	F^2
Data /restraints/parameters	3008 / 1 / 253
Goodness-of-fit on F^2	1.053

R1, wR2 [I>2σ(I)]	0.0311, 0.0813
R1, wR2 (all data)	0.0328, 0.0835
Absolute structure parameter	-0.021(17)
Residual density, e.Å^{-3}	0.414 -0.165

Bond lengths [Å] and angles [°] for **4-43**

S(1)-P(1)	1.9544(12)	P(1)-C(1)	1.823(3)
P(1)-C(111)	1.822(4)	P(1)-C(121)	1.822(3)
O(1)-C(22)	1.418(5)	O(2)-C(22)	1.400(4)
O(1)-C(21)	1.421(4)	O(2)-C(26)	1.453(5)
C(1)-C(6)	1.394(5)	C(3)-C(4)	1.386(5)
C(1)-C(2)	1.410(5)	C(4)-C(5)	1.379(6)
C(2)-C(3)	1.397(5)	C(5)-C(6)	1.389(5)
C(2)-C(21)	1.496(5)		
C(22)-C(23)	1.510(5)	C(24)-C(25)	1.506(5)
C(23)-C(24)	1.519(5)	C(25)-C(26)	1.524(6)
C(111)-C(112)	1.392(5)	C(121)-C(122)	1.385(5)
C(111)-C(116)	1.392(5)	C(121)-C(126)	1.398(5)
C(112)-C(113)	1.377(5)	C(122)-C(123)	1.399(5)
C(113)-C(114)	1.377(6)	C(123)-C(124)	1.376(6)
C(114)-C(115)	1.397(5)	C(124)-C(125)	1.378(6)
C(115)-C(116)	1.379(5)	C(125)-C(126)	1.387(5)

C(111)-P(1)-C(1)	106.64(16)	C(121)-P(1)-C(1)	103.85(13)
C(111)-P(1)-C(121)	105.99(16)	C(1)-P(1)-S(1)	114.43(12)
C(111)-P(1)-S(1)	111.26(12)	C(121)-P(1)-S(1)	113.94(12)
C(2)-C(1)-P(1)	120.9(2)	C(6)-C(1)-P(1)	119.4(3)
C(22)-O(1)-C(21)	113.5(3)	C(22)-O(2)-C(26)	113.4(2)
C(1)-C(2)-C(21)	122.0(3)	C(3)-C(2)-C(21)	119.8(3)
C(6)-C(1)-C(2)	119.7(3)	C(5)-C(6)-C(1)	121.0(3)
C(3)-C(2)-C(1)	118.2(3)	C(22)-C(23)-C(24)	111.6(3)
C(4)-C(3)-C(2)	121.2(3)	C(25)-C(24)-C(23)	109.4(3)
C(5)-C(4)-C(3)	120.5(3)	C(24)-C(25)-C(26)	110.9(3)
C(4)-C(5)-C(6)	119.3(3)	O(2)-C(26)-C(25)	110.5(3)

O(1)-C(21)-C(2)	109.6(3)	O(1)-C(22)-C(23)	106.5(3)
O(2)-C(22)-O(1)	111.6(3)	O(2)-C(22)-C(23)	112.0(3)
C(112)-C(111)-C(116)	119.2(3)	C(122)-C(121)-C(126)	120.2(3)
C(112)-C(111)-P(1)	119.1(3)	C(122)-C(121)-P(1)	119.2(3)
C(116)-C(111)-P(1)	121.7(3)	C(126)-C(121)-P(1)	120.7(2)
C(113)-C(112)-C(111)	120.1(3)	C(121)-C(122)-C(123)	119.2(3)
C(114)-C(113)-C(112)	120.7(3)	C(124)-C(123)-C(122)	120.6(3)
C(113)-C(114)-C(115)	119.7(3)	C(123)-C(124)-C(125)	120.1(3)
C(116)-C(115)-C(114)	119.6(3)	C(124)-C(125)-C(126)	120.4(4)
C(115)-C(116)-C(111)	120.7(3)	C(125)-C(126)-C(121)	119.6(3)

Hydrogen bonds for **4-43** [Å and °].

D-H...A	d(D-H)	d(H...A)	d(D...A)	<(DHA)
C(21)-H(21B)...S(1)	0.99	2.83	3.451(3)	121.1
C(112)-H(112)...S(1)	0.95	2.80	3.299(4)	114.0
C(122)-H(122)...S(1)	0.95	2.88	3.372(4)	113.5
C(21)-H(21B)...S(1)	0.99	2.83	3.451(3)	121.1
C(112)-H(112)...S(1)	0.95	2.80	3.299(4)	114.0
C(122)-H(122)...S(1)	0.95	2.88	3.372(4)	113.5

Crystal data and structure refinement for 4-44

Identification code	**4-44**
Empirical formula	$C_{20}H_{17}O_2$ S
Formula weight	352.36
Temperature, K	150(2)
Wavelength, Å	1.54184
Crystal system	Orthorhombic
Space group	Pbca
a, Å	14.0704(1)
b, Å	14.7015(1)
c, Å	16.8880(1)

α, °	90.0
β, °	90.0
γ, °	90.0
Volume, Å^3	3493.38(4)
Z	8
Density (calc), Mg/m^3	1.340
Abs. coefficient, mm^{-1}	2.580
F(000)	1472
Crystal size, mm^3	0.220 x 0.200 x 0.200
Theta range, °	5.078 - 71.486
Reflections collected	63031
Indpt reflections (R_{int})	3394 (0.0282)
Absorption correction	Multi-scan
Max. / min. transmission	1.0 / 0.75017
Refinement method	F^2
Data /restraints/parameters	3394 / 0 / 218
Goodness-of-fit on F^2	1.046
R1, wR2 [I>2σ(I)]	0.0254, 0.0658
R1, wR2 (all data)	0.0261, 0.0663
Residual density, e.Å^{-3}	0.274 / -0.283

Bond lengths [Å] and angles [°] for **4-44**

S(1)-P(1)	1.9562(4)	P(1)-C(11)	1.8080(12)
P(1)-C(21)	1.8178(12)	P(1)-C(31)	1.8350(12)
O(1)-C(321)	1.2055(16)	O(2)-C(323)	1.4500(16)
O(2)-C(321)	1.3346(16)	C(32)-C(321)	1.4977(17)
C(11)-C(12)	1.3918(17)	C(21)-C(26)	1.3911(17)
C(11)-C(16)	1.3951(16)	C(21)-C(22)	1.3980(17)
C(12)-C(13)	1.3889(18)	C(22)-C(23)	1.3828(18)
C(13)-C(14)	1.3863(19)	C(23)-C(24)	1.3911(19)
C(14)-C(15)	1.3868(19)	C(24)-C(25)	1.382(2)
C(15)-C(16)	1.3854(18)	C(25)-C(26)	1.3903(18)
C(31)-C(36)	1.3960(17)	C(33)-C(34)	1.3873(19)
C(31)-C(32)	1.4099(16)	C(34)-C(35)	1.3815(19)

C(32)-C(33)	1.3892(17)	C(35)-C(36)	1.3927(17)

C(11)-P(1)-S(1)	115.85(4)	C(11)-P(1)-C(21)	104.31(5)
C(21)-P(1)-S(1)	110.50(4)	C(11)-P(1)-C(31)	107.66(5)
C(31)-P(1)-S(1)	113.43(4)	C(21)-P(1)-C(31)	104.06(5)
C(321)-O(2)-C(323)	116.36(11)	O(2)-C(321)-C(32)	110.92(10)
O(1)-C(321)-O(2)	124.70(12)	C(33)-C(32)-C(321)	116.27(11)
O(1)-C(321)-C(32)	124.28(12)	C(31)-C(32)-C(321)	123.66(11)
C(12)-C(11)-C(16)	119.57(11)	C(26)-C(21)-C(22)	119.30(11)
C(12)-C(11)-P(1)	121.68(9)	C(26)-C(21)-P(1)	121.96(9)
C(16)-C(11)-P(1)	118.67(9)	C(22)-C(21)-P(1)	118.73(9)
C(13)-C(12)-C(11)	119.97(11)	C(23)-C(22)-C(21)	120.38(12)
C(14)-C(13)-C(12)	120.12(12)	C(22)-C(23)-C(24)	120.01(12)
C(13)-C(14)-C(15)	120.18(12)	C(25)-C(24)-C(23)	119.88(12)
C(16)-C(15)-C(14)	119.90(12)	C(24)-C(25)-C(26)	120.40(12)
C(15)-C(16)-C(11)	120.27(11)	C(25)-C(26)-C(21)	120.03(12)
C(36)-C(31)-C(32)	118.15(11)	C(34)-C(33)-C(32)	120.94(12)
C(36)-C(31)-P(1)	118.81(9)	C(35)-C(34)-C(33)	119.47(12)
C(32)-C(31)-P(1)	122.56(9)	C(34)-C(35)-C(36)	120.21(12)
C(33)-C(32)-C(31)	120.07(11)	C(35)-C(36)-C(31)	121.11(11)

Crystal data and structure refinement for 4-46

Identification code	**4-46**
Empirical formula	C21 H19 O P S2
Formula weight	382.45
Temperature, K	172.9(7)
Wavelength, Å	1.54184
Crystal system	Monoclinic
Space group	Cc
a, Å	12.9835(2)
b, Å	13.6545(2)
c, Å	10.8818(2)
α, °	90.0
β, °	95.887(2)

γ, °	90.0
Volume, $Å^3$	1918.99(5)
Z	4
Density (calc), Mg/m^3	1.324
Abs. coefficient, mm^{-1}	3.340
F(000)	800
Crystal size, mm^3	0.200 x 0.170 x 0.120
Theta range, °	4.713 to 71.425
Reflections collected	9104
Indpt reflections (R_{int})	3039 (0.0276)
Absorption correction	Sphere
Max. / min. transmission	0.10610 a/ 0.07366
Refinement method	F^2
Data /restraints/parameters	3039 / 2 / 227
Goodness-of-fit on F^2	1.047
R1, wR2 [I>2σ(I)]	0.0446, 0.1196
R1, wR2 (all data)	0.0451, 0.1203
Absolute structure parameter	0.02(3)
Residual density, $e.Å^{-3}$	0.349 / -0.285

Bond lengths [Å] and angles [°] for **4-46**

S(1)-P(1)	1.9530(14)	P(1)-C(111)	1.815(4)
S(2)-C(34)	1.768(5)	P(1)-C(121)	1.816(5)
S(2)-C(33)	1.814(5)	P(1)-C(131)	1.822(4)
O(1)-C(34)	1.195(7)		
C(34)-C(35)	1.508(7)	C(33)-C(132)	1.510(5)
C(111)-C(116)	1.391(6)	C(121)-C(126)	1.397(6)
C(111)-C(112)	1.392(7)	C(121)-C(122)	1.403(7)
C(112)-C(113)	1.388(6)	C(122)-C(123)	1.387(8)
C(113)-C(114)	1.385(8)	C(123)-C(124)	1.369(10)
C(114)-C(115)	1.366(8)	C(124)-C(125)	1.373(11)
C(115)-C(116)	1.404(6)	C(125)-C(126)	1.423(9)
C(131)-C(136)	1.400(5)	C(133)-C(134)	1.384(6)
C(131)-C(132)	1.404(5)	C(134)-C(135)	1.388(6)

C(132)-C(133)	1.407(5)	C(135)-C(136)	1.381(6)

C(34)-S(2)-C(33)	100.6(2)		
C(111)-P(1)-S(1)	111.87(14)	C(111)-P(1)-C(121)	107.38(19)
C(121)-P(1)-S(1)	114.95(15)	C(111)-P(1)-C(131)	105.79(17)
C(131)-P(1)-S(1)	113.24(13)	C(121)-P(1)-C(131)	102.79(18)
C(132)-C(33)-S(2)	112.1(3)	O(1)-C(34)-S(2)	123.8(4)
O(1)-C(34)-C(35)	123.7(5)	C(35)-C(34)-S(2)	112.6(4)
C(116)-C(111)-C(112)	119.7(4)	C(126)-C(121)-C(122)	119.5(5)
C(116)-C(111)-P(1)	123.2(3)	C(126)-C(121)-P(1)	120.2(4)
C(112)-C(111)-P(1)	117.1(3)	C(122)-C(121)-P(1)	120.2(3)
C(113)-C(112)-C(111)	120.1(4)	C(123)-C(122)-C(121)	120.7(5)
C(114)-C(113)-C(112)	119.8(5)	C(124)-C(123)-C(122)	120.1(7)
C(115)-C(114)-C(113)	120.7(4)	C(123)-C(124)-C(125)	120.4(6)
C(114)-C(115)-C(116)	120.1(5)	C(124)-C(125)-C(126)	120.9(5)
C(111)-C(116)-C(115)	119.5(5)	C(121)-C(126)-C(125)	118.3(6)
C(136)-C(131)-C(132)	119.3(3)	C(133)-C(132)-C(33)	117.2(3)
C(136)-C(131)-P(1)	119.6(3)	C(134)-C(133)-C(132)	121.6(4)
C(132)-C(131)-P(1)	121.0(3)	C(133)-C(134)-C(135)	119.4(4)
C(131)-C(132)-C(133)	118.4(3)	C(136)-C(135)-C(134)	120.0(4)
C(131)-C(132)-C(33)	124.4(3)	C(135)-C(136)-C(131)	121.3(4)

Hydrogen bonds for **4-46** [Å and °].

D-H...A	d(D-H)	d(H...A)	d(D...A)	<(DHA)
C(33)-H(33A)...O(1)	0.97	2.33	2.876(5)	115.0
C(33)-H(33B)...S(1)	0.97	2.88	3.449(5)	118.3
C(126)-H(126)...S(1)	0.93	2.93	3.396(7)	112.6

Symmetry transformations used to generate equivalent atoms:

Crystal data and structure refinement for 4-47

Identification code	**4-47**
Empirical formula	C_{21} H_{19} O P S_2
Formula weight	382.45
Temperature, K	180(2)
Wavelength, Å	1.54184
Crystal system	Monoclinic
Space group	$P2_1/c$
a, Å	10.7570(5)
b, Å	7.8455(4)
c, Å	22.8333(12)
α, °	90.0
β, °	91.650(5)
γ, °	90.0
Volume, $Å^3$	1926.20(17)
Z	4
Density (calc), Mg/m^3	1.319
Abs. coefficient, mm^{-1}	3.328
F(000)	800
Crystal size, mm^3	0.300 x 0.250 x 0.200
Theta range, °	3.873 to 71.355
Reflections collected	28522
Indpt reflections (R_{int})	3723 (0.1160)

Absorption correction	Multi-scan
Max. / min. transmission	1.0 / 0.54536
Refinement method	F^2
Data /restraints/parameters	3723 / 0 / 227
Goodness-of-fit on F^2	1.092
R1, wR2 [I>2σ(I)]	0.0648, 0.1651
R1, wR2 (all data)	0.1026, 0.1939
Residual density, e.Å^{-3}	0.601 / -0.432

Bond lengths [Å] and angles [°] for **4-47**

P(1)-S(1)	1.9545(14)	P(1)-C(31)	1.822(4)
P(1)-C(11)	1.820(4)	P(1)-C(21)	1.811(4)
S(2)-C(18)	1.620(5)	C(21)-C(26)	1.394(6)
O(1)-C(18)	1.330(5)	C(22)-C(23)	1.379(6)
O(1)-C(17)	1.448(5)	C(23)-C(24)	1.385(7)
C(11)-C(12)	1.386(5)	C(24)-C(25)	1.383(7)
C(11)-C(16)	1.414(5)	C(25)-C(26)	1.380(6)
C(12)-C(13)	1.389(6)	C(31)-C(32)	1.383(5)
C(13)-C(14)	1.364(7)	C(31)-C(36)	1.389(5)
C(14)-C(15)	1.384(6)	C(32)-C(33)	1.387(6)
C(15)-C(16)	1.393(6)	C(33)-C(34)	1.366(6)
C(16)-C(17)	1.496(6)	C(34)-C(35)	1.384(7)

C(18)-C(19)	1.491(6)	C(35)-C(36)	1.393(6)
C(21)-C(22)	1.388(6)		

C(21)-P(1)-C(11)	105.20(18)	C(21)-P(1)-S(1)	113.02(14)
C(21)-P(1)-C(31)	105.08(18)	C(11)-P(1)-S(1)	113.49(12)
C(11)-P(1)-C(31)	105.67(17)	C(31)-P(1)-S(1)	113.57(13)
C(12)-C(11)-P(1)	119.2(3)	C(16)-C(11)-P(1)	121.6(3)
C(18)-O(1)-C(17)	120.4(3)	C(13)-C(14)-C(15)	120.1(4)
C(12)-C(11)-C(16)	119.1(4)	C(14)-C(15)-C(16)	121.4(4)
C(11)-C(12)-C(13)	121.1(4)	C(15)-C(16)-C(11)	118.3(4)
C(14)-C(13)-C(12)	119.9(4)	C(15)-C(16)-C(17)	120.9(4)
C(11)-C(16)-C(17)	120.7(4)		
O(1)-C(17)-C(16)	111.0(3)	O(1)-C(18)-C(19)	109.0(4)
O(1)-C(18)-S(2)	125.7(3)	C(19)-C(18)-S(2)	125.4(4)
C(22)-C(21)-C(26)	118.9(4)	C(32)-C(31)-C(36)	120.3(4)
C(22)-C(21)-P(1)	119.2(3)	C(32)-C(31)-P(1)	119.4(3)
C(26)-C(21)-P(1)	121.8(3)	C(36)-C(31)-P(1)	120.3(3)
C(23)-C(22)-C(21)	120.3(4)	C(31)-C(32)-C(33)	119.1(4)
C(22)-C(23)-C(24)	120.5(4)	C(34)-C(33)-C(32)	120.8(4)
C(25)-C(24)-C(23)	119.5(4)	C(33)-C(34)-C(35)	120.6(4)
C(26)-C(25)-C(24)	120.2(5)	C(34)-C(35)-C(36)	119.2(4)
C(25)-C(26)-C(21)	120.5(4)	C(31)-C(36)-C(35)	119.9(4)

Hydrogen bonds for **4-47** [Å and °].

D-H...A	d(D-H)	d(H...A)	d(D...A)	<(DHA)
C(17)-H(17A)...S(2)	0.99	2.48	3.008(4)	112.8
C(17)-H(17B)...S(1)	0.99	2.79	3.572(4)	136.0
C(22)-H(22)...S(1)	0.95	2.92	3.390(5)	111.9
C(32)-H(32)...S(1)	0.95	2.92	3.389(4)	111.6

Symmetry transformations used to generate equivalent atoms:

Crystal data and structure refinement for 4-48

Identification code	**4-48**
Empirical formula	$C_{38}\ H_{32}\ P_2\ S_4$
Formula weight	678.81
Temperature, K	173(2)
Wavelength, Å	0.71073
Crystal system	Monoclinic
Space group	$P2_1/c$
a, Å	15.653(2)
b, Å	16.9038(17)
c, Å	12.9632(16)
α, °	90.0
β, °	98.741(12)
γ, °	90.0
Volume, $Å^3$	3390.2(7)
Z	4
Density (calc), Mg/m^3	1.330
Abs. coefficient, mm^{-1}	0.402
F(000)	1416
Crystal size, mm^3	0.24 x 0.16 x 0.15
Theta range, °	1.784 to 25.026
Reflections collected	17094
Indpt reflections (R_{int})	17094
Absorption correction	Multi-scan

Max. / min. transmission	0.71 / 0.76
Refinement method	F^2
Data /restraints/parameters	17094 / 24 / 395
Goodness-of-fit on F^2	1.131
R1, wR2 [I>2σ(I)]	0.1126, 0.2741
R1, wR2 (all data)	0.1293, 0.2878
Residual density, e.Å^{-3}	1.567 / -1.633

Bond lengths [Å] and angles [°] for **4-48**

P(1)-S(1)	1.961(3)	P(1)-C(111)	1.822(8)
P(1)-C(131)	1.822(7)	P(1)-C(121)	1.823(7)
S(2)-P(2)	1.952(3)		
C(112)-C(1)	1.502(12)	C(112)-C(1A)	1.502(12)
C(111)-C(116)	1.401(11)	C(123)-C(124)	1.377(14)
C(111)-C(112)	1.407(11)	C(124)-C(125)	1.376(12)
C(112)-C(113)	1.394(15)	C(125)-C(126)	1.389(11)
C(113)-C(114)	1.377(16)	C(131)-C(136)	1.384(10)
C(114)-C(115)	1.384(15)	C(131)-C(132)	1.400(10)
C(115)-C(116)	1.384(13)	C(132)-C(133)	1.378(11)
C(121)-C(126)	1.384(11)	C(133)-C(134)	1.381(13)
C(121)-C(122)	1.404(11)	C(134)-C(135)	1.384(15)
C(122)-C(123)	1.372(13)	C(135)-C(136)	1.378(12)
C(221)-C(226)	1.390(11)	C(231)-C(236)	1.385(12)
C(221)-C(222)	1.394(11)	C(231)-C(232)	1.400(13)
C(221)-P(2)	1.823(8)	C(231)-P(2)	1.814(8)
C(222)-C(223)	1.388(12)	C(232)-C(233)	1.372(14)
C(223)-C(224)	1.371(15)	C(233)-C(234)	1.36(2)
C(224)-C(225)	1.365(15)	C(234)-C(235)	1.35(2)
C(225)-C(226)	1.384(13)	C(235)-C(236)	1.414(17)
P(2)-C(211)	1.867(15)	P(2)-C(241)	1.793(16)
C(211)-C(216)	1.426(18)	C(241)-C(246)	1.392(19)
C(211)-C(212)	1.427(18)	C(241)-C(242)	1.421(19)
C(212)-C(213)	1.41(2)	C(242)-C(243)	1.37(2)
C(212)-C(2)	1.497(19)	C(242)-C(2A)	1.50(2)

C(2)-S(4)	1.848(13)	C(2A)-S(4A)	1.832(13)
S(4)-S(3)	2.010(6)	S(4A)-S(3A)	2.025(6)
S(3)-C(1)	1.848(9)	S(3A)-C(1A)	1.954(10)
C(213)-C(214)	1.38(2)	C(243)-C(244)	1.37(2)
C(214)-C(215)	1.40(2)	C(244)-C(245)	1.42(2)
C(215)-C(216)	1.397(17)	C(245)-C(246)	1.387(18)

C(131)-P(1)-C(111)	103.2(3)	C(131)-P(1)-S(1)	113.3(2)
C(131)-P(1)-C(121)	106.4(3)	C(111)-P(1)-S(1)	115.9(3)
C(111)-P(1)-C(121)	106.1(3)	C(121)-P(1)-S(1)	111.3(3)
C(113)-C(112)-C(1)	118.6(8)	C(113)-C(112)-C(1A)	118.6(8)
C(111)-C(112)-C(1)	124.0(9)	C(111)-C(112)-C(1A)	124.0(9)
C(116)-C(111)-C(112)	120.4(8)	C(136)-C(131)-C(132)	119.4(7)
C(116)-C(111)-P(1)	118.7(6)	C(136)-C(131)-P(1)	120.4(6)
C(112)-C(111)-P(1)	120.9(6)	C(132)-C(131)-P(1)	120.1(5)
C(113)-C(112)-C(111)	117.3(8)	C(133)-C(132)-C(131)	120.4(7)
C(114)-C(113)-C(112)	122.4(9)	C(132)-C(133)-C(134)	119.5(8)
C(113)-C(114)-C(115)	119.8(10)	C(133)-C(134)-C(135)	120.4(8)
C(116)-C(115)-C(114)	119.8(10)	C(136)-C(135)-C(134)	120.3(8)
C(115)-C(116)-C(111)	120.3(8)	C(135)-C(136)-C(131)	120.0(8)
C(226)-C(221)-C(222)	119.4(8)	C(236)-C(231)-C(232)	118.9(9)
C(226)-C(221)-P(2)	118.4(6)	C(236)-C(231)-P(2)	120.8(8)
C(222)-C(221)-P(2)	122.0(6)	C(232)-C(231)-P(2)	120.2(6)
C(223)-C(222)-C(221)	119.5(9)	C(233)-C(232)-C(231)	119.7(11)
C(224)-C(223)-C(222)	120.4(10)	C(234)-C(233)-C(232)	121.7(13)
C(225)-C(224)-C(223)	120.5(9)	C(235)-C(234)-C(233)	119.7(11)
C(224)-C(225)-C(226)	120.3(9)	C(234)-C(235)-C(236)	121.0(12)
C(225)-C(226)-C(221)	119.9(9)	C(231)-C(236)-C(235)	119.0(12)
C(241)-P(2)-C(221)	104.4(9)	C(241)-P(2)-C(231)	110.8(7)
C(231)-P(2)-C(211)	102.5(6)	C(231)-P(2)-C(221)	102.4(4)
C(221)-P(2)-C(211)	108.5(9)		
C(231)-P(2)-S(2)	112.8(3)	C(241)-P(2)-S(2)	112.4(10)
C(211)-P(2)-S(2)	116.0(9)	C(221)-P(2)-S(2)	113.2(3)
C(216)-C(211)-C(212)	117.0(13)	C(246)-C(241)-C(242)	122.9(14)
C(216)-C(211)-P(2)	119.9(11)	C(246)-C(241)-P(2)	117.0(12)

C(212)-C(211)-P(2)	123.1(12)	C(242)-C(241)-P(2)	119.4(13)
C(213)-C(212)-C(211)	121.3(15)	C(243)-C(242)-C(241)	115.7(15)
C(213)-C(212)-C(2)	115.3(14)	C(243)-C(242)-C(2A)	122.9(14)
C(211)-C(212)-C(2)	123.3(13)	C(241)-C(242)-C(2A)	121.0(13)
C(212)-C(2)-S(4)	105.7(10)	C(242)-C(2A)-S(4A)	115.7(11)
C(2)-S(4)-S(3)	103.4(5)	C(2A)-S(4A)-S(3A)	103.5(5)
C(1)-S(3)-S(4)	97.4(4)	C(1A)-S(3A)-S(4A)	97.9(4)
C(112)-C(1)-S(3)	117.4(6)	C(112)-C(1A)-S(3A)	98.8(6)
C(214)-C(213)-C(212)	119.3(14)	C(244)-C(243)-C(242)	122.5(16)
C(213)-C(214)-C(215)	121.8(14)	C(243)-C(244)-C(245)	121.8(15)
C(216)-C(215)-C(214)	119.0(15)	C(246)-C(245)-C(244)	117.3(16)
C(215)-C(216)-C(211)	121.6(14)	C(245)-C(246)-C(241)	119.6(16)

Crystal data and structure refinement for 4-39

Identification code	**4-39**
Empirical formula	$C_{19}\ H_{17}\ P\ S_2$
Formula weight	680.83
Temperature, K	172(2)
Wavelength, Å	1.54184
Crystal system	Orthorhombic
Space group	Pbca
a, Å	16.97220(10)
b, Å	12.98020(10)
c, Å	30.8344(2)
α, °	90.0
β, °	90.0
γ, °	90.0
Volume, Å3	6792.90(8)
Z	8
Density (calc), Mg/m^3	1.331
Abs. coefficient, mm^{-1}	3.660
F(000)	2848
Crystal size, mm^3	0.42 x 0.28 x 0.08
Theta range, °	2.866 to 71.457

Reflections collected	33609
Indpt reflections (R_{int})	6522 (0.0369)
Absorption correction	Multiscan
Max. / min. transmission	1.0 / 0.12096
Refinement method	F^2
Data /restraints/parameters	6522 / 2 / 403
Goodness-of-fit on F^2	1.026
R1, wR2 [I>2σ(I)]	0.0314, 0.0826
R1, wR2 (all data)	0.0357, 0.0861
Residual density, e.Å^{-3}	0.481 / -0.432

Bond lengths [Å] and angles [°] for **4-39**

P(1)-C(111)	1.8128(17)	P(2)-C(221)	1.8125(18)
P(1)-C(121)	1.8129(16)	P(2)-C(21)	1.8216(17)
P(1)-C(11)	1.8185(16)	P(2)-C(211)	1.8225(19)
P(1)-S(1)	1.9624(6)	P(2)-S(2)	1.9547(6)
S(3)-C(17)	1.8300(19)	S(4)-C(27)	1.8203(19)
C(11)-C(16)	1.399(3)	C(21)-C(26)	1.399(3)
C(11)-C(12)	1.409(2)	C(21)-C(22)	1.412(2)
C(12)-C(13)	1.397(3)	C(22)-C(23)	1.394(3)
C(12)-C(17)	1.509(3)	C(22)-C(27)	1.511(3)
C(13)-C(14)	1.384(3)	C(23)-C(24)	1.381(3)
C(14)-C(15)	1.387(3)	C(24)-C(25)	1.386(3)
C(15)-C(16)	1.386(3)	C(25)-C(26)	1.383(3)
C(111)-C(116)	1.392(2)	C(211)-C(212)	1.391(3)
C(111)-C(112)	1.402(2)	C(211)-C(216)	1.394(3)
C(112)-C(113)	1.380(3)	C(212)-C(213)	1.390(3)
C(113)-C(114)	1.390(3)	C(213)-C(214)	1.374(4)
C(114)-C(115)	1.384(3)	C(214)-C(215)	1.388(3)
C(115)-C(116)	1.393(2)	C(215)-C(216)	1.391(3)
C(121)-C(126)	1.385(2)	C(221)-C(222)	1.394(2)
C(121)-C(122)	1.398(2)	C(221)-C(226)	1.394(3)
C(122)-C(123)	1.388(3)	C(222)-C(223)	1.389(3)
C(123)-C(124)	1.385(3)	C(223)-C(224)	1.383(3)

C(124)-C(125)	1.385(3)	C(224)-C(225)	1.380(3)
C(125)-C(126)	1.388(2)	C(225)-C(226)	1.386(3)

C(111)-P(1)-C(121)	106.74(8)	C(221)-P(2)-C(21)	105.93(8)
C(111)-P(1)-C(11)	106.08(8)	C(221)-P(2)-C(211)	104.84(8)
C(121)-P(1)-C(11)	102.83(7)	C(21)-P(2)-C(211)	107.30(8)
C(111)-P(1)-S(1)	110.56(6)	C(221)-P(2)-S(2)	113.14(6)
C(121)-P(1)-S(1)	114.26(6)	C(21)-P(2)-S(2)	113.41(6)
C(11)-P(1)-S(1)	115.60(6)	C(211)-P(2)-S(2)	111.62(6)
C(16)-C(11)-C(12)	119.54(15)	C(26)-C(21)-C(22)	119.08(16)
C(16)-C(11)-P(1)	118.88(13)	C(26)-C(21)-P(2)	119.26(14)
C(12)-C(11)-P(1)	121.51(13)	C(22)-C(21)-P(2)	121.61(13)
C(13)-C(12)-C(11)	118.35(16)	C(23)-C(22)-C(21)	118.66(16)
C(13)-C(12)-C(17)	117.78(16)	C(23)-C(22)-C(27)	117.34(16)
C(11)-C(12)-C(17)	123.87(15)	C(21)-C(22)-C(27)	124.00(16)
C(14)-C(13)-C(12)	121.65(18)	C(24)-C(23)-C(22)	121.59(18)
C(13)-C(14)-C(15)	119.78(18)	C(23)-C(24)-C(25)	119.70(18)
C(16)-C(15)-C(14)	119.75(18)	C(26)-C(25)-C(24)	119.93(18)
C(15)-C(16)-C(11)	120.91(17)	C(25)-C(26)-C(21)	121.04(18)
C(12)-C(17)-S(3)	113.03(12)	C(22)-C(27)-S(4)	112.60(13)
C(116)-C(111)-C(112)	119.06(16)	C(212)-C(211)-C(216)	119.43(18)
C(116)-C(111)-P(1)	123.24(13)	C(212)-C(211)-P(2)	118.49(15)
C(112)-C(111)-P(1)	117.70(13)	C(216)-C(211)-P(2)	122.06(15)
C(113)-C(112)-C(111)	120.62(17)	C(213)-C(212)-C(211)	120.3(2)
C(112)-C(113)-C(114)	120.01(17)	C(214)-C(213)-C(212)	120.2(2)
C(115)-C(114)-C(113)	119.90(17)	C(213)-C(214)-C(215)	120.1(2)
C(114)-C(115)-C(116)	120.38(17)	C(214)-C(215)-C(216)	120.2(2)
C(111)-C(116)-C(115)	120.03(16)	C(215)-C(216)-C(211)	119.80(19)
C(126)-C(121)-C(122)	120.04(15)	C(222)-C(221)-C(226)	119.14(17)
C(126)-C(121)-P(1)	119.50(13)	C(222)-C(221)-P(2)	121.77(14)
C(122)-C(121)-P(1)	120.46(13)	C(226)-C(221)-P(2)	119.06(13)
C(123)-C(122)-C(121)	119.46(17)	C(223)-C(222)-C(221)	119.99(17)
C(124)-C(123)-C(122)	120.39(18)	C(224)-C(223)-C(222)	120.27(18)
C(123)-C(124)-C(125)	119.98(17)	C(225)-C(224)-C(223)	120.10(18)
C(124)-C(125)-C(126)	120.09(18)	C(224)-C(225)-C(226)	120.05(18)

C(121)-C(126)-C(125)	120.03(17)	C(225)-C(226)-C(221)	120.44(18)

Hydrogen bonds for **4-39** [Å and °].

D-H...A	d(D-H)	d(H...A)	d(D...A)	<(DHA)
S(3)-H(3)...S(1)	1.146(15)	2.694(18)	3.7022(7)	146.2(16)
C(17)-H(17B)...S(1)	0.99	2.96	3.5267(18)	117.1
C(126)-H(126)...S(1)	0.95	2.88	3.3764(17)	114.1
S(4)-H(4)...S(2)	1.182(17)	2.82(2)	3.7905(8)	139.2(18)
C(27)-H(27A)...S(2)	0.99	2.98	3.5449(19)	117.3
C(212)-H(212)...S(2)	0.95	2.75	3.277(2)	115.8
C(226)-H(226)...S(2)	0.95	2.88	3.3639(19)	113.1

Crystal data and structure refinement for 4-38

Identification code	**4-38**
Empirical formula	C_{42} H_{36} Fe P S_4
Formula weight	755.77
Temperature, K	172(1)
Wavelength, Å	1.54184
Crystal system	Triclinic
Space group	P -1
a, Å	9.2536(4)
b, Å	12.6526(6)
c, Å	16.4398(8)
α, °	74.524(4)
β, °	80.988(4)
γ, °	79.780(4)
Volume, $Å^3$	1813.42(15)
Z	2
Density (calc), Mg/m^3	1.384
Abs. coefficient, mm^{-1}	6.128 mm^{-1}
F(000)	786

Crystal size, mm^3	? x ? x ?
Theta range, °	3.662 to 61.452°.
Reflections collected	15255
Indpt reflections (R_{int})	5594 (0.0641)
Absorption correction	Sphere
Max. / min. transmission	0.08470 / 0.01862
Refinement method	F^2
Data /restraints/parameters	5594 / 0 / 433
Goodness-of-fit on F^2	1.072
R1, wR2 [I>2σ(I)]	0.0697, 0.1710
R1, wR2 (all data)	0.0748, 0.1783
Residual density, $e.Å^{-3}$	0.845 / -1.256

Bond lengths [Å] and angles [°] for **4-38**

Cg(1)-Fe(1)	1.630(2)	Cg(2)-Fe(1)	1.650(3)
S(1)-P(1)	1.9584(14)	S(2)-P(2)	1.9583(12)
S(21)-C(21)	1.823(4)	S(21)-C(22)	1.817(4)
P(1)-C(1)	1.796(4)	P(2)-C(211)	1.814(4)
P(1)-C(111)	1.815(4)	P(2)-C(24)	1.819(4)
P(1)-C(121)	1.828(4)	P(2)-C(221)	1.821(4)
C(2)-C(21)	1.496(5)	C(24)-C(25)	1.398(6)
C(22)-C(23)	1.520(6)	C(25)-C(26)	1.383(6)
C(23)-C(28)	1.395(6)	C(26)-C(27)	1.385(7)
C(23)-C(24)	1.407(6)	C(27)-C(28)	1.382(7)
C(111)-C(112)	1.375(6)	C(121)-C(122)	1.382(6)
C(111)-C(116)	1.380(6)	C(121)-C(126)	1.382(6)
C(112)-C(113)	1.374(8)	C(122)-C(123)	1.394(7)
C(113)-C(114)	1.352(7)	C(123)-C(124)	1.362(9)
C(114)-C(115)	1.362(7)	C(124)-C(125)	1.374(9)
C(115)-C(116)	1.382(7)	C(125)-C(126)	1.397(8)
C(211)-C(216)	1.396(6)	C(221)-C(226)	1.384(6)
C(211)-C(212)	1.403(5)	C(221)-C(222)	1.388(6)
C(212)-C(213)	1.380(6)	C(222)-C(223)	1.384(7)
C(213)-C(214)	1.376(6)	C(223)-C(224)	1.372(8)

C(214)-C(215)	1.403(6)	C(224)-C(225)	1.389(7)
C(215)-C(216)	1.372(6)	C(225)-C(226)	1.384(6)

Cg(1)-Fe(1)-Cg(2)	177.64(14)	C(22)-S(21)-C(21)	98.94(18)
C(1)-P(1)-C(111)	103.71(16)	C(1)-P(1)-S(1)	118.10(13)
C(1)-P(1)-C(121)	103.88(17)	C(111)-P(1)-S(1)	113.02(13)
C(111)-P(1)-C(121)	105.33(17)	C(121)-P(1)-S(1)	111.60(14)
C(211)-P(2)-C(24)	107.08(16)	C(211)-P(2)-S(2)	112.92(13)
C(211)-P(2)-C(221)	103.27(17)	C(24)-P(2)-S(2)	113.95(12)
C(24)-P(2)-C(221)	105.39(18)	C(221)-P(2)-S(2)	113.35(13)
C(2)-C(1)-P(1)	128.0(3)	C(5)-C(1)-P(1)	124.5(3)
C(1)-C(2)-C(21)	127.2(3)	C(3)-C(2)-C(21)	125.8(3)
C(2)-C(21)-S(21)	110.0(3)	C(23)-C(22)-S(21)	116.7(3)
C(28)-C(23)-C(24)	118.5(4)	C(24)-C(23)-C(22)	122.0(4)
C(28)-C(23)-C(22)	119.4(4)	C(25)-C(24)-C(23)	119.5(4)
C(23)-C(24)-P(2)	122.1(3)	C(25)-C(24)-P(2)	118.4(3)
C(26)-C(25)-C(24)	121.0(4)	C(28)-C(27)-C(26)	120.3(4)
C(25)-C(26)-C(27)	119.4(4)	C(27)-C(28)-C(23)	121.2(4)
C(112)-C(111)-C(116)	118.5(4)	C(122)-C(121)-C(126)	119.4(4)
C(112)-C(111)-P(1)	119.9(3)	C(122)-C(121)-P(1)	121.4(3)
C(116)-C(111)-P(1)	121.6(3)	C(126)-C(121)-P(1)	119.2(3)
C(113)-C(112)-C(111)	120.0(4)	C(121)-C(122)-C(123)	119.8(5)
C(114)-C(113)-C(112)	121.4(4)	C(124)-C(123)-C(122)	121.0(6)
C(113)-C(114)-C(115)	119.4(4)	C(123)-C(124)-C(125)	119.6(5)
C(114)-C(115)-C(116)	120.2(4)	C(124)-C(125)-C(126)	120.3(5)
C(111)-C(116)-C(115)	120.4(4)	C(121)-C(126)-C(125)	120.0(5)
C(216)-C(211)-C(212)	119.5(3)	C(226)-C(221)-C(222)	120.1(4)
C(216)-C(211)-P(2)	118.7(3)	C(226)-C(221)-P(2)	122.1(3)
C(212)-C(211)-P(2)	121.8(3)	C(222)-C(221)-P(2)	117.9(3)
C(213)-C(212)-C(211)	119.5(4)	C(223)-C(222)-C(221)	119.5(4)
C(214)-C(213)-C(212)	121.0(4)	C(224)-C(223)-C(222)	120.7(4)
C(213)-C(214)-C(215)	119.7(4)	C(223)-C(224)-C(225)	119.8(4)
C(216)-C(215)-C(214)	120.0(4)	C(226)-C(225)-C(224)	120.0(4)
C(215)-C(216)-C(211)	120.3(3)	C(225)-C(226)-C(221)	119.9(4)

Hydrogen bonds for **4-38** [Å and °].

D-H...A	d(D-H)	d(H...A)	d(D...A)	<(DHA)
C(21)-H(21B)...S(1)	0.99	2.80	3.657(4)	144.8
C(212)-H(212)...S(1)	0.95	3.00	3.670(4)	128.5
C(216)-H(216)...S(2)	0.95	2.98	3.423(4)	109.8
C(222)-H(222)...S(2)	0.95	2.85	3.349(5)	113.8

Crystal data and structure refinement for 4-54

Identification code	**4-54**
Empirical formula	C_{25} H_{23} Fe O P S_2
Formula weight	490.37
Temperature, K	172.9(7)
Wavelength, Å	1.54184
Crystal system	Monoclinic
Space group	$P2_1$
a, Å	8.5020(2)
b, Å	10.9304(2)
c, Å	12.3107(3)
α, °	90.0
β, °	104.653(2)
γ, °	90.0
Volume, $Å^3$	1106.83(4)
Z	2
Density (calc), Mg/m^3	1.471
Abs. coefficient, mm^{-1}	8.021
F(000)	508
Crystal size, mm^3	0.700 x 0.400 x 0.300
Theta range, °	3.711 to 71.404
Reflections collected	10883
Indpt reflections (R_{int})	4079 (0.0377)

Absorption correction	Sphere
Max. / min. transmission	0.10610 / 0.02366
Refinement method	F^2
Data /restraints/parameters	4079 / 1 / 272
Goodness-of-fit on F^2	1.073
R1, wR2 [I>2σ(I)]	0.0426, 0.1079
R1, wR2 (all data)	0.0433, 0.1089
Absolute configuration parameter	-0.014(4)
Residual density, e.$Å^{-3}$	0.771 / -0.219

Bond lengths [Å] and angles [°] for **4-54**

Ct1(1)-Fe(1)	1.643(2)	Ct1(2)-Fe(1)	1.661(2)
P(1)-C(1)	1.790(4)	P(1)-S(1)	1.9549(16)
P(1)-C(111)	1.814(4)	P(1)-C(121)	1.814(5)
S(2)-C(21)	1.814(5)	S(2)-C(22)	1.779(6)
O(1)-C(22)	1.193(8)		
C(2)-C(21)	1.497(7)	C(22)-C(23)	1.507(8)
C(111)-C(112)	1.390(7)	C(121)-C(122)	1.388(8)
C(111)-C(116)	1.394(7)	C(121)-C(126)	1.392(7)
C(112)-C(113)	1.389(7)	C(122)-C(123)	1.397(8)
C(113)-C(114)	1.372(9)	C(123)-C(124)	1.373(10)
C(114)-C(115)	1.369(9)	C(124)-C(125)	1.363(11)
C(115)-C(116)	1.400(7)	C(125)-C(126)	1.402(9)

Ct(1)-Fe(1)-Ct(2)	176.45(12)		
C(1)-P(1)-S(1)	117.30(16)	C(1)-P(1)-C(121)	103.3(2)
C(121)-P(1)-S(1)	112.57(16)	C(1)-P(1)-C(111)	104.21(19)
C(111)-P(1)-S(1)	112.00(17)	C(121)-P(1)-C(111)	106.4(2)
C(22)-S(2)-C(21)	101.0(2)		
C(2)-C(1)-P(1)	128.8(4)	C(5)-C(1)-P(1)	123.8(3)
C(1)-C(2)-C(21)	127.9(4)	C(3)-C(2)-C(21)	124.4(4)
C(2)-C(21)-S(2)	110.9(3)	C(23)-C(22)-S(2)	111.5(5)
O(1)-C(22)-S(2)	124.2(4)	O(1)-C(22)-C(23)	124.3(6)
C(112)-C(111)-C(116)	119.4(4)	C(122)-C(121)-C(126)	119.0(5)

C(112)-C(111)-P(1)	119.4(4)	C(122)-C(121)-P(1)	122.0(4)
C(116)-C(111)-P(1)	121.1(4)	C(126)-C(121)-P(1)	118.9(4)
C(113)-C(112)-C(111)	120.0(5)	C(121)-C(122)-C(123)	120.8(5)
C(114)-C(113)-C(112)	120.5(6)	C(124)-C(123)-C(122)	119.7(6)
C(115)-C(114)-C(113)	120.2(5)	C(125)-C(124)-C(123)	120.3(6)
C(114)-C(115)-C(116)	120.5(5)	C(124)-C(125)-C(126)	121.0(6)
C(111)-C(116)-C(115)	119.5(5)	C(121)-C(126)-C(125)	119.4(6)

Hydrogen bonds for **4-54** [Å and °].

D-H...A	d(D-H)	d(H...A)	d(D...A)	<(DHA)
C(21)-H(21A)...O(1)	0.99	2.35	2.905(6)	114.4
C(21)-H(21B)...S(1)	0.99	2.89	3.722(5)	142.7
C(112)-H(112)...S(1)	0.95	2.89	3.352(5)	111.4
C(122)-H(122)...S(2)#1	0.95	2.99	3.699(6)	132.2

Symmetry transformations used to generate equivalent atoms:

#1 -x+1,y+1/2,-z+1

Crystal data and structure refinement for 4-51

Identification code	**4-51**
Empirical formula	$(C_{23}H_{20}F\ PS_2)_{0.84}\ (C_{23}H_{19}FePS_2)_{0.16}$
Formula weight	447.17
Temperature, K	113(2)
Wavelength, Å	0.71073
Crystal system	Monoclinic
Space group	$P2_1/c$
a, Å	8.496
b, Å	13.349
c, Å	18.408
α, °	90.0
β, °	101.950(3)
γ, °	90.0
Volume, $Å^3$	2042.53(2)

Z	4
Density (calc), Mg/m^3	1.454
Abs. coefficient, mm^{-1}	1.026
F(000)	923
Crystal size, mm^3	0.150 x 0.050 x 0.040
Theta range, °	1.899 to 30.757
Reflections collected	42892
Indpt reflections (R_{int})	6179 (0.0707)
Absorption correction	Multi-scan
Max. / min. transmission	0.96 / 0.89
Refinement method	F^2
Data /restraints/parameters	6179 / 0 / 253
Goodness-of-fit on F^2	1.103
R1, wR2 [I>2σ(I)]	0.0481, 0.1134
R1, wR2 (all data)	0.0828, 0.1274
Residual density, $e.Å^{-3}$	0.886 / -0.524

Bond lengths [Å] and angles [°] for **4-51**

Ct(1)-Fe(1)	1.637(1)	Ct(2)-Fe(1)	1.651(1)
P(1)-C(1)	1.795(2)	P(1)-S(1)	1.9566(9)
P(1)-C(11)	1.820(2)	P(1)-C(21)	1.819(2)
C(2)-C(21A)	1.485(4)	C(2)-C(21B)	1.485(4)
C(11)-C(16)	1.382(4)	C(21)-C(22)	1.389(3)
C(11)-C(12)	1.397(3)	C(21)-C(26)	1.391(3)
C(12)-C(13)	1.386(4)	C(22)-C(23)	1.395(4)
C(13)-C(14)	1.382(5)	C(23)-C(24)	1.388(4)
C(14)-C(15)	1.384(4)	C(24)-C(25)	1.378(4)
C(15)-C(16)	1.398(4)	C(25)-C(26)	1.393(4)
C(21A)-S(2A)	1.871(3)	C(21B)-S(2B)	1.516(5)

Ct(1)-Fe(1)-Ct(2)	177.37(6)		
C(1)-P(1)-S(1)	117.10(8)	C(1)-P(1)-C(11)	103.93(11)
C(11)-P(1)-S(1)	112.53(9)	C(1)-P(1)-C(21)	102.15(11)
C(21)-P(1)-S(1)	113.33(8)	C(11)-P(1)-C(21)	106.64(11)

C(2)-C(1)-P(1)	128.24(19)	C(5)-C(1)-P(1)	124.32(19)
C(3)-C(2)-C(21A)	124.8(2)	C(3)-C(2)-C(21B)	124.8(2)
C(1)-C(2)-C(21A)	128.0(2)	C(1)-C(2)-C(21B)	128.0(2)
C(16)-C(11)-C(12)	119.6(2)	C(22)-C(21)-C(26)	119.9(2)
C(16)-C(11)-P(1)	120.72(18)	C(22)-C(21)-P(1)	118.02(18)
C(12)-C(11)-P(1)	119.7(2)	C(26)-C(21)-P(1)	121.90(18)
C(13)-C(12)-C(11)	119.8(3)	C(21)-C(22)-C(23)	119.5(2)
C(14)-C(13)-C(12)	120.5(3)	C(24)-C(23)-C(22)	120.4(2)
C(13)-C(14)-C(15)	119.9(3)	C(25)-C(24)-C(23)	120.1(2)
C(14)-C(15)-C(16)	119.9(3)	C(24)-C(25)-C(26)	120.0(2)
C(11)-C(16)-C(15)	120.2(2)	C(21)-C(26)-C(25)	120.2(2)
C(2)-C(21A)-S(2A)	111.8(2)	C(2)-C(21B)-S(2B)	136.9(3)

Hydrogen bonds for **4-51** [Å and °].

D-H...A	d(D-H)	d(H...A)	d(D...A)	<(DHA)
C(12)-H(12)...S(1)	0.93	2.88	3.358(3)	113.3
C(22)-H(22)...S(1)	0.93	3.00	3.433(3)	110.2
C(12)-H(12)...S(1)	0.93	2.88	3.358(3)	113.3
C(22)-H(22)...S(1)	0.93	3.00	3.433(3)	110.2

Symmetry transformations used to generate equivalent atoms:

Crystal data and structure refinement for 4-56

Identification code	**4-56**
Empirical formula	C_{24} H_{23} Fe P S_2
Formula weight	462.36
Temperature, K	103(2)
Wavelength, Å	0.71073
Crystal system	Monoclinic
Space group	$P2_1/c$
a, Å	10.9637(7)
b, Å	9.5932(7)

c, Å	19.6925(13)
α, °	90.0
β, °	91.522(2)
γ, °	90.0
Volume, $Å^3$	2070.5(2)
Z	4
Density (calc), Mg/m^3	1.483
Abs. coefficient, mm^{-1}	1.015
F(000)	960
Crystal size, mm^3	0.20 x 0.20 x 0.06
Theta range, °	1.858 to 33.748
Reflections collected	64501
Indpt reflections (R_{int})	8236 (0.076)
Absorption correction	Multi-scan
Max. / min. transmission	0.7467 / 0.6845
Refinement method	F^2
Data /restraints/parameters	8236 / 0 / 254
Goodness-of-fit on F^2	1.038
R1, wR2 [I>2σ(I)]	0.0395, 0.1076
R1, wR2 (all data)	0.0614, 0.1229
Residual density, $e.Å^{-3}$	0.596 / -0.882

Bond lengths [Å] and angles [°] for **4-56**

Fe(1)-Ct(1)	1.635(1)	Fe(1)-Ct(2)	1.652(1)
S(1)-P(1)	1.9609(6)	P(1)-C(1)	1.7961(17)
S(2)-C(22)	1.800(2)	P(1)-C(111)	1.8143(16)
S(2)-C(21)	1.8238(18)	P(1)-C(121)	1.8150(17)
C(2)-C(21)	1.498(2)		
C(111)-C(112)	1.396(2)	C(121)-C(126)	1.391(2)
C(111)-C(116)	1.399(2)	C(121)-C(122)	1.398(2)
C(112)-C(113)	1.388(2)	C(122)-C(123)	1.393(3)
C(113)-C(114)	1.392(3)	C(123)-C(124)	1.383(3)
C(114)-C(115)	1.377(3)	C(124)-C(125)	1.384(3)
C(115)-C(116)	1.393(3)	C(125)-C(126)	1.394(2)

Ct(1)-Fe(1)-Ct(2)	176.855(4)		
C(22)-S(2)-C(21)	100.59(9)	C(2)-C(21)-S(2)	113.84(13)
C(1)-P(1)-C(111)	103.57(8)	C(1)-P(1)-S(1)	115.46(6)
C(1)-P(1)-C(121)	105.42(7)	C(111)-P(1)-S(1)	112.82(6)
C(111)-P(1)-C(121)	105.39(7)	C(121)-P(1)-S(1)	113.17(6)
C(1)-C(2)-C(21)	127.16(15)	C(3)-C(2)-C(21)	126.32(15)
C(112)-C(111)-C(116)	119.28(15)	C(126)-C(121)-C(122)	119.31(16)
C(112)-C(111)-P(1)	121.47(12)	C(126)-C(121)-P(1)	119.88(12)
C(116)-C(111)-P(1)	119.23(13)	C(122)-C(121)-P(1)	120.81(13)
C(113)-C(112)-C(111)	120.45(16)	C(123)-C(122)-C(121)	120.16(17)
C(112)-C(113)-C(114)	119.87(17)	C(124)-C(123)-C(122)	120.29(17)
C(115)-C(114)-C(113)	120.01(16)	C(123)-C(124)-C(125)	119.68(17)
C(114)-C(115)-C(116)	120.67(17)	C(124)-C(125)-C(126)	120.65(17)
C(115)-C(116)-C(111)	119.68(16)	C(121)-C(126)-C(125)	119.90(16)

Hydrogen bonds for **4-56** [Å and °].

D-H...A	d(D-H)	d(H...A)	d(D...A)	<(DHA)
C(21)-H(21B)...S(1)	0.99	2.76	3.4920(19)	131.2
C(126)-H(126)...S(1)	0.95	2.96	3.4099(18)	110.3

Symmetry transformations used to generate equivalent atoms:

Crystal data and structure refinement for 4-57

Identification code	**4-57**
Empirical formula	$C_{47}\ H_{42}\ Fe_2\ P_2\ S_4$
Formula weight	908.68
Temperature, K	101(2)
Wavelength, Å	0.71073

Crystal system	Orthorhombic
Space group	$Pna2_1$
a, Å	36.158(7)
b, Å	8.2002(16)
c, Å	14.036(3)
α, °	90.0
β, °	90.0
γ, °	90.0
Volume, $Å^3$	4161.7(14)
Z	4
Density (calc), Mg/m^3	1.450
Abs. coefficient, mm^{-1}	1.009
F(000)	1880
Crystal size, mm^3	0.03 x 0.02 x 0.005
Theta range, °	1.837 to 25.112
Reflections collected	70703
Indpt reflections (R_{int})	7062 (0.266)
Absorption correction	Multi-scan
Max. / min. transmission	0.7401 / 0.5911
Refinement method	F^2
Data /restraints/parameters	7062 / 1 / 262
Goodness-of-fit on F^2	1.113

R1, wR2 [I>2σ(I)]	0.1097, 0.1953
R1, wR2 (all data)	0.1868, 0.2198
Absolute structure parameter	0.02(7)
Residual density, e.Å^{-3}	0.787 and -0.743

Bond lengths [Å] and angles [°] for **4-57**

Fe(1)-Ct(1)	1.950(7)	Fe(2)-Ct(3)	1.950(7)
Fe(1)-Ct(2)	1.950(7)	Fe(2)-Ct(4)	1.950(7)
P(1)-C(111)	1.79(2)	P(2)-C(211)	1.805(18)
P(1)-C(11)	1.793(18)	P(2)-C(21)	1.78(2)
P(1)-C(121)	1.82(2)	P(2)-C(221)	1.824(19)
P(1)-S(1)	1.950(7)	P(2)-S(2)	1.961(8)
S(3)-C(2)	1.78(2)	S(4)-C(3)	1.77(2)
S(3)-C(3)	1.788(19)	S(4)-C(4)	1.79(2)
C(2)-C(12)	1.49(2)	C(4)-C(22)	1.47(2)
C(111)-C(116)	1.39(3)	C(121)-C(126)	1.38(3)
C(111)-C(112)	1.41(3)	C(121)-C(122)	1.43(3)
C(112)-C(113)	1.40(3)	C(122)-C(123)	1.39(3)
C(113)-C(114)	1.37(3)	C(123)-C(124)	1.38(3)
C(114)-C(115)	1.36(3)	C(124)-C(125)	1.37(3)
C(115)-C(116)	1.36(3)	C(125)-C(126)	1.37(3)
C(211)-C(212)	1.35(3)	C(221)-C(222)	1.34(2)

C(211)-C(216)	1.41(3)	C(221)-C(226)	1.42(3)
C(212)-C(213)	1.38(3)	C(222)-C(223)	1.36(3)
C(213)-C(214)	1.37(3)	C(223)-C(224)	1.39(3)
C(214)-C(215)	1.33(3)	C(224)-C(225)	1.36(3)
C(215)-C(216)	1.39(3)	C(225)-C(226)	1.37(3)

C(111)-P(1)-C(11)	106.0(9)	C(21)-P(2)-C(211)	106.0(9)
C(111)-P(1)-C(121)	105.9(9)	C(211)-P(2)-C(221)	102.1(9)
C(11)-P(1)-C(121)	103.3(8)	C(21)-P(2)-C(221)	105.0(10)
C(111)-P(1)-S(1)	111.8(7)	C(211)-P(2)-S(2)	113.5(7)
C(11)-P(1)-S(1)	115.9(7)	C(21)-P(2)-S(2)	116.6(8)
C(121)-P(1)-S(1)	113.1(7)	C(221)-P(2)-S(2)	112.4(6)
Ct(1)-Fe(1)-Ct(2)	102.4(9)	Ct(3)-Fe(2)-Ct(4)	102.4(9)
C(2)-S(3)-C(3)	102.4(9)	C(3)-S(4)-C(4)	102.1(10)
C(12)-C(2)-S(3)	117.9(14)	C(22)-C(4)-S(4)	117.5(14)
S(4)-C(3)-S(3)	119.4(11)		
C(12)-C(11)-P(1)	127.2(14)	C(22)-C(21)-P(2)	125.8(15)
C(15)-C(11)-P(1)	124.3(14)	C(25)-C(21)-P(2)	124.7(15)
C(11)-C(12)-C(2)	129.6(17)	C(21)-C(22)-C(4)	127.5(16)
C(13)-C(12)-C(2)	124.8(17)	C(23)-C(22)-C(4)	126.6(16)
C(116)-C(111)-C(112)	117.5(18)	C(126)-C(121)-C(122)	118.8(18)
C(116)-C(111)-P(1)	121.7(15)	C(126)-C(121)-P(1)	120.3(15)
C(112)-C(111)-P(1)	120.6(15)	C(122)-C(121)-P(1)	121.0(15)

C(113)-C(112)-C(111)	120(2)	C(123)-C(122)-C(121)	119(2)
C(114)-C(113)-C(112)	120(2)	C(124)-C(123)-C(122)	121(2)
C(115)-C(114)-C(113)	121(2)	C(125)-C(124)-C(123)	120(2)
C(114)-C(115)-C(116)	120(2)	C(124)-C(125)-C(126)	120(2)
C(115)-C(116)-C(111)	122.2(19)	C(125)-C(126)-C(121)	121.1(19)
C(212)-C(211)-C(216)	118.0(18)	C(222)-C(221)-C(226)	120.3(18)
C(212)-C(211)-P(2)	124.2(16)	C(222)-C(221)-P(2)	120.7(15)
C(216)-C(211)-P(2)	117.7(16)	C(226)-C(221)-P(2)	118.6(14)
C(211)-C(212)-C(213)	123(2)	C(221)-C(222)-C(223)	122(2)
C(214)-C(213)-C(212)	117(2)	C(222)-C(223)-C(224)	119(2)
C(215)-C(214)-C(213)	122(2)	C(225)-C(224)-C(223)	120(2)
C(214)-C(215)-C(216)	121(2)	C(224)-C(225)-C(226)	122(2)
C(215)-C(216)-C(211)	118(2)	C(225)-C(226)-C(221)	117.4(18)

Hydrogen bonds for **4-57** [Å and °].

D-H...A	d(D-H)	d(H...A)	d(D...A)	<(DHA)
C(2)-H(2A)...S(4)	0.99	2.80	3.346(19)	115.2
C(2)-H(2B)...S(1)	0.99	2.87	3.68(2)	140.0
C(3)-H(3A)...S(2)#1	0.99	2.90	3.61(2)	129.5
C(4)-H(4A)...S(3)	0.99	2.86	3.37(2)	113.0
C(4)-H(4B)...S(2)	0.99	2.80	3.57(2)	135.1
C(216)-H(216)...S(2)	0.95	2.83	3.32(2)	113.7

Symmetry transformations used to generate equivalent atoms:

#1 -x,-y+1,z+1/2